UNIVERSIDAD COMPLUTENSE DE MADRID
FACULTAD DE CIENCIAS QUIMICAS
Departamento de Química Analítica

TESIS DOCTORAL

Desarrollo de biosensores para la determinación de reguladores del apetito en muestras biológica

MEMORIA PARA OPTAR AL GRADO DE DOCTOR

PRESENTADA POR

Gonzalo Martínez García

Directores

Paloma Yáñez-Sedeño Orive
Lourdes Agüí Chicharro
José Manuel Pingarrón Carrazón

Madrid
Ed. electrónica 2019

UNIVERSIDAD COMPLUTENSE DE MADRID
FACULTAD DE CIENCIAS QUÍMICAS
DEPARTAMENTO DE QUÍMICA ANALÍTICA

DESARROLLO DE BIOSENSORES PARA LA DETERMINACIÓN DE REGULADORES DEL APETITO EN MUESTRAS BIOLÓGICAS

Directores:

Dra. Paloma Yáñez-Sedeño Orive
Catedrática de la UCM
Dra. Lourdes Agüí Chicharro
Profesora Titular de la UCM
Dr. José Manuel Pingarrón Carrazón
Catedrático de la UCM

TESIS DOCTORAL PRESENTADA POR

GONZALO MARTÍNEZ GARCÍA

Madrid, 2018

Universidad Complutense de Madrid
Dpto. Química Analítica - Facultad de CC. Químicas - Ciudad Universitaria. 28040 Madrid
Tfno.: 34 913944331 E-mail: depquian@ucm.es

Dª Mª CRUZ MORENO BONDI, CATEDRÁTICA Y DIRECTORA DEL DEPARTAMENTO DE QUÍMICA ANALÍTICA DE LA FACULTAD DE CIENCIAS QUÍMICAS DE LA UNIVERSIDAD COMPLUTENSE DE MADRID

HACE CONSTAR,

Que el trabajo titulado "**DESARROLLO DE BIOSENSORES PARA LA DETERMINACIÓN DE REGULADORES DEL APETITO EN MUESTRAS BIOLÓGICAS**" ha sido realizado bajo la dirección de los doctores**, Paloma Yáñez-Sedeño Orive, Lourdes Agüí Chicharro y José Manuel Pingarrón Carrazón**, profesores de dicho departamento, constituyendo la Tesis Doctoral de su autor.

Madrid, 20 de junio de 2018

Fdo. Mª Cruz Moreno Bondi

Fdo. Paloma Yáñez-Sedeño Orive

Fdo. Lourdes Agüí Chicharro

Fdo. José Manuel Pingarrón Carrazón

Fdo. Gonzalo Martínez García

ÍNDICE

1. SUMMARY 1

1.1. INTRODUCTION 3

1.2. AIMS OF THIS WORK 3

1.3. RESEARCH RESULTS 4

1.4. MILESTONES 4

2. RESUMEN 7

2.1. INTRODUCCIÓN 9

2.2. OBJETIVOS DEL TRABAJO 9

2.3. RESULTADOS 10

2.4. LOGROS 10

3. INTRODUCTION 13

3.1. OBJECTIVE AND WORK PLAN 15

3.2. ELECTROCHEMICAL BIOSENSORS 16

3.3. APPETITE REGULATORS 17

3.4. OBESITY BIOMARKERS 18

3.5. ANALYTES AND THEIR BIOLOGICAL SIGNIFICANCE 21

3.5.1. PEPTIDE HORMONES 21

3.5.1.1. Ghrelin (GHRL) 21

3.5.1.2. Peptide YY (PYY) 24

3.5.1.3. Amylin (AMY) 26

3.5.2. CYTOKINES 29

3.5.2.1. Transforming growth factor β1(TGF-β1) 31

3.5.3. STEROID HORMONES 32

3.5.3.1. Ethynyl estradiol (EE2) 33

3.5.4. KETONE BODIES 33

3.4.4.1. β-hydroxybutyrate (β-HB) 34

3.6. MATERIALS USED FOR THE PREPARATION OF THE ELECTROCHEMICAL SCAFFOLDS 36

3.6.1. MAGNETIC MICROBEADS 36

3.6.2. GRAPHENE AND GRAPHENE HYBRIDS 41

3.6.3. CONDUCTING POLYMERS 48

3.7. STRATEGIES USED FOR THE IMMOBILIZATION ..... OF BIOMOLECULES 51

3.7.1. ELECTROCHEMICAL GRAFTING 51

3.8. REPORTED METHODS FOR THE DETERMINATION OF THE ANALYTES OF INTEREST 56

3.8.1. GHRELIN (GHRL) 56

3.8.2. PEPTIDE YY (PYY) 58

3.8.3. AMYLIN (AMY) 58

3.8.4. TRANSFORMING GROWTH FACTOR β1 (TGF- β1) 61

3.8.5. ETHYNYL ESTRADIOL (EE2) 63

3.8.6. β-HYDROXYBUTYRATE (β-HB) 65

4. PARTE EXPERIMENTAL 69

4.1. INSTRUMENTACIÓN 71

4.1.1. APARATOS 71

4.1.1.1. Otros aparatos 73

4.1.2. ELECTRODOS 73

4.1.3. CÉLULAS ELECTROQUÍMICAS 74

4.1.4. DISPOSITIVOS 75

4.2. REACTIVOS Y DISOLUCIONES 77

4.2.1. MAGNETOINMUNOSENSOR PARA LA DETERMINACIÓN DE GHRL 77

4.2.2. MAGNETOINMUNOSENSOR PARA LA DETERMINACIÓN DE TGF- β1 78

4.2.3. INMUNOSENSOR PARA LA DETERMINACIÓN DE PYY 78

4.2.4. INMUNOSENSOR DUAL PARA LA DETERMINACIÓN SIMULTÁNEA DE GHRL Y PYY 79

4.2.5. INMUNOSENSOR PARA LA DETERMINACIÓN DE EE2 80

4.2.6. BIOSENSOR ENZIMÁTICO PARA LA DETERMINACIÓN DE β-HB 80

4.2.7. INMUNOSENSOR PARA LA DETERMINACIÓN DE AMY 81

4.3. MUESTRAS 82

4.4. PROCEDIMIENTOS EXPERIMENTALES 82

4.4.1. PREPARACIÓN DEL MAGNETOINMUNOSENSOR PARA LA DETERMINACIÓN DE GHRL 82

4.4.1.1. Aplicación a la determinación de GHRL en saliva 84

4.4.2. MAGNETOINMUNOSENSOR PARA LA DETERMINACIÓN DE TGF-β1 84

4.4.2.1. Aplicación a la determinación de TGF-β1 en orina 85

4.4.3. INMUNOSENSOR PARA LA DETERMINACIÓN DE PYY 86

4.4.3.1. Aplicación a la determinación de PYY en suero 88

4.4.4. INMUNOSENSOR PARA LA DETERMINACIÓN SIMULTÁNEA DE GHRL Y PYY 88

4.4.4.1. Aplicación a la determinación de GHRL y PYY en suero y en saliva 90

4.4.5. INMUNOSENSOR PARA LA DETERMINACIÓN DE EE2 90

4.4.5.1. Aplicación a la determinación de EE2 en orina 92

4.4.6. BIOSENSOR ENZIMÁTICO PARA LA DETERMINACIÓN DE β-HB 92

4.4.6.1. Aplicación a la determinación de β-HB en suero 93

4.4.7. INMUNOSENSOR PARA LA DETERMINACIÓN DE AMY 94

4.4.7.1. Aplicación a la determinación de AMY en suero y en orina 95

5.RESULTADOS Y DISCUSIÓN 97

5.1. MAGNETOINMUNOSENSORES 101

5.1.1. MAGNETOINMUNOSENSOR PARA LA DETERMINACIÓN DE GHRL 103

5.1.1.1. Configuración del inmunosensor 104
5.1.1.2. Optimización de las variables experimentales 104
5.1.1.3. Calibrado y características analíticas 112
5.1.1.4. Estudios de selectividad 114
5.1.1.5. Aplicación a la determinación de GHRL en saliva 115
5.1.1.6. Conclusiones 117

5.1.2. MAGNETOINMUNOSENSOR PARA LA DETERMINACIÓN DE TGF-β1 118

5.1.2.1. Configuración del inmunosensor 119
5.1.2.2. Optimización de las variables experimentales 119
5.1.2.3. Calibrado y características analíticas 125
5.1.2.4. Estudios de selectividad 127
5.1.2.5. Aplicación a la determinación de TGF-β1 en orina 128
5.1.2.6. Conclusiones 130

5.2. BIOSENSORES BASADOS EN ELECTRODOS MODIFICADOS CON GRAFENO E HÍBRIDOS DE GRAFENO 131

5.2.1. INMUNOSENSOR PARA LA DETERMINACIÓN DE PYY 133

5.2.1.1. Configuración del inmunosensor 134
5.2.1.2. Optimización de las variables experimentales 134
5.2.1.3. Calibrado y características analíticas 145
5.2.1.4. Estudios de selectividad 148
5.2.1.5. Aplicación a la determinación de PYY en suero 149
5.2.1.6. Conclusiones 151

5.2.2. INMUNOSENSOR DUAL PARA LA DETERMINACIÓN SIMULTÁNEA DE GHRL y PYY 152

5.2.2.1. Configuración del inmunosensor 153
5.2.2.2. Optimización de las variables experimentales 153
5.2.2.3. Calibrados y características analíticas 158
5.2.2.4. Estudios de selectividad 161
5.2.2.5. Aplicación a la determinación de GHRL y PYY en suero y en saliva 162
5.2.2.6. Conclusiones 163

5.2.3. INMUNOSENSOR PARA LA DETERMINACIÓN DE EE2 164

5.2.3.1. Configuración del inmunosensor 165
5.2.3.2. Optimización de las variables experimentales 166
5.2.3.3. Calibrado y características analíticas 174
5.2.3.4. Estudios de selectividad 177
5.2.3.5. Aplicación a la determinación de EE2 en orina 178
5.2.3.6. Conclusiones 180

5.2.4. BIOSENSOR ENZIMÁTICO PARA LA DETERMINACIÓN DE β-HB 181

5.2.4.1. Configuración del biosensor 182
5.2.4.2. Optimización de las variables experimentales 182
5.2.4.3. Calibrado y características analíticas 188
5.2.4.4. Estudios de selectividad 191
5.2.4.5. Aplicación a la determinación de β-HB en suero 192
5.2.4.6. Conclusiones 193

5.3. INMUNOSENSOR ELECTROQUÍMICO BASADO EN UN POLÍMERO CONDUCTOR 195

5.3.1. INMUNOSENSOR PARA LA DETERMINACIÓN DE AMY 197

5.3.1.1. Configuración del inmunosensor 198
5.3.1.2. Optimización de las variables experimentales 198
5.3.1.3. Calibrado y características analíticas 207
5.3.1.4. Estudios de selectividad 210
5.3.1.5. Aplicación a la determinación de AMY en orina y suero 211
5.3.1.6. Conclusiones 212

6. CONCLUSIONS 213

7. BIBLIOGRAFÍA 219

8. GLOSSARY 243

9. PUBLICACIONES 253

INTRODUCTION

AIMS OF THIS WORK

1. SUMMARY

RESEARCH RESULTS

MILESTONES

BIOSENSORS DEVELOPMENT FOR THE DETERMINATION OF APPETITE REGULATORS IN BIOLOGICAL SAMPLES

1.1. INTRODUCTION

Hormones acting as appetite regulators affect the sensations of hunger and satiety. Variations in their levels can cause substancial pathology leading to obesity or anorexia. Therefore, monitoring of such species may lead to appropriate therapies targeted at the underlying disease process. The control center for hunger and satiety is located in the hypothalamus, and circulating peptides play important roles in appetitive behaviors. Among these species, the orexigen ghrelin (GHRL) and anorexigen peptide YY (PYY) together with a related estrogen, ethynyl estradiol (EE2) were analytical objectives in this work.

Regarding obesity, it is currently considered as a chronic inflammatory state in which some biomolecules present at altered levels trigger abnormal functioning of endocrine system. The variation in the concentrations of some of these species is indicative of some health problem related to obesity, such as diabetes; therefore, they can be used as biomarkers for preventive diagnosis. In this work, different types of obesity biomarkers were considered. These were a cytokine related with inflammatory states, transforming growth factor beta 1 (TGF-β1), a ketone body, beta-hydroxybutyrate (β-HB), and a hormone exhibiting similar activity to insulin, amylin (IAPP or AMY).

1.2. AIMS OF THIS WORK

The specific objective of this Thesis was the design, preparation and application of new electrochemical biosensing platforms with analytical utility and capacity for individual and / or multiple determination of biochemical species of interest in the field of appetite regulators and biomarkers of obesity. For this purpose, several configurations were developed in which the use of latest-generation micro- and nanomaterials was proposed as well as novel strategies for immobilizing the bioreactive materials used in each case. All the biosensors designed were applied to the monitoring of analytes scarcely studied for which there were no similar configurations or when existing, the analytical characteristics of the method were significantly improved. Note that, in all cases, the analytical usefulness of these designs was demonstrated by applying them to the analysis of saliva, serum or urine samples that contained physiological concentrations of the species to be determined.

All this research work was carried out by application of the usual methodology in the area of bioanalytical electrochemistry involving the design of the biosensor and the recognition strategy, the optimization of experimental variables, characterization studies, the stablishment of calibration plots and the analytical characteristics, studies of selectivity and application to the analysis of samples.

1.3. RESEARCH RESULTS

Two magnetoimmunosensors using magnetic microbeads functionalized with protein G or carboxylic groups, respectively, for the determination of GHRL in saliva and TGF-β1 in urine were developed.

Four biosensors based on graphene were also developed: An electrochemical platform prepared by grafting of diazonium salt of *p*-ABA onto a glassy carbon electrode modified with reduced graphene oxide (rGO/GCE) was used to prepare an immunosensor for PYY applied to human serum samples. An electrochemical immunosensor for the simultaneous determination of GHRL and PYY in serum and saliva was also prepared using rGO and dual SPCEs as the electrochemical scaffolds. Silver nanoparticles, silica and graphene oxide hybrids were also used to construct an electrochemical immunosensor for monitoring ethynyl estradiol (EE2) in urine. An enzymatic biosensor for the amperometric detection of β-hydroxybutyrate (β-HB) in serum was also implemented. Finally, the use of a carboxyl-functionalized conducting polymer poly(pyrrolepropionic acid) (pPPA) allowed the preparation of an immunosensor for the determination of the hormone AMY in serum and saliva.

1.4. MILESTONES

As major achievements in this Thesis can cite the following:

- An electrochemical immunosensor was first developed for the determination of GHRL using magnetic microparticles whose sensitivity is notably higher than that of commercial ELISA kits and the few immunosensor designs described in the literature. This immunosensor was applied to saliva samples.

- The first immunosensor was designed for the determination of the cytokine TGF-β1 using magnetic microparticles functionalized with carboxyl groups, a polymer of metal complexes to immobilize the capture antibody, and a polymer of peroxidase and streptavidin as a means of amplifying the electrochemical response. The immunosensor was applied to urine samples.

- The first immunosensor was prepared for the determination of PYY using a glassy carbon electrode modified with rGO. For the immobilization of the capture antibody, the electrochemical grafting of a diazonium salt was applied, this allowing the design of a highly sensitive competitive scheme applied to serum samples.

- A method for the simultaneous determination of GHRL and PYY using dual SPCEs modified by grafting a diazonium salt onto rGO was developed for the first time. The limits of detection attained were much lower than those of the immunoassay methods described for the individual determination of each hormone. The multiplex design was applied to serum and saliva.

- Making use for the first time of the AgNPs/SiO_2/GO hybrid onto SPCEs, and applying the grafting method of a diazonium salt to immobilize the capture antibody, an immunosensor was prepared for the determination of EE2 in urine.

- rGO was used for the first time in combination with thionine as a modifier material for SPCEs to develop an enzymatic biosensor for the determination of β-HB applied to serum samples.

- Using the conducting polymer pPPA, the first immunosensor for the determination of AMY hormone was prepared. The capture antibody was covalently immobilized on the surface confined carboxylic groups, and the resulting method, reaching a detection limit much lower than the commercial ELISA kits. It was applied to urine and serum samples.

INTRODUCCIÓN

OBJETIVOS DEL TRABAJO

2. RESUMEN

RESULTADOS EXPERIMENTALES

LOGROS

DESARROLLO DE BIOSENSORES PARA LA DETERMINACIÓN DE REGULADORES DEL APETITO EN MUESTRAS BIOLÓGICAS

2.1. INTRODUCCIÓN

Las hormonas que actúan como reguladores del apetito afectan a las sensaciones de hambre y saciedad. Variaciones en sus niveles pueden originar patologías que lleven a la obesidad o la anorexia. Por ello, la monitorización de estas especies es úitl para encontrar terapias apropiadas para la enfermedad subyacente. El centro de control del hambre y la saciedad se localiza en el hipotálamo, y los péptidos circulantes juegan papeles importantes en el comportamiento relacionado con el apetito. Entre estas especies, las hormonas grelina (GHRL), orexígena, y péptido YY (PYY), anorexígeno, junto con un estrógeno relacionado con ellas, el etinilestradiol (EE2) fueron objetivos analíticos de este trabajo.

En relación a la obesidad, actualmente se considera como un estado inflamatorio crónico en el que algunas moléculas que presentan niveles alterados desencadenan el funcionamiento anormal del sistema endocrino. La variación de la concentración de algunas de estas especies es indicativa de algún problema de salud relacionado con la obesidad como la diabetes. Por ello, éstas pueden ser empleadas como biomarcadores para diagnosis preventiva. En este trabajo, se han considerado diferentes tipos de biomarcadores de obesidad: una citoquina relacionada con el estado inflamatorio, factor de crecimiento transformante beta 1 (TGF-β1); un cuerpo cetónico, beta-hidroxibutirato (β-HB), y una hormona con actividad similar a la insulina, la amilina (AMY).

2.2. OBJETIVOS DEL TRABAJO

El objetivo específico de esta Tesis es el diseño, preparación y aplicación de nuevas plataformas biosensoras de utilidad analítica y capacidad para la determinación individual y/o múltiple de especies de interés bioquímico en el campo de los reguladores del apetito y los biomarcadores de obesidad. Con este propósito, se prepararon varias configuraciones de inmunosensores en las que se propuso el empleo de micro- y nanomateriales de última generación así como nuevas estrategias para la inmovilización de biorreactivos usados en cada caso. Todos los biosensores diseñados se aplicaron a la monitorización de analitos escasamente estudiados para los que no existían configuraciones similares o, en caso de existir, las características analíticas del método fueron mejoradas notablemente. Cabe destacar que, en todos los casos, la utilidad analítica de estos diseños fue demostrada por aplicación al

análisis de saliva, suero u orina que contenían concentraciones a nivel fisiológico de las especies a determinar.

Todas las investigaciones se realizaron aplicando la metodologia usual en el área de los biosensores electroquímicos que implica el diseño del biosensor y la estrategia de reconocimiento, la optimización de las variables experimentales, los estudios de caracterización, el establecimiento de los calibrados y las características analíticas del método, los estudios de selectividad y la aplicación al análisis de muestras.

2.3. RESULTADOS

Se desarrollaron dos magnetoinmunosensores empleando micropartículas magnéticas funcionalizadas con proteína G o con grupos carboxilo, respectivamente, para la determinación de GHRL en saliva y TGF-β1 en orina.

Se prepararon también cuatro biosensores basados en grafeno. Se diseñó una plataforma electroquímica mediante *grafting* de la sal de diazonio del ácido *p*-aminobenzoico (*p*-ABA) (*p*-carboxibencenodiazonio) sobre un electrodo de carbono vitrificado modificado con óxido de grafeno reducido (rGO/GCE) empleada para construir un inmunosensor para PYY, aplicada a muestras de suero humano. También se preparó un inmunosensor electroquímico para la determinación simultánea de GHRL y PYY en suero y en saliva empleando rGO y SPCEs duales como plataformas electroquímicas. Se utilizó el híbrido de nanopartículas de plata, sílice y óxido de grafeno para construir un inmunosensor electroquímico para la monitorización de etinilestradiol (EE2) en orina. También se desarrolló un biosensor enzimático para la detección amperométrica de β-hidroxibutirato (β-HB) en suero. Finalmente, el empleo de un polímero conductor funcionalizado con grupos carboxilo, ácido poli(pirrolpropiónico) (pPPA), hizo posible la preparación de un inmunosensor para la determinación de la hormona amilina (AMY) en suero y en saliva.

2.4. LOGROS

Como principales logros alcanzados en los trabajos realizados en esta Tesis, pueden citarse los siguientes:

- Por primera vez se desarrolló un inmunosensor electroquímico para la determinación de GHRL usando micropartículas magnéticas cuya sensibilidad es notablemente mayor que la de los kits ELISA comerciales y los escasos diseños de inmunosensores decritos en la bibliografía. Este inmunosensor se aplicó al análisis de saliva.

- Se diseñó el primer inmunosensor para la determinación de la citoquina TGF-β1 usando micropartículas magnéticas funcionalizadas con grupos carboxilo empleando un polímero de complejos metálicos para inmovilizar el anticuerpo de captura, así como un polímero de peroxidasa y estreptavidina como un metodo para amplificar la respuesta electroquímica. El inmunosensor se aplicó a muestras de orina.

- Se preparó el primer inmunosensor para la determinación de PYY usando un electrodo de carbono vitrificado modificado con rGO. Se aplicó el método de *grafting* electroquímico de una sal de diazonio, lo que hizo posible el diseño de una configuración competitiva altamente sensible aplicada a muestras de suero.

- Por primera vez se desarrolló un método para la determinación simultánea de GHRL y PYY usando SPCEs duales modificados mediante *grafting* de una sal de diazonio sobre rGO. Los límites de detección obtenidos fueron mucho menores que los de los métodos de inmunoensayo descritos para la determinación individual de cada hormona. Este diseño multiplex se aplicó a suero y saliva.

- Haciendo uso por primera vez del híbrido AgNPs/SiO_2/GO sobre SPCEs, aplicando el método de *grafting* de una sal de diazonio para inmovilizar el anticuerpo de captura, se preparó un inmunosensor para la determinación de EE2 en orina.

- Se utilizó rGO por primera vez en combinación con la tionina como material modificador de SPCEs para desarrollar un biosensor enzimático para la determinación de β-HB aplicado a muestras de suero.

- Se preparó el primer inmunosensor para la determinación de la hormona amilina usando el polímero conductor pPPA. El anticuerpo de captura se inmovilizó covalentemente sobre la superficie modificada con grupos carboxilo, y el método resultante, que presenta un límite de detección mucho menor que el de los kits ELISA comerciales, se aplicó a orina y suero.

OBJECTIVE AND WORK PLAN

ELECTROCHEMICAL BIOSENSORS

APPETITE REGULATORS

OBESITY BIOMARKERS

ANALYTES AND THEIR BIOLOGICAL SIGNIFICANCE

3. INTRODUCTION

MATERIALS USED FOR THE PREPARATION OF THE ELECTROCHEMICAL SCAFFOLDS

STRATEGIES USED FOR THE IMMOBILIZATION OF BIOMOLECULES

REPORTED METHODS FOR THE DETERMINATION OF THE ANALYTES OF INTEREST

3.1. OBJECTIVE AND WORK PLAN

The work presented in this Doctoral Thesis fits into the objectives of the Project CTQ2012-35041 financed by the Spanish Ministry of Economy, Industry and Competitiveness (MINECO), entitled: "New electrochemical biodetection strategies for obesity marker proteins". The specific objective is the design, preparation and application of new electrochemical biosensing platforms with analytical utility and capacity for individual and / or multiple determination of species of biochemical interest in the field of appetite regulators and biomarkers of obesity.

For this purpose, several configurations have been developed in which the use of latest-generation micro- and nanomaterials has been proposed, as well as novel strategies for immobilizing the bioreactive materials used in each case. All the biosensors designed have been applied to the monitoring of analytes scarcely studied for which there were no similar configurations or, where appropriate, the analytical characteristics of the method have been significantly improved. Note that, in all cases, the analytical usefulness of these designs has been demonstrated by applying them to the analysis of saliva, serum or urine samples that contained physiological concentrations of the species to be determined.

All this research work has been carried out by application of the usual methodology in the area of bioanalytical electrochemistry involving the following steps:

1. Design of the biosensor configuration and the recognition strategy.
2. Optimization of the experimental variables involved in the preparation of the biosensor and in the electrochemical detection.
3. Characterization studies.
4. Establishment of calibration plots and the analytical characteristics of the method.
5. Studies of selectivity.
6. Application to the analysis of samples.

3.2. ELECTROCHEMICAL BIOSENSORS

A chemical sensor is a device that transforms chemical information into an analytically useful signal [Thévenot et al., 2001]. They contain usually two basic components: a chemical recognition system (receptor) and a physico-chemical transducer. Biosensors are chemical sensors in which the recognition system utilises a biochemical mechanism. The biological recognition system translates information from the analyte concentration, into an output signal. The main purpose of the recognition system is to provide the sensor with a high degree of selectivity for the analyte to be measured. For this purpose, enzymes or affinity reagents such as antigens, antibodies, or DNA, among others are used. The transducer part of the sensor transfers the signal from the output domain of the recognition system, mostly to the electrical domain.

Biosensor-related research has experienced explosive growth over the last years (see Scheme 1). The main reason is the high applicability to a variety of samples including food, body fluids, cell cultures or environmental samples for the determination of a high number of analytes in different fields. Moreover, the development of biosensors has gone in parallel with that of nanotechnology. In fact, the special properties of nanomaterials have contributed to the rise of biosensors, especially in the case of electrochemical biosensors.

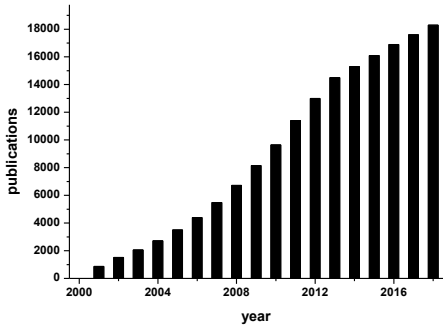

Scheme 1.- *Number of articles per year found in Scopus for the search term "immunosensor".*

An electrochemical biosensor is a biosensor with an electrochemical transducer, and it may be defined as an integrated receptor-transducer device, prepared from a modified electrode coated with a biological receptor. They are characterized by short assay time, simple handling, low cost, small sample requirement, possibility of multiplexing and miniaturization and good performance in complex samples with minimal pre-treatments. Furthermore, a wide variety of nanosized materials with interesting electrochemical properties and ability for immobilizing biomolecules have made it possible to multiply the possibilities of electrochemical biosensors.

3.3. APPETITE REGULATORS

Obesity and cachexia (pathological weight loss) are processes associated to hormones acting as appetite regulators. These hormones act on specific centers in the brain that affect the sensations of hunger and satiety. Mutations or variations in the concentration levels of these hormones or in their receptors can cause substantial pathology leading to obesity or anorexia. Therefore, identification of individuals with specific genetic mutations and monitoring of such species in the organism, may ultimately lead to appropriate therapies targeted at the underlying disease process.

The control center for hunger and satiety is located in the hypothalamus. Part of the hypothalamus, the arcuate nucleus, allows entry through the blood-brain barrier of peripheral peptides and proteins that directly interact with its neurons [Austin & Marks, 2008]. These include neurons expressing peptides that stimulate food intake and weight gain (i.e. neuropeptide Y (NPY) or agouti-related peptide (AgRP)), as well as those expressing peptides which inhibit feeding and promote weight loss such as pro-opiomelanocortin (POMC) and cocaine- and amphetamine-regulated transcript (CART). Together, these neurons and peptides control the sensations of hunger or satiety and ultimately weight gain or weight loss.

NPY is part of the pancreatic polypeptide (PP-) fold peptide family to which also belongs PYY (peptide YY or peptide tyrosine-tyrosine), one of the analytical objectives of this work. Moreover, circulating peptides also play important roles in appetitive behaviors. Among these, as will be seen below, GHRL or growth hormone (GH-) releasing peptide (-RL) (another target hormone in this work), is the only known circulating orexigen, or appetite stimulant. Leptin, produced mainly by the adipose tissue, is another important appetite regulator whose levels do not appear to be driven by meal patterns but by the circadian pattern. This implies that neural and neurohormonal components in the brain may regulate leptin secretion from adipocytes. Interestingly, the levels of these hormones, especially in the case of leptin, have shown to be related with the estrogenic loading and the administration of contraceptives such as ethynyl estradiol (EE2 or EE), also studied in this work.

3.4. OBESITY BIOMARKERS

Biomarkers were defined in 1993 at first time by International Programme on Chemical Safety (IPCS) of World Health Organization and United Nations as: “Any substance, structure, or process that can be measured in the body or its products and influence or predict the incidence of outcome or disease”. In this report, IPCS includes the clinical diagnosis as one of the three uses of biomarkers [IPCS, 1993].

More recently, the scientific journal Nature describes in its web page biomarker as [https://www.nature.com/subjects/biomarkers, 2005]: “A biomarker is a biological characteristic that is objectively measured and evaluated as an indicator of normal biological or pathological processes, or a response to a therapeutic intervention. Examples include patterns of gene expression, levels of a particular protein in body fluids, or changes in electrical activity in the brain”.

Obesity is a pathology involved in numerous comorbidities such as hypertension, diabetes and cardiovascular diseases (CVDs) [Yach et al., 2006] [Lavie et al., 2014]. The World Health Organization (WHO), in its Global Health Observatory, [http://www.who.int/gho/ncd/risk_factors/overweight/en/] considers overweight and obesity like a worldwide epidemic with exponentially increasing incidence, and calls for a global action to prevent this health trouble. The data of 2016 place Spain in the group of countries with the highest overweight, the 61.6% of individuals having a body mass index (BMI) greater than or equal to 25 kg/m^2.

As it is well known, overweight and obesity lead to adverse metabolic effects on blood pressure, cholesterol, triglycerides and insulin resistance. Risks of coronary heart disease, ischemic stroke and type 2 diabetes mellitus increase steadily with increasing BMI also increasing the risk of cancer of breast, colon, prostate, endometrium, kidney and gall bladder. In 2016, 39% of men and 39% of women aged 18+ were overweight and 11% of men and 15% of women were obese (BMI ≥30 kg/m2). Thus, nearly 2 billion adults worldwide were overweight and, of these, more than half a billion were obese. Both overweight and obesity have shown a marked increase over the past 4 decades. Obesity rates in men have risen from around 3% in 1975 and in women from just over 6% in 1975 while overweight has risen over this same time period from 20% in men and from just under 23% in women.

Until recently, obesity was simply considered the result of an inadequate energy balance: greater consumption of food and less expenditure by exercise. However, it is now known that this state is a consequence of many and diverse pathogenic

processes, each of them being complex in its characteristics, and multifactorial. In 2003, Engstrom et al. [Engstrom et al., 2003] studied the association of obesity and the so-called metabolic syndrome with low-grade inflammation. They reported that elevated levels of inflammation-sensitive plasma proteins (ISPs) were associated with future weight gain. This was confirmed by the results obtained in an experiment where five ISPs in 2,821 nondiabetic healthy men (38-50 years of age) were measured and reexamined after a mean follow-up of 6.1 years. The proportion with a large weight gain (75^{th} percentile $\geq$ 3.8 kg) was 21.0, 25.9, 26.8, and 28.3%, respectively, among men with none, one, two, and three or more ISPs in the top quartile. Elevated ISP levels predict a large weight gain in middle-aged men. This data could contribute to relate inflammation, the metabolic syndrome, and cardiovascular disease.

Currently, obesity is considered as a chronic inflammatory state in which some biomolecules present at altered levels trigger abnormal functioning of endocrine system. It has been observed that adipose tissue, apart from acting as an energy reservoir, plays other functions such as the segregation of different hormones or steroids. The variation in the concentrations of some of these species in the organism is indicative of some health problem related to obesity, such as diabetes, therefore, they can be used as biomarkers for preventive diagnosis. Biomarkers of obesity considered so far are of various types [Aleksandrova et al., 2018], and most are also associated with cardiometabolic diseases and obesity-related cancer. Main groups are the following:

- Biomarkers of glucose-insulin homeostasis (insulin and related compounds).
- Adipose tissue biomarkers (adiponectin and related compounds).
- Inflammatory biomarkers (cytokines: TGF-β1, interleukins).
- Omics-based biomarkers (mRNA and metabolites).

The identification and measurement of obesity biomarkers in human circulation have a growing scientific interest for various reasons: since they a) provide compelling evidences into pathophysiologic pathways; b) potentially improve the clinical and public health identification of individuals at risk for disease; c) facilitate monitoring of disease progression and prognosis; d) represent targets for interventions through means of diet, lifestyle, or drug treatment; and e) allow more personalized treatment decisions for individual patients [Pischon, 2009].

As it occurs with other biomarkers, the potential uses and essential features of obesity biomarkers in preclinical and clinical settings are diverse and very important. A summary of them is shown in the Scheme 2 [Aleksandrova et al., 2018].

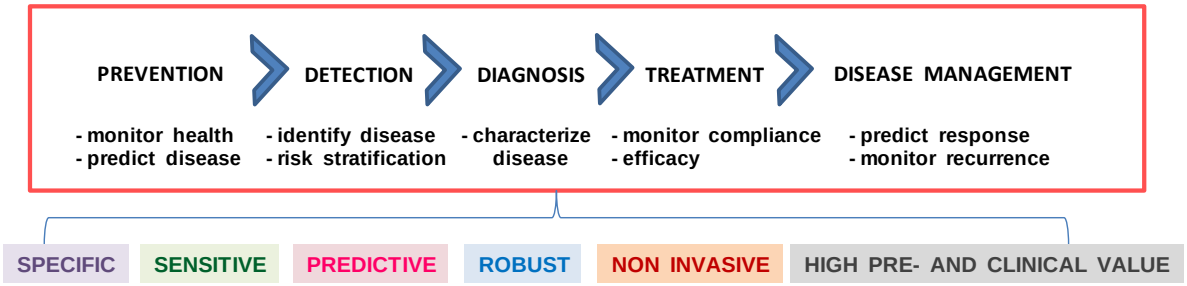

Scheme 2. *Potential uses and essential features of biomarkers in preclinical and clinical settings.*

In this work, electrochemical biosensors for the determination of different types of obesity biomarkers were developed. The selected analytes were: a cytokine related with inflammatory states, transforming growth factor beta 1 (TGF-β1); beta-hydroxy-butyrate (β-HB), the most important ketone body present in human serum, and a hormone exhibiting an activity similar to insulin, the islet amyloid polypeptide amylin (IAPP or AMY). The biological activity of these target compounds, their relationship with other more common biomarkers, and the importance of their determination, are explained individually in Section 3.4.

3.5. ANALYTES AND THEIR BIOLOGICAL SIGNIFICANCE

3.5.1. PEPTIDE HORMONES

These hormones, composed of a more or less longer chain of amino acids, have an effect on the endocrine system. They are water-soluble and act on the surface of target cells via second messengers. Like all peptides and proteins, are synthesized in cells from amino acids according to mRNA transcripts, which in turn are synthesized from DNA templates inside the cell nucleus. Peptide hormones travel through the blood interacting with specific receptor on the surface of their target cells and, then, a second messenger appears in the cytoplasm which triggers signal transduction leading to the cellular responses. Various peptide hormones. i.e. prolactin, adrenocorticotropin (ACTH) and growth hormone (hGH) are secreted from the anterior pituitary, whereas other organs: pancreas, gastrointestinal tract or adipose tissue, also participate in the production of such small proteins through secretion of insulin, cholecystokinin (CCK) and leptin, respectively. The properties of the selected hormones which have been considered as analytical objectives in this work are described below.

3.5.1.1. Ghrelin (GHRL)

GHRL is a peptide hormone containing 28 amino acids (Figure 1) discovered by Kojima and colleagues in 1999 [Kojima et al., 1999]. The name is based on its role as a growth hormone – releasing peptide with reference to the proto-indo-european root *ghre*, meaning to *grow* (**G**rowth **H**ormone **Rel**ease **In**ducing). It is mainly produced by the P/D1 cells lining the fundus of the human stomach [Date et al., 2000] [Peino et al., 2000], and also by the epsilon cells of the pancreas that stimulates hunger. This hormone plays important roles in the gastrointestinal tract stimulating motor activity, gastric contractility and acid secretion [Gröschl et al., 2005] [Masuda et al., 2000]. It represents the only known orexigenic gut hormone identified to date, emerging as the first identified circulating hunger hormone, and acts as an endogenous ligand for the growth hormone secretagogue receptor (GHS-R). GHRL participates in the carbohydrates metabolism and has a direct effect on glucose levels via releasing growth hormone and stimulating glycogenesis [Broglio et al., 2002]. Two forms, acylated and unacylated GHRL, are present in blood serum [Darling et al., 2013], but only the acylated form, with an n-octanoyl group (C8:0) in serine-3 residue, binds with the receptor (GHSR-1a) to activate the release of growth hormone [Trivedi et al., 2012]. Normal levels of total GHRL in human serum are around few hundred pg/mL [Casanueva & Diéguez, 2002] [Vörös et al., 2012] with the deacylated form being clearly predominant [Taskin et al., 2014].

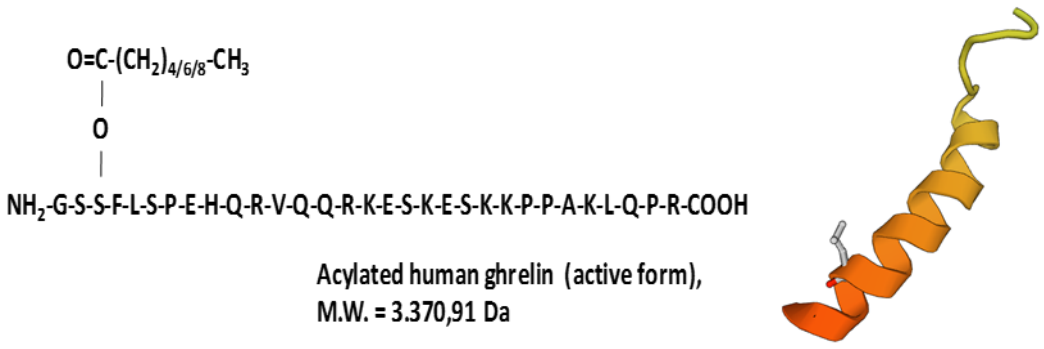

Figure 1.- *Amino acids formula and structure of GHRL peptide. (Modelling using Swiss Model [Expasy]).*

The effects of GHRL on food intake has been thoroughly investigated [Wren et al., 2000]. It is well known that it has potent appetite-stimulation effects in both obese and lean humans. The orexigenic character is manifested by increasing GHRL levels before meals to values that have been shown to cause hunger, and then decreasing (Figure 2) [Kojima & Kangawa, 2008] [Stevanovic et al., 2013]. Thus, endogenous GHRL levels increase during fasting and reduce immediately after food intake fluctuating between around tens and hundreds of pg/mL. This behavior is totally opposed to that of leptin, the peptide hormone produced by adipose tissue which induces satiation.

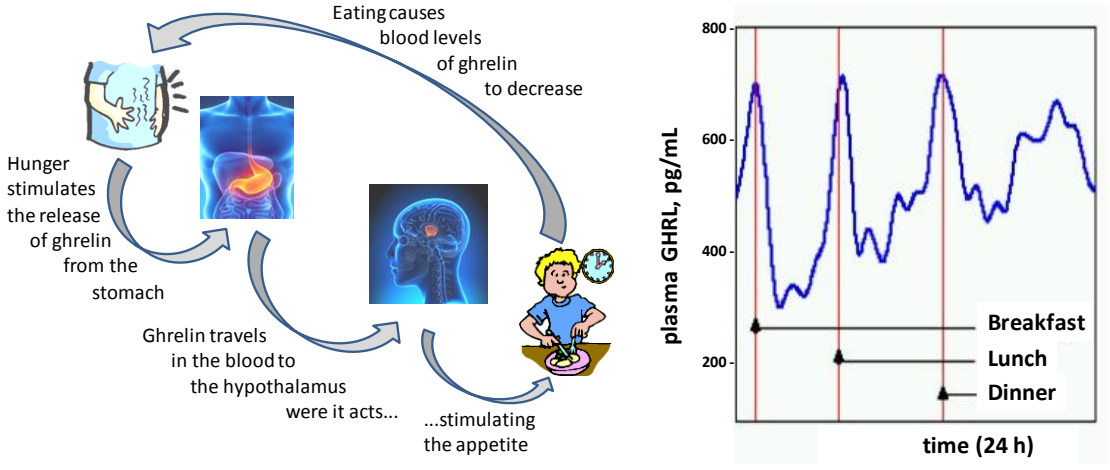

Figure 2.- *Reciprocal effects of hunger and eating on GHRL levels (Right: adapted from [Cummings et al., 2001].*

Interestingly, in obese subjects, the typically expected post-prandial fall in circulating GHRL levels is attenuated, or even absent [English et al., 2002] and, in general, levels of circulating plasma GHRL in obese people are lower than those found in matched lean control subjects [Hameed et al., 2009]. Furthermore, an increase in GHRL plasma levels associated to anorexia nervosa has also been found [Popovic, et al., 2004]. The scheme displayed in Figure 3 shows the effects of GHRL related with appetite regulation in the human organism. Receptors for GHRL are located primarily in the lateral hypothalamus and pituitary. In the hypothalamus arcuate nucleus (ARC), GHRL stimulates the release of neuropeptide Y (NPY) and agouti-related protein (AgRP)-expressing neurons, which increase the appetite, and in turn, it suppresses the release of proopiomelanocortin (POMC) neurons which decrease the appetite.

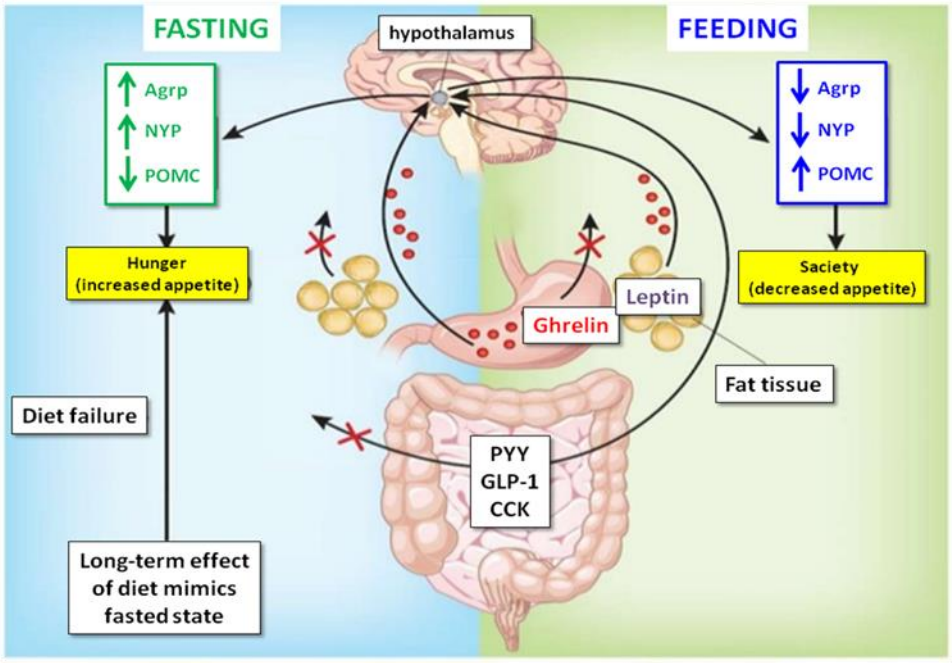

Figure 3.- *Effects of GHRL related with appetite regulation in human organism.*

Other important actions of GHRL has been schematically represented in Figure 4 [De Vriese & Delporte, 2008]. As examples, GHRL affects the carbohydrate and lipid metabolism increasing adiposity, and also exerts influence in the endocrine and exocrine pancreatic functions. This hormone has anti-inflammatory effects and inhibits the production of pro-inflammatory cytokines in human endothelial cells, T-cells and monocytes. Regarding reproductive function, GHRL also inhibits testosterone secretion and may influence the timing of puberty. Furthermore, neurological processes such as memory or learning are also affected by GHRL [Darling et al., 2013].

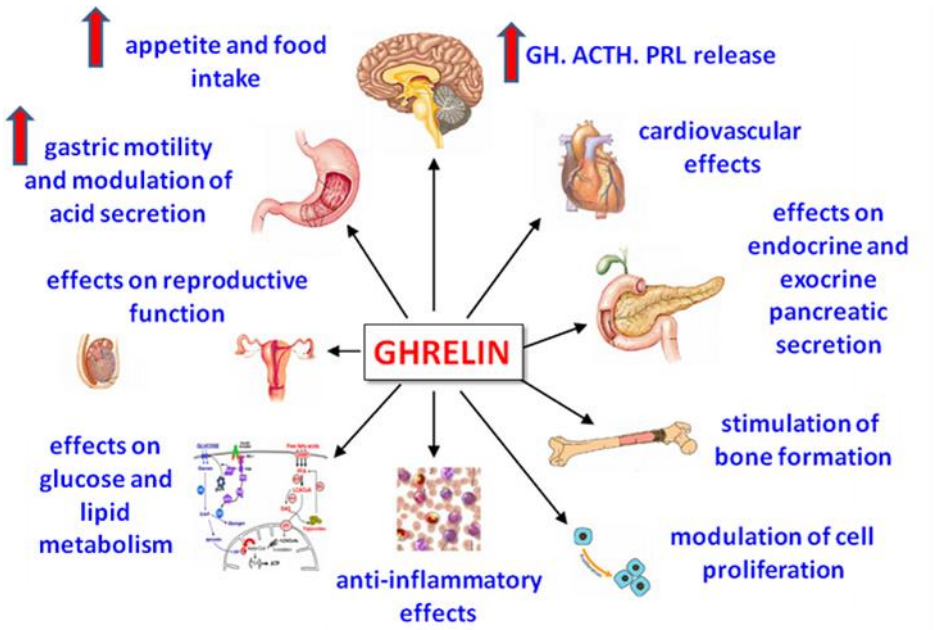

Figure 4.- *Actions of GHRL in the organism [De Vriese & Delporte, 2008].*

3.5.1.2. Peptide YY (PYY)

Peptide YY (Figure 5) is a potent anorexigen belonging to the pancreatic polypeptide family, whose name derives from the tyrosine residues (Tyr or Y) at both its N- and C-termini [Tatemoto & Mutt, 1980]. PYY shows a 70% homology to neuropeptide Y (NPY) and pancreatic polypeptide (PP). It is produced in the gut by the L cells of the terminal ileum and colon, and is secreted to the circulation in response to food [Colon-González et al., 2013] [Adrian et al., 1985]. There are two endogenous forms of the hormone: PYY_{1-36} and PYY_{3-36}, the released $PYY_{1–36}$ being rapidly metabolized by dipeptidyl peptidase-IV to active $PYY_{3–36}$ by removal of two *N* terminal amino acids from the full-length form [Mentlein et al., 1993] [Renshaw & Batterham, 2005]. Although both forms are biologically active, $PYY_{3–36}$ (hereinafter PYY) is the main storage and circulating form and is thought to more actively control food intake [Cooper, 2014]. PYY stimulates gastrointestinal absorption of fluids and electrolytes, reduces gastric and pancreatic secretions, and delays emptying [Adrian et al., 1985]. The effects of PYY on satiety, food intake and body weight have been investigated [Batterham et al., 2003] [Boey et al., 2006]. It is well known that PYY reduces food intake acting on the arcuate nucleus in the hypothalamus (ARC), possibly by inhibiting neuropeptide Y neurons and stimulating POMC expressing neurons via Y2 receptors [Batterham et al., 2002]. However, to date, contradictory results have been published

concerning relationship between PYY and body weight [Cooper, 2014], and it is still investigated [Boey et al, 2006].Furthermore, it has been found [Batterham et al., 2006] that high-protein diets not only reduce adiposity but also enhance PYY synthesis and secretion, and cause greater reduction in hypothalamic expression of NPY. These findings suggested that PYY could mediate both the satiating effects of protein and the associated reduction in long-term adiposity. This behavior has led PYY to become a therapeutic target to reduce hunger and caloric intake [Colon-González et al., 2013]. Also, it was affirmed that abnormalities of the PYY system may be involved in the pathogenesis of obesity condition [Batterham & Bloom, 2003].

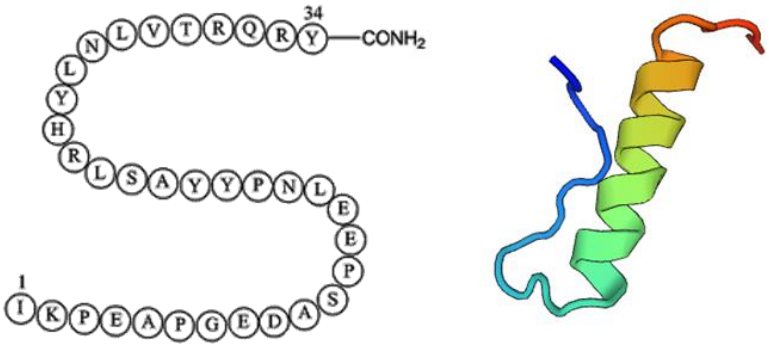

Figure 5.- *Amino acids formula and structure of PYY.*
(Modelling using Swiss Model [Expasy])

The kinetics of PYY secretion and duration of the action differentiate from other classical meal terminating signals such as cholecystokinin (CCK) that acts rapidly to influence the termination of individual meals. In this sense, PYY belongs to the named "long-term regulators" (such as insulin) reflecting body energy stores [Batterham & Bloom, 2003]. Figure 6 shows schematically some interacting hormones involved in the food intake control. In the feeding stage, PYY, CCK and insulin are released and suppress further feeding. Excessive feeding (fat excess) increases leptin production and the inhibition of food intake. In the fasting stage, GHRL is released by the stomach and stimulates the appetite.

Conversely to GHRL, peaks of increased PYY concentrations appear after meals, being the increase proportional to the caloric intake and the food composition. Fat is the most potent stimulus for this response. Concentration levels of PYY in plasma are around 40–70 pg/mL, although variability in circulating levels provides postprandial peaks of about one hundred pg/mL. In obese individuals, their fasting plasma concentration is lower and the response to the intake less intense than the one existing in persons with normal weight. On the contrary, in anorexia nervosa, fasting plasma concentration is greater than in healthy subjects with normal weight [Batterham et al., 2003] [Le Roux et al., 2006].

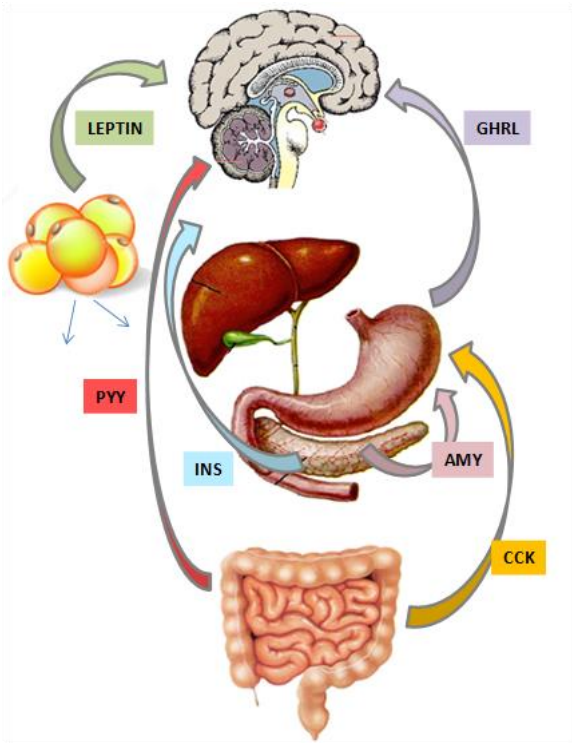

Figure 6.- *Some interacting hormones involved in food-intake control: CCK, cholecystokinin; INS, insulin; AMY, amylin; GHRL, ghrelin; PYY, peptide YY*

3.5.1.3. Amylin (AMY)

Human islet amyloid polypeptide, hIAPP, or amylin (herein AMY), is a 37-residue neuroendocrine peptide hormone co-secreted with insulin from pancreatic islet β-cells (Figure 7). Since its discovery as a hormone in 1986, the effects of AMY in several different organ systems has been investigated [Hay et al., 2015]. Its major role is as a glucoregulatory hormone, being an important regulator of energy metabolism in health and disease. Other AMY actions have also been reported, such as on the cardiovascular system or on bone. AMY acts principally in the circumventricular organs of the central nervous system and functionally interacts with other metabolically active hormones such as cholecystokinin (CCK), leptin, and estradiol. The AMY-based peptide, pramlintide, is used clinically to treat type 1 and type 2 diabetes. Clinical studies in obesity have shown that AMY agonists could also be useful for weight loss, especially in combination with other agents.

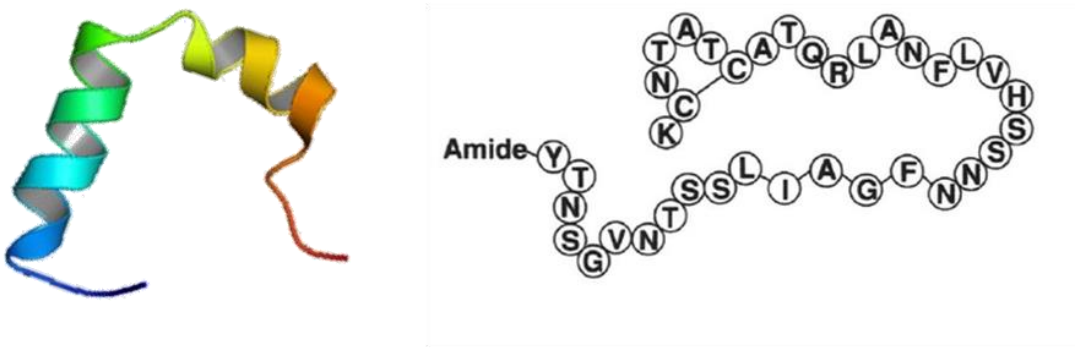

Figure 7.- *Amino acids formula and structure of AMY peptide. (Modelling using Swiss Model [Expasy])*

Like insulin, plasma AMY levels are low during fasting and increase during meals and following glucose administration, being all concentrations directly proportional to body fat. Figure 8 shows the major actions of AMY related with metabolism. AMY, secreted from the pancreas after a meal, circulates in the blood to activate specific receptors in the brainstem. This results in suppression of glucagon release from the pancreas, a reduction in food intake, and gastric emptying [Lutz, 2006]. The net effect of these actions is to decrease blood glucose, associated with longer-term reductions in body weight. It has been suggested that the roles of AMY and insulin for glycemic regulation are complementary [Young, 2005]. As it is well known, insulin facilitates transport of glucose from the bloodstream into peripheral tissues such as skeletal muscle [Carnagarin et al., 2015]. However, blood glucose levels are influenced not only by the transport of glucose into tissue, but also by the entrance of glucose from ingested food into the bloodstream. This side of the equation is controlled, partly, by AMY, which slows gastric emptying [Mietlicki-Baase, 2016], thereby delaying and controlling the entry of nutrients/glucose into the small intestine and subsequently into bloodstream. This effect can be observed when plasma AMY is experimentally increased to levels comparable to those normally observed in a postprandial state [Reidelberger et al., 2001]. Thus, AMY exerts glucoregulatory actions that complement the effects of insulin. In response to nutrient ingestion, circulating AMY concentrations rise rapidly, reaching a peak within 60 minutes and then remaining elevated for up to 4 hours [Koda et al., 1992]. Another difference between insulin and AMY in tissue distribution was described by Banks and Kastin [Banks & Kastin, 1998] and confirms the higher ability of AMY to cross de Blood Brain Barrier (BBB) and its higher presence into the cerebrospinal fluid (CSF).

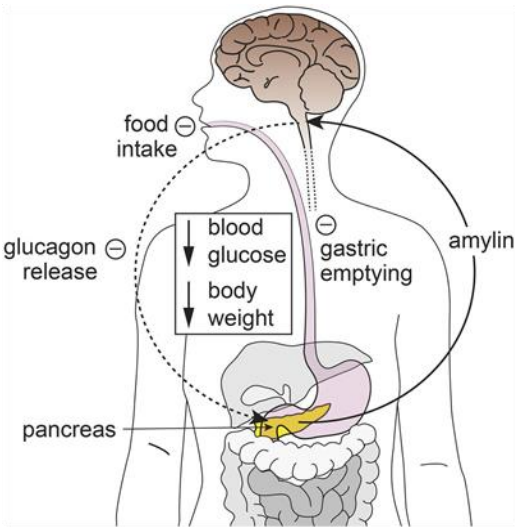

Figure 8.- *Major actions of AMY related with metabolism.*

AMY and insulin are normally co-secreted in a fixed molecular ratio insulin to AMY of between ten and one hundred. However, obesity, diabetes mellitus, or pancreatic cancer all tend to increase the amount of AMY relative to insulin [Cooper et al., 1987]. Studies related to physiology of AMY [Percy et al., 1996] [Castillo et al., 1995] revealed that individuals with type 1 diabetes are AMY deficient [Koda et al., 1992] whereas postmeal secretion of AMY seems to be defective in advanced type 2 diabetes [Sanke et al., 1991]. Contrarily, individuals who are insulin resistant and hyperinsulinemic have high concentrations of AMY in plasma [Kautzky-Willer et al., 1994]. The AMY levels in human serum oscillate around a few tens of pg/mL [Harter et al., 1991] [Butler et al., 1990].

Variable concentrations of AMY in plasma have also been found depending on factors like fasting time or glucose levels in serum. A range of 1 to 90 pg/mL, with a mean of 51 ± 12 pg/mL in lean subjects, has been claimed, these levels increasing in obese patients with normal glucose tolerance, with a mean value about 72 ± 12 pg/mL, although it can be increased to 268 pg/mL in type 1 diabetes patients [Paulsson et al., 2014]. On the contrary, for anorexic patients this range is compressed between 7.8 and 22.0 pg/mL with a mean of 13 ± 1 pg/mL [Wojcik et al., 2010], and urinary levels similar to serum ones [Leckström et al., 1997]. Due to its characteristics, AMY levels have been described as a biomarker of Type 2 Diabetes (T2D) [Patil & Alexandrescu, 2015].

3.5.2. CYTOKINES

Cytokines are low molecular weight bioactive proteins (~6 - 70 kDa) produced by a variety of cells and strongly associated with the immune system [Stenken & Poschenrieder, 2015] [Liu et al, 2016]. They play a critical role in chemically-induced tissue damage repair, cancer development, control of cell replication and apoptosis. In addition, these multipotent modulators are also involved in the pathogenesis of fibrotic diseases, immunological disorders [Danielpour, 1989] and obesity [Samad, 1997] [Sepúlveda-Flores, 2002].

There is enormous clinical interest in cytokines determination as elevated concentrations of these proteins are associated with inflammation or disease progression and, therefore, various types of cytokines are widely used as biomarkers to characterize the immune function, predict diseases and monitor their evolution and treatment. These applications require the availability of highly sensitive analytical methods because cytokines appear into the extracellular milieu at a pM concentration range. As noted, in recent years, several studies have suggested that obesity is associated with an inflammatory process. In fact, obesity has been considered as a low-grade chronic inflammatory pathology characterized by elevated plasma levels of some proinflammatory cytokines such as interleukin 6 (IL-6).

An important issue in the inflammatory state associated with obesity is that it appears to be predominantly provoked and it resides in white adipose tissue, although other key organs may also be involved in the course of inflammation. As indicated, adipose tissue is not only an energy reservoir but a multifunctional endocrine organ secreting a range of bioactive peptides and proteins [Trayhurn & Wood, 2004]. Among them, some inflammatory molecules are expressed and secreted by adipose tissue. These are a heterogeneous group including cytokines, hormones, growth factors, acute phase proteins, prostaglandins, glucocorticoids and sex steroids, with complex effects on the receptor organs liver, pancreas, skeletal muscle, kidneys, hypothalamus and the immune system [Frühbeck et al., 2001].

The excessive intake of nutrients, some infections and oxidative stress can cause an increase in the secretion levels of these cytokines. This lead to chronic inflammation in white adipose tissue favoring the activation and infiltration of mature macrophages. Several studies have shown that increased secretion of cytokines can stimulate preadipocytes and endothelial cells to produce monocyte chemoattractant protein-1 (MCP-1) which attract macrophages to adipose tissue. Once infiltrated, mature macrophages begin to secrete cytokines and chemokines. This pattern of

secretion, together with that produced by adipocytes and other cell types, can perpetuate a vicious circle of recruitment of macrophages and production of inflammatory cytokines, leading to local primary inflammation in adipose tissue. Subsequently, these cytokines secreted by the adipose tissue could trigger the increase of the production of inflammatory proteins in the liver and thus lead to the low-grade systemic inflammation observed in obesity. In addition, this inflammatory state has been proposed as a link with various disorders associated with obesity such as insulin resistance, dyslipidemia, and vascular and liver complications. Thus, several studies have confirmed that the presence of inflammation predicts the future development of type 2 diabetes. The subsequent increase in circulating free fatty acids and the increase in metabolites derived from intracellular fatty acids have been related to the development of insulin resistance in skeletal muscle and in the liver, suggesting that free fatty acids can be an important link between chronic adipose tissue inflammation and systemic insulin resistance [Rana et al., 2007].

Monitoring cell functions and cell-to-cell communication by using their cytokine secretions have enormous value in biology and medicine [O'Shea et al., 2011]. Elevated pro-inflammatory cytokine levels are found in obese patients, in which the concentrations are reduced after surgery-induced weight loss, this contributing to the improvement in the cardiovascular co-morbidity [Catalán et al., 2007]. Chronic systemic inflammation in obesity originates from local immune responses in visceral adipose tissue [Schmidt et al., 2015]; however, assessment of a broad range of inflammation-mediating cytokines and their relationship to physical activity and adipometrics has scarcely been reported to date. Results confirm up-regulation of certain pro- and anti-inflammatory cytokines in obesity. In obese subjects, physical activity may lower levels and thus reduce pro-inflammatory effects of cytokines that may link obesity, insulin resistance and diabetes.

Summarizing, in obesity, alterations of adipokines and several further cytokines are thought to contribute to a low grade inflammation within the adipose tissue affecting the development of several secondary diseases such as metabolic syndrome, insulin resistance, diabetes, and arterial hypertension [Engström et al., 2003]. Changes in cytokine release are related to the infiltration of macrophages into adipose tissue that follow the adipocyte-secretion of chemoattractants and free fatty acids [Maury & Brichard., 2010]. To date, in-vivo serum studies with respect to levels of serum cytokines in subjects suffering from obesity and metabolic syndrome are scarce, the majority being devoted to study the role of interleukins in this disease.

3.5.2.1. Transforming growth factor β1(TGF-β1)

The transforming growth factor-β (TGF-β) family is a collection of structurally related multi-functional cytokines which regulates a wide range of physiological and pathological processes [Martelosi-Cebinelli, 2016]. They are involved in cell-growth, rate of proliferation, differentiation and production of extracellular matrix proteins [Grainger et al., 2000]. Three isoforms (TGF-β1, -β2, and -β3) are present in mammals with some differences in biological activities and also in their potencies. Particularly, TGF-β1 (Figure 9, https://en.wikipedia.org/wiki/TGF_beta_1) is involved in immune and inflammatory responses showing a hundred times more potent behavior as growth inhibitor of hematopoietic stem cells than the others. This cytokine is considered a good biomarker of liver fibrosis [Fallatah, 2014] or bladder carcinoma [Eder et al, 1996]. Increasing evidence also links TGF-β1 to the progression of renal fibrosis and scarring associated with diabetic nephropathy or hypertensive nephrosclerosis [Tsapenko et al, 2013] and glomerulonephritis [Grainger et al, 1995]. TGF-β1 concentration levels between 0.1 and 25 ng/mL have been reported in plasma from healthy individuals [Granger et al, 2000]. The variability observed depends to some extent on the assay type used for the determination.

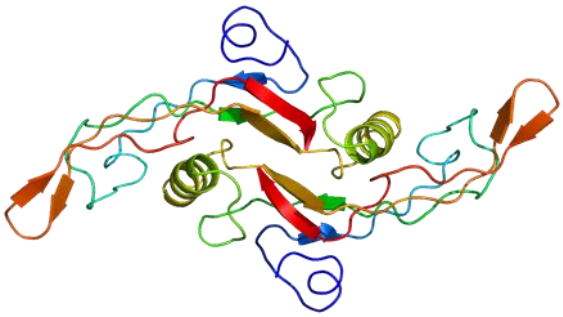

Figure 9.- *TGF-β1 peptide structure.*

Clinical and experimental studies have revealed that obesity is associated with enhanced expression and release of TGF-β1 from adipose tissue [Fain & Madan, 2005], thus, a significant correlation between TGF-β1 levels and adiposity in humans has been found. Production of TGF-β1 in adipose tissue from obese mammals has shown to be increased in about 4 or 5 times. In mice, systemic blockade of TGF-β1 signaling protects them from obesity, diabetes, and hepatic steatosis. Moreover, TGF-β1 regulates glucose tolerance and energy homeostasis and suggest that modulation of TGF-β1 activity might be an effective treatment strategy for obesity and diabetes [Yadav et al., 2011]. The levels of TGF-β1 are not only associated positively with

obesity but also with urinary albumin excretion in patients with hypertension. In addition, obesity may contribute to the impairment of renal dysfunction associated with increased TGF-β1 levels [Torun et al., 2007] [de Jong et al., 2002]. Normal human subjects have between 2.0 and 12.0 ng/ml TGF-β1, in plasma [Wakefield et al., 1995], this cytokine being also present in urine at concentrations between 10 and 50 pg/mL in spite of these values depend on sex, and also on age or ethnicity [Tsapenko, 2013].

3.5.3. STEROID HORMONES

It has been widely accepted that females are partially protected from inflammatory-related diseases [Miller et al., 2012]. At the molecular level, this reduction in disease susceptibility has been suggested to be due to anti-inflammatory properties of estradiol, which has demonstrated activity through direct free radical scavenging, transcription regulation and protein interactions, and also can diminish systemic inflammatory stress.

Understanding of such pathways may provide a basis for the possible use of estrogen and related compounds (i.e. resveratrol) to prevent diseases including weight gain and obesity in peri- and post-menopausal females. However, despite their similarity, controversial effects on metabolism have been reported associated to the use of contraceptives containing synthetic estrogens such as ethynyl estradiol (EE2). With the older high-dose oral contraceptives containing 50 μg EE2 dose or higher, an impaired glucose tolerance test was present in many women where plasma levels of both insulin and blood sugar were elevated [Sağsöz et al., 2009].

Generally, the effect of these drugs produced an increased peripheral insulin resistance. Nowadays, contraceptives containing lower concentration of EE2 (i.e. 30 μg - dose) combined with other drugs such as desogestrel (a molecule of progestin similar to progesterone) or DRSP (1,2-dihydrospirenone) has shown to be associated with none or very slight weight gain. Furthermore, the effects associated with a high concentration of EE2 on glucose and hormones such as leptin or GHRL were also not appreciated when low-dose combined oral contraceptives (COCs) were administered [Soares et al., 2009].

3.5.3.1. Ethynyl estradiol (EE2)

Ethynyl estradiol (herein EE2) (Figure 10) is one of the most potent active synthetic estrogenic hormones. It is a derivate of estradiol, developed in 1938, and is an essential constituent of oral contraceptives, used also to regulate menstrual cyclic disorders [Apelo and Veloso, 1975] and polycystic ovarian syndrome control. Adverse effects of EE2 include accelerated coagulation, risk of venous thrombosis and fibrinolysis [Raps, 2014], and increasing serum lipoprotein levels [Chao, 1979]. Its ability to modify endogenous production of obesity related hormones like GHRL and leptin [Sağsöz et al., 2009] makes EE2 an obesity related molecule. In general, the interaction of estrogens with orexigenic and anorexigenic hormones affects energy balance, food intake, and body fat distribution [Brown & Clegg, 2009]. Although the studies related with these actions are scarce, experimental investigations reveal that the interaction of estrogens with endocrine factors and their receptors in hypothalamus or other body parts is responsible for the regulation of body weight via modulating energy expenditure.

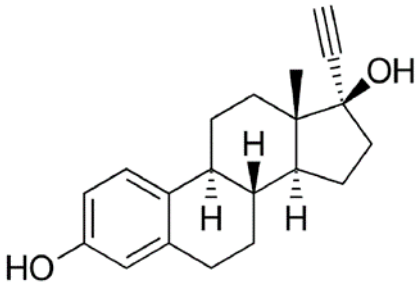

Figure 10.- *Chemical structure of ethynyl estradiol (EE2).*

3.5.4. KETONE BODIES

Ketone bodies (acetoacetate (AcAc), beta-hydroxybutirate (β-HB) and acetone) are produced in liver mitochondria (Figure 11) mainly from the oxidation of fatty acids released from adipose tissue [Persson, 1970]. Acetone, produced in smaller quantities than the others, is exhaled and essentially is unmeasurable in healthy individual [Laffel, 1999] [Cahill & Veech, 2003]. AcAc and β-HB are transported by blood to the extrahepatic tissues, where they are oxidized via the tricarboxylic acid (TCA) cycle to provide the energy required by tissues such as skeletal, heart muscle and renal cortex. Fatty acid oxidation accounts for up to 70% of the ATP produced by the heart, with metabolism of glucose, lactate, amino acids and ketone bodies supplying the rest. However, under specific conditions, like prolonged fasting, type 1 diabetes or

alcoholism, the ketone bodies levels in blood are increased and they can lead to blood acidification through a disease process known as ketoacidosis. This status can produce very dangerous consequences in health, becoming the first cause of mortality in diabetic children. Mild elevation of blood ketone bodies also occurs during the process of normal aging [Sengupta et al., 2010] and during congestive heart failure (HF) [Kupari et al., 1995], however it remains unclear whether this elevation represents an adaptive mechanism required to maintain cell metabolism or actually contributes to the progression of disease.

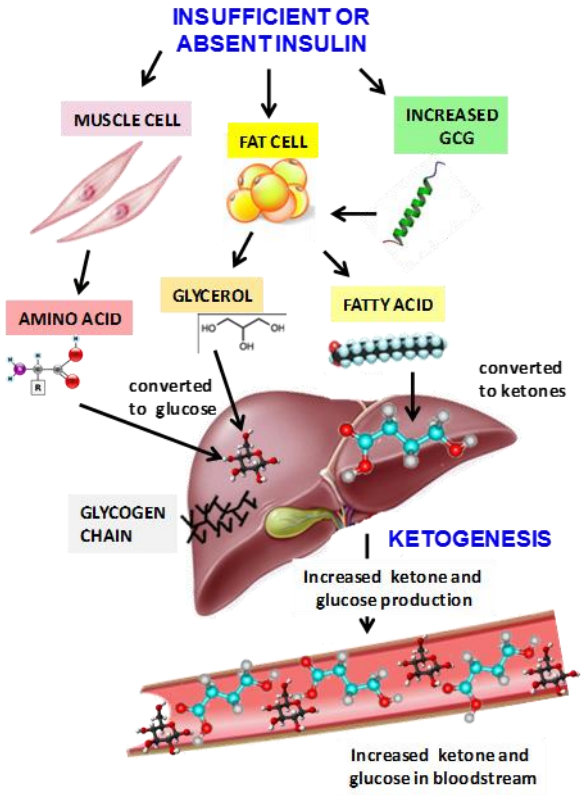

Figure 11.- *Production of ketone bodies. GCG: glucagon*

3.4.4.1. β-hydroxybutyrate (β-HB)

Beta-hydroxybutyrate (Figure 12) is a metabolic intermediate that constitutes ~70% of ketone bodies and acts as an important fuel for some tissues like heart and brain during fasting and starvation. Increased β-HB levels in blood serum result from fatty acids degradation occurring when the body uses these acids instead of carbohydrates for get energy. This situation appears when the individual is undergoing long periods of physical exercise, vomiting or fasting, as well as in type I diabetes mellitus patients with insulin deficiency. During prolonged exercise or maintenance of a low carbohydrate ketogenic diet, the concentration of circulating blood β-HB rises from

~0.1 mM observed in normal fed state to ~1 mM after few hours of fasting, and up to 5–7 mM after prolonged starvation. It is well known that uncontrolled diabetes can lead to the production of acetone (2%), acetoacetate (20%) and 3-HB (78%) from fatty acid catabolism [Wallace & Mattheus, 2004]. If the release of free fatty acids from adipose tissue exceeds the metabolic capacity, as occurs during insulin deficiency of type I diabetes or, less commonly, in the insulin-resistant of type II diabetes, severe and potentially fatal diabetic ketoacidosis may occur where blood β-HB levels can reach up to 25 mM [Lebovitz, 1995] [Cahill and Veech, 2003].

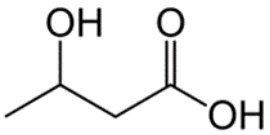

Figure 12.- *Chemical formula of β-hydroxybutyric acid (β-HB).*

Related to obesity, it has been shown that serum levels of β-HB are increased in obese people as compared to lean ones. Since β-HB is one of the biological markers with altered values in patients with morbid obesity, the determination of this marker has a great interest in the control of this and related diseases [Wallace & Matheus, 2004]. Conversely to its adverse effects, recent studies indicate that a mild elevation in β-HB levels could be actually beneficial in certain physiological situations, such as Alzheimer and Parkinson's disease [Kashiwaya et al., 2000] [Tieu et al., 2003] [Reger et al., 2004].

3.6. MATERIALS USED FOR THE PREPARATION OF THE ELECTROCHEMICAL SCAFFOLDS

3.6.1. MAGNETIC MICROBEADS

The so named magnetic microbeads (MBs) are micrometric particles of iron oxide covered with a polymeric thin shell that defines a surface area for interaction by coupling or adsorption with a variety of biomolecules [Centi et al., 2007]. Different kinds of MBs, characterized by possessing different functional groups with ability for interacting with the binding sites of biomolecules are currently commercially available. These include, among others, MBs functionalized with carboxyl, tosyl, or amine groups for covalent immobilization of biomolecules, as well as modified with protein A, protein G or streptavidin for affinity immobilization. In the field of immunosensors, the use of MBs improves the performance of the immunological reaction due to an increase in the surface area and the faster assay kinetics as the reaction takes place in suspension with enhanced probability that antibody-coated magnetic microbeads meet the antigen [Kokkinos et al., 2016]. The selection of adequate coating with proper functional moieties facilitates the specific and oriented bind of an elevated number of capture antibodies. Another advantage of MBs immunosensors is the high simplicity of handling when realizing the successive steps for preparation of the immunoassay by means of employment of attracting magnets. In addition, the use of magnets offers a reduction of matrix effects, as the washing and separation steps which allows the analysis to be made without any pre-enrichment, purification, or pre-treatment steps, are easily allowed [Hervás et al., 2010].

In recent years, a variety of electrochemical immunosensors based on MBs (magnetoimmunosensors) have been described. Most of them have been prepared in combination with screen-printed electrodes by transporting the immunoconjugates from the suspension of bio-functionalized MBs to the electrodic surface and further immobilization by action of a magnetic field (Figure 13). Coupling of electrochemical transduction with the use of magnetic microcarriers is nowadays a well-established methodology which has greatly contributed to significant improvements in the performance of electrochemical immunosensors [Yáñez-Sedeño et al., 2016] because of the easy, fast and selective capture of the specific target molecule from complex samples.The preparation of immunoconjugates on the microparticles avoids the possible non-specific adsorption on the electrode and allows measurements on

complex samples with minimal interferences or passivation of the electrode surface. Also, the need for delicate electrode preparation to enable control of density and orientation of recognition probes at the disposable electrode surface is avoided [Ma et al., 2016].

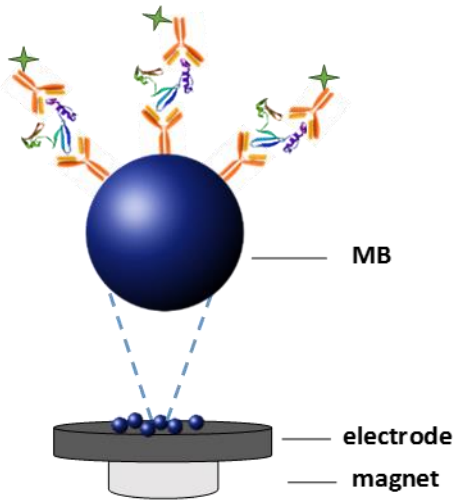

Figure 13.- *Scheme of an electrochemical sandwich-type magnetoimmunosensor.*

In order to give a brief description on the state-of-art of electrochemical magneto-immunosensors, some recent examples of configurations using such strategy have been summarized in Table 1. The selected designs were those developed in the three last years and, as it can be seen, the majority are based on the use of carboxylated magnetic particles for the covalent immobilization of the corresponding capture antibodies and the preparation of sandwich-type configurations after arrangement of magnetoconjugates onto SPCEs. In these designs different enzymatic labels such as horseradish peroxidase (HRP) and alkaline phosphatase (AP), and substrates such as H_2O_2 in the presence of hydroquinone (HQ) and 1-naphthylphosphate (1-NPP), respectively, were used. The electrochemical responses are detected by amperometric and pulse voltammetric techniques. Electroactive molecules such as methylene blue (mB), thionine (THI), and metals (Cd^{2+}, Pb^{2+}) have also been used, the latest by applying stripping methods. The developed magnetoimmunosensors have been used for the determination of analytes of clinical interest, mainly cancer biomarkers such as p53, CA 15-3 or HER-2, or other compounds related to cardiac diseases such as AXL, as well as cells and important molecules in the field of food like toxic *S. Typhi* or allergens (Ara h1 and Ara h2), respectively. These applications have been made mostly in serum samples in the case of analytes of clinical interest, and in a variety of foods in the second case.

Table 1. *Some recent electrochemical immunosensors using functionalized MBs. (See Section 8 for abbreviations).*

Electrode / MBs	Configuration	Technique	Analyte / Sample	Analytical characteristics	Reference
SPCEs array / HOOC-MBs	Sandwich; AuNPs-anti-*S.Typhi*-*S.Typhi*-anti-*S.Typhi*-MBs/SPCEs	μ-fluid. Au^0 ox., DPV det.	*S.Typhi* / milk	D.R: 10-100 cells/mL LOD: 7.7 cells/mL	[de Oliveira et al., 2018]
SPCE/mB/CNTs / HOOC-MBs	Direct assay; mB/CNTs/MBs-anti-*S.Typhi*-*S.Typhi*-anti-*S.Typhi*-SPCE	DPV, mB reduction	*S.Typhi* / milk	D.R: 10-106 CFU/mL LOD: 7.9 CFU/mL	[Ngoensawat et al., 2018]
SPCE / HOOC-MBs	Sandwich; HRP-Strept-Biotin-anti-AXL-AXL-anti-AXL-MBs/SPCE	Amp. -0.2V H_2O_2 / HQ	AXL / human serum	D.R: up 7.5 ng/mL LOD: 74 pg/mL	[Serafín et al., 2017a]
P(1,5DAN)/pPyNW /SPCE/Strept-MBs	Sandwich; HRP-MBs-anti-CA15-3-CA15-3-P(1,5DAN)/pPyNW/SPCE	DPV, H_2O_2 / HQ	CA 15-3 / -	D.R: 0.05 - 20 U/mL LOD: 0.02 U/mL	[Nguyen et al., 2017]
CNTs/SPCE / HOOC-MBs	Sandwich; THI-MSN/pDA-anti-hIgG-hIgG-MBs/CNTs/SPCE	DPV, THI red.	hIgG	D.R: 0.01-100 ng/mL LOD: 5.8 pg/mL	[Lai et al., 2017]
MGCE / HOOC-MBs	Direct assay; S-amlod-anti-S-amlod-MBs/MGCE	SWV, $Fe(CN)_6^{3-/4-}$	S-amlod / medicament	D.R:0.1-1000 ng/mL; LOD: 0.04 ng/mL;	[Zhang et al., 2017]
MFE / anti-hIgG1-MBs	Sandwich; CdSQD/BSA / anti-hIgG1-hIgG1-MBs / MFE	SWASV, Cd^{2+}	hIgG1 / serum	D.R: 0.010-100 ng/mL LOD: 3.4 pg/mL	[Chen & Lu, 2017]
MGCE / Strept-MBs	Sandwich; Pb-NC@BSA- anti-EGFR-EGFR-anti-EGFR-MBs/MGCE	SWASV, Pb^{2+}	EGFR / serum	D.R: 0.4-35 ng/mL LOD: 8 pg/mL	[Mousavi et al., 2017]
SPCEs array / Strept-MBs	Sandwich; AP-Strept-Biotin-HER2-af-HER-HER2-af-Biotin-MBs	DPV, 1-NPP as substrate	HER2 / serum	D.R: 2.0 - 20 ng/mL LOD: 1.8 ng/mL;	[Ilkhani et al., 2016]
SPCE / HOOC-MBs	Sandwich; HRP-anti-p53-p53-anti-p53-MBs/SPCE	Amp. -0.2V H_2O_2 / HQ	p53 / cell lysates	D.R: 5 -150 ng/mL; LOD: 1.29 ng/mL	[Pedrero et al., 2016]

Table 1 (Cont.).- *Some recent electrochemical immunosensors using functionalized MBs.(See Section 8 for abbreviations).*

Electrode / MBs	Configuration	Technique	Analyte / Sample	Analytical characteristics	Reference
SPCE / HOOC-MBs	Sandwich; HRP-anti-α-LA-α-LA-anti-α-LA-MBs/SPCE	Amp. -0.2V H_2O_2 / HQ	α-LA / milk (cow, human breast, infant formula)	D.R: 37-5000 pg/mL; LOD: 11.0 pg/mL; RSD: 8.1%	[Ruiz-Valdepeñas et al., 2016]
SPCE / HOOC-MBs	Sandwich; HRP-anti-CD105-CD105-anti-CD105-MBs/SPCE	Amp. -0.2V H_2O_2 / HQ	CD105 / serum	D.R: 0.8-10.0 ng/ml; LOD: 0.2 ng/mL; RSD: 3.6%	[Torrente-Rodríguez et al., 2016]
dualSPCE / HOOC-MBs	Sandwich; HRP-anti-Ara h1(or 2)-Ara h1(or 2)-anti-Ara h1(or 2)-MBs/SPCE	Amp. -0.2V H_2O_2 / HQ	Ara h1, Ara h2 / food extracts	LR: 60 - 1000; 0.25 - 5 ng/mL; LOD: 18.0; 0.07 ng/mL; RSD: 7.3; 8.9%	[Ruiz-Valdepeñas et al., 2016a]
SPCEs array / protein A-MBs	Competitive; AP-PDBE-anti-PBDE-MBs/SPCE	DPV. 1-NPP as substrate	PBDE / food	D.R: up to 6.9 ng/mL; LOD: 0.18 ng/mL; RSD: 12%	[Bettazzi et al., 2016]
SPCEs array / protein G-MBs	Competitive; HRP-COC-anti-COC-MBs	Amp. H_2O_2 / HQ	COC / urine, saliva, serum	D.R: 0.69 - 57 ng/mL; LOD: 0.09 ng/mL; RSD: 5.5%	[Vidal et al., 2016]
SPCE / HOOC-MBs	Sandwich; HRP-anti-Ara h2-Ara h2-anti-Ara h2-MBs/SPCE	Amp. -0.2V H_2O_2 / HQ	Ara h2 / food extracts	D.R: 87-10000 pg/ml; LOD: 26.0pg/mL; RSD: 3.3%	[Ruiz-Valdepeñas et al., 2015]

In this work, two types of MBs have been used: Protein G functionalized MBs for implementing the immunosensor for the determination of GHRL, and carboxylated MBs for the preparation of the immunosensor of TGF-β1. As it is known, protein G is a cell wall protein found in most species of *Streptococci* that can be used for proper orientation of antibodies. Since protein G exhibits a specific interaction with the Fc portion of Immunoglobulin G (IgG) (Figure 14) [Boyle & Reis, 1987] [Choe et al., 2016], the paratope of IgG can face the opposite side of the protein G-immobilized on solid support with no interference to the antigen binding sites. As a result, protein G mediated antibody immobilization can lead to a highly efficient immunoreaction since in a random orientation of antibodies their Fab fragments may be hidden which resuts in the antibody-antigen binding being hindered.

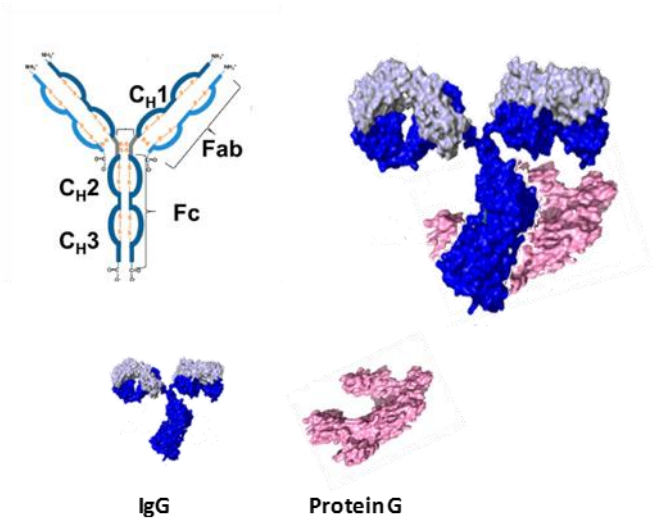

Figure 14.- *Illustration of the different parts of an antibody and IgG-protein G conjugate. Modified from [Choe et al., 2016].*

Regarding carboxylated MBs, they allow the covalent attachment of antibodies to obtain a stable immobilization and a good reproducibility. However, in this case, reduction of binding capability can be observed due to the steric hindrance induced by improper orientation of the immunoreagent. The most used procedure for the covalent attachment consists on the preparation of a succinimidyl ester (-COOSuc) terminated surface layer and reacting it with an amino linker appended to the lysine groups of the protein to form strong covalent peptide bonds. The -COOSuc surface is obtained by reacting a surface bearing carboxyl end groups with an N-hydroxysuccinimide (NHS), in the presence of a water-soluble carbodiimide such as N-ethyl-N´-(3-(dimethylamino) propyl)carbodiimide (EDC) or other similar coupling agents (Figure 15). This reaction is often referred to as surface “activation” [Sam et al., 2010].

One of the main advantages of EDC coupling is its water solubility, which allows direct bioconjugation without prior organic solvent dissolution. However, the coupling reaction has to be carried out fast, as the reactive ester that is formed can be rapidly hydrolyzed in aqueous solutions. The addition of sulfo-NHS (NHSS) estabilizes the amine-reactive intermediate by converting it to an amine-reactive sulfo-NHS ester, thus increasing the efficiency of EDC-mediated coupling reactions. Although prepared sulfo-NHS esters are sufficiently stable to process in a two-step reaction scheme, both groups will hydrolyze within hours or minutes, depending on pH of the reaction solution. The activation reaction with EDC and NHSS is more efficient at pH 4.5-7.2, and EDC reactions are often performed in MES buffer at pH 4.7-6.0.

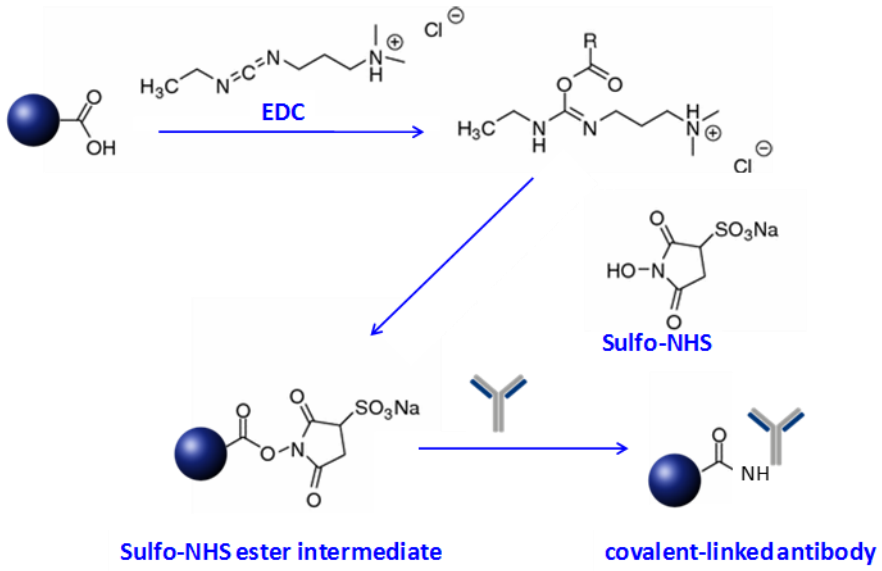

Figure 15.- *Scheme of antibody covalent binding onto HOOC-MBs using EDC/NHSS*

3.6.2. GRAPHENE AND GRAPHENE HYBRIDS

After the "There's plenty of room at the bottom" Feynman's conference in Caltech at the Physics American Society meeting in 1959 [Feynman, 1992], nanomaterials have become a reality and today they have paramount importance in different fields of science including (bio)sensors development. Among the different types, carbon nanomaterials constitute a special group which is presented in all three dimensional classes. The 2D graphene (Gr) [Geim & Novoselov, 2007] is currently one of the most used nanomaterial in (bio)sensing applications. Gr was firstly reported as a single carbon layer of the graphite structure at 2004 by A. Geim and K. Novoselov [Novoselov et al., 2004]. It is described as a one-atom-thick planar sheet of sp^2-bonded carbon atoms densely packed in a honeycomb crystal lattice (Figure 16).

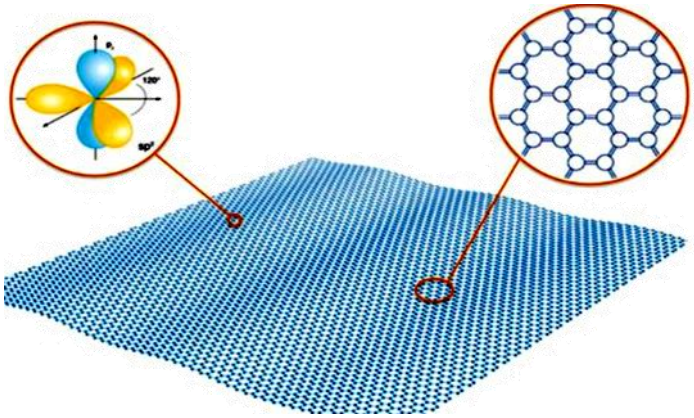

Figure 16.- *Graphene sheet showing each sp^2 hybridized carbon atom, and enlarged section showing the honeycomb crystal lattice.*

The special properties of graphene derive from its honeycomb lattice composed by two equivalent sub-lattices of carbon atoms bonded together with σ bonds [Zhu et al., 2010]. Each atom in the lattice has a π orbital that contributes to a delocalized network of electrons similar to conduction bands in metals. Gr presents a semimetal 0 Gap electronic structure. Important physical properties exploited in electrochemical applications are the extreme large surface area (2630 m^2 g^{-1}) [Geim & Novoselov, 2007], good electrical conductivity, wide potential window, low resistance to charge transfer, and high electrocatalytic activity [Alwarappan et al., 2009]. The high density of defects in the edges of Gr offers active points for the electronic transfer to biomolecules such as redox enzymes [Lawal, 2015]. However, from the practical point of view, the use of graphene in the construction of biosensors is limited by the low solubility of this material in polar and nonpolar solvents, as well as the absence of groups able to achieve an effective immobilization of biomolecules. These problems can be partially solved by chemical modification as, for example, oxidizing it, as commented below.

The different methods for Gr production can be classified into two big generic groups (Figure 17) [Kochmann et al., 2012]: a) top down methods, where graphene is obtained from a precursor. These include chemical and mechanical exfoliation and the reduction of the graphene oxide, and b) bottom up methods in which graphene is produced from carbon atoms like chemical vapour deposition (CVD) and epitaxial growth on CSi methods [Yazdi et al., 2016].

Exfoliation is known as the best method for graphene production, but it suffers from lack of reproducibility. The electrochemical production is achieved by separating the graphene sheets by the application of a potential of about 2eV/nm^2, which overcomes the Van der Waals forces through which graphene sheets interacted. This

"peeling" process can also be carried out by the sonication of graphite and the use of a polar solvent and / or surfactant that prevents graphene sheets from interacting again [Hernández et al., 2008]. Furthermore, the appearance of oxygenated groups is achieved with the chemical synthesis of graphene oxide (GO) by oxidation of graphite mainly by the Hummers method [Hummers & Offeman, 1958] followed by step-wise exfoliation of GO to give aqueous colloidal suspensions by sonication and stirring. Oxygenated groups diminish the interaction between graphite layers and increase the hydrophilic character of the material. The main limitation is the formation of structural defects and vacancies that interrupt the carbonacea sp^2 network, thus get worse the electronic properties. All of these disadvantages can be solved by GO reduction, giving reduced graphene oxide (rGO) which restores a large part of the conductivity and minimizes the drawbacks of low reactivity due to the defects that do not get eliminated [Chua & Pumera, 2014].

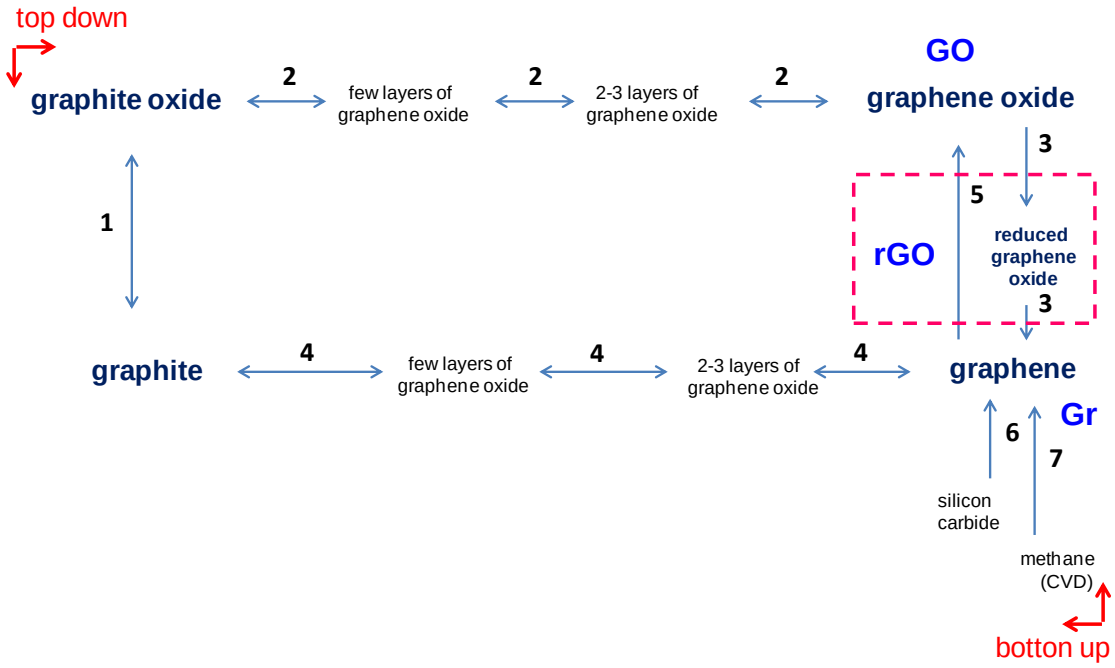

Figure 17.- *Routes for production of graphene-related materials:(1) oxidation of graphite to graphite oxide; (2) step-wise exfoliation of graphite oxide to give graphene oxide in aqueous colloidal suspensions by sonication and stirring; (3) reduction of graphene oxide; (4) mechanical exfoliation of graphite to give graphene (tape method); (5) oxidation of graphene sheets to graphene oxide; (6) thermal decomposition of a SiC wafer; (7) growth of graphene films by chemical-vapor deposition.*

The oxygenated groups present at graphene oxide surface (organic ketones, carboxylic acids and / or epoxy functional groups) can be reduced by applying electrochemical, photochemical, thermal or hydrothermal methods [Wu et al., 2013]. A variety of reducing agents has also been used, the most common being hydrazine monohydrate, sodium borohydride, p-phenylenediamine, hydroquinone and sodium

hydrosulphite [Chen et al., 2010]. However, all these are dangerous to human health and the environment and, therefore, several investigations have been realized in search of finding an ecological and green methodology with non-toxic reagents for GO reduction. Among all the described methods, that proposed by Zhang et al. [Zhang et al., 2010] based on employment of L-ascorbic acid as reducing agent was selected in this work for preparing rGO as it constitutes an environmentally friendly alternative avoiding the use of any toxic or dangerous reagent or solvent that could produce contamination problems.

It is worth mentioning that the synthesis of rGO by any of the existing methods does not allow to obtain totally reduced graphene, although the final product contains less oxygenated moieties than GO. This affects the electrochemical performance in terms of electron transfer rate or adsorption / desorption of molecules, but at the same time provides sites for anchoring to biomolecules facilitating the biosensors developing for detection applications [Wu et al., 2013]. By this way, rGO combines both Gr and GO characteristics and has good conductivity, thermal stability and processing capacity thereby making this material suitable for construction of electrochemical biosensors.

Hybrid nanomaterials were defined as the intentional combination of at least a nanomaterial with one or more materials, at a nanoscale or atomic level of mixture, complementing each other to have new or improved functions and properties which individual components did not possess [Hagiwara & Suzuki, 2000]. Graphene's extremely high specific area and its unique two-dimensional crystal structure makes it one of the more useful support material for combining with nanoparticles or other carbon nanostructures for production of hybrid nanomaterials. Among the variety of such materials prepared from graphene, those based on SiO_2 constitute excellent substrates for the development of electrochemical sensors. The huge conductivity, high surface area, biocompatibility and robustness of graphene, coupled with the physical and chemical resistance of silica, its hydrophylicity, chemical inertness, and the high surface area / volume ratio, all contribute to increase the electroactive surface, thus enhancing sensitivity [Walcarius & Kuhn, 2008]. On the other hand, metallic nanoparticles are characterized by their electrocatalytic ability together with the capacity for adsorption of biomolecules, biocompatibility and high conductivity. In this context, it has been claimed that functionalization of graphene with SiO_2 allows anchoring metal nanoparticles securely onto graphene support with a high dispersion thus enhancing the catalytic performance [Thi Vu et al., 2015].

As it will be seen, a hybrid graphene based-material composed of SiO_2 and silver nanoparticles was prepared in this work for the development of an electrochemical immunosensor for the determination of ethynyl estradiol in urine.

Table 2 summarizes some recent applications of graphene hybrids based-electrochemical immunosensors covering the period 2016-2018, and refers specifically to those designs in which the hybrid materials were used as modifiers of the electrode surface, obviating other configurations in which the main role of these materials is as carrier tags for signal amplification. As it can be seen, metal nanoparticles, mainly AuNPs, have been profusely used for developing electrochemical immunosensors with the goals of improving sensitivity [Anik et al., 2018] [Elshafey et al., 2016], increase the number of sites for immobilization of biorreceptors [Afkhami et al. 2017] [Gao et al., 2016], and accelerate the electron transfer [Han et al., 2016]. Moreover, these nanoparticles also provide a congenial microenvironment for immobilizing biomolecules to retain their bioactivity [Barman et al., 2017]. Conducting polymers have also been used for the preparation of graphene hybrids taking advantage of their redox properties [Yukird et al. 2017], the remarkable electrocatalytic properties [Singal et al., 2017] and the increase of the effective surface area of the electrode that they provide [Sharma et al., 2018]. Other materials used are chitosan, a biodegradable matrix which possess multiple binding groups for bioreagents [Afkhami et al., 2017], magnetic Fe_3O_4 nanoparticles [Sun et al., 2017], and carbon nanotubes [Singal et al., 2016] among others.

As it can be seen, a variety of label-free immunosensors have been developed. These designs avoid the need of labels, so that they simplify the preparation steps and make the detection more cost effective and faster using electrochemical techniques such as DPV or EIS in combination with reversible redox probes such as $Fe(CN)_6^{3-/4-}$ [Elshafey et al., 2016] [Wang et al., 2018]. Finally, as in the case of the designs based on MBs (Section 3.5.1.), the applications of these immunosensors have been basically directed to the determination of biomarkers of cancer or of cardiovascular diseases and to a much lesser extent, to the detection of toxins.

Table 2.- *Some recent electrochemical immunosensors based on graphene and graphene hybrids (See Section 8 for abbreviations).*

Electrode	Configuration	Technique	Analyte / Sample	Analytical characteristics	Reference
AuNPs/PEDOT/ GO/GCE	Label free, AFB1-anti-AFB1--AuNPs/PEDOT/GO/GCE	DPV, $Fe(CN)_6^{3-/4-}$	AFB1 / maize	D.R: 0.5–20 ng/mL, 20–60 ng/mL LOD: 0.109 ng/mL	[Sharma et al., 2018]
AuNPs@MOFs-Fe-NGNRs/GCE	Sandwich, AuPt-MB-anti-Gal-Gal-anti-Gal-3-AuNPs@MOFs-Fe-NGNRs/GCE	DPV, MB	Gal-3 / plasma	D.R: 100 fg/mL - 50 ng/mL LOD: 33.33 fg/mL	[Tang et al., 2018]
AuNPs/Gr/ AuSPE	PNA lectin-neuraminidase-fetuinA-AuNPs/Gr/AuSPE	EIS / $Fe(CN)_6^{3-/4-}$	influenza A virus (neurami-nidase activity) / H9N2	D.R: 10^{-8} - 10^{-1} U/mL LOD: 10^{-8} U/mL	[Anik et al., 2018]
PBSE/Gr/Cu	Label free, CEA-anti-CEA-PBSE/Gr/Cu	EIS / $Fe(CN)_6^{3-/4-}$	CEA / -	D.R: 1.0 - 25.0 ng/mL LOD: 0.23 ng/mL	[Singh et al., 2018]
Ag/MoS_2/rGO/ GCE	Direct, CEA-anti-CEA-Ag/MoS_2/rGO/GCE	Amperom. H_2O_2	CEA / serum	D.R: 0.01 pg/mL - 100 ng/mL LOD: 1.6 fg/mL	[Wang et al., 2018]
Pd@Au@Pt/ rGO/AuE	Label free, anti-CEA-Pd@Au@ Pt/ rGO/AuE; anti-CEA-Pd@Au @Pt/ rGO/AuE	DPV, $Fe(CN)_6^{3-/4-}$	CEA, PSA	D.R:0.012-85 ng/mL (CEA); 0.003- 60 ng/mL (PSA); LOD:8 pg/mL (CEA);2 pg/mL (PSA)	[Barman et al., 2018]
AuNPs@THI/GO/ GCE	Sandwich, PtCu@rGO g-C_3N_4-Ab2 - PSA- Ab1/ AuNPs@THI/GO/GCE	Amperom., red. H_2O_2	PSA / serum	D.R: 50 fg/mL - 40 ng/mL LOD: 16.6 fg/mL	[Feng et al., 2017]
3-MPA-AuNPs/ rGO/SPCE	Sandwich, HRP-ConA-Brett-Ab1-3-MPA-AuNPs/rGO/SPCE	Amperom,	*B. Bruxellensis* / wine	D.R: 10 - 106 CFU/mL LOD: 8 CFU/mL	[Borisova et al., 2017]
AgNPs/Nafion/ Gr/GCE	Label free, MC-LR-Ab1/AgNPs /Nafion/Gr/ GCE	SWV / $Fe(CN)_6^{3-/4-}$	MC-LR / water	D.R: 0.5 - 5000 ng/mL LOD: 0.017 ng/mL	[Zanato et al., 2017]
AuNPs/rGO/AuE	Label free, PSA-anti-PSA-AuNPs/rGO/AuE	DPV, $Fe(CN)_6^{3-/4-}$	PSA / serum	D.R: 6 pg/mL - 30 ng/mL LOD: 3 pg/mL	[Barman et al., 2017]
p(Py/PPA)/Gr/ MWCNTs/GCE	Label free, cTnI-anti-cTnI-p(Py/PPA)/Gr/ MWCNTs/GCE	EIS/ $Fe(CN)_6^{3-/4-}$	cTnI / serum	D.R: 1.0 pg/mL - 10 ng/mL	[Singal et al., 2017]
Chit/AuNPs/Gr/ GCE	Label free, BoNT-A-anti-BoNT-A-Chit/AuNPs/Gr/GCE	EIS, $Fe(CN)_6^{3-/4-}$	BoNT-A / milk, serum	D.R: 0.27 - 268 pg/mL LOD: 0.11 pg/mL	[Afkhami et al., 2017]
AuNPs/Fe_3O_4/ rGO/Nf@GCE	Competitive, HRP-Strept-Biotin-anti-cortisol/ AuNPs/MrGO/ Nf@GCE	DPV, H_2O_2 /*o*-PD	cortisol / serum	D.R: 0.1 - 1000 ng/mL LOD: 0.05 ng/mL	[Sun et al., 2017]
AuNPs/NBA/ ERGO	Label free, CEA-anti-CEA-AuNPs/NBA/ ERGO	DPV, NBA	CEA / serum	D.R: 0.001 - 40 ng/mL LOD: 0.45 pg/mL	[Gao et al., 2016]
AuNPs-Phe-GO/GCE	Sandwich, Fc-GO-anti-cTnI-cTnI-anti-cTnI-AuNPs-Phe-GO/GCE	SWV, Fc	cTnI / serum	D.R: 0.05 - 3 ng/mL LOD: 0.05 ng/mL	[Liu et al., 2016]

Table 2 (Cont.).- *Some recent electrochemical immunosensors based on graphene and graphene hybrids (See Section 8 for abbreviations)*

Electrode	Configuration	Technique	Analyte / Sample	Analytical characteristics	Reference
PMC/GO/AuE	Label free, DENV/PMC/GO/AuE	EIS / $Fe(CN)_6^{3-/4-}$	DENV	D.R: 1 - $2x10^3$ pfu/mL LOD: 0.12 pfu/mL	[Navakula et al., 2017]
anti-NGAL-PANI/Gr/SPCE	Direct, NGAL- anti-NGAL-PANI/Gr/SPCE	Amperom. NGAL	NGAL / urine	D.R: 50 - 500 ng/mL LOD: 21.1 ng/mL;	[Yukird et al., 2017]
rGO/GCE	Sandwich, HRP-anti-AFP- AuNPs/ZnO-anti-AFP-AFP-rGO/GCE	DPV, H_2O_2 TMB	AFP	D.R: 0.02 - 10^4 pg/mL; 10^4-10^5 pg/mL LOD: 0.01 pg/mL	[Fang et al., 2017]
AuNPs-Cyst-gERGO-SPCE	Label free, anti-p53-p53- AuNPs-Cyst-gERGO-SPCE	SWV / $Fe(CN)_6^{3-/4-}$	anti-p53 / serum	D.R: 0.1 - 10 ng/mL LOD: 0.088 ng/mL	[Elshafey et al., 2016]
MPA-PtNPs-pma/ Gr/MWCNTs /GCE	Label free, anti-cTnI-MPA.PtNPs-pma/ Gr/MWCNTs /GCE	EIS / $Fe(CN)_6^{3-/4-}$	cTnI / serum	D.R: 1.0 - 10 ng/mL	[Singal et al., 2016]
CMC/rGO/SPCE	Sandwich, HRP-Strept-Biotin-anti-APNAPN-anti-APN-CMC/rGO/SPCE	Amperom., H_2O_2/HQ	APN / serum	D.R: 0.5 - 10 µg/mL LOD: 61 ng/mL	[Arenas et al., 2016]
PtNPs-Gr/Chit/ IL/GCE	Label free, hCG-anti-hGC-PtNPs-Gr/Chit/IL/GCE	DPV, rutin	hCG / plasma	D.R:0.00106–2.12; 2.12–350 mIU/mL LOD: 0.00035 mIU/mL.	[Roushani & Valipour, 2016]
AuNPs/SnO_2/rGO/ GCE	Sandwich, PdNPs-V_2O_5/MWCNTs-anti-CEA-CEA-anti-CEA-AuNPs/SnO_2/rGO/GCE	Amperom., H_2O_2	CEA / serum	D.R: 0.5pg/mL - 25ng/mL LOD: 0.17pg/mL	[Han et al., 2016]
NH_2-PTC-TEPA-rGO/GCE	Sandwich, C_{60}-AuPt-anti-Vang-Vangl1-anti-Vangl1-NH_2-PTC-TEPA-rGO/GCE	Amperom., H_2O_2	Vangl1 / serum	D.R:0.1-100 pg/mL; 100-450 pg/mL; LOD: 0.03 pg/mL	[Chen et al., 2016]
Protein A-Chit/ mB/GO/dSPCE	Label free, anti-H5N1- (or H1N1) -Protein A-Chit/ mB/GO/SPCE	DPV, mB	influenza A virus (H5N1, H1N1) / serum	D.R: 25 - 500 pM; LOD: 8.3 pM (H5N1); 9.4 pM (H1N1)	[Veerapandian et al., 2016]

3.6.3. CONDUCTING POLYMERS

Polymeric materials in the form of nanoparticles or as film coatings, usually combined with carbon nanotubes, graphene or metallic nanoparticles, have expanded their usefulness for the preparation of electrochemical biosensors. Among them, conducting polymers (CPs) have largely demonstrated their suitability to be used as a matrix to immobilize biomolecules because of the rapid electron transfer and the appropriate ways for immobilization [Teles & Fonseca, 2008]. Electrosynthesis of CPs allows for precise control of probe incorporation to the electrode surfaces and, as the polymer grows in the proximity of the electrode, the molecules are also immobilized very near to such conducting surface. This fact is very important because better currents with a short response time can be obtained. However, not all the strategies developed for the preparation of CPs-based biosensors are suitable for construct electrochemical immunosensors. For example, the simple approach by bioreagents entrampment, profusely used for enzymes, is not recommended in this case, because the antibody–antigen binding can be strongly hindered. Thus, methods for allowing the ordered immobilization of immunoreagents without losing the conductive properties of CPs should be applied. Effective alternatives are the use of CPs containing functional groups for covalent binding of biomolecules. For instance, biotinylated poly(pyrrole) (pPy) copolymerized with pyrrole lactobioamide monomer was used for the construction of an amperometric immunosensor for the detection of cholera antitoxin immunoglobulins [Ionescu et al., 2005]. Another electrochemical immunosensor was prepared by immobilization of a singlechain antibody (ScAb) on a N-alpha bis(carboxymethyl)-L-lysine (ANTA)/Cu^{2+} complex attached to a polypyrrole backbone and applied to the determination of D-dimer, a fibrin degradation product [Chebil et al., 2010]. A method to functionalize pPy with poly(propionic acid) (pPA) through copolymerization was implemented by Hu et al. [Hu et al., 2007], and a label-free SPR immunosensor using goat IgG as a model protein was constructed by covalent immobilization of probes on the resulting pPy/pPA film [Hu et al., 2008]. Using a screen-printed carbon electrode modified with pPy-Py-2-carboxylic acid copolymer, a label-free impedimetric hCG immunosensor was also constructed [Truong et al., 2011].

An amperometric immunosensor for the detection of neomycin was also prepared by covalent immobilization of the antibody onto a glassy carbon electrode modified with gold nanoparticles and electrodeposited poly(2,5-di-(2-thienyl)-1 H-pyrrole-1-(p-benzoic acid) [Zhu et al., 2010a]. Moreover, an electrochemical immunosensor for the hormone leptin was constructed by co-electropolymerization of

pyrrole and pyrrole propylic acid in the presence of gold nanoparticles onto a glassy carbon electrode followed by the covalent attachment of protein G to capture the antibody anti-leptin IgG [Chen et al., 2010a].

Poly(pyrrolepropionic) acid (pPPA) (Figure 18) is a conducting polymer with abundance of carboxyl groups for covalent binding of immunoreagents. Although its conductivity is not very high, relevant characteristics such as the porous structure and hydrophilic property of the films electrodeposited, permit electroactive species to permeate through the polymer film and then generate sensitive electrochemical responses on the electrode surface [Dong et al., 2006].

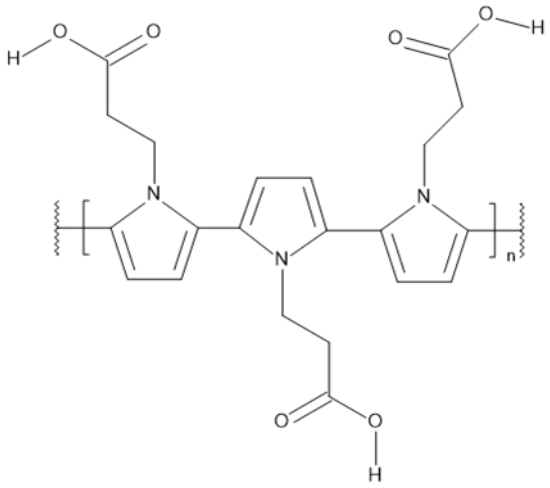

Figure 18. *Structure of poly(pyrrole propionic) acid*

As Table 3 shows, few designs of immunosensors prepared with this polymer have been described so far. Glassy carbon electrodes modified with pPPA were used as platforms for the preparation of amperometric immunosensors using IgG as the target analyte [Dong et al., 2006]. A CNT-*p*PPA network was also proposed for the electrochemical immunoassay of hepatitis B surface antigen [Hu et al., 2011]. More recently, our group has described electrochemical immunosensors based on *p*PPA for the determination of various analytes of clinical interest [Serafín et al., 2014] [Serafín et al., 2014a] [Serafín et al., 2017].

Table 3.- *Some electrochemical immunosensors based on pPPA-modified electrodes. (See Section 8 for abbreviations).*

Electrode	Configuration	Technique	Analyte / Sample	Analytical characteristics	Reference
*p*PPA / SPCE	Sandwich, HRP-Strep. / Biotin–anti- AXL/AXL/anti AXL/*p*PPA / SPCE	Amperom., H_2O_2 / HQ	AXL / serum	D.R: 5 - 700 ng/L LOD: 337 pg/mL; RSD: 3.5%	[Serafín et al., 2017]
*p*PPA / MWCNTs / GCE	Sandwich. HRP-anti-IGF1 / IGF1 / anti-IGF1 / *p*PPA / MWCNTs / GCE	Amperom., H_2O_2 / HQ	IGF1 / serum	D.R: 0.5 – 1000 pg/l LOD: 0.25 pg/ml; RSD: 6%	[Serafín et al., 2014]
*p*PPA / MWCNTs / GCEs	Competitive, AP-anti-PRL / PRL / *p*PPA / MWCNTs / GCE	DPV, 1-NPP	PRL / serum, urine	D.R: 10^{-2}- 10^{5} ng/L LOD: 3 pg/mL; RSD: 2.3%	[Serafín et al., 2014a]
*p*PPA / MWCNTs / GCEs	Sandwich, AP-anti-HBsAg / HBsAg / anti HBsAg / *p*PPA/MWCNTs/GCE	DPV, *p*APP	HBsAg / serum	D.R: 0.001 – 1000 ng/mL LOD: 0.01 ng/mL	[Hu et al., 2011]
*p*PPA/GCE	Sandwich, AP-anti-IgG / IgG / anti IgG / *p*PPA / GCE	DPV / *p*APP	IgG / -	D.R: 10 - 10^{6} pg/mL LOD: 20 pg/mL	[Dong et al., 2006]

3.7. STRATEGIES USED FOR THE IMMOBILIZATION OF BIOMOLECULES

Covalent immobilization of biorecognition elements offers important advantages in the preparation of biosensors. However, as it is well known, binding of biomolecules on the electrode surface requires the presence of reactive functional groups both in the bioreagent and the electrode. In the case of proteins, there are abundant amino groups which may react with oxygen moieties, i.e. carboxyl groups to form amide type bonds. This scheme is usually followed to immobilize proteins covalently for preparation of electrochemical immunosensors. The use of ECD-NHSS chemistry to activate carboxyl groups was described in Section 3.5.1. in the specific case of HOOC-MBs. However, apart from magnetoimmunosensors based on functionalized MBs, the application of this strategy for preparation of integrated immunosensors needs to use electrode materials containing a high amount of oxygenated binding groups. As described above, in this work, two materials of such type, reduced graphene oxide (rGO) and poly(pyrrole propionic) acid (*p*PPA) were used as electrode modifiers for the construction of electrochemical platforms to subsequently bind the immunoreagents. Moreover, another strategy consisted in the incorporation of functional groups to the electrode surface by electrochemical grafting, also used in this work, is discussed in this section.

3.7.1. ELECTROCHEMICAL GRAFTING

Electrochemical grafting was defined as the electrochemical reaction that permits the union of organic molecules onto solid electrode substrates [Bélanger & Pinson, 2011]. This reaction usually involves the transfer of an electron between the organic compound and the electrode. It is a methodology characterized by its simplicity and by the possibility of generating a compact layer with high density of functional groups [Liu et al., 2000]. One of the most commonly used molecules to carry out these proceses is *p*-aminobenzoic acid (*p*-ABA) since it not only provides the necessary carboxylic groups but also they keep oriented them because of the flat structure.

Figure 19 shows the steps involved in the electrochemical grafting of *p*-aminophenyl onto a screen printed carbon electrode [Saby et al., 1997] [Verma et al., 2011]. Firstly, the aryl diazonium salt is prepared in acid medium by reduction of the amino group in the presence of sodium nitrite. Then, by loss of nitrogen, this reaction leads to a radical that is grafted onto the electrode surface by successive cyclic voltammetric scans.

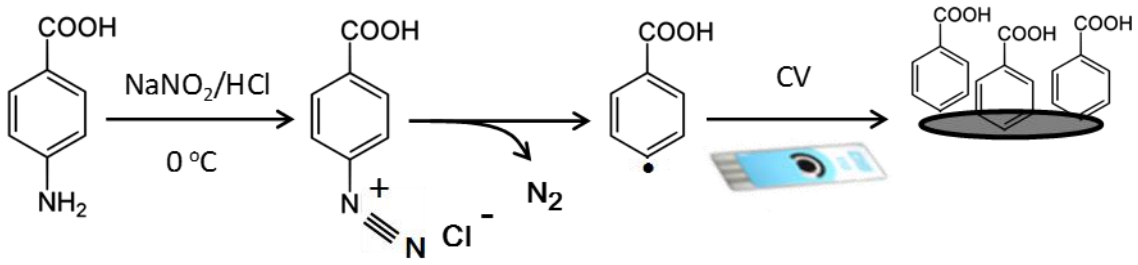

Figura 19.- *Steps involved in the electrochemical grafting of p-carboxyphenyl.*

Since in 1992 Pinson and co-workers [Delamar et al., 1992] described the reaction mechanism for the modification of carbon electrodes by electrochemical reduction of aryldiazonium salts, this chemistry has demonstrated to be an efficient way to introduce many types of functional groups onto a variety of materials, mainly carbon, metals or silicon. [Bélanger & Pinson, 2011]. This electrografting method presents also some advantages: the reaction time scale ranges from seconds to minutes, and the density of the deposited organic layer on the electrode surface can be controlled by a careful selection of the electrografting protocol and time.

In order to illustrate the versatility and analytical utility of this methodology, Table 4 summarizes the characteristics of some recent configurations of electrochemical immunosensors prepared by electrografting of an aryldiazonium salt and subsequent immobilization of immunoreagents. As it can be seen, most strategies involve antibody immobilization onto modified screen-printed electrodes (SPEs). Apart from carbon (SPCEs), other electrode materials such as graphene (GrSPEs) or carbon nanofiber (CnFSPEs) have been used. As modifiers, diazonium salts derived from *p*-ABA (*p*-carboxyphenyl diazonium salt), as well as *p*-aminophenylacetic acid (*p*-APA) and *p*-nitroaniline diazonium salt were used. Antibodies were covalently immobilized onto the electrografted surface using carbodiimide chemistry, and through activation with glutaraldehyde (GA) or aminophenylboronic acid (APBA). For example, a label-free voltammetric immunosensor for the detection of β-lactoglobulin (β-LGB) was developed using SPGrEs grafted with *p*-nitrophenyldiazonium prepared by diazotization of *p*-nitroaniline. After reduction to amine groups and activation with GA, anti-β-LGB was covalently immobilized [Eissa et al., 2012]. A similar strategy was followed by Radi et al. [Radi et al., 2009] using screen-printed gold electrodes (SPAuEs) modified with *p*-nitrophenyl groups assembled from *p*-nitrophenyl diazonium salt for covalent binding of ochratoxin A (OTA) antibodies. A direct competitive-type immunosensor using OTA-HRP was prepared with 3,3′,5,5′-tetramethyl-benzidine (TMB) for the amperometric detection of OTA. SPGrEs grafted with *p*-carboxyphenyl

diazonium salt were also proposed to develop voltammetric immunosensors for the sensitive detection of okadaic acid (OA) [Eissa & Zourob, 2012] and ovalbumin (OVA) [Eissa et al., 2013]. In each case, antibodies were covalently immobilized onto the electrografted electrode via carbodiimide chemistry. Hayat et al. [Hayat et al., 2011] developed another electrochemical immunosensor for OA by covalent immobilization onto SPCEs modified by grafting with *p*-carboxyphenyl followed by covalent bound of hexamethyldiamine (HMDA). An indirect competitive immunoassay was performed using differential pulse voltammetry (DPV) as detection technique. A similar configuration for OA was proposed by the same authors by means of electrochemical impedance spectroscopy (EIS) [Hayat et al., 2012]. A label-free electrochemical immunosensor was also reported for the detection of porcine serum albumin (pSA) using CnFSPEs with grafted *p*-carboxyphenyl [Lim et al., 2016]. Antibodies were covalently immobilized onto the modified electrode and the increase in SWV current of $[Fe(CN)_6]^{3-/4-}$ was measured.

In our group, an immunosensing platform using SPCEs for the covalent immobilization of capture antibodies through grafting of *p*-ABA diazonium salt was developed for the determination of adrenocorticotropin hormone (ACTH) [Moreno-Guzman et al., 2012]. This design involved the use of amino phenylboronic acid for the oriented immobilization of anti-ACTH onto modified SPCEs followed by a competitive immunoassay using alkaline phosphatase-labelled streptavidin and 1-naphtyl phosphate as the enzyme substrate. This strategy was further extended to the construction of a dual electrochemical immunosensor for the simultaneous determination of ACTH and cortisol onto dual screen-printed carbon electrodes (SPdCEs) [Moreno-Guzman et al., 2012a]. Another design was prepared with SPCEs modified with double-walled carbon nanotubes (DWCNTs) previously grafted with *p*-ABA diazonium salt and used for binding adiponectin (APN) antibodies which were also highly oriented by means of Mix&Go chelating polymer [Ojeda et al., 2015].

A simple label-free impedimetric immunosensor for determination of mucin 4 (MUC 4) protein was also described by Hosu et al. [Hosu et al., 2017] using graphite SPEs modified with *p*-APA for antibody immobilization via amidic bond. Recently, [Eissa et al., 2018] a comparative study was performed using six different carbon nanomaterial-modified electrodes (carbon, graphene (Gr), GO, single (SWCNT) and multi-walled (MWCNTs) carbon nanotubes, and carbon nanofiber (CnF)) modified by grafting with *p*-carboxyphenyl to develop immunosensors for detection of survival motor neuron (SMN) protein. Once the antibody was immobilized, results showed that SPCnFE exhibited the best performance for SMN detection by SWV.

Table 4.- *Some immunosensors prepared by grafting of aryldiazonium salts. (See Section 8 for abbreviations).*

Electrode	Configuration	Technique	Analyte / Sample	Analytical characteristics	Reference
Phe-S-AuNPs/ SPCE	Sandwich, HRP-anti BNP- BNP-anti BNP-S-Phe-AuNPs/SPCE	Amperom. H_2O_2 / HQ	BNP / serum	D.R: 0.014 – 15 ng/mL LOD: 4 pg /mL	[Serafín et al., 2018]
p-ABA-g-CnFSPE	Label free, pSA-anti-PSA-*p*-ABA-g-CnFSPE	SWV $[Fe(CN)_6]^{3-/4-}$	SMN / whole blood	D.R: 1.0 pg/mL - 100 ng/mL LOD: 0.75 pg/mL	[Eissa et al., 2018]
p-ABA-g-DWCNTs/ SPdCE	Sandwich, HRP-poly-Strept-Biotin-anti-TNF-TNF-anti-TNF-M&G-*p*-ABA-g-DWCNTs/dSPCE Sandwich, HRP-poly-Strept-Biotin-anti-IL1β-IL1β-anti-IL1β-M&G-*p*-ABA-g-DWCNTs/SPCE	Amperom. H_2O_2 / HQ	TNF-α, IL-1β / serum, saliva	D.R: 1–200 pg/mL (TNF-α); 0.5–100 pg/mL (IL-1β) LOD: 0.85 pg/ mL (TNF-α); 0.38 pg/ mL (IL-1β)	[Sánchez-Tirado et al., 2017]
p-ABA-g-SPCE	Sandwich, V-Phe-SWCNT(-HRP)-anti-TGF-TGF-β1-anti-TGF-Biotin-Strept/SPCE	Amperom. H_2O_2 / HQ	TGF-β1 / saliva	D.R: 2.5–1000 pg/mL LOD: 0.95 pg/ mL	[Sánchez-Tirado et al., 2017a]
p-ABA-g-CnFSPE	Label free, pSA-anti-PSA-*p*-ABA-g-CnFSPE	DPV / $[Fe(CN)_6]^{3-/4-}$	pSA / fresh meat	D.R: 0.5–500 pg/mL LOD: 0.5 pg/mL	[Lim et al., 2016]
p-ABA-g-DWCNTs /SPCE	Sandwich, HRP-Strept-Biotin-APN-anti-APN-M&G-*p*-ABA-gDWCNTs/SPCE	Amperom. H_2O_2 / HQ	APN / serum	D.R: 0.05 –10.0 µg/mL LOD: 14.5 ng/mL	[Ojeda et al., 2015]
p-ABA-g-SPGrE	Label-free, OVA-anti-OVA-*p*-ABA-g-SPGrE	DPV $[Fe(CN)_6]^{3-/4-}$	OVA egg-free cake	D.R: 1.0 pg/mL- 0.5 µg/mL LOD: 0.83 pg/ mL	[Eissa et al., 2013]
p-nitrophenyl-g-SPGrE	Label free, β-LGB-anti-β-LGB-GA-*p*-aminophenyl-g-SPGrE	DPV $[Fe(CN)_6]^{3-/4-}$	β-LGB / cake, cheese, snacks	D.R: 1 - 100 ng/mL LOD: 0.85 pg/mL	[Eissa et al., 2012]
p-ABA-g-SPCE	Sandwich, AP-Strept-Biotin-ACTH-anti-ACTH-4-APBA-*p*-ABA-g-SPCE	DPV / 1-NPP	ACTH / serum	D.R: 0.025–1.0 pg/mL LOD: 18 pg/L	[Moreno-Guzman et al., 2012]

Table 4 (Cont.).- *Some immunosensors prepared by grafting of aryldiazonium salts. (See Section 8 for abbreviations).*

Electrode	Configuration	Technique	Analyte / Sample	Analytical characteristics	Reference
p-ABA-g-SPCE	Label free, OA-anti-OA-*p*-ABA-g-SPCE	EIS $[Fe(CN)_6]^{3-/4-}$	OA/ mussel	D.R: 0.195–12.5 µg/mL LOD: 0.3 µg/L	[Hayat et al., 2012]
p-ABA-g-SPGrE	Label free, competitive, OVA-OA-anti-OA-*p*-ABA-g-SPAuE	SWV $[Fe(CN)_6]^{3-/4-}$	OA/ shellfish tissue	up to 5000 ng/mL 19 ng/L	[Eissa & Zourob, 2012]
p-APA-g-SPGE	Label free, MUC4-anti-MUC4-*p*-APA-g-SPGrE	EIS, $[Fe(CN)_6]^{3-/4-}$	MUC4/ serum	D.R: 1 – 15 µg/mL LOD: 0.33 µg/mL	[Hosu et al., 2017]
p-nitrophenyl-g-SPCE array	Sandwich, HRP-anti-CEA(or anti-AFP)-CEA (or AFP)-anti-CEA (or anti-AFP)-GA-*p*-aminophenyl-g-SPCE	Amperom. H_2O_2 / HQ	CEA, AFP/ serum	D.R: 0.10 – 50 ng/mL LOD:0.03 ng/mL (CEA); 0.05 ng/mL (AFP)	[Qi et al., 2012]
p-ABA-g-dSPCE	Sandwich, AP-Strept-Biotin-ACTH-anti-ACTH-*p*-APBA-*p*-ABA-g-SPCE Competitive, AP-cortisol-anti-cortisol-4-APBA- *p*-ABA-g-SPCE	DPV / 1-NPP	ACTH, cortisol / serum	D.R: $5.0x10^{-5}$ – 0.1 ng/mL (ACTH); 0.1 – 500 ng/mL (cortisol); LOD: 40 pg/L (ACTH); 37 pg/mL (cortisol)	[Moreno-Guzmán et al., 2012a]
p-ABA-g-SPCE	Competitive, AP-IgG-anti-OA-OA-HMDA-*p*-ABA-g-SPCE	DPV, 1-NPP	OA/ mussel	LOD: 1.44 ng/L	[Hayat et al., 2011]
p-nitrophenyl-g-SPAuE	Competitive, HRP-anti-OTA-GA-*p*-amino-phenyl-g-SPAuE	Amperom. TMB	OTA	D.R: up to 60 ng/mL LOD: 12 ng mL−1	[Radi et al., 2009]

3.8. REPORTED METHODS FOR THE DETERMINATION OF THE ANALYTES OF INTEREST

In this section, the methods reported in the literature for the determination of the analytes selected in this work using electrochemical biosensors are briefly described. As can be seen in Tables 5-10, the type of configurations used and the analytical characteristics of the respective procedures were compared to those of some commercial ELISA kits commonly used in clinical analysis.

3.8.1. GHRELIN (GHRL)

Despite its importance, methods for determining GHRL are scarce. Various colorimetric ELISA kits using competitive or sandwich-type assays with anti GHRL, biotinylated immunoreagents, and streptavidin labeled with peroxidase are commercially available, although discrepancies in GHRL quantification using these assays have been reported [Gröschl et al., 2004]. Most of them exhibit dynamic concentration ranges from 0.01 (or 0.1) to 100 (or 1000) ng/mL, with minimum detectable concentrations between 0.05 and 1 ng/mL. The assay time varies from 1 h 45 min to more than 5 h counting from the moment when the immobilization of the capture antibody occurred. Commonly, total GHRL determination is accomplished although some assays for individual acylated or deacylated hormone have also been described. Concerning biosensors, Mascini et al developed a colorimetric microarray detection system for GHRL using aptamers technology, with a linear range between 0.2 and 245.5 ng/mL and a detection limit of 0.2 ng/mL [Mascini et al., 2007]. A Spielgelmer 50-biotin Nox B11, consisted of a RNA molecule made of non-naturally L-nucleotides recognizing five amino acids from the N-terminus of human GHRL was used. The same authors developed an electrochemical aptasensor where the aptamer was adsorbed on the surface of a screen-printed electrode and measurement of the decrease in the guanine oxidation signal in the presence of GHRL was used for quantification. The linear range was from 14 to 100 ng/mL and the detection limit was 8 ng/mL [Mascini et al., 2007a].

.

Table 5.- *Electrochemical biosensors and ELISA kits for the determination of GHRL. (See Section 8 for abbreviations).*

Configuration	Method	LOD, pg/mL	DR, ng/mL	Assay time	Sample	Reference
Wells microarray with immobilized GHRL	Colorim. competitive aptasensor; GHRL + Biotin-aptasensor soln. added to immob. GHRL. Addition of AP-extravidin and 1-NPP.	200	0.2 - 245.5	3 h 30 min	-	[Mascini et al., 2007]
Aptamer adsorbed onto SPCE	Electrochem. competitive aptasensor; SWV responses of guanine inversely related with GHRL concentration	8000	14 - 100	-	-	[Mascini et al., 2007a]
ELISA kit (EK-031-30) Phoenix Pharmaceuticals	Competitive,TMB, H_2O_2 / HRP-Strept-Biotin-GHRL(GHRL)-anti GHRL	130	0.13-1.34	4 h	plasma, serum	www.phoenixpeptide.com/products/view/Assay-Kits/EK-031-30
ELISA kit (LS-F26916) LSBio	Sandwich, TMB, H_2O_2 / HRP-anti GHRL-GHRL-anti GHRL	< 1000	5 -100	2 h 15 min	plasma, cell culture; serum	www.lsbio.com/elisakits/human-ghrelin-elisa-kit-sandwich- elisa-ls-f26916/26916
ELISA kit (E-EL-H1919) Elabscience Biotechnol.	Competitive, TMB, H_2O_2 / HRP-Strept--Biotin-anti GHRL-GHRL	100	0.16 – 10	1 h 45 min	plasma, cell culture; serum	www.elabscience.com/p-human_ghrl(ghrelin)_elisa_kit-17684.html?cpage=1&ctype=s
ELISA kit (EZGRT-89K) Merck	Sandwich,TMB, H_2O_2 / HRP-anti GHRL-GHRL-anti GHRL	50	0.05 – 5	3 h	plasma, serum	www.merckmillipore.com/ES/es/product/Human-Ghrelin-total-ELISA,MM_NF-EZGRT-89K
Human GHRL ELISA BMS2192 Invitrogen	Sandwich, TMB, H_2O_2 / HRP-Strept-Biotin-anti GHRL-GHRL-anti GHRL	11.8	0.016 – 1	3 h 30 min	plasma, serum	www.thermofisher.com/order/catalog/product/BMS2192
GHRL ELISA kit KA 1863 Abnova	Competitive, TMB, H_2O_2/ HRP-Strept-Biotin-GHRL(GHRL)-anti GHRL	161	0.1 -1000	5h 15 min	plasma, serum	www.abnova.com/products/products_detail.asp?catalog_id=KA1863

3.8.2. PEPTIDE YY (PYY)

Various ELISA methods based on similar immunoassay schemes have been developed for the determination of PYY (Table 6). Competitive configurations involving specific PYY antibodies or biotinylated PYY binding, as well as HRP-labeled avidin or streptavidin conjugates, are the most common. These assays allow the determination of PYY in concentration ranges up to 3000 pg/mL, with minimum detectable concentrations varying from 0.5 pg/mL to approximately 80 pg/mL. The times required for these assays are around 2– 5 h, although some assays require more than 20 h or incubate overnight. Among the different assays, it is worth to mention an original configuration based on the use of SULFO-TAG™ label, which generates an electrochemiluminiscent response initiated at the electrode surface of microplates.

3.8.3. AMYLIN (AMY)

As Table 7 shows, various commercial ELISA kits based on competitive strategies for AMY determination using biotinylated antigen are available. The most sensitive configurations exhibit dynamic ranges between 6 and 500 pg/mL, approximately, as well as detectable concentrations typically less than 3 pg/mL. A sandwich-type immunoassay with fluorometric detection was also developed for the detection of AMY in plasma with a dynamic range between 2 and 100 pmol/L and a minimum detectable concentration of 0.5 pmol/L [Percy et al., 1996].

Table 6.- *Electrochemical biosensors and ELISA kits for the determination of PYY. (See Section 8 for abbreviations).*

Configuration	Method	LOD, pg/mL	DR, ng/mL	Assay time, h	Sample	Reference
ELISA kit (48-PYYHU-E01.1) ALPCO	Competitive, TMB, H_2O_2 / HRP-Strept- Biotin-PYY - (PYY)- anti-PYY	82	0.082 – 20	20	plasma, serum	www.alpco.com/store/peptide-yy-elisa-pyy-elisa.html
ELISA kit (EK-59-02) Phoenix Pharmaceuticals	Competitive, TMB, H_2O_2 / HRP-Strept- Biotin-PYY- (PYY) - anti-PYY	60	0.06 - 0.67	4	plasma	www.phoenixpeptide.com/doc/protocol/EK-059-02.pdf
PYY ELISA Kit DEIA477 Creative Diagnostics	Competitive, TMB, H_2O_2 / HRP-Strept- Biotin-PYY- (PYY) - anti-PYY	82	0.082 - 20	22	plasma, serum	www.creative-diagnostics.com/Human-PYY-ELISA-Kit-106173-471.htm
ELISA kit (K151MPD) Meso Scale Discovery	Sandwich, Sulfo-Tag-anti PYY-PYY - anti-PYY-Biotin- Strept	68	0.09 - 3	4	plasma, serum	www.mesoscale.com/products/human-total-pyy-kit-k151mpd/
ELISA kit (EZHPYYT66K) Merck	Sandwich, TMB, H_2O_2 / HRP-Strept - Biotin-PYY - PYY - anti- PYY	6.5	0.014 – 1.8	3	plasma, serum	www.merckmillipore.com/ES/es/product/Human-PYY-Total-ELISA,MM_NF-EZHPYYT66K
ELISA kit (EIA-PYY-1) Ray Biotech	Sandwich, TMB, H_2O_2 / HRP-Strept-Biotin- PYY-PYY- anti - PYY - IgG	5.6	$1 \cdot 10^{-4}$ – 1	>5	plasma, serum	www.raybiotech.com/human-peptide-yy-pyy-eia-kit/
Peptide YY ELISA Kit No. ABIN414478, S	Competitive, TMB, H_2O_2 / HRP-Avidin- Biotin-PYY- (PYY) - anti-PYY	0.48	1.23×10^{-3} - 0.1	2	plasma, serum, cell culture	www.antibodies-online.com/kit/414478/Peptide+YY+ELISA+Kit/

***Table 7.-**. Electrochemical immunosensors and ELISA kits for the determination of AMY. (See Section 8 for abbreviations).*

Configuration	Method	LOD, pg/mL	DR, ng/mL	Assay time	Sample	Reference
ELISA kit (abx051311) Abbexa	Competitive, TMB, H_2O_2 / HRP-AMY (AMY) - anti-AMY	2.26	0.008 – 0.5	2h 30min	serum, plasma, other biolog. fluids	www.abbexa.com/human-amylin-elisa-kit
ELISA kit (CEA812Ra) Cloud-Clone corp.	Competitive, TMB, H_2O_2 / HRP-AMY (AMY) - anti-AMY	2.83	0.006 – 0.5	2	serum, plasma, other biolog. fluids	www.labome.com/product/Cloud-Clone-Corp/CEA812Ra.html
ELISA kit (MBS702315) Mybiosource	Sandwich, TMB, H_2O_2 / HRP-Strept- Biotin-anti AMY-AMY-anti-AMY	11.75	0.047 - 3	4h 30min	serum, plasma, urine	www.mybiosource.com/prods/ELISA-Kit/Human/islet-amyloid-polypeptide/IAPP/datasheet.php?products_id=702315
ELISA kit (EIAM-AMY-1) Ray Biotech	Competitive, TMB, H_2O_2 / HRP-AMY (AMY) - anti-AMY	620	0.1 - 1	>5h	serum, plasma	www.raybiotech.com/files/manual/EIA/EIA-AMY.pdf
ELISA kit (CEA812Hu) Wuhan USCN Business Co.	Competitive, TMB, H_2O_2 / HRP- AMY (AMY) - anti-AMY	2.55	0.006 – 0.5	2h	serum, plasma, other biolog. fluids	http://www.uscnk.com/uscn/ELISA-Kit-for-Islet-Amyloid-Polypeptide-(IAPP)-35976.htm
LSBio HumanIAPP/AMY ELISA Kit (Competitive EIA) LS-F9686	Competitive, HRP-Strept-Biotin-AMY(AMY)-anti-AMY	<6.17	0.006-0.5	1h 50 min	serum, plasma, other biolog. fluids	www.lsbio.com/elisakits/manualpdf/ls-f9686.pdf

3.8.4. TRANSFORMING GROWTH FACTOR β1 (TGF- β1)

The reported methods for the determination of TGF-β1 cytokine were summarized in Table 8.

Immunoassay strategies for the determination of TGF-β1 cytokine based on sandwich-type configurations with peroxidase-labeled or biotinylated anti-TGF-β1 as detection antibodies are employed in commercial ELISA colorimetric kits. These methods are valid for determining TGF-β1 in the range from several tens to thousands of pg/mL with minimum detectable concentrations that can drop to a few units of pg/mL. In the particular case of biosensors for TGF-β1 determination, only two configurations have been found in the literature. An aptasensor involving aptamer-modified Au electrodes integrated with microfluidics was reported. Thiolated aptamers labeled with methylene blue were self-assembled on gold surfaces. The linear range covered up to 250 ng/mL with a detection limit of 1 ng/mL. This device was also used to monitor TGF-β1 release from hepatic cells [Matharu, et al, 2014]. More recently, an impedimetric immunosensor was developed for the determination of TGF-β1 in human serum. A self-assembled monolayer of polyethylene glycol (PEG) prepared onto interdigitated electrodes was used for the covalent immobilization of the antibodies. A linear impedance vs log [TGF-β1] range between 1 and 1000 ng/mL was found with a detection limit of 0.570 ng/mL [Yao et al, 2016].

In our group an electrochemical immunosensor for the determination of TGF-β1 using multi-walled carbon nanotubes (MWCNTs)-modified screen-printed carbon electrodes was developed. MWCNTs were functionalized by means of copper(I) catalyzed azide–alkyne cycloaddition (“click” chemistry) as an efficient strategy for the covalent immobilization of immunoreagents without altering their configurations and preserving their biological activity. Alkyne functionalized IgGs were also prepared and used to assemble IgG-alkyne–azide–MWCNTs conjugates used as scaffolds for the immunosensor preparation. After a blocking step with casein, anti-TGF was immobilized and the target cytokine was sandwiched with biotinylated anti-TGF labeled with poly-HRP labeled streptavidin [Sánchez-Tirado et al., 2016]. More recently (see Table 4), viologen functionalized SWCNTs were also used as carrier nanotags for the electrochemical immunosensing of TGF-β1 [Sánchez-Tirado et al., 2017a].

***Table 8.-**. Electrochemical immunosensors and ELISA kits for the determination of TGF-β1. (See Section 8 for abbreviations).*

Configuration	Method	LOD, pg/mL	DR, ng/mL	Assay time	Sample	Reference
Impedimetric, gold array electrode	Label free, TGF-β1-anti- TGF-β1-HOOC-PEG-HS-Au	586	1-1000	>1h 15 min	serum	[Yao et al., 2016]
Amperometric immunosensor	Sandwich, poly-HRP-Strept-Biotin - anti-TGF-β1-TGF-β1-anti-TGF-β1-IgG-alkyne-azide-MWCNTs/SPCE	1.3	0.005 - 0.2	1h 20 min	serum	[Sánchez-Tirado et al., 2016]
SWV microfluidic aptasensor	Label free, TGF-β1-MB-aptamer-HS-Au	1000	1 - 250	2d (sample)	hepatic stellate cells	[Matharu et al., 2014]
ELISA kit (DB 100B) R&D System	Sandwich, TMB / HRP-Strept-Biotin-anti-TGF-β1-TGF-β1-anti-TGF-β1	15	0.031 - 2	4 h 30 min	serum, plasma, cell cult. Urine	R&D Systems (DB100B) Human TGF-β1 Quantikine ELISA Kit
ELISA kit (ab100647) Abcam	Sandwich, TMB / HRP-Strept- Biotin-anti-TGF-β1-TGF-β1-anti-TGF-β1	80	0.082 - 6	4h 45 min	serum, plasma, cell cult.	http://www.abcam.com/human-tgf-beta-1-elisa-kit-ab100647-protocols.html
ELISA kit (KA0151) Abnova	Sandwich, TMB / HRP-Strept-Biotin-anti-TGF-β1-TGF-β1-anti-TGF-β1	8.6	0.031 - 2	5 h 45 min	serum, plasma, cell cult.	www.abnova.com/products/products_detail.asp?catalog_id=KA0151
ELISA kit (BM 249-4) Thermo Fisher	Sandwich, TMB / HRP-Strept- Biotin-anti-TGF-β1 - TGF-β1- anti TGF-β1	8.6	0.9 – 13.7	5 h 30 min	serum, plasma	www.thermofisher.com/order/catalog/product/BMS249-4
ELISA kit (ADI-900-155) Enzo life sciences	Sandwich, TMB / HRP-IgG -anti-TGF-β1 -TGF-β1 - anti - TGF-β1	3.3	0.031 - 1	4 h	serum, plasma, cell cult.	www.enzolifesciences.com/ADI-900-155/tgf-beta1-elisa-kit/

3.8.5. ETHYNYL ESTRADIOL (EE2)

Table 9 Sumarizes the existing methods for the determination of EE2.

Immunosensor configurations for EE2 were proposed using magnetic microbeads for the preparation of the immunoconjugates and application to the analysis of water. One of these designs, based on functionalized MBs with a synthetic estrogen derivative, was used for competitive immunoassay with anti-EE2, alkaline phosphatase-labeled IgG, and 1-naphthyl phosphate, allowing the determination of the estrogen by SWV with a limit of detection of 10 pg/mL [Kanso et al., 2013]. A competitive microfluidic immunoassay based on the immobilization of anti-EE2 on 3-aminopropyl functionalized magnetic microbeads and amperometric detection using the HRP/H_2O_2/HQ system, was also reported [Martínez et al., 2010].

Various ELISA methods for the determination of EE2 in biological samples or water have also been described. Table 9 summarizes the analytical characteristics of some of these configurations. A typical assay is based on competitive interaction between EE2 and biotinylated EE2 for the binding sites of a pre-coated specific antibody. Colorimetric detection using a peroxidase conjugate, H_2O_2 and TMB, allows the EE2 determination to be performed in a non-linear dynamic range extending up to thousands of pg/mL, and with an analysis time lasting about 2 – 2.5 h [Schneider et al., 2004]. Other immunoassay formats using fluorimetric [Coille et al., 2002] or chemiluminiscence measurements [Schneider et al., 2005] were also described.

Table 9.- *Electrochemical biosensors and ELISA kits for the determination of EE2. (See Section 8 for abbreviations).*

Configuration	Method	LOD, pg/mL	DR, ng/mL	Assay time	Sample	Reference
Biomatik ELISA kit EE2 EKU03983	Competitive, TMB / HRP-Strept-Biotin-EE2 (EE2)- anti-EE2	9.13	0.025-2	2 h	serum, plasma, other biol. fluids	www.biomatik.com/ethynylestradiol-ee-elisa-kit.html
ELISA kit (DEIA06009) Creative Diagnostics	Competitive, TMB / HRP-EE2 (EE2) - anti-EE2	-	(5-300) $x10^4$	2.5 h	serum, plasma	www.creative-diagnostics .com /EE2-EIA-Kit-122944-465.htm
ELISA kit (MBS-2000365) Mybiosource	Sandwich, TMB / HRP-Strep-Biotin-EE2-(EE2)-anti EE2	9.34	0.024 - 2	2 h	biological tissues	www.mybiosource. com/ prods/ELISA-Kit/ General /ethynylestradiol-EE/EE/
ELISA kit (OKCD02267) Aviva Systems biology	Competitive, TMB / HRP-Strep - Biotin-EE2 (EE2)-anti EE2	9.34	0.025 - 2	2.5 h	serum, plasma	www.avivasysbio.com/en/ ethynylestradiol-elisa-kit-okcd02267.html
Magneto-immunosensor, SWV, 1-NPP as substrate	Indirect competitive, AP-IgG-anti-EE2-EE2-MBs/SPCE	10	0.01-1	2h	waters	[Kanso et al., 2013]
Magneto-immunosensor, micro-fluidic, amperometric H_2O_2/HQ	Competitive, HRP-EE2-(EE2)-anti-EE2-MBs/AuE	0.09	10^{-5} - 0.06	30 min	river water	[Martínez et al., 2010]

3.8.6. β-HYDROXYBUTYRATE (β-HB)

Few electrochemical biosensors have been described so far for the determination of β-HB. As Table 10 shows, these are mainly based on the use of dehydrogenase enzymes involving the NAD^+/NADH system. The enzyme β-hydroxybutyrate dehydrogenase (β-HBDH) specifically catalyzes the conversion of the analyte to acetoacetate (AcAc) (Figure 20), leading to the production of NADH which is the electroactive product. The inherent problems related to the large overvoltage for the electrochemical oxidation of NADH, as well as the fouling of the working electrode have been minimized using different electrode materials and redox mediators.

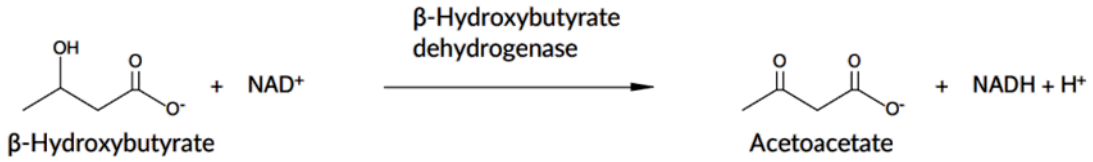

Figure 20.- *β-HB oxidation catalyzed by β-HBDH.*

A method for the determination of β-HB based on the immobilization of β-HBDH onto screen-printed electrodes modified by coenzyme functionalized carbon nanotubes have been described [Khorsand et al., 2013]. The electrocatalytic effect from CNTs allowed to detect NADH at a potential as low as -0.15 V vs Ag/AgCl. An enzyme-based Clark electrode was also used in a bienzyme configuration with β-HBDH in combination with salicylate hydroxylase (SHL). In this design, NADH initiates the irreversible decarboxylation and the hydroxylation of salicylate by SHL in the presence of oxygen, and thus, consumption of dissolved oxygen was detected for the determination of β-HB [Kwan et al., 2006]. A disposable amperometric biosensor with β-HBDH immobilized on screen-printed carbon electrodes (SPCEs) was also prepared using a layer of carboxymethylcellulose (CMC) hydrophilic gel to adsorb the enzyme alongside NAD^+ cofactor and $Fe(CN)_6^{3-}$ as the electron transfer mediator [Li et al., 2005].

Other redox mediators such as 1,10-phenanthroline quinone [Forrow et al., 2005] or Meldola's Blue [Shimomura et al., 2013] have also been used. Recently, an electrochemical biosensor using paper electrodes and 1,10-phenantroline-5,6-dione as the redox mediator was reported for the determination of β-HB in blood [Wang et al., 2016], and a configuration using $[Ru(bpy)_3]^{2+}$ and graphene oxide was described by Veerapandian et al. for the determination of β-HB in bovine serum [Veerapandian et al.,

2016a]. An screen printed electrode fabricated with iridium-carbon particles was also used for the determination of β-HB taking advantage of the electrocatayzed responses of NADH at the modified material [Fang et al., 2008].

Regarding to colorimetric kits, some examples have also been described. Enzymatic schemes using β-HBDH have been proposed based on the synthesis of a coloured product resulted from the oxidized β-HB or the decarboxylation process of acetoacetate to form acetone using a specific enzyme. These methods are characterized by a good sensitivity. Moreover, ELISA kits using β-HB antibodies are also commercially available. As example, Table 10 summarizes the characteristics of a competitive configuration involving biotinylated β-HB and avidin labelled with peroxidase (HRP-Avidin) and colorimetric detection by means of the TMB/H_2O_2 system. All these kits can be applied to analyse serum, plasma and /or urine and other biological fluids.

Table 10.- *Electrochemical biosensors and ELISA kits for the determination of β-HB. 1(See Section 8 for abbreviations).*

Biosensor	Method	Detection	L.R. mM	LOD, μM	Stability	Sample	Reference
β-HBDH /$[Ru(bpy)_3]^{2+}$/ GO/NAD^+/SPCE	Enzyme adsorption, NADH oxid./ $[Ru(bpy)_3]^{2+}$	Amperom. E=+0.06V	0.2 - 2	-	-	Human serum	[Veerapandian et al., 2016a]
1,10-PD/NAD^+/ β-HBDH /SPCE paper	Enzyme adsorption, NADH oxid. / 1,10 PD	Amperom. E=+0.2V	0 - 6	300	-	Human blood	[Wang et al., 2016]
β-HBDH /NAD^+/ SWCNTs/ SPCE	Enzyme adsorption, detect. NADH	CV/ 1 to -1V	0.01 - 0.1	9	180 days	human serum	[Khorsand et al., 2013]
β-HBDH -FSM 8.0 / NAD^+ /MB / SPCE	Enzyme entrampment into mesSiO_2 Detect. NADH/ MB	Amperom. E=-0.05V	0.03 - 8	29.2	> 6 months	-	[Shimomura et al., 2013]
β-HBDH / NAD^+ / SPIrCE / BSA	Enzyme adsorption, NADH oxid.	Amperom. E=+0.2V	0.02 - 10	20	-	bovine serum	[Fang et al., 2008]
Teflon / PCS gel (SHL / β-HBDH) / Clark E	Gel enzyme entrampment (PCS) / Teflon NADH oxid. / SHL O_2 consumption	Amperom, E=+0.6V	0.008 - 0.8	3.9	6 days (90%)	human serum	[Kwan et al., 2006]
1,10-PQ/NAD^+/ β-HBDH/SPCE	NADH oxid. / 1,10-PQ	Amperom. E=+0.2V	up to 6	-	18 months	blood	[Forrow et al., 2005]
β-HBDH / NAD^+ / $Fe(CN)_6^{3-}$ / CMC / SPCE	Enzyme adsorption, NADH oxid./ $Fe(CN)_6^{4-}$	Amperom. E=+0.3V	0.014 - 5.3	14	30 days	human serum	[Li et al., 2005]
ab83390 beta hydroxy-butyrate Assay Kit Abcam	Enzyme biosensor, β-HBDH catal. oxid. + color develop.	Colorim.	0.01-0.2	10	-	serum plasma urine	www.abcam.com/beta-hydroxy-butyrate-beta-hb-assay-kit-colorimetric-ab83390.html
Wako Diagnostics enzyme kit	Enzyme biosensor, β-HBDH catal. oxid. + color develop.	Colorim.	0.003 - 1	0.2	-	plasma, serum	www.wakodiagnostics.com/r_ketone_3hb.html
β-hydroxybutyrate-Colorimetric Assay Kit 700190	Enzyme biosensor, β-HBDH catal. oxid.; NADH react with diahorase + color develop.	Colorim.	0.025 - 0.5	-	-	plasma, serum, urine	www.caymanchem.com/product/700190
LifeSpan beta-hydroxy-butyric ELISA Kit	Immunosensor, competit. HRP-Avidin-Biotin- β-HB (β-HB)-anti-β-HB	Colorim. TMB/H_2O_2	1.56×10^{-4} -0.010	0.156	-	plasma, serum	www.lsbio.com/elisakits/all-species-beta-hydroxybutyric-acid-elisa-kit-competitive-eia-ls-f10582/10582? trid=247

INSTRUMENTACIÓN

REACTIVOS Y
DISOLUCIONES

4. PARTE EXPERIMENTAL

MUESTRAS

PROCEDIMIENTOS
EXPERIMENTALES

4.1. INSTRUMENTACIÓN

4.1.1. APARATOS

Las medidas voltamperométricas se han llevado a cabo utilizando un potenciostato PGSTAT 101 (Autolab) (Figura 21) equipado con el software electroquímico Nova 1.8 de EcoChemie B.V.

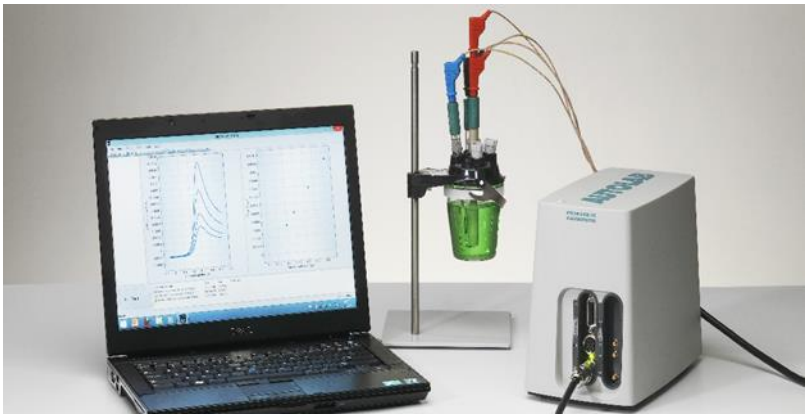

Figura 21.- *PGSTAT 101 (Autolab) utilizado para medidas voltamperométricas.*

También se ha utilizado un analizador electroquímico BAS 100B de la serie 1308 equipado con un software BAS 100/W (Bioanalytical Systems, Inc.) (Figura 22). Este instrumento permite el acoplamiento de una caja de Faraday y un amplificador de corriente PreAmplifier PA-1.

Figura 22.- *BAS 100W (izquierda) y caja de Faraday con amplificador de corriente.*

Las medidas electroquímicas con electrodos duales se han realizado empleando un multipotenciostato 1030 B de CH Instruments provisto de un circuito de adquisición de datos multiplex, de ocho canales (Figura 23).

Figura 23.- *Analizador electroquímico 1030 B (CH Instruments) utilizado para medidas multicanal.*

Las medidas amperométricas se han realizado con un potenciostato portátil InBea de uno o dos canales (según el tipo de medidas) provisto del software IB Graph de InBea Biosensores, S.L. (Figura 24).

Figura 24.- *Potenciostato portátil InBea utilizado para medidas amperométricas.*

Las medidas de impedancia electroquímica para el seguimiento de las etapas de modificación y la caracterización de la superficie electródica se han realizado empleando un potenciostato μAutolab tipo III, controlado por el software FRA2 (Ecochemie) (Figura 25). Este mismo potenciostato se ha utilizado también para realizar medidas voltamperométricas, empleando para ello el software GPES (Ecochemie).

Figura 25.- *Potenciostato µAutolab tipo III utilizado para medidas impedimétricas.*

4.1.1.1. Otros aparatos

− pH-metros de precisión Metrohm Herisau E-510 y Crison Basic 20+ calibrados de la forma usual con disoluciones reguladoras de pH 4.0, 7.0 y 9.0 a 25.0 ± 0.5 °C.

− Baños de ultrasonidos (P-Selecta) y Elmasonic S-60 (Elma).

− Incubador Optic Ivymen System provisto de agitación y sistema de control de temperatura (Comecta S.A.).

− Agitadores Vortex (VELP Scientifica y Heidolph).

− Agitador magnético (P-Selecta Agimatic).

− Centrífugadoras MPW-65R (Med. Instruments) y P-Selecta Cencom.

− Baño termostático P-Selecta Digaterm 100.

4.1.2. ELECTRODOS

Se han empleado electrodos serigrafiados de carbono (SPCEs) marca DropSens (Oviedo, España) de referencia DRP-110 (A = 12.56 mm^2; Ø = 4 mm) y electrodos duales de la misma marca C-1110, con dos superficies elípticas de carbono (A = 5.6 mm^2). Estos electrodos están provistos de un electrodo de pseudorreferencia de plata y de un electrodo auxiliar o contraelectrodo de carbono (Figura 26).

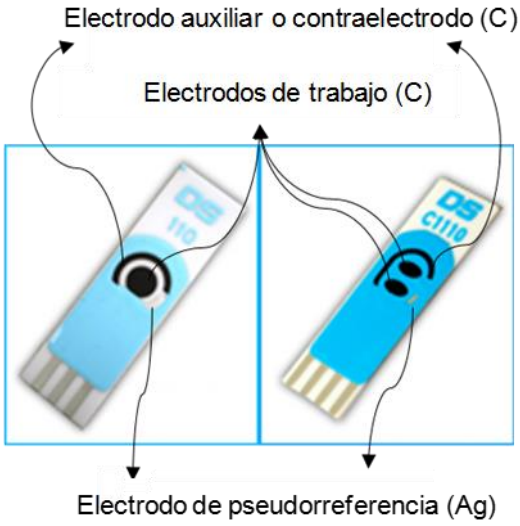

Figura 26.- *Electrodos serigrafiados de carbono sencillo (izda.) y dual.*

Además de los electrodos serigrafiados anteriores, se han utilizado electrodos de carbono vitrificado (GCE) 104 (CH Instruments, Ø=3 mm), electrodos de referencia de Ag / AgCl / KCl 3M MF 2063 (BAS), y electrodos auxiliares de alambre de platino MW 1032 (BAS) (Figura 27). Para el pulido de los GCEs se empleó una suspensión acuosa de alúmina en polvo de 0.3 µm de tamaño de partícula (Metrohm 6.2802.00).

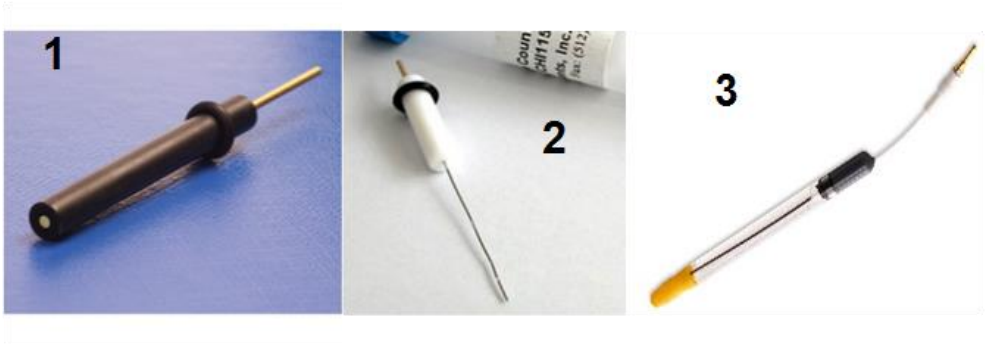

Figura 27.- *Electrodo de trabajo de carbono vitrificado (1); electrodo auxiliar de alambre de platino (2) y electrodo de referencia de Ag/AgCl/KCl (3).*

4.1.3. CÉLULAS ELECTROQUÍMICAS

Las medidas con los electrodos de carbono vitrificado se han realizado en células electroquímicas de 10 mL modelos BAS C2EF-1080 y BAS VC-2, como la que se muestra en la Figura 28a, en la que se aprecia el montaje de tres electrodos con un electrodo de referencia de Ag/AgCl/KCl 3 M y un electrodo auxiliar de alambre de platino. Estas células se utilizaron también para las medidas con los electrodos serigrafiados en modo inmersión.

Además, se utilizaron microcélulas para volúmenes de 50 µL (Figura 28c) para medidas en gota con los electrodos serigrafiados. En el caso del empleo de micropartículas magnéticas, la gota se depositó sobre los electrodos previamente insertados en un bloque de teflón provisto de un imán (DropSens) del modo que se indica en la Figura 28b.

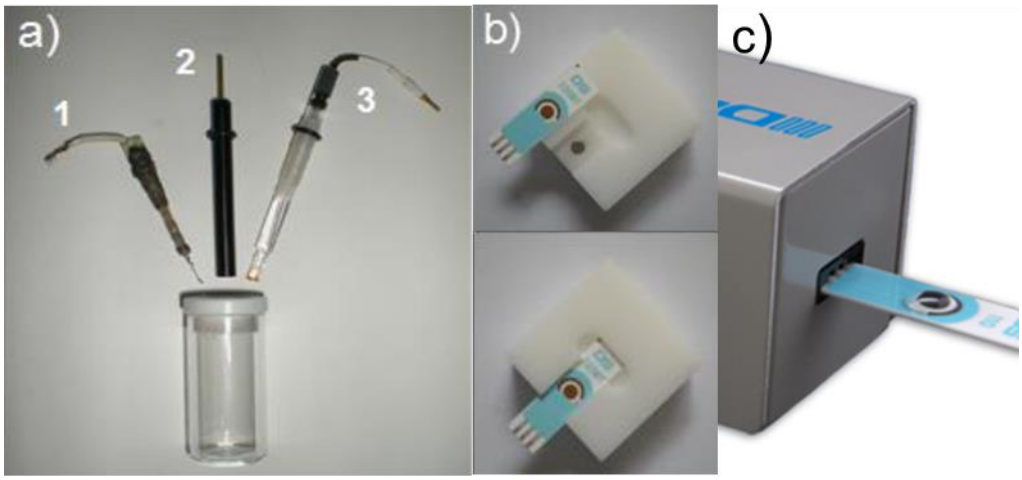

Figura 28.- *(a) Célula electroquímica BAS VC-2 de 10 mL y electrodos utilizados: electrodo auxiliar de Pt (1); electrodo de trabajo (2); electrodo de referencia de Ag/AgCl (3); (b) acoplamiento del electrodo serigrafiado al soporte de magnético de medida; (c) microcélula para medidas en gota sobre electrodos serigrafiados.*

4.1.4. DISPOSITIVOS

− Colector para la recogida de muestras de saliva, Salivette (Sarstedt) (Figura 29).

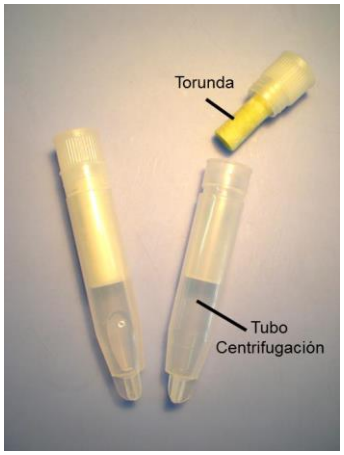

Figura 29.- *Dispositivo colector de saliva Salivette®.*

− Imán de neodimio (AIMAN GZ).

− Separadores magnéticos Dyna MagnsTM-2 (123.21D, Invitrogen Dynal) (Figura 30) y Dynal MPC-S (Dynal Biotech ASA) utilizados para la separación de las micropartículas magnéticas (MBs) durante los procesos de modificación y lavado.

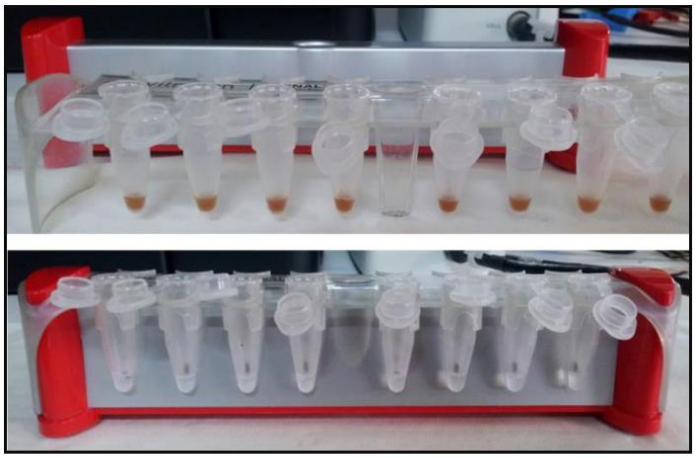

Figura 30.- *Separador magnético Dyna Magns™-2.*

4.2. REACTIVOS Y DISOLUCIONES

En estos apartados se describen los reactivos, materiales y disoluciones principales que se han empleado para la preparación, caracterización y aplicación de los diferentes biosensores desarrollados en este trabajo. Todos los demás reactivos y materiales auxiliares aparecen indicados en las separatas de las publicaciones recogidas al final de esta Memoria.

Todos los productos utilizados, reactivos y disolventes, fueron de calidad analítica. El agua desionizada (18.2 MΩ cm a 25 ºC) se obtuvo empleando un sistema de purificación Millipore Milli-Q. En todos los casos, las medidas electroquímicas se realizaron a temperatura ambiente.

4.2.1. MAGNETOINMUNOSENSOR PARA LA DETERMINACIÓN DE GHRL

Los inmunorreactivos utilizados fueron: antígeno/analito grelina (GHRL), anticuerpo policlonal anti-grelina humana de conejo (anti-GHRL) y grelina biotinilada (Biotin-GHRL) para configurar el diseño competitivo. Todos ellos se obtuvieron de la casa comercial Anaspec. Las disoluciones de estos reactivos se prepararon en regulador fosfato (Scharlab) 0.1M y 0.02% en Tween 20 (Aldrich) de pH 7.4 (regulador B&W). Para hacer posible la detección electroquímica se empleó el conjugado de estreptavidina marcada con fosfatasa alcalina (AP-Strept, Sigma) cuyas disoluciones se prepararon en regulador tris(hidroximetil)-aminometano (Tris, Scharlab) 0.1 M y 0.05% en Tween 20 de pH 7.2. Como sustrato de la enzima fosfatasa alcalina se utilizaron disoluciones de 1-naftilfosfato (1-NPP, Sigma) preparadas en regulador Tris 0.05 M y $MgCl_2$ 10 m M de pH 9.6 (regulador Trizma).

Se utilizaron micropartículas magnéticas funcionalizadas con proteína G, en suspensión, conteniendo 30 mg/mL (Protein G-MBs, Dynal Biotech ASA). Antes de su empleo, la suspensión fue homogeneizada y, para cada ensayo, 1 μL (30 μg) de la misma se transfirió a un tubo eppendorf, lavando dos veces con 50 μL de disolución reguladora B&W.

- Para los estudios de selectividad se prepararon disoluciones patrón de 1000 ng/mL de testosterona (Test, Fluka), progesterona (Prog, Aldrich), hormona de crecimiento humana (hGH, Sigma-Aldrich), prolactina (PRL, Sigma) y hormona folículo-estimulante (FSH,Sigma-Aldrich) en regulador B&W.

4.2.2. MAGNETOINMUNOSENSOR PARA LA DETERMINACIÓN DE TGF- β1

Los inmunorreactivos utilizados fueron: un anticuerpo de captura anti-TGF-β1 humano de ratón (anti-TGF), el antígeno/analito TGF–β1 humano, y el anticuerpo biotinilado de detección, Biotin-anti-TGF humano, para establecer la configuración de tipo sandwich. Todos los reactivos se obtuvieron del kit Duo Sets ELISA Development System (DY240-05) de R&D Systems. Para llevar a cabo la detección electroquímica se utilizaron los conjugados de estreptavidina marcada con peroxidasa (HRP-Strept, Roche) y de estreptavidina marcada con un polímero de peroxidasa (poli-HRP-Strept, Fitzgerald). Como agente bloqueante se utilizó etanolamina (Sigma) en regulador fosfato 0.1 M de pH 8.0. Como sustrato de la enzima peroxidasa se empleó peróxido de hidrógeno (Aldrich, 30% (w/w)), y las medidas electroquímicas se realizaron empleando hidroquinona (HQ, Sigma) como mediador redox.

Se utilizaron micropartículas magnéticas funcionalizadas con grupos carboxilo en suspensión conteniendo 30 mg/mL (HOOC-MBs, Dynabeadss M-270 Carboxylic Acid). Al igual que en el Apartado 4.2.1., antes de su utilización, la suspensión fue homogeneizada y, para cada ensayo, 3 μL (90 μg) se transfirieron a un tubo eppendorf, lavándolas dos veces con 50 μL de disolución reguladora de ácido 2–(N–morfolín) etanosulfónico (MES, Gerbu) 25 mM de pH 5.0. Además de este regulador, también se utlilizaron disoluciones reguladoras de fosfato 0.1 M de pH 8.0 y 0.05 M de pH 6.0, preparadas a partir de Na_2HPO_4 y NaH_2PO_4 (Scharlab) así como un regulador de fosfato salino (PBS) conteniendo Na_2HPO_4 8.1 mM, KH_2PO_4 1.5 mM, NaCl 137 mM y KCl 2.7 mM. A partir de esta, se prepararon disoluciones reguladoras de lavado (WBS) por dilución, añadiendo Tween 20 al 0.05%. Para inmovilizar el anticuerpo de captura en las HOOC-MBs se utilizó el polímero comercial Mix&Go™ (Anteo Diagnostics).

Los estudios de selectividad se realizaron empleando ácido ascórbico (AA, Fluka), ácido úrico (UA, Sigma), creatinina (CR, Sigma), adiponectina (APN, Abcam, interleucina 6 (IL-6, Abcam), interleucina 8 (IL-8, Abcam), y factor de necrosis tumoral alfa (TNF-α, BD Pharmingen).

4.2.3. INMUNOSENSOR PARA LA DETERMINACIÓN DE PYY

Se utilizaron los siguientes inmunorreactivos: anti-péptido YY (3-36) humano (anti-PYY), antígeno/analito péptido YY (3-36) (PYY), y péptido YY biotinilado (Biotin-PYY) para el establecimiento de una configuración competitiva. Todos ellos se obtuvieron de Phoenix Pharmaceuticals, Inc. Para posibilitar la detección

electroquímica se empleó el conjugado de estreptavidina marcada con fosfatasa alcalina (AP-Strept, Sigma), así como 1-naftilfosfato (1-NPP) como sustrato enzimático. Las disoluciones de AP-Strept y la de 1-NPP 0.05 M se prepararon en regulador Trizma. Como agentes bloqueantes se utilizaron etanolamina (Aldrich), albúmina de suero bovino (BSA, Gerbu), y caseína (Thermo Scientific).

Para la modificación de la superficie electródica se empleó óxido de grafeno (GO, NIT.GO.M.140.10, Nanoinnova Technologies). El electrodo modificado se funcionalizó mediante *electrografting* o injerto electroquímico de ácido *p*-aminobenzoico (*p*-ABA, Across) en presencia de $NaNO_2$ 2 mM y HCl 1M. La inmovilización covalente del anticuerpo de captura (anti-PYY) se logró empleando clorhidrato1-etil-3-[3-dimetilaminopropil] carbodiimida (EDC) y N-hidroxi-sulfo-succinimida (NHSS) ambas de Sigma. Las disoluciones se prepararon en regulador fosfato 0.1 M de pH 7.4.

El seguimiento de las etapas de preparación del inmunosensor se realizó empleando disoluciones de ferro- y ferricianuro potásico en medio acuoso 0.1 M en KCl.

Las especies elegidas para estudiar la selectividad del inmunosensor fueron: insulina (INS, Sigma), hormona de crecimiento humana (hGH), hormona folículo-estimulante (FSH), adiponectina (APN), grelina (GHRL) y grelina desacilada (da-GHRL, Anaspec).

4.2.4. INMUNOSENSOR DUAL PARA LA DETERMINACIÓN SIMULTÁNEA DE GHRL Y PYY

Los inmunorreactivos utilizados para la preparación de este inmunosensor han sido descritos en los Apartados 4.2.1. y 4.2.3. Las disoluciones se prepararon en regulador fosfato 0.1 M de pH 7.4, excepto las de AP-Strept y 1-NPP, que se prepararon en regulador Trizma de pH 9.6.

La modificación de las superficies activas del electrodo dual y la inmovilización de los anticuerpos de captura se realizaron del modo que se describe en el Apartado 4.2.3. Al igual que en dicho apartado, el seguimiento de las etapas de preparación del inmunosensor se realizó empleando disoluciones de ferro- y ferricianuro potásico en medio acuoso 0.1 M en KCl.

La posible interferencia en la determinación de ambas hormonas se investigó ensayando varias proteínas: APN, INS, hGH, da-GHRL y FSH.

4.2.5. INMUNOSENSOR PARA LA DETERMINACIÓN DE EE2

Los inmunorreactivos utilizados fueron: el antígeno/analito etinilestradiol (EE2, Aldrich), un anticuerpo de captura anti-etinilestradiol (anti-EE2) y un anticuerpo de detección marcado con peroxidasa (HRP-EE2), ambos de Fitzgerald, para establecer un esquema de immunoensayo tipo sándwich. Las disoluciones se prepararon en regulador fosfato 0.1 M de pH 7.2. Como agente bloqueante se utilizó disolución comercial de caseína en regulador fosfato. Al igual que en el Apartado 4.2.2., como sustrato de la enzima peroxidasa se utilizó H_2O_2 y las medidas electroquímicas se realizaron empleando HQ como mediador redox.

Para la modificación del electrodo se utilizaron los siguientes materiales: oxido de grafeno (GO) obtenido a partir de grafito (Aldrich), tetraetil ortosilicato (TEOS, Sigma-Aldrich), y $AgNO_3$ (Sigma-Aldrich). El electrodo modificado se funcionalizó mediante *electrografting* con *p*-ABA en las condiciones descritas en el Apartado 4.2.2. Para la inmovilización covalente del anticuerpo de captura (anti-EE2) se utilizaron las condiciones descritas en ese mismo apartado. El seguimiento de las etapas de preparación del inmunosensor se realizó, igualmente, empleando disoluciones de ferro- y ferricianuro potásico (Fluka) en medio acuoso 0.1 M en KCl.

Se estudió el efecto sobre la respuesta del inmunosensor de las siguientes especies: cortisol (Cort), β-estradiol (E2), estriol (E3), progesterona (Prog) y testosterona (Test); todos ellos de Sigma.

4.2.6. BIOSENSOR ENZIMÁTICO PARA LA DETERMINACIÓN DE β-HB

Los reactivos utilizados para la preparación del biosensor fueron: enzima β-hidroxibutirato deshidrogenasa de Pseudomonas lemoignei (β-HBDH, ≥ 200 units/mg protein, Aldrich), nicotinamida adenina dinucleótido en forma oxidada (NAD^+, Gerbu), y reducida (NADH, Sigma), y el sustrato/analito, β-hidroxibutirato (β-HB, Alfa Aesar).

Para la modificación del electrodo se utilizó óxido de grafeno (NIT.GO. M.140. 10, Nanoinnova Technologies), empleando ácido ascórbico (AA, Gerbu) y amoniaco (disolución al 32%, Scharlau) para su reducción a óxido de grafeno reducido (rGO). También se utilizó tionina como mediador redox (THI, Aldrich). Las disoluciones se prepararon en regulador fosfato 0.1 M de pH 7.0 que se desoxigenó por burbujeo de nitrógeno durante 15 min antes de su empleo.

Las especies estudiadas como potenciales interferentes fueron: citrato sódico, glutamina, glutamato sódico, succinato sódico, ácido úrico y glucosa, todas ellas de Sigma.

4.2.7. INMUNOSENSOR PARA LA DETERMINACIÓN DE AMY

Los inmunorreactivos utilizados fueron: un anticuerpo monoclonal de captura, anti-amilina humana (anti-AMY) de ratón, el antígeno/analito amilina humana (AMY), y amilina biotinilada (Biotin-AMY) para establecer el esquema competitivo. Todos ellos se obtuvieron del Kit AMY Enzyme Immunoassay (EIA AMY) de RayBio® (RayBiotech, Inc.). Las disoluciones del antígeno (AMY) y del antígeno biotinilado (Biotin-AMY) se prepararon en el diluyente incluido en dicho kit (Assay Diluent B pH 7.5) de RayBiotech. Las disoluciones del anticuerpo anti-AMY se prepararon en el mismo medio, diluyéndose posteriormente hasta la concentración de trabajo deseada con una disolución reguladora 25 mM de ácido 2-(*N*-morfolin)etanosulfónico (MES) (Gerbu) de pH 5.0. También se utilizó una disolución reguladora fosfato de pH 7.4. La inmovilización del anticuerpo de captura en la superficie del electrodo se realizó empleando el polímero Mix&Go™. Para la detección electroquímica se utilizó el conjugado de estreptavidina marcada con peroxidasa (HRP-Strept, Roche). Como bloqueante se empleó una disolución de BSA al 2% (w/v) preparada en el diluyente Assay Diluent B de pH 7.5. Las medidas amperométricas se realizaron empleando disoluciones de H_2O_2 y HQ, como se indica en el Apartado 4.2.2.

Para preparar la superficie electródica se empleó el monómero ácido 1H-pirrol-1-propiónico (PPA) (Sigma-Aldrich, 97%). La electropolimerización a pPPA se realizó empleando disoluciones 0.1 M de PPA en medio acuoso conteniendo KCl 0.5 M (Scharlau, 99.5%).

El seguimiento de las etapas de preparación del inmunosensor se realizó empleando disoluciones de ferro- y ferricianuro potásico preparadas en regulador fosfato 0.05 M de pH 6.0.

Se emplearon disoluciones de ácido ascórbico (AA, Fluka), ácido úrico (UA, Sigma), bilirrubina (BR, Aldrich), colesterol (Chol, Sigma), glucosa (Glu, Panreac) y péptido YY (PYY, Phoenix Pharmaceuticals, Inc.) para estudiar la influencia de estas especies como interferentes potenciales sobre la respuesta del inmunosensor.

4.3. MUESTRAS

El magnetoinmunosensor de GHRL se validó por aplicación a muestras de saliva enriquecida con 0.01, 0.1, 1 y 10 ng/mL de la hormona. El magneto-inmunosensor de TGF-β1 se aplicó a muestras de orina control (Liquichek™, BioRad) contaminada con el analito a niveles de 25, 45 y 100 pg/mL.

El inmunosensor de PYY se aplicó a muestras de suero humano liofilizado (Sigma, S-7394) enriquecidas con 35, 3.5 y 0.35 pg/mL de analito. En el caso del inmunosensor dual de GHRL y PYY se analizaron también estas muestras de suero contaminadas a los niveles de 175, 65 y 6.5 ng/mL (GHRL) y 35, 17.5, 3.5 pg/mL (PYY), así como muestras de saliva enriquecidas con 95 pg/mL (GHRL) y 37.5 pg/mL (PYY). El inmunosensor de EE2 se aplicó al análisis de muestras de orina contaminada a niveles de 0.1, 0.5, 1.0 y 10 ng/mL de analito. La utilidad analítica del inmunosensor de AMY se demostró mediante aplicación a muestras de suero liofilizado (Sigma, S-2257) contaminado a niveles de 1.5 y 8 pg/mL de hormona, así como de orina certificada (Liquichek™) igualmente contaminada a niveles de 0.75 y 4 pg/mL.

Finalmente, el biosensor enzimático para determinación de β-HB se aplicó a muestras de suero humano liofilizado (Sigma, S-2257) contaminadas a niveles de 33 y 290 μM de β-HB.

4.4. PROCEDIMIENTOS EXPERIMENTALES

4.4.1. PREPARACIÓN DEL MAGNETOINMUNOSENSOR PARA LA DETERMINACIÓN DE GHRL

La Figura 31 muestra las etapas de preparación del este inmunosensor. En primer lugar, 30 μg de Protein G-MBs previamente lavadas se suspenden en 10 μL de una disolución de anti-GHRL de 2 μg/mL en un tubo eppendorf (etapa 1 Fig. 31). Después de homogeneizar agitando suavemente en un vórtex durante 15 s, el tubo se sumerge parcialmente en un baño termostático y se incuba 1h a 37 ºC con agitación suave. Seguidamente, se dispone sobre un separador magnético durante 2 min y una vez que el conjugado anti-GHRL-Protein G-MBs se deposita en el fondo del tubo, el líquido sobrenadante se elimina y se aplican dos etapas de lavado con 50 μL de disolución reguladora B&W. Cada una de estas etapas consiste en resuspender los magnetoconjugados en la disolución de lavado y agitar suavemente durante 1 min hasta homogeneización, seguido de la separación magnética por 2 min para decantar la disolución sobrenadante.

A continuación se establece un ensayo competitivo mediante resuspensión del conjugado en 50 µL de una disolución de Biotin-GHRL de 0.01 µg/mL y el analito GHRL (etapa 2 Fig. 31). Después de 45 min de incubación a 37 ºC con agitación suave, el tubo eppendorf se coloca en el separador magnético y se aplican cuatro etapas de lavado, dos de ellas con 100 µL de regulador B&W y otras dos con 150 µL de disolución reguladora Tris. Después, los conjugados Biotin-GHRL(GHRL)-anti-GHRL-Protein-G-MBs se resuspenden en 50 µL de disolución de AP-Strept (etapa 3 Fig. 31) incubando 30 min a 37 ºC en el baño termostático con suave agitación. Una vez transcurrido dicho tiempo, el conjugado resultante, AP-Strept-Biotin-GHRL-(GHRL)-anti-GHRL-Protein-G-MBs se lava dos veces con 150 µL de disolución reguladora Tris y otras dos veces con 200 µL de regulador Trizma, para finalmente ser capturado magnéticamente sobre la superficie del SPCE (etapa 4 Fig. 31). El electrodo debe disponerse de forma horizontal sobre el soporte magnético evitando de este modo variaciones entre medidas del espesor de la capa de micropartículas y/o del área recubierta. Para llevar a cabo la determinación, se depositan en el electrodo 5 µL de una disolución 0.05 M de 1-NPP y se deja estar durante 5 min en la oscuridad a temperatura ambiente. Después se registran los voltamperogramas en diferencial de impulsos en el intervalo de -0.15 a +0.70 V vs Ag.

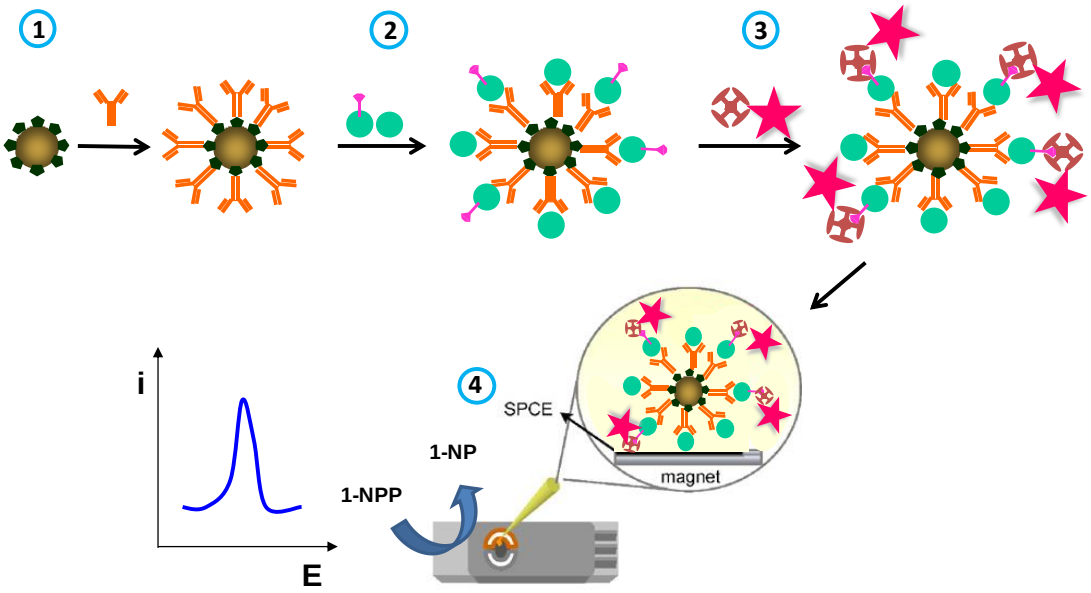

Figura 31.- *Esquema de preparación del magneto-inmunosensor para la determinación de GHRL.*

4.4.1.1. Aplicación a la determinación de GHRL en saliva

Se recogen las muestras de saliva empleando un dispositivo de colección Salivette® (Sarstendt) (Figura 29). Brevemente, el voluntario se introduce en la boca la torunda de algodón, masticándola durante 1 min. Después, el algodón saturado de saliva se inserta en el vial, se sella con la tapa y se centrifuga durante 5 min a 5000 g. A continuación, 1 µL de la muestra contaminada a la concentración deseada (Apartado 4.3.) se mezcla con 3 µL de Biotin-GHRL de 1 µg/mL, diluyendo a 300 µL con el regulador B&W. Para la determinación de GHRL se aplica el procedimiento descrito en el Apartado 4.4.1. a 50 µL de la disolución, y la corriente de pico del voltamperograma se interpola en el calibrado obtenido con disoluciones patrón de GHRL.

4.4.2. MAGNETOINMUNOSENSOR PARA LA DETERMINACIÓN DE TGF-β1

Las etapas de preparación de este inmunosensor se han representado en la Figura 32. Se transfiere en primer lugar una alícuota de 3 µL de la suspensión comercial de HOOC-MBs a un tubo eppendorf lavando dos veces con 50 µL de la disolución reguladora MES a 25 ºC. Cada etapa de lavado consiste en resuspender las MBs en el regulador, agitando a 600 rpm durante 10 min hasta homogeneización, seguido de la separación magnética de las partículas durante 4 min y eliminación de la disolución. Después, se añaden 25 µL de polímero Mix&Go™ (etapa 1 Fig. 32) dejando incubar durante 60 min a 25 °C en agitación a 600 rpm. Seguidamente se aplican dos etapas de lavado con el regulador WBS para, a continuación, añadir 25 µL de una disolución de anti-TGF de 5 µg/mL preparada en regulador MES 25 mM de pH5.0 dejando incubar 60 min a 25 ºC con agitación a 600 rpm. Una vez transcurrido este periodo, los inmunoconjugados anti-TGF-MBs se lavan con 50 µL de regulador MES 25 mM de pH 5.0 y después con 50 µL de PBS 0.1 M de pH 8.0. A continuación se aplica una etapa de bloqueo añadiendo 50 µL de etanolamina 2 M preparada en disolución reguladora PBS 0.1M de pH 8.0 (etapa 2 Fig. 32) dejando incubar durante 60 min. El exceso de etanolamina se elimina lavando primero con 50 µL del mismo regulador y después con 50 µL del regulador WBS.

La conjugación del analito se realiza añadiendo 25 µL de disoluciones patrón de TGF-β1 o las muestras, incubando durante 60 min a 25 °C. Posteriormente se aplican dos etapas de lavado con 50 µL de regulador WBS para añadir después 25 µL de una disolución de Biotin-anti-TGF de 2 µg/mL conteniendo BSA al 1% (etapa 3 Fig. 32) y se deja incubar nuevamente a 25 ºC durante 60 min agitando a 600 rpm. Concluido este periodo de incubación, se aplican otras dos etapas de lavado con 50

µL de regulador WBS seguido de la adición de 25 µL de poli-HRP-Strept en dilución 1/500 e incubación durante 20 min. Finalmente, el conjugado resultante, poli-HRP-Strept-Biotin-anti-TGF-TGF-anti-TGF-MBs, se lava con 50 µL de regulador WBS y la determinación de TGF-β1 se realiza resuspendiendo el conjugado resultante en 45 µL de HQ 0.1 mM, que se depositan en la superficie del SPCE (etapa 4 Fig. 32). Como ya se comentó en el Apartado 4.4.1, el electrodo se mantiene en posición horizontal sobre el soporte magnético con su parte posterior en contacto con el imán. Una vez aplicado el potencial de detección de -200 mV vs Ag, se registra la corriente de fondo hasta que esta se estabiliza (unos 100 s, aproximadamente), y seguidamente se añaden 5 µL de una disolución de H_2O_2 50 mM. Se espera un tiempo de 200 s para que tenga lugar la reacción enzimática completa, y se procede a medir la corriente de reducción de la quinona formada al potencial aplicado.

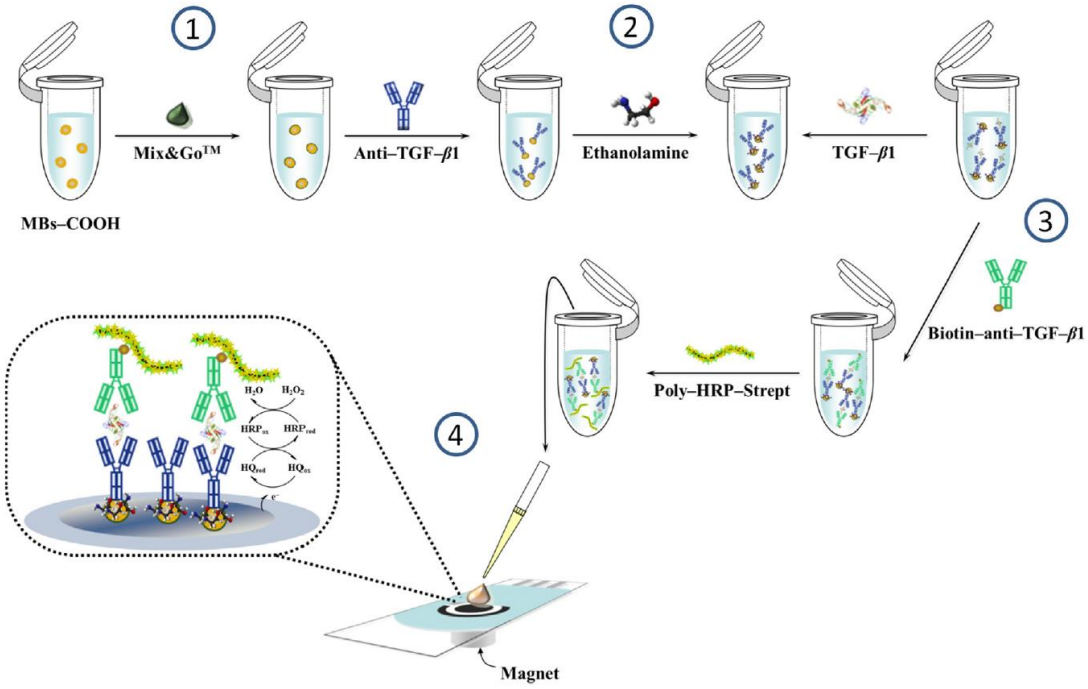

Figura 32.- *Esquema de preparación del magnetoinmunosensor para la determinación de TGF-β1.*

4.4.2.1. Aplicación a la determinación de TGF-β1 en orina

Las muestras de orina control se contaminan con TGF-β1 a los niveles de concentración deseados (Apartado 4.3.) y se diluyen en una proporción 1:3 con regulador fosfato 0.1 M de pH 7.2. La determinación de la citoquina se realiza por aplicación del procedimiento descrito en al Apartado 4.4.2., interpolando la respuesta amperométrica en el calibrado obtenido con patrones de TGF-β1.

4.4.3. INMUNOSENSOR PARA LA DETERMINACIÓN DE PYY

En la Figura 33 se ha representado el esquema seguido para la preparación de este inmunosensor. En primer lugar se prepara el óxido de grafeno reducido (rGO) a partir de 2 mL de una suspensión acuosa de GO de 1 mg/mL a la que se aplica agitación ultrasónica durante 120 min, centrifugando después 10 min a 10.000 g. Una vez descartado el precipitado, el líquido sobrenadante se trata con disolución de amoniaco al 25% hasta alcanzar un pH 9 -10. En este medio se lleva a cabo la reducción del GO mediante adición de ácido ascórbico sólido hasta una concentración final 2 mM. Después de un periodo de reacción de 15 min a 100 ºC, la suspensión de rGO resultante se almacena en la oscuridad a temperatura ambiente. Este producto se repone semanalmente, aunque se ha comprobado su estabilidad durante, al menos, dos semanas.

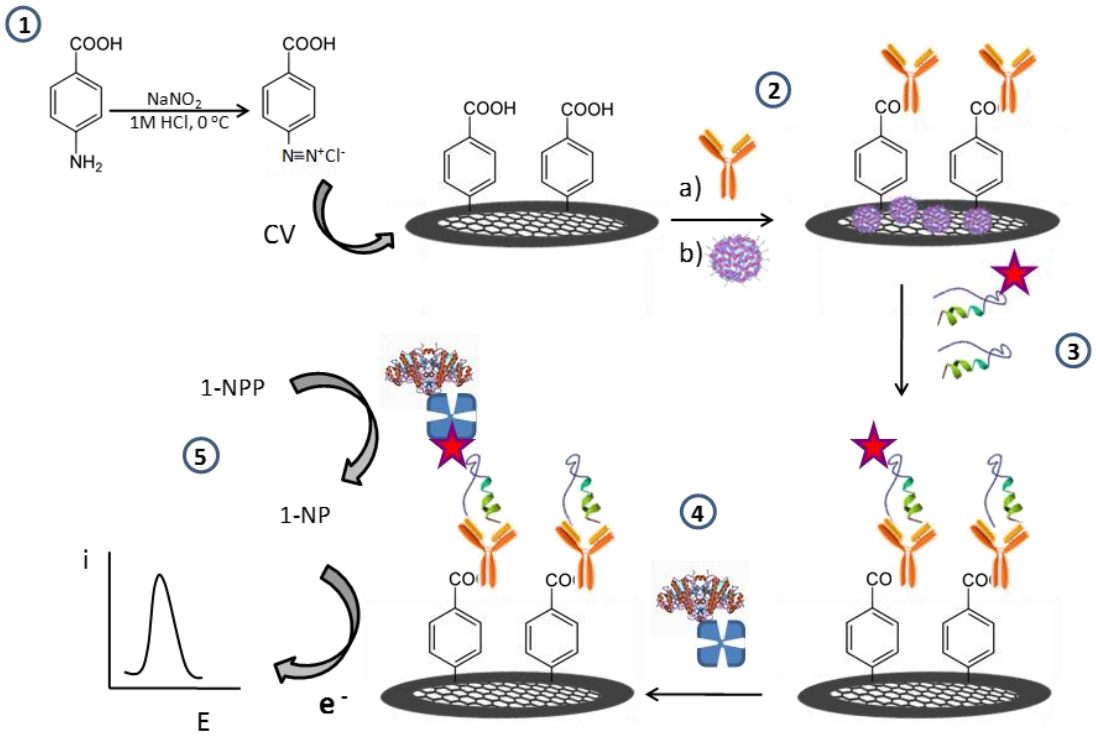

Figura 33.- *Esquema de preparación del inmunosensor para la determinación de PYY.*

Para la modificación de los electrodos (GCEs), primero se limpia la superficie activa mediante pulido con pasta de alúmnina de 0.3 µm durante 1 min, aplicando agitación ultrasónica 30 s en agua, y dejando secar al aire. Después se depositan 10 µL de la suspensión de rGO de 0.5 mg/mL en la superficie del electrodo, dejando secar a temperature ambiente. Aparte se procede a efectuar la reacción de diazotación del ácido *p*-ABA añadiendo gota a gota disolución acuosa de $NaNO_2$ 2 mM sobre la disolución del ácido de 10 mg/mL en medio HCl 1 M enfriada con hielo (la proporción es de 38 mL de $NaNO_2$ por cada 200 mL de *p*-ABA), y se agita durante 10 min para que tenga lugar la reacción (etapa 1 Fig. 33). A continuación, el electrodo rGO/GCE se sumerge en 450 µL de sal de diazonio y se aplican diez barridos cíclicos de potencial desde 0 a -1.0 V vs Ag/AgCl a una velocidad de barrido de potencial ν = 200 mV/s, con el fin de injertar el radical formado a la superficie de carbono.

Una vez preparado, el electrodo modificado resultante, HOOC-Phe-rGO/GCE se lava exhaustivamente con agua y etanol y se deja secar a temperatura ambiente. La activación de los grupos carboxilo se realiza añadiendo 10 µL de una disolución de EDC/NHSS 0.1 M en cada uno de ellos y dejando reaccionar durante 60 min en la oscuridad. Una vez enjuagado con agua y metanol, se deja secar nuevamente a temperatura ambiente y se añaden 10 µL de una disolución de anti-PYY de 20 µg/mL, dejando incubar durante 60 min a 37 ºC (etapa 2 Fig. 33). La etapa siguiente, de bloqueo, se realiza por adición de 20 µL de una disolución comercial de caseína al 0.2% y se incuba durante 60 min a 37 ºC.

A continuación, el ensayo competitivo se establece añadiendo 10 µL de una mezcla de PYY (o la muestra) y Biotin-PYY de 100 ng/mL sobre el bioelectrodo anti-PYY-Phe-rGO/GCE (etapa 3 Fig. 33) dejando incubar 30 min a 37 ºC. Después, se añaden 10 µL de una disolución de AP-Strept de 5 µg/mL (etapa 4 Fig. 33) y se incuba nuevamente durante 30 min a 37 ºC. Finalmente, el inmunosensor se sumerge en 450 µL de disolución reguladora Trizma 50 mM, junto a los electrodos de referencia y auxiliar y la determinación de PYY se realiza añadiendo 50 µL de disolución de 1-NPP 0.05 M que se mantiene en contacto durante 5 min para que tenga lugar la reacción enzimática. Transcurrido este tiempo, se registran los voltamperogramas en diferencial de impulsos en el intervalo de -0.15 a +0.70 V vs Ag/ AgCl a una velocidad de barrido de potencial ν = 20 mV/s, manteniendo ΔE = 50 mV (etapa 5 Fig. 33).

4.4.3.1. Aplicación a la determinación de PYY en suero

Las muestras de suero liofilizado se reconstituyen en 1 mL de regulador fosfato 0.1 M de pH 7.4 mezclando hasta disolución total, y a continuación se contamina con PYY a las concentraciones deseadas (Apartado 4.3). La determinación se realiza aplicando el procedimiento anterior por medida de las corrientes de pico en DPV e interpolación en el intervalo recto del calibrado obtenido con las disoluciones patrón de PYY.

4.4.4. INMUNOSENSOR PARA LA DETERMINACIÓN SIMULTÁNEA DE GHRL Y PYY

El procedimiento de preparación del inmunosensor se ha representado en la Figura 34. Primero se preparan el rGO y la sal de diazonio del *p*-ABA del modo descrito en el Apartado 4.4.3. con ligeros cambios. Brevemente, una alícuota de 2 mL de una suspensión acuosa de GO de 1 mg/mL se agita en el baño de ultrasonidos durante 120 min centrifugando a 10.000 g durante 10 min. Una vez decantado el líquido sobrenadante, el precipitado se trata con amoniaco al 25% hasta un pH 9-10. Seguidamente, la reducción de GO se lleva a cabo en presencia de ácido ascórbico 2 mM manteniendo una temperatura de 95 ºC durante 15 min. Finalmente, la suspensión de rGO se guarda en la oscuridad a temperatura ambiente.

Como en el apartado anterior, la sal de diazonio se prepara añadiendo gota a gota una disolución acuosa de $NaNO_2$ 2 mM a una disolución de *p*-ABA de 10 mg/mL preparada en HCl 1 M (etapa 1 Fig. 34) enfriando con hielo (38 mL $NaNO_2$ por cada 200 mL de *p*-ABA) y dejando reaccionar durante 10 min con agitación. Por separado, 3 µL de la suspensión de rGO se depositan sobre cada superficie activa del electrodo dual y se deja secar a temperatura ambiente. Después, el electrodo modificado se sumerge en la disolución de la sal de diazonio y se aplican diez ciclos de potencial sucesivos entre 0 y -1.0 V vs Ag a una velocidad de barrido de potencial, ν = 200 mV/s. Finalmente, el electrodo modificado se lava a fondo con agua (10 s) y metanol (10 s), y se deja secar a temperatura ambiente.

Para la preparación del inmunosensor dual, en primer lugar se activan los grupos carboxílicos de las superficies activas del electrodo (HOOC- Phe-rGO/SPCE1 y HOOC-Phe-rGO/SPCE2), añadiendo sobre cada una 3 µL de una mezcla EDC/NHSS 0.1 M de cada uno. Esta mezcla se deja reaccionar durante 60 min en la oscuridad. Después de enjuagar con agua y metanol, se deja secar y se procede a inmovilizar los anticuerpos específicos de captura, añadiendo 3 µL de una disolución de anti-GHRL

de 5 μg/mL y 3 μL de una disolución de anti-PYY de 5 μg/mL (etapa 2 Fig. 34), formándose los conjugados anti-GHRL-Phe-rGO/SPCE1 y anti-PYY-Phe-rGO/SPCE2, respectivamente, tras un periodo de incubación de 60 min a 37 ºC.

La etapa de bloqueo se realiza añadiendo 5 μL de una disolución comercial de caseína al 0.2% sobre cada superficie modificada, dejando incubar 60 min a 37 ºC. A continuación se establecen los esquemas de ensayo competitivo (etapa 3 Fig. 34) añadiendo 3 μL de una mezcla de GHRL (o la muestra) y Biotin-GHRL de 0.5 mg/mL, o bien 3 μL de una mezcla de PYY (o la muestra) y Biotin-PYY de 0.1 mg/mL, respectivamente, a los conjugados anti-GHRL-Phe-rGO/SPCE1 y anti-PYY-Phe-rGO/SPCE2, dejando incubar 30 min a 37 ºC. Seguidamente, 10 μL de una disolución de AP-Strept de 5 μg/mL se añaden sobre los conjugados resultantes de la etapa anterior, incubando de nuevo durante 30 min a 37 ºC. Finalmente (etapa 4 Fig. 34), 45 μL de una disolución 50 mM de regulador Trizma y 5 μL de 1-NPP 0.05 M se depositan sobre el electrodo dual y, tras un periodo de espera de 5 min para que la reacción enzimática tenga lugar, se registran los voltamperogramas en diferencial de impulsos en el intervalo de potencial de -0.15 a + 0.70 V vs Ag, a una velocidad de barrido de potencial ν = 20 mV/s, manteniendo ΔE = 50 mV (etapa 4 Fig. 34).

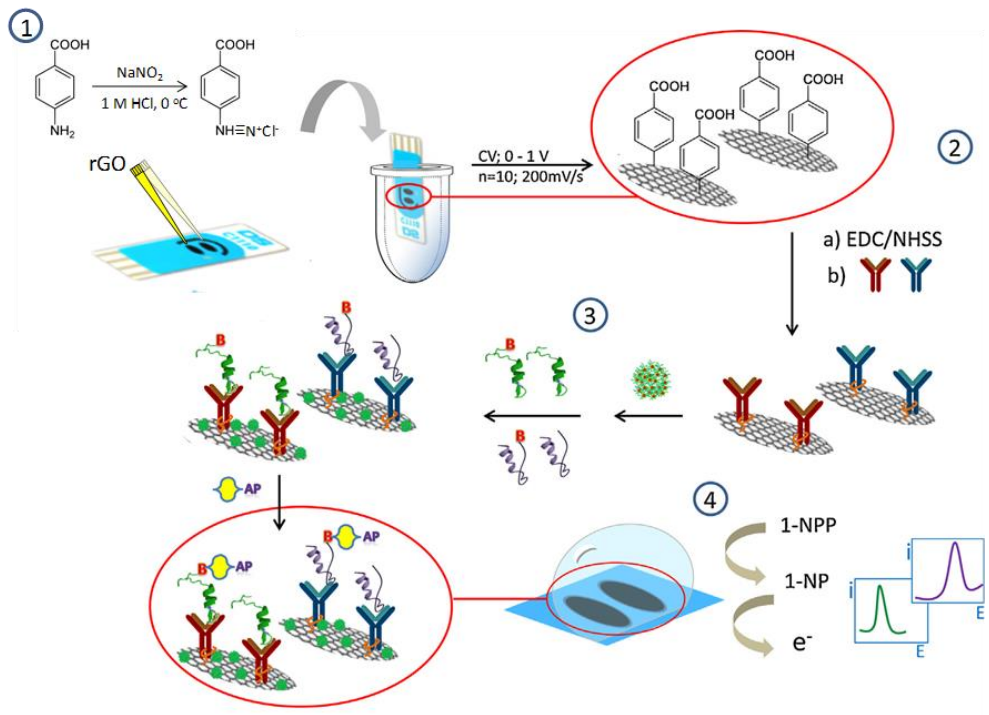

Figura 34.- *Esquema de preparación del inmunosensor dual para la determinación simultánea de GHRL y PYY.*

4.4.4.1. Aplicación a la determinación de GHRL y PYY en suero y en saliva

Para el análisis de las muestras de suero liofilizado, se procede primero a su reconstitución en 1 mL de regulador fosfato 0.1 M de pH 7.4, mezclando hasta total disolución, se alicuota y se congela a -40 ºC hasta su empleo. Una vez contaminado a las concentraciones deseadas (Apartado 4.3), se aplica al suero el procedimiento descrito en el Apartado 4.4.4. midiendo las corrientes de pico en DPV e interpolando en la porción lineal de cada calibrado obtenido con disoluciones patrón. Las muestras de saliva se recogen y contaminan con GHRL y PYY del modo descrito en el Apartado 4.4.3.1., y la determinación de ambas hormonas se realiza inmediatamente después de diluir 1 mL de saliva contaminada con 1 mL de regulador Tris 0.1 M de pH 7.2, aplicando el procedimiento descrito en el Apartado 4.4.4. usando alícuotas de 3-µL de saliva diluida.

4.4.5. INMUNOSENSOR PARA LA DETERMINACIÓN DE EE2

En primer lugar se prepara el material híbrido de óxido de grafeno, sílice y nanopartículas de plata (AgNPs/SiO_2/GO) empleando el método descrito por Cincotto et al. [Cincotto et al., 2014]. El óxido de grafeno se obtiene por el método de Hummers y Offeman [Hummers & Ofeman, 1958]. Brevemente, 10 g de grafito y 10 g de $NaNO_3$ se suspenden en 46 mL de ácido sulfúrico con agitación continua en un baño de hielo. Después, 6.0 g de $KMnO_4$ se añaden lentamente con agitación, y la mezcla de reacción se deja reposar en hielo durante 24 h. Una vez transcurrido este tiempo, se añaden 240 mL de agua y se calienta la suspensión hasta 98 ºC, agitando durante 1 h. Posteriormente, tras la adición de 85 mL de H_2O_2 al 30% (v/v), el producto resultante (GO) se filtra, se lava tres veces con HCl al 5% (v/v), y se seca a 50 ºC durante 48 h.

Para preparar el híbrido SiO_2/GO (ver etapa 1 Fig. 35), se dispersan 4.5 µmol de tetraetil ortosilicato (TEOS) en una mezcla etanol/agua 1/1 con agitación durante 10 min. A continuación se añaden 0.4 mL de agua y 90 mg de GO, se agita la suspensión durante 10 min, y se adicionan 30 mL de ácido fluorhídrico al 47%, agitando en baño de ultrasonidos hasta la formación de un gel. El producto obtenido se conserva a temperatura ambiente durante siete días, finalmente se pulveriza, se lava con etanol en un Soxhlet durante 2 h, y se calienta a 50 °C para evaporar el disolvente residual.

Una vez obtenido el material anterior, el híbrido. AgNPs/SiO_2/GO se prepara añadiendo 0.5 g del mismo a 15 mL de $AgNO_3$ 0.008 M en dimetilformamida (DMF) (etapa 2 Fig. 35). La mezcla se agita en baño de ultrasonidos durante 1 h a 25 °C en la oscuridad y el sólido se recupera por centrifugación, lavando con DMF y por último se mantiene durante 4 h en un hormo a 110 ºC.

Para la preparación del inmunosensor, primero se modifica el electrodo de carbono vitrificado con el material obtenido anteriormente (etapa 3 Fig. 35). Con este objetivo, el electrodo se pule con alúmina, se enjuaga con agua y se agita en ultrasonidos durante 5 min, secando posteriormente al aire. Se aplica a continuación un tratamiento de limpieza electroquímico mediante voltamperometría cíclica en H_2SO_4 0.1 M en el intervalo de potencial de 0 a 1 V vs Ag/AgCl. Después, el electrodo AgNPs/SiO_2/GO/GCE se prepara depositando sobre su superficie 10 µL de una suspensión obtenida por agitación ultrasónica de 0.5 mg de AgNPs/SiO_2/GO en 1mL de DMF, dejando secar toda la noche. La incorporación mediante *electrografting* de la sal de diazonio de *p*-ABA se realiza de forma análoga a la descrita en el Apartado 4.4.2.1. (etapa 4 Fig. 35). Brevemente, se disuelven 20 mg de *p*-ABA en 2 mL de HCl 1M enfriando en hielo. Después se añade gota a gota una disolución acuosa de $NaNO_2$ 2 mM (38 mL $NaNO_2$ por cada 200 mL de *p*-ABA) con agitación constante y se depositan 40 µL de la disolución resultante sobre el electrodo modificado, aplicando diez ciclos de potencial sucesivos en voltamperometría cíclica entre 0.0 y -1.0 V vs Ag/AgCl a ν = 200 mV/s. Finamente, el electrodo se enjuaga con agua.

El anticuerpo de captura se inmoviliza seguidamente (etapa 5 Fig. 35) previa activación de los grupos carboxilo por adición sobre la superficie del electrodo de 10 µL de una mezcla de EDC/NHSS, 0.1 M cada uno de ellos, preparada en medio regulador fosfato 0.1 M de pH 6.0, dejando reaccionar durante 1 h. Después de enjuagar con agua y metanol, 10 µL de una disolución de anti-EE2 de 20 µg/mL se depositan sobre el electrodo y se incuba a 37 ºC durante 45 min. El bloqueo para evitar adsorciones no específicas (etapa 6 Fig. 35) se realiza añadiendo 20 µL de caseína al 1% sobre el bioelectrodo anti-EE2-Phe-AgNPs/SiO_2/GO/GCE, dejando incubar 1h a 37 °C. Finalmente se establece el esquema de inmunoensayo competitivo añadiendo 10 µL de una mezcla de disolución patrón de EE2 o la muestra y HRP-EE2 en dilución 1/100, incubando 1h a 37 °C y enjuagando con regulador fosfato 0.1 M de pH 7.2. La determinación de EE2 se realiza en el mismo medio por amperometría aplicando un potencial de -0.20 V vs Ag/AgCl en presencia de 45 µL de HQ 1 mM tras la adición de 5 µL de H_2O_2 50 mM.

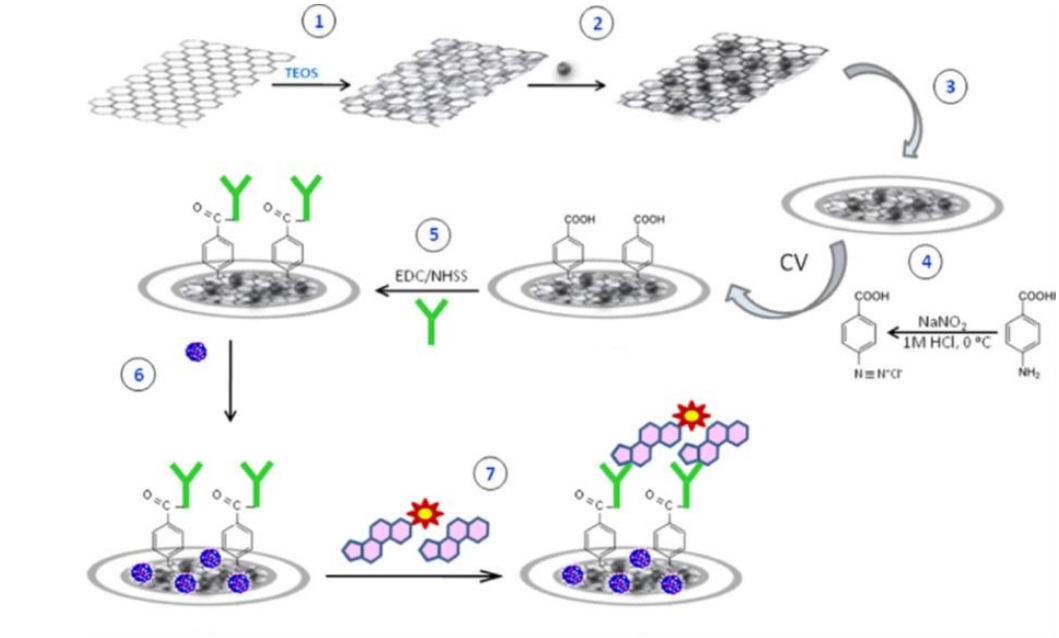

Figura 35.- *Esquema de preparación del inmunosensor para la determinación de EE2.*

4.4.5.1. Aplicación a la determinación de EE2 en orina

Se recogen las muestras de orina, procedentes de una mujer voluntaria sana, y se alicuotan conservándolas a -20 ºC. Seguidamente, las muestras contaminadas a las concentraciones deseadas (Apartado 4.3.) se analizan directamente, sin diluir, aplicando el procedimiento descrito en el Apartado 4.4.5., y la corriente amperométrica se interpola en el calibrado de disoluciones patrón de EE2.

4.4.6. BIOSENSOR ENZIMÁTICO PARA LA DETERMINACIÓN DE β-HB

El esquema de la preparación de este biosensor se ha representado en la Figura 36. Primero se prepara una suspensión de rGO aplicando un procedimiento equivalente al descrito en el Apartado 4.4.3. Brevemente, 2 mL de una suspensión acuosa de GO de 1 mg/mL preparada por agitación ultrasónica durante 4 h, se centrifuga 10 min a 10.000 g y, una vez descartado el precipitado, el líquido sobrenadante se trata con disolución de amoniaco al 25% hasta alcanzar un pH 9 -10. En este medio se lleva a cabo la reducción del GO mediante adición de ácido ascórbico sólido hasta una concentración final 2 mM, manteniendo una temperatura de 100 ºC durante 15 min. Después, la suspensión de rGO resultante se guarda en la oscuridad a temperatura ambiente. Este producto se repone semanalmente, aunque se ha comprobado su estabilidad durante, al menos, dos semanas.

Para la modificación del electrodo serigrafiado, una alícuota de 10 µL de rGO se deposita en el electrodo (etapa 1 Fig. 36) y se deja secar a temperatura ambiente.

Seguidamente se añade el mediador redox, tionina, añadiendo 15 µL de una disolución de THI 1 mM (etapa 2 Fig. 36) que se deja incubar 30 min a temperatura ambiente en humedad. El electrodo modificado THI/rGO/SPCE se lava con agua desionizada y se seca en corriente de nitrógeno. A continuación se prepara en biosensor enzimático depositando 2 µL de una disolución de la enzima β-HBDH de 100 U/mL sobre el electrodo modificado THI/rGO/SPCEs (etapa 3 Fig. 36), dejando secar a 4 ºC.

La determinación de β-HB se realiza depositando 50 µL de una disolución 0.1 mM de NAD^+ en regulador fosfato 0.1 M de pH 7.0 sobre el biosensor, aplicando un potencial de detección de 0.0 V vs Ag (etapa 4 Fig. 36). Una vez que se alcanza una corriente de fondo constante, se añaden 2 µL de disolución patrón de β-HB o la muestra, y se registra la variación de la corriente en estado estacionario.

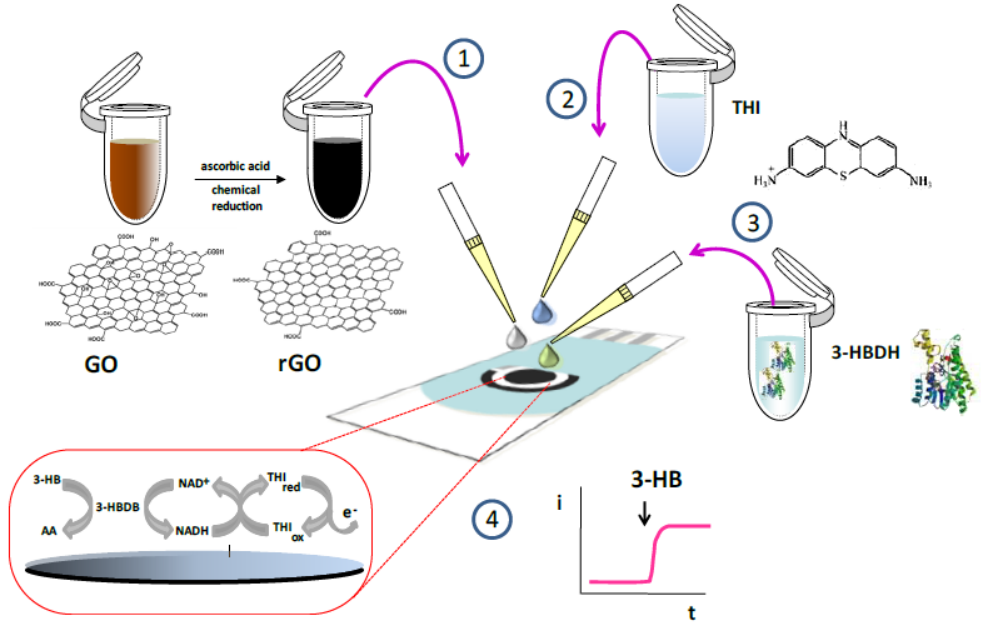

Figura 36.- *Esquema de preparación del biosensor enzimático para la determinación de β-HB.*

4.4.6.1. Aplicación a la determinación de β-HB en suero

El suero liofilizado se reconstituye disolviendo 37 mg del sólido en 500 µL de agua desionizada. A continuación se contamina al nivel requerido (Apartado 4.3.) y se aplica en procedimiento descrito en el Apartado 4.4.6., depositando 25 µL de una disolución 0.2 mM NAD^+ en regulador fosfato 0.1 M de pH 7.0 sobre el electrodo modificado. Una vez estabilizada la corriente de fondo a 0.0 V, se añaden 25 µL de suero contaminado, y se mide la respuesta de oxidación

4.4.7. INMUNOSENSOR PARA LA DETERMINACIÓN DE AMY

En la Figura 37 se ha representado esquemáticamente el procedimiento de preparación de este inmunosensor. En primer lugar se electropolimeriza el monómero sobre la superficie del SPCE (etapa 1 Fig. 37) sumergiendo el electrodo en una disolución de PPA 100 mM conteniendo KCl 0.5 M, por aplicación de 20 ciclos de potencial en voltamperometría cíclica en el intervalo de 0.0 a +0.85 V vs Ag a 100 mV/s. El electrodo modificado resultante, pPPA/SPCEs, se sumerge a continuación en una disolución de HQ 1 mM preparada en regulador fosfato 0.1 M de pH 7.4, y se registra un voltamperograma cíclico control entre −0.2 y +1.0 V vs Ag, a 50 mV/s. A continuación, los grupos carboxilo se activan añadiendo 10 µL de polímero Mix&Go™ sobre el electrodo (etapa 2 Fig. 37) dejando incubar durante 60 min a 25 °C. Finalmente se lava con disolución reguladora MES 25 mM de pH 5.0.

La inmovilización covalente del anticuerpo de captura se realiza depositando 5 µL de una disolución de anti-AMY en dilución 1/100 preparada en regulador MES 25 mM de pH 5.0, incubando durante 60 min a 25°C en ambiente húmedo (etapa 3 Fig 37). Después de una segunda etapa de lavado con el mismo regulador, los grupos activados del bioelectrodo anti-AMY-*p*PPA/SPCEs que no han reaccionado se bloquean por adición de 7.5 µL de BSA al 2% en regulador fosfato 0.1 M de pH 7.4, incubando durante 30 min y lavando nuevamente con la disolución reguladora MES (etapa 4 Fig. 37). Seguidamente, se establece un esquema de inmunoensayo competitivo añadiendo 5 µL de una mezcla de Biotin-AMY de 2.5 ng/mL y el antígeno, AMY, incubando durante 45 min (etapa 5 Fig. 37). Después se añaden 5 µL de una disolución de HRP-Strept en dilución 1/500 (etapa 6 Fig. 37) y, tras 20 min de incubación, el inmunosensor resultante, HRP-Strept-Biotin-AMY-AMY-anti-AMY- pPPA /SPCE se lava con disolución reguladora fosfato 0.1 M de pH 7.4, conservándolo en ambiente húmedo hasta su empleo.

La determinación de AMY se realiza depositando 45 µL de HQ 1.0 mM en regulador fosfato 0.05 M de pH 6.0 sobre el electrodo, midiendo a continuación la respuesta amperométrica a un potencial de -200 mV vs Ag hasta estabilización de la corriente de fondo (unos 100 s). Después se añade una alícuota de 5 µL de H_2O_2 50 mM en regulador fosfato 0.05 M de pH 6.0 y se mide la respuesta electroquímica una vez transcurridos 200 s para que se produzca la reacción enzimática.

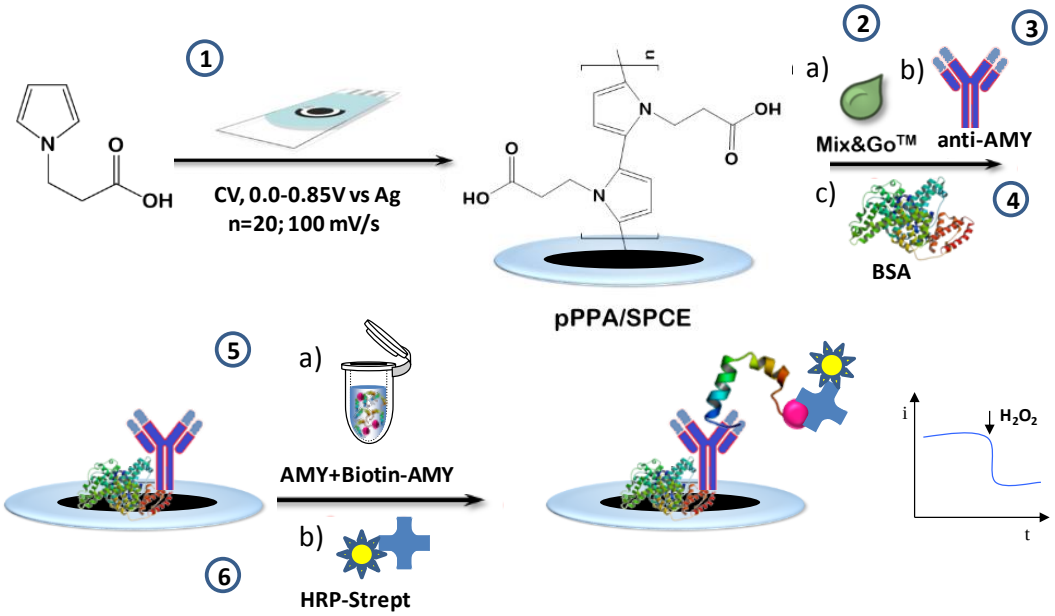

Figura 37.- *Esquema de preparación del inmunosensor para la determinación de AMY.*

4.4.7.1. Aplicación a la determinación de AMY en suero y en orina

El suero liofilizado se reconstituye en agua desionizada, se contamina con AMY a los niveles requeridos (Apartado 4.3.) y se diluye en una proporción 1/10 con el disolvente "Assay Diluent B" de RayBio®. A continuación se aplica el procedimiento descrito en el Apartado 4.4.7. y la respuesta electroquímica se interpola en el calibrado obtenido con disoluciones patrón de AMY.

La muestra de orina control se contamina igualmente a los niveles deseados (Apartado 4.3.) y se diluye en proporción 1/20 con el mismo disolvente, interpolando a continuación la respuesta electroquímica en el calibrado obtenido con disoluciones patrón de AMY.

MAGNETOINMUNOSENSORES

BIOSENSORES BASADOS EN ELECTRODOS MODIFICADOS CON GRAFENO E HÍBRIDOS DE GRAFENO

5.RESULTADOS Y DISCUSIÓN

INMUNOSENSOR ELECTROQUÍMICO BASADO EN UN POLÍMERO CONDUCTOR

Con el fin de alcanzar los objetivos definidos anteriormente, en esta Tesis Doctoral se han preparado varios biosensores electroquímicos para la determinación de reguladores del apetito y biomarcadores de obesidad. Para ello, como se ha señalado, se han utilizado micropartículas magnéticas funcionalizadas y se han construido plataformas biosensoras originales modificadas con grafeno e híbridos de grafeno, así como con un polímero conductor. En la Figura 38 se ha representado un esquema muy simplificado de los diseños desarrollados en este trabajo. Además, se han utilizado métodos originales de inmovilización de biomoléculas sobre la superficie electródica, y se han elegido analitos de interés en el área, para los que no se habían descrito biosensores o, en caso de existir, eran muy escasos o se basaban en otros tipos de transducción. Como se verá, los resultados obtenidos son los primeros descritos en la bibliografía o mejoran, en su caso, los ya publicados. Por otra parte, todos los biosensores desarrollados se han aplicado al análisis de muestras de fluidos biológicos que contenían los analitos a determinar, a los niveles esperables.

En esta parte de Resultados y Discusión, se ha seguido el orden de exposición por tipo de materiales iniciado en la Parte Experimental. De este modo, la información aportada se distribuye, en lo posible, de un modo claro y sistemático.

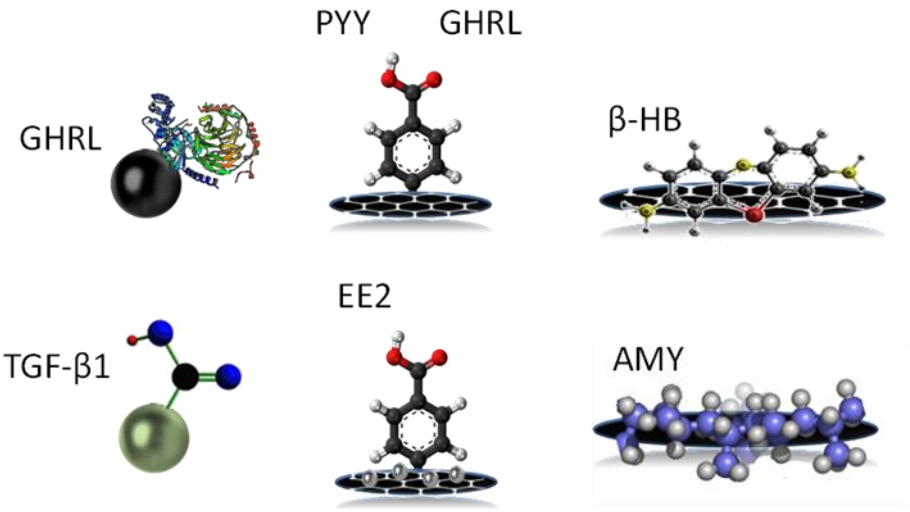

Figura 38.- *Esquema de las partículas magnéticas funcionalizadas y de las plataformas electródicas desarrolladas en este trabajo.*

5.1. MAGNETOINMUNOSENSORES

5.1.1. MAGNETOINMUNOSENSOR PARA LA DETERMINACIÓN DE GHRL

Según se ha descrito en los Apartados anteriores, la grelina (GHRL) es una hormona peptídica descubierta en 1999, producida en el estómago, y que posee propiedades orexígenas. La determinación de los niveles de esta hormona en el organismo tiene un gran interés para el control de la obesidad y enfermedades relacionadas, así como para el seguimiento de los trastornos del apetito y la anorexia. Como se ha visto, la concentración de GHRL circulante varía a lo largo del día, apareciendo picos de máximo coincidentes con las principales ingestas. Los niveles que cabe esperar oscilan entre decenas y centenas de pg/mL en suero humano.

A pesar de su importancia, el número de métodos para la determinación de GHRL es muy escaso. Anteriormente (Apartado 3.7.1.) se han comentado las características de los kits ELISA comerciales basados en ensayos competitivos o de tipo sandwich con diferentes inmunorreactivos, que muestran intervalos dinámicos entre 0.01 ó 0.1 y 100 ó 1000 ng/mL de hormona, con concentraciones mínimas detectables de 0.05 ó 1 ng/mL. Una característica de estos ensayos es el largo tiempo de análisis, que varía entre 1h 30 min y 4 h. En relación a los biosensores, únicamente se ha descrito un aptasensor electroquímico [Mascini et al., 2007a] cuyas características aparecen resumidas en la Tabla 5.

Todo lo dicho justifica la necesidad de desarrollar un inmunosensor sensible, selectivo y fiable para la determinación de GHRL en muestras clínicas, siendo el magnetoinmunosensor electroquímico que se presenta en esta Tesis Doctoral el primero descrito en la bibliografía.

El diseño propuesto combina las ventajas de las micropartículas magnéticas funcionalizadas con proteína G (Protein G-MBs) para la inmovilización específica del anticuerpo, con la realización de un inmunoensayo competitivo seguido de la detección mediante voltamperometría diferencial de impulsos (DPV) de un producto electroactivo. Esta combinación hace que el inmunosensor electroquímico mejore la sensibilidad de los métodos ELISA disponibles y la de otras configuraciones, presentando además una excelente selectividad frente a otras hormonas. Finalmente, como se verá a continuación, el inmunosensor resultó adecuado para la determinación de GHRL en saliva.

5.1.1.1. Configuración del inmunosensor

Las etapas de preparación del inmunosensor electroquímico para la determinación de GHRL aparecen representadas en la Figura 31 de la Parte Experimental. Como puede apreciarse en el esquema (Figura 39), el anticuerpo anti-GHRL se inmoviliza sobre Protein G-MBs y el conjugado anti-GHRL-Protein-G-MBs se captura sobre la superficie de un electrodo serigrafiado de carbono. Una vez que se establece un esquema de inmunoensayo competitivo empleando Biotin-GHRL y AP-Strept, la determinación de la hormona se realiza mediante oxidación en voltamperometría diferencial de impulsos del 1-naftol formado en la reacción enzimática del 1-naftilfosfato empleado como sustrato de la fosfatasa alcalina.

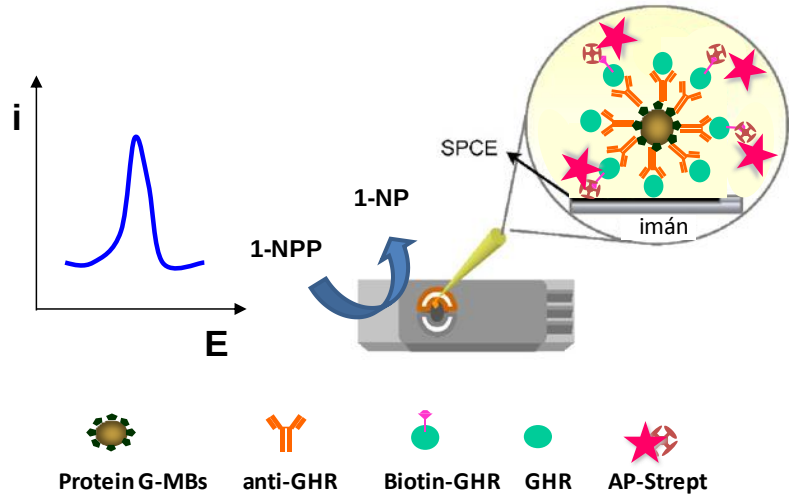

Figura 39.- Esquema y modo de detección del magnetoinmunosensor de GHRL.

5.1.1.2. Optimización de las variables experimentales

Con el criterio de alcanzar la máxima sensibilidad y un amplio intervalo lineal en el calibrado para la determinación de GHRL, se optimizaron las variables implicadas en la preparación y el comportamiento electroquímico del magnetoinmunosensor. Las variables investigadas, los intervalos estudiados y los valores elegidos se resumen en la Tabla 11. A continuación se describen los resultados obtenidos.

- ***Selección del sustrato enzimático***

El desarrollo de inmunosensores electroquímicos con marcador enzimático requiere una adecuada elección del sustrato de la enzima, ya que el producto de la reacción catalizada por la misma será el que genere la respuesta analítica. De este modo, la sensibilidad y selectividad del método dependen en gran medida de esta eleción.

En este caso, la enzima utilizada es la fosfatasa alcalina (AP), que cataliza la reacción de desfosforilación hidrolítica de los arilfosfatos en medio básico, originando fenoles, siendo entonces la oxidación electroquímica de estos productos la que proporciona la señal de corriente. Con el fin de seleccionar el sustrato más apropiado, se investigó la respuesta en voltamperometría cíclica de tres derivados fenólicos que constituyen productos comunes de esta reacción enzimática. Las especies elegidas fueron: fenol, 1-naftol y *p*-aminofenol.

En la Figura 40, los voltamperogramas cíclicos obtenidos sobre el electrodo serigrafiado de carbono en las condiciones indicadas, se comparan con el correspondiente a la disolución de electrólito fondo. Puede observarse cómo las curvas obtenidas presentan características bien diferenciadas.

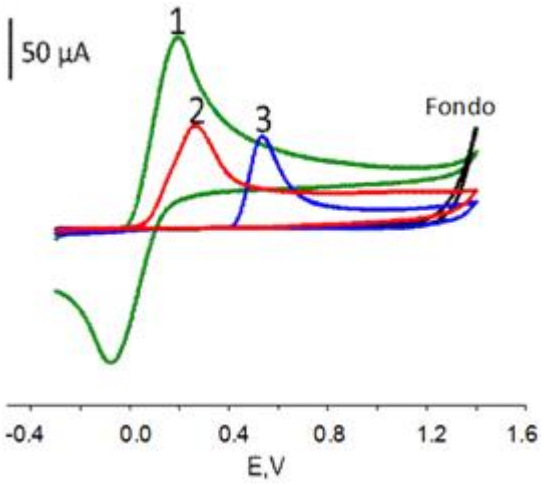

Figura 40.- *Voltamperogramas cíclicos de disoluciones 5 mM de p-aminofenol (verde), 1-naftol (rojo) y fenol (azul). Electrólito fondo (negro)Trizma, pH 9.6*

El pico de oxidación del *p*-aminofenol aparece a un potencial menos positivo que los otros dos compuestos, y presenta la mayor intensidad. Estas características hacen que este derivado fenólico sea, en principio, el más adecuado para los objetivos de elevada selectividad y sensibilidad que se persiguen. Sin embargo, el sustrato correspondiente, *p*-aminofenilfosfato es inestable en disolución alcalina y requiere un tiempo de hidrólisis relativamente elevado (10-12 min). Por tanto, este sustrato no es adecuado, dado que la actividad óptima de la fosfatasa alcalina se alcanza a valores de pH comprendidos entre 9 y 9.6 [Ito et al., 2000] y que se busca una respuesta lo más rápida posible. En relación a las respuestas del 1-naftol y del fenol, ambas poseen valores similares de la intensidad del pico de oxidación, pero el primero aparece a potenciales menos positivos, por lo que se eligió para estudios posteriores. En la Figura 41 se han representado las reacciones enzimática y electroquímica, respectivamente, del sustrato y el producto de hidrólisis.

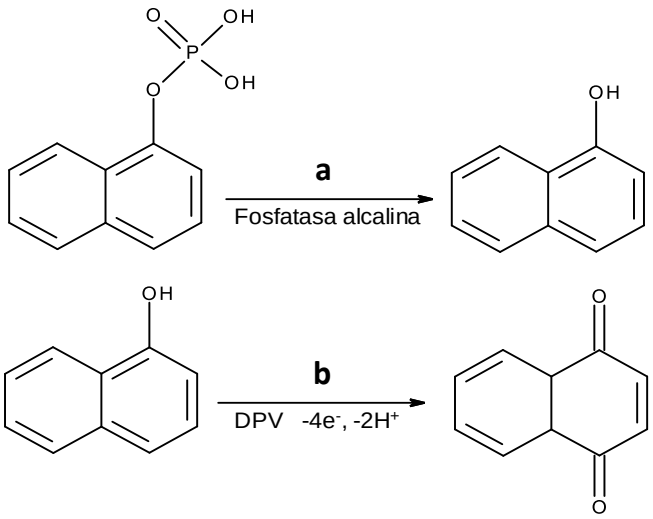

Figura 41.- *Reacción del 1-NPP catalizada por el enzima AP (a) y oxidación electroquímica del 1-NP a 1,4 naftoquinona*

La concentración óptima de 1-NPP para llevar a cabo la detección electroquímica se eligió teniendo en cuenta los resultados de trabajos anteriores [Moreno-Guzmán et al., 2010], seleccionándose el valor 0.05 M, que supone un exceso suficiente como para asegurar que la reacción enzimática depende exclusivamente de la concentración de la enzima. De la misma forma se eligió el tiempo de espera para que transcurra la reacción enzimática, 5 min. Finalmente, el pH de la reacción, 9.6, regulado con Trizma está, como se ha dicho, en el intervalo de actividad óptima de la fosfatasa alcalina [Ito et al., 2000].

- ***Influencia de la cantidad de micropartículas magnéticas***

La cantidad de Protein G-MBs influye notablemente en el funcionamiento del immunosensor ya que de ella depende la carga del anticuerpo de captura inmovilizado. En este estudio se compararon las respuestas voltamperométricas obtenidas con configuraciones preparadas empleando diferentes cantidades de micropartículas funcionalizadas, en ausencia de GHRL, con los resultados que se muestran en la Figura 42.

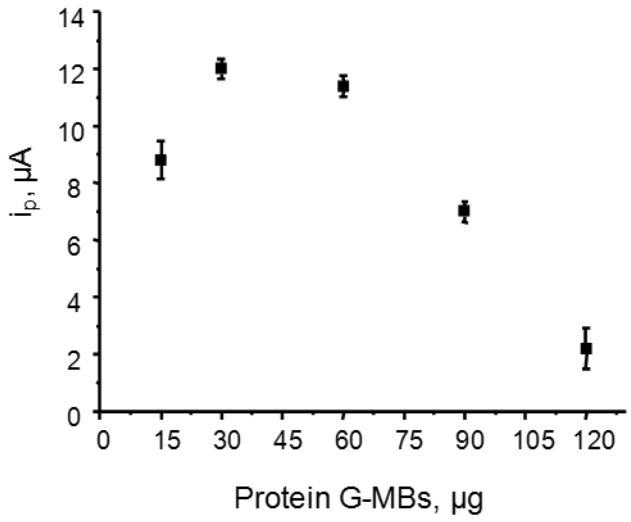

Figura 42.- *Efecto de la cantidad de Protein G-MBs sobre la respuesta del magneto-inmunosensor AP-Strept-Biotin-GHRL(GHRL)-anti-GHRL-Protein-G-MBs/SPCE. Las barras de error corresponden a la desviación estándar (n=3)de las medidas; 10 µg/mL anti-GHRL; 0.01 µg/mL Biotin-GHRL; 1 µg/mL AP-Strept*

Como puede observarse, la mayor corriente de pico se obtiene para 30 µg de Protein G-MBs y disminuye rápidamente para cantidades superiores. Aunque en principio una mayor cantidad de partículas funcionalizadas posibilita la mayor carga de anticuerpo inmovilizado y, por tanto, hace presumible obtener una mayor sensibilidad, sin embargo, una cantidad excesiva de este material da lugar a una disminución de la corriente, debido posiblemente a un impedimento a la transferencia de carga al quedar el electrodo recubierto de una capa aislante [Moreno-Guzmán et al., 2010]. Por ello, la cantidad seleccionada fue de 30 µg. Es importante destacar que, en estas condiciones, la respuesta del inmunosensor en ausencia de anti-GHRL, es decir, la señal inespecífica, es prácticamente nula.

- ***Influencia de la concentración del anticuerpo de captura.***

Se optimizó la cantidad de anticuerpo inmovilizado sobre las partículas magnéticas investigando la respuesta del inmunosensor preparado con 30 µg de Protein G-MBs con los resultados que se muestran en la Figura 43. En todos los casos, la preparación del conjugado anti-GHRL-Protein G-MBs se realizó mediante incubación a una temperatura de 37 ºC durante 1h. Estas condiciones fueron previamente optimizadas estudiando temperaturas entre 10 y 37 ºC, y tiempos de incubación comprendidos entre 10 y 90 min, resultando las elegidas las más adecuadas para la preparación del inmunosensor en el menor tiempo posible.

Como puede verse en la Figura 43a, la corriente de pico aumenta con la concentración de anti-GHRL en todo el intervalo estudiado, aunque la respuesta tiende a estabilizarse a las concentraciones más altas, como corresponde a la saturación de las regiones de unión de las micropartículas funcionalizadas. Como es sabido, en las configuraciones de tipo competitivo, concentraciones menores de anticuerpo proporcionan teóricamente una mayor sensibilidad debido a que se necesita una menor concentración de antígeno/analito para alcanzar la máxima respuesta [Ruth, 2001] [Eguílaz et al., 2010]. Por ello, con el fin de elegir la mejor concentración de anticuerpo de captura, se midió la corriente de pico del magnetoinmunosensor preparado con 2 ó 5 µg/mL de anti-GHRL y diferentes concentraciones de GHRL.

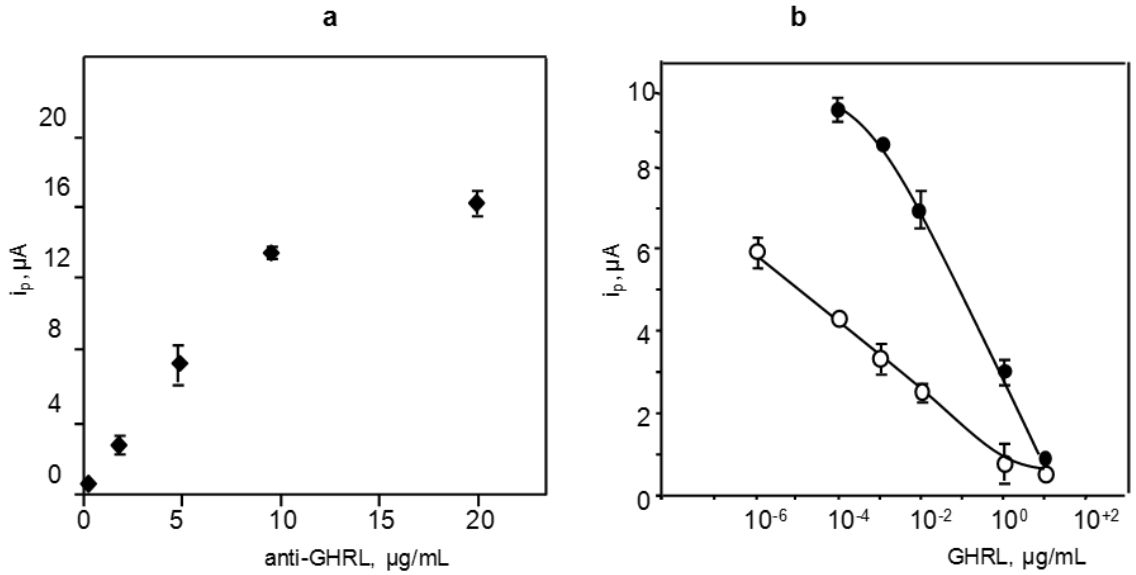

Figura 43.- *Efecto de la concentración de anti-GHRL sobre la respuesta del magneto-inmunosensor AP-Strept-Biotin-GHRL(GHRL)-anti-GHRL-Protein-G-MBs/SPCE: 30 µg Protein G-MBs; 0.01 µg/mL Biotin-GHRL; 1 µg/mL AP-Strept; 0.01 µg/mL GHRL (a); 2 (○) ó 5 (●) µg/mL anti-GHRL (b)*

Los resultados representados en la Figura 43b permiten observar la aparición de respuestas de corriente de mayor magnitud cuando se utiliza el inmunosensor preparado con 5 µg/mL de anticuerpo de captura, obteniéndose una mayor pendiente del tramo recto para concentraciones de GHRL entre 10^{-3} y 10 µg/mL. Sin embargo, cuando se utiliza la concentración menor de anti.GHRL, 2 µg/mL, el intervalo lineal comienza a concentraciones de grelina mucho más bajas, 10^{-6} µg/mL, lo que hace que estas condiciones sean más adecuadas para la determinación de GHRL a los niveles que cabe esperar en muestras clínicas [Casanueva & Diéguez, 2002] [Vörös et al., 2012].

- ***Influencia de la concentración de Biotin-GHRL***

La concentración de antígeno biotinilado, utilizado para establecer el esquema competitivo con la grelina por los sitios de unión del anticuerpo, se optimizó estudiando las repuestas de varios immunosensores preparados con concentraciones de Biotin-GHRL en el intervalo de 0.01 a 0.15 µg/mL con los resultados que se muestran en la Figura 44.

En la Figura 44a se aprecia un aumento de la corriente de pico del inmunosensor al aumentar la concentración de Biotin-GHRL, si bien la variación es mucho más rápida para las concentraciones menores del conjugado y tiende a alcanzar un nivel constante, que probablemente coincide con la saturación de los lugares de unión del anticuerpo de captura.

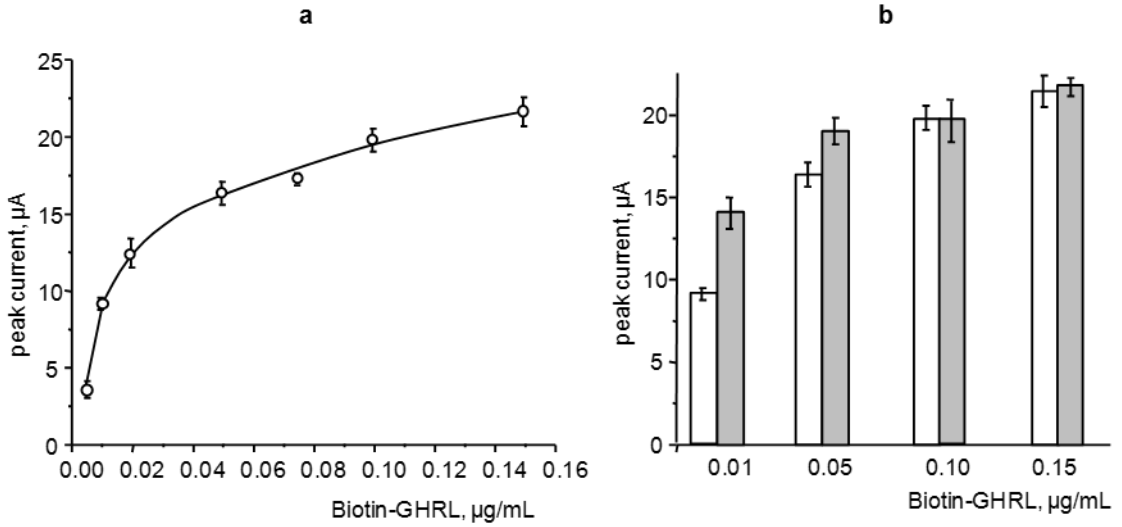

Figura 44.- *Efecto de la concentración de Biotin-GHRL sobre la respuesta del magnetoinmunosensor AP-Strept-Biotin-GHRL(GHRL)-anti-GHRL-Protein-G-MBs/ SPCE: 30 µg Protein G-MBs; 5 µg/mL anti-GHRL; 0.01 µg/mL Biotin-GHRL; 1 µg/mL AP-Strept; 0.01 µg/mL GHRL (a); 0 µg/mL (gris) ó 0.01 µg/mL(blanco) GHRL (b)*

Por otro lado, con el fin de obtener la mayor sensibilidad en el proceso de competición, se evaluó la variación de la respuesta de corriente empleando inmunosensores preparados en ausencia y en presencia de 0.01 µg/mL de GHRL con los resultados representados en la Figura 44b. Como puede verse, a medida que aumenta la concentración de Biotin-GHRL, se reduce la magnitud de los cambios de señal en ausencia y presencia de analito. Esto significa que en las condiciones experimentales utilizadas, la competición más favorable ocurre a bajas concentraciones del conjugado biotinilado, produciéndose ésta aparentemente en un

alto porcentaje. Sin embargo, a concentraciones elevadas de Biotin-GHRL no existen diferencias apreciables entre ambas señales, lo que indica que en esas condiciones no es posible la competición. Estos resultados están de acuerdo con lo esperado, teniendo en cuenta que una elevada concentración de conjugado requiere una alta concentración de antígeno para que se produzca un desplazamiento eficaz en el ensayo competitivo [Eguílaz et al., 2010]. Por tanto, teniendo en cuenta estas observaciones, se eligió una concentración de 0.01 µg/mL de Biotin-GHRL para preparar el inmunosensor. Señalar, además, que la temperatura de incubación para la preparación del inmunosensor fue la misma elegida anteriormente, 37 ºC, habiéndose optimizado el tiempo de incubación en 45 min. Este tiempo permite una buena competición entre GHRL y Biotin-GHRL por las posiciones enlazantes del anticuerpo.

- ***Influencia de concentración y el tiempo de incubación de AP-Strept***

La configuración del magnetoinmunosensor competitivo se completa con el conjugado enzimático AP-Strept responsable de convertir el sustrato en un producto electroactivo. Para optimizar esta variable, se estudió la respuesta del immunosensor preparado con diferentes concentraciones de AP-Strept en el intervalo de 0.5 a 5.0 µg/mL, representándose los resultados obtenidos en la Figura 45a.

Puede verse cómo la respuesta electroquímica aumenta inicialmente hasta una concentración de AP-Strept de 1.0 µg/mL, disminuyendo ligeramente a partir de dicho valor. Por ello, esta fue la concentración elegida como óptima para obtener la mayor sensibilidad en la detección. Por otro lado, como ejemplo de la optimización del tiempo de incubación, en la Figura 45b se han representado las corrientes de pico del registradas mediante DPV para el magnetoinmunosensor preparado en ausencia de GHRL y en presencia de 0.01 µg/mL de hormona, empleando diferentes periodos de incubación de AP-Strept a 37 ºC.

A la vista de los resultados obtenidos se eligió un tiempo de incubación de 30 minutos por corresponder a la mayor diferencia de corrientes de pico en ausencia y presencia de analito.

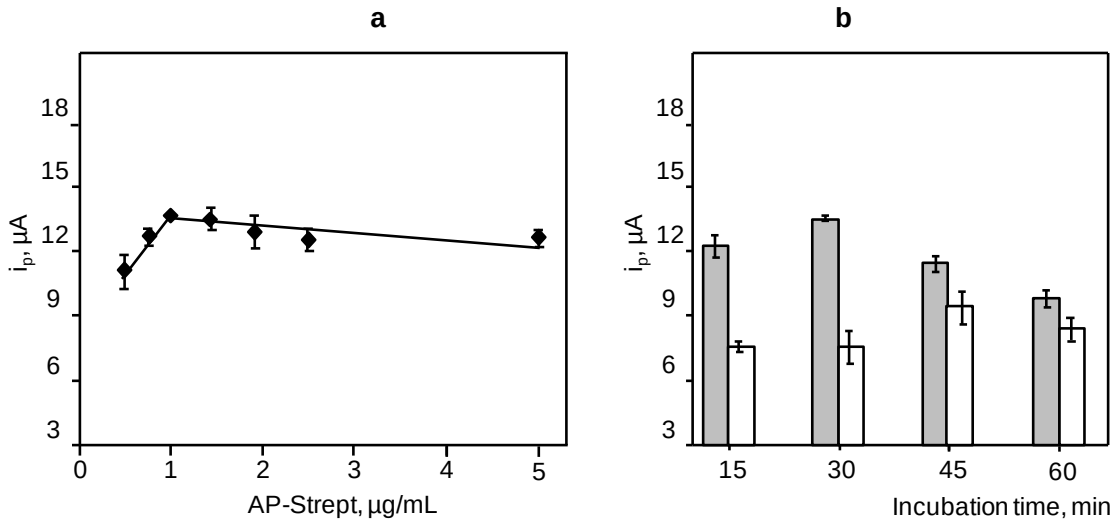

Figura 45.- *Efecto de la concentración de AP-GHRL sobre la respuesta del magneto-inmunosensor AP-Strept-Biotin-GHRL(GHRL)-anti-GHRL-Protein-G-MBs/SPCE:-30 µg Protein G-MBs; 5 µg/mL anti-GHRL; 0.01 µg/mL Biotin-GHRL; 0 µg/mL GHRL (a, b gris) ó 0.01 µg/mLGHRL (b blanco).*

Una vez optimizadas las variables experimentales implicadas en el funcionamiento del magnetoinmunosensor, como resumen, en la Tabla 11 se recogen dichas variables, los intervalos estudiados y los valores óptimos elegidos en cada caso.

Tabla 11.- *Optimización de las variables implicadas en el funcionamiento del immunosensor AP-Strept-Biotin-GHRL-anti-GHRL-Protein G-MBs/SPCE*

Variable	Intervalo estudiado	Valor seleccionado
Protein G-MBs, µg	15 - 120	30
anti GHRL, µg/mL	1 – 20	2
tiempo incubación anti-GHRL, min	15 – 90	60
Biotin-GHRL, µg/mL	0.001 - 0.015	0.01
tiempo incubación Biotin-GHRL, min	15 – 90	45
AP-Strept, µg/mL	0.5 – 1.5	1.0
tiempo incubación AP-Strept, min	15 – 60	30

5.1.1.3. Calibrado y características analíticas

En la Figura 46 se ha representado el calibrado para la determinación de GHRL obtenido en las condiciones experimentales optimizadas anteriormente. Como puede observarse, la forma del mismo es la de una curva sigmoidal decreciente, de acuerdo al tipo de inmunoensayo competitivo de la configuración desarrollada [Tijssen, 1985]. Como puede apreciarse, la concentración de GHRL en dicho calibrado se extiende en un amplio intervalo que abarca desde 10^{-5} hasta 10^{4} ng/mL, habiéndose ajustado la curva mediante regresión no lineal a la ecuación (r = 0.990):

$$i_p = i_{\min} + \frac{i_{max} - i_{min}}{1 + \left(\frac{x}{EC_{50}}\right)^{-h}}$$

donde i_{max} e i_{min} son las corrientes de pico máxima y mínima del calibrado: 5.4 ± 0.3 µA y 0.2 ± 0.4 µA, respectivamente. El valor de EC_{50}, que es la concentración de GHRL correspondiente al 50% de competición, es 2.4 ± 1.5 ng/mL, y la pendiente de Hill, h, en el punto de inflexión de la curva sigmoidal es -0.36 ± 0.08.

Como puede apreciarse, en la porción central de dicha curva existe un intervalo de linealidad $i_p \propto \log$ [GHRL] (r = 0.994) entre 10^{-3} y 10^{3} ng/mL. La pendiente de este tramo lineal es m = -0.95 ± 0.04 µA por década de concentración. Este intervalo es adecuado para la aplicación del inmunosensor a la determinación de GHRL [Casanueva & Diéguez, 2002] [Vörös et al., 2012].

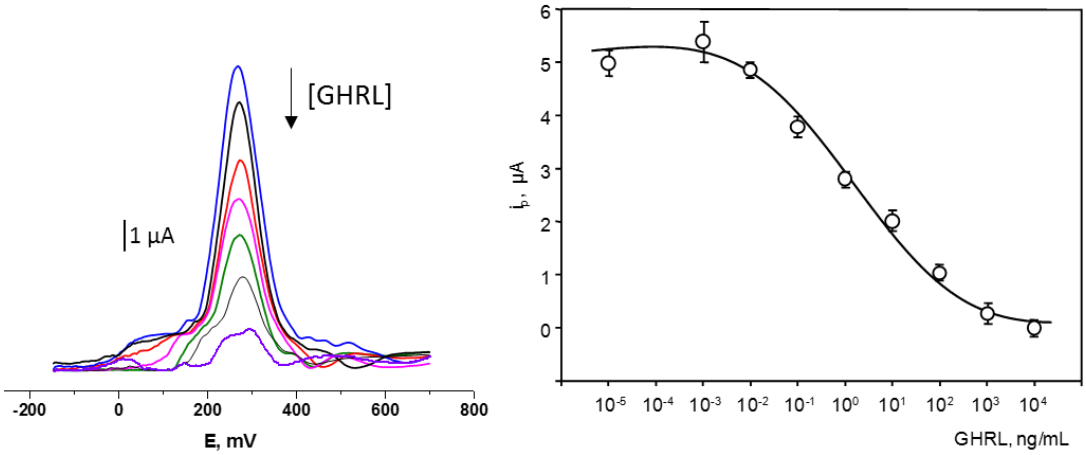

Figura 46.- *Calibrado para la determinación de GHRL con el inmunosensor AP-Strept-Biotin-GHRL(GHRL)-anti-GHRL-Protein G-MBs/SPCE.*

El límite de detección se calculó haciendo uso de la ecuación:

$$LOD = EC_{50}\left(\frac{i_{max} - i_{min}}{i_{max} - i_{min} - 3s} - 1\right)^{-1/h}$$

en la que s es la desviación estándar (n=7) de la corriente de pico medida en ausencia de GHRL, ± 0.24 μA. El valor obtenido, 7 pg/mL GHRL, es mucho menor que los valores de concentración mínima detectable proporcionados por los métodos ELISA comerciales (entre 7 y 140 veces menor), así como también respecto a los de otros métodos descritos en la bibliografía, 0.2 ng/mL [Mascini et al., 2007] y 8 ng/mL [Mascini et al., 2007a]. Cabe destacar que en este último caso, correspondiente al único biosensor electroquímico existente, un aptasensor, el límite de detección alcanzado es más de mil veces superior al obtenido en este trabajo.

La reproducibilidad de las medidas voltamperométricas realizadas en las condiciones experimentales previamente optimizadas, se evaluó llevando a cabo ensayos con diferentes inmunosensores empleando disoluciones conteniendo 1 ng/mL de GHRL. Los resultados obtenidos en el mismo día de trabajo proporcionaron una desviación estándar relativa del 4.1% (n=10). Del mismo modo, se calculó el valor de RSD en diferentes días, obteniéndose un 5.0% (n=9). Estos resultados ponen de manifiesto la buena precisión que presenta la metodología utilizada para la preparación del inmunosensor desarrollado para la determinación de GHRL.

Se estudió también la estabilidad de almacenamiento del conjugado AP-Strept-Biotin-GHRL-anti-GHRL-Protein G-MBs preparando varios inmunoconjugados en el mismo día y conservándolos a 4 ºC en un tubo eppendorf conteniendo regulador Tris 0.1 M 0.05% en Tween 20 de pH 7.2. Después, cada día, un immunoconjugado fue capturado magnéticamente sobre la superficie de un SPCE y se midió la respuesta voltamperométrica en ausencia de GHRL añadiendo 1-NPP 5 mM. Los resultados obtenidos se han representado en la Figura 46, en la que se ha considerado el valor central correspondiente a la media de la corriente en voltamperometría diferencial de impulsos para 10 medidas realizadas el primer día en las mismas condiciones experimentales, para obtener los valores límite superior e inferior situados a tres veces la desviación estándar de dichas medidas (±3s).

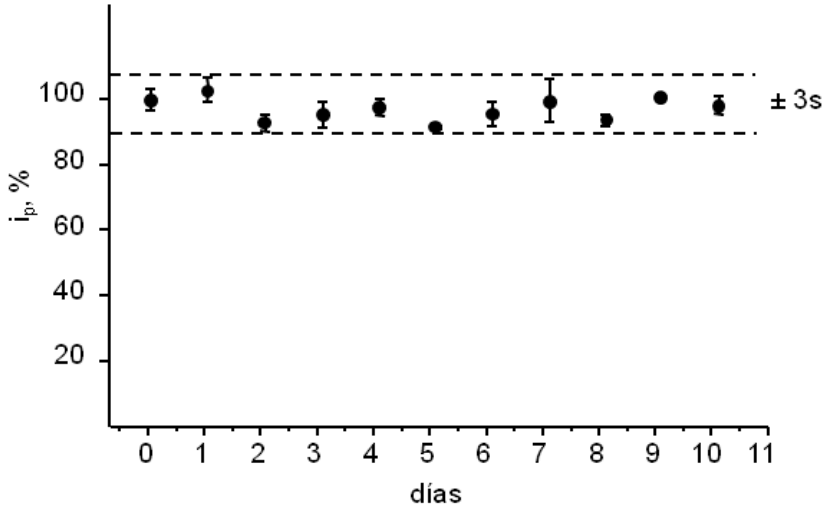

Figura 47.- *Grafico de control para la evaluación de la estabilidad de almacenamiento del conjugado AP-Strept-Biotin-GHRL(GHRL)-anti-GHRL-Protein G-MBs*

Como puede observarse, las respuestas permanecen dentro de los límites del gráfico de control durante al menos diez días, que fue el máximo tiempo de almacenamiento estudiado. Estos resultados demuestran una buena estabilidad del inmunoconjugado a medio plazo, lo que permitiría preparar una serie de ellos, conservarlos en las condiciones indicadas, y utilizarlos posteriormente a demanda, dentro del margen temporal estudiado.

5.1.1.4. Estudios de selectividad

La determinación de GHRL en muestras reales puede verse interferida por la presencia de otras hormonas o proteinas, en general, que puedan interaccionar con el anticuerpo de captura u originar algún tipo de señal electroquímica. Con el fin de aplicar el método desarrollado al análisis de saliva, en este apartado se evaluó la influencia de algunas de ellas sobre la respuesta del inmunosensor. Las especies investigadas fueron: progesterona (Prog), testosterona (Test), prolactina (PRL), hormona folículo estimulante (FSH) y hormona de crecimiento humana (hGH). Para realizar este estudio se preparó una serie de inmunoconjugados incubando en la etapa de competición 1 µg/mL del posible interferente junto a 0.01 µg/mL de Biotin-GHRL en ausencia de GHRL durante el tiempo optimizado (60 min). Los voltamperogramas registrados para cada uno de los inmunosensores así preparados se compararon con los proporcionados por el inmunosensor en ausencia de GHRL y de posible interferente, empleado como blanco. En la Figura 48 se han representado los resultados obtenidos.

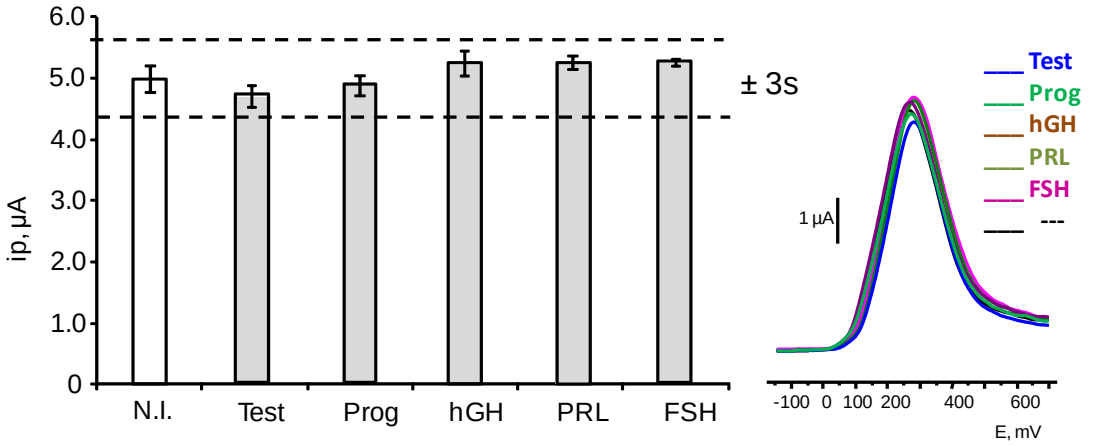

Figura 48.- *Efecto de la presencia de 1 µg/mL de diferentes hormonas en la respuesta voltamperométrica del inmunosensor en ausencia de GHRL*

Como puede apreciarse, los voltamperogramas en diferencial de impulsos son muy parecidos entre sí y prácticamente equivalentes a los del blanco. Además, las señales de corriente obtenidas quedan en todos los casos dentro de los límites situados a ± 3s del valor de la respuesta del inmunosensor en ausencia de GHRL (n=10). Estos resultados demuestran la ausencia de interferencia por parte de los compuestos estudiados, lo que está de acuerdo con la especificidad del anticuerpo de captura utilizado.

5.1.1.5. Aplicación a la determinación de GHRL en saliva

La aplicación a muestras de saliva se considera de gran interés, ya que su recogida es no invasiva, puede disponerse de volúmenes relativamente elevados, y su complejidad es media. El principal problema de su empleo para este tipo de determinaciones, es que las concentraciones que cabe esperar son inferiores a las que están presentes en suero. En este caso, como se ha dicho, la concentración esperable de GHRL en saliva es de algunas centenas de pg/mL [Taskin et al., 2014].

En primer lugar, se estudió la posibilidad de existencia de efecto matriz originado por los componentes de la muestra. Con el fin de evitarlo, al tiempo que ajustar las concentraciones esperables en la saliva a la porción recta del calibrado, se aplicó el factor de dilución 1:300 que se indica en el procedimiento descrito en el Apartado 4.4.1.1. de la Parte Experimental. A continuación se construyó un calibrado en el intervalo lineal de concentraciones de GHRL empleando muestras de saliva contaminadas a las que se aplicó dicho procedimiento. La pendiente del calibrado fue -0.96 ± 0.06 µA, valor muy parecido al obtenido empleando disoluciones patrón de GHRL, -0.95 ± 0.05 µA (ver Figura 49). A pesar de ello, ambas pendientes se

compararon estadísticamente aplicando el ensayo de la t de Student. Como se verá, este ensayo ha sido utilizado también en otras aplicaciones descritas en la Memoria, por lo que en esta parte, en que aparece por primera vez, se describe brevemente el procedimiento seguido.

Inicialmente debe conocerse si las varianzas de las pendientes son homogéneas. Para ello, se calcula $F_{cal} = \frac{s_1^2}{s_2^2} = \frac{0.06^2}{0.05^2} = 1.44$, y de la tabla de valores críticos de *F* para pruebas de dos colas, con *P* = 0.05, $\eta_1 = 4$ y $\eta_2 = 7$, $\upsilon_1 = 4\text{-}2 = 2$ y $\upsilon_2 = 7\text{-}2 = 5$, se obtiene $F_{tab} = 8.434$. Al ser $F_{tab} > F_{cal}$, se demuestra la homogeneidad de las varianzas de las pendientes.

A continuación se aplica el ensayo t para varianzas homogéneas, calculando:

$$t_{cal} = \frac{|b_1 - b_2|}{\sqrt{(s_1^2 - s_2^2)}} = \frac{|-0.96 + 0.95|}{\sqrt{(0.06^2 - 0.05^2\ )}} = 0.30$$

El valor tabulado para un nivel de confianza del 95% y con $\eta_1 + \eta_2 - 2$ niveles de libertad es $t_{(9,\ 0.05)} = 2.26$. Por tanto, como $t_{tab} > t_{cal}$, no existen diferencias significativas entre las pendientes y ambas son estadísticamente similares.

De lo obtenido se deduce que la determinación de GHRL en saliva puede realizarse interpolando las corrientes de pico de los voltamperogramas en diferencial de impulsos en el calibrado de patrones.

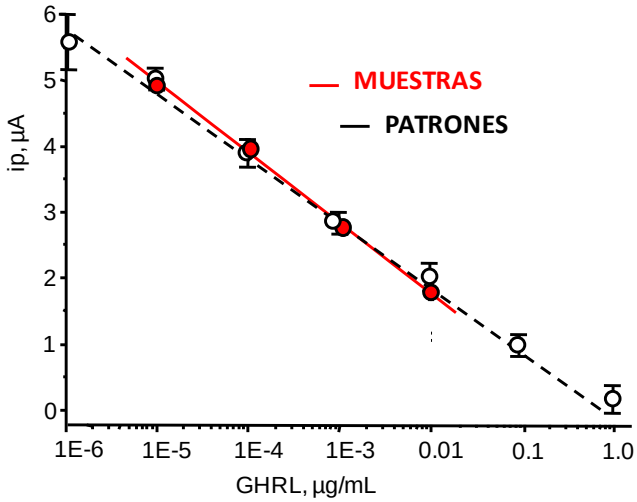

Figura 49.- *Calibrados obtenidos para disoluciones patrón de GHRL (- - -) y para muestras de saliva en dilución 1:300 (—)*

Por último, el método se validó por aplicación a muestras de saliva enriquecidas con GHRL a niveles de concentración de 0.01, 0.1, 1 y 10 ng/mL. Como se describe en la Parte Experimental (Apartado 4.4.1.1.), la saliva se recogió de un voluntario sano empleando un dispositivo Salivette®. Una vez saturado de muestra, el algodón se centrifugó y al líquido se le añadió la cantidad adecuada de hormona y se procedió a aplicar el método con 1 µL de saliva a la que se añadieron 3 µL de BIotin-GHRL de 1 µg/mL, diluyendo a 300 µL con el regulador B&W. Se comprobó que la saliva sin contaminar no contenía GHRL o, al menos, que su concentración no originaba ningún cambio de respuesta con el inmunosensor, y se midieron los voltamperogramas de las muestras enriquecidas, por quintuplicado. Los resultados obtenidos se han resumido en la Tabla 12. Como puede observarse, las recuperaciones alcanzadas se encuentran a niveles próximos al 100% en todos los casos, lo que pone de manifiesto la utilidad analítica del inmunosensor para este tipo de muestras.

Tabla 12.- *Recuperación de GHRL en saliva con el inmunosensor AP-Strept-Biotin-GHRL- anti GHRL- Protein G-MBs / SPCE*

GHRL añadido, ng/mL	GHRL encontrado, ng/mL	Recuperación media, %
0.01	0.010 ± 0.001*	100 ± 10
0.1	0.10 ± 0.01	102 ± 10
1	0.95 ± 0.01	95.3 ± 0.6
10	9.5 ± 0.2	95 ± 2

**ts / √n*

5.1.1.6. Conclusiones

Se ha desarrollado un magnetoinmunosensor electroquímico para la determinación de GHRL que combina las características ventajosas de las micropartículas magnéticas funcionalizadas con Proteína G para la inmovilización del anticuerpo de captura con el empleo de electrodos serigrafiados de carbono. Se ha establecido un esquema de inmunoensayo competitivo empleando la técnica de voltamperometría diferencial de impulsos (DPV), de elevada sensibilidad, para la detección de 1-naftol como producto de la reacción enzimática. Todo ello ha hecho posible alcanzar un bajo límite de detección, inferior al de otros métodos existentes, y aplicar el inmunosensor a la determinación de la hormona en muestras de saliva.

5.1.2. MAGNETOINMUNOSENSOR PARA LA DETERMINACIÓN DE TGF-β1

Como se ha dicho en la Introducción, el factor de crecimiento transformante β1 (TGF-β1), perteneciente a la familia de las citoquinas, desempeña un papel relevante en diversos procesos de tipo inmunológico o inflamatorio, la obesidad o el desarrollo del cáncer. Actualmente existe un enorme interés clínico en la determinación de esta y otras citoquinas consideradas biomarcadores esenciales para la predicción, caracterización y monitorización de enfermedades relacionadas con estos procesos y su tratamiento.

Los niveles séricos normales de TGF-β1 en individuos sanos se sitúan entre 0.1 y 25 ng/mL, si bien se observa alguna variabilidad que depende en cierta medida del tipo de ensayo utilizado para su determinación.

Se han comentado también las características de algunos métodos basados en estrategias de inmunoensayo para la determinación de esta citoquina. Se dispone de algunos kits ELISA comerciales con detección colorimétrica que proporcionan intervalos dinámicos entre varias decenas y miles de pg/mL. Las concentraciones mínimas detectables en estos ensayos se encuentran en el entorno de algunas unidades de pg/mL. También se ha desarrollado un aptasensor (ver Tabla 8), con un límite de detección de 1 ng/mL [Matharu, et al, 2014], y un inmunosensor impedimétrico [Yao et al, 2016]. Finalmente, en nuestro grupo se desarrolló anteriormente un inmunosensor electroquímico basado en la reacción de cicloadición azida-alquino catalizada por Cu(I) (“click” chemistry) [Sánchez-Tirado et al., 2016], con un LOD de 1.3 pg/mL.

En este trabajo se prepara un magnetoinmunosensor amperométrico para la determinación de TGF-β1 empleando micropartículas magnéticas carboxiladas (HOOC-MBs) sobre las que se enlaza covalentemente el anticuerpo anti-TGF haciendo uso del polímero comercial Mix&Go^{TM}. Este polímero contiene varios complejos metálicos seleccionados por su eficiencia para enlazar proteínas y hace posible la inmovilización estable y orientada de los anticuerpos por interacción con sus posiciones Fc. Esto unido a la utilización de un polímero de estreptavidina marcada con peroxidasa (poli-HRP-Strept) para amplificar la señal electroquímica obtenida por medida de la corriente de oxidación de peróxido de hidrógeno mediada por hidroquinona, hace posible alcanzar una elevada sensibilidad, así como aplicar con buenos resultados la configuración desarrollada a la determinación de TGF-β1 en orina.

5.1.2.1. Configuración del inmunosensor

En la Figura 32 de la Parte Experimental se representó el esquema de preparación del magnetoinmunosensor electroquímico desarrollado para la determinación de TGF-β1. Como se ha señalado (ver Figura 50), la preparación de este inmunosensor se basa en la inmovilización del anticuerpo específico anti-TGF sobre las HOOC-MBs seguido del atrapamiento del conjugado sobre un SPCE y el establecimiento de un esquema de tipo sándwich empleando el conjugado Biotin-anti-TGF. Finalmente, la incorporación de poli-HRP-Strept hace posible llevar a cabo la medida amplificada de la respuesta amperométrica a -200 mV vs Ag empleando el sistema H_2O_2/HQ.

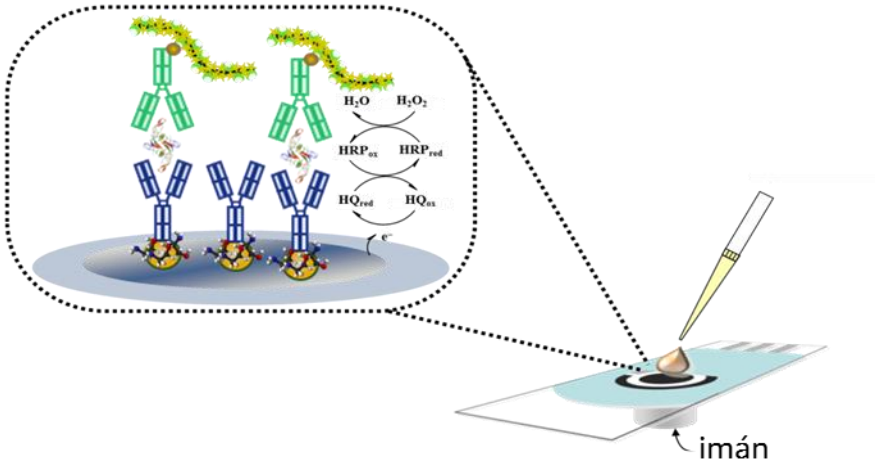

Figura 50.- *Esquema y modo de detección del magnetoinmunosensor de TGF-β1*

5.1.2.2. Optimización de las variables experimentales

Se optimizaron las variables implicadas en la preparación y el funcionamiento del magnetoinmunosensor con el objetivo de alcanzar la sensibilidad y selectividad adecuadas para el análisis de muestras clínicas, así como una buena reproducibilidad de las medidas. Como se verá, el criterio utilizado para seleccionar cada valor fue la obtención de la mayor relación entre las corrientes debidas a interacciones específicas antígeno-anticuerpo y las no específicas (S/N). Los valores óptimos de algunas variables se tomaron de trabajos anteriores realizados en el laboratorio. Es el caso de la cantidad de HOOC-MBs [Ojeda et. al., 2014], el pH y el potencial de medida de la respuesta de oxidación de H_2O_2 en presencia de HQ [Eguílaz et al., 2010], y el volumen de disolución comercial Mix&Go™ [Ojeda et al., 2015]. Por otro lado, los estudios de optimización se realizaron empleando el conjugado HRP-Strept (no el polímero) para marcar el anticuerpo de detección Biotin-anti-TGF, ya que el efecto de las variables estudiadas no depende del tipo de marcador utilizado.

- ***Influencia de la concentración del anticuerpo de captura***

La cantidad de anti-TGF inmovilizada sobre las micropartículas magnéticas HOOC-MBs se optimizó midiendo las respuestas específica e inespecífica (estas últimas sin antígeno) de inmunosensores preparados con concentraciones comprendidas entre 2.5 y 20 µg/mL de anticuerpo, con los resultados que se muestran en la Figura 51.

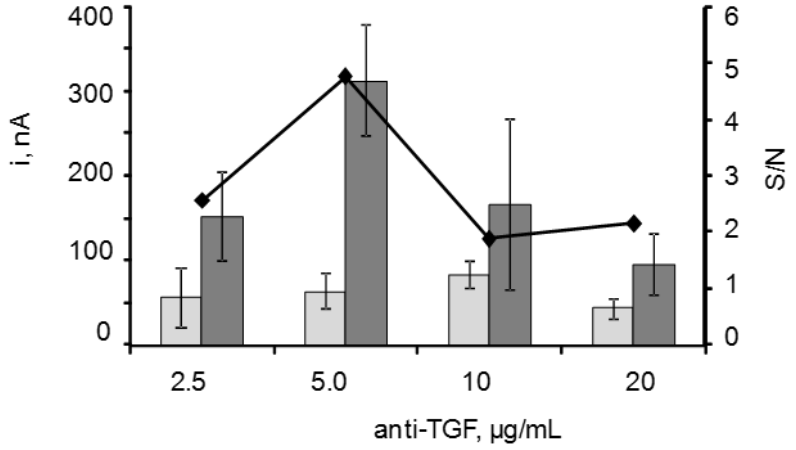

Figura 51.- *Efecto de la concentración de anti-TGF sobre la respuesta del magnetoinmunosensor HRP-Strept-Biotin-anti-TGF-TGF-anti-TGF-MBs/SPCE: 90 µg HOOC-MBs; 25 µL Mix&Go, 60 min; 2.5–20 µg/mL anti-TGF, 60 min; etanolamina 1M, 90 min; Biotin–anti–TGF 2 µg/mL, 60 min; HRP-Strept 1/2000,; 20 min; 125 pg/mL (gris oscuro) ó 0 pg/mL (gris claro) TGF-β1, 60 min. Las barras de error corresponden a la desviación estándar (n=3) de las medidas.*

Como puede observarse, la mayor relación S/N se obtiene para una concentración de anticuerpo de 5 µg/mL. Concentraciones mayores dan lugar a una disminución considerable de la respuesta específica, debido probablemente al impedimento de la reacción electroquímica en presencia de una mayor carga de biomoléculas aislantes en la superficie del electrodo. Por tanto, de acuerdo con estos resultados, se seleccionó el valor mencionado para la preparación del inmunosensor. Por otro lado, se observó que un tiempo de incubación del anticuerpo sobre las HOOC-MBs activadas con Mix&Go™ de 60 min, es suficiente para que tenga lugar la unión covalente del mismo.

- ***Influencia de la concentración de Biotin-anti-TGF***

Para optimizar la concentración del anticuerpo biotinilado se estudió la respuesta electroquímica obtenida con diferentes inmunosensores preparados con concentraciones de Biotin-anti-TGF en el intervalo de 1 a 4 µg/mL. Los resultados representados en la Figura 52 permiten apreciar el incremento de la señal específica y, en menor medida, de la inespecífica al aumentar la concentración de conjugado hasta 2 µg/mL. A partir de esta concentración, la respuesta específica decae y también lo hace la relación S/N. Posiblemente, al igual que en el caso anterior, esta disminución es debida al bloqueo de la superficie del electrodo que dificulta la reacción electroquímica. Por ello, la concentración citada fue elegida para estudios posteriores.

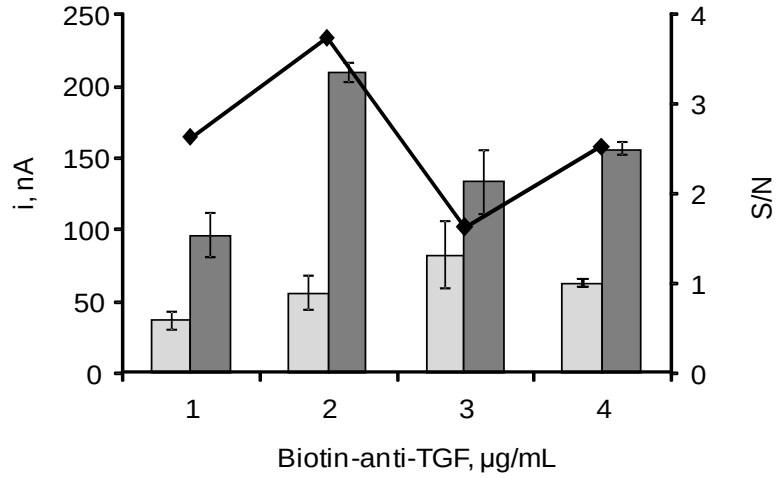

Figura 52.- *Efecto de la concentración de Biotin-anti-TGF sobre la respuesta del magnetoinmunosensor HRP-Strept-Biotin-anti-TGF-TGF-anti-TGF-MBs/SPCE: 90 µg HOOC-MBs; 25 µL Mix&Go, 60 min; 5 µg/mL anti-TGF, 60 min; etanolamina 1M, 90 min; Biotin–anti–TGF 1-4 µg/mL, 60 min; HRP-Strept 1/2000,; 20min; 125 pg/mL (gris oscuro) ó 0 pg/mL (gris claro)TGF-β1, 60 min.*

- ***Optimización de la etapa de bloqueo***

La preparación del magnetoinmunosensor para la determinación de TGF-β1 requirió el empleo de un agente bloqueante para minimizar las adsorciones inespecíficas sobre las HOOC-MBs posteriores a la inmovilización del anticuerpo de captura. El producto elegido para este propósito fue la etanolamina, debido a su probada eficiencia en el bloqueo de las posiciones activas en la superficie de las partículas magnéticas [Campuzano et al., 2014]. Se probaron dos disoluciones de esta amina en concentración 1 y 2 M, empleando tiempos de bloqueo entre 30 y 90 min. Se encontró que la concentración más alta proporcionaba una relación S/N más de 1.3

veces superior. Por otro lado, según se muestra como ejemplo en la Figura 53, se encontró que un tiempo de 60 min era suficiente para obtener un bloqueo efectivo. En estas condiciones, la corriente debida a adsorciones inespecíficas resulta inferior a un 25% de la correspondiente específica para una concentración de TGF-β1 de 125 pg/mL.

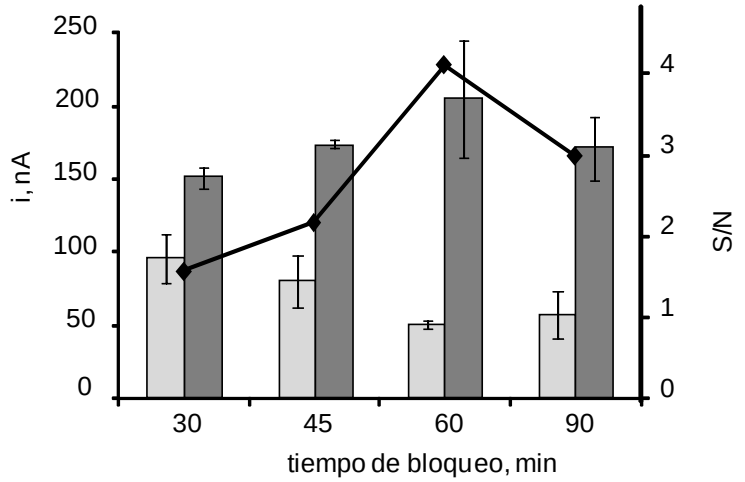

Figura 53.- *Efecto del tiempo de incubación en la etapa de bloqueo: 90 µg HOOC-MBs; 25 µL Mix&Go, 60 min; 5 µg/mL anti-TGF, 60 min; 50 µL etanolamina 2M, 30 - 90 min; 25 µL Biotin–anti–TGF 2 µg/mL, 60 min; 25 µL HRP-Strept en dilución 1/200, 20 min; 125 pg/mL (gris oscuro) ó 0 pg/mL (gris claro) TGF-β1, 60 min.*

- ***Influencia de la concentración de HRP-Strept y de poli-HRP-Strept***

La concentración del conjugado enzimático utilizado para monitorizar la formación del inmunocomplejo se optimizó estudiando la influencia en la respuesta del inmunosensor de disoluciones de HRP-Strept preparadas a diferentes diluciones en el intervalo comprendido entre 1/500 y 1/4000. Los resultados representados en la Figura 54a muestran, como era de esperar, una disminución paulatina de la corriente conforme aumenta la dilución del conjugado en todo el intervalo estudiado. Debido al ligero aumento de la corriente inespecífica a la mayor dilución, la relación S/N adopta un máximo para un valor de 1/2000.

Con el fin de alcanzar la mayor sensibilidad, se utilizó una estrategia de amplificación de la señal electroquímica empleando un conjugado polimérico poli-HRP-Strept en lugar del convencional estudiado anteriormente. Para demostrar el efecto de amplificación conseguido con este conjugado y elegir la concentración más adecuada del mismo, se evaluó el efecto de la dilución de las disoluciones de poli-HRP-Strept en las mismas condiciones experimentales que las utilizadas en el estudio anterior. Los resultados obtenidos aparecen en la Figura 54b.

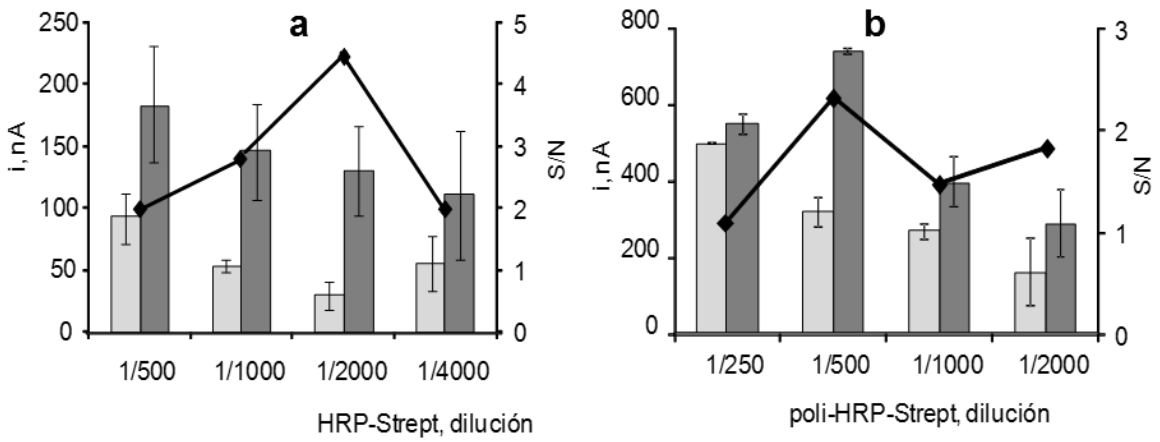

Figura 54.- *Influencia de la concentración de (a) HRP-Strept y (b) poli-HRP-Strept en la respuesta del magnetoinmunosensor: 90 µg HOOC-MBs; 25 µL Mix&Go, 60 min; 5 µg/mL anti-TGF, 60 min; etanolamina 2 M, 60 min; Biotin–anti–TGF 2 µg/mL, 60 min; (a) 125 pg/mL (gris oscuro) ó 0 pg/mL (gris claro) TGF-β1, 60 min; (b) 60 pg/mL (gris oscuro) ó 0 pg/mL (gris claro) TGF-β1, 60 min*

Puede observarse cómo la utilización del polímero poli-HRP-Strept da lugar a un notable incremento de la respuesta electroquímica del inmunosensor en relación a la observada empleando el conjugado convencional. Esto es debido al mayor número de moléculas de peroxidasa disponible para la biocatálisis del sustrato enzimático. En efecto, para una concentración de TGF-β1 inferior a la mitad (60 pg/mL frente a 125 pg/mL), la corriente obtenida a todas las diluciones es apreciablemente superior. En este caso, la mayor relación corriente específica a inespecífica se obtuvo para una dilución de poli-HRP-Strept 1/500 que será la que se utilice en adelante. Por otro lado, un tiempo de incubación de 20 min resultó adecuado para lograr una unión estable al anticuerpo biotinilado.

- ***Inmovilización del anticuerpo anti-TGF***

Como se ha comentado, la inmovilización del anticuerpo de captura sobre las partículas magnéticas carboxiladas se realizó empleando un polímero comercial denominado Mix&Go™ en lugar de los reactivos habituales, EDC y NHSS. Este polímero soluble en agua es un reactivo activador y enlazante de biomoléculas constituido, como se ha dicho, por una serie de complejos metálicos seleccionados por su eficiencia para unirse a las proteínas. Se sabe que este producto utiliza ligandos de pequeño tamaño para ligarse a los dominios Fc de los anticuerpos. En ese sentido, mimetiza a las proteínas A y G originando enlaces estables y orientados con estos inmunorreactivos. Al mismo tiempo, el polímero puede unirse también a grupos

donantes de electrones como los carboxilato presentes en las micropartículas magnéticas, por lo que su comportamiento se asemeja al de un adhesivo intermediario entre la superficie a modificar y la biomolécula. Aparte de estas características, el protocolo de uso de Mix&Go™ es más sencillo y breve que el del método tradicional con EDC y NHSS.

En este trabajo se comparó el comportamiento de los inmunosensores preparados por inmovilización de anti-TGF empleando Mix&Go™ y haciendo uso de la química del EDC/NHSS, en las condiciones y con los resultados que se muestran en la Figura 55.

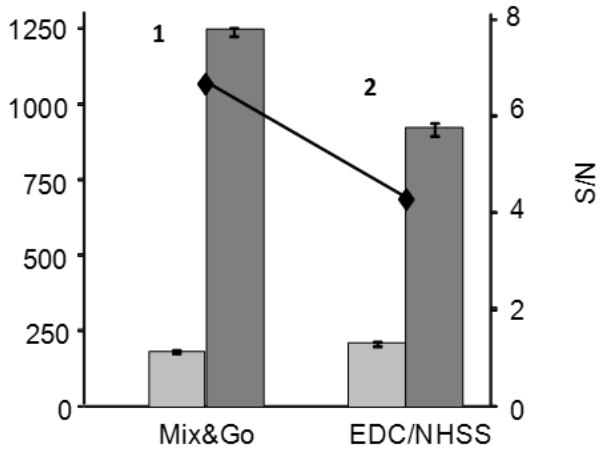

***Figura 55**.- Comparación de las respuestas obtenidas con el inmunosensor poli-HRP-Strept-Biotin-anti-TGF-TGF-anti-TGF-MBs/SPCE preparado empleando (1) Mix&Go™ ó (2) EDC/NHSS para inmovilizar anti-TGF sobre HOOC-MBs: 90 µg HOOC-MBs; 25 µL Mix&Go, 60 min (a); 5 µg/mL anti-TGF, 60 min; etanolamina 2 M, 60 min; Biotin–anti–TGF 2 µg/mL, 60 min; (a) 125 pg/mL (gris oscuro) ó 0 pg/mL (gris claro) TGF-β1, 60 min; (b) 60 pg/mL (gris oscuro) ó 0 pg/mL (gris claro) TGF-β1, 60 min*

Según se muestra, la relación respuesta específica a inespecífica es mucho mayor cuando se utiliza Mix&Go™, resultado que está de acuerdo con otros obtenidos anteriormente [Ojeda et al., 2015], y que se debe probablemente a la orientación del anticuerpo que se consigue empleando este reactivo.

En la Tabla 13 se han resumido los resultados obtenidos en los estudios de optimización de variables.

Tabla 13.- *Optimización de las variables implicadas en el funcionamiento del inmunosensor poli-HRP-Strept- Biotin-anti-TGF-TGF-β1-anti-TGF-MBs/SPCE.*

Variable	Intervalo estudiado	Valor seleccionado
anti-TGF, µg/mL	2.5 – 20	5
Biotin-anti TGF, µg/mL	1 – 4	2
poli-HRP-Strept, dilución	1/2000 – 1/250	1/500
etanolamina, M	1 - 2	2
incubación etanolamina, min	30 – 90	60

5.1.2.3. Calibrado y características analíticas

Empleando inmunosensores preparados en las condiciones óptimas descritas anteriormente, se obtuvo el calibrado que aparece representado en la Figura 56 junto con algunos amperogramas registrados a un potencial de -0.2 V vs Ag. Se trata de una curva sigmoidal creciente, como corresponde a la estrategia de inmunoensayo tipo sandwich empleada.

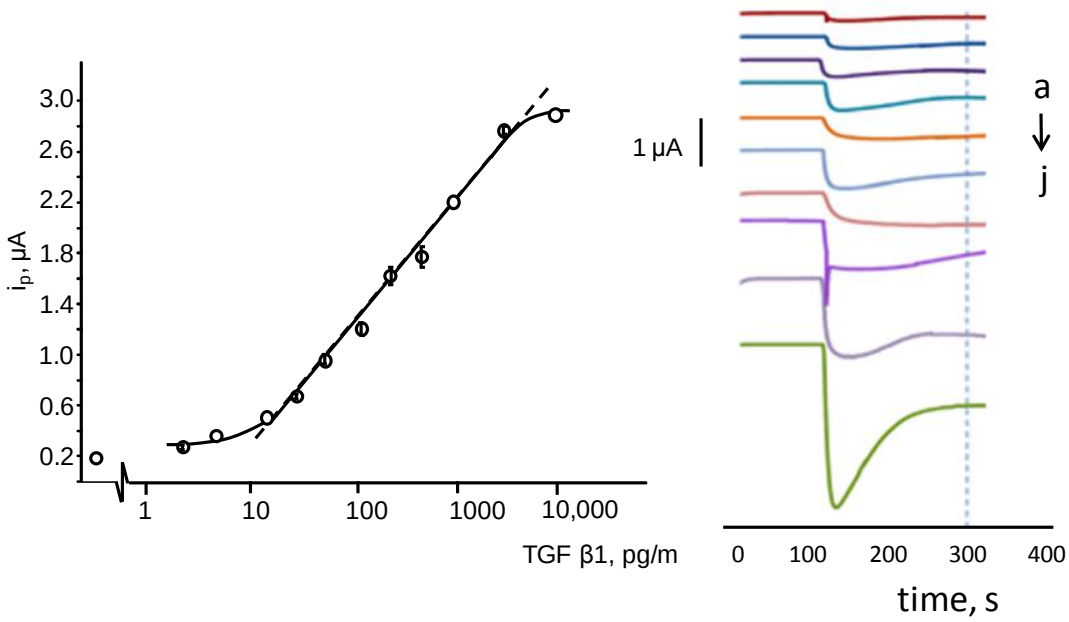

Figura 56.- *Calibrado para la determinación de TGF-β1 con el inmunosensor poli-HRP-Strept-Biotin-anti-TGF-TGF-β1-anti-TGF-MBs/SPCE, y amperogramas para: a) 0; b) 2.5; c)15; d) 30; e) 60; f) 125; g) 250; h) 500; i)1000 y j) 3000 pg/mL TGF-β1; la línea a trazos indica el tiempo de medida.*

La relación entre la corriente en estado estacionario y el logaritmo de la concentración de TGF-β1 en el intervalo de 2.5 a 10,000 pg/mL se ajusta a la ecuación: i, nA = 978 log C (pg/mL) - 734, con r = 0.995. Puede apreciarse también un intervalo de linealidad $i_p \propto$ log [TGF-β1] (r = 0.992) entre 15 y 3000 pg/mL, que es adecuado para la determinación de esta citoquina en muestra reales teniendo en cuenta los niveles esperables en plasma, del orden de unidades de ng/mL [Grainger et al., 1995], o de decenas de pg/mL en orina [Tsapenko et al., 2013].

El límite de detección fue de 10 pg/mL, calculado por aplicación del criterio 3 s_b, donde s_b es la desviación estándar, en unidades de concentración (n=10), de las medidas de la corriente de fondo (0 pg/mL TGF-β1). Este resultado es mucho menor que la concentración mínima detectable por los kits ELISA comerciales (ver Tabla 8 en la Introducción). Por ejemplo, el test colorimétrico RayBio® Human TGF beta 1 ELISA kit (ELH-TGFb1) (www.raybiotech.com/ files/manual/ELISA/ELH-TGFb1.pdf) permite detectar una dosis mínima de 80 pg/mL, calculada como la concentración que proporciona una absorbancia igual a dos veces la desviación estándar del blanco. Por otro lado, el valor obtenido es superior al que se obtiene empleando metodología "click" para la inmovilización del anticuerpo (1.3 pg/mL), pero el intervalo dinámico lineal es mucho más amplio comparado con el de dicho trabajo (5 - 200 pg/mL) [Sánchez-Tirado et al., 2016]. Posiblemente, la menor concentración detectable de TGF-β1 en ese caso se debe al empleo de un electrodo modificado con nanotubos de carbono, de elevada sensibilidad. Finalmente, el LOD alcanzado con el inmunosensor desarrollado en esta Tesis Doctoral es también notablemente inferior al obtenido por un aptasensor (1 ng/mL) [Honkanen et al., 1997] y un inmunosensor impedimétrico más reciente (0.570 ng/mL) [Yao et al., 2016].

La reproducibilidad de las medidas amperométricas realizadas en las condiciones experimentales anteriores se estudió preparando una serie de inmunosensores el mismo día y en días diferentes para medir las respuestas amperométricas de distintas disoluciones sin y con 250 pg/mL deTGF-β1. Los valores de la desviación estándar relativa fueron RSD = 2.9% y 3.9% (n=5), respectivamente, para los ensayos realizados el mismo día, y RSD = 3.7% y 4.2 % (n=5), respectivamente, para las medidas realizadas en diferentes días. Estos resultados demuestran el alto nivel de precisión alcanzado en la preparación y funcionamiento de los inmunosensores desarrollados.

Al igual que en el capítulo anterior, se estudió también la estabilidad de almacenamiento de los conjugados anti-TFG-MBs/SPCE. Para ello, una vez preparados varios de ellos el mismo día, se conservaron en ambiente húmedo a 4 ºC y se emplearon posteriormente para construir el inmunosensor con el que se midieron disoluciones de 250 pg/mL de TGF-β1 en diferentes días. Los resultados obtenidos (Figura 57) muestran cómo las respuestas del inmunosensor permanecen dentro de los límites de control localizados a ± 3s, donde s es la desviación estándar de las medidas (n=10) realizadas el primer día de trabajo, durante al menos 40 días (el máximo periodo de tiempo estudiado), demostrando la buena estabilidad de los conjugados.

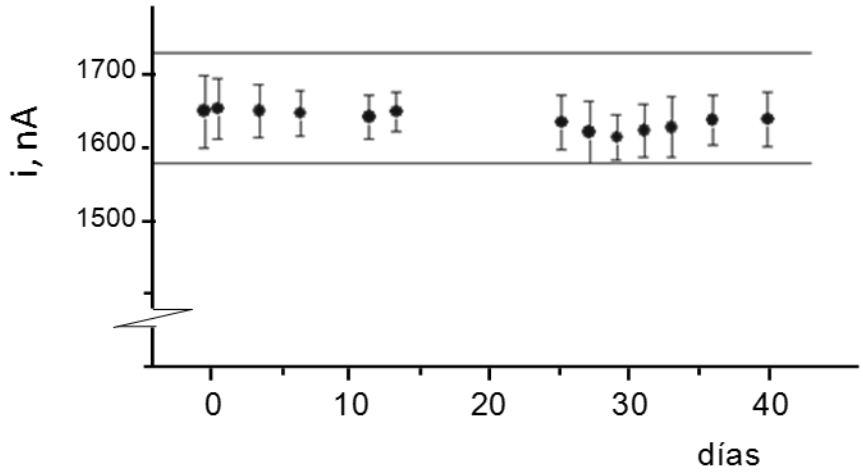

Figura 57.- *Grafico de control para la evaluación de la estabilidad de almacenamiento del conjugado anti-TGF-MBs/SPCE*

5.1.2.4. Estudios de selectividad

Se estudió el efecto sobre la respuesta del inmunosensor de otras sustancias presentes habitualmente en las muestras clínicas usadas para la determinación de TGF-β1. Las especies investigadas fueron ácido ascórbico (AA), ácido úrico (UA), adiponectina (APN), creatinina (CR), factor de necrosis tumoral alfa (TNF), interleucina 6 (IL-6), interleucina 8 (IL-8), todas ellas a las concentraciones que cabe esperar en suero de pacientes sanos. Los resultados obtenidos en la medida de disoluciones preparadas en ausencia de TGF-β1 o en presencia de 25 pg/mL de esta citoquina se han representado en la Figura 58. En ella puede observarse que no existen diferencias apreciales de las respuestas en ausencia y en presencia de interferente, tanto en el caso de las proteínas investigadas como de las sustancias electroactivas, AA y UA, que no ofrecen ningún tipo de respuesta al potencial de medida.

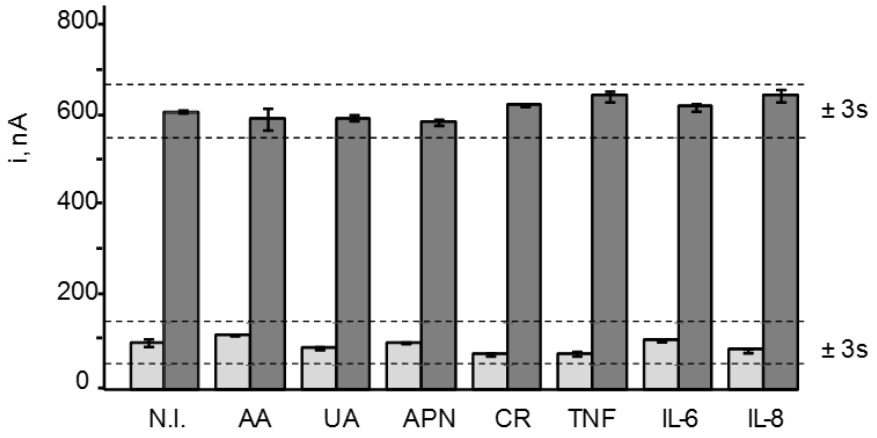

Figura 58.- *Repuestas amperométricas obtenidas con el inmunosensor poli-HRP-Strept-Biotin-anti-TGF-TGF-β1-anti-TGF-MBs/SPCE para 0 (gris claro) y 25 pg/mL (gris oscuro)en presencia de 370 µg/mL AA, 50 µg/mL UA; 200 pg/mL APN; 10 pg/mL CR, 200 µg/mL TNF; 500 pg/mL IL-6; 10 ng/mL IL-8.*

5.1.2.5. Aplicación a la determinación de TGF-β1 en orina

La utilidad analítica del inmunosensor se evaluó por aplicación al análisis de orina enriquecida con TGF-β1 a niveles de 25, 45 y 100 pg/mL. Las muestras ensayadas, de orina control Liquichek™ (Urine Chemistry Control, BioRad) contenían ácido úrico, amilasa, calcio, cloruro, cortisol, creatinina, fósforo, glucosa, magnesio, albúmina, potasio, sodio y urea.

Se investigó la existencia de efecto matriz construyendo diferentes calibrados por adición a la muestra de distintas concentraciones de TGF-β1 en el intervalo de 25 a 250 pg/mL, sin dilución o aplicando factores de dilución de 1:2 y 1:3 con regulador fosfato 0.1 M de pH 7.2. Los resultados obtenidos demostraron que una dilución 1:3 era suficiente como para evitar las diferencias encontradas en las pendientes de los calibrados de las muestras repecto del calibrado de patrones de TGF-β1. Como ejemplo, se muestra la recta obtenida para la dilución escogida, que se compara en la Figura 59 con la porción recta del calibrado representado anteriormente (Figura 56) en el intervalo de 15 a 1000 pg/mL TGF-β1. Puede apreciarse cómo ambas coinciden apreciablemente. No obstante, para confirmar esta coincidencia, de igual modo que en el capítulo anterior, se compararon estadísticamente las pendientes de ambos calibrados, 978 ± 50 y 911 ± 39 nA por década de concentración, respectivamente para los patrones y las muestras de TGF-β1, obteniéndose. t_{tab} = 2.357 y t_{cal} = 1.499, lo que demuestra que no existen diferencias significativas entre ambas, por lo que la determinación en la orina puede realizarse por interpolación directa de las corrientes medidas en el calibrado de disoluciónes patrón.

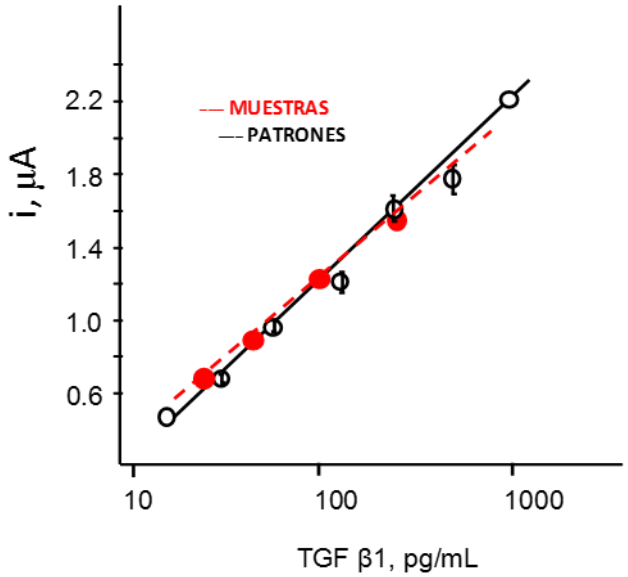

Figura 59.- *Calibrados obtenidos para disoluciones patrón de TGF-β1 (—) y para muestras de orina en dilución 1:3 (- - -)*

De este modo, el método de determinaciión de TGF-β1 se validó por aplicación a muestras de orina enriquecidas a los niveles de concentración señalados, por aplicación del procedimiento descrito en al Apartado 4.4.2. Los resultados obtenidos para la determinación por triplicado a cada concentración se han representado en la Tabla 14, en la que se aprecia que los niveles de recuperación media son en todos los casos próximos al 100%, demostrando así la utilidad del inmunosensor desarrollado al análisis de muestras complejas como es la orina.

Tabla 14.- *Recuperación de TGF-β1 en orina con el inmunosensor poli-HRP-Strept-Biotin-anti-TGF-TGF-β1-anti-TGF-MBs/SPCE*

TGF-β1 añadido, pg/mL	TGF-β1 encontrado, pg/mL	Recuperación media, %
25	25.9 ± 0.5*	103 ± 8
45	44.9 ± 0.3	100 ± 3
100	96 ± 1	97 ± 5

*ts/√n

5.1.2.6. Conclusiones

El magnetoinmunosensor amperométrico puesto a punto en este trabajo para la determinación de TGF-β1 satisface los requisitos de sensibilidad y selectividad para poder se aplicado con excelentes resultados al análisis de muestras de orina sin más tratamiento previo que una simple dilución 1:3 en disolución reguladora fosfato. Probablemente, este buen comportamiento es debido a la combinación del empleo de micropartículas magnéticas carboxiladas unido al del producto comercial Mix&Go™, que da lugar a la inmovilización estable y orientada del anticuerpo de captura, junto a la utilización de la técnica de amperometría y el efecto de amplificación de la corriente que produce el uso del polímero poli-HRP-Strept.

5.2. BIOSENSORES BASADOS EN ELECTRODOS MODIFICADOS CON GRAFENO E HÍBRIDOS DE GRAFENO

5.2.1. INMUNOSENSOR PARA LA DETERMINACIÓN DE PYY

Como se ha descrito en la Introducción, el péptido YY (ver Figura 5) es un potente anorexígeno sintetizado en el intestino, cuya actividad se manifiesta a través de la estimulación de la absorción gastrointestinal de fluidos y electrólitos, la reducción de las secreciones gástrica y pancreática, y la disminución del consumo de alimentos. Esta actividad, contrapuesta a la de la grelina, ha llevado a considerar al PYY como una posible diana terapéutica para la reducción del apetito y el consumo de calorías. La concentración de PYY en plasma oscila normalmente entre 40–70 pg/mL, aunque los niveles circulantes alcanzan valores superiores tras la ingesta y son inferiores en los individuos obesos.

Al igual que en el caso de la GHRL, la determinación de PYY en muestras clínicas tiene interés en el control de la obesidad y enfermedades relacionadas, así como en el seguimiento de los trastornos del apetito.

Se dispone actualmente de métodos de inmunoensayo tipo RIA y ELISA para la determinación de PYY (ver Tabla 6). Entre los kits ELISA comerciales destacan los basados en esquemas competitivos empleando anticuerpos específicos o anticuerpos biotinilados y conjugados HRP-avidina or HRP-estreptavidina y detección colorimétrica empleando H_2O_2 y TMB. Estos ensayos presentan intervalos dinámicos de concentración entre 0.1 - 1 pg/mL y 100 - 1000 pg/mL, con valores mínimos detectables entre 0.5 pg/mL y 3 pg/mL, aproximadamente. Como en otros casos, los tiempos de ensayo son largos, de 3 a 5 horas, e incluso requiriendo tiempos de incubación de más de 20 h.

En este trabajo se desarolló el primer inmunosensor para la determinación de PYY. Destaca en esta configuración el empleo de una plataforma electroquímica novedosa consistente en un electrodo de carbono vitrificado modificado con óxido de grafeno reducido al que se une mediante el método de *grafting* la sal de diazonio del ácido *p*-aminobenzoico. Como se verá, el empleo de esta estrategia unido a la inmovilización del anticuerpo de captura mediante enlace covalente en la superficie del electrodo, confiere al inmunosensor una elevada estabilidad, y hace posible alcanzar una alta sensibilidad y un límite de detección notablemente inferior a los que presentan los métodos de inmunoensayo convencionales.

5.2.1.1. Configuración del inmunosensor

El esquema seguido para la preparación de este inmunosensor aparece representado en la Figura 33 de la Parte Experimental. Como se ha descrito, la plataforma electródica se prepara mediante *grafting* electroquímico del catión diazonio del *p*-ABA sobre el electrodo de carbono vitriicado modificado con óxido de grafeno reducido, obteniéndose la configuración HOOC-Phe-rGO/GCE (ver Figura 60) a la que se une covalentemente el anticuerpo de captura. Después se establece un esquema de inmunoensayo competitivo empleando PYY y Biotin-PYY y el diseño se completa con un conjugado de estreptavidina marcada con fosfatasa alcalina (AP-Strept).

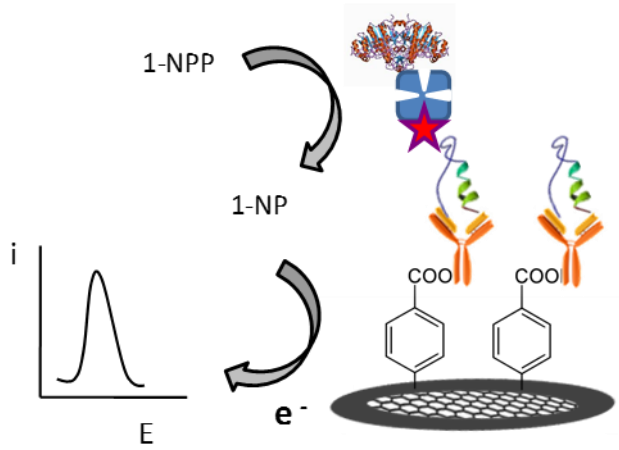

Figura 60.- *Esquema y modo de detección del inmunosensor de PYY.*

5.2.1.2. Optimización de las variables experimentales

La puesta a punto del inmunosensor AP-Strept-Biotin-PYY(PYY)-anti-PYY-Phe-rGO/ GCE requiere una cuidadosa selección de las variables experimentales implicadas en: a) la preparación de los electrodos modificados, y b) la preparación del inmunosensor propiamente dicho. A continuación se describen los estudios de optimización realizados con el objetivo de alcanzar la máxima sensibilidad y un amplio intervalo lineal en el calibrado para la detección del analito.

5.2.1.2.1. Preparación de los electrodos modificados

Las etapas implicadas en la preparación de los electrodos modificados son las siguientes: 1. Obtención del óxido de grafeno reducido (rGO); 2. Preparación de rGO/GCEs; 3. Diazotación de *p*-ABA; 4. *Grafting* electroquímico.

1. Obtención del óxido de grafeno reducido (rGO)

El óxido de grafeno reducido (rGO) se obtuvo a partir de óxido de grafeno (GO) sguiendo el procedimiento descrito en el Apartado 4.4.3. de la Parte Experimental, que se basa en el uso de ácido ascórbico como agente reductor. La elección de este ácido se debe a su demostrada eficiencia en este tipo de reacciones [Fernández-Merino et al., 2010], y a la ventaja de que se trata de un producto natural cuya utilización evita la de otros reactivos tóxicos, como la hidrazina, la hidroxilamina o el borohidruro sódico, usualmente empleados con esta finalidad. Además, como es sabido, las propiedades electrónicas del rGO pueden ser ajustadas en función del grado de reducción del material [Lahaye et al., 2009] y el empleo de un reactivo de un poder reductor medio facilita la optimización de las condiciones experimentales de la reacción para obtener las mejores propiedades electrocatalíticas del producto [Liu et al., 2014].

Se caracterizó el rGO obtenido mediante espectrofotometría UV-visible con los resultados que se han representado en la Figura 61.

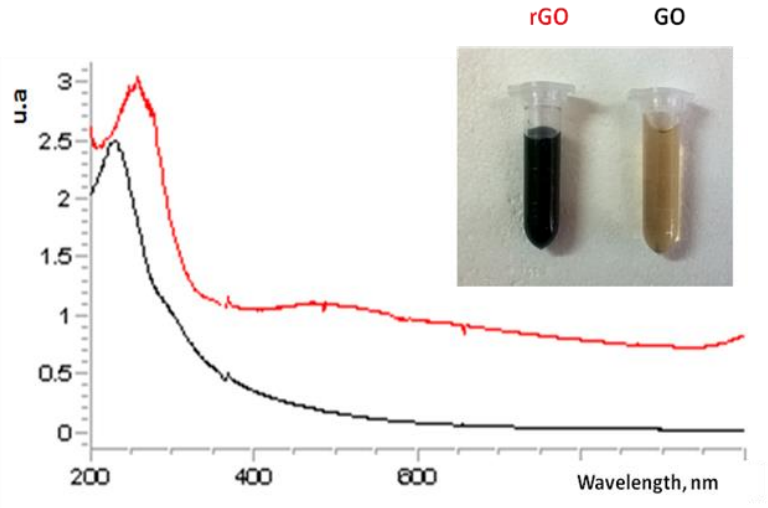

Figura 61.- *Espectros UV-visible y fotografías de GO y rGO en suspensión acuosa*

Como puede observarse, el espectro de GO muestra dos bandas a 230 y 300 nm que corresponden a las transiciones π→π* y n→π*, respectivamente [Sharma et al., 2013]. Tras la reducción a rGO, la segunda desaparece y se produce un desplazamiento batocrómico de la banda π→π* a 241 nm. La posición de esta última se emplea como una prueba del grado de reducción obtenido empleando diferentes reactivos reductores [Fernández-Merino et al., 2010]. Por otro lado, las suspensiones acuosas del rGO son claramente distintas de las de GO y presentan una elevada estabilidad, manteniéndose sin precipitar durante al menos dos semanas. Estos resultados demuestran la eficiencia del método de reducción con ácido ascórbico.

2. Preparación de rGO/GCEs

Los electrodos de carbono vitrificado se modifican simplemente por adición de un pequeño volumen de la suspensión anterior, dejando secar a temperatura ambiente. La cantidad de rGO depositada se optimizó incorporando cada vez sobre el GCE, 10 µL de diferentes suspensiones conteniendo concentraciones distintas de rGO en el intervalo de 0.25 y 1.0 mg/mL Después, a partir de estos electrodos se prepararon varios inmunosensores mediante el procedimiento descrito en el Apartado 4.4.3. de la Parte Experimental, que implica el *grafting* electroquímico de la sal de diazonio del *p*-ABA sobre rGO/GCE y la aplicación de las sucesivas etapas de modificación y de medida que se indican en la Figura 62. En ella se han representado las respuestas específicas e inespecíficas (en ausencia de anti-PYY), así como la relación entre ambas (S/N).

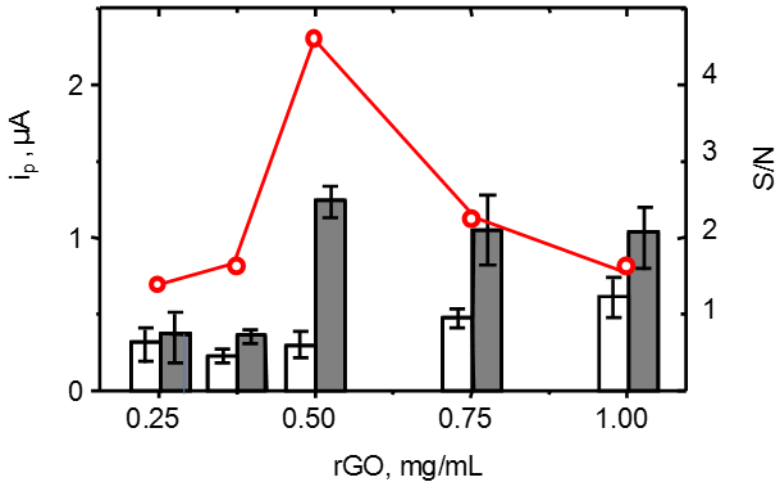

Figura 62.- *Efecto de la cantidad de rGO depositada sobre el GCE en la respuesta del inmunosensor AP-Strept-Biotin-PYY-anti-PYY-Phe-rGO/GCE preparado en ausencia de PYY. 0 µg/mL (blanco) ó 30 µg/mL (gris) anti-PYY, 120 min; BSA 0.1%, 60 min; 100 ng/mL Biotin-PYY, 60 min; 5 µg/mL AP-Strept, 60 min.*

Como puede observarse, la mayor señal específica se alcanza para 0.5 mg/mL de rGO, con una ligera disminución para concentraciones superiores al tiempo que aumenta apreciablemente la señal inespecífica. Estos resultados han llevado a elegir la concentración indicada para la preparación del electrodo.

3. Diazotación de *p*-ABA

Como se ha señalado en la Parte Experimental, de forma independiente a la preparación de los electrodos modificados rGO/GCE se procede a realizar la reacción de diazotación del *p*-ABA en las condiciones indicadas. Se optimizó la concentración de *p*-ABA utilizada en esta reacción con el objetivo de obtener una cantidad adecuada de sal de diazonio para la modificación posterior del electrodo mediante *grafting* electroquímico. En la Figura 63a se han representado los resultados obtenidos en la medida de la respuesta de inmunosensores preparados como en el apartado anterior, utilizando tres concentraciones de *p*-ABA, 10, 20 y 30 mg/mL. Como puede observarse, la mejor relación S/N se obtuvo para una concentración de 20 mg/mL de *p*-ABA. Esta concentración debe proporcionar el adecuado número de radicales carboxifenilo en la superficie del electrodo como para lograr la inmovilización de la cantidad óptima de anticuerpo de captura.

4. *Grafting* electroquímico

Finalmente se optimizaron las condiciones de preparación del radical carboxifenilo y su incorporación a la superficie del electrodo mediante voltamperometría cíclica, estudiando la influencia del número de ciclos de potencial y de la velocidad de barrido de potencial, con los resultados representados, respectivamente, en las Figuras 63b y 63c. Puede apreciarse cómo la mayor relación S/N se obtiene para 10 ciclos, disminuyendo la magnitud de las respuestas electroquímicas para un número más elevado debido probablemente a la menor conductividad del electrodo al aumentar en exceso los grupos carboxilo sobre su superficie. Respecto a la velocidad de barrido de potencial, los mejores resultados se obtuvieron para v = 200 mV/s.

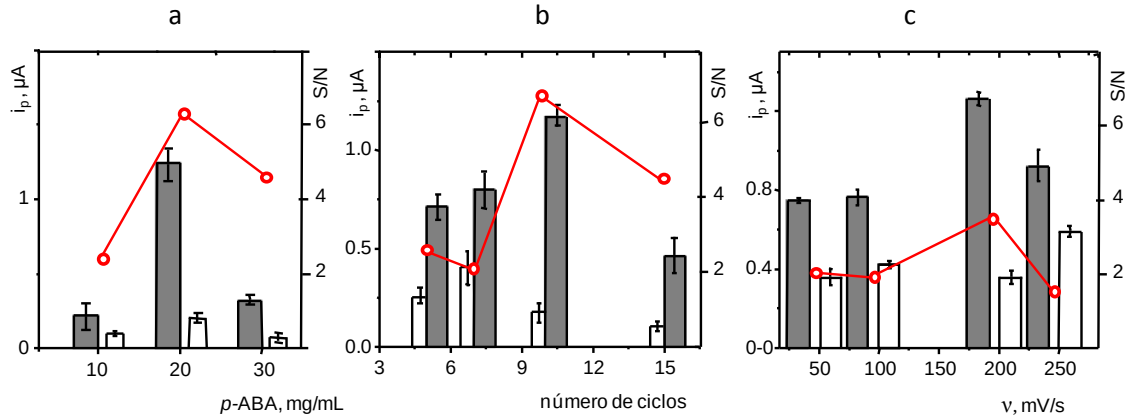

Figura 63.- *Efecto de (a) la concentración de p-ABA, (b) el número de ciclos, y (c) la velocidad de barrido de potencial en la respuesta del inmunosensor AP-Strept-Biotin-PYY(PYY)-anti-PYY-Phe-rGO/GCE preparado en ausencia de PYY. 0 µg/mL (blanco) ó 30 µg/mL (gris) anti-PYY, 120 min; BSA 0.1%, 60 min; 100 ng/mL Biotin-PYY, 60 min; 5 µg/mL AP-Strept, 60 min.*

5.2.1.2.2. Caracterización de la superficie electródica modificada

Una vez preparados, los electrodos modificados con rGO y con el catión diazonio de *p*-ABA se caracterizaron por voltamperometría cíclica (CV) y espectroscopia de impedancia electroquímica (EIS) empleando disoluciones de $Fe(CN)_6^{3-/4-}$ 5 mM en KCl 0.1 M. En la Figura 64a se muestran los voltamperogramas cíclicos registrados sobre el electrodo sin modificar (1) y los electrodos modificados con rGO (2), HOOC-Phe-rGO/GCE (3), y este mismo electrodo una vez activados los grupos carboxílico con el sistema EDC/NHSS (4). Según se aprecia, las corrrientes anódica y catódica sobre el electrodo rGO/GCE (curva 2) son ligeramente superiores a las del GCE (curva 1), obteniéndose las siguientes intensidades de pico: i_{pa} = 109 µA, i_{pc}= 105 µA sobre rGO/GCE, frente a i_{pa} = 98, µA i_{pc}= 91 µA sobre GCE. Como puede observarse, estas corrientes son muy parecidas entre sí, como corresponde al comportamiento cuasi-reversible del sistema electroactivo empleado sobre estos electrodos. Además, en ambos casos, los potenciales de pico anódico y catódico aparecen próximos entre sí, siendo $\Delta E = E_{pa} - E_{pc}$ = 123 mV (rGO/GCE) y 154 mV (GCE). Estos resultados son consecuencia de la elevada conductividad de las superficies electródicas utilizadas, si bien la presencia de rGO, muy conductor, en el electrodo modificado, unido al efecto de difusión a través de los poros de este material, contribuyen a aumentar ligeramente la respuesta electroquímica [Punckt et al., 2013].

El voltamperograma cíclico obtenido tras la aplicación de la etapa de *electrografting* (curva 3) pone de manifiesto el peor comportamiento del sistema $Fe(CN)_6^{3-/4-}$ sobre el electrodo HOOC-Phe-rGO/GCE. Este resultado es consecuencia del aumento de la resistencia a la transferencia de carga sobre la superficie modificada, así como a la repulsión electrostática existente entre la especie electroactiva en disolución y las cargas negativas presentes en el electrodo debido a la disociación de los grupos carboxílico al pH de trabajo. Sin embargo, cuando estos grupos se activan empleando los reactivos EDC y NHSS, se obtiene un voltamperograma mejor definido (curva 4), al menos en la región anódica, como consecuencia de la neutralización de las cargas negativas del electrodo.

Como puede apreciarse en la Figura 64b, los resultados obtenidos por voltamperometría cíclica se confirman mediante aplicación de la técnica EIS. En efecto, los semicírculos que aparecen en los espectros de Nyquist evidencian que la resistencia a la transferencia de carga (R_{CT}) es mucho menor en el electrodo rGO/GCE. Dicha resistencia aumenta solo ligeramente en el electrodo sin modificar, pasando a ser mucho más alta sobre el electrodo HOOC-Phe-rGO/GCE y disminuyendo tras la activación de los grupos carboxilo por las razones ya expuestas. Como conclusión a estos estudios cabe decir que los resultados obtenidos confirman la eficiencia del método de *grafting* electroquímico para la modificación del electrodo.

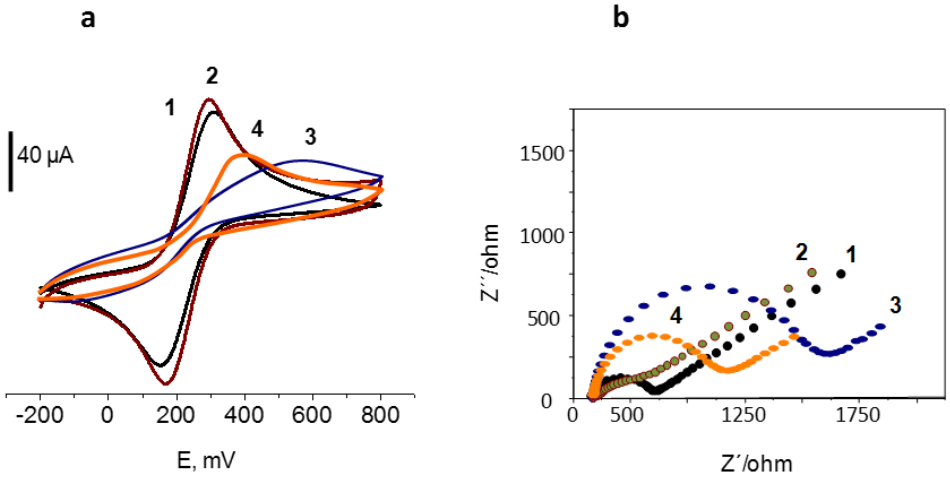

Figura 64. *Voltamperogramas cíclicos (a) y espectros de impedancia (b) obtenidos para: (1) GCE; (2) rGO/GCE; (3) HOOC-Phe-rGO/GCE y (4) HOOC-Phe-rGO/GCE activado con EDC/NHSS. $Fe(CN)_6^{3-/4-}$ 5 mM en KCl 0.1 M*

5.2.1.2.3. Preparación del inmunosensor

Una vez optimizadas las condiciones de preparación del electrodo HOOC-Phe-rGO/GCE, se investigó el efecto de las variables experimentales implicadas en la construcción y el funcionamiento del inmunosensor. En este caso, teniendo en cuenta la elevada conductividad de la superficie electródica, se buscó la mejor relación entre las respuestas específica e inespecífica considerando como tales, respectivamente, la corriente en presencia o ausencia de antígeno biotinilado y, en todos los casos, en ausencia de analito. De este modo, fue posible evaluar de forma más eficaz la existencia de señales debidas a procesos electroquímicos sobre el electrodo y lograr una mejor optimización del bloqueo de su superficie.

- ***Influencia de la concentración y el tiempo de incubación del anticuerpo de captura***

El anticuerpo de captura, anti-PYY, se inmoviliza sobre la superficie del electrodo HOOC-Phe-rGO/GCE mediante unión covalente previa activación de los grupos carboxilo con el sistema EDC/NHSS. Las condiciones experimentales de la activación fueron las mismas que se habían utilizado en otros trabajos anteriores [Moreno-Guzmán et al., 2012], aunque empleando el reactivo N-hidroxisulfo-succinimida, NHSS, más soluble en agua que el equivalente N-hidroxisuccinimida, NHS. Para estudiar el efecto sobre la respuesta del inmunosensor de la cantidad de anti-PYY inmovilizada, se registraron los voltamperogramas en diferencial de impulsos empleando distintos inmunosensores preparados con concentraciones de anticuerpo entre 5 y 30 µg/mL. Los resultados obtenidos se han representado en la Figura 65, en la que se indica también el resto de condiciones experimentales empleadas en la preparación de los inmunosensores.

Como puede observarse (Figura 65a), las respuestas específicas aumentan a medida que lo hace la concentración de anti-PYY hasta 20 µg/mL, manteniéndose prácticamente constantes para concentraciones superiores. Por otro lado, las respuestas inespecíficas se mantienen en un valor relativamente bajo sin modificarse apreciablemente en todo el intervalo estudiado. De acuerdo con estos resultados, se eligió la concentración citada para estudios posteriores. Pueden observarse también (Figura 65b) los resultados obtenidos en el estudio de la influencia del tiempo de incubación del anticuerpo de captura sobre el electrodo HOOC-Phe-rGO/GCE previamente activado, que ponen de manifiesto que un periodo de 60 minutos es el más adecuado por proporcionar la mayor relación S/N.

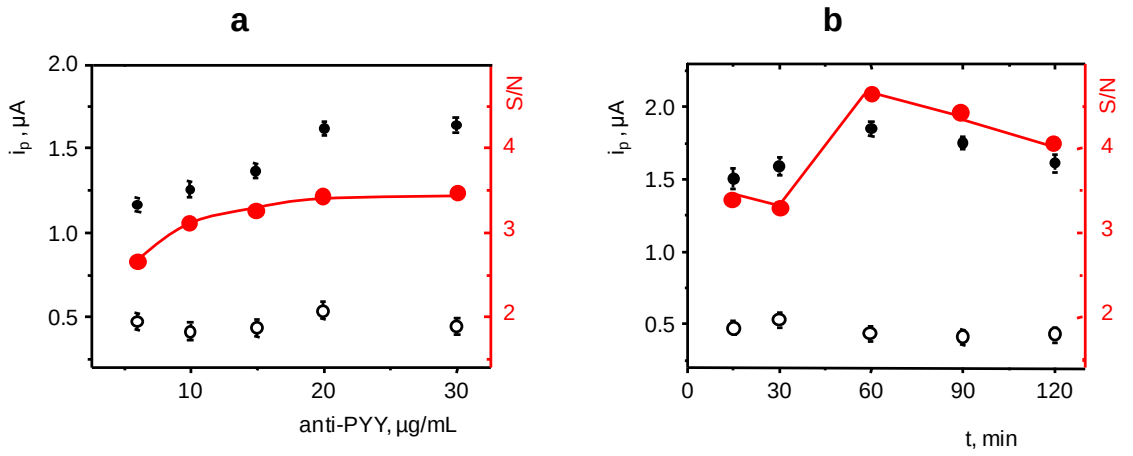

Figura 65.- *Influencia de la concentración (a) y del tiempo de incubación (b) del anticuerpo de captura sobre la respuesta del inmunosensor AP-Strept-Biotin-PYY-anti-PYY-Phe-rGO/GCE: 5 - 30 µg/mL anti-PYY, 120 min (a); 20 µg/mL anti-PYY, 15 - 120 min; 0.1% BSA, 60 min; 0 (o) 100 (●) ng/mL Biotin-PYY, 60 min; 5 µg/mL AP-Strept, 60 min. Todas las etapas de incubación se realizaron a 37 ^{o}C.*

- ***Optimización de la etapa de bloqueo***

En las condiciones elegidas en la etapa anterior, se estudió el tipo de agente bloqueante a utilizar para minimizar las señales inespecíficas sobre el electrodo, así como su concentración y el tiempo de bloqueo. Aunque en los estudios anteriores se empleó una disolución de BSA al 0.1%, en este apartado se evaluó la eficacia de otros dos reactivos usados con frecuencia para esta aplicación: etanolamina y caseína. Se añadieron cada vez 10 µL de la disolución al 0.1% de cada bloqueante sobre el anti-PYY-Phe-rGO/GCE dejando incubar 60 min a 37 ºC. Los resultados, representados en la Figura 66a muestran señales anormalmente altas en presencia de etanolamina, probablemente debido a la inestabilidad del electrodo, así como resultados parecidos empleando BSA y caseína. Sin embargo, la relación S/N es mayor cuando se utiliza este último agente bloqueante, por lo que se eligió la caseína para estudios posteriores. Por otro lado, como se muestra en la Figura 66b, la concentración más adecuada de caseína fue del 0.2%, por proporcionar la mayor relación S/N. Esto mismo ocurre cuando se utiliza un tiempo de incubación de 60 minutos (Figura 66c).

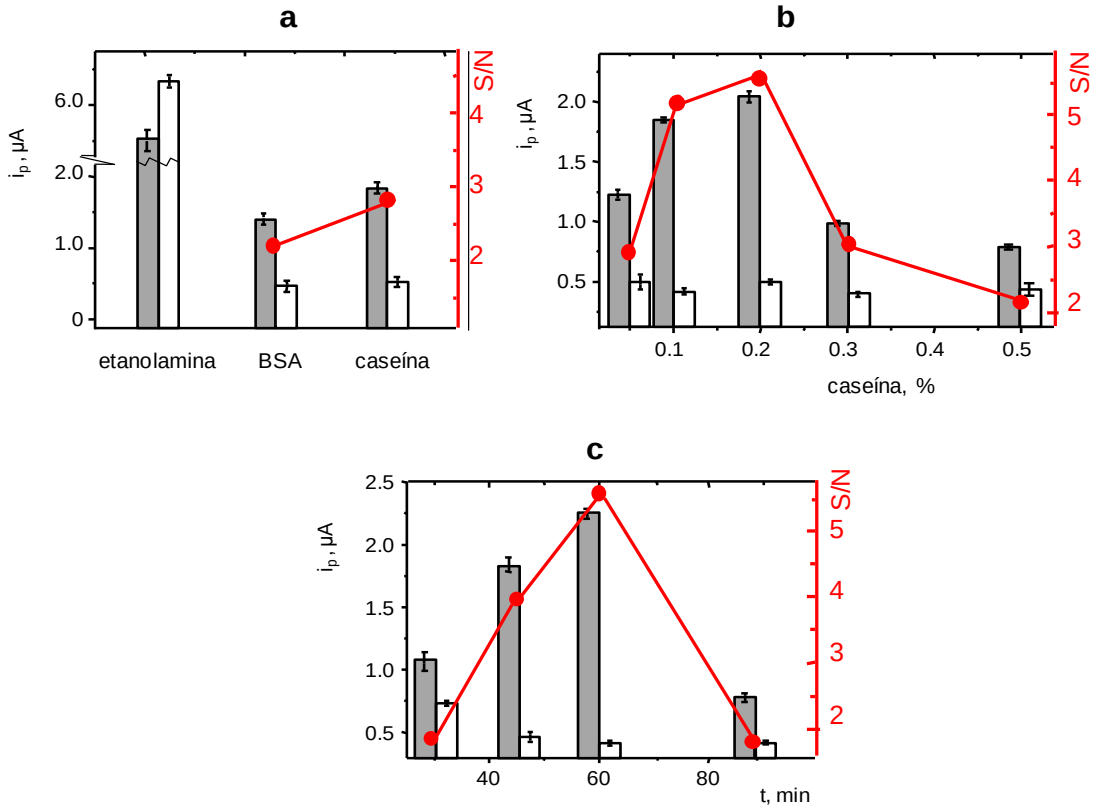

Figura 66.- *Influencia del tipo de agente bloqueante (a), la concentración de caseína (b) y el tiempo de bloqueo (c) sobre la respuesta del inmunosensor AP-Strept-Biotin-PYY-anti-PYY-Phe-rGO/GCE: 20 µg/mL anti-PYY, 60 min; 0.1% agente bloqueante (a); 0.05- 0.5% caseína (b), 60 min (a,b); 0.2% caseína, 20-90 min (c); 0 (blanco) 100 (gris) ng/mL Biotin-PYY, 60 min; 5 µg/mL AP-Strept, 60 min.*

- ***Influencia de la concentración y el tiempo de incubación del antígeno biotinilado***

Para estudiar la influencia de la concentración de antígeno biotinilado, se prepararon varios inmunosensores AP-Strept-Biotin-PYY-anti-PYY-Phe-rGO/GCE incubando el conjugado antti-PYY-Phe-rGO/GCEs en disoluciones de Biotin-PYY a diferentes cioncentraciones en el intervalo de 50 a 400 ng/mL. Como se observa en la Figura 67a, la corriente de pico en DPV aumenta rápidamente con la concentración del bioconjugado hasta 100 ng/mL, permaneciendo prácticamente constante a continuación. Puede verse un comportamiento similar en los valores de la relación S/N ya que en este caso, la respuesta inespecífica adopta un único valor, correspondiente a 0 ng/mL Biotin-PYY. Teniendo en cuenta estos resultados, se eligió la concentración indicada, 100 ng/mL, como la más adecuada para la preparación del inmunosensor. Por otro lado, el tiempo de incubación del conjugado (Figura 67b) exhibe un comportamiento parecido al anterior, encontrándose que 30 min era un periodo suficiente por lo que se seleccionó como óptimo.

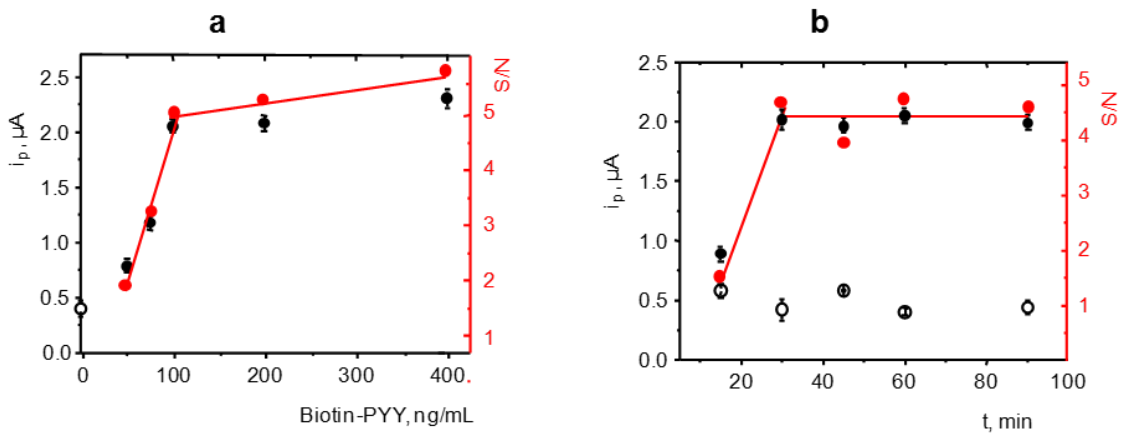

Figura 67.- *Influencia de la concentración de Biotin-PYY (a) y del tiempo de incubación (b) sobre la respuesta del inmunosensor AP-Strept-Biotin-PYY-anti-PYY-Phe-rGO/GCE: 20 µg/mL anti-PYY, 60 min; 0.1% agente bloqueante (a); 0.05 - 0.5% caseína (b), 60 min (a,b); 0.2% caseína, 60 min; 0 (o), 50 - 400 (●) ng/mL Biotin-PYY, 60 min (a); 0 (o), 100 (●) ng/mL Biotin-PYY, 15 - 90 min (b); 5 µg/mL AP-Strept, 60 min; (o)*

- ***Influencia de la concentración y el tiempo de incubación del conjugado AP-Strept***

Con el fin de elegir las mejores condiciones para obtener una buena sensibilidad y un amplio intervalo lineal en el calibrado, se llevó a cabo el estudio del efecto de la concentración de AP-Strept sobre la respuesta del inmunosensor por medida de diferentes disoluciones conteniendo PYY entre 10^{-6} (ó 10^{-7}) y 10^{3} ng/mL con inmunosensores preparados con 7.0, 5.0 y 2.5 µg/mL AP-Strept. Como se muestra en la Figura 68a, la máxima concentración de conjugado AP-Strept (●) no proporciona un calibrado útil para la determinación de PYY debido probablemente a la saturación del bioelectrodo y la consiguiente disminución de la conductividad. Por otro lado, cuando se emplea una concentración de conjugado de 2.5 µg/mL (●), se obtienen respuestas que varían con la concentración de PYY en un intervalo relativamente amplio. Sin embargo, la pendiente del calibrado en la porción recta del mismo es más alta cuando se utiliza una concentración de 5.0 µg/mL de AP-Strept (o), por lo que este valor fue elegido para la preparación del inmunosensor. Por último, respecto al tiempo de incubación de esta proteína marcada, se observó que un periodo de 30 min era apropiado, proporcionando una elevada corriente de pico y una pequeña contirbución a la respuesta inespecífica (Figura 68b).

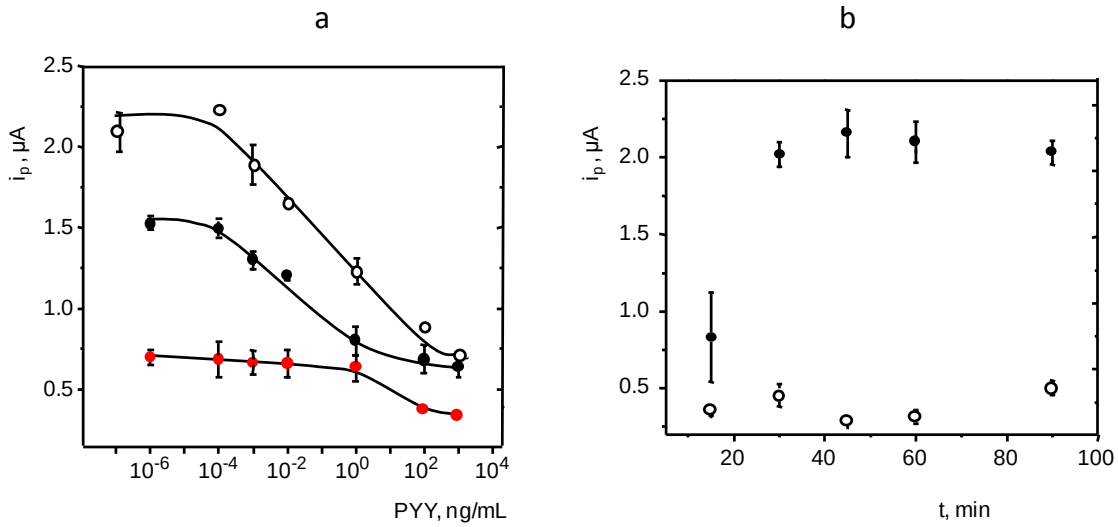

Figure 68.- *Influencia de la concentración de AP-Strept (a) y del tiempo de incubación (b) sobre la respuesta del inmunosensor AP-Strept-Biotin-PYY-anti-PYY-Phe-rGO/ GCE: 20 µg/mL anti-PYY, 60 min; 0.2 % caseína, 60 min; 10^{-6} (ó 10^{-7}) - 10^{3} ng/mL PYY (a); 0 ng/mL PYY (b), 100 ng/mL Biotin-PYY, 60 min; 7.0 (● a), 5 (o a), y 2.5 (● a) µg/mL AP-Strept, 60 min (a), 5 µg/mL AP-Strept (b, 15 - 90 min.*

- ***Influencia de la concentración de 1-NPP y el tiempo de reacción***

Se utilizó 1-NPP como sustrato de la enzima fosfatasa alcalina, estudiándose el efecto de su concentración sobre la respuesta del inmunosensor por medida de voltamperogramas en diferencial de impulsos de disoluciones que contenían diferentes concentraciones de este arilfosfato en el intervalo de 0 a 10 mM (Figura 69a) con inmunosensores preparados en ausencia de PYY. Como puede observarse, la intensidad de pico alcanza valores prácticamente constantes a partir de una concentración 1 mM, siendo ligeramente más alta para 1-NPP 5 mM, que fue el valor escogido. Esta concentración es suficientemente alta como para asegurar que la velocidad de la reacción enzimática dependerá exclusivamente de la concentración de la enzima. Por otro lado, la Figura 69b pone de manifiesto que un tiempo de 5 min es suficiente para que tenga lugar la reacción catalizada por la fosfatasa alcalina.

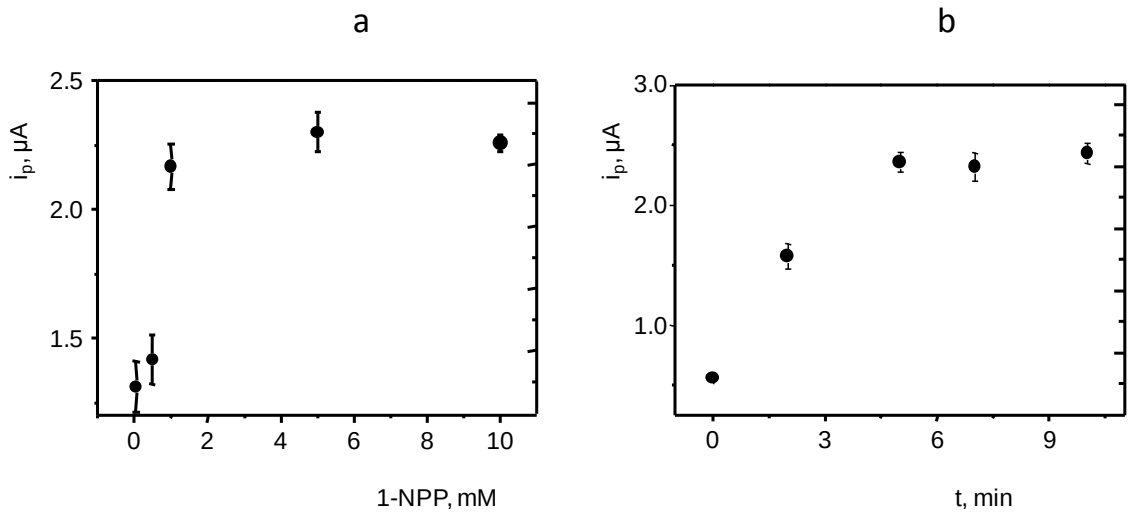

Figure 69.- *Influencia de la concentración de 1-NPP (a) y del tiempo de reacción (b) sobre la respuesta del inmunosensor AP-Strept-Biotin-PYY-anti-PYY-Phe-rGO/ GCE: 20 µg/mL anti-PYY, 60 min; 0.2% caseína, 60 min; 100 ng/mL Biotin-PYY, 60 min; 5 µg/mL AP-Strept, 60 min; 0 - 10 mM 1-NPP, 5 min (a); 1 mM 1-NPP, 0 - 12 min.*

Una vez optimizadas las variables experimentales implicadas en la preparación de los electrodos modificados y en la construcción y el funcionamiento del inmunosensor, como resumen, en la Tabla 15 se recogen dichas variables, los intervalos estudiados y los valores óptimos elegidos en cada caso.

5.2.1.3. Calibrado y características analíticas

El calibrado para la determinación de PYY se ha representado en la Figura 70 junto con algunos de los voltamperogramas en diferencial de impulsos registrados para su obtención. Se trata, como era de esperar según la configuración desarrollada, de una curva sigmoidal decreciente, en la que la variación de la corriente de pico en DPV en función del logaritmo de la concentración de analito se ajusta, de acuerdo con un modelo de regresión no lineal, en el intervalo de 10^{-7} a 10^{4} ng/mL, a la siguiente ecuación (r = 0.995):

$$i_p = i_{\min} + \frac{i_{max} - i_{min}}{1 + \left(\frac{x}{EC_{50}}\right)^{-h}}$$

Esta ecuación tiene la misma forma que la obtenida anteriormente para el calibrado de la GHRL con el magnetoinmunosensor.

Tabla 15.- *Optimización de las variables implicadas en la preparación de los electrodos modificados y en la construcción y el funcionamiento del immunosensor AP-Strept-Biotin-PYY-anti-PYY-Phe-rGO/GCE*

Variable	Intervalo/reactivo estudiado	Valor seleccionado
rGO, mg/mL	0.25 - 1.0	0.5
***p*-ABA, mg/mL**	10 - 30	20
número de ciclos	5 - 15	10
Velocidad de barrido de potencial, mV/s	50 - 250	200
anti-PYY, µg/mL	5 - 30	20
tiempo incubación anti-PYY, min	15 - 120	60
tipo de agente bloqueante	etanolamina, BSA, caseína	caseína
caseína, %	0.05 - 0.5	0.2
tiempo de bloqueo, min	30 - 90	60
Biotin-PYY, ng/mL	50 - 400	100
tiempo incubación Biotin-PYY, min	15 - 90	30
AP-Strept, µg/mL	2.5 – 7	5
tiempo incubación AP-Strept, min	15 - 90	30
1-NPP, mM	0 - 10	1
tiempo de reacción, min	0 - 12	5

En el caso del PYY, los parámetros de la misma son los siguientes: i_{max} e i_{min}, corrientes de pico máxima y mímina del calibrado: 2.40 ± 0.09 µA y 0.57 ± 0.08 µA, respectivamente; el valor de EC_{50} correspondiente a la concentración de PYY para un 50% de competición, es 0.08 ng/mL, y la pendiente de Hill, h= -0.24 ± 0.04. Por otro lado, en la región central de la curva se observa un intervalo en el que la corriente de pico está relacionada linealmente con el logaritmo de la concentración de analito ($i_p \propto \log$ [PYY], r = 0.995) entre 10^{-4} y 10^{2} ng/mL de PYY, con una pendiente de -0.198 ± 0.002 µA por década de concentración. Este intervalo es adecuado para la aplicación del inmunosensor al análisis de muestras de suero, en las que la concentración esperable de esta hormona está situada en torno a 100 pg/mL [Mentlein et al., 1993] [Cahill et al., 2014].

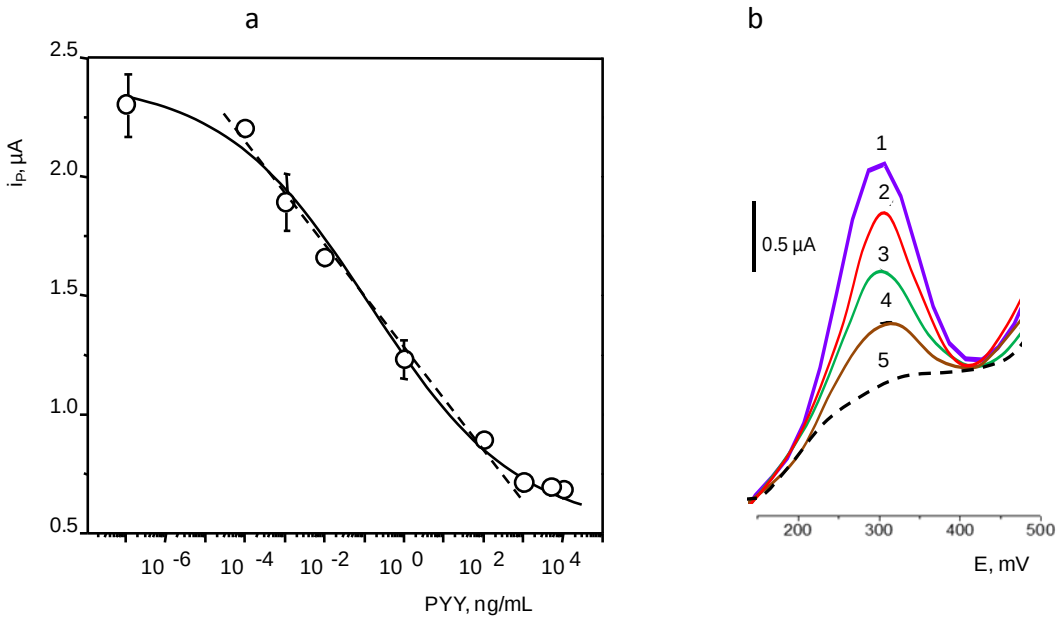

Figura 70.- *Calibrado para la determinación de PYY con el inmunosensor AP-Strept-Biotin-PYY(PYY)-anti-PYY-Phe/rGO/GCE (a), y voltamperogramas en DPV (b) para: 1) 0; 2) 0.01; 3)1.0; 4) 5.0 x 10^4 ng/mL PYY; 5) respuesta inespecífica.*

El límite de detección se determinó empleando la ecuación:

$$LOD = EC_{50}\left(\frac{i_{max} - i_{min}}{i_{max} - i_{min} - 3s} - 1\right)^{-1/h}$$

en la que s es la desviación estándar (n=10) de la corriente de pico medida en ausencia de PYY, ± 0.06 µA. El valor obtenido, 0.01 pg/mL PYY, es mucho menor que la concentración mínima detectable utilizando los kits ELISA comerciales (ver Tabla 6 en la Introducción). Por ejemplo, el valor mínimo encontrado, 0.48 pg/mL [www.antibodies-online.com/kit/414478/Peptide+YY+ ELISA+Kit/] es aproximadamente 50 veces mayor que el obtenido con el inmunosensor. Además, en el intervalo dinámico es mucho más estrecho, así, el kit citado anteriormente, abarca tan solo dos márgenes de concentración (aproximadamente entre 10^{-3} y 0.1 ng/mL). Por otro lado, los tiempos de ensayo son superiores, en general, al requerido para la aplicación del inmunosensor (aproximadamente 2 horas a partir de la inmovilización de anti-PYY), con 3 a 5 h, como se ha señalado, o incluso necesitando tiempos de incubación de más de 20 h.

La reproducibilidad de las medidas realizadas con el inmunosensor se evaluó llevando a cabo ensayos con diferentes inmunosensores en el mismo y en diferentes días, empleando disoluciones preparadas en ausencia y en presencia de 1 ng/mL de PYY. Los valores de RSD obtenidos fueron respectivamente del 4.0 y el 5% (n=5) para

las medidas realizadas el mismo día, y del 5.5% y el 3.2% en diferentes días. Estos resultados revelan la buena precisión alcanzada en la preparación y funcionamiento de la configuración desarrollada. Además, estos valores son muy inferiores a los que proporcionan los kits ELISA, que en general se sitúan en torno al 10 o 15%. Finalmente, otra ventaja del inmunosensor voltamperométrico es que la superficie del electrodo de carbono vitrificado es fácilmente regenerable mediante pulido con alúmina de 3 μm de diámetro durante 1 min, seguido de su enjuague con agua y metanol aplicando agitación ultrasónica y secado bajo radiación IR.

En la Figura 71 se ha representado el gráfico de control construido con el fin de evaluar la estabilidad de almacenamiento del conjugado anti-PYY-Phe-rGO/GCE. Se prepararon varios conjugados el mismo día y se almacenaron a 4 ºC, para posteriormente construir el inmunosensor cada día con uno de ellos y emplearlo para medir la respuesta voltamperométrica en ausencia de PYY. Como puede observarse, las corrientes de pico permanecen entre los límites situados a ± 3 s, siendo s la desviación estándar de las respuestas obtenidas el primer día de trabajo, durante al menos 12 días, máximo periodo de tiempo estudiado.

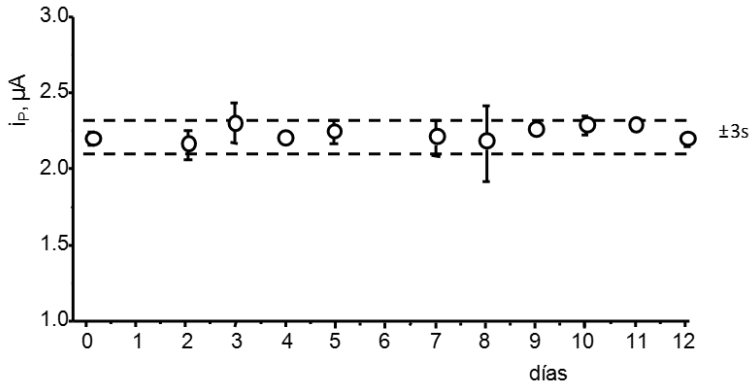

Figura 71.- *Grafico de control para la evaluación de la estabilidad de almacenamiento del conjugado anti-PYY-Phe-rGO/GCE*

5.2.1.4. Estudios de selectividad

Se investigó la influencia varias proteínas, adiponectina (APN), grelina (GHRL), grelina desacilada (da-GHRL), insulina (INS), hormona del crecimiento humana (hGH), y hormona estimulante del folículo (FSH), sobre la respuesta del inmunosensor para la determinaciòn de PYY. Para realizar este estudio se comparó la respuesta voltamperométrica en ausencia de analito con las obtenidas en presencia de cada

compuesto investigado como posible interferencia, a una concentración de 1 μg/mL. Como puede observarse en la Figura 72, no existen diferencias significativas entre las señales obtenidas, lo que demuestra la elevada selectividad del diseño propuesto para la determinación de PYY.

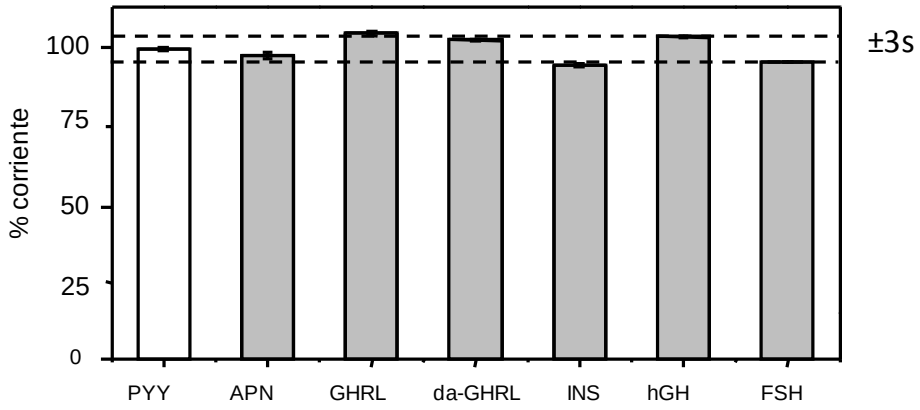

Figura 72.- *Efecto de la presencia de 1 μg/mL de diferentes hormonas en la respuesta voltamperométrica del inmunosensor en ausencia de PYY*

5.2.1.5. Aplicación a la determinación de PYY en suero

El inmunosensor AP-Strept-Biotin-PYY(PYY)-anti-PYY-Phe-rGO/GCE se aplicó a la determinación de la hormona en suero donde, como se ha señalado, los niveles esperables se sitúan al nivel de 100 pg/mL [Mentlein et al., 1993] [Cahill et al., 2014]. Se utilizó el procedimiento descrito en el Apartado 4.4.3. de la Parte Experimental, con 5 μL de la muestra previamente contaminada a la que se añadían 5 μL de Biotin-PYY de 100 ng/mL, incubando posteriormente sobre el conjugado anti-PYY-Phe-rGO/GCE. En primer lugar, se estudió la posibilidad de existencia de efecto matriz en las condiciones indicadas. Para ello se construyó un calibrado en el intervalo lineal de concentraciones de PYY empleando muestras de suero contaminadas con diferentes concentraciones de la hormona a las que se aplicó dicho procedimiento. La pendiente del calibrado fue -0.19 ± 0.01 μA por década de concentración, valor muy parecido al obtenido empleando disoluciones patrón de PYY, -0.198 ± 0.002 μA (ver Figura 73). La comparación entre ambas, aplicando el ensayo de la t de Student, con t_{exp} = 0.853 frente a t_{tab} = 3.355, para n=8, y P=0.05, permitió comprobar la equivalencia estadística de las dos pendientes, lo que descarta la exitencia de efecto matriz, siendo posible, como en otros casos, la determinación directa de PYY en el suero por interpolación de la corriente de pico en DPV en el calibrado de patrones.

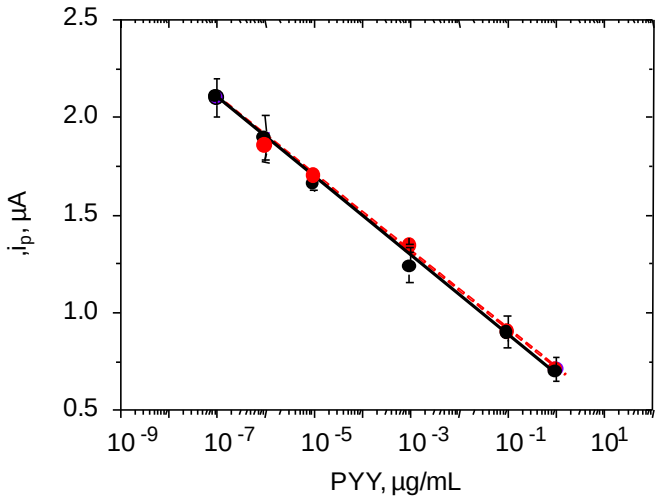

Figura 73.- *Calibrados obtenidos para disoluciones patrón de PYY (——) y para muestras de suero (- - -)*

Los resultados obtenidos se han resumido en la Tabla 16. Como puede observarse, las recuperaciones alcanzadas se encuentran a niveles próximos al 100% en todos los casos, lo que pone de manifiesto la utilidad analítica del inmunosensor para este tipo de muestras.

Tabla 16.- *Determinación de PYY en suero con el inmunosensor AP-Strept-Biotin-PYY(PYY)- anti-PYY- Phe-rGO / SPCE*

PYY añadido, pg/mL	PYY encontrado, pg/mL	Recuperación media, %
0.35	0.348 ± 0.007*	99 ± 2
3.5	3.62 ± 0.06	102 ± 2
35	35 ± 1	99 ± 3

* ± ts / √n

5.2.1.6. Conclusiones

En este trabajo se ha desarrollado el primer inmunosensor electroquímico para la determinación de la hormona anorexígena PYY. Este diseño implica el empleo de electrodos modificados con rGO y funcionalizados mediante *electrografting* con la sal de diazonio del *p*-ABA como plataformas para la inmovilización covalente del anticuerpo específico anti-PYY. El inmunosensor ha demostrado un excelente comportamiento analítico proporcionando calibrados con un amplio intervalo lineal adecuado para la determinación de PYY en muestras clínicas. El bajo límite de detección alcanzado, 0.01 pg/mL, el breve tiempo de análisis y su elevada precisión mejoran notablemente las características analíticas de los kits ELISA disponibles para esta determinación.

5.2.2. INMUNOSENSOR DUAL PARA LA DETERMINACIÓN SIMULTÁNEA DE GHRL y PYY

Como se ha visto en la Introducción, entre las diversas hormonas implicadas en la compleja regulación del apetito y la saciedad, la grelina y el péptido YY son relevantes debido a su importante papel a nivel de hipotálamo y circulación periférica [Kojima et al., 1999] [Batterham et al., 2003]. Ambas poseen actividad contrapuesta, la GHRL como estimulante del apetito, y el PYY como limitante de la ingesta de alimentos y el consumo de calorías.

En los capítulos anteriores se ha puesto de manifiesto la escasez de métodos disponibles para la determinación de estas hormonas tanto de forma individual como conjunta. Sobre esta base, tal como se ha descrito, se concibió la idea de desarrollar un magnetoinmunosensor para GHRL, así como, posteriormente, una plataforma inmunosensora integrada para PYY. Sin embargo, en el seguimiento de los trastornos del apetito, la obesidad y enfermedades relacionadas, la monitorización de más de una especie implicada en el proceso es enormemente valiosa debido al volumen de información que se obtiene. Por ello, dada su importancia, en este trabajo se puso a punto un inmunosensor electroquímico para la determinación simultánea de GHRL y PYY que satisface los requisitos de sensibilidad, selectividad y reproducibilidad para su aplicación al análisis de muestras clínicas. Debido a las ventajas que ofrece el empleo de electrodos serigrafiados para el diseño de configuraciones multiplex, así como a la simplicidad y efectividad del método de *grafting* electroquímico, unido a la elevada conductividad del rGO, se eligió esta estrategia, ya establecida en el capítulo anterior, para desarrollar la configuración que se describe a continuación, basada en el empleo de electrodos serigrafiados de carbono duales (dSPCEs) modificados con rGO y funcionalizados mediante *electrografting* con la sal de diazonio del *p*-ABA, para la inmovilización de los anticuerpos de captura.

Es importante destacar que el inmunosensor fue empleado para la determinación de ambas hormonas en suero y en saliva, demostrando así su utilidad para el análisis de muestras de interés clínico.

5.2.2.1. Configuración del inmunosensor

En la Figura 34 de la Parte Experimental se representó el esquema de las etapas de preparación del inmunosensor. Según se describe, las superficies activas del electrodo dual, una vez modificadas con rGO, se funcionalizan mediante *grafting* electroquímico con la sal de diazonio del *p*-ABA. Con ello se obtienen dos superficies (ver Figura 74) conteniendo grupos carboxifenilo que pueden utilizarse para la unión covalente posterior del anticuerpo específico de cada hormona. Después se establecen los esquemas de inmunoensayo competitivo que implican a cada una de ellas y los respectivos antígenos biotinilados, y se lleva a cabo la determinación mediante voltamperometría diferencial de impulsos por adición de 1-NPP como sustrato de la enzima fosfatasa alcalina.

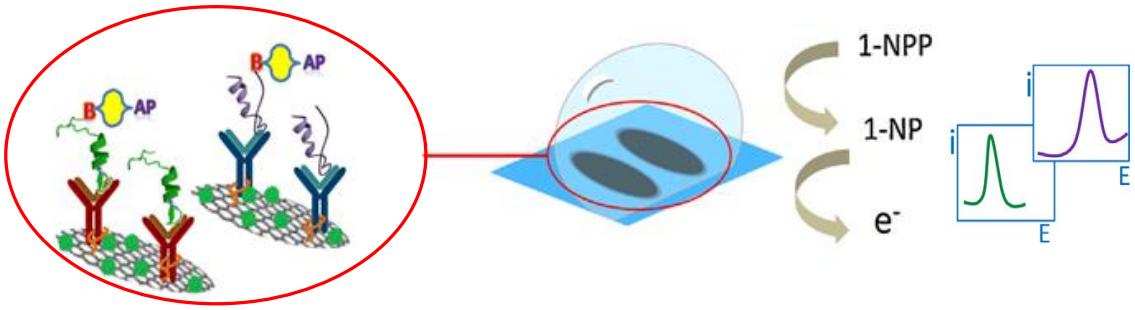

Figura 74.- *Esquema y modo de detección del inmunosensor de GHRL y PYY*

5.2.2.2. Optimización de las variables experimentales

En el capítulo anterior se descrbieron los estudios de optimización de las variables implicadas en la preparación de los electrodos HOOC-Phe-rGO/GCE y en el funcionamiento del inmunosensor AP-Strept-Biotin-PYY(PYY)-anti-PYY-Phe-rGO/ GCE. Por lo tanto, de forma previa a la construcción del inmunosensor dual para la determinación simultánea de GHRL y PYY, se procedió a optimizar las variables que afectan al inmunosensor de GHRL empleando la misma plataforma electródica. Estas variables son: a) la concentración y tiempo de incubación del anticuerpo de captura anti-GHRL, b) la concentración y el tiempo de incubación del conjugado Biotin-GHRL, y c) la concentración y el tiempo de incubación del conjugado AP-Strept. Las demás variables, que afectan a la preparación de los electrodos modificados, la unión covalente del anticuerpo de captura, la etapa de bloqueo, la temperatura de incubación, y la detección electroquímica, fueron las mismas que las elegidas para el inmunosensor de PYY.

- ***Influencia de la concentración y el tiempo de incubación del anticuerpo de captura***

Se estudió la influencia de la cantidad de anticuerpo de captura, anti-GHRL, inmovilizada por unión covalente a la superficie del electrodo modificado, midiendo varios voltamperogramas en diferencial de impulsos con inmunosensores preparados en ausencia de GHRL, depositando cada vez 10 µL de una disolución de anticuerpo en concentración variable entre 1.0 y 20 µg/mL. Como muestra la Figura 75a, la corriente de pico aumenta con la concentración de anticuerpo hasta 5 µg/mL, alcanzando a partir de aquí un valor prácticamente constante que debe corresponder a la saturación de las posiciones de enlace. Por otro lado, la relación S/N adopta el valor máximo para esa concentración de anti-GHRL, por lo que dicho valor se eligió para la preparación del inmunosensor. En estas condiciones, la corriente inespecífica, medida en ausencia de Biotin-GHRL, es de baja magnitud, con valores que representan aproximadamente un 10% del máximo de intensidad de pico. Finalmente, el tiempo de incubación de anti-GHRL se optimizó estudiando periodos comprendidos entre 30 y 90 minutos, obteniendo los resultados representados en la Figura 75b. que permitieron seleccionar 60 min como el más adecuado para estudios posteriores.

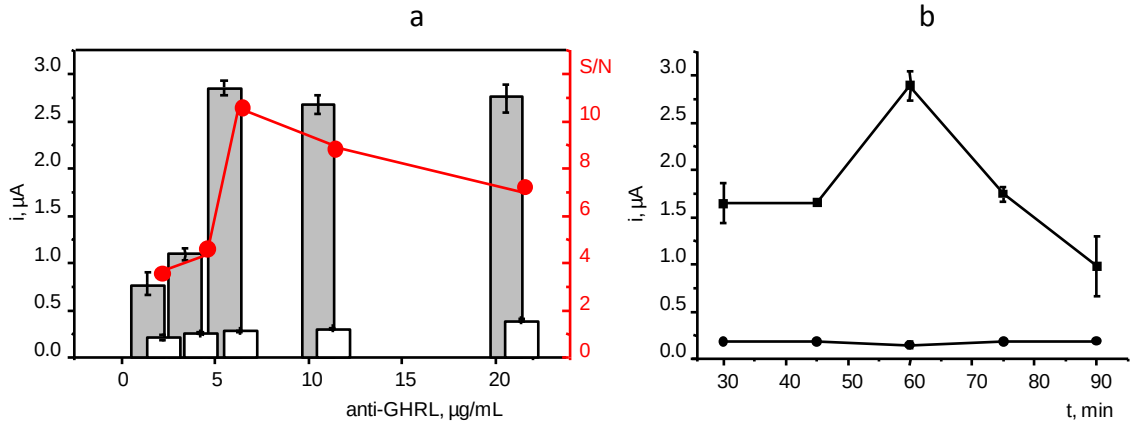

Figura 75. *Influencia de la concentración de anti-GHRL (a) y del tiempo de incubación (b) sobre la respuesta del inmunosensor AP-Strept-Biotin-GHRL-anti-GHRL-Phe-rGO/GCE: 0.5-20 µg/mL anti-GHRL, 60 min (a) 5 µg/mL anti-GHRL, 30 - 90 min; 0.2% caseina, 60 min; 0.5 µg/mL (gris, ■) ó 0 µg/mL (blanco, ●) Biotin-GHRL, 45 min; 5 µg/mL AP-Strept, 30 min.Todas las etapas de incubación se realizan a 37 ºC.*

- ***Influencia de la concentración y el tiempo de incubación del antígeno biotinilado***

Con el fin de optimizar la concentración de Biotin-GHRL, se prepararon distintos inmunosensores incubando el conjugado anti-GHRL-Phe-rGO/GCE en disoluciones de grelina biotinilada en concentraciones comprendidas entre 0.1 y 1.0 µg/mL con los resultados que se muestran en la Figura 76a. Se observa que los valores de la corriente de pico medida en ausencia de GHRL (barras grises) aumentan con la concentración de Biotin-GHRL hasta 0.7 µg/mL, disminuyendo ligeramente después. Por otro lado, las respuestas inespecíficas obtenidas para inmunosensores preparados en ausencia de anti-GHRL (barras blancas) aumentan ligeramente al aumentar la concentración de Biotin-GHRL, obteniéndose valores muy parecidos de la relación S/N para concentraciones de Biotin-GHRL de 0.3 y 0.5 µg/mL. Este último valor fue seleccionado como óptimo para la preparación del inmunosensor. De un modo similar, se estudió la influencia del tiempo de incubación en la disolución de Biotin-GHRL en el intervalo de 15 a 60 minutos, con los resultados mostrados en la Figura 76b. En este caso, se observaron corrientes similares para 30 y 45 minutos, escogiéndose el periodo más breve. 30 minutos, para estudios posteriores.

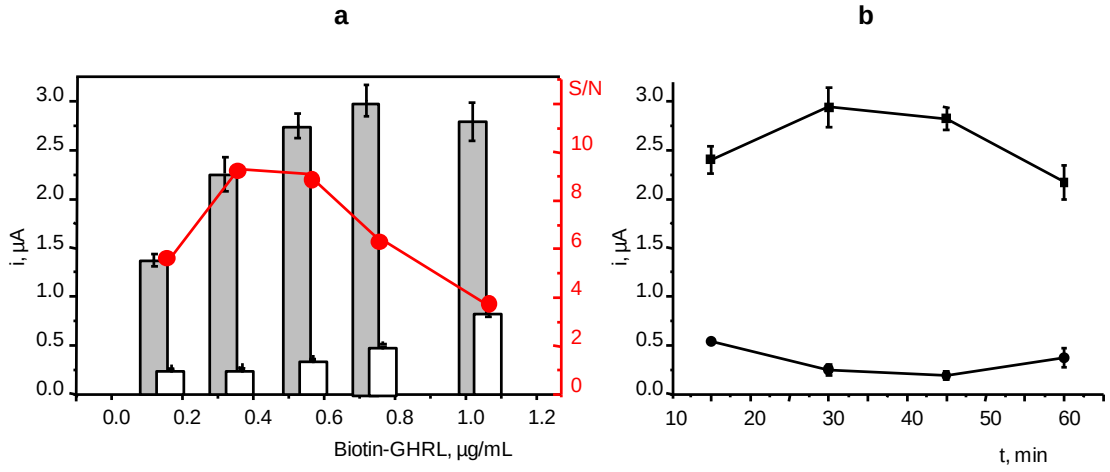

Figura 76.- *Influencia de la concentración de Biotin-GHRL (a) y del tiempo de incubación (b) sobre la respuesta del inmunosensor AP-Strept-Biotin-GHRL-anti-GHRL-Phe-rGO/GCE: 5.0 µg/mL (gris, ■) ó 0 µg/mL (blanco, ●) anti-GHRL, 60 min; 0.2% caseina, 60 min; 0.1-1.0 µg/mL Biotin-GHRL, 45 min (a) 0.5 µg/mL Biotin-GHRL, 15 - 60 min (b); 5 µg/mL AP-Strept, 30 min.*

- ***Influencia de la concentración y el tiempo de incubación del conjugado AP-Strept***

Se prepararon diferentes inmunosensores empleando disoluciones de AP-Strept en concentraciones comprendidas entre 0.5 y 9.0 µg/mL, observándose (Figura 77a) valores máximos de la corriente de pico en ausencia de GHRL a partir de 5 µg/mL. Además, las corrientes inespecíficas (barras blancas) diminuyen paulatinamente al aumentar la concentración de AP-Strept, debido probablemente a una menor conductividad de la superficie del electrodo. Estos resultados han llevado a elegir la concentración citada para estudios posteriores. En cuanto al tiempo de incubación de la disolución de AP-Strept, se evaluó el periodo comprendido entre 15 y 60 min (Figura 77b). Como puede verse, la respuesta inespecífica permanece prácticamente constante en todo el intervalo estudiado, encontrándose la mayor respuesta del inmunosensor para un tiempo de incubación de 30 minutos, que fue elegido como óptimo para su preparación.

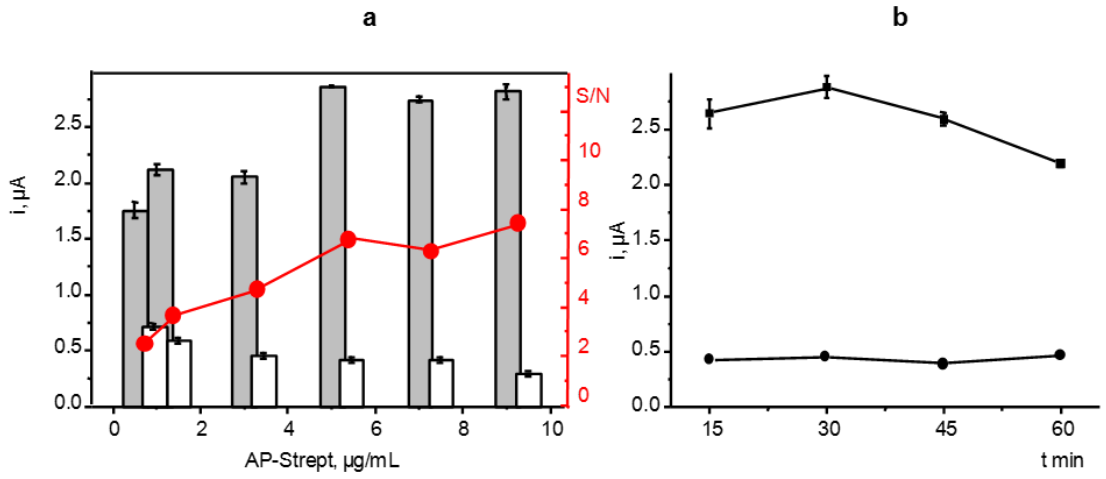

Figura 77. *Influencia de la concentración de AP-Strept (a) y del tiempo de incubación (b) sobre la respuesta del inmunosensor AP-Strept-Biotin-GHRL-anti-GHRL-Phe-rGO/GCE: 5 µg/mL anti-GHRL, 60 min; 0.2% caseina, 60 min; 0.5 µg/mL (gris, ■) ó 0 µg/mL (blanco, ●) Biotin-GHRL, 45 min; 0.5 - 9 5 µg/mL AP-Strept, 30 min (a); 5 µg/mL AP-Strept, 15-60 min (b).*

Una vez completados los estudios de optimización, en la Tabla 17 se resumen las variables investigadas, los intervalos ensayados, y el valor seleccionado en cada caso.

***Tabla* 17.-** Optimización de las variables implicadas en la preparación del inmunosensor AP-Strept-*Biotin-GHRL(GHRL)-anti-GHRL-Phe-rGO/GCE*

Variable	Intervalo/reactivo estudiado	Valor seleccionado
anti-GHRL, µg/mL	1 - 20	5
tiempo incubación anti-GHRL, min	30 - 90	60
Biotin-GHRL, ng/nL	0.1 - 1.0	0.5
tiempo incubación Biotin-GHRL, min	15 - 60	30
AP-Strept, µg/mL	0.5 - 9	5
tiempo incubación AP-Strept, min	15 - 60	30

5.2.2.2.1. Caracterización del inmunosensor

Las etapas implicadas en la preparación del inmunosensor AP-Strept-Biotin-GHRL-anti-GHRL-Phe-rGO/GCE se caracterizaron mediante espectroscopia de impedancia electroquímica (EIS) empleando $Fe(CN)_6^{3-/4-}$ 5 mM en KCl 0.1 M. En la Figura 78 se comparan los espectros de Nyquist registrados sobre GCE (1) y rGO/GCE (2) (Figura 78a). Como era de esperar, se observó una menor resistencia a la transferencia de carga (R_{CT}) sobre el electrodo modificado, debido por un lado a la mayor conductividad y por otro al efecto de difusión a través de los poros del rGO [Punckt et al., 2013]. En la Figura 78b puede apreciarse un fuerte incremento en el valor de la resistencia a la transferencia de carga, con R_{CT} = 5.5 x 10^4 Ω, tras la inmovilización el anitcucerpo de captura, anti-GHRL, lo que confirma la eficiencia del procedimiento de inmovilización. Como era de esperar, las etapas posteriores proporcionan valores aun superiores de R_{CT} como consecuencia de la incorporación de especies no conductoras.

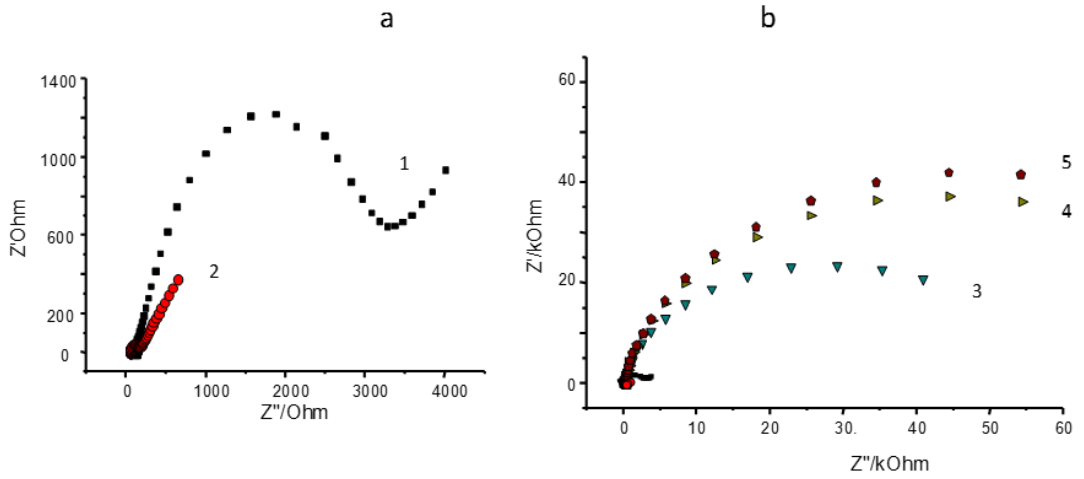

Figura 78.- *Espectros de impedancia obtenidos (a) para: GCE (1); rGO/GCE (2); (b) anti-GHRL-Phe-rGO/GCE (3); Biotin-GHRL-anti-GHRL-Phe-rGO/GCE (4); AP-Strept-Biotin-GHRL-anti-GHRL-Phe-rGO/GCE (5)); $Fe(CN)_6^{3-/4-}$ 5 mM en KCl 0.1 M*

5.2.2.3. Calibrados y características analíticas

Las condiciones experimentales optimizadas para los inmunosensores de PYY (Apartado 5.2.1.) y GHRL de forma individual sobre los electrodos rGO/GCE funcionalizados por *electrografting* con *p*-ABA, se extendieron a la construcción de un inmunosensor para la determinación simultánea de ambas hormonas sobre un electrodo dual serigrafiado de carbono (dSPCE).

En la Figura 79 se han representado los calibrados obtenidos en el intervalo de 10^{-7} a 10^{4} ng/mL de GHRL o PYY, junto con algunos de los voltamperogramas registrados en diferencial de impulsos. Las barras de error corresponden a las medidas realizadas con tres inmunosensores distintos en cada caso. Las dos curvas se ajustan a la ecuación:

$$i_p = i_{\min} + \frac{i_{max} - i_{min}}{1 + \left(\frac{x}{EC_{50}}\right)^{-h}}$$

con valores de $r^2 = 0.991$ (GHRL) y $r^2 = 0.994$ (PYY). Las corrientes máxima y mínima fueron $i_{max} = 2.8 \pm 0.2$ µA, $i_{min} = 0.59 \pm 0.08$ µA, respectivamente para GHRL, e $i_{max} = 3.8 \pm 0.2$ µA, $i_{min} = 0.69 \pm 0.09$ µA para PYY. Los valores de EC_{50} correspondientes al cincuenta por ciento de competición fueron -0.24 ± 0.04 (GHRL) y -0,32 ± 0.05 (PYY), y las pendientes de Hill, h, -0,24 ± 0.04 (GHRL) y -0.32 ± 0.05 (PYY). En este caso se aplicó también un tratamiento de regresión logarítmica de las curvas sigmoidales

representando los valores de Ln (p/1-p) vs Ln x, con p = $(y-i_{min})/(i_{max}-i_{min})$. Con ello, se obtuvieron lineas rectas (r^2 = 0.995 y 0.990, respectivamente) con pendientes de -0.23 (GHRL) y -0.36 (PYY). Estos valores coinciden apreciablemente con los de la pendiente de Hill, h, obtenidos en las ecuaciones de los calibrados anteriores.

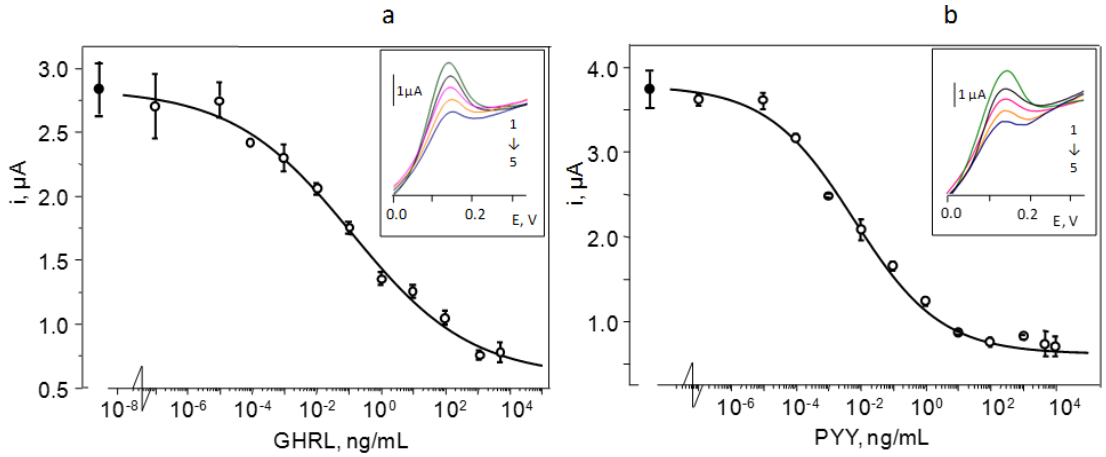

Figura 79.- *Calibrados para la determinación de (a) GHRL y (b) PYY con el inmunosensor dual. Insertos: Voltamperogramas en dierencial de impulsos para: (a) 1) 10^{-3}; 2) 0.01; 3) 0.1; 4) 1.0 y 5) 10 ng/mL GHRL y (b) 1) 10^{-4}; 2) 10^{-3}; 3) 0.01; 4) 0.1 y 5) 1.0 ng/mL PYY.*

El ajuste por mínimos cuadrados de la porción central de cada curva proporcionó calibrados rectos de forma i_p *vs* log [hormona] en los intervalos 10^{-3} a 100 ng/mL GHRL (r^2 = 0.990), y 10^{-4} a 10 ng/mL PYY (r^2 = 0.992). Las pendientes de estos calibrados fueron -246 ± 7 y 422 ± 6 nA por década de concentración, respectivamente. Estos intervalos son adecuados para la aplicación del inmunosensor dual a la determinación de GHRL y PYY en suero [Batterham et al., 2003] [Popovic et al., 2004] [Shiiya et al., 2002] y saliva [Aydin et al., 2005] [Acosta et al., 2011]. Los límites de detección se calcularon como la concentración mínima de cada analito que podía diferenciarse de cero, restando en cada caso el doble de la desviación estándar, 2s, siendo s = ± 0.2 µA para ambas, GHRL y PYY, calculada a partir de la corriente media de disoluciones preparadas en ausencia de hormonas. Los valores calculados, LOD = 1.0 pg/mL GHRL y 0.02 pg/mL PYY están de acuerdo con los calculados empleando la ecuación

$$LOD = EC_{50}\left(\frac{i_{max}-i_{min}}{i_{max}-i_{min}-3s}-1\right)^{-1/h}$$

con la que se obienen los valores de 1.2 pg/mL (GHRL) y 0.06 pg/mL (PYY). Es importante destacar que el límite de detección de GHRL que se alcanza empleando esta configuración es inferior al obtenido con el magnetoinmunosensor descrito anteriormente (Apartado 5.1.1.), así como varios órdenes de magnitud menor que la concentración mínima detectable que proporcionan los kits ELISA disponibles. Por ejemplo, el valor de 161 pg/mL GHRL especificado en el protocolo del RAB0207 Sigma GHRL EIA Kit [www.abnova.com/products/ products_detail.asp? catalog_id = KA1863] es más de 100 veces superior. De forma similar, el valor del límite de detección obtenido para PYY es mucho menor que la concentración mínima detectable con los kits ELISA para esta hormona. Por ejemplo, puede citarse la especificada en el protocolo EIA-PYY-1 Ray Biotech, 5.6 pg/mL [www.raybiotech.com/ human-peptide-yy-pyy-eia-kit/], casi mil veces superior.

La reproducibilidad de las medidas voltamperométricas se evaluó por medida de disoluciones conteniendo 0.1 ng/mL de GHRL ó 0.01 ng/mL PYY con diez inmunosensores preparados en mismo día. Los valores de RSD fueron del 2.9% y el 2.4%, respectivamente. Resultados similares fueron obtenidos también para las medidas realizadas con el inmunosensor dual en diferentes días, siendo RSD = 2.8% para GHRL y RSD = 2.9% para PYY, en ambos casos con n = 8. Estos resultados ponen de manifiesto la buena repetibilidad de las medidas y la elevada precisión alcanzada en la preparación y la utilización de las plataformas inmunosensoras. Por otro lado, se estudió la estabilidad de almacenamiento de los conjugados anti-GHRL-Phe-rGO/SPCE y anti-PYY-Phe-rGO/SPCE. Se prepararon varios el mismo día y se conservaron en el refrigerador a 4 ºC. Después, una vez completada la construcción de cada inmunosensor con 0.1 ng/mL GHRL y 0.01 ng/mL PYY, se midieron las respuestas voltamperométricas en diferentes días con los resultados representados en la Figura 80. Los resultados obtenidos revelan una buena estabilidad en las condiciones de almacenamiento establecidas, manteniéndose las respuestas de corriente dentro de los límites de control (± 3s) durante al menos diez días, que fue el máximo periodo de tiempo estudiado.

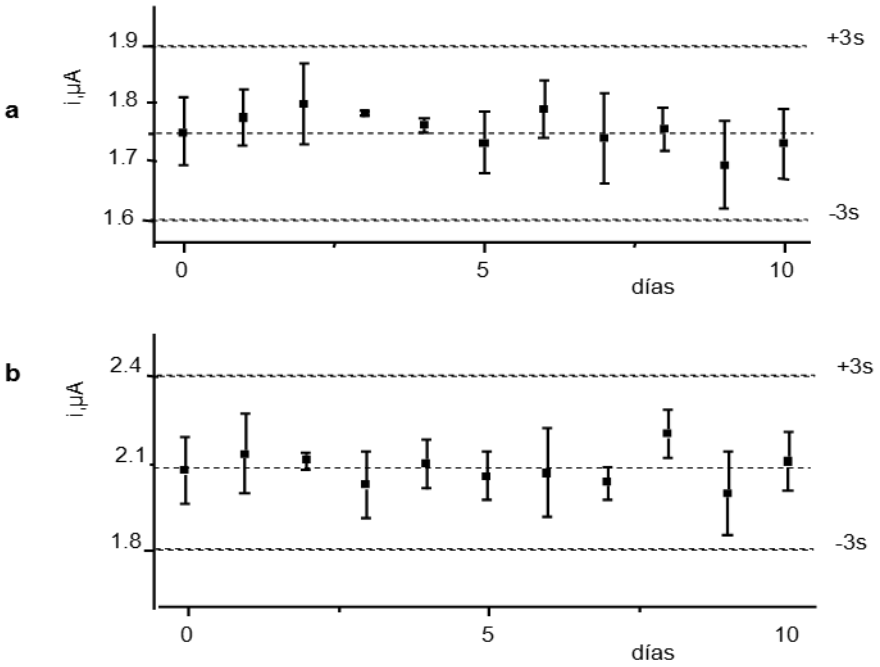

Figura 80.- *Gráficos de control para la evaluación de la estabilidad de almacenamiento de los conjugados anti-GHRL-Phe-rGO/SPCE y anti-PYY-Phe-rGO/SPCE. Cada punto corresponde al valor medio de tres medidas sucesivas para 0.1 ng/mL GHRL (a) y 0.01 ng/mL PYY (b).*

5.2.2.4. Estudios de selectividad

Se investigó el efecto sobre las respuestas del inmunosensor dual de varias proteínas que pueden acompañar a las hormonas GHRL y/o PYY en muestras clínicas. Las especies estudiadas fueron: adiponectina (APN), insulina (INS), hormona de crecimiento humano (hGH), grelina desacilada (da-G), y hormona folículo estimulante (FSH). Las corrientes medidas en ausencia de GHRL y PYY con los inmunosensores AP-Strept-Biotin-GHRL-anti-GHRL-Phe-rGO/SPCE o AP-Strept-Biotin-PYY-anti-PYY-Phe-rGO/SPCE en presencia de cada sustancia potencialmente interferente a una concentración de 1 μg/mL, se compararon con las respuestas obtenidas en ausencia de las mismas. Además, se evaluó también la posible interferencia cruzada ("cross-talking") entre los dos analitos. Como puede observarse (Figura 81) los valores medios de las corrientes de pico aparecen en todos los casos dentro de los límites de control situados a ± 2s, siendo s la desviación estándar de la corriente medida en ausencia de GHRL o PYY (primera medida en cada serie). Estos resultados ponen de manifiesto la excelente selectividad del inmunosensor dual desarrollado para ambas hormonas frente a otras proteínas.

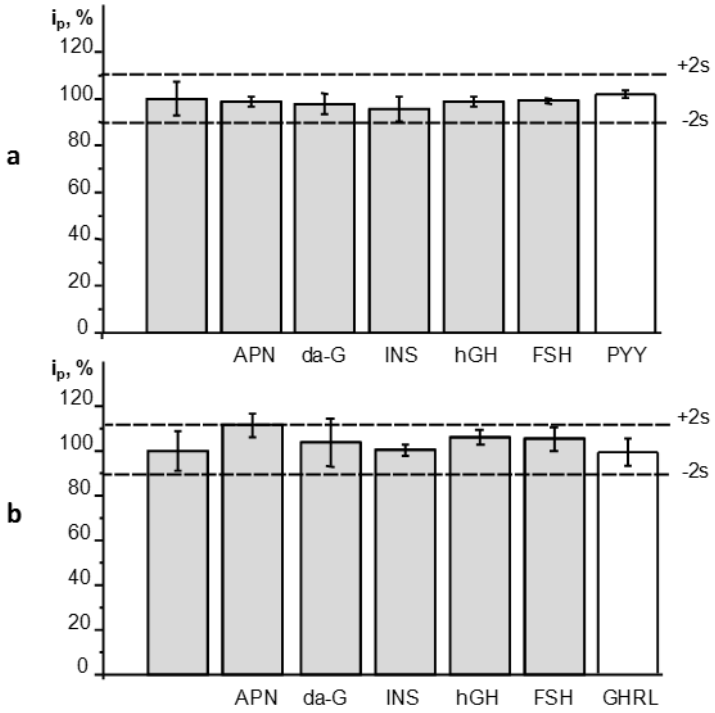

Figura 81.- *Efecto de la presencia de 1 µg/mL de diferentes hormonas en la respuesta voltamperométrica del inmunosensor dual en ausencia de GHRL y PYY*

5.2.2.5. Aplicación a la determinación de GHRL y PYY en suero y en saliva

La utilidad analítica del inmunosensor dual se demostró por aplicación a muestras de suero y saliva enriquecidos con las hormonas a diferentes concentraciones correspondientes a los niveles normales esperables en estos fluidos biológicos. Se aplicaron los protocolos descritos en el Apartado 4.4.4.1. para muestras preparadas según el Procedimiento 4.3. Las alícuotas de suero enriquecido se diluyeron con el mismo volumen de disolución de la hormona biotinilada, estudiándose la posibilidad de existencia de efectos matriz en estas condiciones, por comparación de las pendientes de los calibrados construidos con disoluciones patrón de cada hormona con los obtenidos a partir de las muestras. Los valores obtenidos fueron -233 ± 5 y -410 ± 8 nA por década de concentración, respectivamente para los calibrados de las muestras de GHRL y PYY, muy parecidos a los de los calibrados de patrones, -246 ± 7 y 422 ± 6 nA por década de concentración. La comparación estadística de dichas pendientes por aplicación del test t proporcionó valores de t_{exp} de 1.576 (GHRL) y 1.225 (PYY) inferiores a t_{tab} = 2.776 en ambos casos. Estos resultados demostraron que no existen diferencias significativas entre las pendientes de los calibrados en los dos casos. Por tanto, es posible llevar a cabo la determinación de ambas hormonas por medida de las señales voltamperométricas sobre cada superficie electródica y su interpolación en el calibrado de patrones correspondiente.

En relación a la saliva, las alícuotas de las muestras enriquecidas, diluidas del mismo modo, proporcionaron calibrados con valores de las pendientes de -228 ± 10 y -412 ± 7 nA por década de concentración para GHRL y PYY, respectivamente. Al igual que anteriomente, la comparación estadística de estas pendientes con las de los calibrados de patrones proporcionó valores de t_{exp} =1.37 y 1.08 para GHRL y PYY, respectivamente, inferiores a t_{tab} = 2.776.

En la Tabla 18 se resumen los resultados obtenidos.

Tabla 18.- *Determinación de GHRL y PYY en suero y en saliva con el inmunosensor dual AP-Strept-Biotin-GHRL (PYY)- anti-GHRL (PYY)- Phe-rGO / SPCE*

Muestra	Analito	Añadido, pg/mL	Encontrado, pg/mL	Recuperación media, %
suero	GHRL	175	181 ± 1*	103 ± 1
suero	PYY	17.5	16.6 ± 0.1	95 ± 1
suero	GHRL	65 6.5	65 ± 5 6.3 ± 0.5	99 ± 8 96 ± 7
suero	PYY	35 3.5	34 ± 2 3.6 ± 0.3	98 ± 6 103 ± 8
saliva	GHRL	95	92 ± 4	97 ± 5
saliva	PYY	37.5	37 ± 1	99 ± 3

* ± ts / √n

5.2.2.6. Conclusiones

En este trabajo se ha llevado a cabo por primera vez la determinación simultánea de GHRL y PYY empleando un inmunosensor multiplex en el que las superficies activas de un electrodo dual serigrafiado se modifican con óxido de grafeno reducido y mediante *grafting* con la sal de diazonio del *p*-ABA. La configuración desarrollada hace posible obtener calibrados para ambas hormonas que muestran excelentes características analíticas, alcanzándose límites de detección mucho menores que los obtenidos en los kits ELISA disponibles para cada uno de los compuestos determinados, por separado. Además, la buena reproducibilidad del método es otra característica a destacar. Finalmente, la utilidad del inmunosensor al análisis de muestras clínicas se demostró por aplicación a suero y saliva con buenos resultados.

5.2.3. INMUNOSENSOR PARA LA DETERMINACIÓN DE EE2

En este trabajo se describe la preparación de un inmunosensor electroquímico para la determinación de etinilestradiol (EE2) basado en el empleo de un método de *electrografting* de la sal de diazonio de *p*-ABA sobre un electrodo de carbono vitrificado modificado con nanopartículas de plata (AgNPs), sílice (SiO_2) y óxido de grafeno (GO).

Como se ha indicado en la Introducción, esta hormona es uno de los estrógenos sintéticos más potentes, constituyendo un componente esencial de los anticonceptivos orales. Entre sus efectos adversos se encuentra el aumento de los niveles de lipoproteína sérica [Chao, 1979] y la modificación en los patrones de producción de hormonas relacionadas con la obesidad como grelina y leptina [Sağsöz et al., 2009]. En general, la interacción de los estrógenos con las hormonas orexígenas y anorexígenas afecta al balance de energía, la ingesta de alimentos y la distribución de grasa corporal [Brown & Clegg, 2009]. En la Figura 82, la fórmula estructural del EE2, se compara con la de algunos estrógenos similares. En relación a ellos se sabe que la sustitución del C17 con un grupo etinil le dota de una elevada resistencia a la degradación en el hígado, circunstancia de la que deriva su utilidad como anticonceptivo oral.

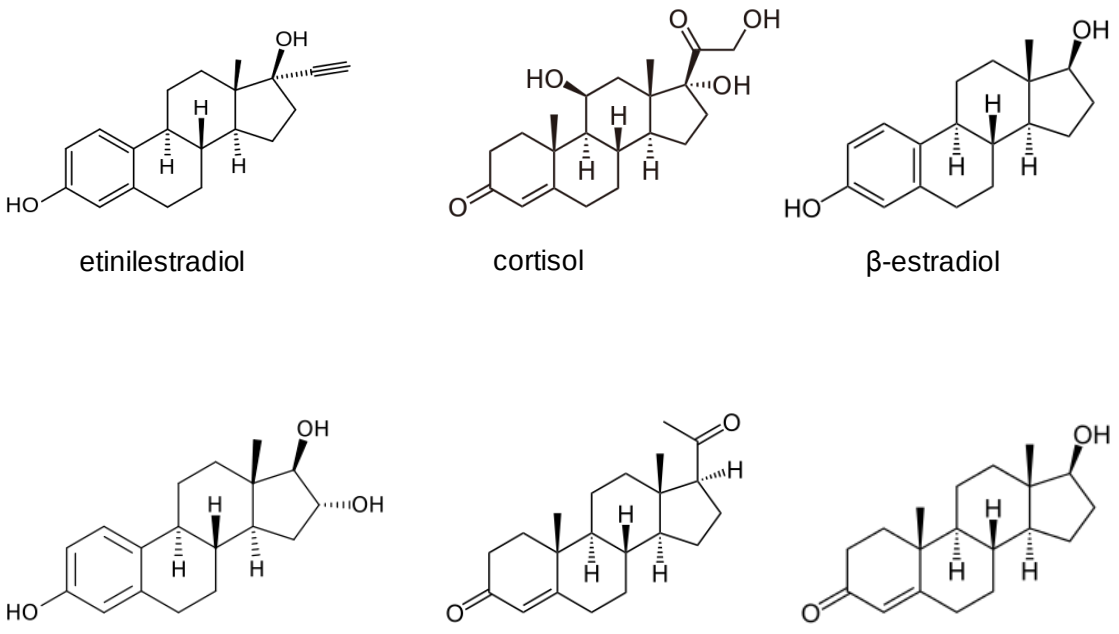

Figura 82. *Fórmulas esrtructurales del EE2 y otros estrógenos.*

En este inmunosensor electroquímico se explora por primera vez la posibilidad de utilizar el material híbrido antes mencionado, AgNPs/SiO_2/GO, para preparar una plataforma sensora adecuada para la inmovilización estable del anticuerpo de captura y la obtención de respuestas electroquímicas sensibles y selectivas. Por un lado, el GO proporciona alta conductividad y elevada área superficial, así como biocompatibilidad y robustez y, por otro, la presencia de SiO_2 aporta una buena resistencia física, hidrofilicidad, inercia química y alta relación área/volumen. Finalmente, las AgNPs se caracterizan por su capacidad electrocatalítica y por su habilidad para la adsorción de biomoléculas, propiedades que van unidas a la elevada conductividad y biocompatibilidad de este nanomaterial.

Es importante señalar que la determinación de EE2 en muestras clínicas tiene un gran interés, no solo en el ámbito de la obesidad y los trastornos alimentarios sino también en relación a otras enfermedades o efectos adversos derivados de su empleo, como la fibrinolisis o la trombosis [WHO Scientific Group, 2011] [Raps et al., 2014]. Existen numerosos métodos dedicados al análisis de estrógenos, incluido el EE2, en muestras ambientales, en las que se consideran contaminantes de gran interés, si bien estos están basados mayoritariamente en técnicas cromatográficas. Sin embargo, se han descrito muy pocos procedimientos aplicables a fluidos biológicos, y casi todos se basan en técnicas de inmunoensayo tipo ELISA. Como se verá, el inmunosensor desarrollado ha permitido llevar a cabo la determinación de EE2 en muestras de orina, con buenos resultados y sin necesidad de tratamiento.

5.2.3.1. Configuración del inmunosensor

En la Figura 35 de la Parte Experimental se representó el esquema de la preparación del inmunosensor para la determinación de EE2. Como ya se indicó, éste consiste en un electrodo de carbono vitrificado modificado con el material híbrido AgNPs/SiO_2/GO que se funcionaliza posteriormente mediante *grafting* electroquímico con la sal de diazonio del *p*-ABA. La inmovilización del anticuerpo de captura, anti-EE2, sobre los grupos carboxilo activados (ver Figura 83), permitió desarrollar una configuración de tipo competitivo empleando EE2 y HRP-EE2.

La determinación del antígeno se llevó a cabo mediante detección amperométrica haciendo uso del esquema de reacciones representado, donde la catálisis enzimática del sustrato origina la oxidación del mediador redox, formándose quinona (HQ_{ox}) cuya reducción electroquímica se detecta sobre la superficie del electrodo a un potencial de -0.2 V vs Ag.

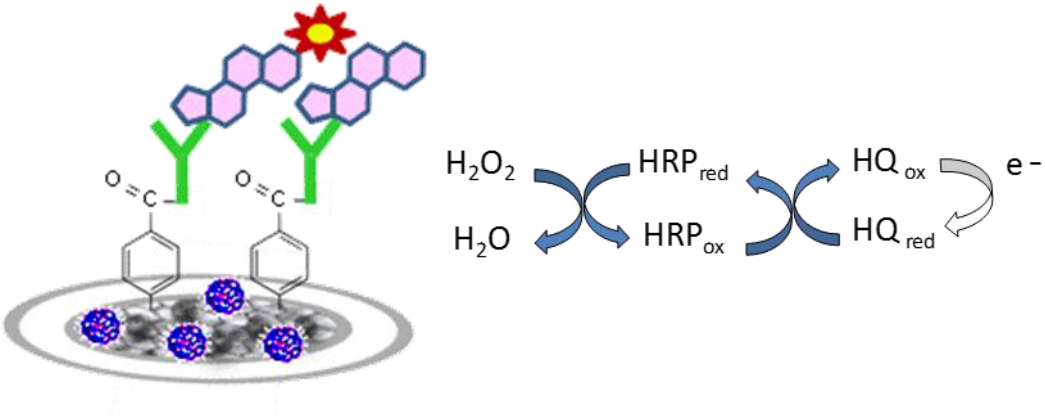

Figura 83.- *Esquema y reacciones de detección del inmunosensor de EE2*

5.2.3.2. Optimización de las variables experimentales

El material híbrido utilizado para la modificación del electrodo se preparó de acuerdo con el procedimiento descrito en el Apartado 4.4.5. de la Parte Experimental empleando el método de [Cincotto et al., 2014]. En este trabajo se eligió el mediador redox utilizado para la detección de la reacción de afinidad sobre el electrodo modificado y se optimizaron las variables implicadas en la preparación del inmunosensor estudiando la concentración y el tiempo de incubación del anticuerpo de captura anti-EE2, y del conjugado HRP-EE2, así como la etapa de bloqueo. Las condiciones experimentales para llevar a cabo la funcionalización del electrodo modificado mediante *electrografting* con *p*-ABA y la activación de los grupos -COOH fueron las empleadas para la preparación de los inmunosensores de GHRL y PYY descritos anteriormente. Finalmente, la detección electroquímica se realizó utilizando las condiciones optimizadas en otros trabajos anteriores para el sistema H_2O_2/HRP/HQ [Eguílaz et al., 2010].

- ***Elección del mediador redox***

Como se ha comentado, la detección electroquímica de la reacción de afinidad se realizó empleando H_2O_2 como sustrato de la peroxidasa en presencia de un mediador redox. En este apartado se estudió el comportamiento voltamperométrico sobre el electrodo modificado de dos especies electroactivas usualmente empleadas con esta finalidad, catecol e hidroquinona, con el objetivo de elegir la más adecuada para alcanzar la mayor sensibilidad y selectividad de la determinación. En la Figura 84 se muestran los voltamperogramas cíclicos obtenidos sobre el electrodo AgNPs/

SiO_2/GO/GCE de disoluciones 1 mM de cada uno de estos compuestos en medio regulador fosfato 0.1 M de pH 7.2. Aunque ambos exhiben un comportamiento cuasi-reversible, los valores de la corriente de pico son mucho mayores en el caso de la hidroquinona, que fue elegida como mediador redox para el trabajo posterior.

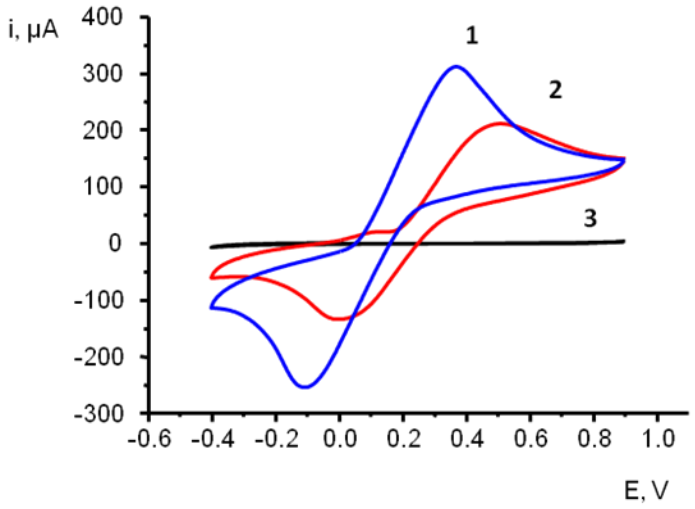

Figura 84.- *Voltamperogramas cíclicos sobre el electrodo AgNPs/SiO_2/GO/GCE de (1) hidroquinona (HQ) 1 mM y (2) catecol 1 mM en medio regulador fosfato 0.1 M de pH 7.2. Corriente de fondo (3); v = 50 mV/s.*

- ***Elección de la plataforma electródica***

Una vez elegido el mediador redox, se comparó el comportamiento de los electrodos modificados GO/GCE, SiO_2/GO/GCE y AgNPs/SiO_2/GO/GCE para su uso como superficies sensoras de la reacción de afinidad, registrando los voltamperogramas cíclicos de una disolución 1 mM de HQ en medio regulador fosfato 0.1 M de pH 7.2. Los resultados representados en la Figura 85 muestran que los potenciales de pico E_{pa} y E_{pc} obtenidos sobre los electrodos preparados en ausencia de AgNPs son similares, con un valor en ambos casos de $\Delta E = E_{pa} - E_{pc}$ de 600 mV aproximadamente. Sin embargo, sobre el electrodo AgNPs/SiO_2/GO/GCE se observó una notable disminución de ΔE, pasando a ser igual a 464 mV, apreciándose al mismo tiempo un incremento en las corrientes de pico de un 27% y un 15% para i_{pa} e i_{pc}, respectivamente. Estos resultados se atribuyen a la actividad electrocatalítica de las AgNPs incorporadas al híbrido SiO_2/GO hacia el proceso electroquímico del sistema quinona / hidroquinona, y están de acuerdo con lo ya observado anteriormente [Cincotto et al., 2014] para el comportamiento electroquímico de otros derivados fenólicos, la dopamina y la epinefrina, sobre el electrodo AgNPs/SiO_2/GO/GCE.

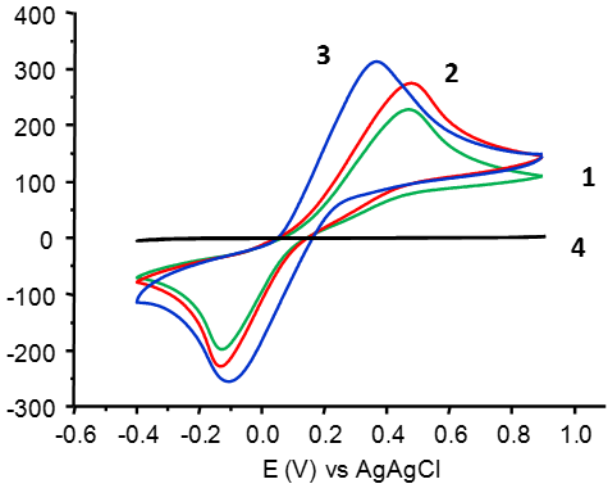

Figura 85. *Voltamperogramas cíclicos de HQ 1 mM sobre los electrodos GO/GCE (1), SiO_2/GO/GCE (2) y AgNPs/SiO_2/GO/GCE (3) en medio regulador fosfato 0.1 M de pH 7.2. Corriente de fondo (4); v = 50 mV/s.*

- ***Inmovilización del anticuerpo de captura***

El anticuerpo anti-EE2 se inmovilizó covalentemente sobre los grupos carboxilo presentes en la superficie del electrodo AgNPs/SiO_2/GO/GCE previa activación de los mismos empleando el sistema EDC/NHSS. Con el fin de demostrar la ventaja de utilizar el electrodo modificado con el material híbrido frente al electrodo sin modificar (GCE) o las configuraciones intermedias (GO/GCE y SiO_2/GO/GCE), se compararon las respuestas amperométricas obtenidas sobre inmunosensores preparados con todos ellos previa incorporación del radical de la sal de diazonio del *p*-ABA y la activación mencionada,. para inmovilizar en cada caso covalentemente el anticuerpo de captura. Como puede observarse (Figura 86a), cuando se utiliza el electrodo AgNPs/SiO_2/GO/GCE, se obtienen las señales más intensas, probablemente como consecuencia tanto de la inmovilización eficiente de anti-EE2 como por el buen comportamiento electroquímico del mediador sobre el material híbrido. Por otro lado, las señales competitivas (barras gris oscuro) fueron de magnitud similar sobre las tres plataformas ensayadas, lo que demuestra una buena tendencia general a competir por parte de EE2 y HRP-EE2 por las posiciones libres del anticuerpo inmovilizado, independientemente de cuál sea la composición del electrodo. Destacar que todas estas señales fueron de pequeña magnitud debido a la concentración relativamente alta de EE2 empleada. Con respecto a las respuestas inespecíficas (barras negras), es decir, las medidas en ausencia de anti-EE2, se observó una mayor magnitud para las obtenidas empleando el inmunosensor preparado con GCE, mientras que las

registradas sobre los electrodos modificados fueron todas ellas similares y de baja magnitud. Posiblemente, este comportamiento se debe a la adsorción del conjugado HRP-EE2, lo que podría explicar también la elevada repuesta competitiva medida sobre el electrodo sin modificar.

Las ventajas de utlizar el método de inmovilización basado en el *electrografting* de la sal de diazonio del *p*-ABA se demostraron por comparación de estos resultados con los que proporciona un inmunosensor preparado por simple adsorption de anti-EE2 sobre la superficie del electrodo modificado con el material híbrido AgNPs/SiO_2/GO (Figura 81b). Puede observarse cómo la respuesta específica sobre el inmmunosensor preparado por simple adsorción del anticuerpo proporciona una corriente específica mucho menor que la medida sobre el inmunosensor preparado por unión covalente, siendo esta similar a la corriente inespecífica. La diferencia de comportamiento encontrada se ha atribuído a la diferente eficiencia de inmovilización que es función de las distintas capacidades de adsorcíon por parte de las superficies ensayadas en ausencia del radical derivado de la sal de diazonio [Mandon et al., 2009]. Sin embargo, es interesante destacar que incluso empleando esta estrategia de inmovilización ineficiente, la competición entre EE2 y HRP-EE2 funciona, si bien lo hace en una extensión limitada (barra gris oscuro). Este comportamiento demuestra la adecuada selección de los inmunorreactivos.

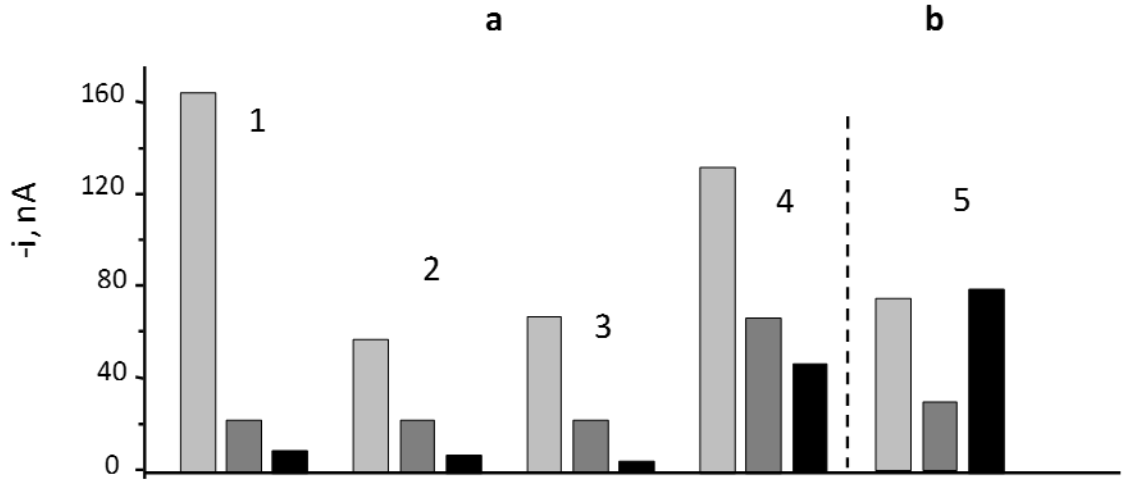

Figura 86.-*Respuestas amperométricas del inmunosensor preparado con el conjugado HRP-EE2(EE2)-anti-EE2: (a) mediante electrografting de p-ABA e inmovilización covalente de anti-EE2 sobre (1) AgNPs/SiO_2/GO/GCE;(2) SiO_2/GO/GCE; (3) GO/GCE; (4) GCE. (b) mediante adsorción de anti-EE2 sobre AgNPs/SiO_2/GO/GCE: respuestas específica (gris claro) y competitiva (gris oscuro), 20 µg/mL anti-EE2; e inespecífica (negro): 0 µg/mL anti-EE2; 0.5 µg/mL EE2 (a, competitivo) 10 µg/mL (b, competitivo) HRP-EE2 en dilución 1/100 (a y b, específica e inespecífica); dilución 1/50 (competitivo).*

- ***Influencia de la concentración y el tiempo de incubación del anticuerpo de captura***

Se estudió la influencia sobre la respuesta del inmunosensor de la cantidad de anticuerpo de captura inmovilizado por unión covalente sobre la superficie del electrodo modificado, empleando disoluciones de anti-EE2 en concentraciones comprendidas entre 0 y 50 µg/mL, aplicando el procedimiento descrito en el Apartado 4.4.5. en ausencia de EE2 y en presencia de HRP-EE2 en dilución 1/100. La detección amperométrica en las condiciones que se indican, proporcionó los resultados que se han representado en la Figura 87a. Como puede verse, la corriente aumenta rápidamente conforme lo hace la concentración del anticuerpo hasta un valor de 20 µg/mL y después permanece prácticamente constante, debido probablemente a la saturación del electrodo. Debido a este comportamiento, dicha concentración fue elegida para la preparación del inmunosensor. Por otro lado, como puede observarse, la respuesta inespecífica obtenida en ausencia de EE2 y de anti-EE2 (aproximadamente igual a 3 nA) representa una corriente cuarenta veces menor que la señal máxima alcanzada con el conjugado HRP-EE2 a la concentración utilizada.

Con respecto al tiempo de incubación, el intervalo estudiado para la optimización de esta variable fue el comprendido entre 0 y 120 min. Los resultados representados en la Figura 87b muestran que en este caso, el periodo de tiempo más apropiado para la inmovilización del anticuerpo de captura es de 45 min.

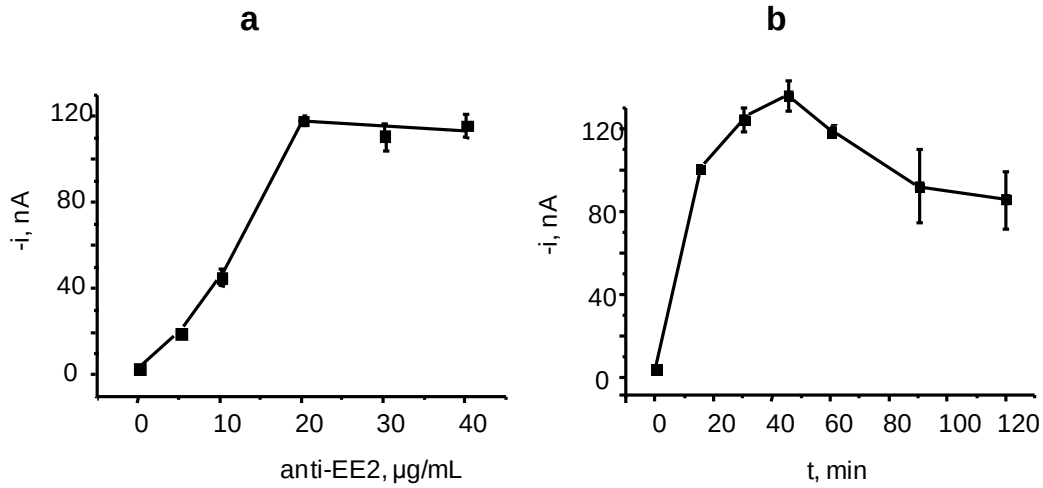

Figura 87.- *Influencia de la concentración de anti-EE2 (a) y del tiempo de incubación (b) sobre la respuesta del inmunosensor HRP-EE2-anti-EE2-Phe-AgNPs/SiO_2/GO/GCE: 0 - 40 µg/mL anti-EE2, 60 min (a); 20 µg/mL anti-EE2, 0-120 min (b); 1% caseína, 60 min; HRP-EE2 en dilución 1/100, 60 min; electrodo modificado con 10 µL de AgNPs/SiO_2/GO de 0.5 mg/mL en DMF. Todas las etapas de incubación se realizaron a 37 ^oC.*

- ***Optimización de la etapa de bloqueo***

Al igual que en los inmunosensores anteriores, en este caso también se aplicó una etapa de bloqueo tras la inmovilización del anticuerpo de captura con el fin de minimizar la adsorción inespecífica de los inmunorreactivos sobre la superficie del electrodo. En primer lugar se optimizó el tipo de agente bloqueante a utilizar estudiando las respuestas del inmunosensor preparado con disoluciones de etanolamina 1 M, BSA al 0.5% o caseína al 1% en medio regulador fosfato 0.1 M de pH 7.2. Se observó que en presencia de etanolamina, las respuestas amperométricas eran poco reproducibles, obteniéndose corrientes estacionarias inestables y continuamente decrecientes.

En la Figura 88a se comparan las señales específicas (barras grises) del inmunosensor preparado en presencia de anti-EE2 y en ausencia de EE2, inespecíficas (barras negras) en ausencia de ambos, y las respuestas competitivas, en presencia de anti-EE2 y EE2 (barras blancas). Puede observarse cómo la señal inespecífica más baja se obtuvo con el inmunosensor preparado con caseína, que muestra además la mayor relación señal específica a inespecífica. En estas condiciones, tal como se aprecia en la Figura 88b, se estudió la influencia del tiempo de incubación en el intervalo de 30 a 75 minutos, observándose que el valor óptimo, por la mejor relación respuesta específica a inespecífica, es de 60 minutos.

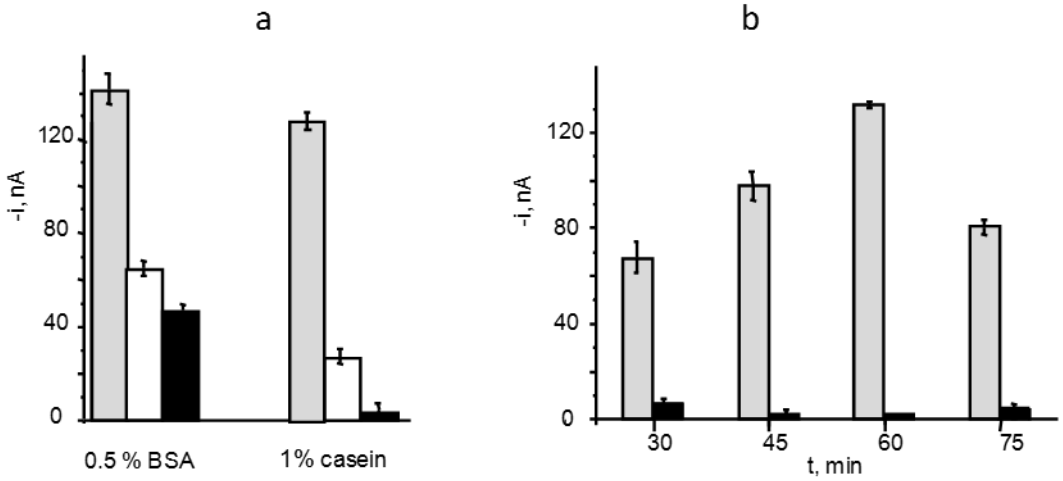

Figura 88.- *Influencia del tipo de agente bloqueante (a) y del tiempo de incubación de la caseína (b) sobre la respuesta del inmunosensor HRP-EE2(EE2)-anti-EE2-Phe-AgNPs/ SiO_2/GO/ GCE: 20 µg/mL anti-EE2, 60 min; 0 µg/mL EE2 (gris); 20 µg/mL anti-EE2, 60 min; 0.5 µg/mL EE2, 60 min (blanco); 0 µg/mL anti-EE2, 0 µg/mL EE2, (negro); HRP-EE2 en dilución 1/100, 60 min. Ver Fig.87 y el texto para las demás condiciones.*

- ***Influencia de la concentración y el tiempo de incubación del conjugado HRP-Strept***

La configuración del inmunosensor competitivo para la determinación de EE2 se completa con el conjugado HRP-Strept, en el que la etiqueta enzimática es la responsable de catalizar la oxidación del sustrato, peróxido de hidrógeno, que en presencia de hidroquinona dará lugar a la formación de quinona, cuya reducción electroquímica se detecta sobre la superficie del electrodo a un potencial de -0.2 V vs Ag. Para optimizar la concentración de este conjugado, se estudió la respuesta del immunosensor preparado con disoluciones de HRP-Strept a diferentes diluciones en el intervalo de 1/200 a 1/50, representándose los resultados obtenidos en la Figura 89a.

Puede verse cómo el máximo de corriente se alcanza para una dilución 1/100, valor que coincide con la mayor relación S/N. Por ello, esta fue la concentración elegida como óptima para obtener la mayor sensibilidad en la detección. Por otro lado, en las condiciones experimentales elegidas, se estudió la influencia del tiempo de incubación del conjugado HRP-Strept a 37 ºC en el intervalo comprendido entre 30 y 75 min. En este caso (Figura 89b), los resultados obtenidos llevaron a elegir un tiempo de incubación de HRP-Strept de 60 minutos a 37 ºC.

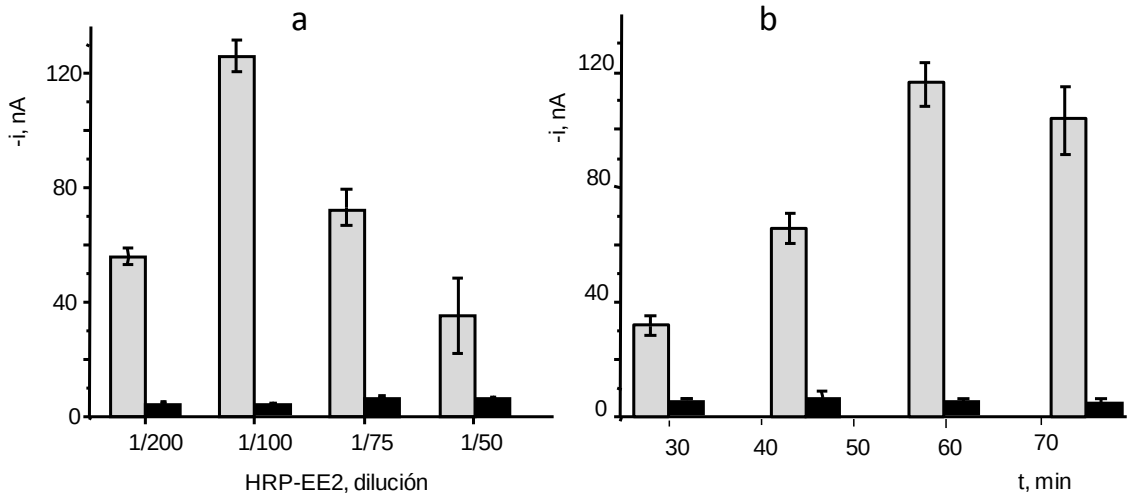

***Figura 89**.- Influencia de la concentración de HRP-EE2 (a) y el tiempo de incubación (b) sobre la respuesta del inmunosensor HRP-EE2(EE2)-anti-EE2-Phe-AgNPs/ SiO_2/GO/ GCE: 20 µg/mL anti-EE2, 60 min; 0 µg/mL EE2 (gris); 0 µg/mL anti-EE2, 0 µg/mL EE2, (negro); HRP-EE2 en dilución 1/200 -1/50, 60 min (a); HRP-EE2 en dilución 1/100, 30 -75 min (b);. Las demás condiciones son las mismas que en la Fig.87.*

Una vez completados los estudios de optimización, en la Tabla 19 se resumen las variables investigadas, los intervalos ensayados, y el valor seleccionado en cada caso.

Tabla 19.- *Optimización de las variables implicadas en la preparación del inmunosensor HRP-EE2(EE2)-anti-EE2-Phe-AgNPs/SiO_2/GO/ GCE*

Variable	Intervalo/reactivo estudiado	Valor seleccionado
anti-EE2, µg/mL	0 - 50	20
tiempo incubación anti-EE2, min	0 - 120	45
tipo de agente bloqueante	etanolamina, caseína, BSA	caseína
tiempo incubación caseína, min	30 - 75	60
HRP-EE2, dilución	1/200 - 1/50	1/100
tiempo incubación HRP-EE2, min	30 - 75	60

5.2.3.2.1. Estudios de caracterización

Los electrodos modificados se caracterizaron por espectroscopia de impedancia electroquímica empleando disoluciones de $Fe(CN)_6^{3-/4-}$ 5 mM en KCl 0.1 M, con los resultados que se han representado en la Figura 90. Como puede observarse, la curva de Nyquist registrada sobre el electrodo GO/GCE (curva1), muestra un valor de la resistencia a la transferencia de carga, R_{CT} = 1362 Ω, mucho mayor que la que se obtiene sobre el electrodo SiO_2/GO/GCE (curva 2), R_{CT} = 331 Ω, disminuyendo esta ligeramente sobre el electrodo AgNPs/SiO_2/GO/GCE (curva 3), con R_{CT} = 233 Ω. Este comportamiento se explica teniendo en cuenta que la presencia del óxido de grafeno unido a la estructura porosa de la matriz de sílice proporciona una mayor conductividad, incrementada posteriormente por la incorporación de las nanopartículas de plata. Finalmente, la inmovilización del anticuerpo de captura para obtener el inmunosensor anti-EE2-Phe-AgNPs/SiO_2/GO/GCE produjo un fuerte incremento de R_{CT}, con un valor de 23.3 kΩ, debido al carácter aislante de la biomolécula. Este último resultado, además, demuestra la utilidad de la superficie electródica empleada y del método de *electrografting* utilizado para la construcción de la superficie inmunosensora.

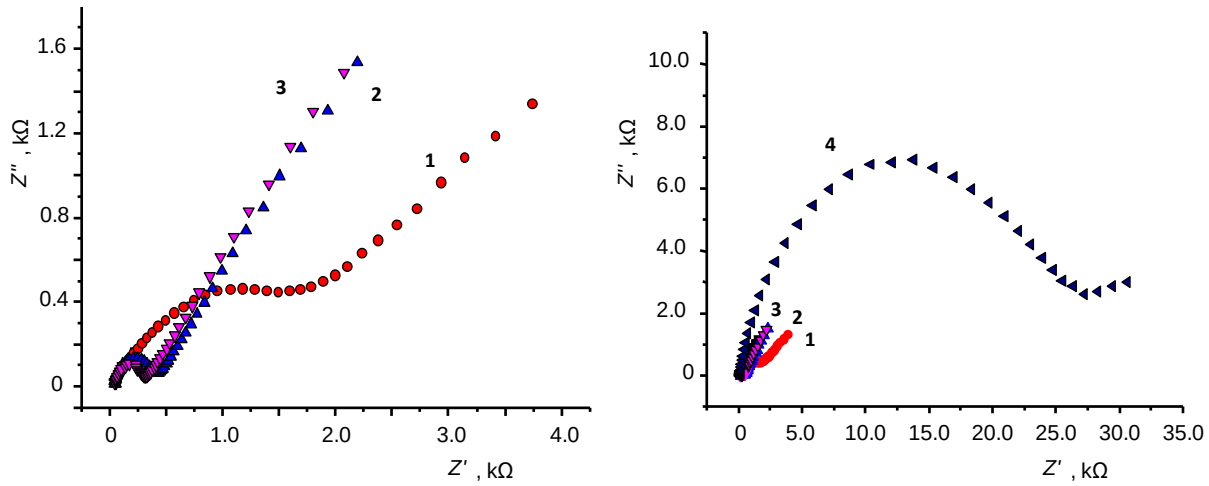

Figura 90.- *Espectros de impedancia electroquímica registrados sobre los electrodos GO/GCE (1), SiO_2/GO/GCE (2), AgNPs/SiO_2/GO/GCE (3) y anti-EE2-Phe-AgNPs/ SiO_2 /GO/GCE (4) $Fe(CN)_6^{3-/4-}$ 5 mM 0.1M KCl.*

5.2.3.3. Calibrado y características analíticas

En la Figura 91 se ha representado el calibrado obtenido para EE2 empleando el inmunosensor HRP-EE2(EE2)-anti-EE2-Phe-AgNPs/SiO_2/GO/GCE, observándose la dependencia de la respuesta amperométrica con el logartimo de la concentración en el intervalo comprendido entre 5 x 10^{-4} y 5 x 10^3 ng/mL de hormona. Al igual que en otros casos, las barras de error corresponden a las medidas realizadas con tres electrodos modificados diferentes. La curva sigmoidal obtenida se ajustó mediante regresión no lineal (r^2 = 0.994) a la ecuación:

$$i_p = i_{\min} + \frac{i_{max} - i_{min}}{1 + \left(\frac{x}{EC_{50}}\right)^{-h}}$$

donde i_{max} = 155.6 nA e i_{min} = 6.1 nA, son los valores de intensidad máximo y mínimo de la curva, respectivamente. Por otro lado, el valor de EC_{50} fue de 3.3 ng/mL, que es la concentración de EE2 para un 50% de competición, mientras que para la pendiente de Hill, que determina la curvatura del sigmoide [Lu et al., 2007] se obtuvo h= -0.57.

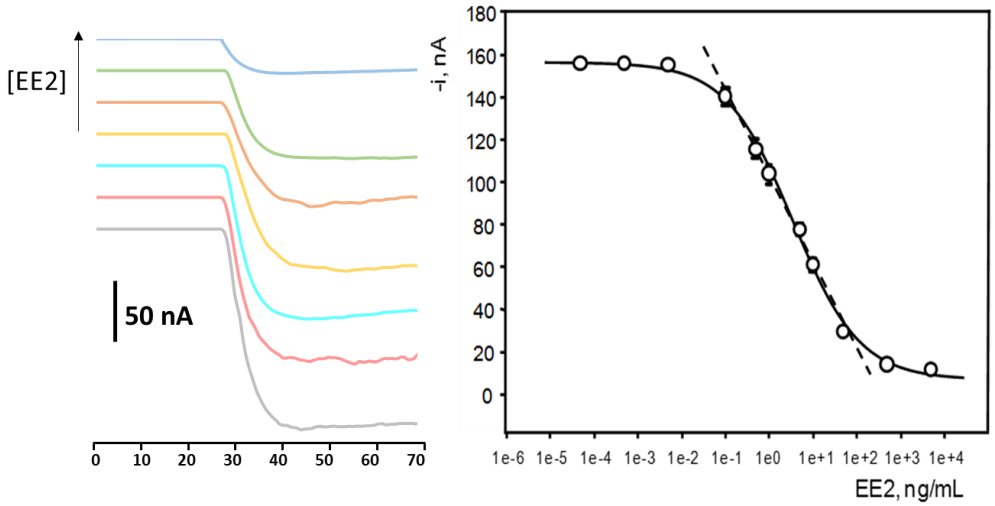

Figura 91.- *Calibrado para la determinación de EE2 con el inmunosensor HRP-EE2(EE2)-anti-EE2-Phe-AgNPs/SiO_2/GO/GCE. Amperogramas obtenidos para diferentes concentraciones de EE2: azul 500 ng/mL; verde 100 ng/mL; naranja 50 ng/mL; amarillo 10 ng/mL; turquesa 5 ng/mL; rosa 1 ng/mL y gris 0.1ng/mL.*

El ajuste por mínimos cuadrados de la porción recta de dicha curva proporcionó un intervalo regido por la ecuación i vs. log [EE2] (r^2=0.994) entre 0.1 y 50 ng/mL, con una pendiente de 4171 nA por década de concentración. El límite de detección se calculó como la menor concentración de EE2 que puede diferenciarse de cero, y se obtuvo restando dos veces la desviación estándar (2 s, siendo s = ± 4.7 nA) del valor medio de la corriente proporcionada por una disolución preparada en ausencia de EE2. El valor obtenido fue 0.065 ng/mL EE2, muy parecido al resultado de 0.063 ng/mL que se obtiene con la ecuación:

$$LOD = EC_{50}\left(\frac{i_{max} - i_{min}}{i_{max} - i_{min} - 3s} - 1\right)^{-1/h}$$

En este caso también se aplicó un tratamiento de ajuste por regresión logística (logit) de la curva, representando *Ln (p/1-p) vs Ln x, siendo* $p=(y-i_{min})/(i_{max}-i_{min})$ con los resultados que aparecen en la Figura 92.

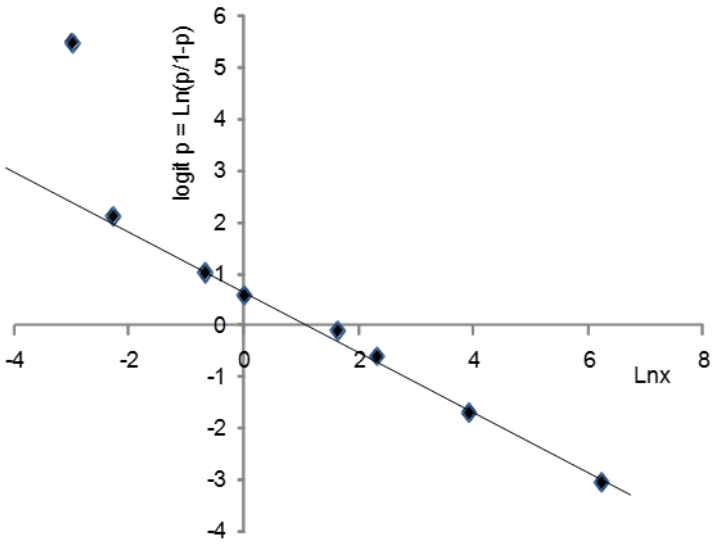

Figura 92.- *Representación de Ln (p/1-p) vs Ln x, con x = [EE2] en ng/mL*

Como puede observarse, se obtuvo una línea recta que se desvía de la linearidad por debajo de una concentración de EE2, x = 0.05 ng/mL. La pendiente de dicha recta fue de -0.59, valor que coincide apreciablemente con la pendiente de Hill, h, obtenida anteriormente.

Es importante señalar que las características analíticas del inmunosensor son adecuadas para la determinación de EE2 en muestras biológicas en las que la concentración se encuentra en el margen de las decenas de ng/mL [Schneider et al., 2004]. El intervalo dinámico del calibrado es mucho más amplio que el reportado por los kits ELISA disponibles (ver Tabla 9 en la Introducción), pero el límite detección alcanzado por el inmunosensor corresponde a una concentración más alta que la concentración mínima detectable encontrada con los métodos de inmunoensayo ELISA, 9.3 pg/mL aproximadamente, y que la obtenida por el método descrito por [Martínez et al., 2010] (0.09 pg/mL). Sin embargo, esta comparación no es enteramente correcta ya que se han empleado distintos criterios para obtener los valores.

La reproducibilidad de las medidas realizadas con el inmunosensor se evaluó mediante la obtención de una serie de amperogramas de disoluciones de EE2 de 0.1 ng/mL con inmunosensores preparados en el mismo o en diferentes días. Los valores de la RSD fueron del 4.5% (n=10) y del 5.4% (n=10), respectivamente. Estos resultados revelan la buena precisión alcanzada en la preparación de la plataforma electródica y en la medida electroquímica con el bioelectrodo desarrollado. En relación a la estabilidad de almacenamiento de los conjugados anti-EE2-AgNPs/SiO_2/

GO/GCE, conservados a 4 ºC, ésta se evaluó en ausencia de EE2, midiendo la respuesta amperométrica de los inmunosensores preparados a partir de ellos, por adición del agente bloqueante y el conjugado de detección, HRP-EE2. Los resultados obtenidos (Figura 93) muestran que la corriente inicial del inmunosensor se mantiene durante al menos 15 días dentro de los límites del gráfico de control, situados a ± 3s, donde s es la desviación estándar de las medidas (n=10) obtenidas el primer día de trabajo. Este resultado indica una buena estabilidad del conjugado desarrollado, y pone de manifiesto la posibilidad de preparar una serie de ellos, mantenerlos a baja temperatura, y utilizarlos cuando sea necesario realizar las medidas con el inmunosensor completo.

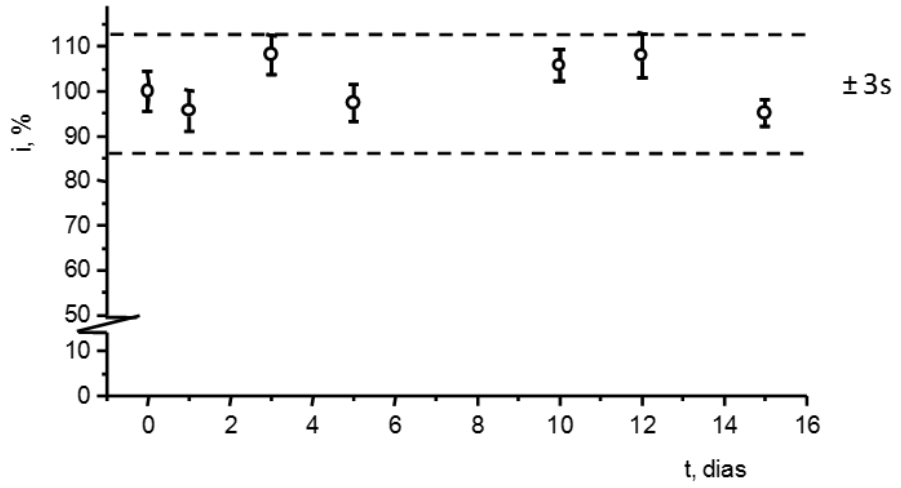

Figura 93.- *Gráfico de control para la evaluación de la estabilidad de almacenamiento del conjugado anti-EE2-Phe-AgNPs/GO/SiO_2/SPCE. Cada punto corresponde al valor medio de tres medidas sucesivas en ausencia de EE2*

5.2.3.4. Estudios de selectividad

Varias hormonas esteroideas relacionadas con el EE2 fueron ensayadas como potenciales interferentes del método de determinación del analito empleando el inmunosensor desarrollado en el trabajo. Las especies investigadas fueron: cortisol, β-estradiol (E2), estriol (E3), progesterona y testosterona (ver estructuras en la Figura 82). El efecto de la presencia de cada hormona se estudió por medida de las corrientes sobre el inmunosensor preparado a partir de conjugados anti-EE2(EE2)-Phe-AgNPs/SiO_2/ GO/GCE con 1 ng/mL de EE2 o del compuesto interferente.

En la Figura 94 se han representado los resultados obtenidos, observándose cómo únicamente el β-estradiol (E2) y la testosterona (TEST) originan porcentajes de corriente relativa ligeramente por encima del límite correspondiente a ± 2s. Este fenómeno fue observado también en otros trabajos empleando diferentes metodologías. Por ejemplo, el E2 mostraba una mayor reactividad cruzada que otras hormonas estrogénicas en el método ELISA para EE2 descrito por el grupo de Schneider, utilizando detección espectrofotométrica o quimioluminiscente [Schneider et al., 2004]. Estos dos compuestos son estructuralmente similares, siendo E2 el producto de la reacción de aromatización de la testosterona, con el grupo hidroxi en la posición C-17 y ningún otro grupo funcional incorporado a ese anillo (Figura 82). Por ello, puede concluirse que el anticuerpo utilizado es capaz de discriminar los antígenos basándose en estas diferencias.

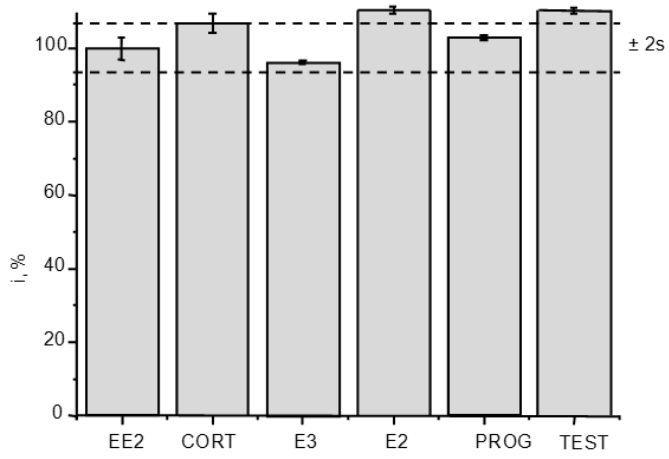

Figura 94.- *Efecto de la presencia de 1 ng/mL de distintas hormonas en la respuesta amperométrica del inmunosensor HRP - EE2 (EE2) - anti - EE2 - Phe - AgNPs / GO / SiO_2 / SPCE*

5.2.3.5. Aplicación a la determinación de EE2 en orina

La utilidad analítica del inmunosensor HRP-EE2-anti-EE2(EE2)-Phe-AgNPs/ SiO_2/GO/GCE para la determinación de EE2 en muestras biológicas se demostró por aplicación al análisis de orina contaminada con la hormona a cuatro niveles de concentración: 0.1, 0.5, 1.0 and 10 ng/mL. En primer lugar se realizaron varios análisis de las muestras de orina sin contaminar para verificar la ausencia de EE2, no encontrándose en ellas concentraciones detectables. Posteriormente, se aplicó el procedimiento descrito en la Parte Experimental, analizando las muestras sin tratamiento previo. Con el fin de evaluar la posible existencia de efecto matriz, se

compararon los calibrados obtenidos con disoluciones patrón de EE2 y con las muestras de orina contaminadas con EE2 en el intervalo de 0.1 a 50 ng/mL. Como puede observarse en la Figura 95, ambas rectas son muy parecidas, solapando prácticamente entre sí.

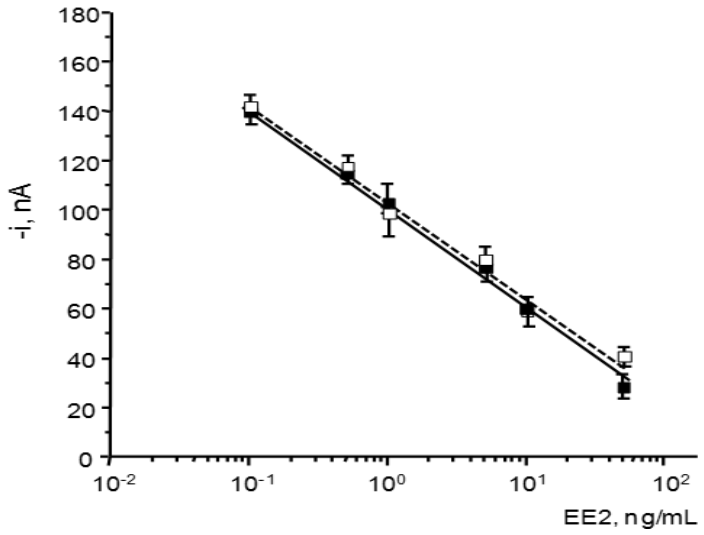

Figura 95.- *Calibrados para EE2 construidos con el inmunosensor HRP-EE2(EE2)-anti-EE2-Phe-AgNPs/SiO_2/GO/GCE inmunosensor: (—■—) disoluciones patrón de EE2; (- -□- -) muestras de orina.*

Las pendientes de ambos calibrados: 38 ± 2 nA por década de concentración para las muestras y 41 ± 1 nA por década de concentración para los patrones se compararon estadísticamente aplicando el test t en las mismas condiciones que en los casos anteriores, obteniéndose un valor de t_{exp} = 1.34, inferior al valor tabulado, t_{tab} = 2.306, para n = 8, a un nivel de significación de 0.05. Estos resultados indican que no existen diferencias significativas entre los dos valores de las pendientes, por lo que es posible realizar la determinación de EE2 en la muestra por interpolación directa de la corriente proporcionada por el inmunosensor en el calibrado de patrones. En estas condiciones, los resultados obtenidos en el análisis de las muestras de orina se han resumido en la Tabla 20, en la que se observan buenas recuperaciones a todos los niveles de concentración ensayados, con valores comprendidos entre 96 ± 1% y 100 ± 1%, para cinco réplicas de cada una de ella.

Tabla 20.- *Determinación de EE2 en orina con el inmunosensorHRP-EE2-anti-E2/AgNPs/SiO_2/GO/GCE*

EE2 añadido, ng/mL	EE2 encontrado, pg/mL	Recuperación media, %
0.1	0.098 ± 0.002*	99 ± 2
0.5	0.50 ± 0.01	102 ± 2
1.0	0.98 ± 0.02	99 ± 3
5.0	4.8 ± 0.1	96 ± 1

*± ts / √n

5.2.3.6. Conclusiones

En este trabajo se ha preparado un inmunosensor electroquímico para la determinación de EE2. En la configuración desarrollada, por primera vez se ha explorado la posibilidad de emplear el material híbrido AgNPs/SiO_2/GO para la construcción de este tipo de sensores de afinidad diseñando una estategia de inmovilizaciñon del anticuerpo de captura por *electrografting* de *p*-ABA y activación de los grupos carboxilo con el sistema EDC/NHSS. El uso de esta configuración unido al esquema de inmunosensayo competitivo establecido y la excelente respuesta electroquímica obtenida para la reacción del peróxido de hidrógeno catalizada por la peroxidasa en presencia de hidroquinona, sobre el electrodo modificado, han hecho posible poner a punto un método para la determinación de EE2 en un intervalo lineal comprendido entre 1 y 50 ng/mL, con un límite de detección de 0.065 ng/mL. Estas características, junto a la elevada precisión y selectividad que presenta el inmunosensor, lo hacen adecuado para determinar la hormona en muestras de orina.

5.2.4. BIOSENSOR ENZIMÁTICO PARA LA DETERMINACIÓN DE β-HB

Como se ha señalado en la Introducción, la determinación de compuestos cetónicos en sangre es una potente herramienta para detectar procesos de cetoacidosis peligrosos para la salud. En este contexto, los niveles de β-hidroxibutirato (β-HB), uno de los principales cuerpos cetónicos en el organismo, se han establecido en diferentes márgenes relacionados con distintos tipos de enfermedades, como por ejemplo entre 1.1 y 3 mM para la hipercetonemia, o por encima de 3 mM en el caso de la cetoacidosis diabética (DKA) [Wallace et al., 2004] [Laffel, 1999]. La concentración de β-HB presenta, además, valores alterados en los pacientes con obesidad mórbida [Rodríguez-Gallego et al., 2015], otro aspecto de gran importancia que demuestra el alto interés clínico que posee la puesta a punto de métodos para la determinación de este compuesto.

En el Apartado 3.7.6. se describieron las características de algunos métodos disponibles para esta aplicación, la mayor parte basados en el empleo de la enzima β-hidroxibutirato deshidrogenasa (β-HBDH) y el sistema NAD^+/NADH. Como se ha dicho, esta enzima cataliza específicamente la transformación del analito a acetoacetato en presencia de NAD^+, produciendo NADH que es el producto detectable. Como en otros casos, debido a los problemas de alto potencial de oxidación y de ensuciamiento de los electrodos que conlleva esta detección, es preciso utilizar materiales de electrodo adecuados y/o mediadores redox para mejorar la selectividad del método y la reproducibilidad de las medidas.

En el trabajo realizado en esta Tesis Doctoral, se construyó una plataforma electroquímica empleando SPCEs modificados con óxido de grafeno reducido (rGO) para la preparación de un biosensor enzimático usando β-HBDH y NAD^+, en el que la detección de NADH se lleva a cabo usando tionina (THI) como mediador redox. La mejora en la velocidad de transferencia de carga del proceso de oxidación del NADH que provoca el empleo del electrodo modificado con rGO, unido a la presencia de THI, con la notable disminución del potencial de detección, ha hecho posible determnar β-HB en suero humano a niveles clínicamente relevantes.

5.2.4.1. Configuración del biosensor

En la Figura 36 de la Parte Experimental se representó el esquema de preparación y funcionamiento del biosensor enzimático para β-HB que, como se ha señalado, implica la inmovilización de la enzima β-HBDH sobre el electrodo serigrafiado modificado con rGO y THI. Tras la adición de β-HB o la muestra, en presencia del cofactor NAD^+, fue posible detectar el NADH generado a un potencial de 0.0 V vs Ag, basándose en la siguiente serie de reacciones:

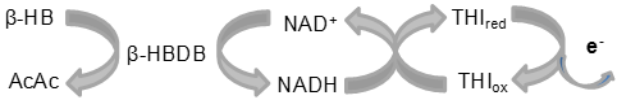

donde la enzima cataliza la oxidación del sustrato a aceto acetato (AcAc), produciéndose la reducción del mediador (THI_{ox}) por acción del NADH, lo que hace posible finalmente la reacción electroquímica de oxidación de THI_{red}, que es la especie que genera la respuesta analítica sobre el bioelectrodo.

5.2.4.2. Optimización de las variables experimentales

Se optimizaron las variables implicadas en la preparación del electrodo modificado y del biosensor enzimático. Aparte de la cantidad de rGO depositada sobre el electrodo, que fue la utilizada en un trabajo anterior [Martínez-García et al., 2016], las variables investigadas fueron: a) el potencial de medida, b) la cantidad de tionina y el tiempo de adsorción, c) la cantidad de enzima y d) el valor de pH.

- ***Elección del potencial de medida***

En primer lugar se estudió el comportamiento electroquímico del electrodo modificado mediante voltamperometría cíclica. En la Figura 96 se comparan los voltamperogramas obtenidos sobre el electrodo rGO/SPCE (curva a) y sobre el mismo electrodo modificado por adición de 15 µL de THI 1 mM (THI/rGO/SPCE, curva b) en medio regulador fosfato 0.1 M de pH 7.0. Como puede observarse, los picos anódico y catódico de THI aparecen respectivamente a potenciales de 0.0 V y -0.2 V correspondiendo a la oxidación y la reducción del mediador redox.

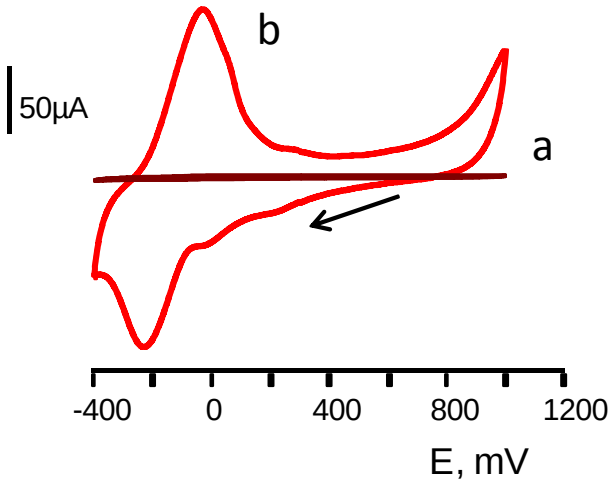

Figura 96.- *Voltamperogramas cíclicos de: a) rGO/SPCE; b) THI/rGO/SPCE en disolución reguladora fosfato 0.1 M de 7.0. Más información en el texto.*

Con el fin de investigar la respuesta del mediador en la superficie del electrodo, se evaluó el efecto de la velocidad de barrido de potencial en el intervalo de 5 a 200 mV/s mediante voltamperometría cíclica sobre el electrodo THI/rGO/SPCE con los resultados representados en la Figura 97.

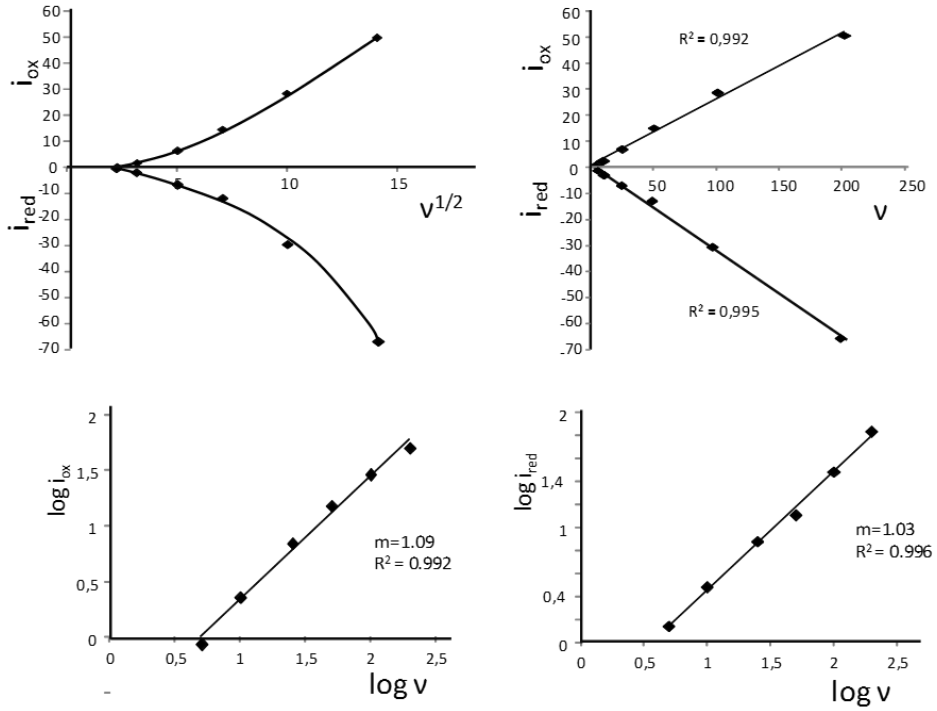

Figura 97.- *Estudio del efecto de la velocidad de barrido de potencial en CV sobre la respuesta del electrodo THI/rGO/SPCE. Disolución reguladora fosfato 0.1 M de 7.0.*

Como puede apreciarse, los picos de oxidación y de reducción de la tionina (THI) mostraron una dependencia lineal con la velocidad de barrido de potencial (r^2 = 0.992 (ox) y r^2 = 0.995 (red)), mientras que la representación de la corriente frente a la raiz cuadrada de la velocidad de barrido originó lineas curvas. Además, la representación logarítmica log i vs. log v proporcionó rectas (r^2 = 0.992 (ox) y r^2 = 0.996 (red)) con valores de la pendiente de 1.09 (ox) y 1.03 (red). Estos resultados demostraron el control superficial de la respuesta electroquímica de THI.

Teniendo en cuenta el comportamiento del electrodo modificado, se eligió un potencial de detección de 0.0 V vs Ag para realizar las medidas. En estas condiciones se obtuvieron calibrados para NADH sobre el electrodo THI/rGO/SPCE en el intervalo de 0.1 a 1.0 mM, observándose un buen ajuste a la ecuación: i, μA = (0.19 ± 0.01) [NADH, mM] + (0.018 ± 0.007) (r^2 = 0.990). Es importante señalar, a efectos comparativos, que la pendiente de este calibrado es aproximadamente quince veces mayor que la obtenida sobre un electrodo serigrafiado fabricado con partículas de indio-carbono, m= 0.013 μA/mM, diseñado para la determinación de β-HB, aplicando un potential de detección de +0.2 V vs Ag/AgCl [Fang et al., 2008].

- ***Influencia de la cantidad de THI y del tiempo de adsorción***

El efecto de la cantidad de mediador redox presente en la superficie del electrodo THI/rGO/SPCE se evaluó midiendo la corriente de disoluciones de NADH 0.2 mM sobre electrodos preparados empleando diferentes concentraciones de THI en el intervalo de 0.1 a 5.0 mM.

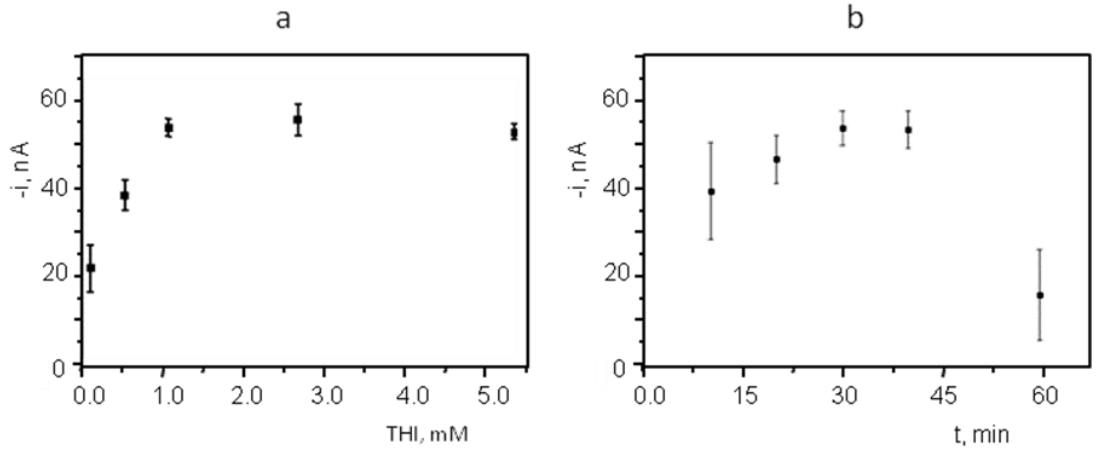

Figura 98.- *Efecto de la cantidad de THI (a) y del tiempo de adsorción (b) sobre la respuesta del electrodo THI/rGO/SPCE.*

Como puede observarse en la Figura 98a, la señal de oxidación aumenta hasta una concentración de THI 1 mM, permaneciendo después prácticamente constante para concentraciones superiores. Se observó también (Figura 98b) que en estas condiciones, un tiempo de 30 minutos era suficiente para asegurar una adsorción estable del mediador en el electrodo.

- ***Influencia de la cantidad de enzima***

El efecto sobre la respuesta del biosensor de la cantidad de β-HBDH adsorbida en el electrodo modificado se evaluó preparando varios bioelectrodos con disintas cantidades de enzima en el intervalo de 0.01 a 0.6 unidades, por medida de disoluciones que contenían NAD^+ 0.1 mM y β-HB 0.040 mM. Los resultados representados en la Figura 99 muestran cómo las repuestas óptimas se alcanzan para 0.2 unidades de β-HBDH, cantidad que coincide apeciablemente con la empleada para preparar otros biosensores descritos para β-HB. El rápido decaimiento de la corriente medida para mayores cantidades de enzima se debe probablemente a la disminuciòn de la conductividad originada por la presencia de una capa de biomoléculas aislantes en la superficie del electrodo.

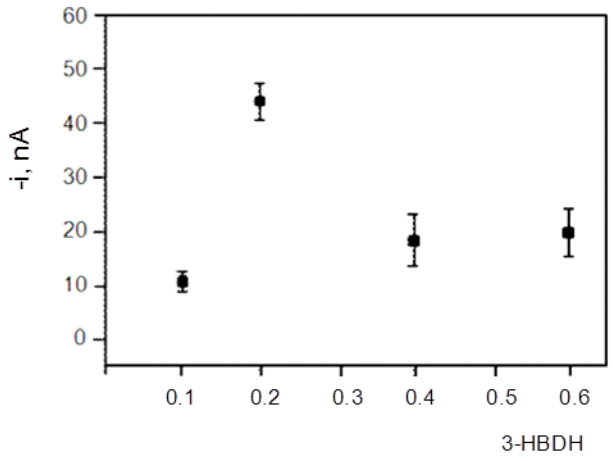

Figura 99.- *Efecto de la cantidad de β-HBDH sobre la respuesta del biosensor β-HBDH/THI/rGO/SPCE.*

- ***Influencia del pH***

Para estudiar el efecto del pH sobre la respuesta del biosensor, se emplearon diferentes disoluciones reguladoras fosfato 0.1 M preparadas a pHs comprendidos entre 5.0 y 9.0, midiendo la señal amperométrica en presencia de NAD^+ 0.1 mM y β-HB 0.040 mM. Los resultados que se muestran en la Figura 100a permiten observar corrientes de mayor magnitud a pH comprendidos entre 7.0 y 8.0. Para elegir el valor óptimo, en un experimento aparte se registraron las respuestas del electrodo THI/rGO/SPCE correspondientes a la adición de NADH 20 μM a diferentes pHs (Figura 100b). Puede apreciarse cómo a pH 7.0, la reproducibilidad de los amperogramas es mayor. Por ello, el valor citado fue el elegido para estudios posteriores. Debe señalarse también que, en las condiciones elegidas, la respuesta del bioelectrodo es rápida, alcanzándose el 95% de la corriente máxima en 7 segundos.

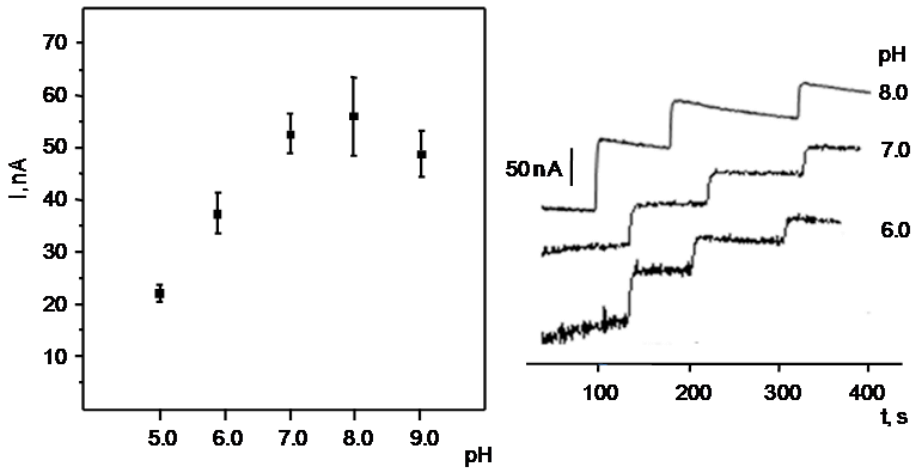

Figura 100.- *Efecto del pH en la respuesta del biosensor y señales amperométricas de NADH 20 μM sobre el electrodo THI/rGO/SPCE*

5.2.4.2.1. Estudios de caracterización

Se empleó la técnica de espectroscopia de impedancia electroquímica para caracterizar la superficie del biosensor. Como puede observarse en la Figura 101a, los espectros de Nyquist obtenidos con los bioelectrodos β-HBDB/rGO/SPCE y β-HBDB/THI/rGO/SPCE en disoluciones 0.1 M KCl, mostraron líneas con el valor de la pendiente mucho mayor que la unidad, lo que revela un comportamiento asimilable al de un condensador ideal, sin que se observen diferencias apreciables en presencia de THI. Por otro lado, cuando se emplearon disoluciones de $Fe(CN)_6^{3-/4-}$ 1 mM en KCl 0.1 M (Figura 100b), los dos bioelectrodos mostraron el comportamiento esperado para

una transferencia de carga controlada por difusión. Además, un pequeño semicírculo aparece a las frecuencias más altas, que es menos aparente sobre el electrodo preparado con THI. Este comportamiento se debe probablemente a la existencia de defectos en forma de pequeños poros o a un espesor no uniforme del recubrimiento electródico, pero no se puede atribuir a un diferente comportamiento electroquímico de la sonda electroactiva sobre los electrodos.

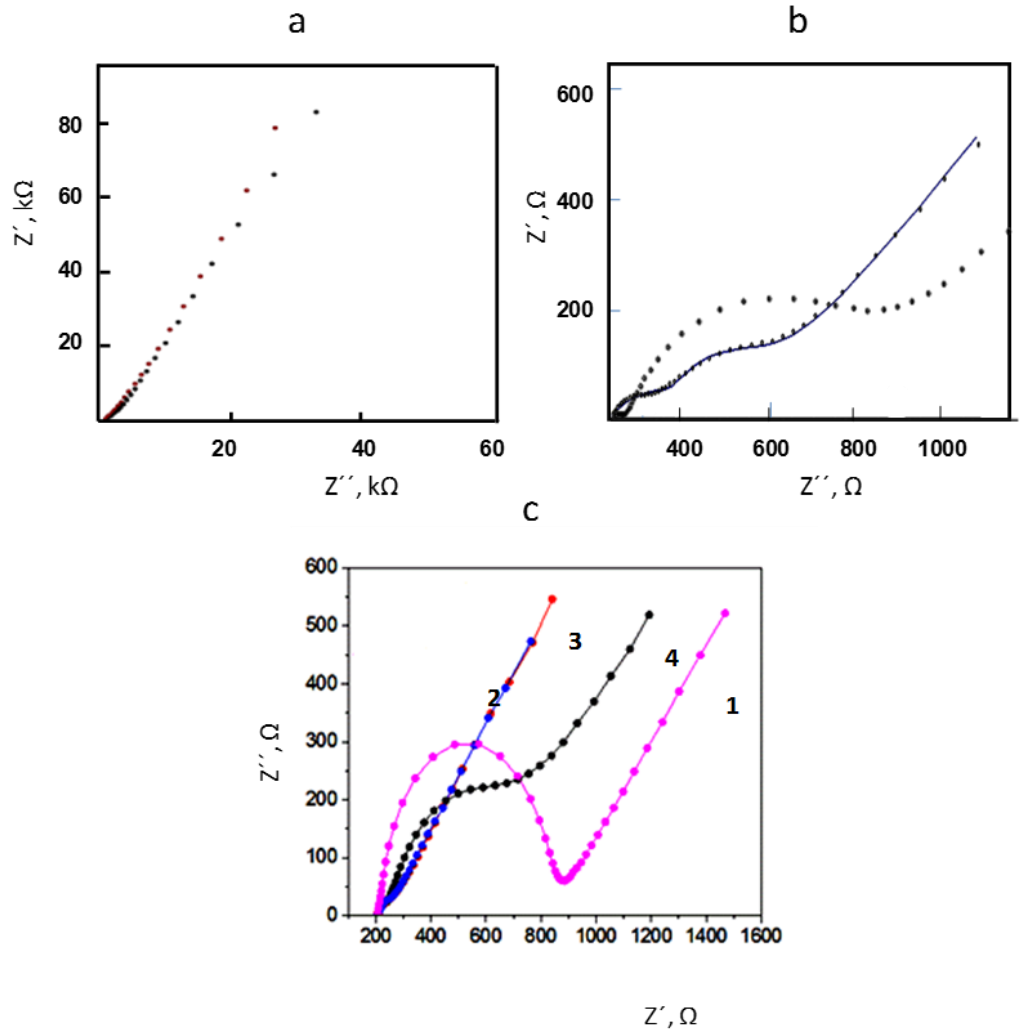

Figura 101.- *Curvas de Nyquist obtenidas sobre (a) β-HBDH/THI/rGO/SPCE (negro) y β-HBDH/rGO/SPCE (rojo) en KCl 0.1 M; (b) β-HBDH/THI/rGO/SPCE (••••) y β-HBDH/rGO/SPCE (—) en $Fe(CN)_6^{3-/4-}$ 1 mM en KCl 0.1 M; (c) SPCE (1); rGO/SPCE (2); THI/rGO/SPCE (3); β-HBDH/THI/rGO/SPCE (4) en $Fe(CN)_6^{3-/4-}$ 1 mM en KCl 0.1 M*

Las distintas etapas de preparación del biosensor se estudiaron también mediante EIS empleando $Fe(CN)_6^{3-/4-}$ 1 mM en KCl 0.1 M. En la Figura 101c se han representado los espectros de impedancias registrados sobre SPCE (curva 1), rGO/SPCE (curva 2), THI/rGO/SPCE (curva 3), y β-HBDH/THI/rGO/ SPCE (curva 4). Como puede apreciarse, la resistencia a la transferencia de carga sobre el SPCE (638

Ω) es notablemente superior a las que presentan los electrodos rGO/SPCE y THI/rGO/SPCE (87 y 94 Ω, respectivamente) como consecuencia de la presencia de rGO que proporciona una elevada conductividad al electrodo modificado. Destacar que la presencia del mediador redox, THI, prácticamente no afecta al valor de R_{CT}. Por último, como era de esperar, la inmovilización de la enzima provoca un aumento de la resistencia a la transferencia de carga, siendo R_{CT} = 1547 Ω, debido a la presencia de una capa aislante en la superficie del electrodo. Este resultado confirma la adecuada adsorción de la enzima en la superficie del electrodo modificado.

5.2.4.3. Calibrado y características analíticas

En la Figura 102 se ha representado el calibrado para la determinación de β-HB con el biosensor β-HBDH/THI/rGO/SPCE. Como puede observarse, el calibrado lineal se extiende entre 0.003 y 0.400 mM (r^2 = 0.992) con valores de la pendiente y la ordenada en el origen de 110 ± 4 nA/mM y 0.6 ± 3 nA, respectivamente. El límite de detección se calculó con el criterio de $3s_b/m$, donde s_b es la desviación estándar (n=10) obtenida por medida de la corriente de diez disoluciones preparadas en ausencia de β-HB, y m es la pendiente del calibrado. Se obtuvo un valor de LOD = 0.001 mM, muy inferior a los obtenidos usando otros biosensores (ver Tabla 10 en la Introducción). El límite de cuantificación, calculado como 10 s_b/m, fue 0.003 mM.

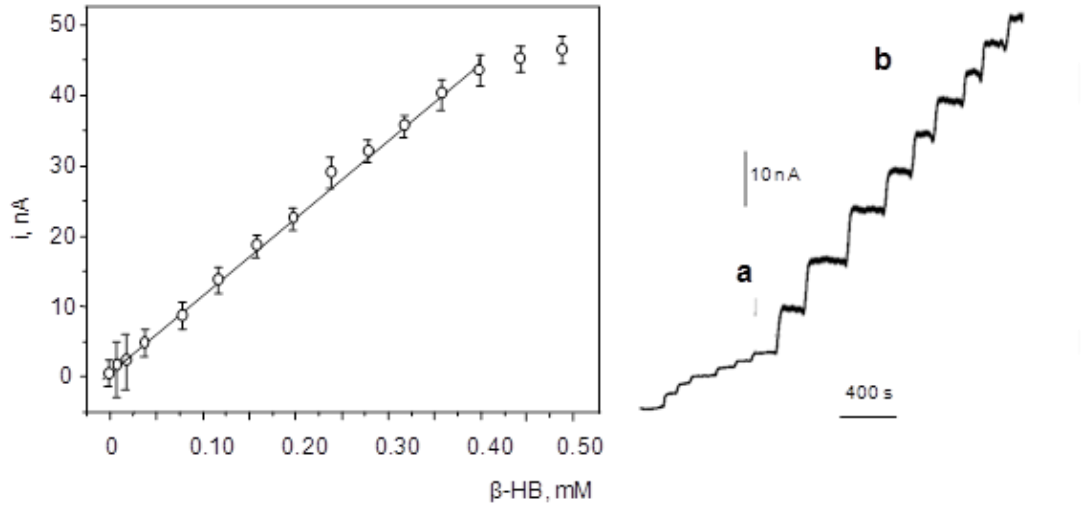

Figura 102.- *Calibrado para β-HB obtenido con el biosensor β-HBDH/THI/rGO/SPCE, y algunas respuestas amperométricas para adiciones de (a) 100 μM and (b) 20 μM β-HB. Las barras de error corresponden a ± s (n=3).*

Las características analíticas del biosensor enzimático son adecuadas para la determinación de β-HB en suero humano, donde las concentraciones se encuentran a nivel mM [Fernández-Merino et al., 2010]. Cuando estas características se comparan con las de los kits ELISA para esta determinación, se aprecian ciertos aspectos ventajosos. Por ejemplo, el intervalo lineal del biosensor, comprendido entre 0.003 y 0.400 mM, es más amplio que el que presenta el kit colorimétrico ab83390 de Abcam (ver Tabla 10), entre 0.01 y 0.1 mM. Por otro lado, el límite de detección obtenido, 0.001 mM es menor que el alcanzado en dicho kit (10 µM).

Se investigó la precisión en la preparación del electrodo enzimático y en las medidas empleando, en primer lugar, diez biosensores distintos preparados aplicando el mismo protocolo en diferentes días, para registrar las corrientes amperométricas de disoluciones de β-HB 0.200 mM. En estas condiciones se obtuvo un valor de RSD = 4.5%. Este resultado demuestra una buena reproducibilidad en la preparación del biolectrodo. Por otro lado, la precisión de las medidas realizadas con un mismo biosensor se estudió empleando diez disoluciones distintas de β-HB 0.200 mM, obteniéndose una valor de RSD = 2.5%, resultado que pone de manifiesto la buena repetibilidad de las medidas con un único biosensor. También se evaluó la estabilidad de almacenamiento a 4 ºC del biosensor β-HBDH/THI/rGO/SPCE, midiendo en diferentes días las respuestas amperométricas de disoluciones de β-HB 0.1 mM con un biosensor preparado en las condiciones experimentales óptimas. Los resultados representados en la Figura 103 ponen de manifiesto que la respuesta inicial del biosensor permanece durante 20 días dentro de los límites del gráfico de control situados a ± 3s, siendo s la desviación estándar de las medidas realizadas el primer día de trabajo (n = 10). Por tanto, puede decirse que el biosensor posee una buena estabilidad de almacenamiento.

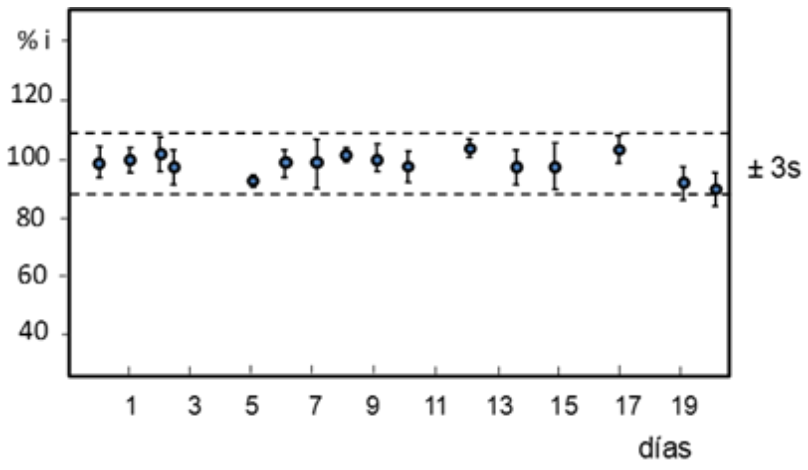

Figura 103.- *Gráfico de control para la evaluación de la estabilidad de almacenamiento del biosensor β-HBDH/THI/rGO/SPCE.*

- ***Parámetros cinéticos***

Se comprobó que la reacción enzimática sobre el biosensor β-HBDH/THI/rGO/SPCE se ajustaba bien al modelo cinético de Michaelis-Menten, según demuestra el cálculo del parámetro "x" (1.05 ± 0.07) a partir de la represenctación de Hill ([log (i_{max}/1)-1] vs. log [β-HB] (Figura 104). Por ello, se efectuó el cáculo de la constante aparente K_M^{app} haciendo uso de la representación de Lineweaver-Burk, obteniéndose un valor de 1.50 ± 0.03 mM. Este resultado es notablemente inferior a los obtenidos por inmovilización de β-HBDH sobre un electrodo serigrafiado de iridiio, 2.3 mM [Fang et al., 2008], sobre sílice mesoporosa FSM8.0, 2.8 mM [Forrow et al., 2005], o sobre un electrodo de carbono platinado, 5.4 mM [McNeil et al., 1990]. Este resultado pone de manifiesto la elevada afinidad de la enzima por el sustrato cuando se inmoviliza sobre el electrodo modificado.

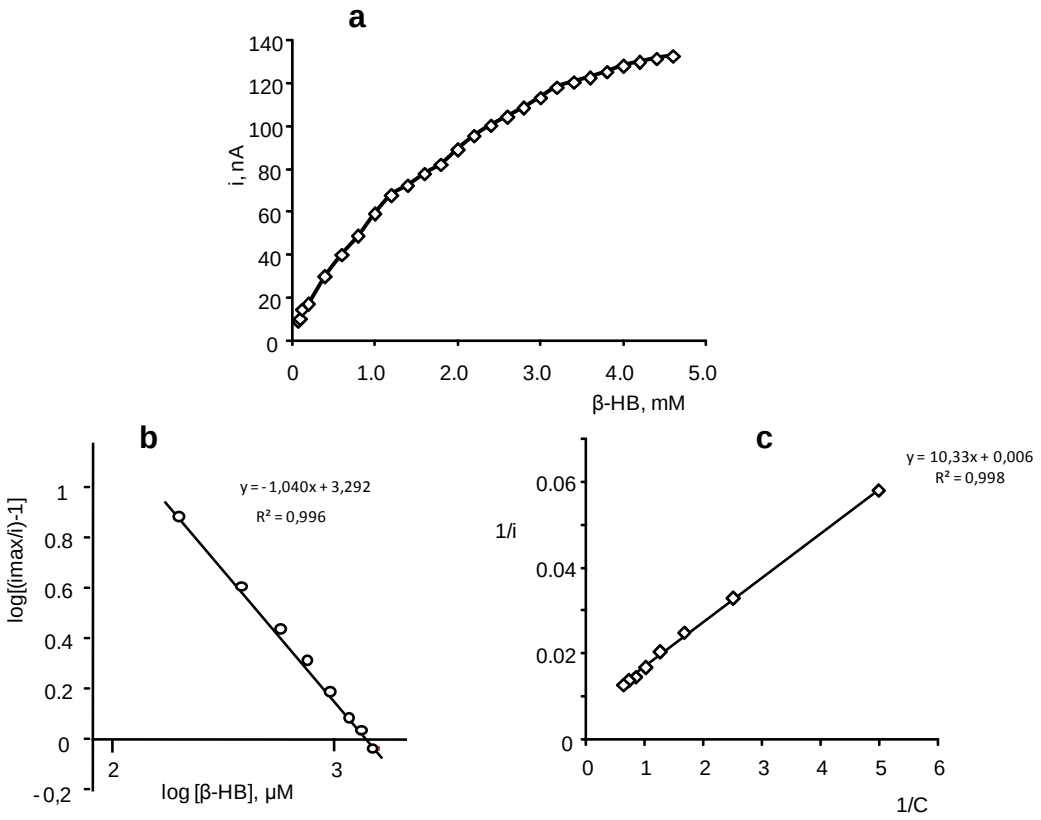

Figura 104.- *Representaciones utilizadas para el cálculo de la constante aparente de Michaelis-Menten: a) calibrado para β-HB; b) gráfico de Hill; c) gráfico de Lineweaver-Burk.*

5.2.4.4. Estudios de selectividad

Se estudió la influencia sobre la respuesta del biosensor enzimático de varios compuestos que pueden estar presentes en las muestras de suero para la determinación de β-HB. Las especies ensayadas fueron: citrato, glutamina, glutamato, succinato, ácido ascórbico, ácido úrico y glucosa. Para ello, se midió la corriente del biosensor β-HBDH/THI/rGO/SPCE en las condiciones óptimas y en ausencia de analito, empleando disoluciones de cada uno de los interferentes a concentraciones del orden del nivel normal esperable en el suero de individuos sanos. La Figura 105 muestra las respuestas amperométricas obtenidas, que se comparan con la de β-HB 0.020 mM.

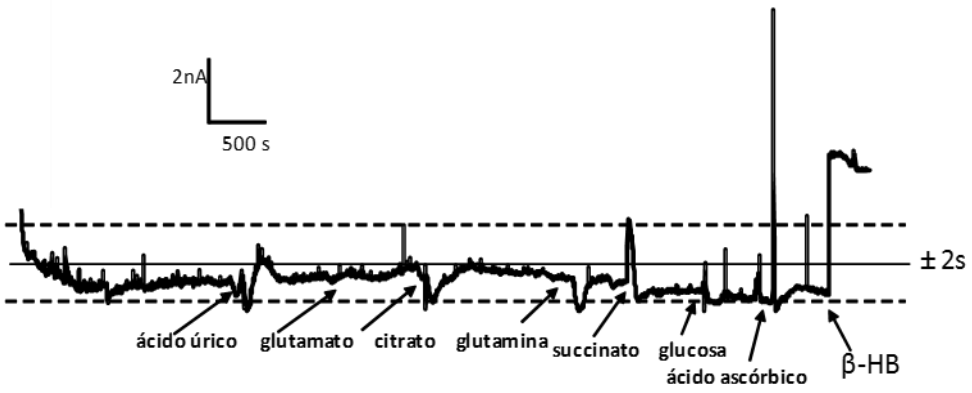

Figura 105.- *Respuestas amperométricas obtenidas sobre el biosensor β-HBDH/THI/rGO/SPCE para ácido úrico 0.178 mM, glutamato 0.103 mM; citrato 0.060 mM; glutamina 0.067 mM; succinato 0.0083 mM; glucosa 0.0073 mM; ácido ascórbico 0.057 mM y β-HB 0.020 mM.*

Como puede observarse, los compuestos ensayados produjeron ligeras variaciones en la corriente de fondo, todas ellas dentro del intervalo ± 2s de dicha señal, excepto el ácido ascórbico que, a la concentración estudiada, originó una repuesta de magnitud elevada. Esto se debe probablemente a la oxidación de esta especie electroactiva al potencial empleado para la detección. A título comparativo, decir que la corriente obtenida para una concentración de ácido ascórbico 0.057 mM equivale a la proporcionada por β-HB 0.040 mM. A pesar de existir esta interferencia, como se verá a continuación, en el análisis del suero humano utilizado para la validación del método no se observó la aparición de ninguna corriente de oxicación de magnitud significativa.

5.2.4.5. Aplicación a la determinación de β-HB en suero

La utilidad del biosensor para el análisis de muestras clínicas se demostró aplicándolo a la determinación de β-HB en suero. Primero se estudió la posible existencia de efecto matriz comparando las pendientes del calibrado de patrones (Apartado 5.2.4.3.) y del obtenido por adiciones de disolución patrón del analito en el intervalo de 0.01 a 0.400 mM sobre una muestra de suero a la que se aplicó el Procedimiento descrito en el Apartado 4.4.6. de la Parte Experimental. Tal como se indica, dicho procedimiento implica la dilución del suero con el mismo volumen de una disolución 0.2 mM de NAD^+ en regulador fosfato de pH 7.0. En estas condiciones, la pendiente obtenida para el calibrado de adiciones sobre la muestra fue igual a 66 ± 4 nA/mM, valor que es significativamente diferente a la del calibrado patrón, 110 ± 4 nA/mM (ver Figura 106). Esta diferencia pone de manifiesto la necesidad de utilizar el método de adiciones patrón para la determinación de β-HB en el suero. Hay que destacar que no se observó ningún incremento de la señal de corriente sobre la señal del fondo que pudiera estar causada por la presencia de compuestos interferentes en el suero. Así, la señal proporcionada por el suero sin contaminar, 0.4 ± 0.1 nA, es incluso menor que la que proporciona el electrólito fondo, regulador fosfato, utilizado para obtener el calibrado de patrones, 0.6 ± 0.3 nA.

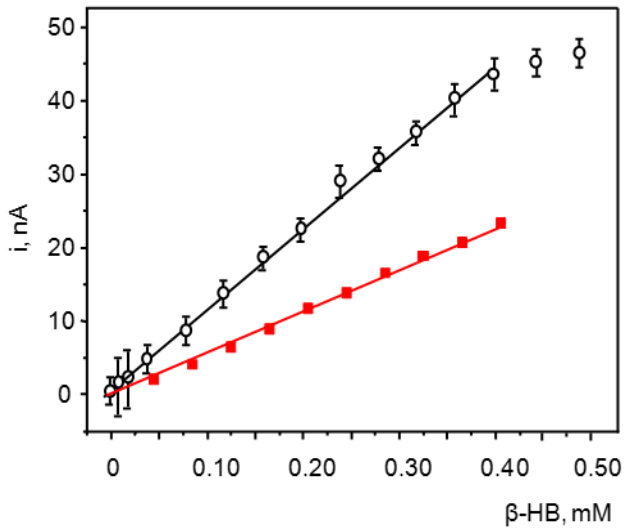

Figura 106.- *Calibrados para β-HB construidos con el biosensor β-HBDH/THI/ rGO/SPCE (—○—)disoluciones patrón de β-HB; (—■—) muestra de suero.*

La aplicación del método se realizó sobre muestras de suero contaminadas con β-HB en concentración 0.033 mM y 0.290 mM, niveles inferiores a los esperados en pacientes con problemas de salud causados por hipercetonemia o cetoacidosis diabética. Evidentemente, otras muestras más concentradas podrían analizarse también sin más que aplicar la dilución adecuada. Como se muestra en la Tabla 21, los resultados obtenidos por quintuplicado proporcionaron recuperaciones muy próximas al 100%, demostrando la utilidad del biosensor desarrollado para la aplicación a este tipo de muestras.

Tabla 21.- *Determinación de β-HB en suero con el biosensor β-HBDH/THI/ rGO/SPCE*

β-HB, mM	β-HB encontrado, mM	Recuperación media, %
0.033	0.032 ± 0.003*	98 ± 8
0.290	0.294 ± 0.015	101 ± 5

*± ts / √n

5.2.4.6. Conclusiones

En este trabajo se puso a punto un método simple de preparación de un biosensor electroquímico enzimático para la determinación de β-HB en suero humano. En el diseño de este biosensor se aprovecharon las ventajas del empleo de electrodos serigrafiados de carbono modificados con óxido de grafeno reducido, que dan lugar a una elevada la velocidad de transferencia electrónica en la oxidación de NADH, así como también a las del uso de tionina como mediador redox, que permite utilizar un potencial de detección de 0.0 V vs Ag. El biosensor demostró buenas características analíticas en términos de intervalo de linealidad, elevada sensibilidad y bajo límite de detección en comparación con otras configuraciones existentes para la determinación de β-HB. Finalmente, se demostró la utilidad del método desarrollado aplicándolo a muestras de suero diluidas sin necesidad de preparación previa.

5.3. INMUNOSENSOR ELECTROQUÍMICO BASADO EN UN POLÍMERO CONDUCTOR

5.3.1. INMUNOSENSOR PARA LA DETERMINACIÓN DE AMY

La hormona amilina (AMY), como se ha señalado, se secreta conjuntamente con la insulina (INS), y está implicada en diversos procesos relacionados con el apetito, la saciedad y la adiposidad. Sus niveles en plasma son bajos en los periodos de ayuno y aumentan en las comidas, así como tras la administración de glucosa, siendo en todos los casos proporcionales al contenido de grasa corporal. La relación INS/AMY se mantiene aproximadamente fija en un valor entre 10 y 100 en los individuos sanos, pero la obesidad, la diabetes y otras enfermedades tienden a incrementar la cantidad de amilina respecto a la de insulina. Además, la variación en la concentración de esta hormona posee valor diagnóstico en situaciones de resistencia a la insulina, o en pacientes hiperinsulinémicos [Castillo et al., 1995]. Como referencia, indicar que los niveles de amilina en suero humano oscilan en torno a unas pocas decenas de pg/mL [Percy et al., 1996] [Harter et al., 1991].

Al igual que en otros casos, a pesar de la importancia de esta hormona, prácticamente no se dispone de métodos para su determinación. Ya se han comentado las características de los kits ELISA disponibles (Tabla 7). Entre ellos, los de mayor sensibilidad poseen intervalos dinámicos en el entorno de los pg/mL, y requieren tiempos de ensayo de dos a cinco horas, aproximadamente.

El inmunosensor propuesto en este trabajo es el primero que se desarrolla para esta aplicación. Posee una característica destacable, que es el empleo de un polímero conductor como material modificador de la superficie del SPCE, sobre el que se inmoviliza el anticuerpo de captura. El uso de polímeros conductores para la preparación de plataformas inmunosensoras requiere disponer de grupos funcionales adecuados para la inmovilización, como es el caso del ácido poli(pirrolpropílico) (pPPA), que posee una elevada concentración de grupos carboxilo adecuados para la unión covalente del anticuerpo.

Como se verá, el esquema competitivo puesto a punto, y la detección amperométrica de la respuesta del peróxido de hidrógeno mediada por la hidroquinona sobre la superficie del biosensor permitió establecer un calibrado con un amplio margen de linealidad, y alcanzar un límite de detección de 0.92 fg/mL. Por último, el inmunosensor resultó adecuado para la determinación de AMY en muestras de orina y de suero.

5.3.1.1. Configuración del inmunosensor

Las etapas de preparación del inmunosensor electroquímico para la determinación de AMY se muestran en el esquema de la Figura 37 de la Parte Experimental. El anticuerpo anti-AMY se inmoviliza sobre el SPCE modificado con pPPA, se bloquea con BSA y se establece un esquema de inmunoensayo competitivo empleando Biotin-AMY y HRP-Strept (Figura 107). La determinación de la hormona se realiza amperométricamente empleando el sistema H_2O_2/HQ.

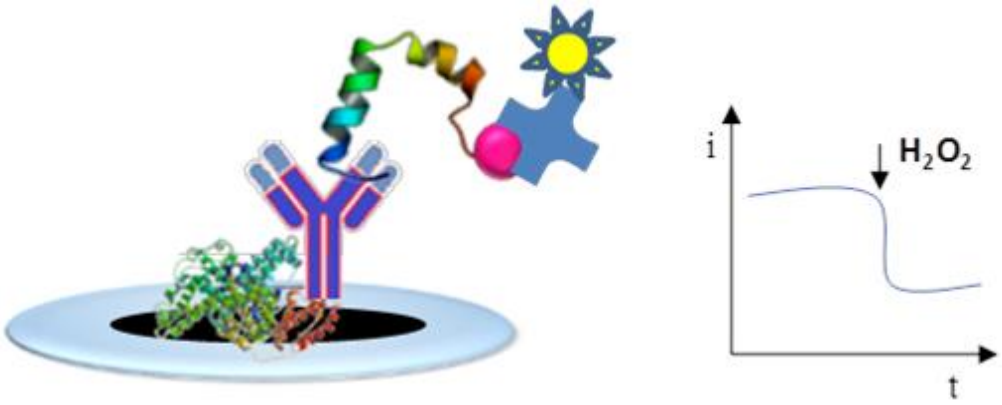

Figura 107.- *Esquema y modo de detección del inmunosensor de AMY.*

5.3.1.2. Optimización de las variables experimentales

Las variables implicadas en la preparación y el funcionamiento del inmunosensor se optimizaron con el criterio de alcanzar la máxima sensibilidad y un amplio intervalo lineal en el calibrado para la determinación de AMY. La modificación del electrodo por electropolimerización de PPA se realizó en las condiciones experimentales optimizadas en investigaciones anteriores [Serafín et al., 2017]. En este trabajo se optimizó el modo de inmovilización y la concentración del anticuerpo de captura, la etapa de bloqueo, la cantidad de antígeno biotinilado, la de conjugado HRP-Strept y el tiempo de competición. A continuación se describen los resultados obtenidos, resumiéndose estos en la Tabla 22.

- ***Elección del modo de inmovilización del anticuerpo de captura***

Como es sabido, la estrategia de inmovilización utilizada habitualmente sobre superficies funcionalizadas con grupos carboxilo se basa en la activación previa de dichos grupos con el sistema EDC/NHSS, seguido de la formación de uniones tipo amida con los restos amina de las proteínas. En este trabajo, al igual que en el caso del magnetoinmunosensor para TGF-β1 (ver Apartado 5.1.2.2), dicha estrategia se comparó con el empleo del polímero de complejos metálicos Mix&Go™ para la inmovilización del anticuerpo de captura anti-AMY sobre el electrodo funcionalizado con pPPA. Como se ha señalado, el producto utilizado está formado por una serie de complejos metálicos seleccionados por su elevada eficiencia para enlazar proteínas [Ooi et al., 2014], orientando y proporcionando una alta estabilidad a la configuración resultante [Muir et al., 2007].

En la Figura 108 se comparan las respuestas amperométricas del inmunosensor HRP-Strept-Biotin-AMY(AMY)-anti-AMY-pPPA/SPCE preparado por inmovilización covalente de anti-AMY empleando las dos alternativas. Como puede verse, el uso del polímero Mix&Go™ proporcionó una mayor diferencia (un 14% más) entre las respuestas en ausencia y en presencia de antígeno, demostrando así la utilidad de este material para el desarrollo de esta configuración.

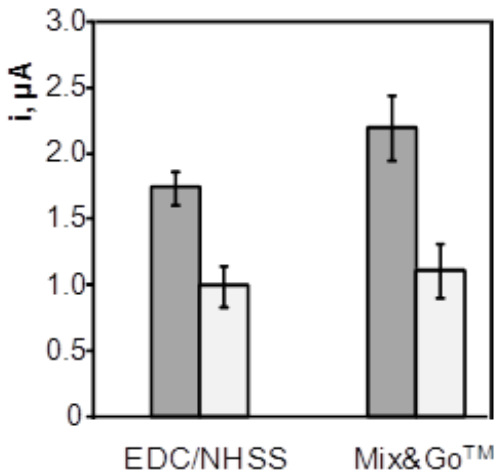

Figura 108.- *Respuestas amperométricas del inmunosensor HRP-Strept-Biotin-AMY (AMY)-anti-AMY-pPPA/SPCE en función de la estrategia de inmovilización de anti-AMY: 5 µL EDC/NHSS 100 mM, 30 min ó 10 µL Mix&Go™, 60 min; anti-AMY en dilución 1/100, 60 min; BSA 2%, 30 min; Biotin-AMY 2.5 ng/mL + 0 (gris) ó 1.25 (blanco) pg/mL AMY, 60 min; HRP-Strept en dilución 1/500, 20 min.*

- ***Influencia de la concentración del anticuerpo de captura***

Se optimizó la cantidad de anticuerpo inmovilizado sobre el electrodo modificado con pPPA, con los resultados que se han representado en la Figura 109. Como puede verse, la corriente obtenida en ausencia de antígeno (gris) aumenta al disminuir la dilución de anti-AMY hasta una relación 1/100, disminuyendo posteriormente debido a la saturación de las regiones de unión en la superficie del electrodo. Por otro lado, la respuesta del inmunosensor en presencia de 1.25 pg/mL de AMY (blanco) permanece prácticamente constante por debajo de una dilución 1/200. Como resultado, la mayor relación entre ambas señales de obtiene para una dilución 1/100, que fue la elegida para estudios posteriores.

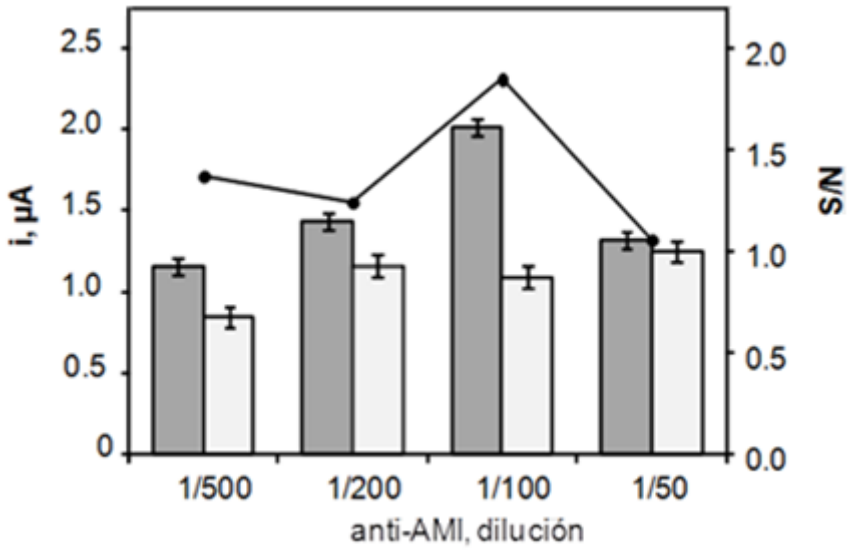

Figura 109.- *Efecto de la dilución de anti-AMY sobre la respuesta del inmunosensor HRP-Strept-Biotin-AMY(AMY)-anti-AMY-pPPA/SPCE: 10 µL Mix&Go^{TM}, 60 min; anti-AMY en dilución 1/500 - 1/50, 60 min; BSA 2%, 30 min; 2.5 ng/mL Biotin-AMY+ 0 (gris) ó 1.25 (blanco) pg/mL AMY, 45 min; HRP-Strept en diución 1/500, 20 min.*

- ***Optimización de la etapa de bloqueo***

Con el fin de bloquear las posiciones activas remanentes en la superficie del biosensor, minimizando en lo posible las adsorciones inespecíficas, se ensayó el empleo de dos agentes bloqueantes empleados habitualmente, BSA y caseína, a las concentraciones usuales, así como sus mezclas, evaluando su influencia sobre la respuesta del inmunosensor. Los resultados obtenidos en este estudio se han representado en la Figura 110, en la que se observa un mejor comportamiento para

los ensayos realizados en presencia de BSA y en ausencia de caseína. Por otro lado, la concentración del 2% de esta proteína fue la que proporcionó una mayor diferencia entre las señales preparadas en ausencia y en presencia de AMY, por lo que estas condiciones fueron las elegidas para bloquear la superficie del inmunosensor.

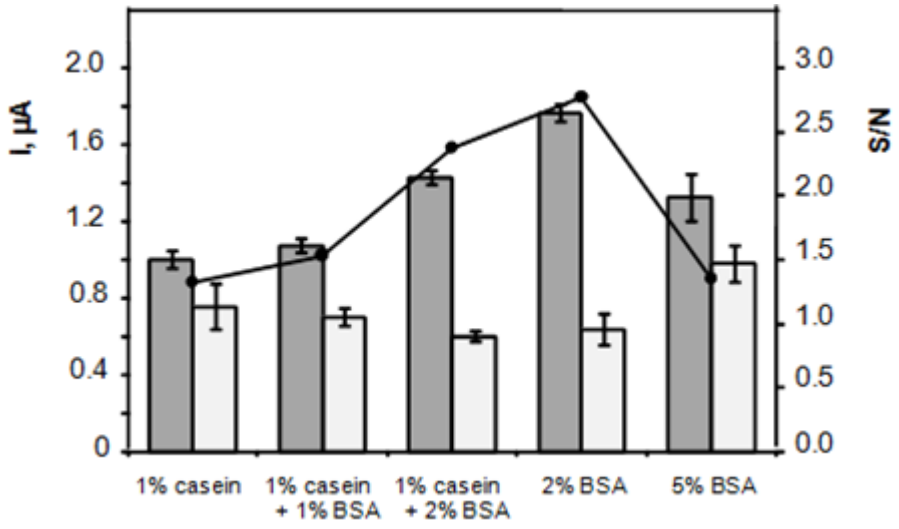

Figura 110.- *Influencia del tipo y la concentración de agente bloqueante sobre la respuesta del inmunosensor HRP-Strept-Biotin-AMY (AMY)-anti-AMY-pPPA/SPCE: 10 µL Mix&Go^{TM}, 60 min; anti-AMY en dilución 1/100, 60 min; BSA 0 -5% + Caseina 0 – 1%, 30 min; Biotin-AMY 2.5 ng/mL + 0 (gris) ó 1.25 (blanco) pg/mL AMY, 60 min; HRP-Strept en dilución 1/500, 20 min.*

- ***Influencia de la concentración de Biotin-AMY***

La concentración de antígeno biotinilado utilizado para establecer el esquema competitivo con la amilina por los sitios de unión del anticuerpo, se optimizó estudiando las repuestas de varios inmunosensores preparados con concentraciones de Biotin-AMY en el intervalo de 1 a 7.5 ng/mL con los resultados que se muestran en la Figura 111. En ella se aprecia, a partir de 2.5 ng/mL de conjugado, una menor diferencia entre las respuestas en ausencia y en presencia de antígeno al aumentar la concentración de conjugado, lo que está de acuerdo con una menor competición por parte de la amilina. Teniendo en cuenta que en ese intervalo la corriente en ausencia de AMY permanece prácticamente constante, se eligió la concentración citada, 2.5 ng/mL de Biotin-AMY para la preparación del inmunosensor.

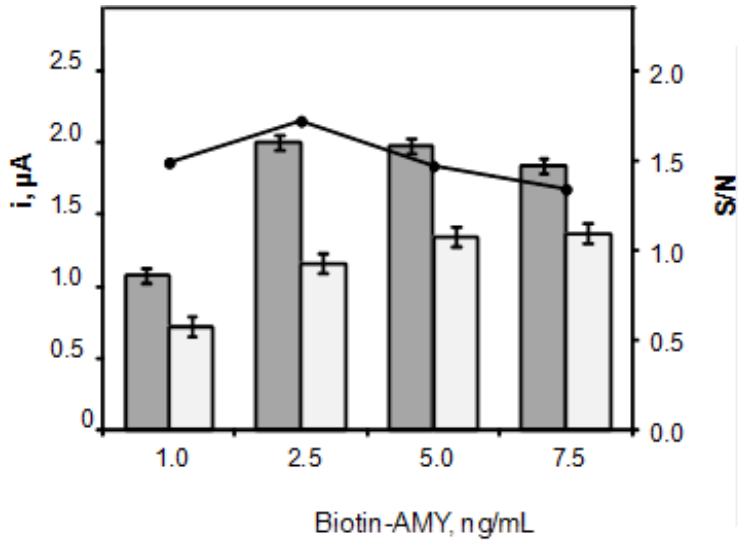

Figura 111.- *Efecto de la concentración de Biotin-AMY sobre la respuesta del inmunosensor HRP-Strept-Biotin-AMY(AMY)-anti-AMY-pPPA/SPCE: 10 µL Mix&Go^{TM} , 60 min; anti-AMY en dilución 1/100, 60 min; BSA 2%, 30 min; 1.0 - 7.5 ng/mL Biotin-AMY + 0 (gris) ó 1.25 (blanco) pg/mL AMY, 45 min; HRP-Strept en diución 1/500, 20 min.*

- ***Influencia de concentración de HRP-Strept***

La configuración del inmunosensor competitivo se completa con el conjugado enzimático HRP-Strept responsable de convertir el sustrato en un producto electroactivo. Para optimizar esta variable, se estudió la respuesta del immunosensor preparado con disoluciones de este conjugado a diferente dilución en el intervalo 1/250 a 1/2000, en ausencia y en presencia de 1.25 pg/mL de AMY, representándose los resultados obtenidos en la Figura 112.

Puede verse cómo, tal como era de esperar, las respuestas del inmunosensor en presencia y ausencia de AMY disminuyen a medida que aumenta la dilución del conjugado, debido a que existe una menor concentración de enzima para catalizar la respuesta del peróxido de hidrógeno en presencia de HQ. Por otro lado, dentro de esta tendencia, se observó la mayor relación entre ambas señales de corriente para una dilución 1/500, que fue la elegida como óptima para alcanzar la mayor sensibilidad.

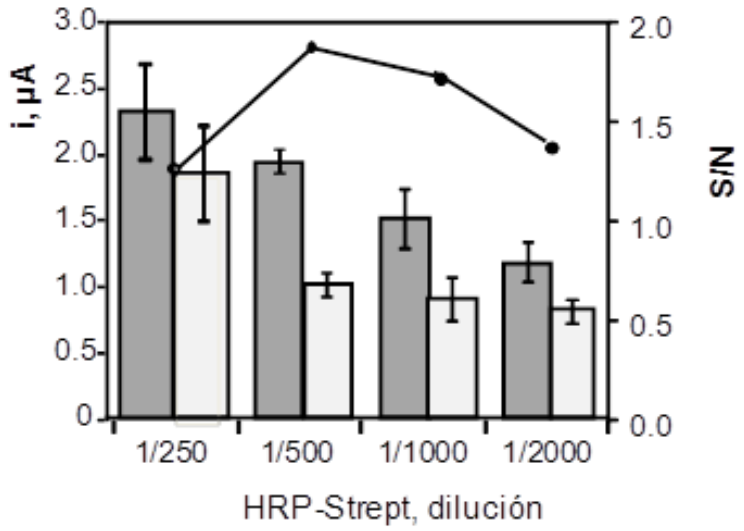

Figura 112.- *Efecto de la dilución de HRP-Strept sobre la respuesta del inmunosensor HRP-Strept-Biotin-AMY(AMY)-anti-AMY-pPPA/SPCE: 10 µL Mix&Go^{TM} , 60 min; anti-AMY en dilución 1/100, 60 min; BSA 2%, 30 min; 2.5 ng/mL Biotin-AMY + 0 (gris) ó 1.25 (blanco) pg/mL AMY, 45 min; HRP-Strept en diución 1/250 - 1/2000, min.*

- ***Optimización del tiempo de competición***

El tiempo de competición es el lapso durante el que el antígeno y el antígeno biotinilado compiten por los sitios de unión del anticuerpo. Los resultados obtenidos en la optimización de esta variable se han representado en la Figura 113. Puede observarse un incremento progresivo de la respuesta del inmunosensor, tanto en ausencia (sin competición) como en presencia de AMY, como corresponde a la inmovilización de una mayor cantidad de Biotin-AMY, responsable de la incorporación del conjugado enzimático, y de la corriente. Debido a que con un tiempo de 45 minutos se obtenía una mayor relación de señales, se eligió este intervalo como el más adecuado para una buena competición.

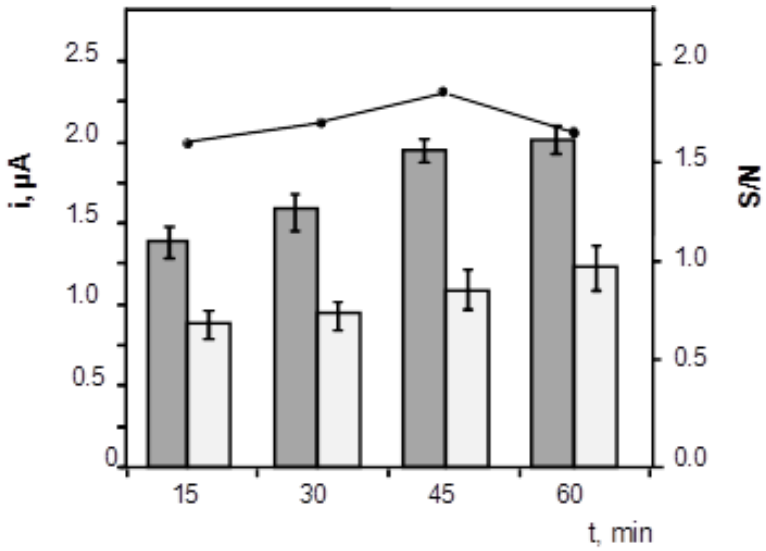

Figura 113.- *Efecto del tiempo de competición sobre la respuesta del inmunosensor HRP-Strept-Biotin-AMY(AMY)-anti-AMY-pPPA/SPCE: 10 µL Mix&Go™ , 60 min; anti-AMY en dilución 1/100, 60 min; BSA 2%, 30 min; 2.5 ng/mL Biotin-AMY + 0 (gris) ó 1.25 (blanco) pg/mL AMY, 15 - 60 min; HRP-Strept en diución 1/500, 20 min.*

Una vez optimizadas las variables experimentales implicadas en el funcionamiento del inmunosensor, como resumen, en la Tabla 22 se recogen dichas variables, los intervalos estudiados y los valores óptimos elegidos en cada caso.

Tabla 22.- *Optimización de las variables implicadas en el funcionamiento del immunosensor HRP-Strept-Biotin-AMY(AMY)-anti-AMY-pPPA/SPCE*

Variable	Especie/Intervalo estudiado	Valor seleccionado
anti-AMY, dilución	1/500 - 1/50	1/100
agente bloqueante	caseína, BSA	BSA
Biotin-AMY, ng/mL	1.0 - 7.5	2.5
HRP-Strept, dilución	1/250 - 1/2000	1/500
tiempo de competición, min	15 - 60	45

5.3.1.2.1. Estudios de caracterización

Las etapas de preparación del inmunosensor se caracterizaron por espectroscopia de impedancia electroquímica y voltamperometría cíclica, empleando disoluciones de $Fe(CN)_6^{3-/4-}$ 2 mM en regulador fosfato 0.05 M de pH 6.0. En la Figura 114 aparecen los resultados obtenidos mediante EIS, en forma de diagramas de Nyquist. Como puede observarse, la curva registrada sobre el electrodo pPPA/SPCE (curva 2) presenta una resistencia a la transferencia de carga mayor (R_{CT} = 7835 Ω) que el electrodo sin modificar (curva 1), con R_{CT} = 1226 Ω, debido a la baja conductividad del polímero pPPA [Dong et al., 2008] y a la repulsión electrostática entre el compuesto electroactivo y los grupos carboxilo disociados presentes en la superficie del electrodo al pH de trabajo. La adición de Mix&Go™ origina un brusco descenso del valor de R_{CT} hasta 978 Ω (curva 3), debido probablemente a la neutralización de cargas. Después, la resistencia a la transferencia de carga va aumentando tras la inmovilización del anticuerpo de captura (curva 4), R_{CT} = 1723 Ω, y la adición del agente bloqueante, BSA (curva 5), R_{CT} = 2342 Ω, debido al carácter aislante de ambas biomoléculas. Sin embargo, la incorporación del antígeno biotinilado y la formación del complejo con el conjugado HRP-Strept (curvas 6 y 7, respectivamente) dan lugar a diagramas de Nyquist con una forma similar a la de una superficie conductora. Este comportamiento se debe probablemente a la presencia de AMY cargada positivamente en el electrodo AMY-anti-AMY-pPPA/SPCE al pH de trabajo, ya que el punto isoeléctrico de la amilina es 8.9 [Li et al., 2012]. De este modo, se produce atracción electrostática entre las cargas de distinto signo y la transferencia de carga se ve favorecida. Este efecto parece ser suficientemente intenso como para evitar un aumento significativo en el valor de R_{CT} tras la incorporación del conjugado de estreptavidina.

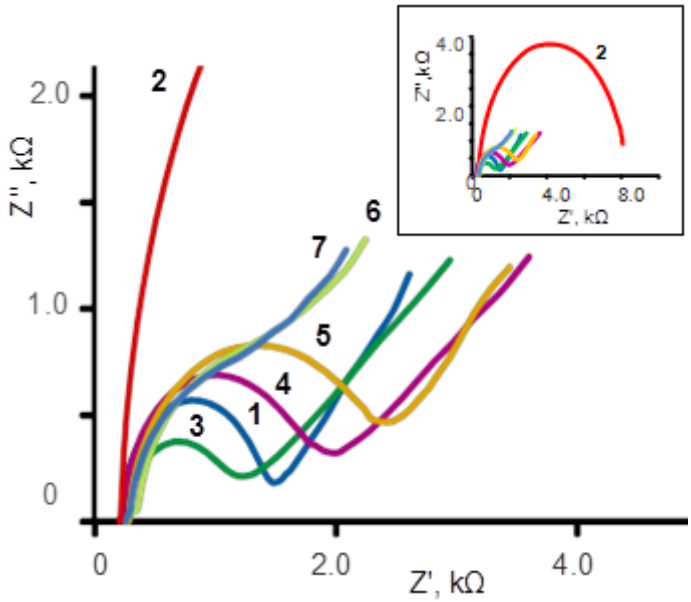

Figura 114.- *Espectros de Nyquist de $Fe(CN)_6^{3-/4-}$ 2 mM en regulador fosfato 0.05 M de pH 6.0: SPCE (1); pPPA/SPCE (2); Mix&Go-pPPA/SPCE (3); anti-AMY-pPPA/SPCE (4); BSA/anti-AMY-pPPA/SPCE (5); Biotin-AMY(AMY)-anti-AMY-pPPA/SPCE (6); HRP-Strept-Biotin-AMY(AMY)-anti-AMY-pPPA/SPCE (7).*

El comportamiento observado anteriormente fue corroborado mediante voltamperometría cíclica (Figura 115). El voltamperograma obtenido sobre el electrodo sin modificar, SPCE (curva 1) muestra los picos de oxidación y reducción característicos del sistema $Fe(CN)_6^{3-/4-}$ que aparecen a valores de los potenciales de pico de +0.24 and +0.16 V vs Ag, respectivamente, con corrientes de pico anódico y catódico de 72 y 60 µA. La modificación posterior con pPPA (curva 2) origina una disminución de las corrientes de pico y un aumento en la separación de los potenciales de pico, que se atribuyen a la baja conductividad relativa del polímero y al efecto de repulsión electrostática antes comentado. Asimismo, la incorporaction de Mix&Go™ (curva 3) permite apreciar un comportamiento más parecido al del electrodo sin modificar, atribuido a la neutralización de cargas. Seguidamente, las curvas 4 y 5 correspondientes a la incorporación sucesiva de anti-AMY y Biotin-AMY exhiben pequeños cambios asociados a respuestas menos reversibles debido a la presencia de capas aislantes de espesor creciente en la superficie del electrodo. Finalmente, el comportamiento que muestran los voltamperogramas 6 y 7 está de acuerdo con lo observado mediante EIS.

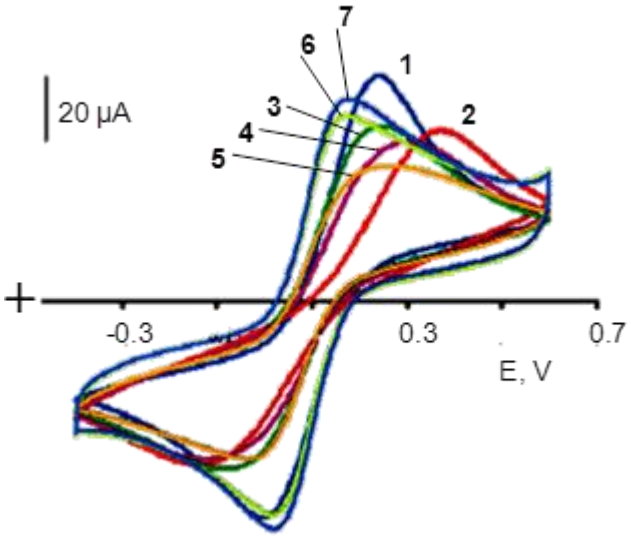

Figure 115. *Voltamperogramas cíclicos de $Fe(CN)_6^{3-/4-}$ 2 mM en regulador fosfato 0.05 M de pH 6.0: SPCE (1); pPPA/SPCE (2); Mix&Go-pPPA/SPCE (3); anti-AMY-pPPA/ SPCE (4); BSA/anti-AMY-pPPA/SPCE (5); Biotin-AMY(AMY)-anti-AMY-pPPA/ SPCE (6); HRP-Strept-Biotin-AMY(AMY)-anti-AMY-pPPA/SPCE (7).*

5.3.1.3. Calibrado y características analíticas

En la Figura 116 se ha representado el calibrado para la determinación de AMY obtenido en las condiciones experimentales optimizadas anteriormente. Como era de esperar, se obtiene una curva sigmoidal decreciente en el intervalo de concentración comprendido entre 10^{-5} hasta 10^{4} pg/mL, habiéndose ajustado la curva mediante regresión no lineal (r^2 = 0.994) a la ecuación:

$$i_p = i_{\min} + \frac{i_{max} - i_{min}}{1 + \left(\frac{x}{EC_{50}}\right)^{-h}}$$

donde i_{max} = 2.07 ± 0.05 µA e i_{min} = 0.26 ± 0.6 µA, el valor de EC_{50}, 0.44 ± 0.1 pg/mL, y la pendiente de Hill, en el punto de inflexión de la curva, h = -0.35 ± 0.04. Por otro lado, el intervalo lineal $i_p \propto \log$ [AMY] (r^2 = 0.990) se extiende entre 0.001 y 50 pg/mL. Este intervalo es adecuado para la determinación de AMY en suero humano, en el que, como se ha señalado, los niveles normales se encuentran en torno a las decenas de pg/mL [Hay et al., 2015] [Harter et al., 1991].

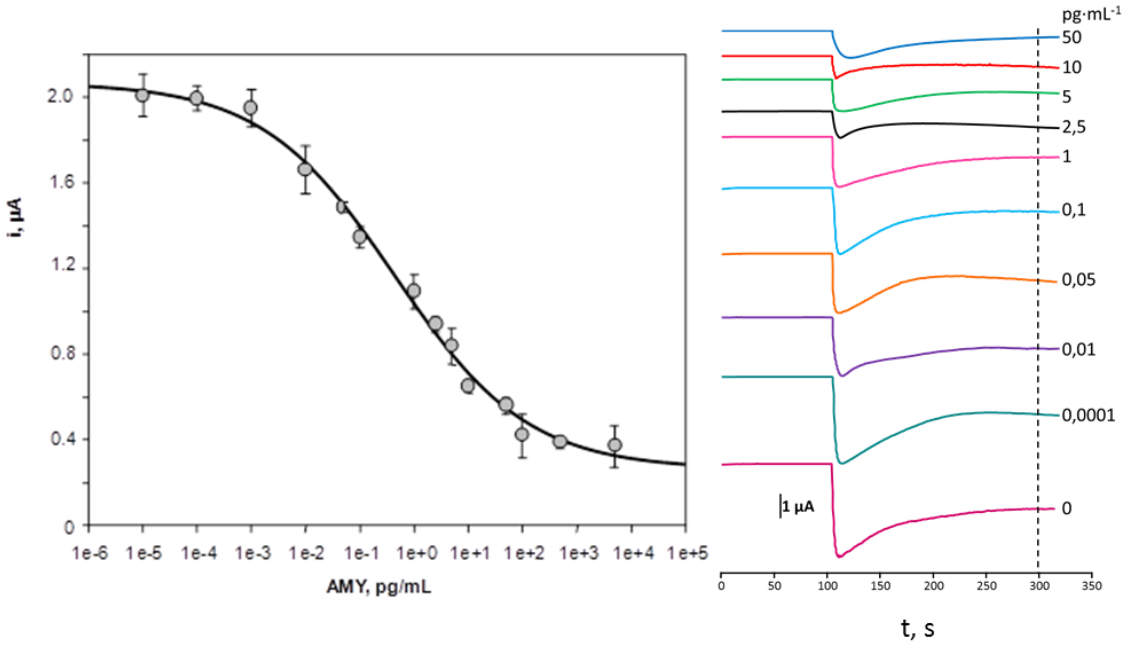

Figura 116.- *Calibrado para la determinación de AMY con el inmunosensor HRP-Strept-Biotin-AMY(AMY)-anti-AMY-pPPA/SPCE*

Al igual que en otros casos, el límite de detección, 0.92 fg/mL, se calculó haciendo uso de la ecuación:

$$LOD = EC_{50}\left(\frac{i_{max} - i_{min}}{i_{max} - i_{min} - 3s} - 1\right)^{-1/h}$$

donde s es la desviación estándar (n=10) del valor del cero (la corriente amperométrica medida en ausencia de AMY), ± 0.12 µA. Es importante destacar que esta concentración es mucho menor que la concentración mínima detectable empleando los kits ELISA comerciales basados en inmunorreactivos similares: 0.62 ng/mL [https://www.raybiotech.com/files/manual/EIA/EIA-AMY.pdf] y 6.17 pg/mL [https://www.lsbio.com/elisakits/manualpdf/ls-f9686.pdf]. También cabe señalar que el intervalo lineal se extiende a lo largo de casi cinco órdenes de magnitud, que es un margen mucho más amplio que los de los métodos ELISA, con intervalos dinámicos usualmente comprendidos entre 1 y 1000 ng/mL [https://www.raybiotech.com/files/manual/EIA/EIA-AMY.pdf] o desde 6.17 a 500 pg/mL [https://www.lsbio.com/elisakits/manualpdf/ls-f9686.pdf]. Además, el tiempo de ensayo es muy superior en algunos de estos kits, extendiéndose, por ejemplo, a 3 h y 5 min en el de RayBiotech citado

anteriormente, contando a partir de la inmovilización del anticuerpo de captura. Por otra parte, la simplicidad y facilidad de uso del inmunosensor desarrollado, así como la posibilidad de desarrollar sistemas de detección multiplex hace más atractivo su uso en comparación con las metodologías ELISA convencionales.

Se evaluó la reproducibilidad de las medidas amperométricas en ausencia y en presencia de 0.1 pg/mL de AMY, con cinco inmunosensores diferentes preparados el mismo día. En estas condiciones, se obtuvieron valores de RSD del 5.9% y el 5.5%, respectivamente. Por otro lado, para las medidas realizadas con cinco inmunosensores distintos preparados en diferentes días, las desviaciones estándar relativas fueron del 6.8% y el 7.4%, respectivamente.

En la Figura 117 se han representado los resultados obtenidos en el estudio de la estabilidad de almacenamiento del inmunoconjugado BSA/anti-AMY-pPPA/SPCE que se realizó preparando varios bioelectrodos el mismo día, almacenándolos a -20 ºC hasta su empleo. A partir de ese momento, durante varios días se completaron las construcciónes de varios inmunosensores HRP-Strept-Biotin-AMY-anti-AMY-pPPA/SPCE, en ausencia de AMY, y se realizaron las medidas de acuerdo con el procedimiento previamente optimizado. Como puede verse, el gráfico de control representado muestra cómo las respuestas de corriente permanecen dentro de los límites situados a ± 3s, donde s es la desviación estándar de las medidas (n=10) realizadas el primer día de trabajo, durante 35 días, periodo que pone de manifiesto la excelente estabilidad de almacenamiento del inmunosensor.

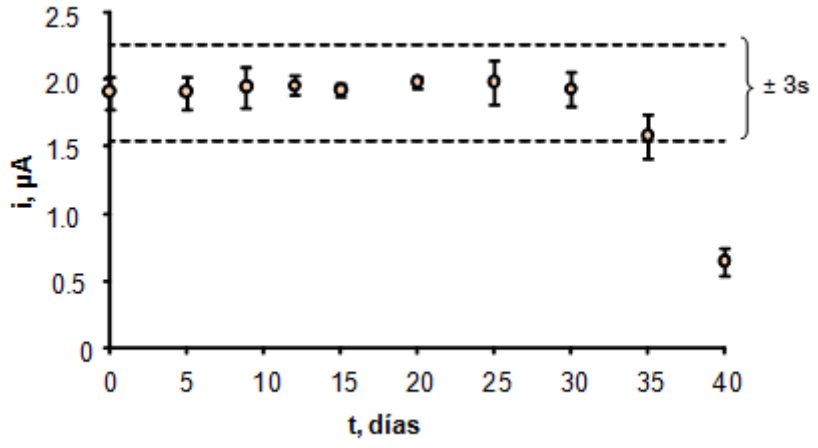

Figura 117.- *Grafico de control para la evaluación de la estabilidad de almacenamiento del conjugado HRP-Strept-Biotin-AMY-anti-AMY-pPPA/SPCE*

5.3.1.4. Estudios de selectividad

La selectividad del método para la determinación de AMY empleando el inmunosensor desarrollado en este trabajo se evaluó por medida de disoluciones preparadas en ausencia y en presencia de 1.0 pg/mL de amilina así como en ausencia y en presencia de compuestos potencialmente interferentes, proteínas y especies electroactivas, que pueden acompañar al analíto en las muestras de interés. Los compuestos ensayados y sus concentraciones fueron: ácido ascórbico (AA, 370 µg/mL), ácido úrico (UA, 50 µg/mL), bilirrubina, (BR, 3.4 µg/mL), colesterol (Chol, 20 µg/mL), glucosa (Glu, 1.3 mg/ml), y péptido YY (PYY, 100 pg/mL). Las concentraciones elegidas corresponden aproximadamente a los niveles fisiológicos normales de cada especie en suero humano.

Como puede observarse en la Figura 118, en ninguno de los casos existen diferencias significativas entre las corrientes medidas, permaneciendo todos los valores medios de las mismas dentro de los límites de ± 2s señalados en la gráfica. Este resultado demuestra la elevada selectividad del anticuerpo utilizado, del inmunosensor y del método empleado en su conjunto.

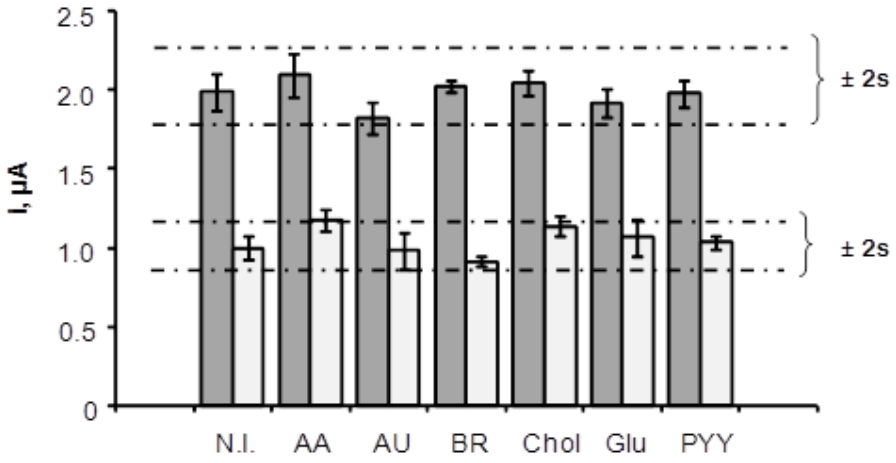

Figura 118.- *Efecto de la presencia de ácido ascórbico (AA), ácido úrico (UA), bilirrubina (BR), colesterol (Chol), glucosa (Glu), y péptido YY (PYY) (ver el texto para las concentraciones) sobre las respuestas amperométricas medidas con el inmunosensor HRP-Strept-Biotin-AMY(AMY)-anti-AMY-pPPA/SPCE para 0.0 (gris) ó 1.0 (blanco) pg/mL AMY.*

5.3.1.5. Aplicación a la determinación de AMY en orina y suero

La utilidad del inmunosensor HRP-Strept-Biotin-AMY(AMY)-anti-AMY-pPPA /SPCE para el análisis de muestras reales se estudió aplicándolo a la determinación de AMY en orina y suero. Como en otros casos, la posibilidad de existencia de efecto matriz se evaluó en ambos casos midiendo las muestras contaminadas con AMY en el intervalo de 0.001 a 1 pg/mL (orina) y de 0.001 a 10 pg/mL (suero) diluidas con diferentes volúmenes del diluyente "Assay Diluent B" del kit de inmunorreactivos utilizado (ver procedimiento descrito en el Apartado 4.4.7.1. de la Parte experimental. Los resultados obtenidos (ver Figura 119) pusieron de manifiesto que una dilución 1/20 para la orina y 1/10 para el suero eran suficientes para evitar el efecto matriz, lográndose la práctica coincidencia de las pendientes de estos calibrados con la de los patrones de AMY.

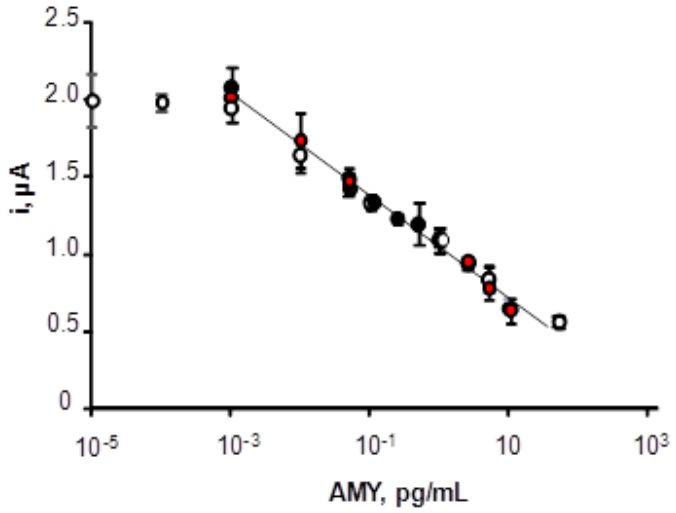

Figura 119.- *Calibrados para la determinación de AMY con el inmunosensor HRP-Strept-Biotin-AMY(AMY)-anti-AMY-pPPA/SPCE:○disoluciones patrón; ● orina; ● suero.*

En efecto, las pendientes de los calibrados de las muestras fueron -327 ± 22 (orina) y -336 ± 12 (suero) µA por década de concentración, valores que se compararon estadísticamente con la del calibrado de patrones, 307 ± 8 µA por década de concentración, aplicando el test t de Student. Los resultados de esta comparación para α=0.05 y n=12, proporcionaron valores de t_{exp} = 0.832 y 2.005, respectivamente, para orina y suero, que son menores que el valor tabulado, t_{tab} = 2.179. Por tanto, la determinación de AMY en las muestras se realizó directamente por interpolación de la corriente amperométrica medida con el inmunosensor en el calibrado de patrones.

Los resultados obtenidos en el análisis de orina y suero contaminados con 15 y 80 pg/mL de amilina, respectivamente, aparecen resumidos en la Tabla 23. Puede observarse la obtención de recuperaciones en el intervalo del 94 al 102%, que demuestran la utilidad del método desarrollado para la determinación de bajas concentraciones de esta especie en este tipo de muestra sin necesidad de tratamiento previo salvo la dilución.

Tabla 23.- *Determinación de AMY en orina y en suero con el inmunosensor HRP-Strept-Biotin-AMY(AMY)-anti-AMY-pPPA/SPCE*

Sample	[AMY], pg/mL	[AMY] encontrado, pg/mL*	Recuperación, %
orina	0.75	0.75 ± 0.05	100 ± 7
	4.0	4.1 ± 0.2	102 ± 4
suero	1.5	1.4 ± 0.1	94 ± 7
	8.0	8.0 ± 0.4	100 ± 6

*± ts / √n

5.3.1.6. Conclusiones

Se ha desarrollado el primer inmunosensor electroquímico para la determinación de AMY que combina las ventajas de utilizar un electrodo serigrafiado modificado con un polímero rico en grupos carboxilo con el empleo de un polímero enlazante para la unión estable y orientada del anticuerpo de captura, y la medida amperométrica de la señal del peróxido de hidrógeno mediada por la hidroquinona. Una vez establecido el ensayo competitivo entre AMY y Biotin-AMY, el inmunosensor resultante permitió alcanzar un bajo límite de detección, muy inferior al de los sistemas ELISA comerciales y aplicar con buenos resultados el método a la determinación de la hormona en muestras de suero y orina.

6. CONCLUSIONS

Partial conclusions to the research work done in this Doctoral Thesis have been exposed through the different sections where the achievements have been highlighted and the characteristics of the methods have been compared with other previously used methodologies. A summary of those conclusions is as follows:

An electrochemical magnetoimmunosensor has been developed for the determination of GHRL that combines the advantageous characteristics of the functionalized magnetic microparticles with Protein G for the immobilization of the capture antibody with the use of carbon-screened electrodes. A competitive immunoassay scheme has been established using the high sensitivity differential pulse voltammetry (DPV) technique for the detection of 1-naphthol as a product of the enzymatic reaction. All this has made it possible to reach a lower limit of detection, lower than that of other existing methods, and apply the immunosensor to the determination of the hormone in saliva samples.

The amperometric magnetoimmunosensor developed in this work for the determination of TGF-β1 satisfies the requirements of sensitivity and selectivity to be applied with excellent results to the analysis of urine samples without further pretreatment than a simple dilution 1:3 in regulatory solution phosphate. Probably, this good behavior is due to the combination of the use of carboxylated magnetic microparticles together with that of the commercial product Mix & Go ™, which results in stable and targeted immobilization of the capture antibody, together with the use of the amperometry technique and the effect of amplification of the current produced by the use of poly-HRP-Strept polymer.

The first electrochemical immunosensor for the determination of the anorexigenic hormone PYY has been developed. This design involves the use of electrodes modified with rGO and functionalized by electrografting with the diazonium salt of *p*-ABA as platforms for the covalent immobilization of the anti-PYY specific antibody. The immunosensor has demonstrated excellent analytical performance by providing calibrations with a broad linear range suitable for the determination of PYY in clinical samples. The low detection limit reached, 0.01 pg/mL, the short analysis time and its high precision significantly improve the analytical characteristics of the ELISA kits available for this determination.

Tthe simultaneous determination of GHRL and PYY was carried out for the first time using a multiplex immunosensor in which the active surfaces of a screen-printed dual electrode are modified with reduced graphene oxide and by grafting with the diazonium salt of *p*-ABA. The developed configuration makes it possible to obtain

calibration plots for both hormones showing excellent analytical characteristics, and reaching detection limits much lower than those obtained in the ELISA kits available for each of the determined compounds, separately. In addition, the good reproducibility of the method is another feature to be highlighted. Finally, the utility of the immunosensor to the analysis of clinical samples was demonstrated by application to serum and saliva with good results.

An electrochemical immunosensor has been prepared for the determination of EE2. In the developed configuration, for the first time the possibility of using the hybrid material AgNPs / SiO2 / GO for the construction of this type of affinity sensors was explored by designing an immobilization strategy of the capture antibody by electrografting of p-ABA and activation of the carboxyl groups with the EDC / NHSS system. The use of this configuration together with the competitive immunoassay scheme established, and the excellent electrochemical response obtained on the modified electrode for the reaction of hydrogen peroxide catalyzed by peroxidase in the presence of hydroquinone, have made it possible to develop a method for the determination of EE2 in a linear range comprised between 1 and 50 ng/mL, with a limit of detection of 0.065 ng/mL. These characteristics, together with the high precision and selectivity that the immunosensor presents, make it suitable for determining the hormone in urine samples.

A simple method for preparing an enzymatic electrochemical biosensor for the determination of β-HB in human serum was developed. This biosensor takes advange of properties of screen-printed carbon electrodes modified with reduced graphene oxide, which give rise to a high rate of electronic transfer in the oxidation of NADH, as well as those of the use of thionine, used as a redox mediator, allowing the application of a detection potential of 0.0 V vs. Ag. The biosensor demonstrated good analytical characteristics in terms of linear range, high sensitivity and low limit of detection compared to other existing configurations for the determination of β-HB. Finally, the usefulness of the method developed was demonstrated by applying it to diluted serum samples without the need for prior preparation.

The first electrochemical immunosensor for the determination of AMY has been developed which combines the advantages of a screen-printed electrode modified with a polymer rich in carboxyl groups with those derived from the use of a binding polymer for the stable and oriented immobilization of the capture antibody and the measurement of amperometric responses of hydrogen peroxide mediated by hydroquinone. Once the competitive assay between AMY and Biotin-AMY was established, the resulting immunosensor allowed to reach a low limit of detection, much

lower than that of commercial ELISA systems and to apply the method with good results to the determination of the hormone in serum samples and urine.

As a general conclusion it can be said that the studies implemented have demonstrated the usefulness of the electrochemical biosensors for the monitoring of species of interest in clinical samples belonging to a little explored area of appetite regulators and biomarkers of obesity. In particular, the advantages of using functionalized magnetic microparticles, graphene and other materials, as well as novel immobilization procedures to construct electrochemical platforms useful for the preparation of stable, sensitive and selective biosensors have been proven.

It is worth noting the construction of the first electrochemical immunosensors for the determination of AMY, GHRL and PYY, as well as the first multiplex configuration for the simultaneous determination of these last two hormones. In addition, the first magnetoimmunosensor for the cytokine TGF-β1 has been prepared, and the hybrid material AgNPs/SiO_2/GO has been used for the first time for the implementation of an immunosensor for ethynyl estradiol. Moreover, the combination of reduced graphene oxide and thionine for the development of an enzymatic biosensor for β.hydroxybutyrate has also been used for the first time.

As indicated in each case, the analytical characteristics of the methods elaborated in this work has been shown that improve those of existing methods, mainly in terms of sensitivity, linear range, analysis time and reproducibility.

Finally, all biosensors have demonstrated their practical utility by application to biological samples for the determination of the analytes at physiological levels in serum, urine and / or saliva.

7. BIBLIOGRAFÍA

[Acosta et al., 2011] A. Acosta, M.D. Hurtado, O. Gorbatyuk, M. La Sala, D. Duncan, G. Aslanidi, M. Campbell-Thompson, L. Zhang, H. Herzog, A. Voutetekis, B.J. Baum, S. Zolotukhin, Salivary PYY: A putative bypass to saciety, PLoS ONE 6 (2011) e26137.

[Adrian et al., 1985] T.E. Adrian, G.L. Ferri, A.J. Bacarese-Hamilton, H.S. Fuessi, J.M. Polak, S.R. Bloom, Human distribution and release of a putative new gut hormone, peptide YY, Gastroenterology, 89 (1985) 1070

[Afkhami et al., 2017] A. Afkhami, P. Hashemi, H. Bagheri, J. Salimian, A. Ahmadi, T. Madrakian, Impedimetric immunosensor for the label-free and direct detection of botulinum neurotoxin serotype A using Au nanoparticles/graphene-chitosan composite. Biosens. Bioelectron, 93 (2017) 124.

[Aleksandrova et al., 2018] K.Aleksandrova, D.Mozaffarian, T. Pischon, Addressing the perfect storm: Biomarkers in obesity and pathophysiology of cardiometabolic risk. Clin. Chem. 64 (2018) 1.

[Alwarappan et al., 2009] S. Alwarappan, A. Erdem, C. Liu, C.-Z. Li, Probing the electrochemical properties of graphene nanosheets for biosensing applications. J. Phys. Chem. C, 113 (2009) 8853.

[Anik et al., 2018] Ü. Anik, Y.Tepeli, M. Sayhi, J. Nsirib, M.F. Diouani, Towards the electrochemical diagnostic of influenza virus: development of a graphene–Au hybrid nanocomposite modified influenza virus biosensor based on neuraminidase activity. Analyst, 143 (2018) 150.

[Apelo and Veloso, 1975] R. Apelo, I. Veloso, Clinical experience with ethynyl estradiol and D-norgestrel as an oral contraceptive. Fertil.Steril, 26 (1975) 283.

[Arenas et al., 2016] C.B.Arenas, E.Sánchez-Tirado, I.Ojeda, C.A.Gómez-Suárez, A. González-Cortés, R.Villalonga, P.Yáñez-Sedeño, J.M.Pingarrón, An electrochemical limmunosensor for adiponectin using reduced graphene oxide–carboxymethyl-cellulose hybrid as electrode scaffold. Sens. Actuators B 223 (2016) 89.

[Austin & Marks, 2008] J. Austin, D. Marks, Hormonal regulators of appetite. Int. J. Pediatr. Endocrinol, 1 (2009) 141753.

[Aydin et al., 2005] S. Aydin, I. Halifeoglu, I.H. Ozercan, F. Erman, N. Kilic, N. Ilhan, Y. Ozkan, N. Akpolat, L. Sert, E. Caylak, A comparison of leptin and ghrelin levels in plasma and saliva of young healthy subjects. Peptides 26 (2005) 647–652.

[Banks & Kastin, 1998] W.A. Banks, A.J. Kastin, Differential permeability of the blood-brain barrier to two pancreatic peptides: insulin and amylin. Peptides, 19 (1998) 883.

[Barman et al., 2017] S. C. Barman, M. F. Hossain, J.Y. Park, Gold nanoparticles assembled chemically functionalized reduced graphene oxide supported

electrochemical immunosensor for ultra-sensitive prostate cancer detection, J. Electrochem. Soc., 164 (2017) B234

[Barman et al., 2018] S. C. Barman, M. F. Hossain, H. Yoon, J.Y. Park, Trimetallic Pd@Au@Pt nanocomposites platform on -COOH terminated reduced graphene oxide for highly sensitive CEA and PSA biomarkers detection. Biosens. Bioelectron. 100 (2018) 16.

[Batterham et al., 2002] R.L. Batterham, M.A. Cowley, C. J. Small, H. Herzog, M.A. Cohen, C.L. Dakin, A.M. Wren, A.E. Brynes, M.J. Low, M.A. Ghatei, R.D. Cone, S.R. Bloom. Nature, 418 (2002) 650.

[Batterham et al., 2003] R.L. Batterham, M.A. Cohen, S.M. Ellis, C.W. Le Roux, D.J. Withers, G.S. Frost, M.A. Ghatei, S.R. Bloom, Inhibition of food intake in obese subjects by peptide YY3-36. New England J. Med., 349 (2003) 941.

[Batterham & Bloom, 2003] R. L. Batterham, S.R. Bloom, The gut hormone peptide YY regulates appetite, Ann. N.Y. Acad. Sci., 994 (2003) 162.

[Batterham et al., 2006] R. L. Batterham, H. Heffron, S. Kapoor, J. E. Chivers, K. Chandarana, H. Herzog, C. W. Le Roux, E. L. Thomas, J. D. Bell, D. J. Withers, Critical role for peptide YY in protein-mediated satiation and body-weight regulation. Cell Metabolism., 4 (2016) 223.

[Bélanger & Pinson, 2011] D. Bélanger, J. Pinson, Electrografting: A powerful method for surface modification. Chem. Soc. Rev., 40 (2011) 3995.

[Bettazzi et al., 2016] F. Bettazzi, T. Martellini, W.L. Shelver, A. Cincinelli, E. Lanciotti, I. Palchetti, Development of an electrochemical immunoassa for the detection of polybrominated diphenyl ethers (PBDEs). Electroanalysis, 28 (2016) 1817.

[Boey et al., 2006] D. Boey, L. Heilbronn, A. Sainsbury, R. Laybutt, A. Kriketos, H. Herzog, L. V. Campbell. Neuropeptides, 40 (2006) 317.

[Boyle & Reis, 1987] M.D.P. Boyle, K.J. Reis, Bacterial Fc receptors. Biotechnology, 5 (1987) 697.

[Broglio et al., 2002] F. Broglio, A. Benso, C. Gottero, F. Prodam, S. Grottoli, F. Tassone, M. Maccario, F.F. Casanueva, C. Diéguez, R. Deghenghi, E. Ghigo, E. Arvat, Effects of glucose, free fatty acids or arginine load on the GH-releasing activity of ghrelin in humans. Clin. Endocrinol., 57 (2002) 265.

[Brown & Clegg, 2009] L.M. Brown, D.J. Clegg, Central effects of estradiol in the regulation of adiposity. J. Steroid Biochem. Mol. Biol. 122 (2010) 65.

[Borisova et al., 2017] B. Borisova, M.L.Villalonga, M. Arévalo-Villena, A. Boujakhrout,& A. Sánchez, C.Parrado, J. M. Pingarrón, A. Briones-Pérez, R. Villalonga, Disposable electrochemical immunosensor for Brettanomyces bruxellensis based on nanogold-

reduced graphene oxide hybrid nanomaterial. Anal. Bioanal. Chem., 409 (2017) 5667.

[Butler et al., 1990] P. C. Butler, J. Chou, W. Bradford Carter, Y.-N. Wang, B.-H. Bu, D. Chang, J.-K. Chang, R.A. Rizza, Effects of meal ingestion on plasma amylin concentration in NIDDM and nondiabetic humans. Diabetes, 29 (1990) 752.

[Cahill et al., 2014] F. Cahill, Y.Ji, D. Wadden, P. Amini, E. Randell, S. Vasdev, W. Gulliver, G. Sun, The association of serum total peptide YY (PYY) with obesity and body fat measures in the CODING study. PLoS One, 9 (2014) e95235.

[Cahill & Veech, 2003] G.F. Jr., Cahill, R.L. Veech, Ketoacids? Good medicine? Trans. Am. Clin. Climatol. Assoc. 114 (2003) 149.

[Campuzano et al., 2014] S. Campuzano, V. Salema, M. Moreno-Guzmán, M. Gamella, P.Yáñez-Sedeño, L.A. Fernández, J.M.Pingarrón, Disposable amperometric magnetoimmunosensors using nanobodies as biorecognition element. Determination of fibrinogen in plasma. Biosens. Bioelectron., 52 (2014) 255.

[Carnagarin et al., 2015] R. Carnagarin, A.M. Dharmarajan, C.R. Dass, Molecular aspects of glucose homeostasis in skeletal muscle - A focus on the molecular mechanisms of insulin resistance. Mol. Cell Endocrinol., 417 (2015) 52.

[Casanueva & Diéguez, 2002] F.F. Casanueva, C. Diéguez, Ghrelin: the link connecting growth with metabolism and energy homeostasis. Rev. Endocr. Metab. Disord., 3 (2002) 325.

[Castillo et al., 1995] M.J. Castillo, A.J. Scheen, P.J. Lefèbre, Amylin/islet amyloid polypeptide: biochemistry, physiology, patho-physiology. Diabet Metab., 21 (1995) 3.

[Catalán et al., 2007] V. Catalán, J.Gómez-Ambrosi, B. Ramírez, F.Rotellar, C. Pastor. C. Silva, et al., Ob. Surg., 17 (2007)1464.

[Centi et al., 2007] S. Centi, S. Laschi, M. Mascini, Improvement of analytical performances of a disposable electrochemical immunosensor by using magnetic beads. Talanta, 73 (2007) 394.

[Chao, 1979] Y. Chao, E.E. Windier, G.C. Chen, R.J. Have, Hepatic Catabolism of Rat and Human Lipoproteins in Rats Treated with 17 Ethynyl Estradiol. J. Biol. Chem., 22 (1979) 11360.

[Chebil et al., 2010] S. Chebil I.Hafaiedh H.Sauriat-Dorizon N.Jaffrezic-Renault A.Errachid Z.Ali H.Korri-Youssoufi, Electrochemical detection of D-dimer as deep vein thrombosis marker using single-chain D-dimer antibody immobilized on functionalized polypyrrole. Biosens. Bioletectron. 26 (2010) 736.

[Chen et al., 2010] W. Chen, L. Yan, P. R.Bangal, Preparation of graphene by the rapid and mild thermal reduction of graphene oxide induced by microwaves. Carbon, 48 (2010) 1146.

[Chen et al., 2010a] W. Chen, Y. Lei, C.M. Li, Regenerable leptin immunosensor based on protein G immobilized Au-pyrrole propylic acid-polypyrrole nanocomposite. Electroanalysis, 22 (2010) 1078.

[Chen et al., 2016] Q. Chen, C. Yu, R. Gao, L. Gao, Q.Li, G.Yuan, J. He, A novel electrochemical immunosensor based on the rGO-TEPA-PTC-NH2 and AuPtmodified C60 bimetallic nanoclusters for the detection of Vangl1, a potential biomarker for dysontogenesis. Biosens. Bioelectron., 79 (2016) 364.

[Chen & Lu, 2017] Z. Chen, M. Lu, Novel electrochemical immunoassay for human IgG1 using metal sulfide quantum dot-doped bovine serum albumin microspheres on antibody-functionalized magnetic beads. Anal. Chim. Acta, 979 (2017) 24.

[Choe et al., 2016] W. Choe, T.A. Durgannavar, S.J. Chung, Fc-Binding Ligands of Immunoglobulin G: An Overview of High Affinity Proteins and Peptides. Naturals, 9 (2016) 994.

[Chua & Pumera, 2014] C. K. Chua, M. Pumera, Chemical reduction of graphene oxide: a synthetic chemistry viewpoint. Chem. Soc. Rev., 43 (2014) 291.

[Cincotto et al., 2014] F.H.Cincotto, T.C.Canevari, A.M.Campos, R.Landers, S.A.S.Machado, Simultaneous determination of epinephrine and dopamine by electrochemical reduction on the hybrid material SiO_2/graphene oxide decorated with Ag nanoparticles. Analyst, 139 (2014) 4634.

[Coille et al., 2002] I. Coille, S. Reder, S. Bucher, G.Gauglitz, Comparison of two fluorescence immunoassay methods for the detection of endocrine disrupting chemicals in water. Biomol. Eng., 18 (2002) 273.

[Colon-González et al., 2013] F. Colon-Gonzalez, G. W. Kim, J. E. Lin, M. A. Valentino, S. A. Waldman, Obesity pharmacotherapy: What is next? Mol. Aspects Med., 34 (2013) 71.

[Cooper et al., 1987] G. Cooper, A. Willis, A. Clark, R. Turner, R. Sim, K. Reid, Purification and characterization of a peptide from amyloid-rich pancreases of type 2 diabetic patients. Proc Natl Acad Sci, 84 (1987) 8628.

[Cooper, 2014] J.A. Cooper, Factors affecting circulating levels of peptide YY in humans: a comprehensive review. Nutrition Research Reviews, 27 (2014) 186.

[Cummings et al., 2001] D.E. Cummings, J.Q. Purnell, R.S. Frayo, K. Schmidova, B.E. Wisse, D.S. Weigle, A preprandial rise in plasma ghrelin levels suggests a role in meal initiation in humans. Diabetes, 50 (2001) 1714.

[Danielpour, 1989] D. Danielpour, L.L. Dart, K.C. Flanders, A.B. Roberts, M.B. Sporn, Immunodetection and Quantitation of the Two Forms of Transforming Growth Factor-Beta (TGF-β1 and TGF-β2) Secreted by Cells in Culture. J. Cell. Physiol, 138 (1989) 79.

[Darling et al., 2013] J.E. Darling, E.P. Prybolsky, M. Sieburg, J.L. Hougland, A fluorescent peptide substrate facilitates investigation of ghrelin recognition and acylation by ghrelin O-acyltransferase. Anal. Biochem., 437 (2013) 68.

[Date et al., 2000] Y. Date, M. Kojima, H. Hosoda, A. Sawaguchi, M.S. Mondal, T. Suganuma, S. Matsukura, K. Kangawa, M. Nakazato, Ghrelin, a novel growth hormone-releasing acylated peptide, is synthesized in a distinct endocrine cell type in the gastrointestinal tracts of rats and humans. Endocrinol., 141 (2000) 4255.

[de Jong et al., 2002] P.E. de Jong PE, Verhave JC, Pinto-Sietsma SJ, Hillege HL; PREVEND study group. Obesity and target organ damage: the kidney. Int. J. Obes. Relat. Metab. Disord., 26 (2002) 21.

[de Oliveira et al., 2018] T. R. de Oliveira, D. H. Martucci, R. C. Faria, Simple disposable microfluidic device for Salmonella typhimurium detection by magneto-immunoassay. Sens. Actuators B, 255 (2018) 684.

[De Vriese & Delporte, 2008] C. De Vriese, C. Delporte, Ghrelin: A new peptide regulating growth hormone release and food intake. Int. J. Biochem. Cell Biol., 40 (2008) 1420.

[Delamar et al., 1992] M. Delamar, R. Hitmi, J. Pinson, J.M. Saveant, Covalent modification of carbon surfaces by grafting of functionalized aryl radicals produced from electrochemical reduction of diazonium salts. J. Am. Chem. Soc., 114 (1992) 5883.

[Dong et al., 2006] H. Dong, C.M. Li, W. Chen, Q. Zhou, Z. X. Zeng, J.H.T. Luong, Sensitive amperometric immunosensing using polypyrrolepropylic acid films for biomolecule immobilization. Anal. Chem., 78 (2006) 7424.

[Dong et al., 2008] H. Dong, X. Cao, C.M. Li, W. Hu, An in situ electrochemical surface plasmon resonance immunosensor with polypyrrole propylic acid film: Comparison between SPR and electrochemical responses from polymer formation to protein immunosensing. Biosens. Bioelectron., 23 (2008) 1055.

[Eder et al, 1996] I.E. Eder, A. Stenzl, A. Hobisch, M.V. Cronauer, G. Bartsch, H. Klocker, Transforming growth factors-beta 1 and beta 2 in serum and urine from patients with bladder carcinoma. J. Urol., 156 (1996) 953.

[Eguílaz et al., 2010] M. Eguílaz, M. Moreno-Guzmán, S. Campuzano, A. González-Cortés, P. Yáñez-Sedeño, J.M. Pingarrón, An electrochemical immunosensor for

testosterone using functionalized magnetic beads and screen-printed carbon electrodes. Biosens. Bioelectron., 26 (2010) 517.

[Eissa et al., 2012] S. Eissa, C. Tlili, L. L'Hocine, M. Zourob, Electrochemical immunosensor for the milk allergen β-lactoglobulin based on electrografting of organic film on graphene modified screen-printed carbon electrodes. Biosens. Bioelectron., 38 (2012) 308.

[Eissa & Zourob, 2012] S. Eissa, M.A. Zourob, A graphene-based electrochemical competitive immunosensor for the sensitive detection of okadaic acid in shellfish. Nanoscale, 4 (2012) 7593.

[Eissa et al., 2013] S. Eissa, L. L'Hocineb, M. Siaj, M. Zourob, Graphene-based label-free voltammetric immunosensor for sensitive detection of the egg allergen ovalbumin. Analyst, 7 (2013) 4378.

[Eissa et al., 2018] S. Eissa, N. Alshehri, A.M. Abdel Rahman, M. Dasouki, K.M. Abu Salah, M. Zourob, Electrochemical immunosensors for the detection of survival motor neuron (SMN) protein using different carbon nanomaterials-modified electrodes. Biosens. Bioelectron., 101 (2018) 282.

[Elshafey et al., 2016] R. Elshafey, M.Siaj, A. C. Tavares, Au nanoparticle decorated graphene nanosheets for electrochemical immunosensing of p53 antibodies for cancer prognosis. Analyst, 141 (2016) 2733.

[English et al., 2002] P.J. English, M.A. Ghatei, I.A. Malik, S.R. Bloom, J.P. Wilding, Food fails to suppress ghrelin levels in obese humans. J. Clin. Endocrinol. Metab., 87 (2002) 2984.

[Engström et al., 2003] G. Engström, B. Hedblad, L. Stavenow, P. Lind, L. Janzon, F. Lindgärde, Inflammation-sensitive plasma proteins are associated with future weight gain. Diabetes, 52 (2003) 2097.

[Fain & Madan, 2005] J.N. Fain, D.S. Tichansky, A.K. Madan, Transforming growth factor beta1 release by human adipose tissue is enhanced in obesity. Metabolism, 54 (2005) 1546.

[Fallatah, 2014] H.I. Fallatah, Noinvasive fiomarkers of fiver fibrosis: an overview. Ad. Hepatol., 2014 ID 357287.

[Fang et al., 2008] L. Fang, S.-H. Wang, C.-C. Liu, An electrochemical biosensor of the ketone 3-β-hydroxybutyrate for potential diabetic patient management. Sens. Actuators B, 129 (2008) 818.

[Fang et al., 2017] X. Fang, J. Liu, J. Wang, H. Zhao, H. Ren, Z. Li, Dual signal amplification strategy of Au nanopaticles/ZnO nanorods hybridized reduced graphene nanosheet and multienzyme functionalized Au@ZnO composites for

ultrasensitive electrochemical detection of tumor biomarker. Biosens. Bioelectron., 97 (2017) 218.

[Feng et al., 2017] J. Feng, Y. Li, M. Li, F. Li, J. Han, Y. Dong, Z. Chen, P. Wang, H. Liu, Q. Wei, A novel sandwich-type electrochemical immunosensor for PSA detection based on PtCu bimetallic hybrid (2D/2D) rGO/g-C3N4. Biosens. Bioelectron., 91 (2017) 441.

[Fernández-Merino et al., 2010] M. J. Fernández-Merino, L. Guardia, J. I. Paredes, S. Villar-Rodil, P. Solís-Fernández, A. Martínez-Alonso, J. M. D. Tascón, Vitamin C is an ideal substitute for hydrazine in the reduction of graphene oxide suspension. J. Phys. Chem. C, 114 (2010) 6426.

[Feynman, 1992] R.P. Feynman, "There's plenty of room at the bottom". A reprint of the talk. J. Microelectromechanical Systems, 1 (1992) 60.

[Forrow et al., 2005] N.J. Forrow, G.S. Sanghera, S.J. Walters, J.L. Watkin, Development of a commercial amperometric biosensor electrode for the ketone d-3-hydroxybutyrate. Biosens. Bioelectron., 20 (2005) 1617.

[Frühbeck et al., 2001] G. Frühbeck, J. Gomez-Ambrosi, F.J. Muruzabal, M.A. Burrell, The adipocyte: a model for integration of endocrine and metabolic signaling in energy metabolism regulation. Am. J. Physiol. Endocrinol. Metab., 280 (2001) 827.

[Gao et al., 2016] Y.-S. Gao, X.-F. Zhu, J.-K. Xu, L.-M. Lu, W.-M. Wang, T.-T. Yang, H.-K. Xing, Y.-F. Yu, Label-free electrochemical immunosensor based on Nile blue A-reduced graphene oxide nanocomposites for carcinoembryonic antigen detection. Anal. Biochem., 500 (2016) 80.

[Geim & Novoselov, 2007] A.K. Geim, K.S. Novoselov, The rise of graphene. Nature Mat., 6 (2007) 183.

[Grainger et al., 1995] D.J. Grainger, B.R. Kemp, J.C. Metcalfe, A.C. Liu, R.M. Lawn, N.R. Williams, A.A. Grace, et al. Nat. Med., 1 (1995) 74.

[Grainger et al., 2000] D. J. Grainger, D. E. Mosedale, J. C. Metcalfe, TGF-b in blood: a complex problem. Cytokine Growth Factor Rev., 11 (2000) 145.

[Gröschl et al., 2004] M. Gröschl, M. Uhr, T. Kraus, Evaluation of the comparability of commercial ghrelin assays. Clin. Chem., 20 (2004) 457.

[Gröschl et al., 2005] M. Gröschl, H. G. Topf, J. Bohlender, J. Zenk, S. Klussmann, J. Dötsch, W. Rascher, M. Rauh, Identification of ghrelin in human saliva: production by the salivary glands and potential role in proliferation of oral keratinocytes. Clin. Chem., 51 (2005) 997.

[Hagiwara & Suzuki, 2000] Y. Hagiwara, H. Suzuki, Fracture Mechanics, Ohmsha, Tokyo, Japan, 135–138, 2000.

[Hameed et al., 2009] S. Hameed, W.S. Dhillo, S.R. Bloom, Gut hormones and appetite control. Oral Dis., 15 (2009) 18.

[Han et al., 2016] J. Han, L. Jiang, F. Li, P. Wang, Q. Liu, Y. Dong, Y. Li, Q. Wei, Ultrasensitive non-enzymatic immunosensor for carcino-embryonic antigen based on palladium hybrid vanadium pentoxide / multiwalled carbon nanotubes. Biosens. Bioelectron., 77 (2016) 1104.

[Harter et al., 1991] E. Harter, T. Svoboda, B. Ludvik, M. Schuller, B. Lell, E. Kuenburg, M. Brunnbauer, W. Woloszcruk, E. Prager, Basal and stomulated plasma levels of pancreatic amylin indicate its co-secretion with insulin in humans. Diabetologia, 34 (1991) 52.

[Hay et al., 2015] D.L. Hay, S. Chen, T.A. Lutz, D.G. Parkes, J.D. Roth, Amylin: Pharmacology, Physiology, and Clinical Potential. Pharmacol. Rev., 67 (2015) 564.

[Hayat et al., 2011] A. Hayat, L. Barthelmebs, A. Sassolas, J.-L. Marty, An electrochemical immunosensor based on covalent immobilization of okadaic acid onto screen printed carbon electrode via diazotization-coupling reaction. Talanta, 85 (2011) 513.

[Hayat et al., 2012] A. Hayat, L. Barthelmebs, J.-L. Marty, Electrochemical impedimetric immunosensor for the detection of okadaic acid in mussel simple. Sens. Actuators B Chem., 171 (2012) 810.

[Hernández et al., 2008] Y. Hernández, V. Nicolisi, M. Lotya, F.M. Blighe, Z. Sun et al., High - production of graphene by liquid - phase exfoliation of graphite. Nature Nanotech. 3 (2008) 563.

[Hervás et al., 2010] M. Hervás, M.A. López, A. Escarpa, Simplified calibration and analysis on screen-printed disposable platforms for electrochemical magnetic bead-based inmunosensing of zearalenone in baby food samples. Biosens. Bioelectron., 25 (2010) 1755.

[Honkanen et al., 1997] E. Honkanen, A.M. Teppo, T. Törnroth, P.H. Groop, C. Grönhagen-Riska, Urinary transforming growth factor-beta 1 in membranous glomerulonephritis. Nephrol. Dial. Transplant., 12 (1997) 2562.

[Hosu et al., 2017] O. Hosu, M.Tertiş, G. Melinte, R. Săndulescu, C. Cristea, Mucin 4 immunosensor based on p-aminophenylacetic acid grafting on carbon electrodes as immobilization platform. Proc. Technol., 27 (2017) 110.

[Hu et al., 2007] W. Hu, C. M. Li, X. Cui, H. Dong, Q. Zhou, In Situ Studies of Protein Adsorptions on Poly(pyrrole-co-pyrrole propylic acid) Film by Electrochemical Surface Plasmon Resonance. Langmuir, 23 (2007) 2761.

[Hu et al., 2008] W. Hu, C.M. Li, H. Dong, Poly(pyrrole-co-pyrrole propylic acid) film and its application in label-free surface plasmon resonance immunosensors. An. Chim. Acta., 630 (2008) 67.

[Hu et al., 2011] Y. Hu, Z. Zhao, Q. Wan, Facile preparation of carbon nanotube conducting polymer network for sensitive electrochemical immunoassay of Hepatitis B surface antigen in serum. Bioelectrochem., 81 (2011) 59.

[Hummers & Offeman, 1958] W.S. Hummers, R.E. Offeman, Preparation of graphitic oxide. J. Am. Chem. Soc., 80 (1958) 1339.

[Ilkhani et al., 2016] H. Ilkhani, A. Ravalli, G.Marrazza, Design of an affibody-based recognition strategy for human epidermal growth factor receptor 2 (HER2) detection by electrochemical biosensors. Chemosensors, 4 (2016) 23.

[Ionescu et al., 2005] R.E. Ionescu, C. Gondran, S. Cosnier, L.A. Gheber, R.S. Marks, Comparison between the performances of amperometric immunosensors for cholera antitoxin based on three enzyme markers. Talanta 66 (2005)15.

[IPCS, 1993] WHO International Programme on Chemical Safety Biomarkers and Risk Assessment: Concepts and Principles. 1993. Retrieved from http://www.inchem.org /documents/ehc/ehc/ehc155.htm.

[Ito et al., 2000] S. Ito, S. Yamazaki, K. Kano, T. Ikeda, Highly sensitive electrochemical detection of alkaline phosphatase. Anal. Chim. Acta, 424 (2000) 57.

[Kanso et al., 2013] H. Kanso, L. Barthelmebs, N. Inguimbert, T. Noguer, Immunosensors for estradiol and ethynyl estradiol based on new synthetic estrogen derivatives: Application to wastewater analysis. Anal.Chem., 85 (2013) 2397.

[Kashiwaya et al., 2000] Y. Kashiwaya, T. Takeshima, N. Mori, K. Nakashima, K. Clarke, R.L. Veech, D-beta-hydroxybutyrate protects neurons in models of Alzheimer's and Parkinson's disease. Proc. Natl. Acad. Sci., 97 (2000) 5440.

[Kautzky-Willer et al., 1994] A. Kautzky-Willer, K. Thomaseth, G. Pacini, M. Clodi, B. Ludvik, C. Streli, W. Waldhäusl, R. Prager, Role of islet amyloid polypeptide secretion in insulin-resistant humans. Diabetologia, 37 (1994) 188.

[Khorsand et al., 2013] F. Khorsand, M.D. Azizi, A. Naeemy, B. Larijani, K. Omidfar, An electrochemical biosensor for 3-hydroxybutyrate detection based on screen-printed modifed by coenzyme functionalized carbon nanotubes. Mol. Biol. Rep., 40 (2013) 2327.

[Kochmann et al., 2012] S. Kochmann, T. Hirsch, O.S.Wolfbeis, Graphenes in chemical sensors and biosensors. TrAC Trends in Analytical Chemistry, 39 (2012) 87.

[Koda et al., 1992] J.E. Koda, M. Fineman, T.J. Rink, G.E. Dailey, D.B. Muchmore, L.G. Linarelli, Amylin concentrations and glucose control. Lancet, 339 (1992) 1179.

[Kojima et al., 1999] M. Kojima, H. Hosoda, Y. Date, M. Nakazato, H. Matsuo, K. Kangawa, Ghrelin is a growth-hormone-releasing acylated peptide from stomach. Nature, 402 (1999) 656.

[Kojima & Kangawa, 2008] M. Kojima, K. Kangawa, Structure and function of ghrelin. Results Probl. Cell Differ., 46 (2008) 89.

[Kokkinos et al., 2016] C. Kokkinos, A. Economou, M.I. Prodromidis, Electrochemical immunosensors: critical survey of different architectures and transduction strategies, TrAC. Trends Anal. Chem., 79 (2016) 88.

[Kupari et al., 1995] M. Kupari, J. Lommi, M. Ventilä, U. Karjalainen, Breath acetone in congestive heart failure. Am. J. Cardiol., 76 (1995) 1076.

[Kwan et al., 2006] R.C.H. Kwan, P.Y.T. Hona, W.C. Maka, L.Y. Lawa, J. Huc, R. Renneberg, Biosensor for rapid determination of 3-hydrybutyrate using bienzyme system. Biosens. Bioelectron., 21 (2006) 1101.

[Laffel, 1999] L. Laffel, Use of a point-of-care beta-hydroxybutyrate sensor for detection of ketonemia in dogs. Diabetes/Metab. Res. Rev., 15 (1999) 412.

[Lahaye et al., 2009] R. J. W. E., Lahaye, H.K., Jeong, C.Y. Park, Y.H. Lee, Density functional theory study of graphite oxide for different oxidation levels. Phys. Rev. B, 79 (2009) 125435.

[Lai et al., 2017] G. Lai, M. Zheng , W. Hu , A. Yu, One-pot loading high-content thionine on polydopamine-functionalized mesoporous silica nanosphere for ultrasensitive electrochemical immunoassay. Biosens. Bioelectron., 95 (2017) 15.

[Lavie et al., 2014] C.J.Lavie, P.A. McAuley, T. S. Church, R. V. Milani, S. N. Blair, Obesity and Cardiovascular Diseases: Implications Regarding Fitness, Fatness, and Severity in the Obesity Paradox. J. Am. Coll. Cardiol., 63 (2014) 1345.

[Lawal, 2015] A.T. Lawal, Synthesis and utilisation of graphene for fabrication of electrochemical sensors. Talanta, 131 (2015) 424.

[Lebovitz, 1995] H.E. Lebovitz, Diabetic ketoacidosis. Lancet, 345 (1995) 767.

[Le Roux et al., 2006] C.W. Le Roux, R. L. Batterham, S. J. Aylwin, M. Patterson, C.M. Borg, K.J. Wynne, et al., Attenuated peptide YY release in obese subjects is associated with reduced satiety. Endrocrinology, 147 (2006) 3.

[Leckström et al., 1997] A. Leckström, K. Bjorklund, J. Permert, R. Larsson, P. Westermark, Renal elimination of islet amyloid polypeptide. Biochem Biophys Res Commun, 239 (1997) 265.

[Li et al., 2005] G. Li, N.Z. Ma, Y. Wang, A new handheld biosensor for monitoring blood ketones. Sens. Actuators B, 109 (2005) 285.

[Li et al., 2012] S. Li, M. Micic, J. Orbulescu, J.D. Whyte, R.M. Leblanc, Human islet amyloid polypeptide at the air–aqueous interface: a Langmuir monolayer approach. J. R. Soc. Interface, 9 (2012) 3118.

[Lim et al., 2016] S.A. Lim, U.A. Minhaz, A label free electrochemical immunosensor for sensitive detection of porcine serum albumin as a marker for pork adulteration in raw meat. Food Chem., 206 (2016) 197.

[Liu et al., 2000] J. Liu, L. Cheng, B. Liu, S. Dong, Covalent modification of a glassy carbon surface by 4-aminobenzoic acid and its application in fabrication of a polyoxometalates-consisting monolayer and multilayer films. Langmuir, 16 (2000) 7471.

[Liu et al., 2014] J. Liu, C. Hu, J. Xu, F. Jiang, F. Chen, Enhanced photocatalytic performance of partially reduced graphene oxide under simulated solar light through loading gold nanoparticles. Mater. Lett., 134 (2014) 134.

[Liu et al., 2016] G.Liu, M. Qi, Y. Zhang, C. Cao, E. M. Goldys, Nanocomposites of gold nanoparticles and graphene oxide towards an stable label-free electrochemical immunosensor for detection of cardiac marker troponin-I. Anal. Chim. Acta, 909 (2016) 1.

[Lu et al., 2007] H. Lu, M.P. Kreuzer, K.Takkinen, G.G.Guilbault, A recombinant Fab fragment-based electrochemical immunosensor for the determination of testosterone in bovine urine. Biosens. Bioelectron., 22 (2007)1756.

[Lutz, 2006] T.A. Lutz, Amylinergic control of feeding. Physiol. Behav., 89 (2006) 465.

[Ma et al., 2016] W. Ma, B. Situ, W. Lv., B. Li, X. Yin, P. Vadgama, L. Zheng, W. Wang, Electrochemical determination of microRNAs based on isothermal strand-displacement polymerase reaction coupled with multienzyme functionalized magnetic micro-carriers. Biosens. Bioelectron., 80 (2016) 344.

[Mandon et al., 2009] C.A. Mandon, L.J.Blum, C.A.Marquette, Aryl diazonium for biomolecules immobilization. Chem.Phys.Chem.,10 (2009) 3273.

[Martelosi-Cebinelli, 2016] Martelossi-Cebinelli, Paiva-Trugilo, B. Garcia, B. de Oliveira, TGF-β1 functional polymorphisms: a review. Eur. Cytokine. Netw., 27 (2016) 81.

[Martínez et al., 2010] N.A.Martínez, R.J.Schneider, G.A. Messina, J.Raba, Modified paramagnetic beads in a microfluidic system for the determination of ethynyl estradiol (EE2) in river water samples. Biosens. Bioelectron., 25 (2010) 1376.

[Martínez-García et al., 2016] G. Martínez-García, L. Agüí, P. Yáñez-Sedeño, J.M. Pingarrón, Multiplexed electrochemical immunosensing of obesity-related hormones at grafted graphene-modified electrodes. Electrochim.Acta, 202 (2016) 209.

[Mascini et al., 2007] M. Mascini, G. G. Guilbault, S. J. Lebrun, D. Compagnone, Colorimetric microarray detection system for ghrelin using aptamer-technology. Anal. Lett., 2007, 40, 1386.

[Mascini et al., 2007a] M. Mascini, K. Papamichael, I. Mevola, M. Pravda, G. G. Guilbault, Ghrelin detection using spiegelmer-capture molecules. Anal. Lett., 2007, 40, 403.

[Masuda et al., 2000] Y. Masuda, T. Tanaka, N. Inomata, N. Ohnuma, S. Tanaka, Z. Itoh, H. Hosoda, M. Kojima, K. Kangawa, Ghrelin stimulates gastric acid secretion and motility in rats. Biochem. Biophys. Res. Commun., 276 (2000) 905.

[Matharu, et al, 2014] Z. Matharu, D. Patel, Y. Gao, A. Haque, Q. Zhou, A. Revzin, Detecting Transforming Growth Factor-β Release from liver cells using an aptasensor integrated with microfluidics. An.Chem., 86 (2014) 8865.

[Maury & Brichard., 2010] E. Maury, S.M. Brichard, Adipokine dysregulation, adipose tissue inflammation and metabolic syndrome. Mol. Cell Endocrinol., 314 (2010) 1.

[McNeil et al., 1990] C.J. McNeil, J.A. Spoors, J.M. Cooper, K.G.M.M. Alberti, W.H. Mullen, Amperometric biosensor for rapid measurement of 3-hydroxybutyrate in undiluted whole blood and plasma. Anal. Chim. Acta, 237 (1990) 99.

[Mentlein et al., 1993] R. Mentlein, P. Dahms, D. Grandt, R. Krüger, Proteolytic processing of neuropeptide Y and peptide YY by dipeptidyl peptidase IV. Regul. Pept., 49 (1993) 133.

[Mietlicki-Baase, 2016] E.G. Mietlicki-Baase, Amylin-mediated control of glycemia, energy balance, and cognition. Physiol. Behav., 162 (2016) 130.

[Miller et al., 2012] C. N. Miller, L. M. Brown, S. Rayalam, M. A. Della-Fera, C.A. Baile, Estrogens, inflammation and obesity: an overview. Front. Biol., 7 (2012) 40.

[Moreno-Guzmán et al., 2010] M. Moreno-Guzmán, M. Eguílaz, S. Campuzano, A. González-Cortés, P. Yáñez-Sedeño, J.M. Pingarrón, Disposable immunosensor for cortisol using functionalized magnetic particles. Analyst, 135 (2010) 1926.

[Moreno-Guzmán et al., 2012] M. Moreno-Guzmán, I. Ojeda, R. Villalonga, A. González-Cortés, P. Yáñez-Sedeño, J.M. Pingarrón, Ultrasensitive detection of adrenocorticotropin hormone (ACTH) using disposable phenylboronic-modified electrochemical immunosensors. Biosens. Bioelectron., 35 (2012) 82.

[Moreno-Guzmán et al., 2012a] M. Moreno-Guzmán, A. González-Cortés, P. Yáñez-Sedeño, J.M. Pingarrón, Multiplexed ultrasensitive determination of adreno-corticotropin and cortisol hormones at a dual electrochemical immunosensor. Electroanalysis, 24 (2012) 1100.

[Mousavi et al., 2017] M. F. Mousavi, S. Mirsian, A. Noori, H. Ilkhani, M.Sarparast, N. Moradi, S. Z. Bathaie, M. A. Mehrgardi, BSA-templated Pb nanocluster as a

biocompatible signaling probe for electrochemical EGFR immunosensing. Electroanalysis, 29 (2017) 861.

[Muir et al., 2007] W. Muir, M.C. Barden, S.P. Collett, A.-D. Gorse, R. Monteiro, L. Yang, N.A. McDougall, S. Gould, N.J. Maeji, High-throughput optimization of surfaces for antibody immobilization using metal complexes. Anal. Biochem., 363 (2007) 97.

[Navakula et al., 2017] K. Navakula, C. Warakulwit,, P. Yenchitsomanus, A. Panya, P. A. Lieberzeit, C. Sangma, A novel method for dengue virus detection and antibody screening using a graphene-polymer based electrochemical biosensor. Nanomed.: Nanotechnol. Biol. Med.,13 (2017) 549.

[Ngoensawat et al., 2018] U.Ngoensawat, P. Rijiravanich, W. Surareungchai, M. Somasundrum, Electrochemical immunoassay for Salmonella Typhimurium based on an immuno-magnetic redox label. Electroanalysis, 30 (2018) 146.

[Nguyen et al., 2017] V.-A. Nguyen, H. L. Nguyen, D.T. Nguyen, Q. P. Do, L.D. Tran, Electrosynthesized poly(1,5-diaminonaphthalene)/polypyrrole nanowires bilayer as an immunosensor platform for breast cancer biomarker CA 15-3, Curr. Appl. Phys., 17 (2017) 1422.

[Novoselov et al., 2004] K. S. Novoselov, A. K. Geim, S. V. Morozov, D. Jiang, Y. Zhang, S. V. Dubonos, I. V. Grigorieva, A.A. Firsov, Electric Field Effect in Atomically Thin Carbon Films. Science, 22 (2004) 666.

[Ojeda et al., 2014] I. Ojeda, M. Moreno-Guzmán, A. González-Cortés, P. Yáñez-Sedeño, J.M. Pingarrón, Electrochemical magnetoimmunosensor for the ultrasensitive determination of interleukin-6 in saliva and urine using poly-HRP-streptavidin conjugates as labels for signal amplification. Anal. Bioanal. Chem., 406 (2014) 6363.

[Ojeda et al., 2015] I. Ojeda, M. Barrejón, L.M. Arellano, A. González-Cortés, P. Yáñez-Sedeño, F. Langa, J.M. Pingarrón, Grafted-double walled carbon nanotubes as electrochemical platforms for immobilization of antibodies using a metallic-complex chelating polymer: Application to the determination of adiponectin cytokine in serum. Biosens. Bioelectron., 74 (2015) 24.

[Ooi et al., 2014] H.W. Ooi, S.J. Cooper, C.-Y. Huang, D. Jennins, E. Chung, N.J. Maeji, A.K. Whittaker, Coordination complexes as molecular glue for immobilization of antibodies on cyclic olefin copolymer surfaces. Anal. Biochem., 456 (2014) 6.

[O'Shea et al., 2011] J. J. O'Shea, M. Gadina, Y.Kanno. Cytokine signalin: Birth of a Pathway. J. Immunol., 187 (2011) 5475.

[Patil & Alexandrescu, 2015] S.M. Patil, A.T. Alexandrescu, Charge-Based Inhibitors of Amylin Fibrillization and Toxicity. J. Diabet. Res., 2015 (2015) ID 946037.

[Paulsson et al., 2014] J. F. Pailsson, J. Ludvigsson, A. Carlsson, R. Casas, G. Forsander, E. A. Ivarsson, et al., High plasma levels of islet amyloid polypeptide in young with new-onset of type 1 diabetes mellitus. Plos One, 9 (2014) e93053.

[Pedrero et al., 2016] M. Pedrero, F. J. Manuel de Villena, C. Muñoz-San Martín, S. Campuzano, M. Garranzo-Asensio, R. Barderas, J.M. Pingarrón, Disposable amperometric immunosensor for the determination of human P53 protein in cell lysates using magnetic micro-carriers. Biosensors, 6 (2016) 56.

[Peino et al., 2000] R. Peino, R. Baldelli, J. Rodriguez-Garcia, S. Rodriguez-Segade, M. Kojima, K. Kangawa, E. Arvat, E. Ghigo, C. Diéguez, F.F. Casanueva, Ghrelin-induced growth hormone secretion in humans. Eur. J. Endocrinol., 143 (2000) R11.

[Percy et al., 1996] A. J. Percy, D.A. Trainor, J. Rittenhouse, J. Phelps, J.E. Koda, Development of sensitive immunoassays to detect amylin and amylin-like peptides in unextracted plasma. Clin. Chem., 42 (1996) 576.

[Persson, 1970] B. Persson, Determination of plasma acetoacetate and D-β-hydroxy butyrate in new-born infants by an enzymatic fluorometric micro-method. Scand J Clin Lab Invest, 25(1970) 9.

[Pischon, 2009] T. Pischon, Use of obesity biomarkers in cardiovascular epidemiology. Dis Markers, 26 (2009) 247.

[Popovic et al., 2004] V. Popovic, M. Svetel, M. Djurovic, S. Petrovic, M. Doknic, S. Pekic, D. Miljic, N. Milic, J. Glodic, C. Dieguez, F. F. Casanueva, V. Kostic, Circulating and cerebrospinal fluid ghrelin and leptin: potential role in altered body weight in Huntington's disease. Eur. J. Endocrinol., 151 (2004) 451.

[Punckt et al., 2013] C. Punckt, M.A. Pope I.A. Aksay, On the electrochemical response of porous functionalized graphene electrodes. J. Phys. Chem. C, 117 (2013) 16076.

[Qi et al., 2012] H. Qi, C. Ling, Q. Ma, Q. Gao, C. Zhang, Sensitive electrochemical immunosensor array for the simultaneous detection of multiple tumor markers. Analyst, 137 (2012) 393.

[Radi et al., 2009] A.-E., Radi,.X. Muñoz-Berbel, M. Cortina-Puig, J.-L. Marty, An electrochemical immunosensor for ochratoxin A based on immobilization of antibodies on diazonium-functionalized gold electrode. Electrochim. Acta, 54 (2009) 2180.

[Rana et al., 2007] J. S. Rana, M. Nieuwdorp, J.W. Jukema, J.J. Kastelein, Cardiovascular metabolic syndrome - an interplay of, obesity, inflammation, diabetes and coronary heart disease. Diabetes Obes. Metab., 9 (2007) 218.

[Raps et al., 2014] M. Raps, J.Curvers, F.M.Helmerhorst, B.E.P.B. Ballieux, J.Rosing, S.Thomassen, F.R.Rosendaal, H.A.A.M.van Vliet, Thyroid function, activated protein

C resistance and the risk of venous thrombosis in users of hormonal contraceptives. Thromb. Res. 133 (2014) 640.

[Rauf et al., 2018] S. Raufa, G.K. Mishra, J.A. Rupesh, K.Mishra, K.Y. Goud, M.A.H. Nawaz, J.L. Marty, A. Hayat, Carboxylic group riched graphene oxide based disposable electrochemical immunosensor for cancer biomarker detection. Anal. Biochem. 545 (2018) 13.

[Reger et al., 2004] M.A. Reger, S.T. Henderson, C. Hale, B. Cholerton, L.D. Baker, G. S. Watson, et al. Effects of beta-hydroxybutyrate on cognition in memory-impaired adults. Neurobiol. Aging, 25 (2004) 311.

[Reidelberger et al., 2001] R.D. Reidelberger, U. Arnelo, L. Granqvist, J. Permert, Comparative effects of amylin and cholecystokinin on food intake and gastric emptying in rats. Am. J. Physiol. Regul. Integr. Comp. Physiol., 280 (2001) R605.

[Renshaw & Batterham, 2005] D. Renshaw, R.L. Batterham, Peptide YY: a potential therapy for obesity. Curr. Drug Targets, 6 (2005) 171.

[Rodríguez-Gallego et al., 2015] E. Rodríguez-Gallego, M. Guirro, M. Riera-Borrull, A. Hernández-Aguilera, R. Mariné-Casadó, S. Fernández-Arroyo, R. Beltrán-Debón, F. Sabench, M. Hernández, et al., Mapping of the circulating metabolome reveals α-ketoglutarate as a predictor of morbid obesity-associated non-alcoholic fatty liver disease. Int. J. Obes., 39 (2015) 279.

[Roushani & Valipour, 2016] M. Roushani, A. Valipour, Using electrochemical oxidation of Rutin in modeling a novel andsensitive immunosensor based on Pt nanoparticle and graphene–ionicliquid–chitosan nanocomposite to detect human chorionicgonadotropin. Sens. Actuators B, 222 (2016) 1103.

[Ruiz-Valdepeñas et al., 2015] V. Ruiz-Valdepeñas, S. Campuzano, A. Pellicano, R.M. Torrente-Rodríguez, A.J. Reviejo, M.S. Cossio, J.M. Pingarrón, Sensitive and selective magnetoimmunosensing platform for determination of the food allergen Ara h 1. Anal. Chim. Acta, 880 (2015) 52.

[Ruiz-Valdepeñas et al., 2016] V. Ruiz-Valdepeñas, S. Campuzano, R.M. Torrente-Rodríguez, A.J. Reviejo, J.M. Pingarrón, Electrochemical magnetic beads-based immunosensing platform for the determination of α-lactalbumin in milk. Food. Chem., 213 (2016) 595.

[Ruiz-Valdepeñas et al., 2016a] V. Ruiz-Valdepeñas Montiel, R. M.Torrente-Rodríguez, S. Campuzano, A. Pellicanò, Á. J. Reviejo, M. Stella Cosio, J. M. Pingarrón, Simultaneous determination of the main peanut allergens in foods using disposable amperometric magnetic beads-based Immunosensing platforms. Chemosensors, 5 (2016) 11.

[Ruth, 2001] A. Ruth, Clinical measurements of steroid metabolism, Best Pract. Res. Clin. Endocrinol. Metab., 15 (2001)1.

[Saby et al., 1997] C. Saby, B. Ortiz, G.Y. Champagne, D. Bélanger, Electrochemical modification of glassy carbon electrode using aromatic diazonium salts. 1. Blocking effect of 4-nitrophenyl and 4-carboxyphenyl groups. Langmuir, 13 (1997) 6805.

[Sağsöz et al., 2009] N. Sağsöz, Z. Orbak, V.Noyan, A. Yücel, B.Ucxar, L. Yıldız, The effects of oral contraceptives including low-dose estrogen and drospirenone on the concentration of leptin and ghrelin in polycystic ovary syndrome. Fertility and Sterility, 92 (2009) 660.

[Sam et al., 2010] S. Sam, L. Touahir, S. Andres, P. Allongue, J.-N. Chazalviel, A. C. Gouget-Laemmel, C. Henry de Villeneuve, A. Moraillon, F. Ozanam, N. Gabouze, S. Djebbar, Semiquantitative study of the EDC/NHS activation of acid terminal groups at modified porous silicon surfaces. Langmuir, 26 (2010) 809.

[Samad, 1997] F. Samad, K. Yamamoto, M. Pandey, D.J. Loskutoff, Elevated Expression of Transforming Growth Factor-β in Adipose Tissue from Obese Mice. Mol.Med., 1 (1997) 37.

[Sánchez-Tirado et al., 2016] E. Sánchez-Tirado, A. González-Cortés, P. Yáñez-Sedeño, J. M. Pingarrón, Carbon nanotubes functionalized by click chemistry as scaffolds for the preparation of electrochemical immunosensors. Application to the determination of TGF-beta 1 cytokine. Analyst, 141 (2016) 5730.

[Sánchez-Tirado et al., 2017] E. Sánchez-Tirado, C. Salvo, A. González-Cortés, P. Yáñez-Sedeño, F. Langa, J.M. Pingarrón, Electrochemical immunosensor for simultaneous determination of interleukin-1 beta and tumor necrosis factor alpha in serum and saliva using dual screen printed electrodes modified with functionalized double–walled carbon nanotubes. Anal. Chim. Acta, 959 (2017) 66.

[Sánchez-Tirado et al., 2017a] E. Sánchez-Tirado, L. M. Arellano, A. González-Cortés, P. Yáñez-Sedeño, F. Langa, J.M. Pingarrón, Viologen-functionalized single-walled carbon nanotubes as carrier nanotags for electrochemical immunosensing. Application to TGF-β1 cytokine. Biosens. Bioelectron., 98 (2017) 240.

[Sanke et al., 1991] T. Sanke, T. Hanabusa, Y. Nakano, C. Oki, K. Okai, S. Nishimura, M. Kondo, K. Nanjo, Plasma islet amyloid polypeptide (amylin) levels and their responses to oral glucose in type-2 (non-insulin-dependent) diabetic patients. Diabetologia, 34 (1991) 129.

[Schmidt et al., 2015] F. M. Schmidt, J. Weschenfelder, C. Sander, J. Minkwitz, J.Thormann, T. Chittka, et al., Inflammatory cytokines in general and central obesity and modulating effects of physical activity. PLoS One, 10 (2015) e0121971.

[Schneider et al., 2004] C. Schneider, H.F.Schöler, R.J.Schneider, A novel enzyme-linked immunosorbent assay for ethynyl estradiol using a long-chain biotinylated EE2 derivative. Steroids, 69 (2004) 245.

[Schneider et al., 2005] C. Schneider, H.F.Schöler, R.J.Schneider, Direct sub-ppt detection of the endocrine disruptor ethynyl estradiol in water with a chemiluminescence enzyme-linked immunosorbent assay. Anal. Chim. Acta, 551 (2005) 92.

[Sengupta et al., 2010] S. Sengupta, T.R. Peterson, M. Laplante, S. Oh, D.M. Sabatini, mTORC1 controls fasting-induced ketogenesis and its modulation by ageing. Nature, 468 (2010)1100.

[Sepúlveda-Flores, 2002] R.N. Sepúlveda-Flores, L. Vera-Cabrera, J.P. Flores-Gutiérrez, H. Maldonado-Garz, R. Salinas-Garza, P. Zorrilla-Blanco, F.J. Bosques-Padilla, Obesity-related non-alcoholic steatohepatitis and TGF-β1 serum levels in relation to morbid obesity. Ann. Hepatol., 1 (2002) 36.

[Serafín et al., 2014] V. Serafín, L. Agüí, P. Yáñez-Sedeño, J.M. Pingarrón, Electrochemical immunosensor for the determination of insulin-like growth factor-1 using electrodes modified with carbon nanotubes–poly(pyrrole propionic acid) hybrids. Biosens. Bioelectronics, 52 (2014) 98.

[Serafín et al., 2014a] V. Serafín, L. Agüí, P. Yáñez-Sedeño, J.M. Pingarrón, Determination of prolactin hormone in serum and urine using an electrochemical immunosensor based on poly(pyrrolepropionic acid)/carbon nanotubes hybrid modified electrodes. Sens. Actuator B, 195 (2014) 404.

[Serafín et al., 2017] V. Serafín, R.M. Torrente-Rodríguez, M. Batlle, P. García de Frutos, S. Campuzano, P. Yáñez-Sedeño, J.M. Pingarrón, Electrochemical immunosensor for receptor tyrosine kinase AXL using poly(pyrrolepropionic acid)-modified disposable electrodes. Sens. Actuators B, 240 (2017) 1251.

[Serafín et al., 2017a] V. Serafín, R. M. Torrente-Rodríguez, M. Batlle, P. García de Frutos, S. Campuzano, P. Yáñez-Sedeño, J. M. Pingarrón, Comparative evaluation of the performance of electrochemical immunosensors using magnetic microparticles and nanoparticles. Application to the determination of tyrosine kinase receptor AXL. Microchim. Acta, 184 (2017) 4251.

[Serafín et al., 2018] V. Serafín, R. M. Torrente-Rodríguez, A. González-Cortés, P. García de Frutos, M. Sabaté, S. Campuzano, P. Yáñez-Sedeño, J.M. Pingarrón, An electrochemical immunosensor for brain natriuretic peptide prepared with screen-printed carbon electrodes nanostructured with gold nanoparticles grafted through aryl diazonium salt chemistry. Talanta, 179 (2018) 191.

[Sharma et al., 2013] P. Sharma, G. Darabdhara, T. M. Reddy, A. Borah, P. Bezboruah, P. Gogoi, N. Hussain, P. Sengupta, M. R. Das, Synthesis, characterization and catalytic application of Au NPs-reduced graphene oxide composites material: an eco-friendly approach. Catal. Commun., 40 (2013) 139.

[Sharma et al., 2018] A. Sharma, A. Kumar, R. Khan, A highly sensitive amperometric immunosensor probe based on gold nanoparticle functionalized poly (3, 4-ethylenedioxythiophene) doped with graphene oxide for efficient detection of aflatoxin B1. Synth. Met., 235 (2018) 136.

[Shiiya et al., 2002] T. Shiiya, M. Nakazato, M. Mizuta, Y. Date, M.S. Mondal, M. Tanaka, S.-I. Nozoe, H. Hosoda, K. Kangawa, S. Matsukura, Plasma ghrelin levels in lean and obese humans and the effect of glucose on ghrelin secretion. J. Clin. Endocrinol. Metab., 87 (2002) 240.

[Shimomura et al., 2013] T. Shimomura, T. Sumiya, M. Ono, T. Ito, T.A. Hanaoka, A novel, disposable, screen-printed amperometric biosensor for ketone 3-β-hydroxybutyrate fabricated using a 3-β-hydroxybutyrate dehydrogenase–mesoporous silica conjugate. Anal. Bioanal. Chem., 405 (2013) 297.

[Singal et al., 2016] S. Singal, A.K Srivastava, B. Gahtori, Rajesh, Immunoassay for troponin I using a glassy carbon electrode modified with a hybrid film consisting of graphene and multiwalled carbon nanotubes and decorated with platinum nanoparticles. Microchim. Acta, 183 (2016) 1375.

[Singal et al., 2017] S. Singal, A.K. Srivastava, Rajesh, Electrochemical impedance analysis of biofunctionalized conducting polymer-modified graphene-CNTs nanocomposite for protein detection. Nano-Micro Lett., 9 (2017) 7.

[Soares et al., 2009] G. M. Soares, C. S. Vieira, W. de Paula Martins, R. M. dos Reis, M.F.S. de Sa´, R.A. Ferriani, Metabolic and cardiovascular impact of oral contraceptives in polycystic ovary syndrome. Int. J. Clin. Pract., 63 (2009) 160.

[Stenken & Poschenrieder, 2015] J.A. Stenken, J. Poschenrieder, Bioanalytical chemistry of cytokines. A review. Anal.Chim. Acta, 853 (2015) 95.

[Stevanovic et al., 2013] D. Stevanovic, V. Trajkovic, S. Müller-Lühlhoff, E. Brandt, W. Abplanalp, C. Bumke-Vogt, B. Liehl, P. Wiedmer, K. Janjetovic, V. Starcevic, A.F.H. Pfeiffer, H. Al-Hasani, M. H. Tschöp, T.R. Castañeda, Ghrelin-induced food intake and adiposity depend on central mTORC1/S6K1 signaling. Mol. Cell. Endocrinol., 381 (2013) 280.

[Sun et al., 2017] B. Sun, Y. Gou, Y. Ma, X. Zheng, R. Bai, A. Attia, A. Abdelmoaty, F. Hua, Investigate electrochemical immunosensor of cortisol based on gold nanoparticles/magnetic functionalized reduced graphene oxide. Biosens Bioelectron., 88 (2017) 55.

[Tang et al., 2018] Z.Tang, J. He, J. Chen, Y. Niu, Y. Zhao, Y. Zhang, C. Yu, A sensitive sandwich-type immunosensor for the detection of galectin-3 based on N-GNRs-Fe-MOFs@AuNPs nanocomposites and a novel AuPt methylene blue nanorod. Biosens. Bioelectron., 101 (2018) 253.

[Tatemoto & Mutt, 1980] K. Tatemoto, V. Mutt, Isolation of two novel candidates for finding naturally occurring polypeptides. Nature, 285 (1980) 417.

[Taskin et al., 2014] E. Taskin, B. Atli, M. Kiliç, Y. Sari, S. Aydin, Serum, urine, and saliva levels of ghrelin and obestatin pre- and post-treatment in pediatric epilepsy. Pediatric Neurol., 51 (2014) 365.

[Teles & Fonseca, 2008] F.R.R. Teles, L.P. Fonseca, Applications of polymers for biomolecule immobilization in electrochemical biosensors. Mater. Sci. Eng. C., 28 (2008) 1530.

[Thévenot et al., 2001] D.R. Thévenot, K. Toth, R.A. Durst, G.S. Wilson, Electrochemical biosensors: recommended definitions and classification, Biosens. Bioelectron. Technical report 16 (2001) 121–131

[Thi Vu et al., 2015] T.H. Thi Vu, T.T. Thi Tran, H.N. Thi Le, L.T. Tran, P.H.T. Nguyen, H.T. Nguyen, N. Q. Bui, Solvothermal synthesis of Pt-SiO2 / graphene nanocomposites as efficient electrocatalysts for methanol oxidation. Electrochim. Acta, 161 (2015) 335.

[Tieu et al., 2003] K. Tieu, C. Perier, C. Caspersen, P. Teismann, D.C. Wu, S.D. Yan et al. D-beta-hydroxybutyrate rescues mitochondrial respiration and mitigates features of Parkinson disease. J. Clin. Invest., 112 (2003) 892.

[Tijssen, 1985] P. Tijssen, “Practice and theory of enzyme immunoassays”, en R.H. Burdon, P.H. van Lnippenberg, eds. “Laboratory Techniques in Biochemistry and Molecular Biology”, 15 (1985) 414.

[Torrente-Rodríguez et al., 2016] R. M. Torrente-Rodríguez, S. Campuzano, V. Ruiz-Valdepeñas Montiel, M. Pedrero, M. J. Fernández-Acenero, R. Barderas, J. M. Pingarrón, Rapid endoglin determination in serum samples using an amperometric magneto-actuated disposable immunosensing platform. J. Pharm. Biomed. Anal., 129 (2016) 288.

[Torun et al., 2007] D.Torun, R. Ozelsancak, I. Turan, H. Micozkadioglu, S. Sezer, F.N. Ozdemir, The relationship between obesity and transforming growth factor beta on renal damage in essential hypertension. Int. Heart J., Nov., 56 (2007) 733.

[Trayhurn & Wood, 2004] P.Trayhurn, I.S. Wood, Adipokines: inflammation and the pleiotropic role of white adipose tissue. Br. J. Nutr., 92 (2004) 347.

[Trivedi et al., 2012] A.Trivedi, S. Babic, J.-P. Chanoine, Pitfalls in the determination of human acylated ghrelin plasma concentrations using a double antibody enzyme immunometric assay. Clin. Biochem., 45 (2012) 178.

[Truong et al., 2011] L.T.N. Truong, M. Chikae, Y. Ukita, Y. Takamura, Labelless impedance immunosensor based on polypyrrole-pyrolecarboxylic acid copolymer for hCG detection. Talanta, 85 (2011) 2576.

[Tsapenko et al., 2013] M.V. Tsapenko, R.E. Nwoko, T.M. Borland, N.V. Voskoboev, A. Pflueger, A.D. Rule, J.C. Lieske. Clin. Biochem., 46 (2013) 1430.

[Veerapandian et al., 2016] M. Veerapandian, R. Hunter, S. Neethirajan, Dual immunosensor based on methylene blue - electroadsorbed graphene oxide for rapid detection of the influenza A virus antigen. Talanta, 155 (2016) 250.

[Veerapandian et al., 2016a] M. Veerapandian, R. Hunter, S. Neethirajan, Ruthenium dye sensitized graphene oxide electrode for on-farm rapid detection of beta-hydroxybutyrate. Sens. Actuators B, 228 (2016) 180.

[Verma et al., 2011] P. Verma, P. Maire, P. Novák, Concatenation of electrochemical grafting with chemical or electrochemical modification for preparing electrodes with specific surface functionality. Electrochim. Acta, 56 (2011) 3555.

[Vidal et al., 2016] J.C. Vidal, J.R. Bertolin, L. Bonel, L. Asturias, M.J. Arcos-Martinez, J.R. Castillo, A multi-electrochemical competitive immunosensor for sensitive cocaine determination in biological samples. Electroanalysis, 28 (2016) 685.

[Vörös et al., 2012] K. Vörös, Z. Prohászka, E. Kaszás, A. Alliquander, A. Terebesy, F. Horváth, L. Janik, A. Sima, J. Forrai, K. Cseh, L. Kalabay, Serum ghrelin level and TNF-α/ghrelin ratio in patients with previous myocardial infarction. Arch. Med. Res., 43 (2012) 548.

[Wakefield et al., 1995] L.M. Wakefield, J.J. Letterio, T. Chen, D. Danielpour, R.S. Allison, L.H. Pai, A.M. Denicoff, M.H. Noone, K.H. Cowan, J.A. O'Shaughnessy, Transforming growth factor-beta1 circulates in normal human plasma and is unchanged in advanced metastatic breast cancer. Clin. Cancer Res., 1 (1995) 129.

[Walcarius & Kuhn, 2008] A. Walcarius, A. Kuhn, Ordered porous thin films in electrochemical analysis. Trac-Trends Anal. Chem., 27 (2008) 593.

[Wallace & Mattheus, 2004] T.M. Wallace, D.R. Mattheus. Recent advances in the monitoring and management of diabetic ketoacidosis. QJM, 97 (2004) 773.

[Wang et al., 2016] C.C. Wang, J.W. Hennek, A. Ainla, A.A. Kumar, W.J. Lan, J. Im., B.S. Smith, M. Zhao, G.M. Whitesides, A paper-based ``pop-up´´ electrochemical device for analysis of beta-hydroxybutyrate. Anal. Chem., 88 (2016) 6326.

[Wang et al., 2018] Y. Wang, Y. Wang, D. Wu, H. Ma, Y. Zhang, D. Fan, X. Pang, B. Du, Q. Wei, Label-free electrochemical immunosensor based on flower-

likeAg/MoS2/rGO nanocomposites for ultrasensitive detection ofcarcinoembryonic antigen. Sens. Actuators B, 255 (2018) 125.

[WHO Scientific Group, 2011] Cardiovascular disease and steroid hormone contraception, Report of a WHO Scientific Group, 877 [i–vii], 2011. pp. 1–89.

[Wojcik et al., 2010] M.H Wojcik, E. Meenaghan, E. A Lawson, M.Misra, A.Klibanski, K. K Miller, Reduced amylin levels are associated with low bone mineral density in women with anorexia nervosa. Bone, 46 (2010) 796.

[Wren et al., 2000] A.M. Wren, C.J. Small, H.L.Ward, K.G. Murphy, C.L. Dakin, S. Taheri, A.R. Kennedy, G.H. Roberts, D.G. Morgan, M.A. Ghateis, S.R. Bloom, The novel hypothalamic peptide ghrelin stimulates food intake and growth hormone secretion. Endocrinol., 141 (2000) 4325.

[Wu et al., 2013] S. Wu, Q. He, C.Tan, Y. Wang, H. Zhang, Graphene-based electrochemical sensors. Small, 9 (2013) 1160.

[Yach et al., 2006] D. Yach, D. Stuckler, K.D. Brownell, Epidemiologic and economic consequences of the global epidemics of obesity and diabetes. Nature Med., 12 (2006) 62.

[Yadav et al., 2011] H. Yadav, C. Quijano, A. K. Kamaraju, O. Gavrilova, R. Malek, W. Chen, P. Zerfas, D. Zhigang, E. C. Wright, et al., Protection from obesity and diabetes by blockade of TGF-b/Smad3 signaling. Cell Metabolism, 14 (2011) 67.

[Yáñez-Sedeño et al., 2016] P. Yáñez-Sedeño, S. Campuzano, J.M. Pingarrón, Magnetic particles coupled to disposable screen printed transducers for electrochemical biosensing. Sensors, 16 (2016) 1585.

[Yao et al., 2016] Y. Yao, J. Bao, Y. Lu, D. Zhang, S. Luo, X. Cheng, Q. Zhang, S. Li, Q. Liu, Biomarkers of liver fibrosis detecting with electrochemical immunosensor on clinical serum. Sens. Actuators B, 222 (2016) 127.

[Yazdi et al., 2016] Yazdi, G.R. T. Iakimov, R. Yakimova, Epitaxial graphene on SiC: A review of growth and characterization. Crystals, 6 (2016) 53.

[Young, 2005] A. Young, Amylin and the integrated control of nutrient influx. Adv. Pharmacol., 52 (2005) 67.

[Yukird et al., 2017] J. Yukird, T. Wongtangprasert, R. Rangkupan, O. Chailapakul, T. Pisitkun, N. Rodthongkum, Label-free immunosensor based on graphene / polyaniline nanocomposite for neutrophil gelatinase-associated lipocalin detection. Biosens. Bioelectron., 87 (2017) 249.

[Zanato et al., 2017] N. Zanato, L. Talamini, T. R. Silva, I. Cruz Vieira, Microcystin-LR label-free immunosensor based on exfoliated graphite nanoplatelets and silver nanoparticles. Talanta, 175 (2017) 38.

[Zhang et al., 2010] J. Zhang, H. Yang, G. Shen, P. Cheng, J. Zhang, S. Guo, Reduction of graphene oxide via L-ascorbic acid. Chem.Com., 46 (2010) 1112.

[Zhang et al., 2017] L. Zhang, P. Song, H. Long, M. Meng, Y. Yin, R. Xi, Magnetism based electrochemical immunosensor for chiral separation of amlodipine. Sens. Actuators B, 248 (2017) 682.

[Zhu et al., 2010] Y. Zhu, S. Murali, W. Cai, X. Li, J. W. Suk, J. R. Potts, R.S. Ruoff, Graphene and graphene oxide: Synthesis, properties, and applications. Adv. Mat., 22 (2010) 3906.

[Zhu et al., 2010a] Y. Zhu, J.I. Son, Y.-B. Shim, Label-free detection of kanamycin based on the aptamer-functionalized conducting polymer / gold nanocomposite. Biosens. Bioelectron., 26 (2010) 1002.

8. GLOSSARY

-A-

AA: ascorbic acid

AcAc: acetoacetate

ACTH: adrenocorticotropin hormone

AFB1: aflatoxin B

AFP: α-fetoprotein

AgRP: agouti-related peptide

AMY: amylin

AP: alkaline phosphatase

APBA: aminophenylboronic acid

APN: adiponectin

ARC: arcuate nuclei

AuNPs: gold nanoparticles

AuSPE: screen-printed gold electrodes

AXL: receptor tyrosine kinase

-B-

BMI: body mass index

BNP: brain natriuretic peptide

BoNT-A: botulinum neurotoxin A

BR: billirubin

BSA: bovine serum albumin

-C-

CA 15 3: carbohydrate antigen 15 3

CART: cocaine and amphetamine-regulated transcript

CD 105: endoglyn

CEA: carcioembryonic antigen

CFU: colony forming units

Chit: chitosan

CHOL: cholesterol

CLK: cholecystokinin

CMC: carboxymethylcellulose

CnFSPE: carbon nanofibre screen printed electrode

CNTs: carbon nanotubes

COC: cocaine

COCs: combined oral contraceptives

CPs: conducting polymers

CR: creatinine

CSF: cerebrospinal fluid

cTnI: *cardiac t*roponin I

CV: cyclic voltammetry

-D-

da-GHRL: deacylated ghrelin

DENV: dengue virus

DMF: dimethylformamide

DPV: differential pulse voltammetry

D.R: dynamic range.

DRSP: 1,2-dihydrospirenone

dSPCE: double screen-printed carbon electrode

DWCNTs: double-walled carbon nanotubes

-E-

E2: β-estradiol

E3: estriol

EDC:N-ethyl-N´-(3-(dimethyl aminopropyl)carbodiimide

EE: ethynyl estradiol

EE2: ethynyl estradiol

EGFR: epidermal growth factor receptor (HER1)

EIA: enzyme immunoasay

EIS: electrochemical impedance spectroscopy

ELISA: enzyme linked immunosorbent assay

ERGO: electrochemical reduced graphene oxide

-F-

FSH: follicle-stimulating hormone

FSM8.0: mesoposrous silica

-G-

GA: glutaraldehyde

GAL-3: galectin-3

GCE: glassy carbon electrode

GCG: glucagon

GHRL: ghrelin

GHS-R: growth hormone secretagogue receptor

GO: graphene oxide

Gr: graphene

-H-

HBsAg: hepatitis B surface antigen

β-HB: beta hydroxybutyrate

β-HBDH: β-hydroyibutyrate dehydrogenase

hCG: human chorionic gonadotropin

hGH: human growth hormone

HMDA: hexamethylenediamine

HQ: hydroquinone

HRP: horseradish peroxidase

-I-

IAPP: isletamyloid polipeptide

IGF1: insulin-like growth factor 1

IL: ionic liquid

IL-1β: interleukin 1beta

IL-6; IL-8: interleukin 6 or 8

INS: insulin

ISPs: inflammation-sensitive plasma proteins

-L-

α-LA: a*lpha*-lactalbumin

β-LGB: beta lactoglobulin

LOD: limit of detection

LR: linear range

-M-

mB: methylene blue

MB: Meldola´s blue

MBs: magnetic microbeads

MC-LR: microcystin-LR

MCP-1: monocyte chemoattractant protein1

MES: 2-(N-morpholino)ethanesulfonic acid

MFE: mercury film electrode

MGCE: magnetic glassy carbon electrode

MPA: 3-mercaptopropionic acid

MUC4: mucin 4

-N-

NAD^+: nicotinamide adenine dinucleotide (oxidized)

NADH: nicotinamide adenine dinucleotide (reduced)

NBA: Nile blue A

Nf: Nafion

NGAL: neutrophil gelatinase-associated lipocalin

NHS: N-hydroxysuccinimide

NHSS: N-hidroxi-sulfo-succinimide

1-NP: 1-naphthylphenol

1-NPP: 1-naphthylphosphate

NPY: neuropeptide Y

-O-

OA: okadaic acid

OTA: ochratoxin A

OVA: ovoalbumin

-P-

p-ABA: p-aminobenzoic acid

p-APBA: p-aminophenylboronic acid

PANI: poly(aniline)

p-APP: p-amino phenyl phosphate

PBSE: 1- pyrenebutanoic acid succinimidyl ester

PCS: polycarbamoyl sulfonate

1,10-PD: 1,10-phenanthroline-5,6-diol

o-PD: o-phenylenediamine

p(1,5DAN): poly(1,5-diamino-naphthalene)

PBDE: polybrominated diphenyl ether

PEDOT: 3,4-poly(ethylene-dioxythiophene)

PEG: polyethylene glycol

Phe: phenyl

PMC: polymer-based composite

PNA: peanut agglutinin (lectin)

POMC: proopiomelanocortin

PP: pancreatic polypeptides

pPA: polypropionic acid

PPA: pyrrolepropionic acid

p(1,5-DAN): poly(1,5-diamino-naphtalene)

pPy: polypyrrole

pPyNW: polypyrrole nanowires

1,10-PQ: 1,10-phenanthroline quinone

PRL: prolactin

Prog: progesterone

pSA: porcine serum albumin

PSA: prostate specific antigen

PtNPs: platinum nanoparticles

PTC-NH_2: 3,4,9,10-perylene-tetra-carboxylicdianhydride

PYY: peptide YY

-Q-

QD: quantum dot

-R-

rGO: reduced graphene oxide

RSD: relative standard deviation.

-S-

S-amlod: S-amlodipine

SCAb: singlechain antibody

SHL: salicylate hydroxylase

SMN: survival motor neuron protein

SPCE: screen printed carbon electrode

SPIrCE: iridium-doped screen printed carbon electrode

SWCNTs: single walled carbon nanotubes

SWV: square wave voltammetry

-T-

T2D: type 2 diabetes

TCA: tricarboxylic acid

TEPA: tetraethylene pentamine

Test: testosterone

TGF-β1: transforming growth factor beta 1

THI: thionine

TMB: 3,3`,5,5`tetramethyl benzidine

TNF-α: tumor necrosis factor alpha

-U-

UA: uric acid

-W-

WHO: world health organization

9. PUBLICACIONES

The research work presented has given rise to the following publications:

1. G. Martínez-García, V. Serafín, L. Agüí, P.Yáñez-Sedeño, J.M.Pingarrón, Electrochemical immunosensor for the determination of total ghrelin hormone in saliva, ELECTROANALYSIS, 27 (2015) 1119-1126.

2. E. Sánchez-Tirado, G. Martínez-García, A. González-Cortés, P.Yáñez-Sedeño, J. M. Pingarrón, Electrochemical immunosensor for sensitive determination of transforming growth factor (TGF)- β1 in urine, BIOSENSORS AND BIOELECTRONICS, 88 (2017) 9 – 14.

3. S. Guerrero, G. Martínez-García, V. Serafín, L. Agüí, P.Yáñez-Sedeño, J.M.Pingarrón, Electrochemical immunosensor for sensitive determination of the anorexigen peptide YY at grafted reduced graphene oxide electrode platforms, ANALYST, 140 (2015) 7527-7533 (portada del volumen).

4. G. Martínez-García, L. Agüí, P.Yáñez-Sedeño, J. M. Pingarrón, Multiplexed electrochemical immunosensing of obesity-related hormones at grafted graphene-modified electrodes, ELECTROCHIMICA ACTA, 202 (2016) 209 – 215.

5. F. H. Cincotto, G. Martínez-García, P.Yáñez-Sedeño, T. C. Canevari, S. A. S. Machado, J. M. Pingarrón, Electrochemical immunosensor for ethinylestradiol using diazonium salt grafting onto silver nanoparticles-silica-graphene oxide hybrids, TALANTA, 147 (2016) 328 - 334.

6. G. Martínez-García, E. Pérez-Julián, L. Agüí, N. Cabré, J. Camps, P. Yáñez-Sedeño, J. M. Pingarrón, An electrochemical enzyme biosensor for 3-hydroxybutyrate detection based on screen-printed electrodes modified by reduced graphene oxide and thionine, BIOSENSORS**, 7 (2017) 50** doi:10.3390/bios7040050 (portada del volumen).

7. G. Martínez-García, E. Sánchez-Tirado, A. González-Cortés, P. Yáñez-Sedeño, J. M. Pingarrón, Electrochemical bioplatform using carboxylated porous polymer for determination of the obesity biomarker amylin, MICROCHIMICA ACTA, 185 (2018) 323

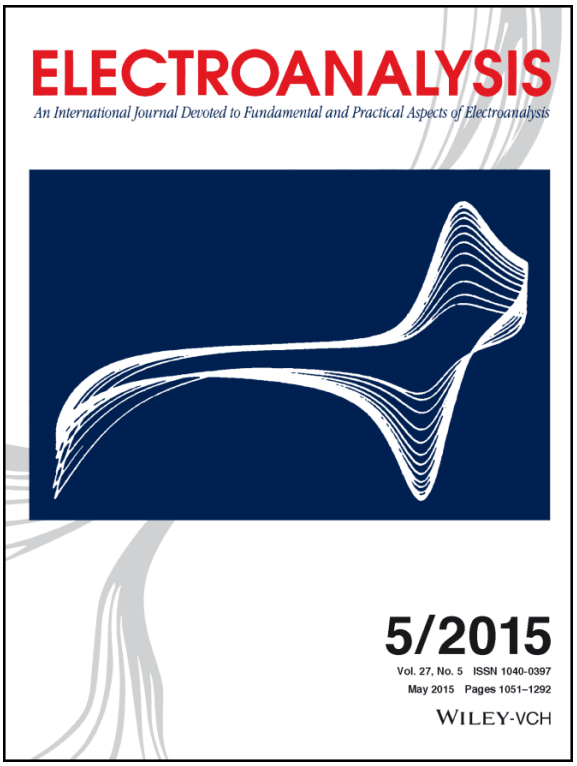

9.1. ELECTROCHEMICAL IMMUNOSENSOR FOR THE DETERMINATION OF TOTAL GHRELIN HORMONE IN SALIVA.

Full Paper Wiley Online Library ELECTROANALYSIS

DOI: 10.1002/elan.201400662

Electrochemical Immunosensor for the Determination of Total Ghrelin Hormone in Saliva

Gonzalo Martínez-García,[a] Verónica Serafín,[a] Lourdes Agüí,[a] Paloma Yáñez-Sedeño,*[a] and José M. Pingarrón[a]

Abstract: An electrochemical immunosensor for ghrelin (GHRL) determination in saliva is reported. Anti-GHRL was immobilized onto Protein G-magnetic beads and a competitive immunoassay involving biotinylated GHRL and alkaline phosphatase-streptavidin was implemented. Once conjugate was magnetically captured on a screen-printed carbon electrode, GHRL quantization was accomplished by DPV of 1-naphtol formed upon addition of 1-naphtyl phosphate. A linear range between 10^{-3} and 10^{3} ng/mL GHRL, and a *LOD* of 7 pg/mL, much smaller than those from commercial ELISA kits, were found. The usefulness of the immunosensor was demonstrated by analyzing human saliva spiked with GHRL at 0.01, 0.1, 1 and 10 ng/mL.

Keywords: Ghrelin · Immunosensor · Magnetic particles · Screen-printed electrodes · Saliva

1 Introduction

Ghrelin (GHRL) is a peptide hormone containing 28 amino acids discovered by Kojima in 1999 [1]. It is produced mainly in the stomach [2,3] and plays important roles in the gastrointestinal tract stimulating motor activity, gastric contractility and acid secretion [4,5]. GHRL participates in carbohydrates metabolism and has a direct effect on glucose levels via releasing growth hormone and stimulating glucogenesis [6]. Two forms, acylated and unacylated ghrelin, are present in blood serum [7], but only the acylated form binds with the receptor (GHSR-1a) to activate the release of growth hormone [8]. Normal levels of total GHRL in human serum are around few hundred pg/mL [9,10] with the deacylated form being clearly predominant [11]. The effects of ghrelin on food intake are thoroughly investigated [12]. It exhibits an orexigenic character, with increasing GHRL levels before meals to values that have been shown to stimulate appetite, and then decreasing [13,14]. It has also been observed an increase in GHRL plasma levels associated to anorexia nervosa, as well as lower levels in obese subjects [15]. Other important actions of GHRL affect neurological processes such as memory or learning [7].

Despite its importance, methods for determining GHRL are scarce. Various colorimetric ELISA kits using competitive or sandwich-type assays with anti-GHRL, biotinylated immunoreagents, and streptavidin labeled with peroxidase are commercially available, although discrepancies in GHRL quantification using these assays have been reported [16]. Most of them exhibit dynamic concentration ranges from 0.01 (or 0.1) to 100 (or 1000) ng/mL, with minimum detectable concentrations between 0.05 and 1 ng/mL. The assay time varies from 1 h 30 min to 4 h counting since the moment when the immobilization of the capture antibody occurred. Commonly, total GHRL is accomplished although some assays for individual acylated or deacylated hormone have also been described. For example, an enzyme immunometric assay (EIA) for acylated GHRL was developed using a sandwich configuration with an acetylcholinesterase FAb' conjugate and colorimetric detection using the Ellman's reagent [17]. An important drawback of this kind of determinations is that acylated GHRL is rapidly degraded by deacylation and proteolysis, so that samples must be treated by addition of protease inhibitors immediately after the collection, and the plasma samples must be acidified [8].

Concerning biosensors, Mascini et al developed a colorimetric microarray detection system for GHRL using aptamers technology, with a linear range between 0.2 and 245.5 ng/mL and a detection limit of 0.2 ng/mL [18]. The same authors developed an electrochemical aptasensor where the aptamer was adsorbed on the surface of a screen-printed electrode and measurement of the decrease in the guanine oxidation signal in the presence of GHRL. The linear range was from 14 to 100 ng/mL and the detection limit was 8 ng/mL [19].

In this paper, we describe the preparation of an electrochemical immunosensor for GHRL suitable to be applied for the direct determination of the hormone in saliva. It has been reported that GHRL is produced not only in the stomach but also in human salivary glands [4]. Interestingly, the GHRL concentration found in serum, urine and saliva has demonstrated to be equivalent [11] and, therefore, saliva can be considered as a suitable biological

[a] G. Martínez-García, V. Serafín, L. Agüí, P. Yáñez-Sedeño, J. M. Pingarrón
Department of Analytical Chemistry, Faculty of Chemistry, University Complutense of Madrid
28040-Madrid, Spain
*e-mail: yseo@quim.ucm.es

fluid for the diagnosis based on GHRL levels, with the advantage of the non-invasive collection protocol. The developed methodology makes use of protein G-functionalized magnetic microparticles as support for anti-GHRL immobilization. A competitive immunoassay involving Biotin-GHRL and streptavidin labeled with alkaline phosphatase (AP-Strept) was employed. The resulting conjugate was captured on the surface of a screen-printed carbon electrode with a small magnet and GHRL quantization was accomplished by differential pulse voltammetry of 1-naphtol formed upon addition of the AP substrate 1-naphtyl phosphate. The methodology allows measurements to be carried out with a small solution volume. Moreover, as the product of the enzyme reaction is generated close to the electrode surface, diffusion limitations of electroactive species are minimized, thus enabling low detection limits to be achieved.

2 Experimental

2.1 Reagents and Solutions

Ghrelin (GHRL, deacylated), Biotin-GHRL, and anti-GHRL (rabbit polyclonal-Ab) were from Anaspec. Solutions were prepared in 0.1 M phosphate (Scharlab) and 0.02 % Tween 20 buffer solution of pH 7.4 (B&W buffer). Streptavidin labeled with alkaline phosphatase (AP-Strept) and 1-naphtyl phosphate (1-NPP) were from Sigma. AP-Strept solutions were prepared in 0.1 M Tris (Scharlab) and 0.05 % Tween 20 buffer of pH 7.2 (Tris buffer). 1-NPP solutions were prepared in 0.05 M Tris and 10 mM $MgCl_2$ of pH 9.6 (Trizma buffer). Stock 1000 ng/mL and more diluted solutions of testosterone (Fluka, 99 %), progesterone (Aldrich, 98 %), human growth hormone (hGH, Sigma-Aldrich), prolactin (PRL, Sigma), and follicle stimulating hormone (FSH) in B&W buffer solution were also prepared and used for the study of interferences. Magnetic beads functionalized with protein G (Protein G-MBs, 30 mg/mL) were from Dynal Biotech ASA. Before use, Protein G-MBs suspensions were homogenized and, for each test, 1 μL (30 μg) was transferred to an eppendorf tube and washed twice with 50 μL of B&W buffer solution.

2.2 Samples

Saliva samples were collected from a volunteer using a Salivette collection device (Sarstedt). Briefly, the volunteer rinsed the mouth thoroughly with water and then inserted the cotton swab into the mouth and chewed for 1 min. Then, the swap saturated with saliva was inserted into de vial, sealed with the cap and centrifuged for 5 min at 5000 g.

2.3 Apparatus and Electrodes

All electrochemical measurements were carried out using a BAS 100 B potentiostat provided with BAS 100/W (Bioanalytical System) software for electrochemical analysis. Screen-printed carbon electrodes (SPCEs, DRP 110, 4 mm diameter) were from Drop Sens (Oviedo, Spain). They included a silver pseudo-reference electrode and a carbon counter electrode. A magnetic support for SPEs (Drop Sens), a P-Selecta ultrasonic bath, a Heidolph Reax Top homogenizer for small samples, a magnetic separator Dynal MPC-S (Dynal Biotech ASA) and a P-Selecta Digaterm 100 thermostated bath were also used.

2.4 Immunoassay Procedure

30 μg of previously washed Protein G-MBs were suspended in 10 μL of a 2 μg/mL anti-GHRL solution in an eppendorf tube,. After homogenization by gentle stirring in a vortex for 15 s, the tube was partially immersed in a thermostated bath and incubated 1 h at 37 °C under gentle stirring. Then, the tube was placed on the magnetic separator for 2 min. Once anti-GHRL-Protein G-MBs were deposited on the bottom of the tube the supernatant was removed and two washing steps, each with 50 μL of B&W buffer, were applied to the modified MBs. Each washing step consisted of a re-suspension of the MBs in the washing solution and gentle stirring for 1 min (up to homogenization) followed by separation with the magnet for 2 min to remove the solution. The competitive assay was implemented by re-suspension of the anti-GHRL-Protein G-MBs in 50 μL of 0.01 μg/mL Biotin-GHRL or Biotin-GHRL/target GHRL mixture solution. After 45 min incubation at 37 °C under gentle stirring, the tube was placed on the magnetic separator and four washing steps, twice with 100 μL of the B&W buffer and twice with 150 μL of Tris buffer solution, were applied. Thereafter, the conjugates were re-suspended in 50 μL of AP-Strept and incubated 30 min at 37 °C in the thermostated bath under gentle stirring. Subsequently, the AP-Strept-Biotin-GHRL-anti-GHRL-Protein G-MBs were washed twice with 150 μL Tris buffer solution, and twice with 200 μL of Trizma buffer, and 50 μL of the suspension were magnetically captured onto the surface of the SPCE. In order to do that in a reproducible way, the SPCE was kept horizontal in the magnetic support thus avoiding variations in the MBs-layer thickness or spreading area on the electrode surface between measurements. Then, 5 μL of a 0.05 M 1-NPP solution were deposited on the electrode and allowed to stand for 5 min in the darkness at room temperature. Thereafter, differential pulse voltammograms were recorded over the −0.15 to +0.70 V potential range.

2.5 Determination of GHRL in Saliva

The samples were prepared as described in Section the 2.2. 50-μL aliquots of centrifuged saliva were spiked with GHRL at the desired concentration and then 1 μL of the resulting solution was mixed with 3 μL of 1 μg/mL Biotin-GHRL. The mixture was diluted up to 300 μL with the B & W buffer and the procedure described in Section 2.4

was applied using 50 µL of such solution. GHRL determination was accomplished by interpolation of the measured DPV peak current values into the linear portion of the calibration plot constructed with GHRL standard solutions.

3 Results and Discussion

The biosensing approach used in this work is schematically illustrated in Figure 1. Oriented immobilization of anti-GHRL antibodies was accomplished onto Protein G-MBs due to the Protein G binding ability with the Fc region of antibodies. Subsequently, a competitive assay between target GHRL and Biotin-GHRL for the binding sites of the immobilized Abs was performed. After incubation with AP-Strept, the MBs bearing the immunoconjugates were captured magnetically on the surface of a SPCE and the determination of GHRL was carried out by recording differential pulse voltammograms for the 1-naphtol (1-NP) generated in the enzyme reaction with AP after addition of 1-naphtyl phosphate (1-NPP) as the substrate.

3.1 Optimization of the Experimental Variables

All variables concerning the preparation and the electrochemical performance of the immunosensor were optimized. The amount of Protein G-MBs used has an important influence regarding the possibility of immobilizing a large amount of the capture antibody without loss of sensitivity. The DPV peak current value showed a higher value when using 30 µg of Protein G-MBs (1 µL of the MBs suspension) than for 60 µg, probably as a consequence of the increase in the electron transfer resistance as increasing the amount of insulating material [20]. It is important to remark that, with the mentioned MBs loading, practically negligible unspecific voltammetric signals were observed in the absence of anti-GHRL. The effect of the antibody loading was evaluated by testing the response of immunosensors fabricated with 30 µg of Protein G-MBs and using 0.01 µg/mL Biotin-GHRL, 0.01 µg/mL GHRL and 1 µg/mL AP-Strept. This study was made by preparing the anti-GHRL-Protein G-MBs conjugates at 37 °C with 1 h incubation. Both temperature and incubation time were optimized by testing the response of different immunosensors prepared at 10, 25 and 37 °C, and

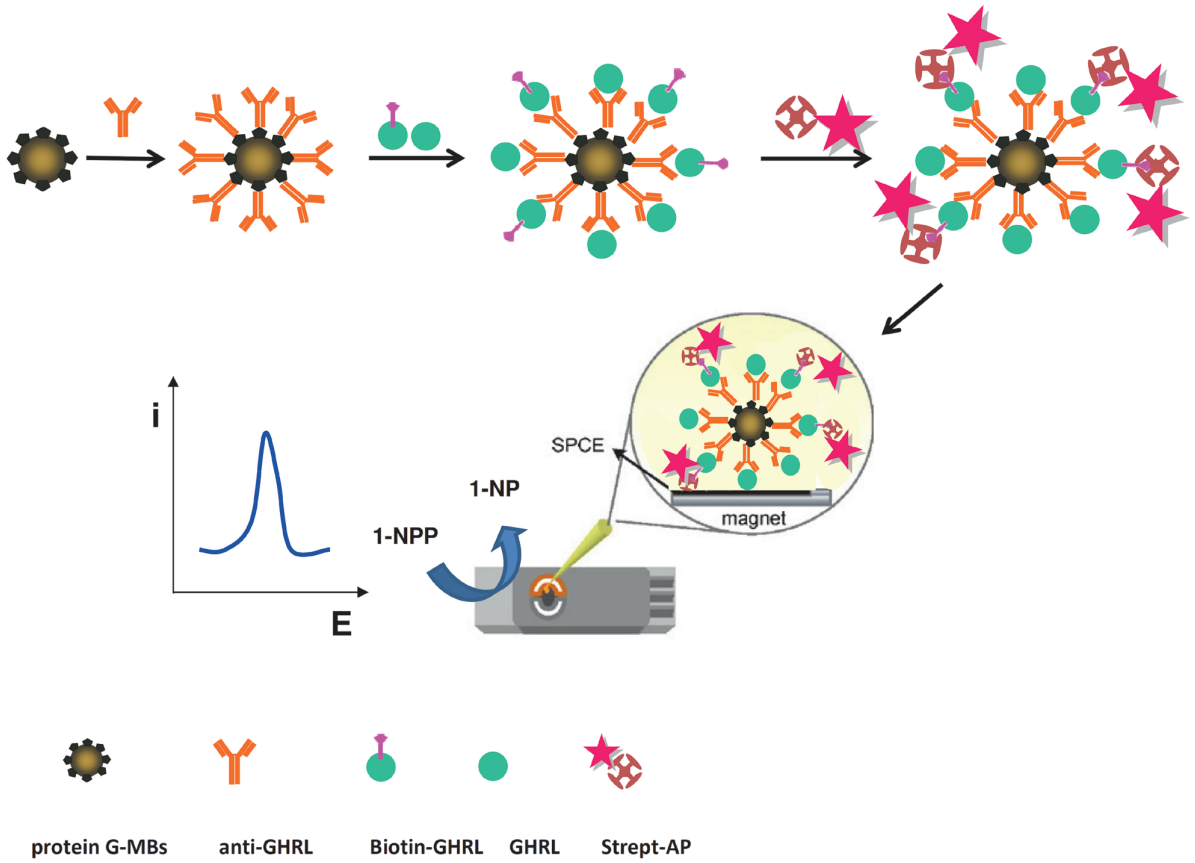

Fig. 1. Schematic display of the steps involved in the preparation and electrochemical transduction of an immunosensor for ghrelin using AP-Strept-Biotin-GHRL-anti-GHRL-Protein G-MBs immunoconjugates.

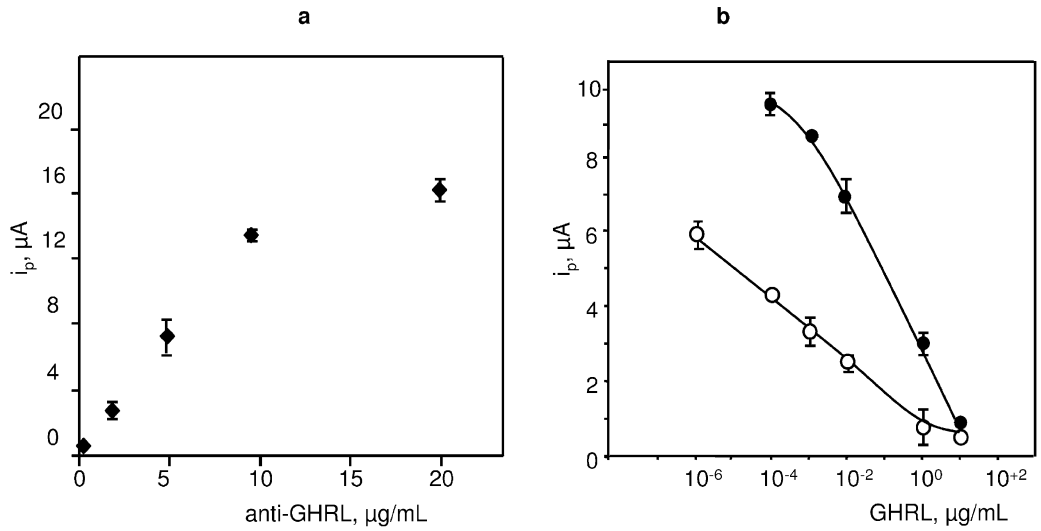

Fig. 2. Effect of the anti-GHRL loading onto protein G-MBs on the DPV peak current obtained for immunoassays performed with 30 µg of Protein G-MBs, 0.01 µg/mL Biotin-GHRL, 1 µg/mL AP-Strept and 0.01 µg/mL GHRL (a); 10^{-6}–10 µg/mL GHRL using 2 (○) or 5 (●) µg/mL anti-GHRL (b).

using incubation times between 10 and 90 min. Figure 2a shows as the measured peak current increased with the Ab loading and leveled off for approximately 20 µg/mL anti-GHRL indicating saturation of the functionalized microparticles. Taking into account that, theoretically, lower amounts of antibody should allow the achievement of a higher sensitivity because less analyte would be required to reach the plateau of maximal response [21,22], DPV peak currents were measured for different GHRL concentrations with two different immunosensors prepared with 2 or 5 µg/mL anti-GHRL (Figure 2b). As it can be observed, the immunosensor prepared with 5 µg/mL antibody exhibited larger peak current values for all the antigen concentrations tested and, accordingly, a larger slope value for the linear portion of the calibration plot covering a range of GHRL concentrations between 10^{-3} and 10 µg/mL. Conversely, the immunosensor prepared with 2 µg/mL anti-GHRL provided smaller currents and a lower slope but, in this case, the linear range extended from a GHRL concentration as low as 10^{-6} µg/mL. Such behavior makes the immunosensor prepared with the lower anti-GHRL concentration more suitable

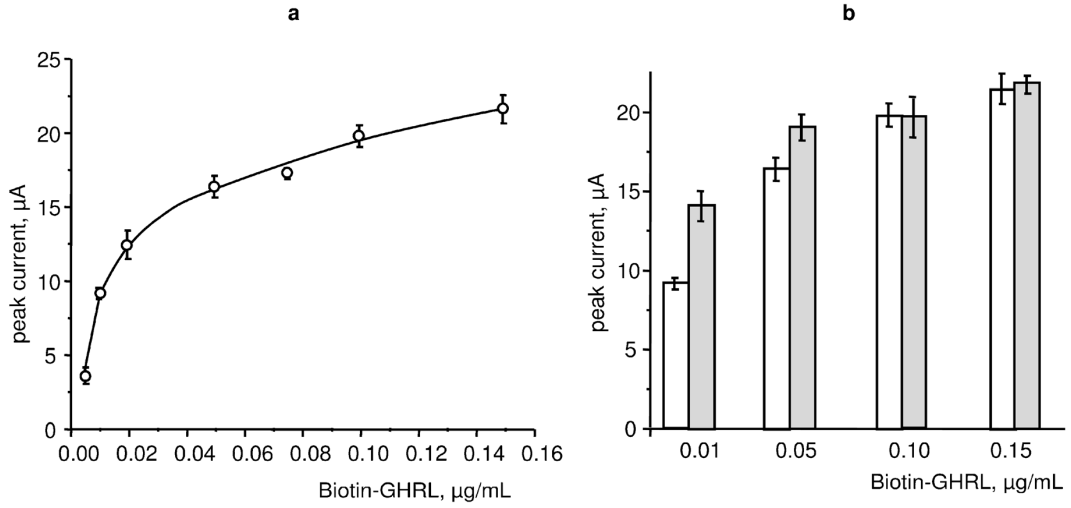

Fig. 3. Effect of the Biotin-GHRL concentration used in immunoassay on the DPV peak current measured with the anti-GHRL-Protein G-MBs immunosensor; 30 µg of Protein G-MBs; 5 µg/mL anti-GHRL; 0.01 µg/mL GHRL; 1 µg/mL AP-Strept (a). Peak current values measured in absence of GHRL (grey) and in the presence of 0.01 µg/mL GHRL (white) (b).

for the determination of GHRL in clinical samples, since, as it has been mentioned above, normal levels of the hormone are around few hundred pg/mL [9,10]. Using these experimental conditions, the incubation step was found to provide optimal results when it was carried out at 37 °C for 60 min (results not shown).

The Biotin-GHRL concentration used to perform competition was also optimized. Various AP-Strept-Biotin-GHRL-anti-GHRL-Protein G-MBs immuno-conjugates were prepared using different Biotin-GHRL solutions with concentrations in the 0.01–0.15 μg/mL range. As it can seen in Figure 3a the i_p values increased with the Biotin-GHRL concentration over the whole tested range, although the variation rate was faster for the lower concentrations and tended to level off at higher concentrations as expected due to the saturation of the antibody binding sites. Moreover, Figure 3b compares the peak current values measured with immunosensors in the presence of no target GHRL (grey columns) or 0.01 μg/mL GHRL (white columns). As it can be observed, the biggest difference between both voltammetric responses occurred for a 0.01 μg/mL conjugate concentration indicating a significant extent of the competition process. On the contrary, no significant differences were apparent for 0.10 or 0.15 μg/mL Biotin-GHRL concentrations. These results are in agreement with the expected behavior considering that larger conjugate concentration in solution would require larger antigen concentration for effective displacement in the competitive assay. According to these observations, a 0.01 μg/mL Biotin-GHRL was selected for further work. An incubation period of 45 min at 37 °C was shown to be appropriate to allow an adequate competition between GHRL and Biotin-GHRL for the binding positions of the antibody (results not shown).

The competitive assay was monitored using AP-Strept to be bound to Biotin-GHRL conjugate. The AP-Strept concentration was optimized by measuring the voltammetric responses recorded with different immunosensors incubated with AP-Strept in the 0.5 to 5.0 μg/mL range. Figure 4a displays the results obtained with no GHRL. As it can be seen, after an initial increase up to 1.0 μg/mL, the peak current remained practically constant for larger conjugate concentrations. Therefore, 1.0 μg/mL AP-Strept, which probably corresponded to saturation of the Biotin-GHRL, was selected. Moreover, Figure 4b compares the DPV peak currents measured in the absence of GHRL and in the presence of 0.01 μg/mL Biotin-GHRL for different incubation times with AP-Strept at 37 °C. An incubation period of 30 min was selected for this step.

Finally, the concentration of 1-NPP used as substrate in the AP enzyme reaction was that optimized previously, 5 mM, which was a sufficient excess to ensure that the enzyme reaction depended only on the AP concentration. The time allowing the enzyme reaction to proceed, 5 min, was also taken from the same previous work, whereas the reaction pH was 9.6 which corresponded to optimal AP activity [23].

3.2 Analytical Characteristics

Figure 5 shows the calibration plot constructed for GHRL under the optimized working conditions stated above. The GHRL concentration tested ranged between 10^{-5} and 10^{4} ng/mL. The i_p vs. GHRL concentration curve was fitted by non-linear regression using the Sigma Plot data analysis software. The adjusted equation ($r = 0.990$) was:

$$i_p = i_{min} + \frac{i_{max} - i_{min}}{1 + \left(\frac{x}{EC_{50}}\right)^{-h}}$$

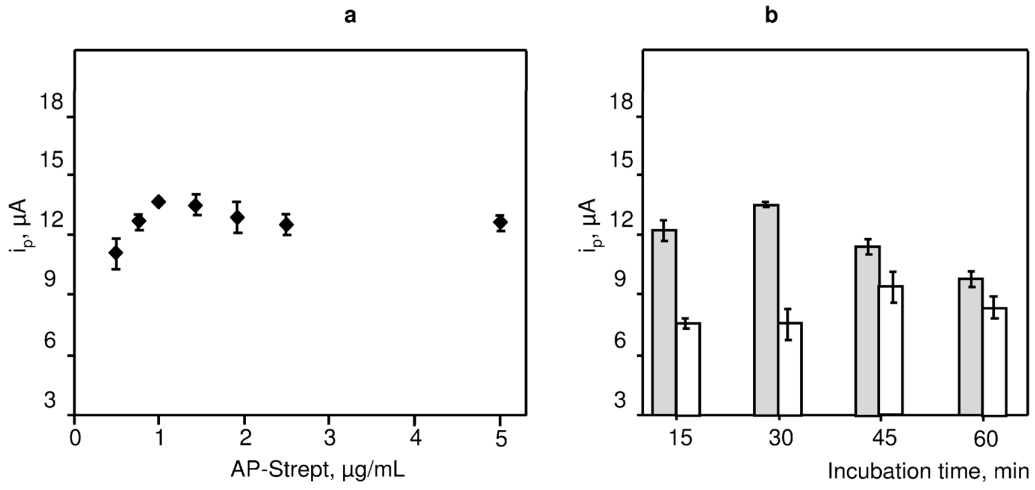

Fig. 4. (a) Influence of the AP-Strept concentration on the DPV peak current measured with the Biotin-GHRL-anti-GHRL-protein G-MBs immunosensor without GHRL; 30 μg of Protein G-MBs, 5 μg/mL anti-GHRL. (b) Effect of the incubation time with AP-Strept in the presence of 0.01 μg/mL GHRL (white) or in the absence of GHRL (grey) (b).

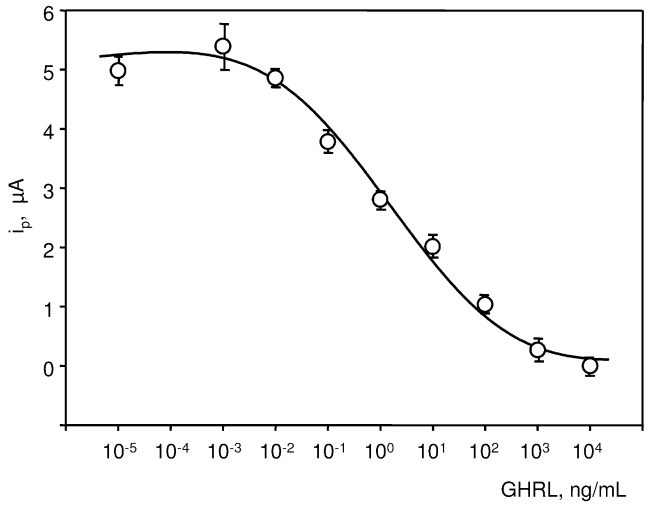

Fig. 5. Calibration plot constructed for GHRL with the AP-Strept-Biotin-GHRL-anti-GHRL-Protein G-MBs/SPCE.

where i_{max} and i_{min} were the maximum and minimum peak current values of the calibration graph: 5.4 ± 0.3 μA and 0.2 ± 0.4 μA, respectively. The EC_{50} value, which is the GHRL concentration corresponding to a fifty per cent competition, was 2.4 ± 1.5 ng/mL, and the Hill slope, h, at the inflection point of the sigmoid curve was −0.36 ± 0.08. The range of linearity (r = 0.994) was found to be between 10^{-3} and 10^{3} ng/mL which is adequate for the analysis of clinical samples [9,10].

The limit of detection was calculated according to the equation:

$$LOD = EC_{50}\left(\frac{i_{max} - i_{min}}{i_{max} - i_{min} - 3s} - 1\right)^{-1/h}$$

where s is the standard deviation (n = 7) of the zero value (the i_p value measured in the absence of GHRL), ± 0.24 μA. It is important to remark that the obtained value, 7 pg/mL, is much smaller than the *LOD* values reported for the commercially available ELISA kits (ranging between 7 and 140 times smaller), as well as with respect to the values obtained with the immunosensors described in the literature, 0.2 ng/mL [18] and 8 ng/mL [19]. The reproducibility of the DP voltammetric measurements was evaluated by carrying out assays with different immunosensors for solution containing a 1.0 ng/mL GHRL concentration level on the same day. A value of the relative standard deviation (*RSD*) of 4.1 % (n = 10) was obtained. Moreover, the storage stability of the AP-Strept-Biotin-GHRL-anti-GHRL-Protein G-MBs conjugates was also tested by preparing various immunoconjugates on the same day and storing them at 4 °C in eppendorf tubes containing Tris buffer. Then, everyday one immunoconjugate was magnetically captured onto the surface of a SPCE and the voltammetric response for 5 mM 1-NPP with no target GHRL was recorded. Figure 6 shows the corresponding control chart constructed by setting the mean value of ten measurements made on the first day of the set of experiments as the central value and the upper and lower control limits as ± 3s of this central value. As it can be observed, the obtained voltammetric responses remained within the control limits for at least ten days (largest storage time tested) thus indicating a good storage stability of the prepared immunoconjugates.

3.3 Selectivity

The selectivity of the magnetoimmunosensor toward GHRL was tested against other proteins such as testosterone (Test), progesterone (Prog), human growth hormone (hGH), prolactin (PRL) and follicle stimulating hormone (FSH). The DP voltammetric responses obtained with the AP-Strept-Biotin-GHRL-anti-GHRL-Protein G-MBs in the presence of 1 ng/mL of each potential interfering compound were compared with that obtained without GHRL. All voltammograms exhibited similar shapes, with peak current values within ± 4.7 %, to that recorded with no target analyte thus demonstrating a high selectivity of the developed immunosensor against other hormones.

3.4 Determination of GHRL in Saliva

The usefulness of the immunosensor for the analysis of real samples was demonstrated by analyzing human saliva from a healthy volunteer. Although it has been reported that GHRL can be present in saliva in a content of few hundred pg/mL [11], this concentration being clearly detectable by the immunosensor, no significant endogenous GHRL signals were found in the tested saliva. Therefore, saliva samples were spiked with the analyte at four different concentration levels, 0.01, 0.1, 1 and 10 ng/mL. The

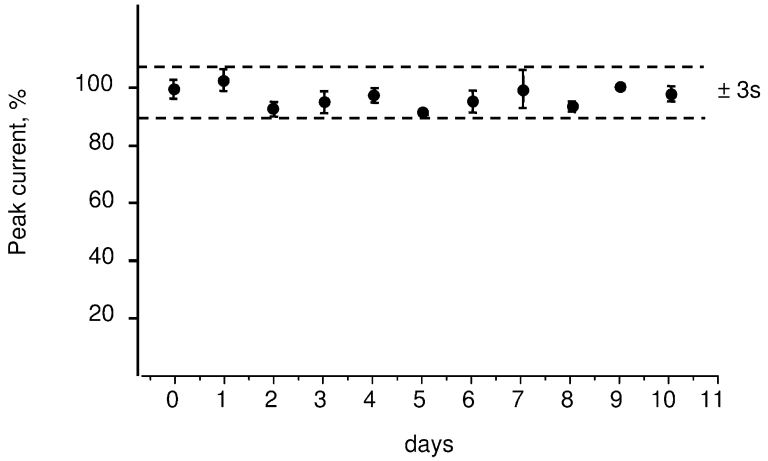

Fig. 6. Control chart constructed to check the storage stability of AP-Strept-Biotin-GHRL-anti-GHRL-Protein G-MBs conjugates upon storage at 4 °C in Tris buffer. The central value was set as the average DP voltammetric response for ten measurements of different 5 mM 1-NPP solutions containing no GHRL; upper and lower limits of control were set as ± three times the standard deviation of these measurements.

possibility of a matrix effect was evaluated by constructing a calibration plot in the linear range of GHRL concentrations from spiked saliva samples to which the procedures described in Sections 2.4 and 2.5 were applied. The slope value obtained, -0.96 ± 0.06, was not statistically different (by application of the Student t test) to that shown in Figure 5 from GHRL standard solutions, -0.95 ± 0.04 indicating that no matrix effect was apparent. Accordingly, the determination of GHRL could be carried out by interpolation of the voltammetric responses for the samples into the calibration plot constructed with GHRL standards. The obtained results are summarized in Table 1. As it can be observed, recovery values ranged between 95 % and 102 % demonstrating clearly the usefulness of the developed immunosensor for the determination of the hormone at low concentration levels in saliva with practically no sample treatment.

Table 1. Determination of GHRL in saliva with the AP-Strept-Biotin-GHRL-anti-GHRL-Protein G-MBs/SPCE immunosensor.

Sample	Added GHRL (ng/mL)	Found GHRL (ng/mL)	Mean recovery (%)
1	0.01	0.010 ± 0.001	100 ± 10
2	0.1	0.10 ± 0.01	102 ± 10
3	1	0.95 ± 0.01	95.3 ± 0.6
4	10	9.5 ± 0.2	95 ± 2

4 Conclusions

An electrochemical immunosensor for the determination of the hormone ghrelin has been implemented by coupling the advantageous characteristics of Protein G-functionalized magnetic beads for the specific antibody immobilization, a competitive immunoassay and differential pulse voltammetric transduction at disposable screen-printed carbon electrodes. The approach allows an improved sensitivity to be obtained with respect to commercially available ELISA kits and other immunosensors described in the literature as well as an excellent selectivity against other hormones. The developed immunosensor has been shown to be useful for the quantification of ghrelin in human saliva samples at low concentration levels thus representing an appropriate analytical tool for monitoring this hormone in relation with different important diseases.

Acknowledgements

Financial support from the *Spanish Ministerio de Economía y Competitividad* (Project CTQ 2012-35041) and *Comunidad de Madrid S2013/MIT-3029*, Programme NANOAVANSENS are gratefully acknowledged.

References

[1] M. Kojima, H. Hosoda, Y. Date, M. Nakazato, H. Matsuo, K. Kangawa, *Nature* **1999**, *402*, 656.
[2] Y. Date, M. Kojima, H. Hosoda, A. Sawaguchi, M. S. Mondal, T. Suganuma, S. Matsukura, K. Kangawa, M. Nakazato, *Endocrinology* **2000**, *141*, 4255.
[3] R. Peino, R. Baldelli, J. Rodriguez-Garcia, S. Rodriguez-Segade, M. Kojima, K. Kangawa, E. Arvat, E. Ghigo, C. Diéguez, F. F. Casanueva, *Eur. J. Endocrinol.* **2000**, *143*, R11.
[4] M. Gröschl, H. G. Topf, J. Bohlender, J. Zenk, S. Klussmann, J. Dötsch, W. Rascher, M. Rauh, *Clin. Chem.* **2005**, *51*, 997.
[5] Y. Masuda, T. Tanaka, N. Inomata, N. Ohnuma, S. Tanaka, Z. Itoh, H. Hosoda, M. Kojima, K. Kangawa, *Biochem. Biophys. Res. Commun.* **2000**, *276*, 905.
[6] F. Broglio, A. Benso, C. Gottero, F. Prodam, S. Grottoli, F. Tassone, M. Maccario, F. F. Casanueva, C. Diéguez, R. De-

ghenghi, E. Ghigo, E. Arvat, *Clin. Endocrinol.* **2002**, *57*, 265.
[7] J. E. Darling, E. P. Prybolsky, M. Sieburg, J. L. Hougland, *Anal. Biochem.* **2013**, *437*, 68.
[8] A. Trivedi, S. Babic, J.-P. Chanoine, *Clin. Biochem.* **2012**, *45*, 178.
[9] F. F. Casanueva, C. Diéguez, *Rev. Endocr. Metab. Disord.* **2002**, *3*, 325.
[10] K. Vörös, Z. Prohászka, E. Kaszás, A. Alliquander, A. Terebesy, F. Horváth, L. Janik, A. Sima, J. Forrai, K. Cseh, L. Kalabay, *Arch. Med. Res.* **2012**, *43*, 548.
[11] E. Taskin, B. Atli, M. Kiliç, Y. Sari, S. Aydin, *Pediatric Neurol.* **2014**, *51*, 365.
[12] A. M. Wren, C. J. Small, H. L. Ward, K. G. Murphy, C. L. Dakin, S. Taheri, A. R. Kennedy, G. H. Roberts, D. G. Morgan, M. A. Ghateis, S. R. Bloom, *Endocrinology* **2000**, *141*, 4325.
[13] M. Kojima, K. Kangawa, *Results Probl. Cell Differ.* **2008**, *46*, 89.
[14] D. Stevanovic, V. Trajkovic, S. Müller-Lühlhoff, E. Brandt, W. Abplanalp, C. Bumke-Vogt, B. Liehl, P. Wiedmer, K. Janjetovic, V. Starcevic, A. F. H. Pfeiffer, H. Al-Hasani, M. H. Tschöp, T. R. Castañeda, *Mol. Cell. Endocrinol.* **2013**, *381*, 280.
[15] V. Popovic, M. Svetel, M. Djurovic, S. Petrovic, M. Doknic, S. Pekic, D. Miljic, N. Milic, J. Glodic, C. Dieguez, F. F. Casanueva, V. Kostic, *Eur. J. Endocrinol.* **2004**, *151*, 451.
[16] M. Gröschl, M. Uhr, T. Kraus, *Clin. Chem.* **2004**, *50*, 457.
[17] C. Prudom, J. Liu, J. Patrie, B. D. Gaylinn, K. E. Foster-Schubert, D. E. Cummings, M. O. Thorner, H. M. Geysen, *J. Clin. Endocrinol. Metab.* **2010**, *95*, 2351.
[18] M. Mascini, G. G. Guilbault, S. J. Lebrun, D. Compagnone, *Anal. Lett.* **2007**, *40*, 1386.
[19] M. Mascini, K. Papamichael, I. Mevola, M. Pravda, G. G. Guilbault, *Anal. Lett.* **2007**, *40*, 403.
[20] M. Moreno-Guzmán, M. Eguílaz, S. Campuzano, A. González-Cortés, P. Yáñez-Sedeño, J. M. Pingarrón, *Analyst* **2010**, *135*, 1926.
[21] A. Ruth, *Best Pract. Res. Clin. Endocrinol. Metab.* **2001**, *15*, 1.
[22] M. Eguílaz, M. Moreno-Guzmán, S. Campuzano, A. González-Cortés, P. Yáñez-Sedeño, J. M. Pingarrón, *Biosens. Bioelectron.* **2010**, *26*, 517.
[23] S. Ito, S. Yamazaki, K. Kano, T. Ikeda, *Anal. Chim. Acta* **2000**, *424*, 57.

Received: November 5, 2014
Accepted: November 21, 2014
Published online: March 18, 2015

9.2. ELECTROCHEMICAL IMMUNOSENSOR FOR SENSITIVE DETERMINATION OF TRANSFORMING GROWTH FACTOR (TGF)- β1 IN URINE

Biosensors and Bioelectronics 88 (2017) 9–14

Contents lists available at ScienceDirect

Biosensors and Bioelectronics

journal homepage: www.elsevier.com/locate/bios

Electrochemical immunosensor for sensitive determination of transforming growth factor (TGF) - β1 in urine

E. Sánchez-Tirado, G. Martínez-García, A. González-Cortés, P. Yáñez-Sedeño *, J.M. Pingarrón

Department of Analytical Chemistry, Faculty of Chemistry, University Complutense of Madrid, 28040 Madrid, Spain

ARTICLE INFO

Article history:
Received 29 March 2016
Received in revised form
11 May 2016
Accepted 30 May 2016
Available online 31 May 2016

Keywords:
Transforming growth factor-β1 (TGF-β1)
Electrochemical immunosensor
Signal amplification
Urine

ABSTRACT

The first amperometric immunosensor for the quantification of TGF-β1, a cytokine proposed as a biomarker for patients having or at risk for renal disease, is described in this work. The immunosensor design involves disposable devices using carboxylic acid-functionalized magnetic microparticles supported onto screen-printed carbon electrodes and covalent immobilization of the specific antibody for TGF-β1 using Mix&Go polymer. A sandwich-type immunoassay was performed using biotin-anti-TGF and conjugation with peroxidase-labeled streptavidin (poly-HRP-Strept) polymer. Amperometric measurements were carried out at −0.20 V by adding hydrogen peroxide solution onto the electrode surface in the presence of hydroquinone as the redox mediator. The calibration plot allowed a range of linearity extending between 15 and 3000 pg/mL TGF-β1 which is adequate for the determination of the cytokine in plasma and urine. The limit of detection, 10 pg/mL, is notably improved with respect to those obtained with ELISA kits. The usefulness of the immunosensor for the determination of low TGF-β1 concentrations in real samples was evaluated by analyzing spiked urine at different pg/mL concentration levels.

1. Introduction

Cytokines are low molecular weight bioactive proteins produced by many different cells and strongly associated with the immune system (Stenken and Poschenrieder, 2015) (Liu et al., 2016). There is enormous clinical interest in cytokines determination as elevated concentrations of these proteins are associated with inflammation or disease progression and, therefore, various types of cytokines are widely used as biomarkers to characterize the immune function, predict diseases and monitor their evolution and treatments. These applications require the availability of highly sensitive analytical methods because cytokines appear into the extracellular milieu at pM concentration range.

The transforming growth factor-β (TGF-β) family is a collection of structurally related multi-functional cytokines which regulates a wide range of physiological and pathological processes. They are involved in cell-growth, rate of proliferation, differentiation and production of extracellular matrix proteins (Grainger et al., 2000). Three isoforms (TGF-β1, -β2, and -β3) are present in mammals with some differences in biological activities and also in their potencies. Particularly, TGF-β1 is involved in immune and inflammatory responses showing a hundred times more potent behavior as growth inhibitor of hematopoeitic stem cells than the others. This cytokine has been considered as a good biomarker of liver fibrosis (Fallatah, 2014) or bladder carcinoma (Eder et al., 1996). Increasing evidence also links TGF-β1 to the progression of renal fibrosis and scarring associated with diabetic nephropathy or hypertensive nephrosclerosis (Tsapenko et al., 2013) and glomerulonephritis (Grainger et al., 1995). TGF-β1 concentration levels between 0.1 and 25 ng/mL have been reported in plasma from healthy individuals (Grainger et al., 2000). The variability observed depends to some extent on the assay type used for the determination. Circulating levels of TGF-β1 increase in patients suffering various types of cancer in addition to the aforementioned kidney diseases, and are severely depressed in advanced atherosclerosis (Matharu et al., 2014).

Despite its importance, relatively few methods are available for the determination of this cytokine. Immunoassay strategies based on sandwich-type configurations with peroxidase-labeled or biotinylated anti-TGF-β1 as detection antibodies are employed in commercial ELISA colorimetric kits. These methods are valid for determining TGF-β1 in the range from several tens to thousands of pg/mL with minimum detectable concentrations that can drop to a few units of pg/mL. In the particular case of biosensors for TGF-β1 determination, only two configurations have been found in the literature. An aptasensor involving aptamer-modified Au electrodes integrated with microfluidics was reported. Thiolated aptamers labeled with methylene blue were self-assembled on gold

* Corresponding author.
E-mail address: yseo@quim.ucm.es (P. Yáñez-Sedeño).

http://dx.doi.org/10.1016/j.bios.2016.05.093
0956-5663/

surfaces. The linear range covered up to 250 ng/mL with a detection limit of 1 ng/mL. This device was used to monitor TGF-β1 release from hepatic cells (Matharu, et al., 2014). Very recently, an impedimetric immunosensor was developed for the determination of TGF-β1 in human serum. A self-assembled monolayer of polyethylene glycol (PEG) prepared onto interdigitated electrodes was used for the covalent immobilization of the antibodies. A linear impedance vs log [TGF-β1] range between 1 and 1000 ng/mL was found with a detection limit of 0.570 ng/mL (Yao et al., 2016). However, biosensors exhibiting higher sensitivity are needed to be applied to clinical samples containing very low TGF-β1 concentrations. For example, in urine this cytokine ranges typically between 10 and 50 pg/mL and it has been proposed as a biomarker for patients having or at risk for renal disease (Tsapenko et al., 2013) (Grainger et al., 1995) (Honkanen et al., 1997). Obviously, it is also mostly important the noninvasive nature of collecting urine sample and therefore its usefulness to be employed with point of care devices.

In this work, the first amperometric immunosensor for the quantification of TGF-β1 is described, with the objective of developing a sensitive, reliable, and robust analytical tool for the determination of this cytokine in complex clinical samples. The immunosensor implies a disposable device using carboxylic acid-functionalized magnetic microparticles supported onto screen-printed carbon electrodes. These magnetic beads have demonstrated to be powerful tools for the preparation of electrochemical immunosensors enabling minimization of matrix effects in the analysis of complex samples (Zacco et al., 2006), (Ruiz-Valdepeñas Montiel et al., 2015). Covalent immobilization of the specific antibody for TGF-β1 (anti-TGF) was performed using Mix&Go, a polymer containing several metallic complexes selected for their efficiency to bind proteins (Ojeda et al., 2015). A sandwich-type immunoassay was designed using biotin-anti-TGF, and conjugation with peroxidase-labeled streptavidin (poly-HRP-Strept) polymer was used as to amplify the electrochemical detection. Amperometric measurements were performed by adding hydrogen peroxide solution onto the electrode surface in the presence of hydroquinone as the redox mediator. The analytical usefulness of the immunosensor was demonstrated by application to urine samples containing different TGF-β1 concentrations at the pg/mL level.

2. Experimental

2.1. Reagents and solutions

Human TGF–β1, mouse capture antibody (anti-TGF), and chicken biotinylated antibody (Biotin-anti-TGF) were from R&D Systems and included in the DuoSet® ELISA Development System (DY240-05). Horseradish peroxidase-labeled streptavidin (HRP-Strept) (Roche), poly-HRP-Strept (85-R200) (Fitzgerald), carboxylic acid-functionalized magnetic beads (HOOC-MBs) (Dynabeads® M–270 Carboxylic Acid, 2.8 μm diameter, 30 mg/mL), and Mix&Go™ polymer from Anteo Diagnostics, were also used. Buffer solutions used were: 0.1 M phosphate buffer solution of pH 8.0 and 0.05 M phosphate buffer solution of pH 6.0 prepared from Na_2HPO_4 and NaH_2PO_4; saline phosphate buffer of pH 7.2 (PBS) containing 8.1 mM Na_2HPO_4, 1.5 mM KH_2PO_4, 137 mM NaCl, and 2.7 mM KCl; washing buffer solution (WBS) prepared from the latter PBS by dissolving 0.05% Tween 20; 25 mM MES buffer solution of pH 5.0 prepared from *2*–(*N*–morpholine) ethanosulfonic acid (Gerbu). Hydrogen peroxide (Aldrich, 30% (w/w) and hydroquinone (Sigma) were also used. 2 M ethanolamine (Sigma) prepared in 0.1 M phosphate buffer solution of pH 8.0 was used as blocking solution. Ascorbic acid (AA) (Fluka), uric acid (UA) and creatinine (CR) (Sigma), adiponectin (APN), interleukin 6 (IL–6) and interleukin 8 (IL–8) (Abcam), and tumor necrosis factor alpha (TNF–α) (BD Pharmingen) were tested as potential interferents. Deionized water was obtained from a Millipore Milli-Q purification system (18.2 M Ω cm at 25 °C).

2.2. Apparatus and electrodes

Amperometric measurements were performed using an INBEA potentiostat provided by the IbGraph software. Screen-printed carbon electrodes (SPCEs, 110 DRP, ϕ 4 mm) from DropSens (Oviedo, Spain) were used as working electrodes. These electrodes are provided with a silver pseudo-reference electrode and a carbon counter electrode. Incubation steps were performed at 25 °C using an Optic Ivymen System constant temperature incubator shaker (Comecta S. A.) and pH measurements were made using a Crison Basic 20+ pHmeter. A P-Selecta ultrasonic bath, a magnetic separator (DynaMagn®, Invitrogen Dynal), and a Vortex homogenizator from Heidolph were also used. All experiments were performed at room temperature.

2.3. Procedures

2.3.1. Preparation of the poly-HRP-Strept/Biotin-anti-TGF/TGF-β1/anti-TGF-MBs-conjugates

3 μL of the commercial HOOC-MBs suspension were transferred into a 1.5 mL Eppendorf tube and washed twice with 50 μL of MES buffer solution at 25 °C. Each washing step consisted of a re-suspension of the functionalized MBs in the buffer solution and stirring at 600 rpm for 10 min (up to homogenization) followed by magnetic separation for 4 min and removal of the solution. Next, 25 μL of Mix&Go were added and incubated for 60 min at 25 °C under stirring at 600 rpm. Thereafter, two washing steps with WBS were carried out and, further, 25 μL of a 5 μg/mL anti–TGF solution prepared in 25 mM MES buffer solution of pH 5.0 were added, allowing incubation for 60 min at 25 °C under stirring at 600 rpm. Then, the immunoconjugates were washed firstly with 50 μL of 25 mM MES buffer solution of pH 5.0 and, secondly, with 50 μL of 100 mM PBS of pH 8.0. Next, a blocking step by incubation of the anti–TGF-MBs conjugate with 50 μL of 2 M ethanolamine solution prepared in 0.1 M PBS of pH 8.0 was applied for 1 h. Thereafter, the excess of ethanolamine was removed by washing successively with 50 μL of the same PBS buffer and with 50 μL of the WBS. Bioconjugation of the target cytokine was carried out by adding 25 μL of a TGF-β1 standard solution or the sample and incubating for 60 min at 25 °C. Two washings with 50 μL WBS were performed and 25 μL of a 2 μg/mL Biotin–anti–TGF-β1 solution containing 1% BSA were added and incubated for 60 min at 25 °C under stirring at 600 rpm. Then, two washing steps with 50 μL WBS were applied followed by the addition of 25 μL of 1/500 diluted poly–HRP–Strept in PBS, and incubation for 20 min. Finally, two more washing steps with 50 μL WBS were applied. All buffer solutions used were those recommended by the supplier of DuoSet® ELISA Development System (DY240–05).

2.3.2. Determination of TGF-β1

The as prepared poly-HRP-Strept/Biotin-anti-TGF/TGF-β1/anti-TGF-MBs were re-suspended in 45 μL of 1 mM hydroquinone and transferred onto the surface of the SPCE. This was done by keeping the SPCE horizontal and placing a neodymium magnet on the bottom part of the electrode to locate in a reproducible way the biofunctionalized MBs onto the working electrode surface area. A detection potential of −200 mV was applied and the background current was recorded until stabilization (100 s approximately). Further, a 5 μL aliquot of 50 mM hydrogen peroxide solution was added and, after a period of 200 s for the enzymatic reaction to

take place, the reduction current of the formed quinone was measured.

2.3.3. Analysis of spiked urine

The procedure described above was applied to urine samples which were spiked with TGF-β1 at final concentrations of 25, 45 or 100 pg/mL. No pretreatment was required except a 1:3 dilution with 0.1 M PBS of pH 7.2. The determination of TGF-β1 was carried out by interpolation of the amperometric responses for the samples into the calibration plot constructed with TGF-β1 standards.

3. Results and discussion

Fig. 1 shows schematically the different steps involved in the preparation and functioning of the poly-HRP-Strept/Biotin-anti-TGF/TGF-β1/anti-TGF-MBs/SPCE immunosensor. Covalent immobilization of capture antibodies onto carboxylic acid-functionalized magnetic microparticles (step 1) was carried out by using the polymer Mix&Go. This polymer uses ligands to bind Fc domains that mimic those binding domains from proteins A and G (Ooi et al., 2014), and can also interact strongly with electron donating moieties such as dissociated carboxyl groups. Therefore, combination of HOOC-MBs with the use of Mix&Go for antibody immobilization resulted in a convenient methodology to be applied as a general route for the preparation of electrochemical immunosensors (Ojeda et al., 2015). Capture antibodies immobilization was followed by a blocking step with ethanolamine (step 2) and the implementation of a sandwich-type immunoassay employing a biotinylated secondary antibody and poly-HRP-Strept for signal amplification (step 3). The use of poly-HRP-Strept instead of conventional HRP-Strept conjugate has demonstrated to be advantageous for the design of sensitive electrochemical immunosensors as multiple HRP molecules are available to biocatalyze H_2O_2 reduction (Ojeda et al., 2014). Once the MBs bearing the immuno-conjugates were transferred to the surface of SPCE, hydrogen peroxide was added (step 4) and the amperometric response at −200 mV in the presence of hydroquinone was measured according to the reactions displayed in Fig. 1.

3.1. Optimization of the experimental variables involved in the preparation of the immunosensor

The effect of the different variables involved in the preparation of the TGF-β1 immunosensor on the corresponding analytical responses was studied. The amount of Mix&Go used was that optimized previously in our group (Ojeda et al., 2015) and, in these studies, conventional HRP-Strep was used to label the detection antibody since the effect of the other variables should not depend on the type of label employed.

The anti-TGF loading on the carboxylic acid-functionalized MBs was optimized by measuring the specific and unspecific responses (without sandwiched antigen) with antibody concentrations ranging between 2.5 and 20 μg/mL. Fig. 2(a) shows as the largest specific-to-unspecific current ratio was obtained for a 5 μg/mL antibody concentration. Higher concentrations produced a significant decrease of the specific response most likely due to hindering of the electrochemical reaction in the presence of a large biomolecule loading. Accordingly, such a concentration was selected to construct the immunosensor. Optimization of the incubation time for this step (results not shown) led us to select 60 min for the covalent binding of the antibody.

Ethanolamine was chosen as the blocking agent to minimize unspecific adsorptions onto HOOC-MBs after anti-TGF binding due to its proved efficiency for this purpose (Ojeda et al., 2014). In order to optimize this blocking step, 1 and 2 M ethanolamine solutions and different incubation times over 30–90 min range were tested. Fig. 2(b) and (c) show as an effective blocking was reached using a 2 M ethanolamine solution for 60 min. Under these conditions, the current due to unspecific adsorption was less than 25% than that measured for such a low TGF-β1 concentration as 125 pg/mL.

The Biotin-anti-TGF concentration was also optimized by testing the electrochemical responses measured with different

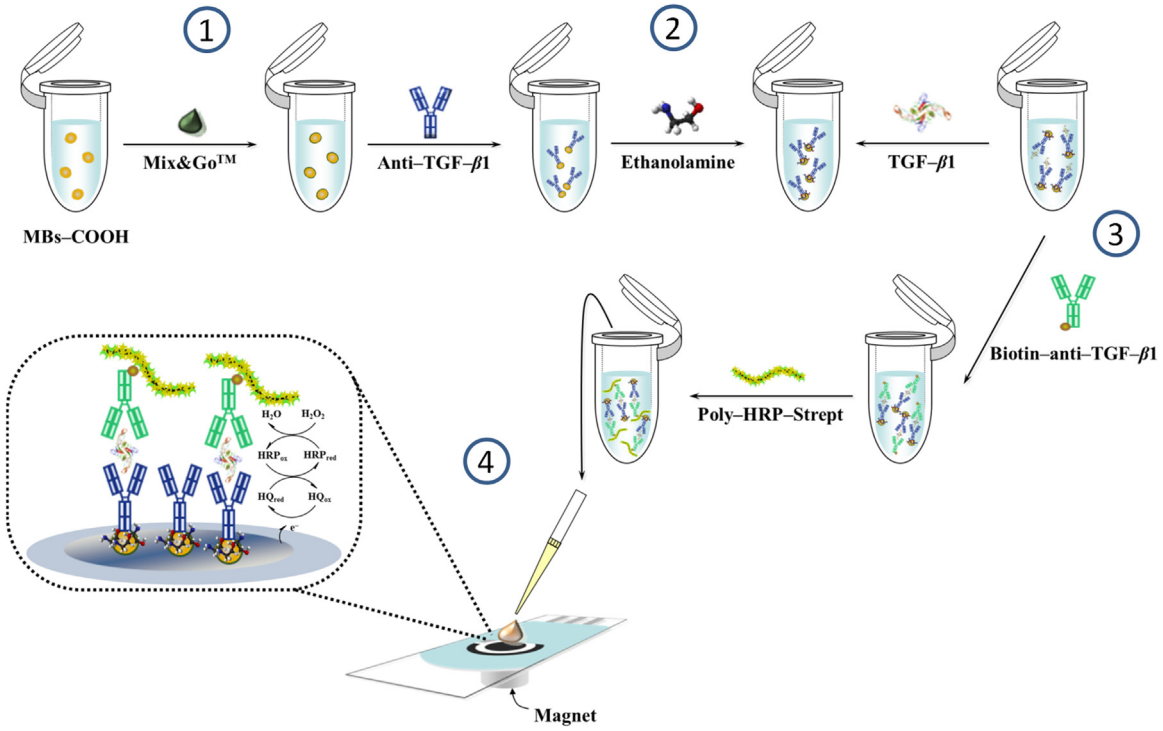

Fig. 1. Schematic display of the different steps involved in the preparation of the amperometric immunosensor for TGF-β1.

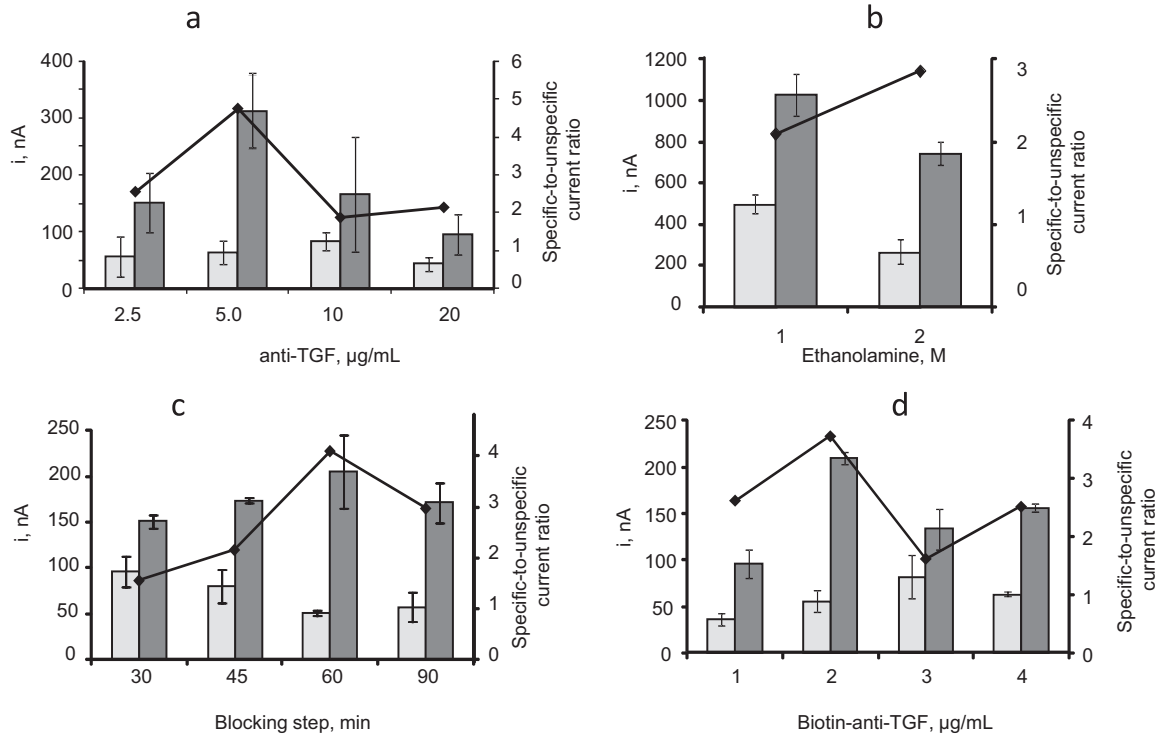

Fig. 2. Effect of the anti-TGF loading (a), the blocking agent concentration (b), the incubation time in the blocking step (c) and the concentration of Biotin-anti-TGF (d) on the amperometric response obtained with the TGF-β1immunosensor. 3 µL HOOC-MBs; 25 µL Mix&Go, 60 min; (a) 2.5–20 µg/mL anti-TGF, 60 min; 50 µL 1 M ethanolamine, 90 min; 25 µL 2 µg/mL Biotin–anti–TGF, 60 min; 25 µL 1/2000 dilution HRP-Strept; 20 min; (b) 5 µg/mL anti-TGF, 60 min; 50 µL 1 or 2 M ethanolamine, 90 min; (c) 50 µL 1 M ethanolamine, 30–90 min; 25 µL 2 µg/mL Biotin–anti–TGF, 60 min; 25 µL 1/2000 dilution HRP-Strept, 20 min; (d) 5 µg/mL anti-TGF, 60 min; 50 µL 1 M ethanolamine, 60 min; 25 µL 1–4 µg/mL Biotin-anti-TGF, 60 min; 25 µL 1/2000 dilution HRP-Strept, 20 min 25 µL 125 pg/mL TGF-β1 (dark grey) and 0 pg/mL TGF-β1 (light grey), 60 min; $E_{app} = -200$ mV. See the text for more information. Triplicate measurements with error bars at ± s values.

immunosensors prepared with conjugate loadings over the 1-4 µg/mL range. Results obtained (Fig. 2(d)) showed an increase in the amperometric response with increasing the Biotin-anti-TGF concentration between 1 and 2 µg/mL. Larger concentrations produced smaller and rather similar responses suggesting saturation of the antibodies binding sites. Accordingly, 2 µg/mL was

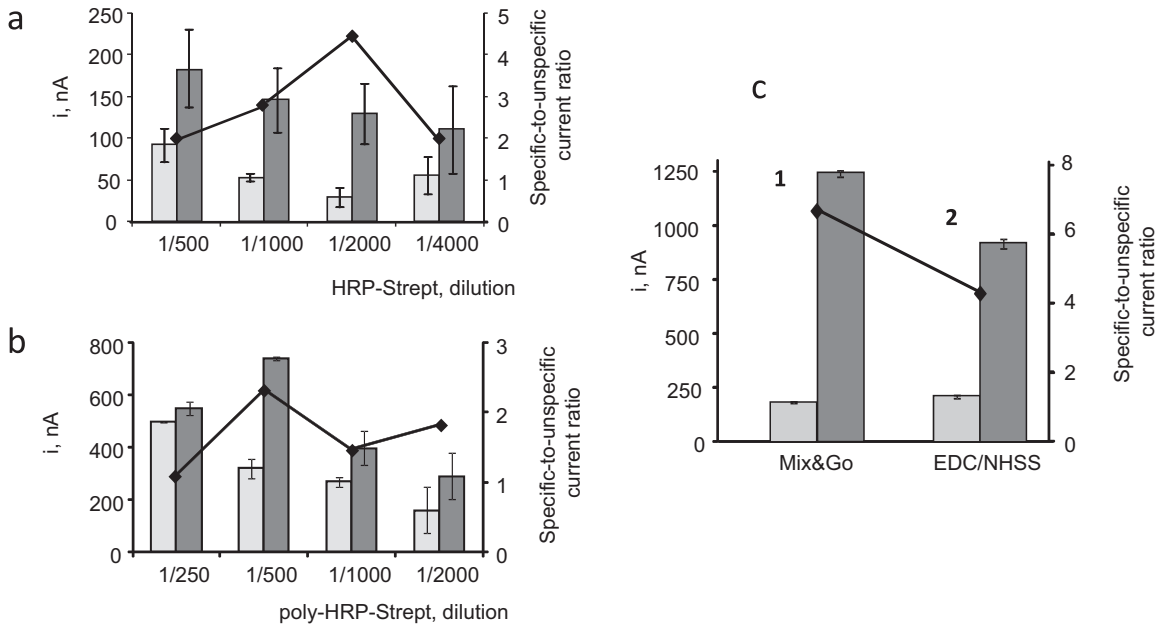

Fig. 3. Comparative responses of the TGF-β1 immunosensor when different loadings of HRP-Strept (a) and poly-HRP-Strept (b) were used to label the biotinylated anti-TGF detection antibody: 25 µL 125 pg/mL TGF-β1 (dark grey) or 0 pg/mL TGF-β1 (light grey), 60 min; 25 µL HRP-Strept, 20 min (a); 25 µL 60 pg/mL TGF–β1 (dark grey) or 0 pg/mL TGF-β1 (light grey), 60 min; 25 µL poly. HRP-Strept, 20 min (b); 3 µL HOOC-MBs; 25 µL Mix&Go, 60 min; 25 µL 5 µg/mL anti-TGF, 60 min; 50 µL 1 M ethanolamine, 90 min; 25 µL 2 µg/mL Biotin-anti-TGF, 60 min (c) amperometric currents for 25 µL of 125 pg/mL (dark grey) or 0 (light grey) TGF–β1, 60 min, measured with immunosensors prepared by covalent immobilization of anti-TGF onto HOOC-MBs using Mix&Go (1) or by activation with EDC/NHSS (2). 3 µL HOOC-MBs; 25 µL Mix&Go, 60 min or 25 µL 25 mg/mL EDC/NHSS, 60 min; 50 µL 2 M ethanolamine, 60 min; 25 µL 2 µg/mL Biotin–anti–TGF–β1, 60 min; 25 µL, 1/500 poly–HRP–Strept, 20 min; $E_{app} = -200$ mV. See the text for more information. Results for triplicate analysis with error bars at ± s values.

chosen as the optimal conjugate concentration. Regarding the incubation time for this step (results not shown), a period of 60 min was shown be enough to allow binding of all biotinylated antibodies to TGF-β1 antigen.

In order to get the highest possible sensitivity to achieve the goal mentioned in the Introduction for this work, an electrochemical signal amplification strategy was implemented by labeling the detection antibody with a peroxidase-streptavidin polymer instead of conventional HRP-Strept. This strategy has demonstrated to enhance sensitivity in the preparation of electrochemical immunosensors since multiple HRP molecules are available to be used in the biocatalysis of the enzyme substrate (Ojeda et al., 2014). The foreseen amplification effect provoked by the use of poly-HRP-Strept was confirmed by comparing the responses obtained with both conjugates. Fig. 3(a) shows the results when HRP-Strept was employed with dilution factors ranging from 1/500 to 1/4000. The specific response for a TGF-β1 concentration of 125 pg/mL slightly decreased when the conjugate concentration was lower while the best specific-to-unspecific current ratio was obtained for a 1/2000 HRP-Strept dilution. When poly-HRP-Strept was employed, a remarkable larger current was measured (Fig. 3(b)) for a TGF-β1 concentration of 60 pg/mL, thus demonstrating the achieved amplification in the electrochemical response. In this case, the largest specific-to-unspecific current ratio occurred for a 1/500 dilution factor and, as it could be expected, it was significantly smaller than that occurring with HRP-Strept. In both cases, an incubation time of 20 min was enough for binding with the biotinylated secondary antibody.

As commented above, the strategy for binding capture antibodies to carboxylic acid-functionalized MBs implied the use of the Mix&Go polymer. This was claimed as an efficient strategy for the stable and oriented binding of antibodies (Ojeda et al., 2015) and, in this case, it was demonstrated by comparing the immunosensor response when anti-TGF antibodies were covalently immobilized using Mix&Go, with that obtained when conventional EDC/NHSS chemistry was employed for the antibody binding. As Fig. 3(c) shows, a remarkably enhanced specific-to-background current was apparent when anti-TGF was immobilized using Mix&Go, probably as a consequence of the suitable orientation of the antibody provided by this polymer.

3.2. Analytical characteristics of the immunosensor

Fig. 4 shows the calibration plot for TGF-β1 constructed with the developed immunosensor under the optimized working conditions. Error bars were calculated from measurements carried out with three different immunosensors in each case. The steady state current vs. logarithm of TGF-β1 concentration followed the adjusted equation $I(nA) = 978 \log C(pg/mL) - 734$ ($r^2 = 0.991$), with a range of linearity extending between 15 and 3000 pg/mL TGF-β1. This range covers more than two orders of magnitude and it is adequate for the determination of the cytokine in real samples taking into account the expected concentrations, at ng/mL level in plasma (Grainger et al., 1995), or tens of pg/mL in urine (Tsapenko et al., 2013). The limit of detection, 10 pg/mL, was calculated by applying the 3 s_b criterion, where s_b was estimated as the standard deviation in concentration units (n = 10) of measured blank currents (0 ng/mL TGF-β1). The analytical characteristics achieved with the proposed immunosensor improve notably those reported for the commercial ELISA kits. For example, RayBio® Human TGF-beta1 ELISA kit (ELH-TGFb1) claims (⟨www.raybiotech.com/files/manual/ELISA/ELH-TGFb1.pdf⟩) for a minimun detectable dose (analyte concentration resulting in an absorbance equal to 2 s higher than that of the blank) of 80 pg/mL, which is eight times higher than that achieved in this work. The immunosensor exhibits also remarkably higher sensitivity than that reported for both the aptasensor (LOD of 1 ng/mL) (Honkanen et al., 1997) and the impedimetric imunosensor (LOD = 0.570 ng/mL) (Yao et al., 2016).

The reproducibility of the amperometric responses obtained with different immunosensors was evaluated. Sets of immunosensors were prepared on the same day and on different days using a new anti-TGF-MBs/SPCE in each case. The relative standard deviation (RSD) (n = 5) values were 2.9% and 3.9% for the assays performed on the same day in the absence and in the presence of 250 pg/mL TGF-β1, respectively, whereas RSD (n = 5) values were 3.7% and 4.2%, respectively, for the measurements made on different days. These results revealed the good level of precision achieved in the fabrication and functioning of the proposed immunosensing platform. Moreover, the storage ability of anti-TGF-MBs/SPCE conjugates was also tested. Different anti-TGF-MBs/SPCE were prepared on the same day, stored under humidity conditions at 4 °C, and employed to prepare immunosensors to measure 250 pg/mL TGF-β1 on different days. The results obtained (not shown) indicated that the immunosensor responses remained within the control limits, located at ± 3 s, were s was the standard deviation of the measurements (n = 10) carried out on the first working day, for at least 30 days (no longer storage times were tested) demonstrating the good stability of the anti-TGF-MBs/SPCE conjugates.

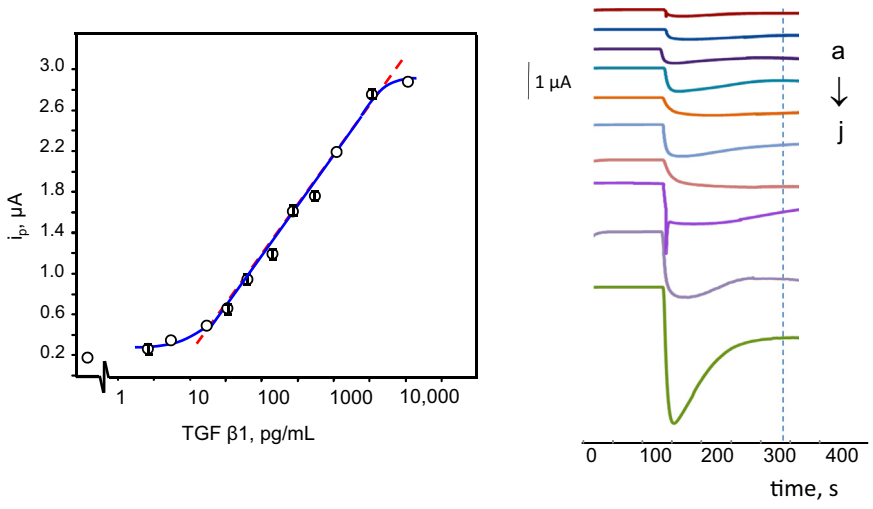

Fig. 4. Calibration plot construted for TGF-β1 by amperometry at the poly-HRP-Strept/Biotin-anti-TGF/TGF-β1/anti-TGF-MBs/SPCE immunosensor. Amperograms recorded for a) 0; b) 2.5; c) 15; d) 30; e) 60; f) 125; g) 250; h) 500; i) 1000; j) 3000 pg/mL TGF-β1. Dotted line indicates the time of measurement.

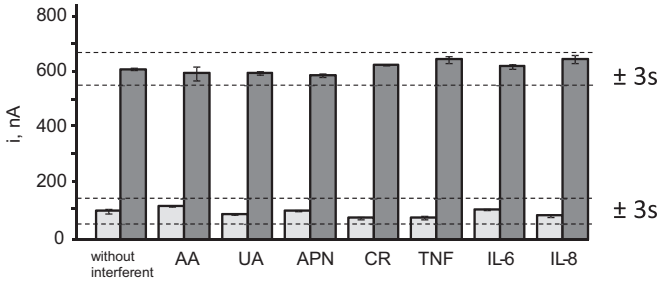

Fig. 5. Amperometric responses measured with the poly-HRP-Strept/Biotin-anti-TGF/TGF-β1/anti-TGF-MBs/SPCE immunosensor for 0 (light grey) and 25 pg/mL TGF-β1 (dark grey) in the presence of 370 μg/mL ascorbic acid (AA), 50 μg/mL uric acid (AU), 200 pg/mL adiponectin (APN), 10 pg/mL creatinine (CR), 200 pg/mL tumor necrosis factor alpha (TNF), 500 pg/mL interleukin 6 (IL-6), and 10 ng/mL interleukin 8 (IL-8).

Table 1
Determination of TGF-β1 in spiked urine with the poly-HRP-Strept/Biotin-anti-TGF/TGF-β1/anti-TGF-MBs/SPCE immunosensor.

TGF-β1, pg/mL	TGF-β1found, pg/mL	Recovery, %
25	25.9 ± 0.5	103 ± 8
45	44.9 ± 0.3	100 ± 3
100	96 ± 1	97 ± 5

The used antibody also exhibited a great selectivity against other proteins. Fig. 5 displays the immunosensor responses in the absence and in the presence of 25 pg/mL TGF-β1, and in the presence of ascorbic acid (AA), uric acid (UA), adiponectin (APN), creatinine (CR), tumor necrosis factor alpha (TNF), interleukin 6 (IL-6) or interleukin 8 (IL-8) at the expected concentrations in healthy patients. As it is clearly seen, no significant differences were apparent in any case. Interestingly, due to the detection potential value used, no interference from electroactive substances such as ascorbic and uric acids was observed.

3.3. Determination of TGF-β1 in spiked urine

The usefulness of the immunosensor for the determination of low TGF-β1 concentrations in real samples was evaluated by analyzing spiked urine following the procedure described in section 2.3.3. The sample used was Liquichek™ Urine Chemistry Control (BioRad) containing uric acid, amilase, calcium, chloride, cortisol, creatinine, phosphorous, glucose, magnesium, albumin, potassium, sodium, and urea, and it was spiked with TGF-β1 at 25, 45 or 100 pg/mL concentration levels.

The possibility of a matrix effect was evaluated by constructing calibration graphs in urine by spiking it with TGF-β1 concentrations ranging between 25 and 250 pg/mL and applying 0, 1:2 and 1:3 dilution ratios with 0.1 M PBS of pH 7.2. The results obtained revealed that a 1:3 dilution was enough to avoid significant matrix effects since the slope of the calibration plot, 911 nA per decade of concentration, was not statistically different from that obtained with TGF-β1 standards. Accordingly, the determination of TGF-β1 in urine could be accomplished by interpolation of the current measured with the immunosensor in the 1:3 diluted samples into calibration plot prepared with standards. No other sample pretreatment was needed in any case. Table 1 summarizes the results obtained in the analysis of spiked urine with recoveries near to 100% in all cases, thus demonstrating the suitability of the approach to determine low TGF-β1 concentrations in a complex biological fluid such urine is.

4. Conclusions

The first amperometric immunosensor for the quantification of the cytokine TGF-β1, proposed as a biomarker for patients having or at risk for renal disease, is described in this work. The rational design of the immunosensor involving stable and oriented immobilization of the specific antibodies on carboxylic acid-functionalized MBs by using the polymer Mix&Go, and an electrochemical signal amplification strategy by labeling the detection antibody with a peroxidase-streptavidin polymer, allowed remarkably improved analytical characteristics to be obtained with respect to ELISA kits or previous methods. Combining these benefits, a calibration plot suitable for the determination of the cytokine in plasma and urine is achieved. This allowed the determination of TGF-β1 concentrations in urine at the pg/mL concentration level with no sample treatment except a 1:3 dilution with buffer solution. The obtained results show that the initial objective of developing a sensitive, reliable, and robust analytical tool for the determination of this cytokine in complex clinical samples, and, therefore, suitable to develop point-of-care devices is reasonably achieved.

Acknowledgments

Financial support of Spanish Ministerio de Economía y Competitividad, Research Project CTQ2015–70023-R, and NANOAVANSENS Program from Comunidad de Madrid (S2013/MT-3029) is gratefully acknowledged.

References

Eder, I.E., Stenzl, A., Hobisch, A., Cronauer, M.V., Bartsch, G., Klocker, H., 1996. J. Urol. 156, 953–957.
Fallatah, H.I., 2014. Advances in. Hepatology, 357287.
Grainger, D.J., Kemp, B.R., Metcalfe, J.C., Liu, A.C., Lawn, R.M., Williams, N.R., Grace, A.A., Schofield, P.M., Chauhan, A., 1995. Nat. Med. 1, 74–79.
Grainger, D.J., Mosedale, D.E., Metcalfe, J.C., 2000. Cytokine Growth Factor Rev. 11, 133–145.
Honkanen, E., Teppo, A.-M., Törnroth, T., Groop, P.-H., Grönhagen-Riska, G., 1997. Nephrol. Dial. Transpl. 12, 2562–2568.
Liu, G., Qi, M., Hutchinson, M.R., Yang, G., Goldys, E.M., 2016. Biosens. Bioelectron. 79, 810–815.
Matharu, Z., Patel, D., Gao, Y., Haque, A., Zhou, Q., Revzin, A., 2014. Anal. Chem. 86, 8865–8872.
Ojeda, I., Moreno-Guzmán, M., González-Cortés, A., Yáñez-Sedeño, P., Pingarrón, J. M., 2014. Anal. Bioanal. Chem. 406, 6363–6371.
Ojeda, I., Barrejón, M., Arellano, L.M., González-Cortés, A., Yáñez-Sedeño, P., Langa, F., Pingarrón, J.M., 2015. Biosens. Bioelectron. 74, 24–29.
Ooi, H.W., Cooper, S.J., Huang, C.-Y., Jennins, D., Chung, E., Maeji, N.J., Whittaker, A. K., 2014. Anal. Biochem. 456, 6–13.
Ruiz-Valdepeñas Montiel, V., Campuzano, S., Pellicanò, A., Torrente-Rodríguez, R.M., Reviejo, A.J., Cosio, M.S., Pingarrón, J.M., 2015. Anal. Chim. Acta 880, 52–59.
Stenken, J.A., Poschenrieder, A.J., 2015. Anal. Chim. Acta 853, 95–99.
Tsapenko, M.V., Nwoko, R.E., Borland, T.M., Voskoboev, N.V., Pflueger, A., Rule, A.D., Lieske, J.C., 2013. Clin. Biochem. 46, 1430–1435.
Yao, Y., Bao, J., Lu, Y., Zhang, D., Luo, S., Cheng, X., Zhang, Q., Li, S., Liu, Q., 2016. Sens. Actuators, B 222, 127–132.
Zacco, E., Pividori, M.I., Alegret, S., Galve, R., Marco, M.P., 2006. Anal. Chem. 78, 1780–1788.
⟨www.raybiotech.com/files/manual/ELISA/ELH-TGFb1.pdf⟩.

9.3. ELECTROCHEMICAL IMMUNOSENSOR FOR SENSITIVE DETERMINATION OF THE ANOREXIGEN PEPTIDE YY AT GRAFTED REDUCED GRAPHENE OXIDE ELECTRODE PLATFORMS.

Analyst

PAPER

View Article Online
View Journal | View Issue

Cite this: *Analyst*, 2015, **140**, 7527

Electrochemical immunosensor for sensitive determination of the anorexigen peptide YY at grafted reduced graphene oxide electrode platforms†

S. Guerrero, G. Martínez-García, V. Serafín, L. Agüí, P. Yáñez-Sedeño* and J. M. Pingarrón

Received 13th June 2015,
Accepted 30th July 2015

DOI: 10.1039/c5an01185j

www.rsc.org/analyst

The first electrochemical immunosensor for the determination of peptide YY is reported in this paper. A novel electrochemical platform, prepared by the electrochemical grafting of the diazonium salt of 4-aminobenzoic acid onto a reduced graphene oxide-modified glassy carbon electrode, was used, on which the covalent immobilization of specific anti-PYY antibodies was accomplished. The HOOC-Phe-rGO/GCEs were characterized using cyclic voltammetry and electrochemical impedance spectroscopy. The different variables affecting the preparation of the modified electrodes and the performance of the immunosensor were optimized. Under the optimized conditions, a calibration plot for PYY showing a linear range extending between 10^{-4} and 10^{2} ng mL^{-1} was found. This range is adequate for the determination of this protein in real samples, since the expected concentration in human serum is around 100 pg mL^{-1}. The limit of detection was 0.01 pg mL^{-1} of PYY. The immunosensor exhibited good reproducibility of the PYY measurements, excellent storage stability and selectivity, as well as a shorter assay time than those of ELISA kits. The usefulness of the immunosensor for the analysis of real samples was demonstrated by analyzing human serum samples spiked with PYY at three concentration levels.

Introduction

Peptide YY is a potent anorexigen belonging to the pancreatic polypeptide family. It is produced in the gut by the L cells of the terminal ileum and colon and is secreted into the circulatory system in response to food.[1,2] There are two endogenous forms of the hormone: PYY_{1-36} and PYY_{3-36}, released PYY_{1-36} is rapidly metabolized by dipeptidyl peptidase-IV to active PYY_{3-36} through the removal of the two *N* terminal amino acids from the full length form.[3,4] Although both forms are biologically active, PYY_{3-36} (hereinafter PYY) is the main storage and circulating form and is thought to more actively control food intake.[5] PYY stimulates the gastrointestinal absorption of fluids and electrolytes, reduces gastric and pancreatic secretions, and delays emptying.[2] The effects of PYY on satiety, food intake and body weight have been investigated.[6,7] Although to date contradictory results have been published concerning the relationship between PYY and body weight,[5] it is well known that PYY reduces food intake by acting on the arcuate nucleus in the hypothalamus, possibly by inhibiting neuropeptide Y neurons and stimulating POMC expressing neurons *via* the Y2 receptors.[8] This behavior has led to PYY becoming a therapeutic target for reducing hunger and calorie intake.[1]

Despite its importance, methods for determining PYY are restricted to RIA or ELISA immunoassays. A variety of commercial ELISA kits are available. These are mainly based on competitive schemes involving specific PYY antibodies or biotinylated PYY binding, as well as HRP-labeled avidin or streptavidin conjugates and colorimetric detection after hydrogen peroxide and TMB addition. These assays allow the determination of PYY in concentration ranges from 0.1–1 pg mL^{-1} to 100–1000 pg mL^{-1}, with minimum detectable concentrations of 0.5 pg mL^{-1} to approximately 3 pg mL^{-1}. The times required for these assays are around 2.5–3.5 h.

The scientific and technological advances shown by graphene in recent years are enormous. Due to its remarkable physical properties, this material has largely proven to be extremely versatile and suitable for electroanalytical applications.[9] The use of graphene in the preparation of electrochemical biosensors commonly requires modifying an electrode surface with colloidal suspensions of this material. Graphene suspensions are prepared from graphene oxide (GO) using chemical

Department of Analytical Chemistry, Faculty of Chemistry, University Complutense of Madrid, 28040-Madrid, Spain. E-mail: yseo@quim.ucm.es

†Electronic supplementary information (ESI) available. See DOI: 10.1039/c5an01185j

methods which typically involve the reduction of dispersed single-layer GO sheets to form stable rGO suspensions. In this paper we have introduced a green alternative for rGO preparation using the natural antioxidant ascorbic acid as a reducing agent, which demonstrated good efficiency for such a purpose.[10] Glassy carbon electrodes were then modified with the as prepared rGO and the resulting rGO/GCEs were used as platforms for the development of the first electrochemical immunosensor for PYY. The protocol for the immobilization of immunoreagents on the rGO/GCEs involved the grafting of free radicals onto the electrode surface.[11,12] Specifically, the diazonium salt of 4-amino benzoic acid (4-ABA) was electrochemically reduced at the electrode surface, resulting in the covalent attachment of 4-carboxy phenyl to the rGO/GCE.[13] Then, anti-PYY antibodies were covalently immobilized onto the modified electrode, and a competitive immunoassay involving PYY and biotinylated PPY (Biotin-PYY) was performed. The determination of PYY was carried out by differential pulse voltammetry using alkaline phosphatase-labeled streptavidin (AP-Strept) and 1-naphthyl phosphate (1-NPP) as the enzyme substrate. AP catalyzes the hydrolysis of 1-NPP to 1-naphtol and the electrochemical oxidation of this compound on the electrode surface is measured by DPP.

Experimental

Reagents and solutions

Peptide YY (PYY) (3-36) (human) purified IgG antibodies (antiPYY), peptide YY (PYY) (3-36) (human), and biotinylated-PYY (Biotin-PYY) (3-36) (human) were purchased from Phoenix Pharmaceuticals, Inc. The graphene oxide (NIT.GO.M.140.10) was from Nanoinnova Technologies. Alkaline phosphatase labelled-streptavidin (AP-Strept), 1-naphthyl phosphate (1-NPP), 1-ethyl-3-[3-dimethylaminopropyl]carbodiimide hydrochloride (EDC), and *N*-hydroxysulfo-succinimide (NHSS) were from Sigma. 4-Aminobenzoic acid (ABA) was from Acros. Ethanolamine (ETA, Aldrich), bovine serum albumin (BSA) from Gerbu, and casein from Thermo Scientific were used as blocking agents. A 0.1 M phosphate buffer solution (PBS) of pH 7.4 was prepared from sodium di-hydrogen phosphate and di-sodium hydrogen phosphate (Scharlau). A 50 mM tris (tris (hydroxymethyl)amino-methane, Sigma) buffer solution containing 10 mM of $MgCl_2$ (Panreac) at pH 9.6 (Trizma) was also used. All reagent solutions were prepared in 0.1 M PBS except the AP-Strept and 0.05 M 1-NPP solutions, which were prepared in Trizma buffer. Insulin, human growth hormone (hGH) and follicle stimulating hormone (FSH), all from Sigma-Aldrich, and adiponectin (APN, Abnova), ghrelin (GHRL) and des-acyl-ghrelin (da-GHRL, Anaspec), were tested as potential interfering compounds. De-ionized water was obtained from a Millipore Milli-Q purification system (18.2 MΩ cm).

Apparatus

Voltammetric measurements were carried out using a BAS (Bioanalytical System) 100 B potentiostat accompanied by BAS 100/W software for the electrochemical analysis. A three electrode (BAS VC-210-mL) glass electrochemical cell was used. Modified 3 mm diameter CHI 104 glassy carbon electrodes from CH Instruments were used as the working electrodes. The reference electrode was an Ag/AgCl/KCl 3M BAS MF 2063 and the auxiliary electrode was a BAS MW 1032 Pt wire. A P-Selecta ultrasonic bath, a Vortex (Heidolph) stirrer and a precision Metrohm Herisau E-510 pH-meter were also used.

Procedures

Preparation of rGO. 2 mL of a 1 mg mL^{-1} GO aqueous dispersion was sonicated for 120 min and then centrifuged at 10 000 g for 10 min. The precipitate was discarded and the supernatant was treated with a 25% NH_3 solution to achieve a pH of 9–10. Then, the reduction of GO was performed by adding solid ascorbic acid up to a 2 mM final concentration and letting it react at 100 °C for 15 min. The resulting rGO dispersion was left in the dark at room temperature. The product was replenished every week, although it was stable for at least two weeks.

Preparation of the immunosensors. Fig. 1 shows the steps involved in the modification of the electrodes and preparation of the immunosensors. Firstly, the diazonium salt was prepared by adding dropwise a 2 mM $NaNO_2$ aqueous solution to a 1 mg mL^{-1} ABA solution prepared with 1 M HCl and cooled with ice (38 mL of $NaNO_2$ for each 200 mL of ABA). The reaction was allowed to proceed for 10 min under stirring. Separately, glassy carbon electrodes were polished with 0.3 μM alumina slurries for 1 min, sonicated for 30 s in water and dried in air. Then, 10 μL of a 0.5 mg mL^{-1} rGO suspension were deposited onto the electrode surface and, after drying at room temperature, the rGO/GCEs were immersed in 450 μL of the diazonium salt. Ten successive voltammetric cycles from 0 to −1.0 V *vs.* Ag/AgCl (ν = 200 mV s^{-1}) were carried out to allow electrochemical grafting. The resulting HOOC-Phe-rGO/GCE modified electrodes were washed thoroughly with water and ethanol and dried at room temperature.

The activation of the carboxylic groups was achieved by dropping 10 μL of an EDC/NHSS (0.1 M each) aqueous solution onto the HOOC-Phe-rGO/GCEs and leaving them to react for 1 h in the dark. After rinsing them with water and methanol and allowing them to dry, 10 μL of a 20 μg mL^{-1} anti-PYY solution was casted onto the electrode and left to stand for 1 h at 37 °C. Then, 20 μL of a 0.2% casein blocking solution was deposited onto the electrode and incubation was allowed for 1 h at 37 °C. A competitive immunoassay was performed by spotting 10 μL of a mixed solution of PYY (or the sample) and 100 ng mL^{-1} of Biotin-PYY onto the anti-PYY-Phe-rGO/GCE, then allowing incubation for 30 min at 37 °C. Thereafter, 10 μL of 5 μg mL^{-1} AP-Strept was added to the Biotin-PYY-anti-PYY-Phe-rGO/GCE followed by incubation for 30 min at 37 °C. Finally, the immunosensor was immersed in 450 μL of 50 mM Trizma buffer solution, and 50 μL of 0.05 M 1-NPP solution was added. After a delay time of 5 min to allow the enzyme reaction to take place, differential pulse voltammograms were

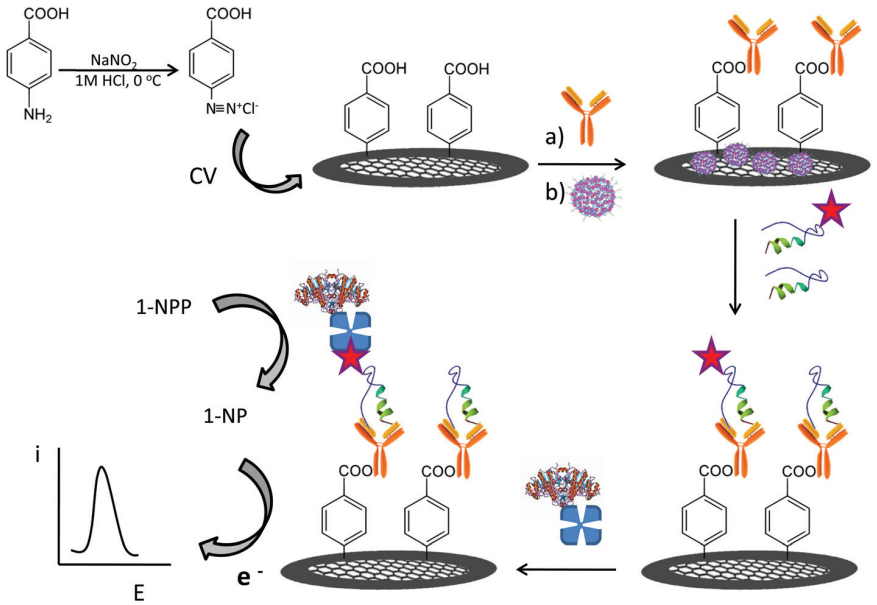

Fig. 1 Schematic display of the different steps involved in the construction of an electrochemical immunosensor for PYY involving the grafting of 4-ABA diazonium salt onto a rGO-modified GCE and the covalent immobilization of anti-PYY.

recorded over the −0.15 to + 0.70 V range to obtain the electroanalytical signals, using ΔE = 50 mV and ν = 20 mV s^{-1}.

Determination of PYY in spiked serum samples

Lyophilized human serum S-7394 from Sigma containing no PPY was reconstituted in 1 mL of 0.1 M PBS solution of pH 7.4 by mixing up to total dissolution and subsequently spiked with the target analyte at 0.35, 3.5 and 35 pg mL^{-1} concentration levels. PYY determination was performed by applying the procedure described above, and the peak current values measured by DPV were interpolated into the linear portion of a calibration plot constructed using the PYY standard solutions.

Results and discussion

In order to develop the first electrochemical immunosensor for PYY, we have designed an approach whose rationale is based on the immobilization of specific capture antibodies, using a grafting strategy *via* the diazonium salt of 4-amino benzoic acid, onto a tailor-made electrode surface modified with rGO in order to take advantage of the well known properties of this nanomaterial (high conductivity and large specific surface area), which enhances the performance of electrochemical biosensors. Moreover, the electrode modification involved a green route using ascorbic acid as the reducing agent.

Preparation of rGO

The procedure described in the Experimental section was followed for the preparation of rGO from graphene oxide. In this procedure, ascorbic acid was used as the reducing agent due to the high efficiency demonstrated in the reduction of GO[10] together with the advantage of substituting other commonly used toxic reagents such as hydrazine, hydroxylamine or sodium borohydride for this natural and inexpensive antioxidant. Furthermore, it is well known that the electronic properties of rGO can be tuned on the basis of the extent of the reduction process.[14] In this sense, the use of a mild reducing agent such as ascorbic acid allows an easy optimization of the experimental conditions for the reduction reaction to get the optimal electrocatalytic properties.[15,16]

The as obtained rGO was characterized by UV-vis spectrophotometry. Fig. S1 in the ESI† shows two peaks at 230 and 300 nm corresponding to the $\pi \rightarrow \pi^*$ and $n \rightarrow \pi^*$ transitions, respectively, in the unreduced GO spectrum.[17] Upon reduction of GO with ascorbic acid, the $n \rightarrow \pi^*$ peak partially disappears and a red-shift of the $\pi \rightarrow \pi^*$ peak to 241 nm occurs. This peak position has been used as a convenient probe of the reduction degree achieved using different reducing reagents.[10] Furthermore, the aqueous ascorbic-reduced GO suspension was clearly different from that of the unreduced GO (inset in Fig. S1†), and exhibited long-term stability without observing precipitation for several weeks. These results demonstrate the efficiency of the method used for the reduction of GO.

Preparation of the modified electrodes

The preparation of the modified electrodes required optimization of (a) the loading of rGO onto the GCE surface, (b) the ABA concentration and (c) the number of cycles and potential scan rate used during the electrochemical grafting of the rGO/

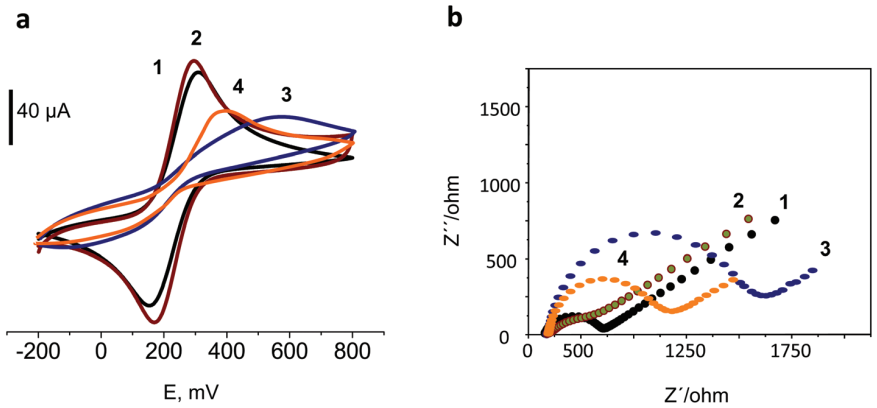

Fig. 2 Cyclic voltammograms (a) and Nyquist plots obtained by electrochemical impedance spectroscopy (b) for the (1) bare GCE, (2) rGO/GCE, (3) HOOC-Phe-rGO/GCE and (4) HOOC-Phe-rGO/GCE activated with EDC/NHSS, in 5 mM $Fe(CN)_6^{3-/4-}$ 0.1 M KCl solution.

GCE. Detailed information on the optimization of these steps can be found in the ESI.†

Once prepared, the rGO/GCEs were characterized by cyclic voltammetry and electrochemical impedance spectroscopy (EIS) using 5 mM $Fe(CN)_6^{3-/4-}$ as the redox probe in 0.1 M KCl. Fig. 2a displays the typical cyclic voltammograms recorded from the (1) bare GCE, (2) rGO/GCE, (3) HOOC-Phe-rGO/GCE, and (4) HOOC-Phe-rGO/GCE activated with EDC/NHSS. As can be seen, slightly larger voltammetric peaks and a smaller electron transfer resistance (Fig. 2b) were observed for the rGO/GCE with respect to the unmodified GCE, which could be attributed to both the larger conductivity and/or porous diffusion effects of the functionalized graphene electrodes.[18] Conversely, electrochemical grafting resulted in a poorer voltammetric behavior and a large increase in the electron transfer resistance as a consequence of the electrostatic repulsion between the redox probe and the negatively charged carboxylate groups. However, when the carboxyl moieties were activated using the EDC/NHSS reagents, a semicircle with a shorter diameter appeared as a consequence of the neutralization of the negative charges on the carboxylate groups (curve 4). Equivalent behavior can also be observed by cyclic voltammetry. These results confirm the successful modification of the electrode surface through electrochemical grafting with the diazonium salt.

Immunosensor preparation

All the experimental variables involved in the immunosensor construction and therefore affecting its analytical performance were investigated. These variables were (a) the loading of anti-PYY and the incubation time, (b) the blocking step, (c) the loading of biotin-PYY and the incubation time, (d) the loading of AP-Strept and the incubation time and (e) the concentration of 1-NPP and the time for the enzyme reaction to proceed. Detailed information on the results obtained in these studies can be found in the ESI† and are summarized in Table S1.†

Analytical characteristics of the immunosensor for PYY

Once all the working conditions were optimized, a calibration plot of PYY with the AP-Strept-Biotin-PYY-anti-PYY-Phe-rGO/GCE immunosensor was constructed showing the expected inverse peak current *vs.* log PYY concentration relationship for the competitive immunoassay (Fig. 3a). The i_p *vs.* PYY concentration curve was fitted by a non-linear regression using Sigma Plot data analysis software. The error bars displayed were calculated from measurements obtained from three different immunosensors and the concentrations of PYY tested ranged between 10^{-7} and 10^{4} ng mL^{-1}. The corresponding equation is:

$$y = \frac{i_{max} - i_{min}}{1 + (EC_{50}/x)^{h}} + i_{min}$$

The maximal and minimal current values were: i_{max} = 2.40 ± 0.09 μA and i_{min} = 0.57 ± 0.08 μA. The EC_{50} value, corresponding to the PYY concentration at fifty per cent competition, was 0.08 ng mL^{-1}, and the Hill slope was h = −0.24 ± 0.04. A linear range (r = 0.995) between 10^{-4} and 10^{2} ng mL^{-1} of PYY was observed. This range is adequate for the clinical determination of PYY when taking into account the expected concentrations in human serum (around 100 pg mL^{-1}).[3,19] The limit of detection was calculated to be 0.01 pg mL^{-1} of PYY according to the equation:

$$LOD = EC_{50}\left(\frac{i_{max} - i_{min}}{i_{max} - i_{min} - 3s} - 1\right)^{-1/h}$$

where s is the standard deviation, ±0.06 μA, of the i_p values measured for solutions (n = 10) containing no PYY (zero value).

Some of the recorded DP voltammetric traces are displayed in Fig. 3b. The reproducibilities of the peak current measurements for solutions containing no PYY and 1.0 ng mL^{-1} of PYY, were tested using different immunosensors on the same

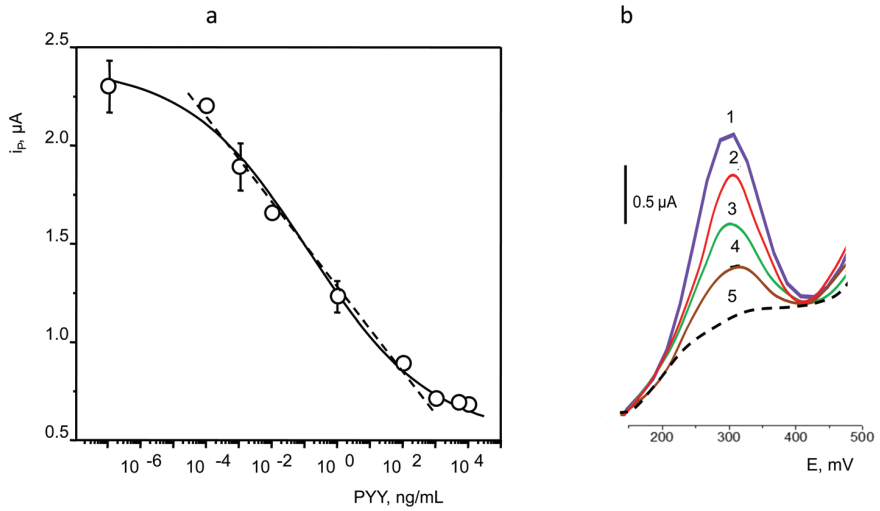

Fig. 3 Calibration plot for PYY (a) and differential pulse voltammograms (b) for (1) 0, (2) 0.01, (3) 1.0, (4) 5.0×10^4 ng mL^{-1} of PYY and (5) unspecific adsorption at the AP-Strept-Biotin-PYY-anti-PYY-Phe-rGO/GCE immunosensor. See text and Table S1† for the experimental conditions.

day and on different days. A new anti-PYY-Phe-rGO/GCE conjugate was assembled for each measurement. Relative standard deviation (RSD) values of 4.0 and 5.0% (n = 5) were found, respectively, for the assays performed on the same day, whereas the RSD values were 5.5% in the absence of PYY and 3.2% for 1.0 ng mL^{-1} of PYY when the measurements were carried out on different days. These results reveal the good reproducibility achieved for the fabrication and functioning of the proposed immunosensing platform.

The comparison of the analytical performance of the AP-Strept-Biotin-PYY-anti-PYY-Phe-rGO/GCE immunosensor *versus* that reported for commercial ELISA kits allows us to point out the following advantages. Firstly, the assay time is considerably shorter. In fact, once the antibody was immobilized, measurements could be made in two hours in contrast to colorimetric kits which take longer than three hours. Examples are the Enzyme Immunoassay Kit from RayBio® or the Abnova KA1686 for human, mouse or rat PYY that require 3 h 45 min. Furthermore, the accessible dynamic range with these kits ranges from 1 to 1000 pg mL^{-1}, which is a much narrower range than that achieved with the developed immunosensor. Moreover, the minimum detectable concentration achievable with such commercial kits, 2.84 pg mL^{-1}, is more than three hundred times larger than the detection limit achieved with the immunosensor, and the precision of these kits, with CV < 10% (intra-assay) or CV < 15% (inter-assay), is worse than that obtained in this work. Another noticeable advantage is the reusability of the electrochemical platforms employed for the construction of the immunosensor. The regeneration of the GCE surface could be accomplished simply by polishing for one minute with 3-micron alumina and rinsing for 30 s each with water and methanol under ultrasonic stirring followed by drying under IR irradiation.

The storage stability of the anti-PYY-Phe-rGO/GCE conjugate was also investigated. In order to do that, different bioelectrodes were prepared on the same day and stored in a refrigerator at 4 °C. Each bioelectrode was used to construct the corresponding immunosensor and to measure the voltammetric response for 5 mM 1-NPP in the absence of PYY. The results obtained (not shown) revealed the high stability of this configuration, since the measured peak currents remained within the control limits set at ±3 × the standard deviation of the responses obtained on the first day of the study for at least 12 days (no longer periods of storage time were tested).

Selectivity of the immunosensor

Various proteins: adiponectin (APN), ghrelin (GHRL), desoctanoyl ghrelin (do-GHRL), insulin (INS), human growth hormone (hGH) and follicle stimulating hormone (FSH) were tested as potential interfering substances for the determination of PYY using the developed immunosensor. The selectivity evaluation was accomplished by comparing the immunosensor response to 0 μg mL^{-1} of PYY with those measured in the presence of each tested compound at a concentration of 1 μg mL^{-1}. Fig. 4 clearly shows that no significant differences in the measured responses were apparent in any case, thus demonstrating the high selectivity of the proposed configuration for PYY determination.

Determination of PYY in spiked serum samples

The applicability of the immunosensor for the determination of PYY in human serum was demonstrated by analyzing a commercial human serum sample containing no PYY spiked with the hormone at three different concentration levels: 0.35, 3.5 and 35 pg mL^{-1}. As described in the Experimental section, the samples were analyzed without any treatment except for

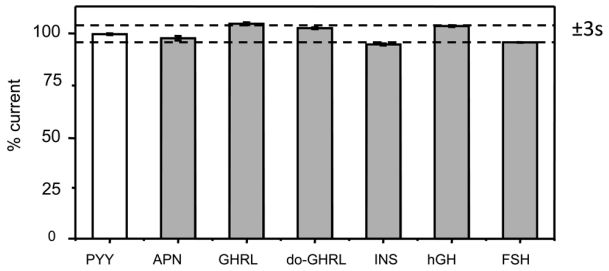

Fig. 4 Effects of the presence of APN, GHRL, do-GHRL, INS, hGH and FSH on the differential pulse voltammetric responses obtained for 0 μg mL^{-1} of PYY with the AP-Strept-Biotin-PYY-anti-PYY-Phe-rGO/GCE immunosensor.

Table 1 Determination of PYY in spiked serum samples with the AP-Strept-Biotin-PYY-anti-PYY-Phe-rGO/GCE immunosensor

Sample	PYY, pg mL^{-1}	PYY found, pg mL^{-1}	Mean PYY[a], pg mL^{-1}	Mean recovery, %
1	35	35, 33, 35, 36	35 ± 1	99 ± 3
2	3.5	3.55, 3.67, 3.58, 3.67	3.62 ± 0.06	102 ± 2
3	0.35	0.342, 0.358, 0.348, 0.345	0.348 ± 0.007	99 ± 2

[a] Mean value ± $ts/\sqrt{n}$.

dilution. In order to evaluate potential matrix effects, a calibration plot for PYY in serum was constructed by appropriate dilution. Fig. S8† shows a comparison between the calibration plots obtained from standard PYY solutions and from the diluted samples. The slope value calculated for the linear portion of this calibration was 0.19 ± 0.01 μA per decade of concentration. A statistical comparison using the Student *t*-test with the slope value of the linear range corresponding to the calibration graph prepared with the PYY standards, 0.198 ± 0.002 μA per decade of concentration, showed that t_{exp}, 0.853, was lower than the tabulated value of 2.365, for $n = 8$, at a 0.05 significance level, indicating that no significant difference existed between the slope values. Accordingly, significant matrix effects could be discarded and the determination of PYY in human serum could be carried out simply by the interpolation of the amperometric measurements from the samples into the calibration plot constructed from the standards. Table 1 summarizes the results obtained. It can be observed that satisfactory recoveries were obtained for four replicates and for all the tested concentration levels, with recoveries ranging between 99 ± 3 and 102 ± 3%.

Conclusions

The first electrochemical immunosensor for the determination of the anorexigen PYY is described in this work. The immunosensor design involved the use of modified electrodes as scaffolds to covalently immobilize capture antibodies and a competitive immunoassay involving PYY and biotinylated PPY. The immunosensor exhibited an excellent analytical performance with a broad calibration linear range between 10^{-4} and 10^{2} ng mL^{-1}, which is adequate for the determination of PYY in real samples, and a low detection limit of 0.01 pg mL^{-1}. The immunosensor also exhibited remarkably higher sensitivity, better precision and a shorter assay time than those of available ELISA kits, and its applicability was demonstrated by analyzing human serum samples spiked with PYY at three concentration levels.

Acknowledgements

The financial support of the Spanish Ministerio de Economía y Competitividad, Research Project CTQ2012-35041, and the NANOAVANSENS Program from Comunidad de Madrid (S2013/MT-3029) are gratefully acknowledged.

References

1 F. Colon-Gonzalez, G. W. Kim, J. E. Lin, M. A. Valentino and S. A. Waldman, *Mol. Aspects Med.*, 2013, **34**, 71.
2 T. E. Adrian, G. L. Ferri, A. J. Bacarese-Hamilton, H. S. Fuessi, J. M. Polak and S. R. Bloom, *Gastroenterology*, 1985, **89**, 1070.
3 R. Mentlein, P. Dahms, D. Grandt and R. Krüger, *Regul. Pept.*, 1993, **49**, 133.
4 D. Renshaw and R. L. Batterham, *Curr. Drug Targets*, 2005, **6**, 171.
5 J. A. Cooper, *Nutr. Res. Rev.*, 2014, **27**, 186.
6 R. L. Batterham, M. A. Cohen, S. M. Ellis, C. W. Le Roux, D. J. Withers, G. S. Frost, M. A. Ghatei and S. R. Bloom, *N. Engl. J. Med.*, 2003, **349**, 941.
7 D. Boey, L. Heilbronn, A. Sainsbury, R. Laybutt, A. Kriketos, H. Herzog and L. V. Campbell, *Neuropeptides*, 2006, **40**, 317.
8 R. L. Batterham, M. A. Cowley, C. J. Small, H. Herzog, M. A. Cohen, C. L. Dakin, A. M. Wren, A. E. Brynes, M. J. Low, M. A. Ghatei, R. D. Cone and S. R. Bloom, *Nature*, 2002, **418**, 650.
9 M. Pumera, A. Ambrosi, A. Bonanni, E. L. K. Chng and H. L. Poh, *TrAC, Trends Anal. Chem.*, 2014, **29**, 954.
10 M. J. Fernández-Merino, L. Guardia, J. I. Paredes, S. Villar-Rodil, P. Solís-Fernández, A. Martínez-Alonso and J. M. D. Tascón, *J. Phys. Chem. C*, 2010, **114**, 6426.
11 G. Liu, E. Luais and J. J. Gooding, *Langmuir*, 2011, **27**, 4176.
12 M. Moreno-Guzmán, I. Ojeda, R. Villalonga, A. González-Cortés, P. Yáñez-Sedeño and J. M. Pingarrón, *Biosens. Bioelectron.*, 2012, **35**, 82.
13 J. Liu, L. Cheng, B. Liu and S. Dong, *Langmuir*, 2000, **16**, 7471.

14 R. J. W. E. Lahaye, H. K. Jeong, C. Y. Park and Y. H. Lee, *Phys. Rev. B: Condens. Matter*, 2009, **79**, 125435.
15 T. W. Lu, R. B. Zhang, C. Y. Hu, F. Chen, S. W. Duo and Q. H. Hu, *Phys. Chem. Chem. Phys.*, 2013, **15**, 12963.
16 J. Liu, C. Hu, J. Xu, F. Jiang and F. Chen, *Mater. Lett.*, 2014, **134**, 134.
17 P. Sharma, G. Darabdhara, T. M. Reddy, A. Borah, P. Bezboruah, P. Gogoi, N. Hussain, P. Sengupta and M. R. Das, *Catal. Commun.*, 2013, **40**, 139.
18 C. Punckt, M. A. Pope and I. A. Aksay, *J. Phys. Chem. C*, 2013, **117**, 16076.
19 F. Cahill, Y. Ji, D. Wadden, P. Amini, E. Randell, S. Vasdev, W. Gulliver and G. Sun, *PLoS One*, 2014, **9**, e95235.

Electronic Supplementary Material (ESI) for Analyst.

SUPPLEMENTARY MATERIAL

1. Characterization of ascorbic acid-reduced GO by UV/vis spectrophotometry

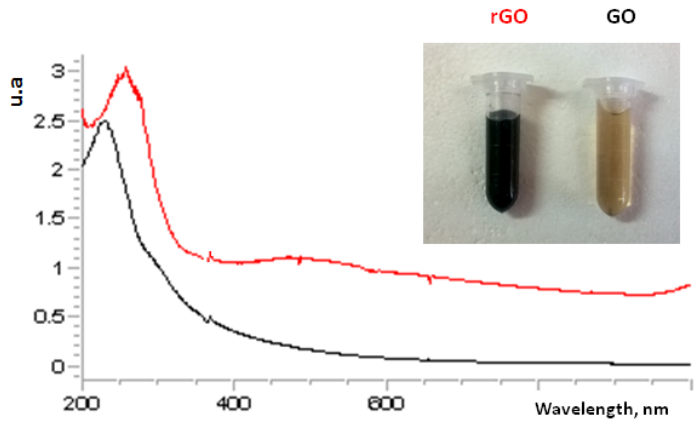

Figure S1. UV/visible spectra and pictures of unreduced GO (black) and ascorbic acid - reduced GO (red) aqueous suspensions. For more information, see Results and Discussion section in the main Manuscript.

2. Optimization of the variables affecting the preparation of modified electrodes.

a) Loading of rGO on the GCE surface

Optimization of this variable was carried out by depositing 10 µL of rGO suspensions with concentrations ranging between 0.25 and 1.0 mg/mL on the GCE. Then, different immunosensors were prepared by applying the procedure described in the Experimental section involving 4-ABA grafting and successive modification with 10 µL of 30 µg/mL anti-PYY (2 h incubation), 10 µL of 0.1 % BSA as blocking agent (1 h), 10 µL of 100 ng/mL Biotin-PYY (1 h) and, finally, 10 µL of 5 µg/mL AP-Strept (1 h). All incubation steps were performed at 37 ^{o}C. Once the immunosensors were prepared, differential pulse voltammograms were recorded according to the protocol described in the Experimental section. Figure S2a shows the specific and unspecific (in the absence of anti-PYY) responses obtained in the absence of target PYY. The immunosensor reached the maximal specific signal for a 0.5 mg/mL rGO concentration with a slight decrease for larger loadings which is probably due to a higher electron transfer resistance associated to large amounts of immobilized antibody. Conversely,

unspecific responses increased notably with rGO concentration which led us to select 0.5 mg/mL rGO as the concentration to get the largest specific/unspecific currents ratio.

b) ABA concentration

The effect of ABA concentration used for grafting at rGO/GCE was also evaluated. Figure S2b shows the responses of the immunosensors prepared similarly to that described in section (a) for three different ABA concentrations, 10, 20 and 30 mg/mL. Clearly, better signal-to-background current ration was obtained when using 20 mg/mL ABA indicating that an adequate number of carboxy phenyl radicals were grafted on the electrode surface allowing a suitable loading of the covalently immobilized antibody.

c) *Number of cycles and potential scan rate for the electrochemical grafting of ABA onto rGO/GCE*

Electrochemical grafting of carboxy phenyl radical onto rGO/GCE was carried out by immersing the modified electrode in the diazonium salt solution and performing successive cyclic voltammetric scans between 0 and -1.0 V vs. Ag/AgCl. The number of these scans was also optimized (Figure S2c). The largest specific-to-unspecific current ratio was obtained for 10 cycles. Probably, under these conditions, a sufficiently large loading of carboxyl moieties grafted onto the modified electrode surface was achieved then ensuring an appropriate covalent binding of antibodies. A higher number of voltammetric scans produced a decrease in the immunosensor responses probably as a consequence of the lower modified electrode conductivity due to an extensive grafting of carboxyl groups. Furthermore, the effect of the potential scan rate on the immunosensor responses was also tested. As it can be seen in Figure S2d, best results were achieved for ν = 200 mV/s.

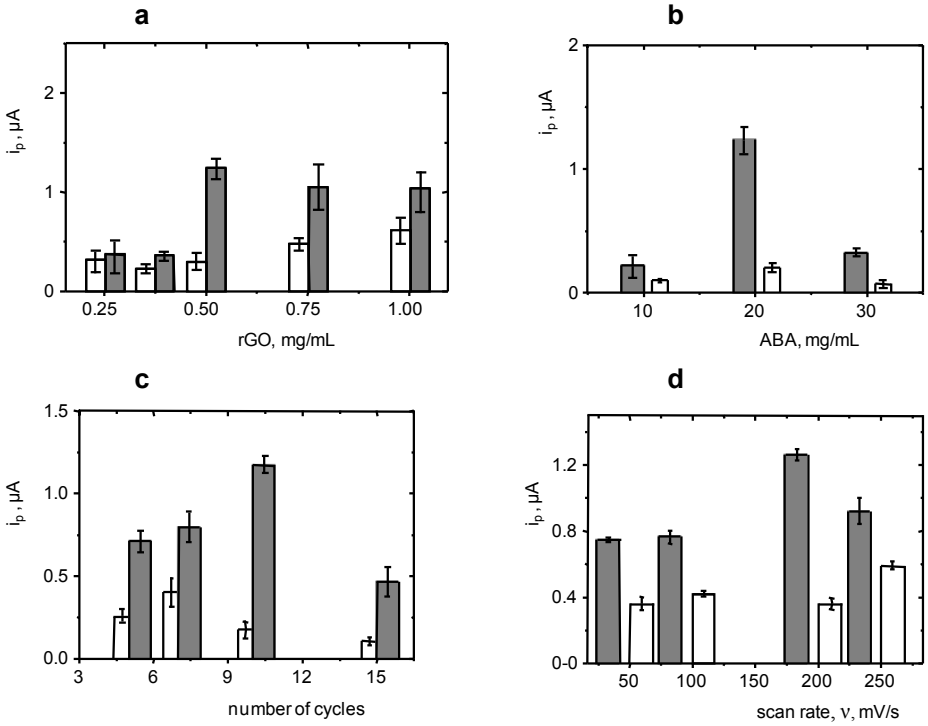

Figure S2. Effect of: the loading of rGO onto GCE (a), ABA concentration (b), the number of cycles (c) and the potential scan rate for the electrochemical grafting of ABA onto rGO/GCE electrodes (d), on the electrochemical responses of AP-Strept-Biotin-PYY-anti-PYY-Phe-rGO/GCE immunosensor in the absence of target PYY. See the text and the Experimental section in the main manuscript for more information.

3. Optimization of the experimental variables involved in the immunosensor preparation

a) Loading of anti-PYY and incubation time

The effect of the amount of immobilized antibody onto HOOC-Phe-rGO/GCE on the immunosensor voltammetric response was tested using different anti-PYY concentrations in the 5 to 30 µg/mL range. All other immunoreagent concentrations and incubation times are the same that those specified in paragraph 2a. Figure S3a shows as the specific responses increased with the antibody concentration up to 20 µg/mL then levelling off for larger loadings. The small unspecific responses exhibited negligible change over the whole concentration range. Accordingly, 20 µg/mL anti-PYY was selected for further work. Regarding the antibody incubation time (Figure 2b), the largest specific-to-unspecific current ratio was obtained for 60 min, this value being selected for the preparation of the anti-PYY-Phe-rGO/GCE conjugates.

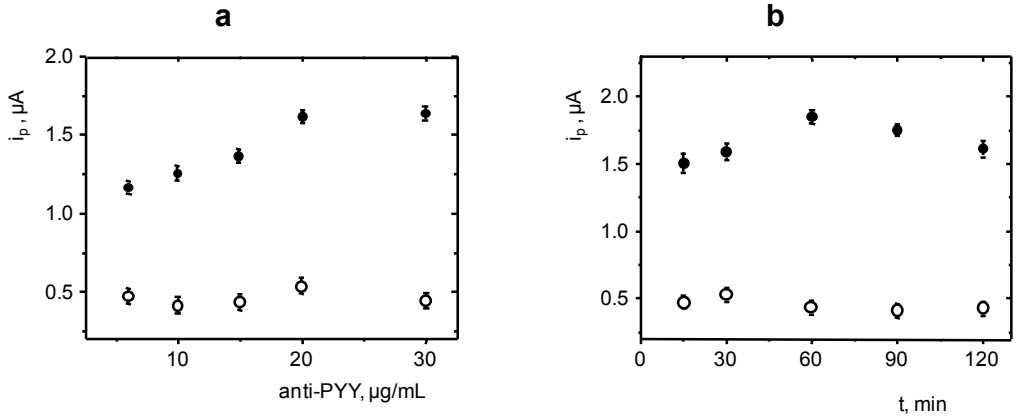

Figure S3. Effect of: the anti-PYY loading (a) and the time for incubation of anti-PYY onto Phe-rGO/GCE (b) on the electrochemical responses of the AP-Strept-Biotin-PYY-anti-PYY-Phe-rGO/GCE immunosensor in the absence of target PYY. See the text and the Experimental section in the main manuscript for more information.

b) Optimization of the blocking step

In order to minimize unspecific adsorptions of immunoreagents on the electrode surface, various blocking strategies were evaluated. Although previous optimization studies were made using 0.1 % BSA as the blocking agent, other suitable reagents for this purpose (ethanolamine (ETA) and casein in addition to BSA) were tested. The protocol consisted of adding 10 µL of a 0.1% blocking solution onto the anti-PYY-Phe-rGO/GCE allowing incubation for a pre-established time of 1 h at 37 ^{o}C. The results are shown in Figure S4a and revealed that both specific and unspecific responses were much larger when ETA was used, probably as a consequence of the instability of the electrode coating with this compound. The best specific-to-unspecific responses ratio was achieved using casein and, therefore, it was selected as the blocking agent for further work. Its concentration and time for incubation were also checked. Figure S4b shows as the largest specific-to-unspecific ratio was found for a 0.2% casein concentration. Moreover, 60 min incubation allowed a specific response to be obtained more than 5 times larger than that corresponding to nonspecific interactions (Figure S4c).

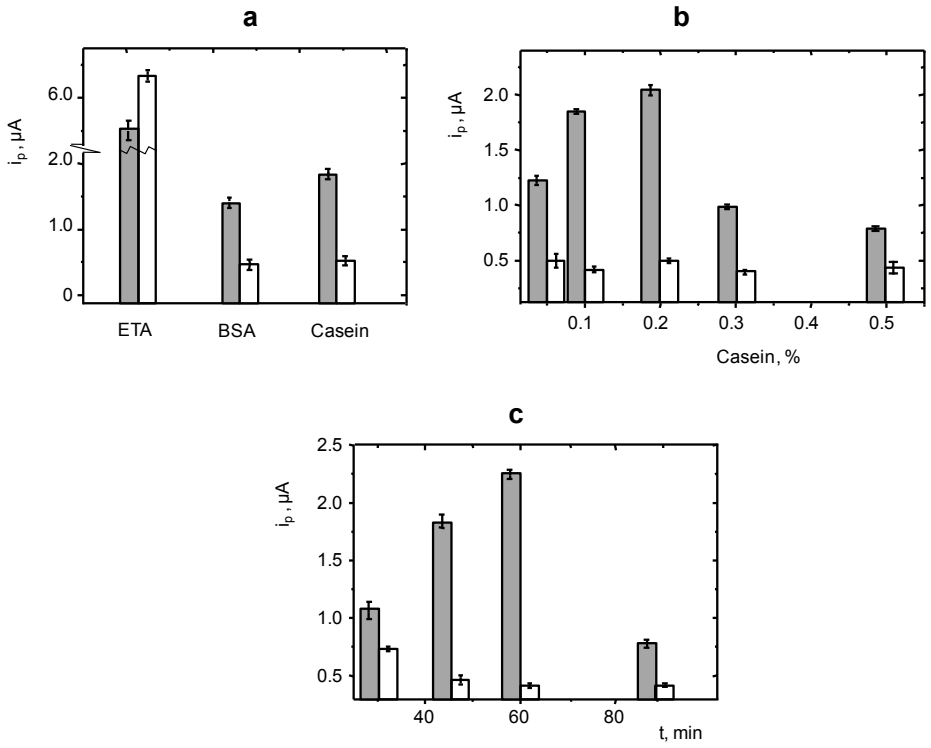

Figure S4. Effect of: the type of blocking agent used (a), the concentration of casein (b) and the time for incubation of casein (c) onto anti-PYY-Phe-rGO/GCE, in the electrochemical responses of AP-Strept-Biotin-PYY-anti-PYY-Phe-rGO/GCE immunosensor in the absence of target PYY. See the text and the Experimental section in the main manuscript for more information.

c) Loading of Biotin-PYY and incubation time

Different AP-Strept-Biotin-PYY-anti-PYY-Phe-rGO/GCE immunosensors were prepared by incubating anti-PYY-Phe-rGO/GCEs in Biotin-PYY solutions with concentrations ranging between 50 and 400 ng/mL. The measured DPV peak current values increased sharply with the Biotin-PYY concentration from 50 to 100 ng/mL and then leveled off, whereas the unspecific currents practically did not vary over the whole tested concentrations range (Figure S5a). Accordingly, 100 ng/mL was selected for further work. In addition, 30 min was shown to be a sufficient incubation time in the Biotin-PYY solution (Figure S5b).

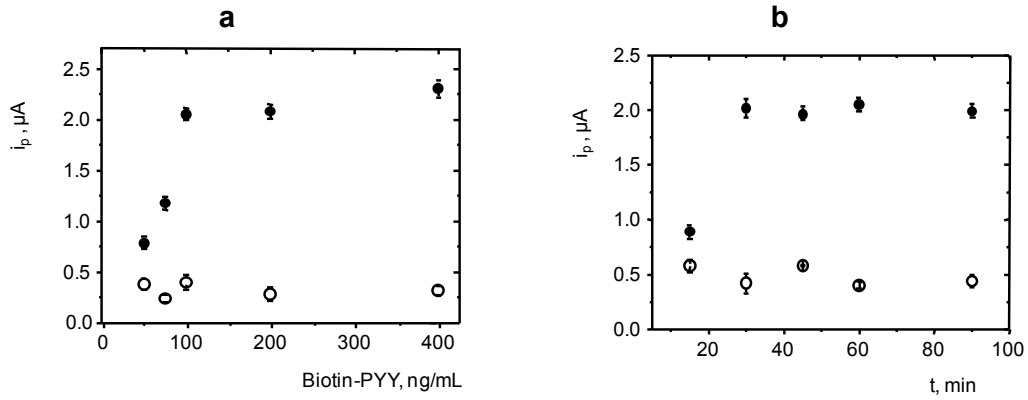

Figure S5. Effect of: the loading of Biotin-PYY (a), and the time for incubation of Biotin-PYY onto anti-PYY-Phe-rGO/GCE (b), on the electrochemical responses of AP-Strept-Biotin-PYY-anti-PYY-Phe-rGO/GCE immunosensors in the absence of target PYY. See the text and the Experimental section in the main manuscript for more information.

d) Loading of AP-Strept and incubation time.

The effect of the AP-streptavidin loading was checked by constructing calibration plots for PYY over the 10^{-6} (or 10^{-7}) to 10^{3} ng/mL concentration range, with AP-Strept-Biotin-PYY-anti-PYY-Phe-rGO/GCE immunosensors prepared with 7.0, 5.0 and 2.5 µg/mL AP-Strept. As it can be seen in Figure S6a, the largest used AP-Strept loading did not provide a useful calibration graph probably due to saturation of the bioelectrode and a decrease in conductivity. Although 2.5 µg/mL AP-Strept allowed responses varying with PYY concentration in a wide range, the largest slope value for the linear portion of the calibration plot was obtained using 5.0 µg/mL AP-Strept and then this value was selected for further work. Regarding the time for incubation with of this labeled protein, Figure S5b shows that 30 min was an appropriate time to obtain a good specific-to-unspecific current ratio.

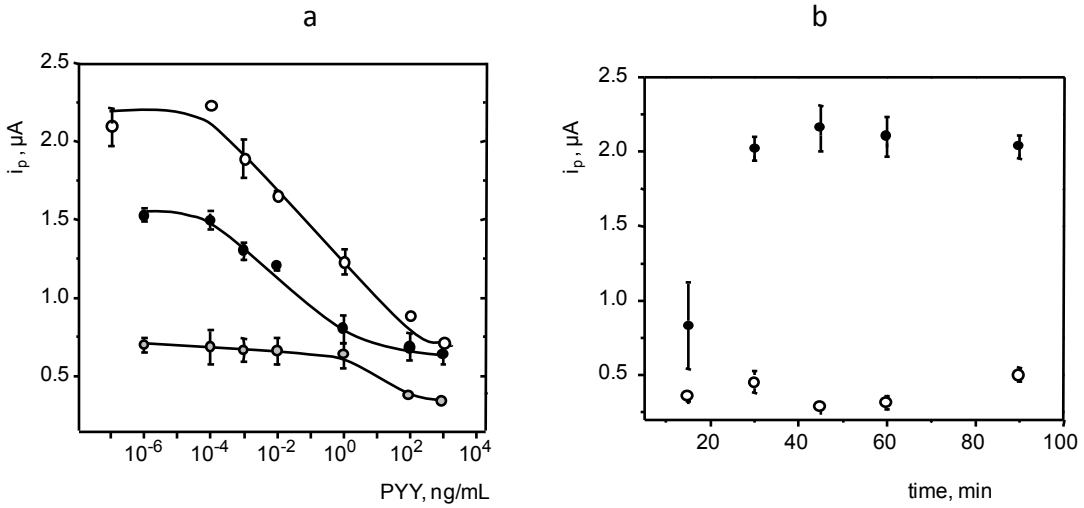

Figure S6. Effect on the electrochemical responses of AP-Strept-Biotin-PYY-anti-PYY-Phe-rGO/GCE immunosensors in the absence of target PYY of: the 5.0 (white dots) 2.5 (black), and 7.0 (grey) µg/mL AP-Strept loading (a), and the time for incubation of AP-Strept onto Biotin-PYY-anti-PYY-Phe-rGO/GCE (b). See the text and the Experimental section in the main manuscript for more information.

e) Concentration of 1-NPP and time for the enzyme reaction to proceed

The influence of AP substrate concentration on the differential pulse voltammetric responses measured with the AP-Strept–Biotin-PYY-anti-PYY-Phe-rGO/GCE immunosensor was also studied. Figure S7a shows as the largest peak current value was obtained for 5 mM 1-NPP, which represents a relatively high concentration then ensuring that the enzyme reaction rate depended only on the enzyme concentration. Moreover, Figure S7b shows that 5 min were sufficient to allow the reaction catalyzed by AP enzyme to be proceeded.

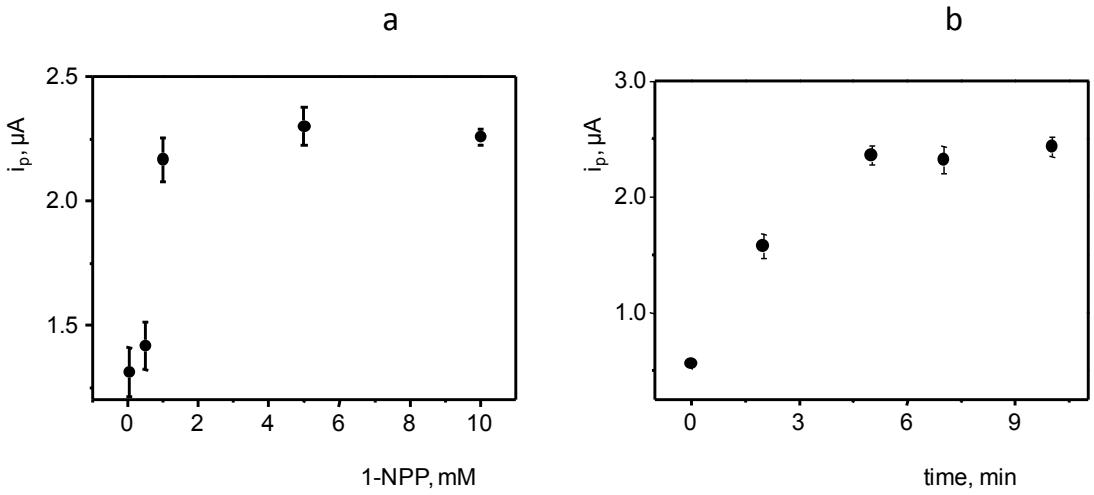

Figure S7. Effect on the electrochemical responses of AP-Strept-Biotin-PYY-anti-PYY-Phe-rGO/GCE immunosensors in the absence of target PYY of: the concentration of 1-NPP (a), and the time for the enzyme reaction to proceed (b). See the text and Experimental section in the main manuscript for more information.

Table S1. Optimization of the experimental variables affecting the preparation of grafted ABA-rGO/GCE and the performance of the AP-Strept-Biotin-PYY-anti-PYY-Phe-rGO/GCE immunosensors

Variable	Tested range	Selected value
rGO, mg/mL	0.25 - 1.0	0.5
ABA, mg/mL	10 - 30	20
Number of CV cycles	5 - 15	10
Potential scan rate, mV/s	50 - 250	200
anti-PYY, µg/mL	5 - 30	20
Incubation time for anti-PYY, min	15 - 120	60
Blocking agent type	Ethanolamine, BSA, casein	casein
Casein, % (w/v) in PBS	0.05 - 0.5	0.2
Incubation time for blocking, min	30 - 90	60
Biotin-PYY, ng/mL	50 - 400	100
Incubation time for Biotin-PYY, min	15 - 90	30
AP-Strept, µg/mL	2.5 - 7	5
Incubation time for AP-Strept,	15 - 90	30

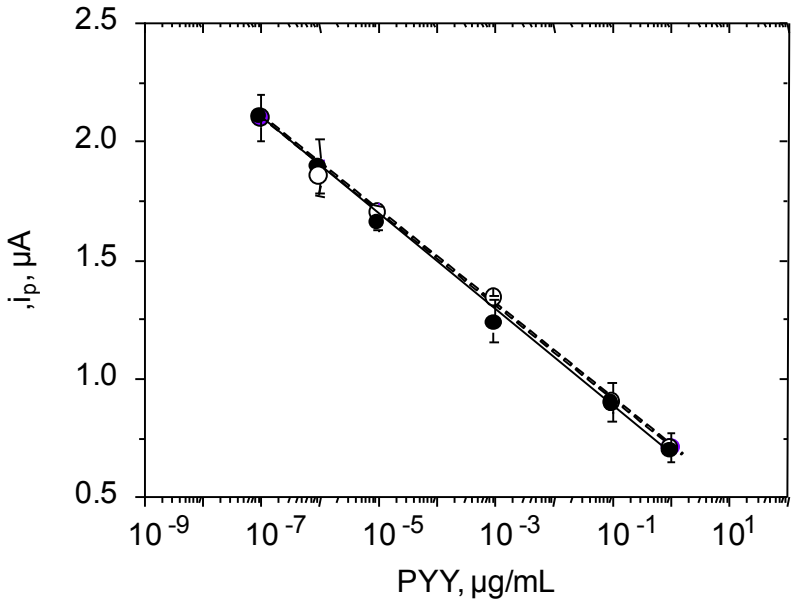

Figure S8. Calibration plots for PYY at the AP-Strept-Biotin-PYY-anti-PYY-Phe-rGO/GCE immunosensor: (—•—) standard PYY solutions; (**- - o - -**) serum samples.

9.4. MULTIPLEXED ELECTROCHEMICAL IMMUNOSENSING OF OBESITY-RELATED HORMONES AT GRAFTED GRAPHENE-MODIFIED ELECTRODES

Electrochimica Acta 202 (2016) 209–215

Contents lists available at ScienceDirect

Electrochimica Acta

journal homepage: www.elsevier.com/locate/electacta

Multiplexed electrochemical immunosensing of obesity-related hormones at grafted graphene-modified electrodes

G. Martínez-García, L. Agüí, P. Yáñez-Sedeño*, J.M. Pingarrón

Department of Analytical Chemistry, Faculty of Chemistry, University Complutense of Madrid, 28040 Madrid, Spain

ARTICLE INFO

Article history:
Received 28 January 2016
Received in revised form 23 March 2016
Accepted 24 March 2016
Available online 6 April 2016

Keywords:
Ghrelin
Peptide YY
appetite
obesity
electrochemical immunosensor
multiplex

ABSTRACT

An electrochemical immunosensor was prepared for the simultaneous determination of two hormones, ghrelin (GHRL) and peptide YY (PYY), which play important roles in the regulation of hunger and saciety. Dual screen-printed carbon electrodes modified with reduced graphene oxide (rGO) were used as scaffolds for the immobilization of the corresponding capture antibodies. Grafting of the diazonium salt of 4-aminobenzoic acid (4-ABA) on the modified electrode surfaces allowed covalent immobilization of antibodies. Competitive immunoassays were employed and the affinity reactions were monitored by differential pulse voltammetry upon addition of 1-naphthyl phosphate. Under the optimized working conditions, linear current vs. log [hormone] plots extending between 10^{-3} and 100 ng/mL GHRL ($r^2 = 0.990$), and 10^{-4} and 10 ng/mL PYY ($r^2 = 0.992$) were obtained. These ranges are adequate for the determination of both hormones at clinical levels in serum and saliva. An excellent analytical performance in terms of detection limit, reproducibility of the measurements, storage stability and selectivity against other proteins was achieved. The usefulness of the approach was demonstrated by its application to spiked human serum and saliva.

1. Introduction

Among the various hormones involved in the complex regulation of hunger and saciety, ghrelin and peptide YY are noteworthy since they play important roles at the levels of hypothalamus and peripheral circulation [1–3]. Ghrelin (growth hormone-releasing peptide, GHRL) is a peptide hormone containing 28 amino acids secreted in the stomach that acts in the gastrointestinal tract as a stimulant of motor activity, acid secretion and gastric contractility [4]. GHRL levels have shown to be increased before meals to concentrations sufficient to stimulate appetite, and then decreasing [5]. Peptide YY (peptide tyrosine tyrosine, PYY) consisted of 36-amino-acid peptide with a carboxy-terminal tyrosine amide synthesized by endocrine cells in the lower intestine. It acts as a regulator of pancreatic and gastrointestinal functions [6], and plays an important role upon saciety by limiting meal size and overall calorie intake [7,8]. Conversely to GHRL, peaks of increased PYY concentrations appear after meals [9]. From a clinical point of view, the levels of these hormones have been found to be elevated in anorexic patients, while lower levels appear in obese subjects [10].

GHRL concentration in plasma shows great variability depending on the individual and also on the method used for its determination. Values of several units [11] or tenths of ng/mL [12,13] have been found in healthy individuals. In addition, GHRL levels undergo postprandial falls and preprandial rises in circulating levels with peaks around 700 pg/mL in breakfast, lunch and dinner [13]. Regarding PYY, concentration levels in plasma are around 40–70 pg/mL [2]. In this case, variability in circulating levels is lower, with postprandial peaks reaching values around a hundred pg/mL [9].

It is also important to highlight that both hormones can be determined in saliva, this making this fluid, whose extraction is not invasive, a convenient and alternative sample for diagnosis. Salivary concentrations of 183–190 pg/mL GHRL [13] or 15–75 pg/mL PYY [14] have been reported in the literature.

Despite their clinical relevance, methods for determining these hormones are scarce. Various colorimetric ELISA kits for GHRL using competitive or sandwich-type assays with anti-GHRL, biotinylated immunoreagents, and streptavidin labeled with peroxidase are commercially available. Usually, calibration plots show dynamic concentrations ranging from 0.01 (or 0.1) to 100 (or 1000) ng/mL, with minimum detectable concentrations between 0.05 and 1 ng/mL. The assay time varies from 1 h 30 min to 4 h counting from the moment when the antibody was immobilized.

* Corresponding author.
E-mail address: yseo@quim.ucm.es (P. Yáñez-Sedeño).

http://dx.doi.org/10.1016/j.electacta.2016.03.140
0013-4686/

Moreover, ELISA methods based on similar immunoassay schemes for PYY are also available. Competitive configurations involving specific PYY antibodies or biotinylated PYY binding, as well as HRP-labeled avidin or streptavidin conjugates, are the most common. These assays allow the determination of PYY in concentration ranges from 0.1–1 pg/mL to 100–1000 pg/ mL, with minimum detectable concentrations varying from 0.5 pg/mL to approximately 3 pg/mL. The times required for these assays are around 2.5–3.5 h. A scarce number of biosensors for these hormones have been reported in the literature. An example is the colorimetric microarray detection system for GHRL using aptamers technology developed by Mascini et al. [15], with a linear range between 0.2 and 245.5 ng/mL and a detection limit of 0.2 ng/mL,. The same authors proposed also an electrochemical aptasensor involving measurement of the decrease in the guanine oxidation signal in the presence of GHRL with a linear range from 14 to 100 ng/mL and a detection limit of 8 ng/mL [16]. Recently, our group reported the preparation of an electrochemical magnetic immunosensor for GHRL involving anti-GHRL immobilization onto Protein G-magnetic beads and competitive immunoassay using biotinylated GHRL and alkaline phosphatase-streptavidin conjugate. Differential pulse voltammetry of 1-naphthol formed upon addition of 1-naphthyl phosphate allowed the determination of the hormone to be performed in a linear range between 10^{-3} and 10^{3} ng/mL, and a limit of detection of 7 pg/mL [17].

Electrochemical grafting consisting of covalent modification of carbon surfaces by aryl radicals generated from the electrochemical reduction of diazonium salts [18] has demonstrated to be an excellent strategy for immobilization of biomolecules [19–21]. Our group has reported various electrochemical immunosensors designs using such strategy by means of 4-aminobenzoic acid (4-ABA) grafted onto screen-printed electrodes [22–24]. More recently, reduced graphene oxide (rGO)/glassy carbon modified electrodes were also used as electrochemical platforms for grafting with 4-ABA to develop a voltammetric immunosensor for PYY [25]. Following a competitive immunoassay configuration, a calibration plot for PYY with a linear range extending between 10^{-4} and 10^{2} ng/mL, and a limit of detection of 0.01 pg/ mL PYY were obtained.

In this paper, we report the preparation of electrochemical immunosensors for the simultaneous determination of GHRL and PYY which satisfies the requirements of sensitivity, selectivity and reproducibility needed for clinical applications. Screen-printed electrodes modified with reduced graphene oxide (rGO) were used as scaffolds for the immobilization of capture antibodies. The diazonium salt of 4-ABA was electrochemically grafted at the electrode surfaces, resulting in the covalent attachment of 4-carboxy phenyl moiety to the rGO/SPCE. Then, the immunoreagents were covalently immobilized onto the modified electrodes, and competitive immunoassays involving the hormones and the respective biotinylated antigens were performed. Differential pulse voltammetry upon 1-naphtyl phosphate addition was employed to monitor the affinity reactions. The usefulness of the approach was demonstrated by its application to spiked human serum and saliva.

2. Experimental

2.1. Apparatus and electrodes

Electrochemical measurements with dual electrodes were carried out using a 1030 B Multi-potentiostat from CH Instruments provided with a multiplexed data adquisition circuitry (8 channels). A BAS 100B potentiostat provided with a BAS C2EF-1080 cell stand was also used for the electrochemical measurements with glassy carbon electrodes. Dual screen-printed electrodes (C 1110 DropSens) consisted of two elliptic carbon working electrodes with surface area of 5.6 mm^2, a carbon counter electrode and a silver pseudo-reference electrode. Modified 3-mm diameter CHI104 glassy carbon electrodes from CH Instruments, Ag/AgCl/

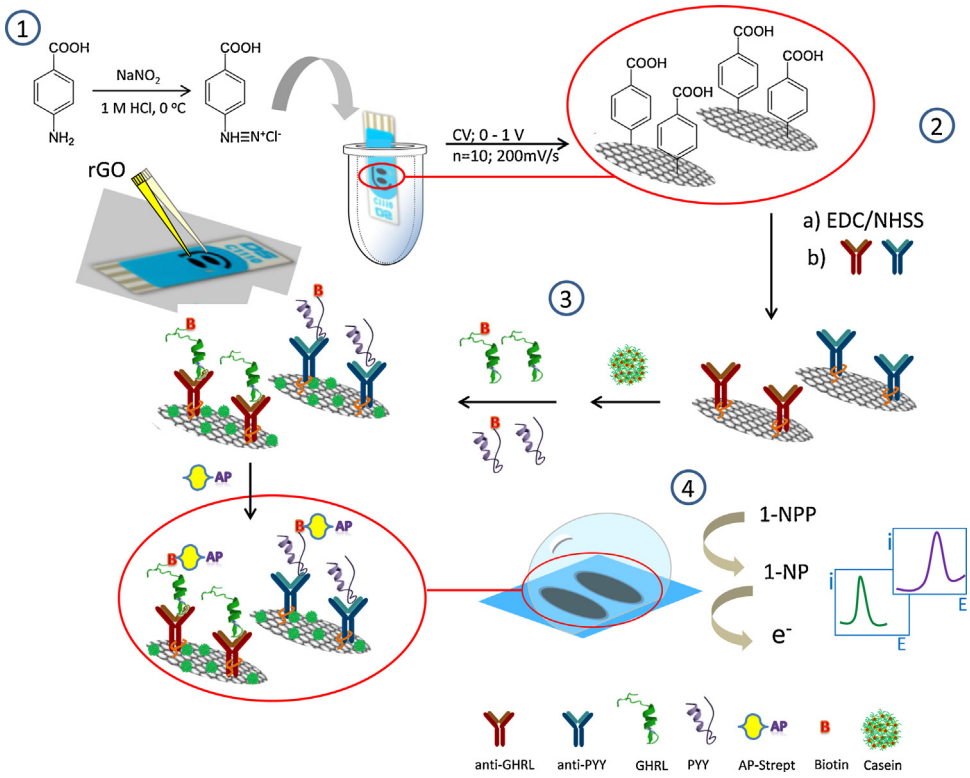

Fig. 1. Schematic display of the different steps involved in the preparation and funcioning of the dual GHRL and PYY immunosensors.

KCl 3 M BAS MF 2063 reference electrode and a BAS MW 1032 Pt wire as auxiliary electrode were also used. All electrochemical experiments were performed at room temperature. A P-Selecta ultrasonic bath, a Vortex (Heidolph) stirrer and a precision Metrohm Herisau E-510 pH-meter were also used.

2.2. Reagents and solutions

Ghrelin (GHRL) rabbit polyclonal antibody (anti-GHRL), GHRL, and biotinylated-GHRL (Biotin-GHRL) were from Anaspec. Peptide YY (3-36) purified IgG antibody (anti-PYY), peptide YY (3-36) (PYY), and biotinylated-PYY (3-36) (Biotin-PYY) were purchased from Phoenix Pharmaceuticals, Inc. Graphene oxide (NIT.GO. M.140.10) was from Nanoinnova Technologies. Alkaline phosphatase labeled-streptavidin (AP-Strept), 1-naphthyl phosphate (1-NPP), 1-ethyl-3-[3-dimethylaminopropyl]carbodiimide hydrochloride (EDC), and N-hydroxysulfo-succinimide (NHSS) were from Sigma. 4-aminobenzoic acid (ABA) was from Across. Ethanolamine (ETA, Aldrich), bovine serum albumin (BSA) from Gerbu, and casein from Thermo Scientific were used as blocking agents. A 0.1 M phosphate buffer solution of pH 7.4 (PBS) was prepared from sodium di-hydrogen phosphate and di-sodium hydrogen phosphate (Scharlau). A 50 mM Tris (tris(hydroxymethyl)amino-methane, Sigma) buffer solution containing 0.05% Tween 20 (Panreac) of pH 7.2, and a 50 mM Tris buffer solution containing 10 mM $MgCl_2$ (Sigma) of pH 9.6 (Trizma) was also used. All reagents solutions were prepared in PBS except AP-Strept and 1-NPP solutions which were prepared in Tris buffer and Trizma buffer, respectively. Insulin, human growth hormone (hGH) and follicle stimulating hormone (FSH), all from Sigma-Aldrich, as well as adiponectin (APN, Abnova), were tested as potentially interfering compounds. De-ionized water was obtained from a Millipore Milli-Q purification system (18.2 MΩ cm).

2.3. Procedures

2.3.1. Preparation of modified electrodes

The method described in [25] with slight changes was followed for the preparation of rGO as well as for grafting of the 4-ABA diazonium salt onto carbon electrodes. Briefly, 2 mL of a 1 mg/mL GO aqueous dispersion were sonicated for 120 min, and then centrifuged at 10,000 g for 10 min. The precipitate was discarded and the supernatant liquid was treated with a 25% NH_3 solution up to pH 9-10 (3.5 μL). Further reduction of GO was performed in the presence of 2 mM ascorbic acid, by keeping a temperature of 95 °C during 15 min. Finally, rGO dispersion was left in the dark at room temperature. The product was replenished every week although it was stable for at least two weeks. Fig. 1 schematizes the procedure followed for modification of dual SPCEs. In step 1, diazonium salt was prepared by adding dropwise 2 mM $NaNO_2$ aqueous solution to a 1 mg/mL 4-ABA solution prepared in 1 M HCl and cooled with ice (38 mL $NaNO_2$ for each 200 mL 4-ABA). The reaction was allowed to proceed during 10 min under stirring. Separately, 3 μL of rGO were deposited onto each working electrode and allowing drying at room temperature. Thereafter, the rGO-modified dual electrode was immersed into the diazonium salt solution and ten successive voltammetric cycles from 0 to −1.0 V (ν = 200 mV/s) were scanned. Finally, the modified SPCEs were washed thoroughly with water (10 s) and methanol (10 s), and dried at room temperature.

2.3.2. Preparation of the immunosensors

Steps 2 to 4 schematizes graphically the protocols employed for the preparation of the dual GHRL and PYY immunosensor. Surface confined carboxylic groups were activated by dropping 3 μL of an EDC/NHSS (0.1 M each) aqueous solution onto each 4-carboxy phenyl-rGO/SPCE modified working electrode (HOOC-Phe-rGO/$SPCE_1$ and HOOC-Phe-rGO/$SPCE_2$) and left to react for 1 h in the dark. After rinsing with water and methanol and allowing drying, immobilization of the capture antibodies was accomplished by casting 3 μL of a 5 μg/mL anti-GHRL solution and 3 μL of a 5 μg/mL anti-PYY solution onto the respective electrodes and left stand for 1 h at 37 °C. Then, 5 μL of a 0.2% casein blocking solution were deposited onto each modified working electrode and incubation was allowed for 1 h at 37 °C. Competitive immunoassays were carried out (step 3 in Fig. 1) by spotting 3 μL of a mixture solution of GHRL (or the sample) and 0.5 μg/mL biotinylated-GHRL (Biotin-GHRL), or 3 μL of a mixture of PYY (or the sample) and 0.1 μg/mL Biotin-PYY onto anti-GHRL-Phe-rGO/$SPCE_1$ and anti-PYY-Phr-rGO/$SPCE_2$, respectively, allowing incubation for 30 min at 37 °C. Thereafter, 10 μL of a 5 μg/mL AP-Strept were dropped onto both Biotin-GHRL-anti-GHRL-Phe-rGO/$SPCE_1$ and Biotin-PYY-anti-PYY-Phe-rGO/$SPCE_2$, and incubation was performed for 30 min at 37 °C. Finally (step 4 in Fig. 1), 45 μL of 50 mM Trizma buffer solution, and 5 μL of 0.05 M 1-NPP solution were deposited on the dual immunosensor and, after a delay time of 5 min for the enzyme reaction to take place, differential pulse voltammograms were recorded over the −0.15 to + 0.70 V range, using ΔE = 50 mV and ν = 20 mV/s. The incubation temperature used in all the steps was that recommended in protocols of commercial ELISA kits.

2.3.3. Analysis of spiked human serum

Samples were lyophilized human serum (S-7394, Sigma) spiked with the hormones at different concentrations. The solid serum was reconstituted in 1 mL of 0.1 M PBS solution of pH 7.4 by mixing up to total dissolution, aliquoted and frozen at −40 °C until assayed. Subsequently, serum was spiked with the target analytes, and determination was performed by applying the procedure described above, the peak current values measured by DPV being interpolated into the linear portion of the calibration graph constructed using the standard solutions.

2.3.4. Analysis of spiked saliva

Saliva samples obtained from a lab researcher were collected using a SalivetteR collection device (Sarstedt). Briefly, the volunteer rinsed the mouth thoroughly with water and then inserted the cotton swab into the mouth and chewed for 1 min. Then, the swap saturated with saliva was inserted into the vial, sealed with the cap and centrifuged for 5 min at 5000 x g. The determination was performed immediately by diluting 1 mL of spiked saliva with 1 mL 0.1 M Tris buffer of pH 7.2 and applying the procedure described above using 3-μL aliquots of the diluted saliva.

3. Results and Discussion

The strategy employed in this work involved covalent immobilization of capture antibodies onto rGO-modified carbon electrodes grafted with p-ABA diazonium salt. This strategy takes advantage of the well-known enhancement of electron transfer processes occurring on rGO-modified electrode surfaces and the high availability of surface confined carboxyl groups, suitable for covalent immobilization of biomolecules, provided by the grafting reaction.

The protocols are described in the Experimental section and schematically displayed in Fig. 1. After a subsequent blocking step of the remaining active free sites on the electrode surface with casein, competitive assays involving the target hormones and biotinylated derivatives for the binding sites of the immobilized antibodies were accomplished. A further conjugation with AP-Strept allowed the voltammetric determination of GHRL and

PYY to be performed using 1-NPP as AP substrate and measuring the peak current, recorded by differential pulse voltammetry, corresponding to the electrochemical oxidation of the generated enzyme reaction product, 1-naphthol.

3.1. Optimization of the experimental variables involved in the preparation of the dual immunosensor

Variables involved in the preparation of a PYY immunosensor by immobilizing anti-PYY on rGO/glassy carbon electrodes grafted with 4-ABA were optimized in a previous work [25]. Therefore, prior to the optimization of the dual configuration for the simultaneous determination of GHRL and PYY, the variables affecting the response of a GHRL immunosensor prepared using the same modified electrode surface were checked and optimized. These included: a) the antibody loading onto HOOC-Phe-rGO/GCE and the time for incubation; b) the Biotin-GHRL loading onto anti-GHRL-Phe-rGO/GCE immunosensor and the time for incubation, and c) the Strept-AP loading onto Biotin-GHRL-anti-GHRL-Phe-rGO/GCE immunosensor and the time for incubation. Other variables involved in the preparation of modified electrodes, covalent binding of antibodies, blocking step and electrochemical detection were the same than those employed with the PYY immunosensor. Details on these optimization studies are provided in Supplementary material and in Figs. S1-S3 and summarized in Table 1.

The different steps involved in the preparation of the immunosensor were characterized by electrochemical impedance spectroscopy (EIS) using 5 mM $Fe(CN)_6^{3-/4-}$ as redox probe in 0.1 M KCl. Fig. 2a displays the Nyquist plots recorded at both bare GCE (1) and rGO/GCE (2). As expected, a smaller electron transfer resistance (R_{CT}) was observed at rGO/GCE with respect to the unmodified GCE which can be attributed to both the larger conductivity and/or the porous diffusion effects of the functionalized graphene electrodes [26]. The Nyquist plots recorded after the sequential immobilization of the biomolecules (Fig. 2b). showed a large increase in the measured R_{CT} value ($5.5 \times 10^4\ \Omega$) upon immobilization of the capture antibody (anti-GHRL) thus confirming the efficiency of the immobilization procedure. As expected, further steps implied in the immunosensors preparation gave rise to larger R_{CT} values as a consequence of the non-conducting compounds incorporation.

3.2. Simultaneous determination of GHRL and PYY at disposable dual immunosensors

The working conditions optimized for both immunosensors prepared individually at modified rGO/GCE were extended to the construction of the dual SPCE immunosensor. Fig. 3 shows the calibration plots obtained for both hormones in the 10^{-7} to 10^4 ng/mL concentration range together with some of the DPV curves recorded for different GHRL and PYYconcentrations. As it can be seen, curves exhibited the expected behavior for competitive immunoassays. The current vs. analyte concentration were fitted by non-linear regression using the Sigma Plot data analysis software with the adjusted equation:

$$y = i_{min} + \left[(i_{max} - i_{min})/1 + (x/E_{50})^{-h}\right]$$

Values of r^2 were 0.991 and 0.994 for GHRL and PYY, respectively, and error bars displayed were calculated from measurements carried out with three different dual immunosensors. The maximal and minimal current values were 2.8 ± 0.2 μA and 0.59 ± 0.08 μA, respectively, for GHRL, and 3.8 ± 0.2 μA and 0.69 ± 0.09 μA for PYY. The EC_{50} values, corresponding to GHRL or PYY concentrations exhibiting fifty per cent competition, were 0.08 ng/mL and 0.005 ng/mL, respectively. The Hill slope values (h) were -0.24 ± 0.04 (GHRL) and -0.32 ± 0.05 (PYY). Logit transformation of the sigmoidal curves by plotting *Ln (p/1-p) vs Ln x*, with $p = (y - i_{min})/(i_{max} - i_{min})$, provided linear graphs ($r^2 = 0.995$ and 0.990, respectively) with slopes values of −0.23 (GHRL) and −0.36 (PYY), which is in agreement, as expected, with the h values calculated above.

Least square fitting of the curves provided linear current vs. log [hormone] plots extending between 10^{-3} and 100 ng/mL GHRL ($r^2 = 0.990$), and 10^{-4} and 10 ng/mL PYY ($r^2 = 0.992$). The slope values of such calibration plots were -246 ± 7 nA and -422 ± 6 nA, respectively, expressed as the current variation per decade of hormone concentration. These ranges are adequate for the determination of both hormones at clinical levels taking into account the expected concentrations in serum [2,11,12] and saliva [13,14].

The limits of detection were calculated as the lowest concentrations that could be differentiated from zero. They were determined by subtracting two times the standard deviations, 2s, with $s = \pm 0.2$ μA for both GHRL or PYY, from the mean current of solutions in absence of hormones. The calculated values were 1.0 pg/mL GHRL and 0.02 pg/mL PYY. These values were in good agreement with those calculated (1.2 pg/mL (GHRL) and 0.06 pg/mL (PYY) from the equation [27]:

$$LOD = EC_{50}\ \{[(i_{max}\text{-}i_{min})/(i_{max}\text{-}i_{min}\text{-}3s)]\text{-}1\}^{-1/h}$$

Interestingly, the achieved LOD value for GHRL is much lower than those previously reported [15,16], and is also various orders of magnitude lower than the minimum detectable concentration provided by ELISA kits methods. For example, a value of 161 pg/mL is specified in RAB0207 Sigma Ghrelin EIA Kit ptotocol. Moreover, the obtained LOD is also remarkably lower than that reported by our group using electrochemical immunosensors based on magnetic particles (GHRL), 7 pg/mL [17]. Similarly, regarding PYY, the LOD achieved with the developed dual immunosensor is much better than the minimum detectable concentration attributed to commercial ELISA kits such as RayBio® or Abnova KA1686 (2.84 pg/mL).

The reproducibility of the voltammetric measurements for 0.1 ng/mL GHRL or 0.01 ng/mL PYY was tested with ten different dual immunosensors prepared on the same day. The RSD values obtained were 2.9% and 2.4%, respectively. Similar RSD values were calculated from measurements performed with dual immunosensors prepared in different days (n = 8), 2.8% for GHRL and 2.9% for PYY. These results revealed both the good repeatability of measurements and reproducibility achieved in the fabrication and functioning of the proposed immunosensing platforms.

The storage stability of the anti-GHRL-Phe-rGO/SPCE and anti-PYY-Phe-rGO/SPCE conjugates was also investigated. Different dual bioelectrodes were prepared on the same day and stored in a refrigerator at 4 °C. Each immunosensor was used to measure the voltammetric response for 0.1 ng/mL GHRL or 0.01 ng/mL PYY. The results obtained in Fig. 4 revealed a high storage stability of the prepared configurations, with the DPV peak currents remaining within the control limits set at ±3 x standard deviation of the

Table 1
Optimization of the experimental variables affecting the performance of the AP-Strept-Biotin-GHRL-anti-GHRL-Phe-rGO/GCE immunosensor.

Variable	Tested range	Selected value
anti-GHRL, μg/mL	1-20	5
Incubation time for anti-GHRL, min	30-90	60
Biotin-GHRL, ng/mL	0.1-1.0	0.5
Incubation time for Biotin-GHRL, min	15-60	30
AP-Strept, μg/mL	0.5-9	5
Incubation time for AP-Strept, min	15-60	30

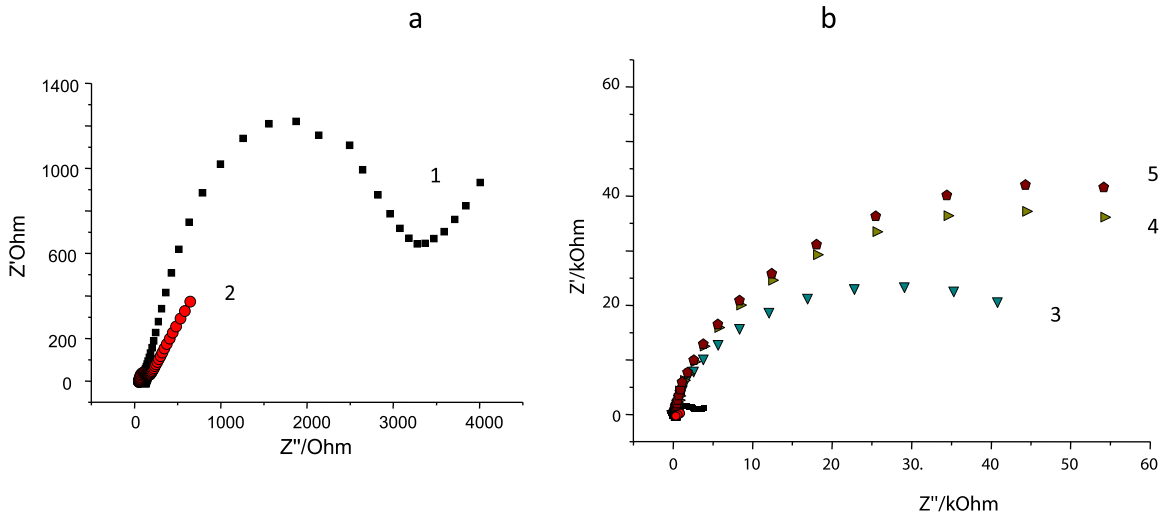

Fig. 2. Nyquist plots obtained by electrochemical impedance spectroscopy at: (1) GCE; (2) rGO/GCE (a); and (3) anti-GHRL-Phe-rGO/GCE; (4) Biotin-GHRL-anti-GHRL-Phe-rGO/GCE; (5) AP-Strept- Biotin-GHRL-anti-GHRL-Phe-rGO/GCE in 5 mM $Fe(CN)_6^{3-/4-}$ in 0.1 M KCl solution.

responses obtained on the first day of the study, for at least 10 days (no longer period of storage time was tested).

3.3. Selectivity

Various proteins that may be found together with GHRL and/or PYY in clinical samples, adiponectin (APN), insulin (INS), human growth hormone (hGH), deacylated GHRL (DA-G), and follicle stimulant hormone (FSH), were checked as potential interfering compounds for the quantification of each target hormone at the dual immunosensor. The currents measured in the absence of GHRL or PYY with the AP-Strept- Biotin-GHRL-anti-GHRL-Phe-rGO/SPCE or AP-Strept- Biotin-PYY-anti-PYY-Phe-rGO/SPCE immunosensors in the presence of the respective interfering substances at a concentration level of 1 μg/mL, were compared with those measured without the tested interfering protein. Moreover, the possible cross-talking between the two target hormones was evaluated. Fig. 5 shows clearly as the mean values of the measured steady state currents were in all cases within the $\pm 2 \times$ standard deviation range of the current measured in absence of GHRL or PYY (first bar in each series), this reflecting an excellent selectivity of the developed dual immunosensor for both hormones against other proteins.

3.4. Determination of GHRL and PYY in spiked human serum and saliva

The usefulness of the developed dual immunosensor for the analysis of real samples was investigated by analyzing human serum and saliva spiked with the hormones at different concentrations corresponding with normal levels expected in these biological fluids. The analysis protocol was described in sections 2.4.3 and 2.4.4. In the case of human serum, an aliquot was 1:1 diluted with the respective biotinylated hormone. The possibility of occurring matrix effects was evaluated by comparing the slopes values of the calibration plots constructed with standard solutions with those obtained from the spiked sample solutions. The slope values of the calibrations plots obtained with these spiked samples were -233 ± 5 nA and -410 ± 8 nA for GHRL and PYY, respectively. A Student t-test provided t_{exp} values of 1.576 (GHRL) and 1.225 (PYY) which were lower than the tabulated value of Student t for n = 5, α=0.05, t_{tab} = 2.776. These results demonstrated that no significant matrix effect was observed in the analysis of serum samples when the described methodology was applied. It is important to note that this methodology involved only a 1:1 serum dilution with the biotinylated antigen conjugate as sample treatment.

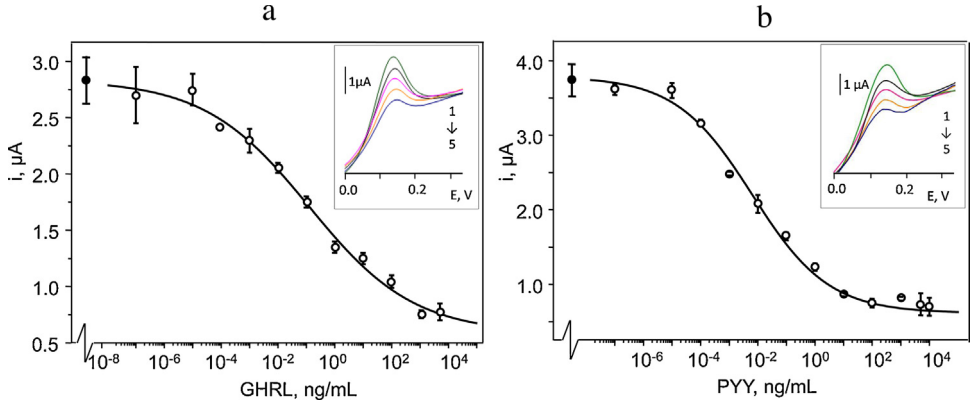

Fig. 3. Calibration plots constructed for GHRL (a) and PYY (b) with the dual immunosensors. Insets: Differential pulse voltammograms recorded for: 10^{-3} (1), 0.01 (2), 0.1 (3), 1.0 (4) and 10 ng/mL (5) GHRL (a), and 10^{-4} (1), 10^{-3} (2), 0.01 (3), 0.1 (4), and 1.0 (5) ng/mL PYY (b).

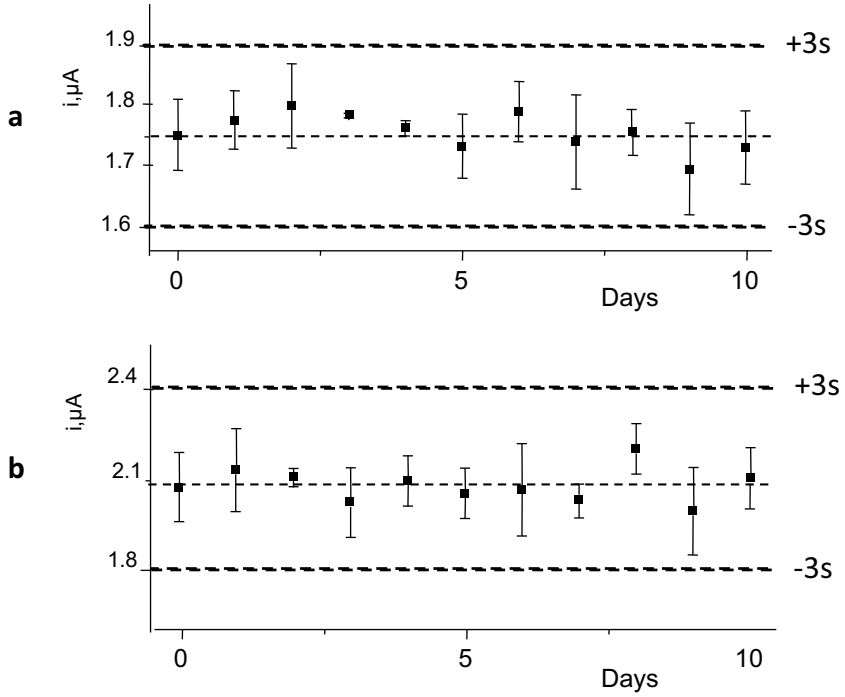

Fig. 4. Control charts constructed to evaluate the storage stability of anti-GHRL-Phe-rGO/SPCE and anti-PYY-Phe-rGO/SPCE conjugates. Each point corresponds to the mean value of three successive measutements for 0.1 ng/mL GHRL (a) or 0.01 ng/mL PYY (b).

Regarding saliva, the protocol described in Procedure 2.4.4 involving a 1:1 sample dilution with 0.1 M Tris buffer of pH 7.2, gave rise to slope values of calibration plots constructed from spiked samples of -228 ± 10 nA (GHRL) and -412 ± 7 nA (PYY), respectively. Similarly to serum samples, a statistical comparison with the slopes obtained from the calibration plots with standards provided t_{exp} of 1.37 and 1.08 for GHRL and PYY, respectively. Both values were also lower than $t_{tab} = 2.776$. Therefore, again no relevant matrix effect was apparent in the analysis of saliva under the working conditions used.

Accordingly, the determination of GHRL and PYY in spiked serum or saliva was accomplished by simple interpolation of the measured i_p values into the respective calibration plot constructed with standard solutions. The results obtained for different target analyte concentration levels are summarized in Table 2. As it can be seen, recovery values ranged between 96 and 103%, with no significant differences due to the different nature of biological sample analyzed, thus demonstrating the suitability of the approach for the accurate analysis of these two biomarkers in human serum and saliva.

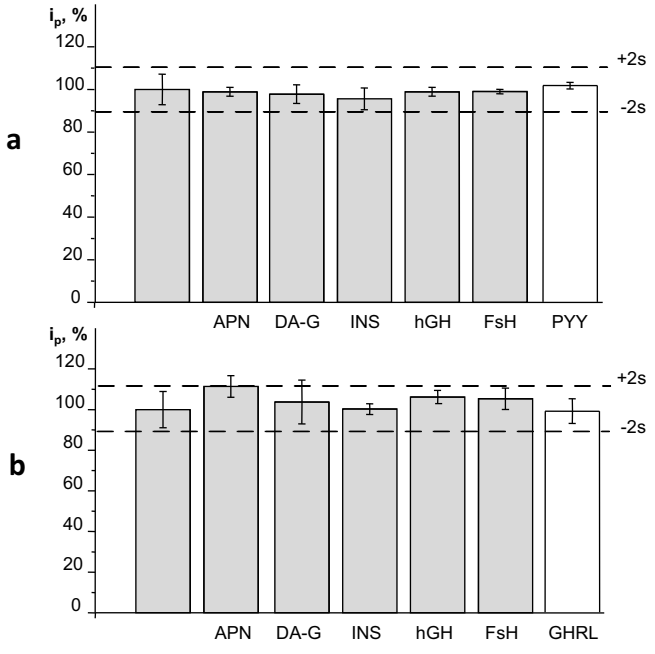

Fig. 5. Effect of the presence of APN, DA-G, INS, hGH, FsH and PYY (a) or GHRL (b), on the differential pulse voltammetric responses obtained with the dual immunosensor for 0 μg/mL GHRL (a) or PYY (b).

4. Conclusions

A dual electrochemical immunosensor for the simultaneous determination of the obesity biomarkers ghrelin and peptide PYY has been developed using screen-printed carbon electrodes modified with reduced graphene oxide (rGO) as scaffolds for the covalent immobilization of capture antibodies through a 4-ABA diazonium salt grafting strategy. The immunosensor exhibited excellent analytical capabilities, allowing detection limits for the

Table 2
Determination of GHRL and PYY in spiked human serum and saliva with the developed dual immunosensor at grafted graphene-modified electrodes.

Sample	Analyte	Added, pg/mL	Found, ng/mL*	Recovery, %
serum	GHRL	175	181 ± 1	103 ± 1
serum	PYY	17.5	16.6 ± 0.1	95 ± 1
serum	GHRL	65	65 ± 5	99 ± 8
		6.5	6.3 ± 0.5	96 ± 7
serum	PYY	35	34 ± 2	98 ± 6
		3.5	3.6 ± 0.3	103 ± 8
saliva	GHRL	95	92 ± 4	97 ± 5
saliva	PYY	37.5	37 ± 1	99 ± 3

*mean value $\pm s_{n-1}$ ($n = 3$).

target analytes to be obtained which are much lower than the minimum detectable concentrations reported for commercial ELISA kits. Moreover, an excellent reproducibility of the measurements obtained with both dual immunosensors prepared on the same day and on different days, and an excellent selectivity against other proteins were also important analytical characteristics. The usefulness of the developed immunosensor for the analysis of real samples was demonstrated by analyzing spiked human serum and saliva with minimal sample treatment. No apparent matrix effect was apparent with both types of samples and the achieved recoveries demonstrated the suitability of the approach for the accurate analysis of these two biomarkers in human serum and saliva.

Acknowledgments

Financial support of Spanish Ministerio de Economía y Competitividad, Research Project CTQ2015-70023-R, and CTQ2015-71955-REDT, and NANOAVANSENS Program from Comunidad de Madrid (S2013/MT-3029) is gratefully acknowledged.

Appendix A. Supplementary data

Supplementary data associated with this article can be found, in the online version, at http://dx.doi.org/10.1016/j.electacta.2016.03.140.

References

[1] T. Riediger, C. Bothe, C. Becskei, T.A. Lutz, Peptide YY directly inhibits ghrelin-activated neurons of the arcuate nucleus and reverses fasting-induced c-Fos expression, Neuronendocrinol. 79 (2004) 317–326.
[2] R.L. Batterham, M.A. Cohen, S.M. Ellis, C.W. Le Roux, D.J. Withers, G.S. Frost, M. A. Ghatei, S.R. Bloom, Inhibition of food intake in obese subjects by peptide YY_{3-36}, N. Engl. J. Med. 349 (2003) 941–948.
[3] M. Kojima, H. Hosoda, Y. Date, M. Nakazato, H. Matsuo, K. Kangawa, Ghrelin is a growth-hormone-releasing acylated peptide from stomach, Nature 402 (1999) 656–660.
[4] Y. Masuda, T. Tanaka, N. Inomata, N. Ohnuma, S. Tanaka, Z. Itoh, H. Hosoda, M. Kojima, K. Kangawa, Ghrelin stimulates gastric acid secretion and motility in rats, Biochem. Biophys. Res. Commun. 276 (2000) 905–908.
[5] M. Kojima, K. Kangawa, Structure and function of ghrelin, Results Probl. Cell Differ. 46 (2008) 89–115.
[6] K. Kohri, K. Nata, H. Yonekura, A. Nagai, K. Konno, H. Okamoto, Cloning and structural determination of human peptide YY cDNA and gene, Biochim. Biophys. Acta 1173 (1993) 345–349.
[7] I.P. Wong, P.A. Baldock, H. Herzog, Gastrointestinal peptides and bone health, Curr. Opin. Endocrinol. Diabetes Obes. 17 (2010) 44–50.
[8] E.C. Khor, N.K.Y. Wee, P.A. Baldock, Influence of hormonal appetite and energy regulators on bone, Curr. Osteoporos. Rep. 8 (2013) 194–202.
[9] B.R. Hill, M.J. de Souza, D.A. Wagstaff, N.I. Williams, The impact of weight loss on the 24-h profile of circulating peptide YY and its association with 24-h ghrelin in normal weight premenopausal women, Peptides 49 (2013) 81–90.
[10] Y. Zhang, R. Proenca, M. Maffei, M. Barone, L. Leopold, J.M. Friedman, Positional cloning of the mouse *obese* gene and its human homologue, Nature 372 (1994) 425–432.
[11] V. Popovic, M. Svetel, M. Djurovic, S. Petrovic, M. Doknic, S. Pekic, D. Miljic, N. Milic, J. Glodic, C. Dieguez, F.F. Casanueva, V. Kostic, Circulating and cerebrospinal fluid ghrelin and leptin: potential role in altered body weight in Huntington's disease, Eur. J. Endocrinol. 151 (2004) 451–455.
[12] T. Shiiya, M. Nakazato, M. Mizuta, Y. Date, M.S. Mondal, M. Tanaka, S.-I. Nozoe, H. Hosoda, K. Kangawa, S. Matsukura, Plasma ghrelin levels in lean and obese humans and the effect of glucose on ghrelin secretion, J. Clin. Endocrinol. Metab. 87 (2002) 240–244.
[13] S. Aydin, I. Halifeoglu, I.H. Ozercan, F. Erman, N. Kilic, N. Ilhan, Y. Ozkan, N. Akpolat, L. Sert, E. Caylak, A comparison of leptin and ghrelin levels in plasma and saliva of young healthy subjects, Peptides 26 (2005) 647–652.
[14] A. Acosta, M.D. Hurtado, O. Gorbatyuk, M. La Sala, D. Duncan, G. Aslanidi, M. Campbell-Thompson, L. Zhang, H. Herzog, A. Voutetekis, B.J. Baum, S. Zolotukhin, Salivary PYY: A putative bypass to saciety, PLoS ONE 6 (2011) e26137.
[15] M. Mascini, G.G. Guilbault, S.J. Lebrun, D. Compagnone, Colorimetric microarray detection system for ghrelin using aptamer-technology, Anal. Lett. 40 (2007) 1386–1399.
[16] M. Mascini, K. Papamichael, I. Mevola, M. Pravda, G.G. Guilbault, Grelin detection using spiegelmer-capture molecules, Anal. Lett. 40 (2007) 403–405.
[17] G. Martínez-García, V. Serafín, L. Agüí, P. Yáñez-Sedeño, J.M. Pingarrón, Electrochemical immunosensor for the determination of total ghrelin hormone in saliva, Electroanalysis 27 (2015) 1119–1126.
[18] P. Allongue, M. Delamar, B. Desbat, O. Fagebaume, R. Hitmi, J. Pinson, J.M. Saveant, Covalent modification of carbon surfaces by aryl radicals generated from the electrochemical reduction of diazonium salts, J. Am. Chem. Soc. 119 (1997) 201–207.
[19] A. Hayat, L. Barthelmebs, A. Sassolas, J.-L. Marty, An electrochemical immunosensor based on covalent immobilization of okadaic acid onto screen printed carbon electrode via diazotization-coupling reaction, Talanta 85 (2011) 513–518.
[20] A.-E. Radi, X. Muñoz-Berbel, V. Lates, J.-L. Marty, Label-free impedimetric immunosensor for sensitive detection of ochratoxin A, Biosens. Bioelectron. 24 (2009) 1888–1892.
[21] B.P. Corgier, C.A. Marquette, L.J. Blum, Diazonium-protein adducts for graphite electrode microarrays modification: Direct and addressed electrochemical immobilization, J. Am. Chem. Soc. 127 (2005) 18328–18332.
[22] M. Moreno-Guzmán, I. Ojeda, R. Villalonga, A. González-Cortés, P. Yáñez-Sedeño, J.M. Pingarrón, Ultrasensitive detection of adrenocorticotropin hormone (ACTH) using disposable phenylboronic-modified electrochemical immunosensors, Biosens. Bioelectron. 35 (2012) 82–86.
[23] M. Moreno-Guzmán, A. González-Cortés, P. Yáñez-Sedeño, J.M. Pingarrón, Multiplexed ultrasensitive determination of adrenocorticotropin and cortisol hormones at a dual electrochemical immunosensor, Electroanalysis 5 (2012) 1100–1108.
[24] I. Ojeda, J. Lopez-Montero, M. Moreno-Guzman, B.C. Janegitz, A. González-Cortes, P. Yáñez-Sedeño, J.M. Pingarrón, Electrochemical immunosensor for rapid and sensitive determination of estradiol, Anal. Chim. Acta 743 (2012) 117–124.
[25] S. Guerrero, G. Martínez-García, V. Serafín, L. Agüí, P. Yáñez-Sedeño, J.M. Pingarrón, Electrochemical immunosensor for sensitive determination of the anorexigen peptide YY at grafted reduced graphene oxide electrode platforms, Analyst 140 (2015) 7527–7533.
[26] C. Punckt, M.A. Pope, I.A. Aksay, On the electrochemical response of porous functionalized graphene electrodes, J. Phys. Chem. C 117 (2013) 16076–16086.
[27] H. Lu, M.P. Kreuzer, K. Takkinen, G.G. Guilbault, A recombinant Fab fragment-based electrochemical immunosensor for the determination of testosterone in bovine urine, Biosens.Bioelectron. 22 (2007) 1756–1763.

SUPPLEMENTARY INFORMATION

Optimization of the experimental variables involved in the preparation of the immunosensor for GHRL

a) Effect of the anti-GHRL loading onto Phe/rGO/GCE; effect of the incubation time

The influence of the amount of antibody immobilized by covalent binding onto the electrode surface modified with 4-ABA diazonium salt was evaluated by checking the voltammetric response obtained with different immunosensors, in the absence of GHRL, constructed upon deposition of 10 μL of anti-GHRL solutions prepared in the 1.0 to 20 μg/mL concentration range, and applying the procedure described in section 2.4.3 with 0.5 μg/mL Biotin-GHRL and 5 μg/mL Strept-AP. Figure S1a shows as the measured i_p value increased with the antibody loading up to 5 μg/mL reaching a saturated response for larger loadings. Therefore, this value was selected for the preparation of the immunosensor. Furthermore, the current measured in the absence of Biotin-GHRL, which corresponded to unspecific interactions, represented less 10% of the maximum current. The time for incubation of anti-GHRL was also optimized over the 30 to 90 min range. The results (Figure S1b) indicated an optimum time for incubation of 60 min.

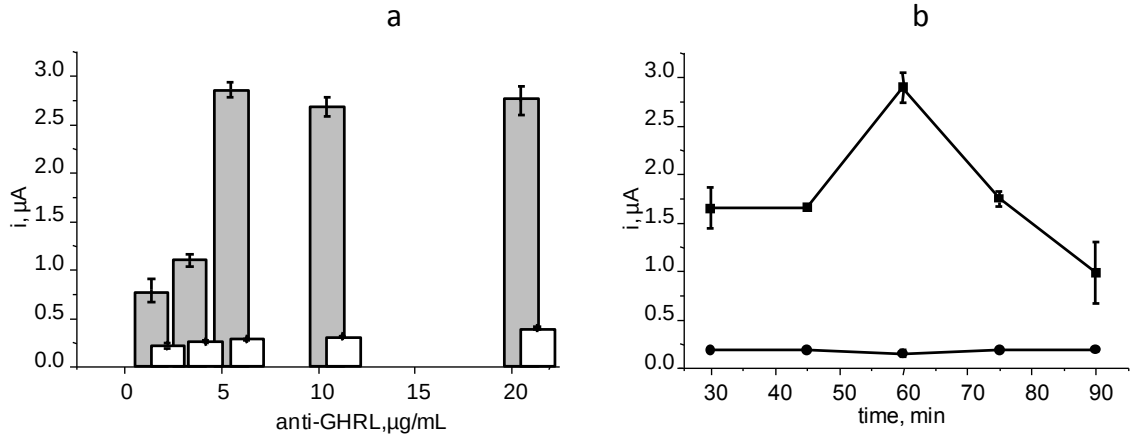

Figure S1. Effect of a) the anti-GHRL loading over the 0.5-20 μg/mL concentration range incubated for 1 h at 37ºC, and b) the time for incubation of anti-GHRL (5 μg/mL), on the DP voltammetric responses measured with the Biotin-GHRL-anti-GHRL-Phe-rGO/GCE immunosensor: 10 μL of a 0.5 mg/mL rGO dispersion, 0.5 μg/mL (grey, ■) or 0 μg/mL (white, ●) Biotin-GHRL incubated for 45 min at 37ºC; 0.2% casein incubated for 1 h at

37 ºC; 5µg/mL AP-Strept incubated for 30 min at 37 ºC; 5 mM 1-NPP, 5 min reaction time at room temperature; DPV, -0.2- +0.7 V; 50 mV/s (b) 20 µg/mL anti-GHRL.

b) Effect of the Biotin-GHRL concentration and the time for incubation onto anti-GHRL-Phe-rGO/GCE

In order to optimize the concentration of Biotin-GHRL, different AP-Strept–Biotin-GHRL-anti-GHRL–Phe-rGO/GCE immunosensors were prepared by incubating in Biotin-GHRL solutions with concentrations ranging from 0.1 to 1.0 µg/mL. The ip values measured in the absence of GHRL (grey bars) showed an increase from 0.1 to 0.7 µg/mL and a slight decrease for higher Biotin-GHRL concentrations (Figure S2a). Furthermore, the results obtained for immunosensors prepared in the absence of anti-GHRL (white bars) showed a slight increase with the Biotin-GHRL concentration. As it can be observed, the largest difference between currents was obtained when using 0.5 µg/mL Biotin-GHRL and, thus, it was selected for further work. Moreover, the incubation time in the Biotin-GHRL solution was also evaluated in the 15 to 60 min interval (Figure S2b) by testing the voltammetric signal obtained with AP-Strept-Biotin-GHRL-anti-GHRL–Phe-rGO/GCE immunosensors in the absence of GHRL. Similar differences between specific and unspecific currents were observed at 30 and 45 min and, therefore, the shorter time, 30 min, was selected as the incubation time to be used.

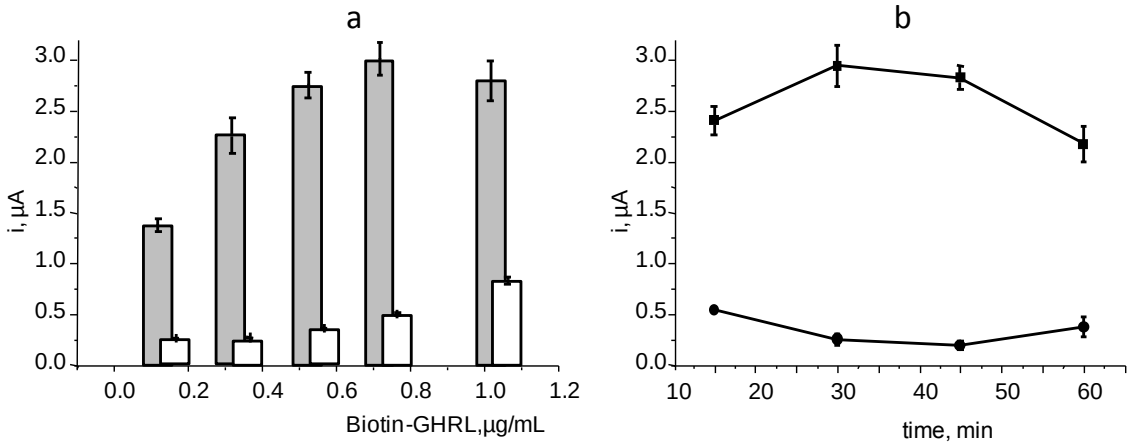

Figure S2. Effect of a) the Biotin-GHRL loading over the 0.1-1.0 µg/mL concentration range incubated for 45 min at 37ºC, and b) the time for incubation of Biotin-GHRL (0.5 µg/mL) on the DP voltammetric responses measured with the Biotin-GHRL-anti-GHRL-Phe-rGO/GCE immunosensor: 10 µL of a 0.5 mg/mL rGO dispersion; 5.0 µg/mL (grey,

■) or 0 μg/mL (white, ●) anti-GHRL incubated for 1 h at 37ºC. Other conditions as in Fig. S1.

c) Effect of the Strept-AP loading onto Biotin-GHRL-anti-GHRL-Phe-rGO/GCE immunosensor and the time for incubation

Different AP-Strept–Biotin-GHRL-anti-GHRL–Phe-rGO/GCE immunosensors were prepared by incubating into AP-Strept solutions in the 0.5 - 9.0 μg/mL concentration range (Figure S3a). Maximum i_p values were obtained in the absence of GHRL (grey bars) with a conjugate concentration of 5 μg/mL. Moreover, the unspecific currents (white bars) slightly decreased as AP-Strept loading increased. These results led us to select the above mentioned AP-Strept concentration for further work. Regarding the incubation time in the AP-Strept solution, a range between 15 to 60 min was tested. As it is shown in Figure S3b, the largest difference between specific and unspecific currents measured at the AP-Strept-Biotin-GHRL-anti-GHRL–Phe-rGO/GCE immunosensor was reached at 30 min, and, therefore, this incubation time was selected.

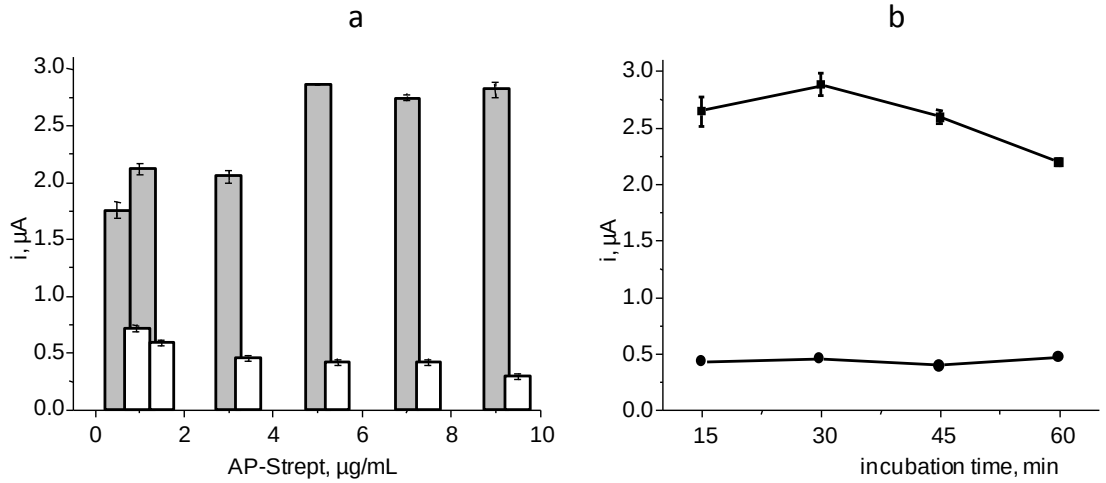

Figure S3. Effect of a) the AP-Strept loading over the 0.5-9.0 μg/mL concentration range incubated for 30 min at 37ºC, and b) the time for incubation of AP-Strept (5μg/mL), on the DP voltammetric responses measured with the Biotin-GHRL-anti-GHRL-Phe-rGO/GCE immunosensor: 10 μL of a 0.5 mg/mL rGO dispersion; 5.0 μg/mL (grey, ■) or 0 μg/mL (white, ●) anti-GHRL incubated for 1 h at 37ºC. Other conditions as in Fig. S2.

9.5. ELECTROCHEMICAL IMMUNOSENSOR FOR ETHYNYL ESTRADIOL USING DIAZONIUM SALT GRAFTING ONTO SILVER NANOPARTICLES-SILICA–GRAPHENE OXIDE HYBRIDS

Talanta 147 (2016) 328–334

Contents lists available at ScienceDirect

Talanta

journal homepage: www.elsevier.com/locate/talanta

Electrochemical immunosensor for ethinylestradiol using diazonium salt grafting onto silver nanoparticles-silica–graphene oxide hybrids

Fernando H. Cincotto [a], Gonzalo Martínez-García [c], Paloma Yáñez-Sedeño [c,*], Thiago. C. Canevari [b], S.A.S. Machado [a], José M. Pingarrón [c]

[a] Institute of Chemistry, State University of São Paulo, São Carlos, Brazil
[b] Engineering School, Mackenzie Presbiterian University, São Paulo, Brazil
[c] Department of Analytical Chemistry, Faculty of Chemistry, University Complutense of Madrid, Madrid, Spain

ARTICLE INFO

Article history:
Received 10 August 2015
Received in revised form
18 September 2015
Accepted 24 September 2015
Available online 1 October 2015

Keywords:
Ethinylestradiol
EE2
Electrochemical immunosensor
Silver nanoparticles
Graphene oxide
Urine

ABSTRACT

This work describes the preparation of an electrochemical immunosensor for ethinylestradiol (EE2) based on grafting of diazonium salt of 4-aminobenzoic acid onto a glassy carbon electrode modified with silver nanoparticles/SiO_2/graphene oxide hybrid followed by covalent binding of anti-ethinylestradiol (anti-EE2) to activated carboxyl groups. A competitive immunoassay was developed for the determination of the hormone using peroxidase-labeled ethinylestradiol (HRP-EE2) and measurement of the amperometric response at −200 mV in the presence of hydroquinone (HQ) as redox mediator. The calibration curve for EE2 exhibited a linear range between 0.1 and 50 ng/mL (r^2=0.996), with a detection limit of 65 pg/mL. Interference studies with other hormones related with EE2 revealed the practical specificity of the developed method for the analyte. A good reproducibility, with RSD=4.5% (n=10) was also observed. The operating stability of a single bioelectrode modified with anti-EE2 was maintained at least for 15 days when it was stored at 4 °C under humid conditions between measurements. The developed immunosensor was applied to the analysis of spiked urine with good results.

1. Introduction

Ethinylestradiol (EE2) is one of the most potent synthetic estrogenic hormones. It is an essential constituent of oral contraceptives widely prescribed in women [1,2]. Adverse effects of EE2 include accelerated coagulation and fibrinolysis. Furthermore, use of combined hormonal contraceptives has shown to be associated with increased risk of venous thrombosis depending on estrogen concentration [3,4]. EE2 is rapidly absorbed orally, yielding a peak in plasma between 1 and 2 h after taking [5]. A major challenge is the presence of residues of EE2 and its derivatives in the environment coming from excretions, where negative impact on the reproductive system in wildlife and human can be produced [6].

The relevance of EE2 determination both in biological and environmental samples has made available a large number of analytical methods. In addition to chromatography using GC or HPLC coupled to at least one mass spectrometer, various immunoassay methods have been developed. RIA and ELISA methods were reported early to determine EE2 in body fluids [7,8]. Currently, various ELISA kits are available for the analysis of biological samples or water. Table 1 summarizes the analytical characteristics of some of these configurations. A typical assay is based on competitive interaction between EE2 and biotinylated EE2 for the binding sites of a pre-coated specific antibody. Colorimetric detection using a peroxidase conjugate, H_2O_2 and TMB, allows the EE2 determination to be performed in a non-linear dynamic range extending up to thousands of pg/mL, and with an analysis time lasting about 2–2.5 h [6]. Other immunoassay formats using fluorimetric [9] or chemiluminiscence measurements [10] were also described. A competitive microfluidic immunoassay based on the immobilization of anti-EE2 on 3-aminopropyl functionalized magnetic beads and amperometric detection, was also reported [11]. Regarding immunosensors, a configuration was proposed using magnetic beads functionalized with a synthetic estrogen derivative. Competitive immunoassay with anti-EE2, alkaline phosphatase-labeled IgG, and 1-naphthyl phosphate, allowed the determination of the estrogen with a limit of detection of 10 pg/mL using square wave voltammetric detection [12].

Hybrid materials prepared from graphene and SiO_2 constitute excellent substrates for the development of electrochemical sensors. The huge conductivity, high surface area, biocompatibility and robustness of graphene, coupled with the physical and chemical resistance of silica, its hydrophylicity, chemical inertness, and the high surface area/volume ratio, all contribute to increase the electroactive surface, thus enhancing sensitivity [13]. On the

* Corresponding author.

http://dx.doi.org/10.1016/j.talanta.2015.09.061
0039-9140/

Table 1
Analytical performance of some methods based on immunoassay for the determination of ethinylestradiol (EE2)

Configuration and methodology	Dynamic range, pg/mL	LOD, pg/mL	Reproducibility, RSD,%	Total time, min	Application	Ref.
CEK510Ge ELISA kit (Uscn) Immobilization of monoclonal anti-EE2. Competitive immunoassay between biotin-EE2 and EE2. Addition of HRP-avidin. Colorimetric detection using H_2O_2 and TMB	24.6–2000	9.28	< 10% (intra-assay) < 12% (inter-assay)	≈ 120	Biological fluids	
ABIN1873485 (Abyntek) Immobilization of monoclonal anti-EE2. Competitive immunoassay between biotin-EE2 and EE2. Addition of HRP-avidin. Colorimetric detection using H_2O_2 and TMB	24.7–2000	9.28	< 10% (intra-assay) < 12% (inter-assay)	150	Biological fluids	
R-Biopharma™ Ridascreen ELISA Kit. Competitive immunoassay between EE2 and HRP-EE2. Colorimetric detection using H_2O_2 and TMB	up to 8100	370	< 10% (intra-assay) < 10% (inter-assay)	150	Bovine urine	
Ecologiena™ EE2 ELISA Kit (Tokiwa Chemical Industries). Competitive immunoassay between EE2 and HRP-EE2. Colorimetric detection using H_2O_2 and TMB	50–3000	–	< 10%	150	Water	–
Competitive ELISA immunoassay using a biotinylated EE2 derivative and HRP-streptavidin. Colorimetric detection using H_2O_2 and TMB	22–1200	14 ($S/N=3$)	< 5%	120	Water	[6]
Competitive immunoassay using total internal reflection fluorescence (TIRF) with Cy5 labeled antibody, or energy transfer (ETIA) with Cy5 labeled EE2 or Cy5.5 labeled antibody	60–1.8×10^4 (TIRF); 40–2×10^5 (ETIA)	70 (TIRF) 10 (ETIA			Waste water	[9]
Competitive ELISA immunoassay using a HRP-EE2-6-CMO conjugate and chemiluminescence detection.	0.8–100	0.2 ± 0.1	< 10%	40	Water	[10]
Competitive microfluidic immunoassay using EE2 and HRP-EE2. Immobilization of anti-EE2 on 3-aminopropyl-MBs. Amperometric detection with H_2O_2 and catechol at a gold electrode.	0.01–60	0.09	4.1% (intra-assay) 5.8% (inter-assay)	30	River water	[11]
Electrochemical AP-IgG-anti-EE2-EE2-hexa-MBs/SPCE immunosensor. Competitive immunoassay using anti-EE2, AP-IgG and 1-NPP. SWV detection	0.1–5×10^4	10	–	120	Waters	[12]
Electrochemical HRP-EE2-anti-EE2/AgNPs/SiO_2/GO/GCE immunosensor. Competitive immunoassay between EE2 and HRP-EE2. Amperometry with H_2O_2 using HQ as redox mediator.	10^2–5×10^4	65	4.5% (intra-assay) 5.4% (inter-assay)	120	Human urine	This work

Key: HRP, horseradish peroxidase; TMB, tetramethylbenzidine, EE2-6-CMO, 1,3,5(10)-estratrien-17-ethinyl-3,17-diol-6-one-6-carboxymethyloxime, 1-NPP, 1-naphthyl phosphate.

other hand, metallic nanoparticles are characterized by their electrocatalytic ability together with the capacity for adsorption of biomolecules, biocompatibility and high conductivity. In this context, it has been claimed that functionalization of graphene with SiO_2 allows anchoring metal nanoparticles securely onto graphene support with a high dispersion thus enhancing the catalytic performance [14]. Despite their properties, only few examples of the use of metallic nanoparticles /silica/graphene hybrids can be found in the literature in connection to the preparation of electrochemical (bio)sensors. A hybrid material prepared with gold nanoparticles (AuNPs) immobilized onto mesoporous silica-coated reduced graphene oxide (rGO) was reported for cancer cell detection through hydrogen peroxide sensing [15]. Moreover, an interleukin-6 (IL-6) electrochemical immunosensor was prepared making use of AuNPs-graphene-silica sol–gel as immobilization biointerface and AuNP-poly-dopamine (PDA) @carbon nanotubes as the label of HRP-bound antibodies [16]. Recently, Cincotto et al. [17] reported the synthesis and characterization of AgNPs/SiO_2/GO hybrid and the preparation of a voltammetric sensor for the simultaneous determination of epinephrine and dopamine in urine. A good distribution of silver nanoparticles in the SiO_2/GO material was found with a synergistic effect among the hybrid components producing electrocatalytic activity toward the electrochemical responses thus leading to a high sensitivity and selectivity.

The work described in this manuscript faces the double objective of addressing the lack of immunosensors for the determination of EE2, and explores for the first time the ability of AgNPs/SiO_2/GO hybrids for the preparation of electrochemical immunosensors. The designed strategy for capture antibodies immobilization involved 4-aminobenzoic acid (ABA) grafting onto AgNPs/SiO_2/GO glassy carbon (GCE) modified electrodes by electrochemical reduction of the corresponding diazonium salt. This strategy provided a suitable surface for covalent attachment of the capture antibody allowing the development of a competitive immunoassay for the determination of the hormone using peroxidase-labeled ethinylestradiol (HRP-EE2), and measuring the amperometric response at −200 mV upon addition of H_2O_2 in the presence of hydroquinone (HQ) as redox mediator.

2. Experimental

2.1. Reagents and solutions

Graphite (Aldrich), tetraethylorthosilicate (TEOS, Sigma-Aldrich, 98%) and silver nitrate (Sigma-Aldrich, 99%) were used for the synthesis of the hybrid material. 4-aminobenzoic acid (ABA, Across), 1-ethyl-3-[3–dimethylaminopropyl]carbodiimide hydrochloride (EDC, Sigma) and N-hydroxysulfo-succinimide (NHSS, Sigma), were also used. Ethinylestradiol (EE2, Aldrich), anti-ethinyl-estradiol (anti-EE2), and HRP-labeled ethinylestradiol (HRP-EE2), both from Fitzgerald, were the reagents used for the immunosensor preparation. 0.1 M phosphate buffer solutions of pH 7.2 (PBS) and pH 6.0 were prepared from NaH_2PO_4 and Na_2HPO_4 (Scharlau, 99%). Blocker casein in PBS (Thermo), hydroquinone (HQ, Sigma), and H_2O_2 (Scharlau, 35%) were also employed.

Cortisol, β-estradiol (E2), estriol (E3), progesterone (Prog) and testosterone (Test), all from Sigma, were tested as potential interfering compounds. Solutions of each compound at a 10^{-3} μg/mL concentration in PBS were prepared. All other chemicals and solvents used were of analytical-reagent grade and distilled water was obtained from a Milli-Q purification system (Millipore, Bedford, NA, USA).

2.2. Apparatus

Voltammetric measurements were carried out using a PGSTAT 101 potentiostat from Autolab controlled by Nova 1.6 electrochemical software (EcoChemie B.V.). A dual-channel ultrasensitive INBEA potentiostat (Inbea biosensores S.L. Spain) was used for amperometric measurements. A three electrodes (BAS VC-2 10-mL) glass electrochemical cell was used. Modified 3-mm diameter CHI 104 glassy carbon electrodes from CH Instruments were utilized as working electrodes. The reference electrode was an Ag/AgCl/KCl 3 M BAS MF 2063 and the auxiliary electrode was a BAS MW1032 Pt wire. All the electrochemical experiments were performed at room temperature. A P-Selecta ultrasonic bath, an Optic Ivymen System constant temperature incubator shaker (Comecta S.A.), and a P-Selecta Agimatic magnetic stirrer, all distributed by Scharlab, Madrid, Spain, were also used.

2.3. Procedures

2.3.1. Preparation of AgNPs/SiO_2/GO Hybrid

The method used was that reported in Ref. [17]. Briefly, 10 g of each graphite and $NaNO_3$ were dispersed in 46 mL of concentrated sulfuric acid by continuous stirring in an ice bath. Then, 6.0 g of $KMnO_4$ were slowly added under stirring, and the reaction mixture was kept on ice for 24 h. Thereafter, 240 mL of water were added and temperature of the stirred solution was raised to 98 °C for 1 h. After addition of 85 mL of 30% (v/v) H_2O the resulting product (GO) was filtered, washed three times with 5% (v/v) HCl, and dried at 50 °C for 48 h.

The SiO_2/GO hybrid was prepared by dispersing 4.5 μmol of TEOS in 1/1 (v/v) ethanol under stirring for 10 min. Then, 0.4 mL of water and 90 mg of GO were added. The suspension was stirred for 10 min and 30 μL of hydrofluoric acid (47%) were added under sonication until gel formation. The obtained gel was stored at room temperature for up to seven days and then grounded. The resulting powder was washed with ethanol in a Soxhlet for 2 h, and heated at 50 °C to evaporate residual solvent.

AgNPs/SiO_2/GO was prepared by adding 0.5 g of SiO_2/GO to 15 mL of an 8×10^{-3} M $AgNO_3$ solution in dimethylformamide (DMF). The mixture was sonicated for 1 h at 25 °C in the dark and the solid was recovered by centrifugation, washed with DMF, and treated at 110 °C for 4 h in a furnace.

2.3.2. Preparation of the EE2 immunosensor

The GCE surface was polished with 0.3 μm alumina slurries, rinsed thoroughly with deionized water, sonicated for 5 min in ethanol and 5 min in water, and dried in air. Then, the polished electrode was electrochemically cleaned by repetitive cyclic voltammetry in 0.1 M sulfuric acid over the 0–1 V vs. Ag/AgCl potential range. AgNPs/SiO_2/GO/GCEs were prepared by suspending 0.5 mg AgNPs/SiO_2/GO in 1 mL DMF and sonicating for 10 min. Then, 10 μL of the resulting suspension were dropped onto the GCE surface and the modified electrode allowed to dry overnight.

Grafting of 4-aminobenzoic acid (ABA) diazonium salt was performed as follows (see Fig. 1). Firstly, 20 mg of ABA were dissolved in 2 mL of 1 M HCl and cooled with ice. Then, the diazonium salt was prepared by adding 2 mM $NaNO_2$ aqueous solution dropwise to this solution (38 μL for each 200 μL) with constant stirring. Next, 40 μL from the resulting solution were placed onto the modified electrode and ten successive voltammetric cycles between 0.0 and-1.0 V at $\nu = 200$ mV/s were carried out. Thereafter, the modified electrodes were washed thoroughly with water and methanol and dried at room temperature. In a second step, 10 μL of an EDC/NHSS (0.1 M each) aqueous solution prepared in 0.1 M phosphate buffer of pH 6.0 were placed onto the modified electrode and left to react for 1 h. After rinsing with water and methanol, and drying, 10 μL of a 20 μg/mL anti-EE2 solution were dropped onto the electrode and incubated at 37 °C for 45 min. Then, 20 μL of a 1% casein blocking solution were deposited onto the anti-EE2-Phe-AgNPs/SiO_2/ GO/GCE, and left to incubate for 1 h at 37 °C. In order to perform the competitive assay, 10 μL of a mixture of the appropriated standard EE2 solution (or the sample) and 1/100 diluted HRP-EE2 were placed onto the electrode surface and incubated for 1 h at 37 °C. After each modification step, the modified electrode was washed with 0.1 M PBS of pH 7.2. EE2 determination was accomplished in the same buffer solution by amperometric detection at −0.20 V in the presence of 45 μL of 1 mM HQ after addition of 5 μL of 50 mM H_2O_2.

2.3.3. Determination of EE2 in urine

Urine samples were collected from a healthy adult female volunteer. Samples were aliquoted and stored at −20 °C, and

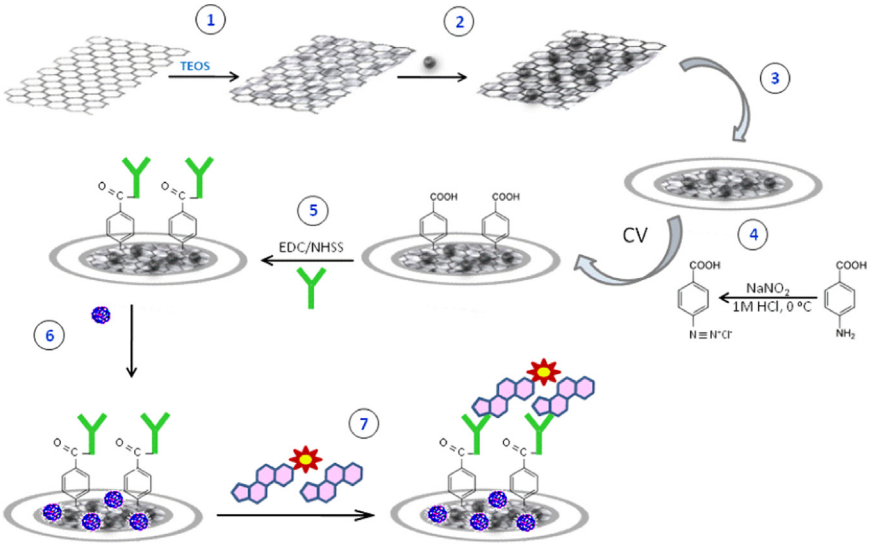

Fig. 1. Schematic display of the different steps involved in the preparation of the immunosensor for EE2: (1) synthesis of SiO_2/GO; (2) preparation of AgNPs/SiO_2/ GO hybrid; (3) adsorption of AgNPs/SiO_2/GO onto GCE; (4) grafting of 4-ABA diazonium salt onto AgNPs/SiO_2/GO/GCE; (5) activation of carboxyl groups and covalent immobilization of anti-EE2; (6) blocking with casein; (7) competitive assay between EE2 and HRP-EE2.

analyzed directly upon dilution with buffer. It would be mentioned that all ethical and human rights guidelines in the sampling procedure were obeyed. The determination of EE2 was made by applying the experimental procedure described above to samples spiked with the hormone at 0.1; 0.5; 1.0 and 10 ng/mL concentration levels.

3. Results and discussion

As it was commented in the Introduction section, this work explores for the first time the ability of AgNPs/SiO_2/GO hybrids for the preparation of electrochemical immunosensors, which can be justified by the synergistic effect found by Cincotto et al. among the hybrid components giving rise to enhanced electrocatalysis [17]. AgNPs/SiO_2/GO was prepared by mixing SiO_2/GO gel with silver ions dissolved in DMF and sonicated for 1 h in the dark. This method led to the production of DMF radicals which were responsible for the formation of silver nanoparticles [18]. Characterization of this material by electron microscopy and X-ray techniques revealed the presence of graphene sheets incorporated in the silica matrix together with homogeneously distributed silver nanoparticles with a diameter around 20 nm [17]. Then, AgNPs/SiO_2/GO/GCEs were prepared by dropping 10 μL of AgNPs/SiO_2/GO hybrid suspènded in DMF on the GCE surface and allowing to dry overnight.

Fig. 1 illustrates the steps involved in the preparation of the developed immunosensor. As it was also described in Section 2.3.2, diazotized ABA was obtained by reaction with sodium nitrite in hydrochloride acid and the resulting 4-carboxybenzenediazonium ion solution was dropped onto the modified electrode surface. Cyclic voltammetric scans between 0.0 and −1.0 V at ν=200 mV/s completed the grafting process. Thereafter, surface-confined carboxyl groups were activated with EDC/NHSS and anti-EE2 antibodies were covalently attached to the electrode through the formation of amide bonds. After a blocking step with casein, a competitive assay between EE2 and HRP-EE2 for the binding sites of the immobilized antibodies was accomplished. Hydrogen peroxide was used as the HRP substrate to detect the immunosensing event in the presence of hydroquinone, by measuring the amperometric response at −200 mV vs Ag/AgCl.

3.1. Electrochemical characterization

As commented above, the affinity reaction was electrochemically monitored using H_2O_2 as HRP substrate and a redox mediator. This was selected by checking the cyclic voltammetric responses recorded at the AgNPs/SiO_2GO/GCE from 1 mM solutions of hydroquinone (HQ) or catechol in 0.1 M PBS as they are commonly employed for this purpose. Although Fig. 2a shows that both compounds exhibited a quasi-reversible behavior at the modified electrode, the peak current values were considerably larger for HQ, which was the selected for further work. Moreover, CVs for 1 mM HQ solutions were recorded at GO/GCE, SiO_2/GO/GCE and AgNPs/SiO_2/GO/GCE for comparison purposes. As it can be observed, the peak potential values obtained at the electrodes prepared without AgNPs were similar, with peak-to-peak separation (ΔE) of ca. 600 mV in both cases. However, a significant decrease of 136 mV in the ΔE value was produced at the AgNPs/SiO_2/GO/GCE and the peak current values were also larger (27% and 15% for the anodic and cathodic peaks, respectively). These observations are in agreement with those previously reported for the electrochemical behavior of dopamine and epinephrine [17] and were attributed to the presence of AgNPs onto SiO_2/GO/GCE enhancing the electrocatalytic ability of the hybrid nanomaterial towards the quinone/hydroquinone electrochemical process.

Furthermore, the different modified electrodes were characterized by electrochemical impedance spectroscopy using 5 mM $Fe(CN)_6^{3-/4-}$ 0.1 M KCl as electrochemical probe. Fig. 3 shows the Nyquist plots recorded at GO/GCE (curve 1), SiO_2/GO/GCE (curve 2) and AgNPs/SiO_2/GO/GCE (curve 3). As it can be seen, the charge transfer resistance at the GO/GCE (R_{CT}=1362 Ω) is significantly higher than that at SiO_2/GO/GCE (R_{CT}=331 Ω), and decreased slightly after further modification with AgNPs (R_{CT}=233 Ω). These results can be explained taking into account the presence of graphene sheets incorporated into the porous of the silica matrix, thus providing a good conductivity for the SiO_2/GO modified electrode. Furthermore, the R_{CT} value increased dramatically upon immobilization of anti-EE2 (curve 4), with R_{CT}=23342 Ω, because of the partially insulating barrier on the electrode surface due to the proteins immobilization.

3.2. Capture antibodies immobilization

Covalent binding of anti-EE2 can be achieved by carbodiimide chemistry with the activated carboxylic moieties present on the grafted electrode surface thus assuring stable immobilization [19]. The advantage of using the AgNPs/SiO_2/GO hybrid surface compared to bare GCE or intermediate assemblies is demonstrated by comparing the amperometric measurements recorded at immunosensors prepared by grafting of 4-ABA diazonium salt and covalent immobilization of anti-EE2 antibody onto the AgNPs/SiO_2/GO/GCE and onto SiO_2/GO/GCE, GO/GCE and bare GCE (Fig. 4A). As it can be seen, the AgNPs/SiO_2/GO/GCE immunosensor provided remarkably larger specific responses (corresponding to

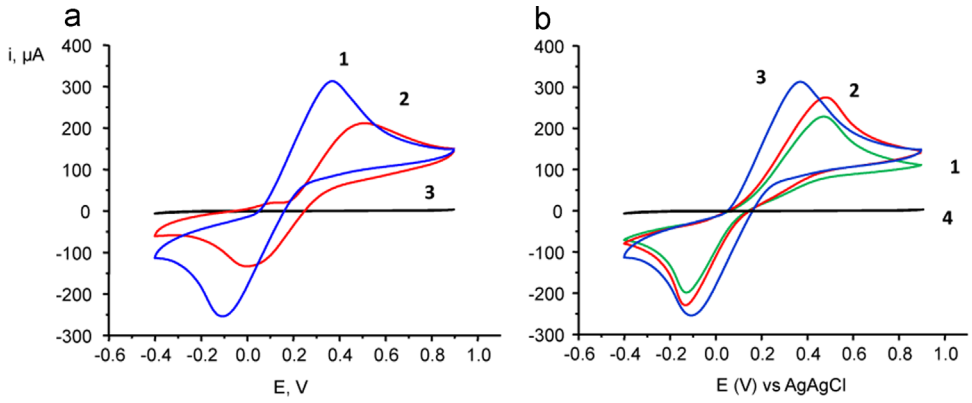

Fig. 2. Cyclic voltammograms recorded at the AgNPs/SiO_2/GO/GCE (A) for 1 mM hydroquinone (1) and catechol (2) in 0.1 M PBS pH 7.2; (3) background current. (B) for 1 mM hydroquinone at (1) GO/GCE, (2) SiO_2/GO/GCE and (3) AgNPs/SiO_2/GO/GCE; (4) background current; ν=50 mV/s.

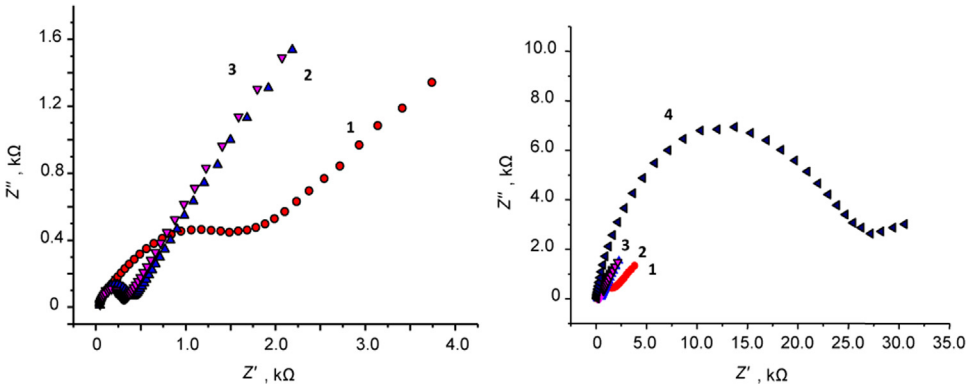

Fig. 3. Nyquist plots recorded at GO/GCE (1); SiO_2/GO/GCE (2); AgNPs/SiO_2/GO/GCE (3) and anti-EE2-Phe-AgNPs/SiO_2/GO/GCE (4). 5 mM $Fe(CN)_6^{3-/4-}$ 0.1 M KCl.

HRP-EE2 interaction at anti-EE2-Phe-AgNPs/ SiO_2/GO/GCE) as a consequence of both the efficient immobilization of anti-EE2 and the improved electrochemical behavior found with the hybrid nanomaterial. Moreover, competitive signals (dark grey bars) were similar with the three nanostructured immunosensors thus indicating that a good competition between HRP-EE2 and EE2 for the binding sites of the immobilized antibodies occurred regardless the electrode composition. These responses were of small magnitude as corresponds to the relatively high EE2 concentration used. Regarding unspecific signals (black bars), i.e. those measured in the absence of capture antibody, low and similar values were observed at all the nanostructured electrodes while it was much larger at the bare GCE probably due to the adsorption of HRP-EE2 conjugate which also would explain the large competitive signal measured with the unmodified electrode.

Moreover, the benefits of the selected immobilization approach on the immunoassay performance were verified by comparing it with the results obtained by simple adsorption of anti-EE2 on the hybrid-modified electrode surface (Fig. 4B). As it is clearly observed, the immunosensor prepared by simple adsorption of the antibody onto AgNPs/SiO_2/GO/GCE showed a much lower specific current than that measured with the immunosensor constructed by covalent anti-EE2 immobilization and, furthermore, it was similar to that corresponding to unspecific interactions. This different behavior should be attributed to the differences in antibody immobilization efficiency which may be also related to the different surface property due to the absence of the aryldiazonium layer [22]. However, it is interesting to note that even with this inefficient immobilization strategy, the competition still works although in a limited extension (dark grey column in Fig. 4B) which proved the suitable selection of immunoreagents.

3.3. Optimization of the experimental variables involved in the immunosensor preparation

The experimental conditions used to carry out grafting, i.e. diazotation and activation of carboxyl groups, were the same than those optimized by our group in the preparation of an electrochemical immunosensor for adrenocorticotropin [19]. Moreover, other variables affecting the performance of the developed immunosensor were optimized. These studies involved the evaluation of (i) the loading of antibody at AgNPs/SiO_2/GO/GCE and the time for incubation; (ii) the blocking step; (iii) the HRP-EE2 loading onto the anti-EE2/AgNPs/SiO_2/GO/GCE and the time for incubation. Details on these optimization studies are provided in Supplementary material and in Fig S1–S3. A summary of the results is made in Table 2.

3.4. Analytical characteristics for EE2 determination

Fig. 5 shows the dependence of the biosensor amperometric response with EE2 concentration over the 5×10^{-4}–5×10^{3} ng/mL under the optimized experimental conditions. Error bars were calculated for measurements carried out with three different modified electrodes. As expected, a sigmoidal shape typical of a competitive enzyme immunoassay, in which binding of the antigen-enzyme conjugate (HRP-EE2) is inhibited by the addition of free antigen (EE2), and the concentration is inversely proportional to the free antigen added, was obtained [20]. The current vs. EE2 concentration was fitted by non-linear regression with the adjusted four parameters equation (r^2=0.994):

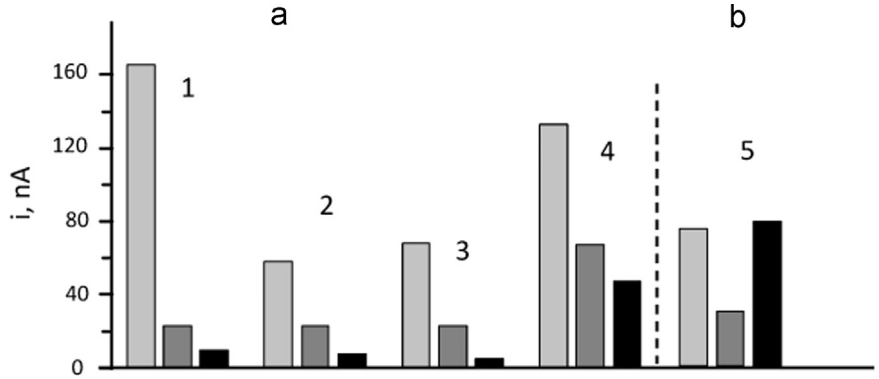

Fig. 4. Amperometric responses recorded at immunosensors prepared (A) by grafting of 4-ABA diazonium salt and covalent immobilization of anti-EE2 antibody onto (1) AgNPs/SiO_2/GO/GCE; (2) SiO_2/GO/GCE; (3) GO/GCE; (4) GCE, and (B) by adsorption of anti-EE2 antibody onto AgNPs/SiO_2/GO/GCE: specific (light grey), competitive (dark grey) and unspecific (black) responses. Anti-EE2, 20 μg/mL (0 μg/mL unspecific); EE2 (competitive): 0.5 μg/mL (A), 10 μg/mL (B); HRP-EE2: 1/100 dilution (A); 1/100 dilution (B) (specific and unspecific), 1/50 dilution (competitive). See text for other conditions.

Table 2
Optimization of the performance conditions of the HRP-EE2-anti-EE2/AgNPs/ SiO_2/GO/GCE immunosensor.

Variable	Tested range	Selected value
Anti-EE2, μg/mL	0–50	20
Incubation time for anti-EE2, min	0–120	45
Blocking agent type	Ethanolamine, casein, BSA	casein
Incubation time for blocking, min	30–75	60
HRP-EE2, dilution	1/200–1/50	1/100
Incubation time for HRP-anti-APN, min	30–75	60

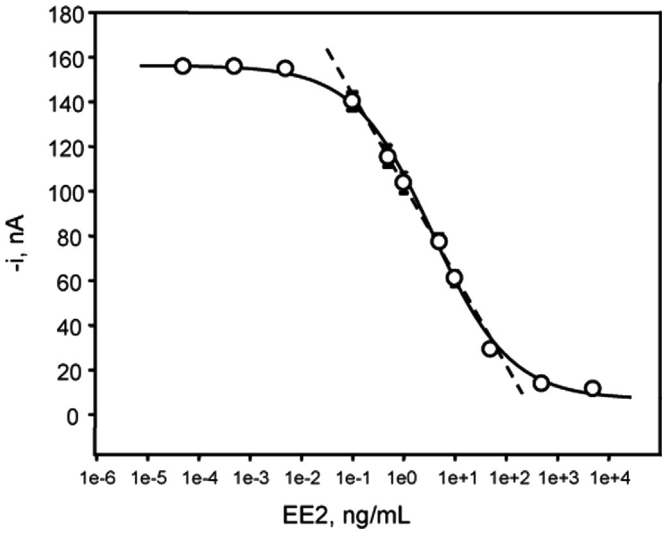

Fig. 5. Calibration plot for EE2 at the anti-EE2-Phe-AgNPs/SiO_2/GO/GCE immunosensor. See text and Table 2 for the experimental conditions.

$$y = i_{min} + \frac{i_{max} - i_{min}}{1 + (\frac{x}{E50})^{-h}}$$

where i_{max}=155.6 nA and i_{min}=6.1 nA were the maximum and minimum current values of the calibration curve. The EC_{50} value, corresponding to the EE2 concentration for a fifty per cent inhibition, was 3.3 ng/mL, while the Hill slope, h, which determines the curvature of the calibration graph and gives an idea of the assay sensitivity (with optimum values close to unity [21]) was −0.57. Logit transformation of the sigmoidal curve by plotting $\mathrm{Ln}\frac{p}{1-p}$ vs $\mathrm{Ln}\,x$, with $p = (y - i_{min})/(i_{max} - i_{min})$ provided a linear graph that deviated from linearity for EE2 concentration lower than 0.05 ng/mL. The slope of such line was −0.59, which appreciably coincides with the h value mentioned above.

Least square fitting of the curve provided a linear current vs. log [EE2] plot (r^2=0.994) extending between 0.1 and 50 ng/mL with a slope value of 41 ± 1 nA, expressed as the current value per decade of EE2 concentration. The limit of detection was calculated as the lowest EE2 concentration that could be differentiated from zero. It was determined by subtracting two times the standard deviations (2 s, with $s = \pm$ 4.7 nA) from the mean current of solutions containing no EE2. The calculated value was 0.065 ng/mL EE2 which is in agreement with the LOD value, 0.063 ng/mL, calculated from the equation [21]:

$$LOD = EC_{50}\left(\frac{i_{max} - i_{min}}{i_{max} - i_{min} - 3s} - 1\right) - \frac{1}{h}$$

The reproducibility of the measurements carried out with the immunosensor was also evaluated. Amperometric measurements for 0.1 ng/mL EE2 were made with immunosensors prepared on the same day or on five different days. The RSD values obtained were 4.5% (n=10) or 5.4% (n=10), respectively.

The achieved analytical characteristics of the immunosensor are suitable for the determination of EE2 in biological samples where concentrations in the range of tenths of ng/mL are found [6]. The linear range of the calibration plot is much wider and the precision much higher than that reported with the ELISA kits. However, the detection limit obtained with the immunosensor is higher than the so-called minimum concentration detectable with the colorimetric assay (9.28 pg/mL) as well as the value obtained using the microfluidic immunoassay (0.09 pg/mL) [11]. Nevertheless, this comparison is not entirely correct since different criteria were used to calculate the mentioned values.

The storage stability at 4 °C of anti-EE2/AgNPs/SiO_2/GO/GCE conjugates was evaluated by measuring the amperometric response of immunosensors prepared after adding the blocking agent and the HRP-EE2 conjugate. The results obtained (not shown) revealed that the initial response of the immunosensor was maintained within the limits of control set at ± 3 times the standard deviation of the measurements (n=10) carried out on the first day, during at least 15 days after the immunosensor preparation, thus showing a good storage stability.

3.5. Interferences study

Various steroid hormones structurally related with ethinylestradiol such as cortisol, β-estradiol (E2), estriol (E3), progesterone and testosterone (see Fig S5 for the structures), were tested as potential interfering compounds. The effect of the presence of each compound was evaluated from the currents measured, under the optimal experimental conditions, using HRP-EE2-anti-EE2/AgNPs/SiO_2/GO/GCE conjugates for 1 ng/mL EE2 and interfering compound. Fig. 6 shows as only E2 and testosterone gave rise to relative current percentages very slightly above the limit corresponding to the ± 2 s range. This was also observed using other methodologies. For example, E2 showed higher cross-reactivity than that from other estrogenic hormones in the ELISA methods described by Schneider´s group using spectrophotometric or chemiluminiscent detection [7,13]. Both compounds are structurally similar, being E2 the product of testosterone aromatization reaction, with the hydroxy group at the C-17 position and no other functional group incorporated into such a ring. Therefore, it can be concluded that the selected antibody is able to discriminate on the basis of these differences.

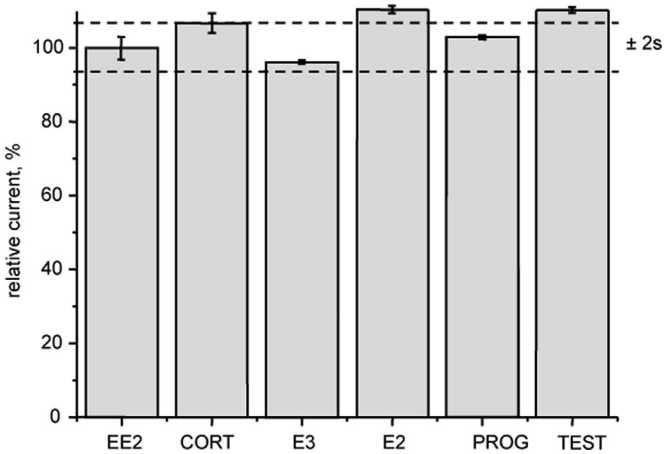

Fig. 6. Effect of the presence of cortisol, E3, E2, progesterone and testosterone on the amperometric responses obtained for 0 ng/mL EE2 with the anti-EE2-Phe-AgNPs/SiO_2/GO/GCE immunosensor.

Table 3
Determination of EE2 in spiked urine with the HRP-EE2-anti-EE2/AgNPs/SiO_2/GO/GCE immunosensor.

Sample	EE2 added, ng/mL	EE2 found, ng/mL	EE2, mean value, ng/mL[1]	Recovery, %
1	0.1	0.097; 0.100; 0.095;0.098; 0.098	0.098 ± 0.002	98 ± 2
2	0.5	0.50; 0.51; 0.51;0.50; 0.50	0.50 ± 0.01	100 ± 1
3	1.0	0.97; 1.0; 0.95:0.98; 0.98	0.98 ± 0.02	98 ± 2
4	5.0	4.8; 4.7; 5.0; 4.8; 4.9	4.8 ± 0.1	96 ± 1

[a] mean value ± $ts/\sqrt{n}$.

3.6. Determination of EE2 in spiked urine

The applicability of the HRP-EE2-anti-EE2/AgNPs/SiO_2/ GO/GCE immunosensor for the determination of EE2 in biological samples was demonstrated by analyzing urine which was spiked with the hormone at four different concentration levels: 0.1, 0.5, 1.0 and 10 ng/mL. Previously, blanks of unspiked diluted urine were tested and no detectable content of the hormone was found. Then, as it was described in the Experimental section, the spiked samples were analyzed without any treatment step except dilution. In order to evaluate the existence of potential matrix effect, a calibration plot for EE2 in urine was constructed by appropriate dilution. Figure S5 displays the overlapped calibration plots constructed with standard EE2 solutions and from the diluted urine samples. The slope value calculated for the linear portion of this latter calibration plot was 38 ± 2 nA per decade of concentration. A statistical comparison using the Student *t*-test with the slope value of the calibration graph prepared with EE2 standards, 41 ± 1 nA per decade of concentration, showed that t_{exp}, 1.34, was lower than the tabulated value, 2.306, for $n=8$, at a 0.05 significance level, indicating that no no significant differences existed between both slope values. Accordingly, significant matrix effect could be discarded and the determination of EE2 in human urine could be carried out simply by interpolation of the amperometric measurements from the sample solutions into the calibration plot constructed with standards. Table 3 summarizes the results obtained. As it can be observed, satisfactory recoveries, ranging between $96 \pm 1\%$ and $100 \pm 1\%$, were obtained for five replicates and for all the tested concentration levels.

4. Conclusions

An electrochemical immunosensor has been developed for the amperometric determination of the estrogenic hormone ethinylestradiol. The biosensor design explores for the first time the ability of prepared AgNPs/SiO_2/GO hybrids as a convenient scaffold for such purpose. Capture antibodies were covalently immobilized on activated 4-aminobenzoic acid grafted onto AgNPs/SiO_2/GO glassy carbon modified electrodes by electrochemical reduction of the corresponding diazonium salt. This immunoelectrode design together with the competitive immunoassay developed making use of peroxidase-labeled ethinylestradiol allowed the determination of the hormone over the 0.1–50 ng/mL linear concentration range and with a detection limit of 0.065 ng/mL. These characteristics along with the high precision and selectivity exhibited by the immunosensor makes it highly appropriate for the determination of the estrogenic hormone in biological samples. This was demonstrated by analyzing human urine samples spiked with the analyte at four different concentration levels ranging from 0.1 to 10 ng/mL.

Acknowledgments

Financial support of Spanish Ministerio de Economía y Competitividad, Research ProjectCTQ2012-35041, and NANOAVANSENS Program from Comunidad de Madrid (S2013/MT-3029) is gratefully acknowledged.

Appendix A. Supplementary material

Supplementary data associated with this article can be found in the online version at doi:10.1016/j.talanta.2015.09.061.

References

[1] P.R. Galvinas, W. Moreira da Silva, V.M. Rezende, R.A. Moreno, J. Chromatogr. B 877 (2009) 3601.
[2] S.J. Keam, A.J. Wagstaff, Treat. Endocrinol. 2 (2003) 49.
[3] Cardiovascular disease and steroid hormone contraception, Report of a WHO Scientific Group, 877 [i–vii], 2011. pp. 1–89.
[4] M. Raps, J. Curvers, F.M. Helmerhorst, B.E.P.B. Ballieux, J. Rosing, S. Thomassen, F.R. Rosendaal, H.A.A.M. van Vliet, Thromb. Res. 133 (2014) 640–644.
[5] A. Baumann, A. Fuhrmeister, M. Brudny-K, I. Cippel, C. Draeger, T. Bunte, W. Kuhnz, Contraception 54 (1996) 234.
[6] C. Schneider, H.F. Schöler, R.J. Schneider, Steroids 69 (2004) 245.
[7] K. Fotherby, J.O. Akpoviroro, L. Siekmann, H. Breuer, J. Steroid Biochem. 14 (1981) 499.
[8] R.L. Tacey, W.J. Harman, L.L. Kelly, J. Pharm. Biomed. Anal. 12 (1994) 1303.
[9] I. Coille, S. Reder, S. Bucher, G. Gauglitz, Biomol. Eng. 18 (2002) 273.
[10] C. Schneider, H.F. Schöler, R.J. Schneider, Anal. Chim. Acta 551 (2005) 92.
[11] N.A. Martínez, R.J. Schneider, G.A. Messina, J. Raba, Biosens. Bioelectron. 25 (2010) 1376.
[12] H. Kanso, L. Barthelmebs, N. Inguimbert, T. Noguer, Anal. Chem. 85 (2013) 2397.
[13] A. Walcarius, A. Kuhn, Trac-Trends Anal. Chem. 27 (2008) 593.
[14] T.H. Thi Vu, T.T. Thi Tran, H.N. Thi Le, L.T. Tran, P.H.T. Nguyen, H.T. Nguyen, N. Q. Bui, Electrochim. Acta 161 (2015) 335.
[15] S.K. Maji, S. Sreejith, A.K. Mandal, X. Ma, Y. Zhao, ACS Appl. Mater. Interfaces 6 (2014) 13648.
[16] G. Wang, X. He, L. Chen, Y. Zhu, X. Zhang, Coll. Surf. B: Biointerfaces 116 (2014) 714.
[17] F.H. Cincotto, T.C. Canevari, A.M. Campos, R. Landers, S.A.S. Machado, Analyst 139 (2014) 4634.
[18] I. Pastoriza-Santos, L.M. Liz-Marzán, Langmuir 15 (1999) 948.
[19] I. Ojeda, J. López-Montero, M. Moreno-Guzman, B.C. Janegitz, A. González-Cortés, P. Yáñez-Sedeño, J.M. Pingarrón, Anal. Chim. Acta 743 (2012) 117.
[20] P. Tijssen, Practice and theory of enzyme immunoassays, in: R.H. Burdon, P. H. van Knippenberg (Eds.), Laboratory Techniques in Biochemistry and Molecular Biology, vol. 15, Elsevier, Amsterdam, 1985, p. 19.
[21] H. Lu, M.P. Kreuzer, K. Takkinen, G.G. Guilbault, Biosens. Bioelectron 22 (2007) 1756.
[22] C.A. Mandon, L.J. Blum, C.A. Marquette, Chem. Phys. Chem. 10 (2009) 3273.

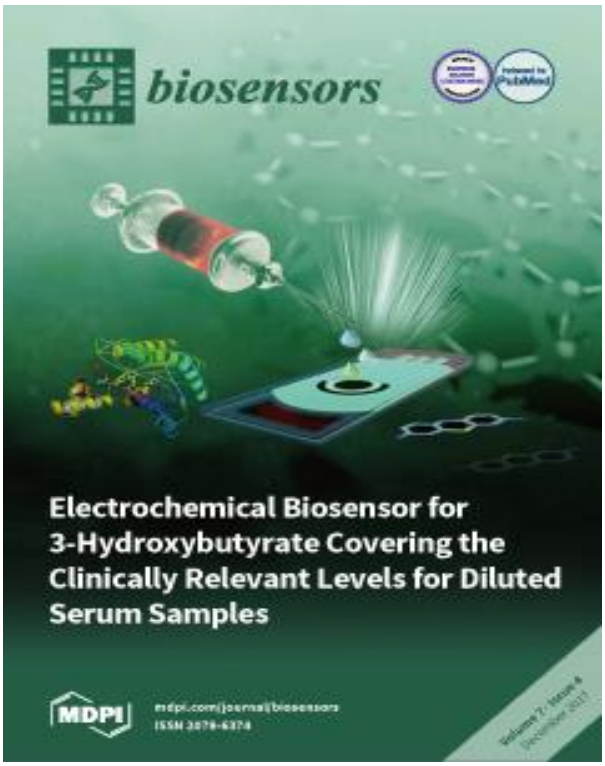

9.6. AN ELECTROCHEMICAL ENZYME BIOSENSOR FOR 3-HYDROXYBUTYRATE DETECTION USING SCREEN-PRINTED ELECTRODES MODIFIED BY REDUCED GRAPHENE OXIDE AND THIONINE

biosensors

MDPI

Article

An Electrochemical Enzyme Biosensor for 3-Hydroxybutyrate Detection Using Screen-Printed Electrodes Modified by Reduced Graphene Oxide and Thionine

Gonzalo Martínez-García [1], Elena Pérez-Julián [1], Lourdes Agüí [1], Naomí Cabré [2], Jorge Joven [2], Paloma Yáñez-Sedeño [1,*] and José Manuel Pingarrón [1]

[1] Departamento de Química Analítica, Facultad de CC. Químicas, Universidad Complutense de Madrid, E-28040 Madrid, Spain; quimigon@gmail.com (G.M.-G.); elena.epj@hotmail.com (E.P.-J.); malagui@quim.ucm.es (L.A.); pingarro@quim.ucm.es (J.M.P.)

[2] Unitat de Recerca Biomèdica (URB-CRB), Antic Hospital Universitari de Sant Joan c/Sant Joan s/n, 43201 Reus, Spain; noemi.cabre@gmail.com (N.C.); jjoven@grupsagessa.com (J.J.)

* Correspondence: yseo@quim.ucm.es; Tel.: +34-91-394-4317; Fax: +34-91-394-4329

Received: 23 October 2017; Accepted: 10 November 2017; Published: 11 November 2017

Abstract: A biosensor for 3-hydroxybutyrate (3-HB) involving immobilization of the enzyme 3-hydroxybutyrate dehydrogenase onto a screen-printed carbon electrode modified with reduced graphene oxide (GO) and thionine (THI) is reported here. After addition of 3-hydroxybutyrate or the sample in the presence of NAD^+ cofactor, the generated NADH could be detected amperometrically at 0.0 V vs. Ag pseudo reference electrode. Under the optimized experimental conditions, a calibration plot for 3-HB was constructed showing a wide linear range between 0.010 and 0.400 mM 3-HB which covers the clinically relevant levels for diluted serum samples. In addition, a limit of detection of 1.0 μM, much lower than that reported using other biosensors, was achieved. The analytical usefulness of the developed biosensor was demonstrated via application to spiked serum samples.

Keywords: 3-hydroxybutyrate; graphene; thionine; electrochemical biosensor; diabetic ketoacidosis

1. Introduction

Blood ketone testing is considered a useful tool to detect potentially life-threatening ketoacidosis. The levels of 3-hydroxybutyrate (3-HB), one of the major ketone compounds in blood, are established between 1.1 and 3 mM in clinically significant hyperketonemia and above 3 mM in diabeticketoacidosis (DKA) [1,2]. Increased 3-HB levels in blood serum result from fatty acids degradation occurring when the body uses these acids instead of carbohydrates toobtainenergy. This situation appears when the individual is undergoing long periods of physical exercise, vomiting or fasting, as well as in type I diabetes mellitus patients with insulin deficiency. It is well known that uncontrolled diabetes can lead to the production of acetone (2%), acetoacetate (20%), and 3-HB (78%) from fatty acid catabolism [1]. Moreover,3-HB is one of the biological markers with altered values in patients with morbid obesity, the determination of this marker having a great interest in the control of this and related diseases [3].

On the other hand, it is widely accepted that the excellent properties of graphene such as large surface area, good electrical conductivity, wide potential window, low resistance to charge transfer, good electrocatalytic activity, and ease of functionalization and mass production, make this nanomaterial an excellent choice to construct electrochemical scaffolds to be used in the preparation of sensitive and reliable electrochemical biosensors. Furthermore, graphene possesses a high density of defects at the edges, which act as active points for the electron transfer to biomolecules such as redox enzymes [4]. Despite these unique characteristics, the use of graphene in the construction of

enzyme biosensors is limited by the low solubility of this nanomaterial in polar and nonpolar solvents and the absence of functional groups, which makes the efficient immobilization of biomolecules difficult. Chemical modification of graphene is used to partially solve these drawbacks. For example, the presence of hydrophilic oxygenated groups in graphene oxide (GO) decreases the interaction between graphite layers, although the formation of structural defects and vacancies that interrupt the carbonaceous sp^2 network leads to a worsening of the nanomaterial electronic properties. Reduction of GOrestores a large part of the conductivity, while some defects are not eliminated, and can minimize the problems of low reactivity [5]. The reduction of the oxygenated groups in GO can be performed electrochemically [6] or chemically using any reducing agent such as hydrazine, sodium borohydride, *p*-phenylenediamine, hydroquinone, or sodium hydrosulfite [7]. In order to avoid the use of toxic reagents, and perform a green reduction, Zhang et al. proposed the use of L-ascorbic acid as the reducing agent [8]. Although the resulting rGO still contains oxygenated functional groups, they are in much smaller number than those in the original GO suchthat this material combines both graphene and GO characteristics showing good conductivity and providing sites for anchoring to enzymes or other species specific for detection applications [9].

Few electrochemical biosensors have been reported in the literature for the determination of 3-HB. Table 1 shows thatmost of them used the enzyme 3-hydroxybutyrate dehydrogenase (3-HBDH) and involved the NAD^+/NADH system. The enzyme 3-HBDH specifically catalyzes the conversion of the analyte to acetoacetate (AA), leading to the production of NADH, which is anelectroactive detectable product. The inherent problems related to the large overvoltage for the electrochemical oxidation of NADH, as well as the fouling of the working electrode have been minimized using different electrode materials and redox mediators. In this context, the immobilization of 3-HBDH onto screen-printed electrodes modified by coenzyme functionalized carbon nanotubes was used [10]. The electrocatalytic effect of carbon nanotubes allowed the detection of NADH to be carried out at a potential of −0.15 V vs. Ag/AgCl, and the determination of 3-HB between 10 and 100 μM witha limit of detection (LOD) value of 9 μM. An enzyme-based Clark electrode was used in a bienzyme configuration with 3-HBDH and salicylate hydroxylase (SHL). In this biosensor, once 3-HB was dehydrogenated in the presence of 3-HBDH and NAD^+, the generated NADH was consumed by reaction with salycilate catalyzed by SHL in the presence of oxygen. Consumption of dissolved oxygen was monitored amperometrically for the determination of 3-HB [11]. A disposable amperometric biosensor with 3-HBDH immobilized on screen-printed carbon electrodes (SPCEs) was prepared using a layer of carboxymethylcellulose (CMC) hydrophilic gel to adsorb the enzyme alongside NAD^+ cofactor and $Fe(CN)_6{}^{3-}$ as the electron transfer mediator [12]. Other redox mediators such as 1,10-phenanthroline quinone [13] or Meldola Blue [14] have also been used. Recently, an electrochemical biosensor prepared with paper electrodes and 1,10-phenantroline-5,6-dione as the redox mediator was reported for the determination of 3-HB in blood [15]. Moreover, a configuration using $[Ru(bpy)_3]^{2+}$ and graphene oxide was described by Veerapandian et al. for the determination of 3-HB in cow serum [16]. A screen-printed electrode fabricated with iridium–carbon particles was also used for the determination of 3-HB taking advantage of the electrocatayzed responses of NADH at the modified material [17].

Table 1. Some electrochemical enzyme biosensors for the determination of 3HB.

Electrode	Biosensor Fundamentals	Technique/E Detec.	Linear Range /LOD, mM	Sample	Ref.
3-HBDB/NAD^+/SWCNTs/SPCE	3-HB + NAD^+ (3-HBDH)→NADH. Detect. NADH	CV/−150 mV vs. Ag/AgCl	0.01–0.1/0.009	human serum	[10]
Clark electrode	3-HB + NAD^+ (3-HBDH)→NADH NADH+O_2(SHL)→NAD^+ Detect. O_2 consumption	amperom.−600mV vs. Ag/AgCl	0.008–0.8/0.0039	spiked human serum	[11]
3-HBDB/NAD^+/$Fe(CN)_6^{4-}$/CMC/SPCE	3-HB + NAD^+ (3-HBDH)→NADH Detect. NADH with $Fe(CN)_6^{4-}$	amperom. +300 mV vs. Ag/AgCl	0.014–5.3/0.014	human serum	[12]
1,10-PQ/NAD^+/3-HBDH/SPCE	3-HB + NAD^+ (3-HBDH)→NADH Detect. NADH with 1,10-PD	+200 mV vs. Ag/AgCl	0–6/-	spiked blood	[13]
3-HBDH–FSM8.0/NAD+/MB/SPCE	3-HB + NAD^+ (3-HBDH)→NADH Detect. NADH with MB	amperom. −50 mV vs. Ag/AgCl	0.03–8/0.0292	-	[14]
1,10-PD/NAD^+/3-HBDH/EPAD	3-HB + NAD^+ (3-HBDH)→NADH Detect. NADH with 1,10-PD	amperom. +200 mV	0–6/0.3	spiked whole blood	[15]
3-HBDH/$[Ru(bpy)_3]^{2+}$/GO/NAD^+/SPCE	3-HB + NAD^+ (3-HBDH) → NADH. Detect. NADH with $[Ru(bpy)_3]^{2+}$	amperom. +60 mV vs. Ag/AgCl	0.2–2.0/-	bovine serum	[16]
SPIrCE	3-HB + NAD^+ (3-HBDH)→NADH Detect. NADH	amperom. +200 mV vs. Ag/AgCl (T = 37.5 °C)	0–10/-	bovine serum	[17]
3-HBDH/THI/rGO/SPCE	3-HB + NAD^+ (3-HBDH)→NADH Detect. NADH with THI	amperom. 0 mV vs. Ag	0.003–0.4/0.001	spiked human serum	This work

CMC: carboxymethyl cellulose; EPAD: electrochemical paper-based analytical device; FSM8.0: mesoporous silica; MB: Meldola Blue; 1,10-PD: 1,10-phenanthroline-5,6-diol; 1,10-PQ: 1,10-phenanthroline quinone; SPIrC: carbon-ink containing iridium; THI: thionine; LOD: limit of detection.

In this work, we describe an electrochemical platform prepared with SPCEs modified with reduced graphene oxide (rGO) for the construction of a 3-HBDH enzyme biosensor and detection of NADH in the presence of NAD^+, using thionine (THI) as the redox mediator. Graphene-modified electrodes have been demonstrated to provoke a remarkable enhancement in the electron transfer rate of NADH oxidation probably because of the existence of defects providing many active sites at the electrode surface [18,19]. Moreover, among the different redox mediators used to electrocatalyze the electrochemical oxidation of NADH, THI has been shown to decrease the corresponding detection potential up to −0.1 V on CNT-modified electrodes [20]. The as prepared enzyme bioelectrode allows for the determination of 3-HB at clinically relevant levels in diluted human.

2. Experimental

2.1. Apparatus

Amperometric measurements were made with a BAS electrochemical analyzer model 100 B (1308 series) coupled to a Faraday cage and a current amplifier PreAmplifier PA-1 provided with the BAS 100/W electrochemical analysis software. Impedimetric measurements were made using a μAutolab type 3 potentiostat controlled by the FRA2 software (Ecochemie). This instrument was also used for voltammetric measurements using the GPES software (Ecochemie). Screen-printed carbon electrodes (SPCEs, 110 DRP, 4 mm Ø, were purchased from DropSens (Oviedo, Spain). These electrodes include a silver pseudoreference electrode and a carbon counter electrode. SPCEs modified with rGO and thionine were used as the working electrodes. A precision Crison Basic 20+ pH-meter, a P-Selecta Ultrasons ultrasonic bath, a P-Selecta Digaterm 100 thermostatic bath, a Vortex Wizard (VELP Scientifica, Usmate, Italy) stirrer, and a centrifuge MPW-G5R MedInstrument were also used.

2.2. Reagents and Solutions

The enzyme 3-hydroxybutyrate dehydrogenase (3-HBDH) from *Pseudomonas lemoignei* lyophilized powder, ≥200 units/mg protein, and thionine were from Aldrich (Madrid, Spain). 3-HB (Alfa Aesar, 98%), NAD^+ (Gerbu, 99.6%), and NADH (Sigma, 97%) were also used. Graphene oxide (NIT.GO.M.140.10) was from (Madrid, Spain). Ascorbic acid (Gerbu, >99%) and ammonia solution (Scharlau, 32%) were used for the preparation of rGO. Sodium citrate (99%), glutamine (99%), glutamate (98%), succinate (98%), uric acid (99%), and glucose (99.5%), all from Sigma (Madrid, Spain), were tested as interferents. A 0.1 M phosphate buffer solution of pH 7.0 (PBS) was prepared from sodium di-hydrogen phosphate (Scharlau, 98%–100%) and di-sodium hydrogen phosphate (Scharlau, 99%). Before using, the buffer solutions were deoxygenated by bubbling nitrogen for 15 min. De-ionized water was obtained from a Millipore Milli-Q purification system (18.2 MΩ cm).

2.3. Samples

Samples analyzed were lyophilized human serum (S2257, Sigma, Madrid, Spain) spiked with 0.033 and 0.290 mM 3-HB.

2.4. Procedures

2.4.1. Preparation of Enzyme Biosensors

A 1 mg mL^{-1} GO aqueous dispersion in de-ionized water was prepared by ultrasonic stirring for 4 h, and then centrifuged at 10,000× *g* for 10 min. The precipitate was discarded and the supernatant liquid was treated with a 25% NH_3 solution up to pH 9–10. Further reduction of GO was performed in the presence of 2 mM ascorbic acid by maintaininga temperature of 100 °C for 15 min. Then, rGO dispersion was left in the dark at room temperature. The product was replenished every week although it was stable for at least two weeks. Finally, a 10 μL aliquot of rGO was dropped onto the electrode surface and allowed drying at room temperature. The redox mediator, thionine, was subsequently incorporated onto the rGO/SPCEs surface by deposition of 15 μL of a 1 mM THI solution and incubation for 30 min at room temperature in humid ambient. The modified electrodes were washed with de-ionized water and dried with nitrogen stream. Then, 3-HBDH/THI/rGO/SPCEs were prepared by casting 2 μL of a 100 U/mL enzyme solution onto THI/rGO/SPCEs surface and allowed drying at 4 °C. Amperometric measurements with the as prepared biosensor were carried out by depositing 50 μL of a 0.1 mM NAD^+ solution in phosphate buffer of pH 7.0 and applying a detection potential of 0.0 V vs. Ag pseudoreference electrode. After reaching a constant current base line, 2 μL of 3-HB standard solution or the sample were added, and the steady state oxidation current was measured.

2.4.2. Analysis of Human Serum

Lyophilized serum was reconstituted by dissolving 37 mg of the solid in 500 μL of deionized water. Then, the same procedure described in Section 2.4.1 was followed. In this case, 25 μL of a 0.2 mM NAD^+ solution in phosphate buffer of pH 7.0 were deposited, and, once the background current recorded at 0.0 V was stabilized, 25 μL of spiked serum were added and the corresponding oxidation current measured. The determination of 3-HB was accomplished by applying the standard additions method, which involved four successive additions of 0.020 mM 3-HB each.

3. Results and Discussion

Figure 1 shows schematically the steps involved in the preparation and functioning of the electrochemical enzyme biosensor. As indicated in Section 2.4.1, rGO was firstly prepared from commercial GO using ascorbic acid as the reducing agent [21]. Step 1 involved dropping a 10μL aliquot of therGO dispersion on the SPCE surface. Thereafter, the electrode was modified sequentially with

15 µL THI (Step 2) and 3-HBDH (Step 3) solutions. Amperometric responses were obtained according to the sequence of reactions shown in Figure 1 after addition of NAD^+ and the 3-HB standard solution or the sample. Once the enzyme reaction takes place, the generated NADH chemically reduces THI and the electrochemical oxidation of THI_{red} was amperometrically monitored at 0.0 V vs. Ag pseudo reference electrode.

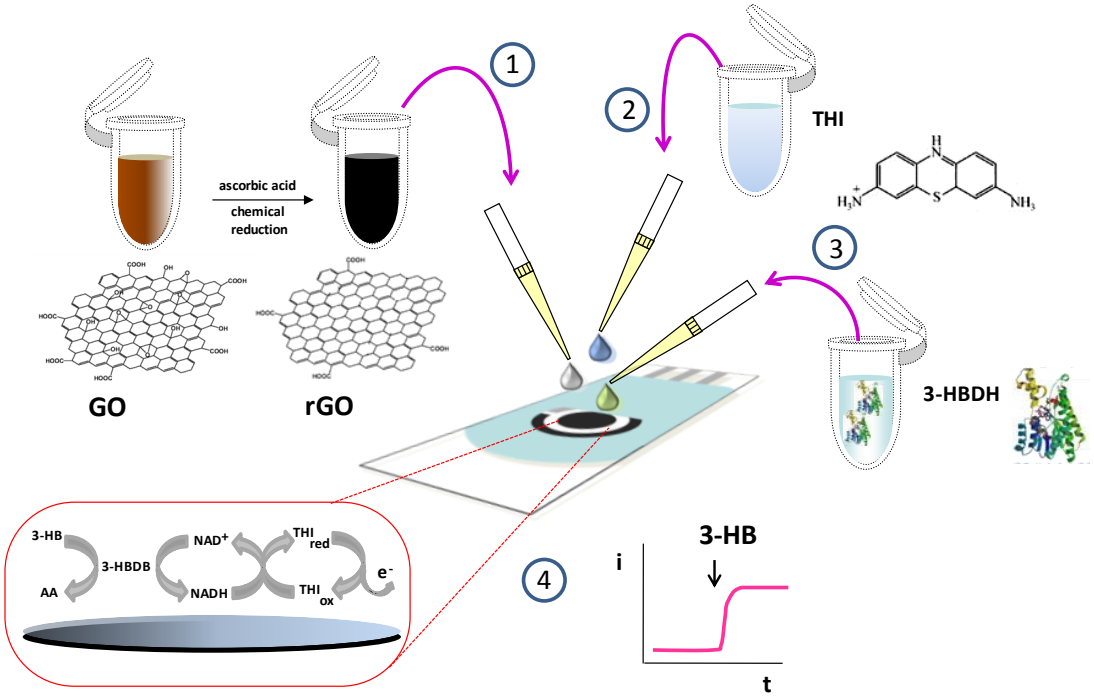

Figure 1. Scheme of the steps involved in the preparation and functioning of the 3-hydroxybutyrate dehydrogenase (3-HBDH)/thionine (THI)/reduced graphene oxide (rGO)/screen-printed carbon electrode (SPCE) biosensor.

3.1. Optimization of the Variables Involved in the Preparation and Performance of the Biosensor

The variables involved in the preparation of the 3-HBDB/THI/rGO/SPCE biosensor were optimized. The detection potential was selected taking into account the electrochemical behavior of THI at the rGO/SPCEs. Figure 2 shows cyclic voltammograms of rGO/SPCE (Curve a) and rGO/SPCE modified by dropping 15 µL of 1 mM THI (Curve b) in a 0.1 M phosphate buffer solution of pH 7.0. As can be seen, anodic and cathodic peaks of THI appeared respectively at 0.0 V and −0.2 V corresponding to the oxidation and reduction responses of the redox mediator. Thus, 0.0 V was chosen as the optimum potential to be used.

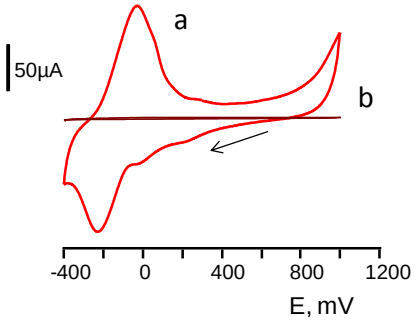

Figure 2. Cyclic voltammograms from 1000 to −400 mV of THI/rGO/SPCE (**a**) andrGO/SPCE (**b**) in a 0.1 mol L^{-1} phosphate buffer solution of pH 7.0. See the text for more information.

In order to investigate the electrochemical response of THI at the electrode surface, a study of the effect of the potential scan rate in the 5–200 mV/s range was performed on the CVs of THI/rGO/SPCE. Both oxidation and reduction peak currents showed a linear dependence with the scan rate (R^2 = 0.992 (ox) and R^2 = 0.995 (red)), whereas curves were obtained by plotting current vs. square root of the scan rate. Moreover, the log i vs. log v plots were linear (R^2 = 0.992 (ox) and R^2 = 0.996 (red)) with slope values of 1.09 (ox) and 1.03 (red). These results demonstrated that the electrochemical response of THI is surface-controlled.

Regarding the rGO loading on the SPCE, the selected value was that optimized previously by our group [22]. Using these experimental variables, calibration plots of NADH at THI/rGO/SPCE in the 0.1–1.0 mM range were obtained following the equation I, μA = (0.19 ± 0.01) [NADH, mM] + (0.018 ± 0.007) (R^2 = 0.990). For comparison, the value of the slope is approximately 15times greater than that found in the literature using a screen-printed electrode fabricated with iridium–carbon particles (m = 0.013 μA/mM) and a potential value of +0.2 V vs. Ag/AgCl [17].

The effect of the THI loading was checked by measuring the current from a 0.2 mM NADH solution at THI/rGO/SPCEs prepared with different THI concentrations in the 0.1–5.0 mM range. As is shown in Figure 3a, a sharp increase in the oxidation current was observed when the THI concentration increased up to 1 mM and leveled off for larger concentrations. Using 1 mM THI, an incubation time of 30 min was found to be sufficient to ensure a successful adsorption of the redox mediator. The effect of the enzyme loading on the amperometric response of the biosensor was also evaluated by preparing biosensors with different enzyme loadings over the 0.01–0.6 units range in the presence of 0.1 mM NAD^+ and 0.040 mM 3-HB. Figure 3b shows thatoptimal responses were obtained with 0.2 3-HBDH units, which is similar to thoseemployed in other reported biosensors for 3-HB. The sharp decrease in the measured current for larger 3-HBDH loadings is most likely due to the decrease in conductivity caused by high biomolecule loadings on the electrode surface. Moreover, this optimal enzyme loading was verified upon constructing calibrations plots for 3-HB over the 0–0.1 mM range with biosensors prepared with enzyme loadings in the above-mentioned range. A larger slope value for the calibration was obtained with 0.1 U 3-HBDH.

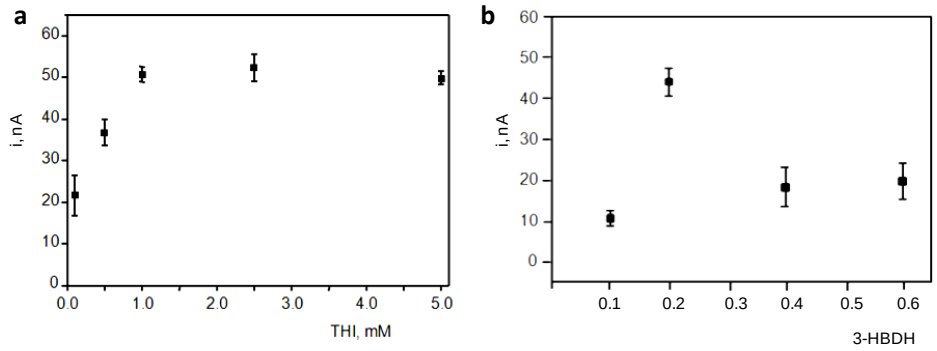

Figure 3. Effect of the THI and enzyme loadings on the amperometric responses measured with THI/rGO/SPCE (**a**) and 3-HBDH/THI/rGO/SPCE biosensors (**b**).

The effect of pH on the enzyme electrode response was also studied in 0.1M phosphate buffer solutions with pH ranging between 5.0 and 9.0. Figure 4 shows thatlarger currents were measured at 7.0–8.0 pH values. Furthermore, amperograms corresponding to additions of 20 μM NADH in the optimal experimental conditions revealed a better reproducibility of the responses recorded at pH 7.0; thus, this pH value was selected for further work. Under the optimized experimental conditions, the enzyme biosensor exhibited a rapid response reaching 95% of the maximum current in 7 s.

Characterization of the electrode surfaces was performed by electrochemical impedance spectroscopy. As can be observed in Figure 5a, the EIS spectra obtained at 3-HBDB/rGO/SPCE and 3-HBDB/THI/rGO/SPCE biosensors in 0.1 M KCl solutions prepared in the absence of redox

probe exhibited lines with the slope value much higher than 1, revealing a behavior tending to that of an ideal capacitor. No differentiated electrochemical process was observed in the presence of THI. Furthermore, when using solutions containing 1 mM $Fe(CN)_6^{3-/4-}$ as the redox probe (Figure 5b), both bioelectrodes showed the expected behavior for a diffusion-controlled electron transfer. Moreover, a small semicircle appeared at the higher frequencies, which is less apparent at the electrode prepared with THI. This behavior is probably due to the existence of film defects such as pinholes or to a non-uniform thickness throughout the substrate, but it cannot be attributed to a different electroactive behavior of the redox probe on the electrodes. The different steps involved in the preparation of the enzyme biosensor were also monitored by means of electrochemical impedance spectroscopy using 1 mM $Fe(CN)_6^{3-/4-}$ in 0.1 M KCl as the redox probe. Figure 5c shows the Nyquist plots recorded at the bare SPCE (Curve 1), rGO/SPCE (Curve 2), THI/rGO/SPCE (Curve 3), and 3-HBDB/THI/rGO/SPCE (Curve 4). As can be seen, the charge transfer resistance at the bare SPCE (638Ω) is significantly higher than that at rGO/SPCE or THI/rGO/SPCE (87 and 94 Ω, respectively) as a consequence of the presence of rGO providing a high conductivity for the modified electrode. The deposition of the redox mediator practically did not affect the electron transfer resistance. Moreover, as expected, the enzyme immobilization provoked an increase in the R_{CT} value (1547 Ω) due to the partial insulation of the electrode surface, thus confirming the successful adsorption of the protein on the modified electrode.

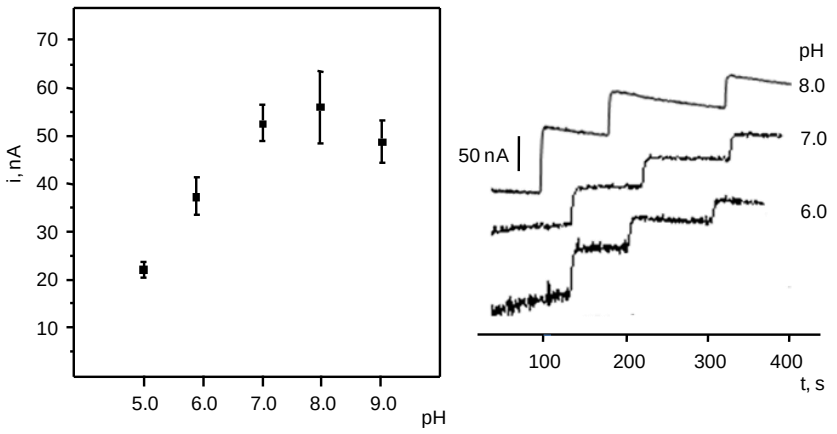

Figure 4. Effect of pH on the biosensor response. See the text for more information.

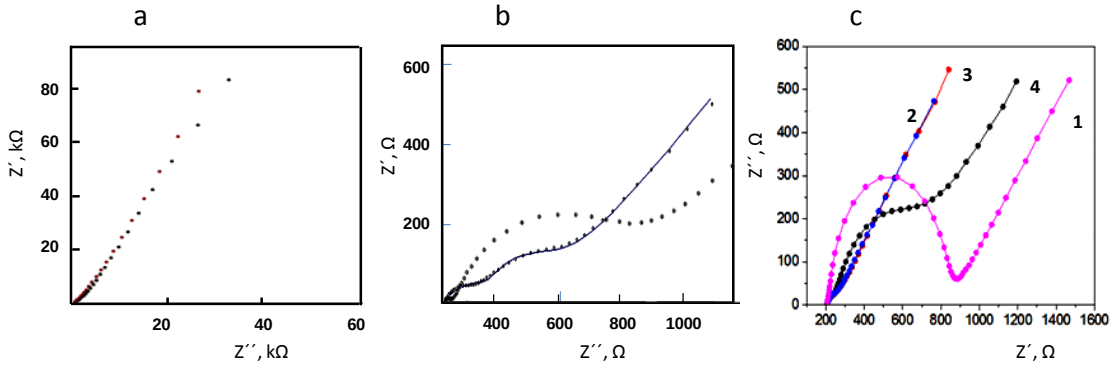

Figure 5. Nyquist plots recorded at (**a**) 3-HBDB/THI/rGO/SPCE (black) and 3-HBDB/rGO/SPCE (red) in 0.1 M KCl; (**b**) 3-HBDB/THI/rGO/SPCE (o oo o) and 3-HBDB/rGO/SPCE (——) in 1 mM $Fe(CN)_6^{3-/4-}$; (**c**) SPCE (1), rGO/SPCE (2), THI/rGO/SPCE (3), and 3-HBDB/THI/rGO/SPCE (4), using 1 mM $Fe(CN)_6^{3-/4-}$ in 0.1 M KCl. Bias potential = 0.125 V.

3.2. Analytical Figures of Merit of the Biosensor

The calibration plot for 3-HB constructed with the 3-HBDB/THI/rGO/SPCE biosensor is displayed in Figure 6. The linear range extends between 0.003 and 0.400 mM (r^2 = 0.992) with a slope and intercept values of 110 ± 4 nAmM and 0.6 ± 3 nA, respectively. The LOD was calculated according to the $3s_b/m$ criterion, where s_b was estimated as the standard deviation (n = 10) from the mean current of solutions containing no 3-HB, and m was the slope of the linear calibration range. An LOD value of 0.001 mM, which is significantly lower than those reported using other biosensor configurations, was obtained (see Table 1). The limit of quantification ($10\ s_b/m$) was 0.003 mM.

The enzyme reaction occurring at the 3-HBDB/THI/rGO/SPCE biosensor fitted well into Michaelis–Menten kinetics, as demonstrated by calculation of the "x" parameter (1.05 ± 0.07) from the corresponding Hill's plot ([log ($i_{max}/1$) - 1] vs. the log of 3-HB concentration). Therefore, the apparent Michaelis–Menten constant (K_M^{app}) was calculated from the Lineweaver–Burk plot. The K_M^{app} value obtained was 1.50 ± 0.03 mM. This value is significantly lower than that reported by immobilization of 3-HBDH onto a thick film screen-printed iridium-modified electrode, 2.3 mM [16], or in mesoporous silica (FSM8.0), 2.8 mM [13], and much lower than that obtained when a platinized activated carbon electrode was used as immobilization surface, 5.4 mM [23]. The low K_M^{app} value obtained indicates a high affinity of the enzyme for the substrate when it is immobilized on the rGO-modified electrode.

Amperometric currents measured for 0.200 mM 3-HB with 10different biosensors prepared with the same protocol provided an RSD value of 4.5%, thus showing a good reproducibility both in the preparation procedure of the enzyme electrodes and in the amperometric transduction. Importantly, the analytical characteristics of the enzyme biosensor are suitable for the determination of 3-HB in human serum where concentrations are in the range of mM units [1]. When the analytical figures of merit of the enzyme electrode are compared with data provided by commercial kits for 3-HB determination, some noticeable differences become apparent. These kits claim for dynamic ranges usually covering from hundreds to tenths mM. For example, the ab83390 (colorimetric) enzymatic kit from Abcam [24] reports a 0.01–0.1 mM linear range, while the fluorimetricab180876 kit [25] provides a linear range of 0.002–0.01 mM. Therefore, it can be concluded that the range of linearity provided by the enzyme biosensor (0.003–0.400 mM) is wider. In addition, the limits of detection and quantification achieved are lower (or much lower in the case of colorimetric detection) At this point, it is important to note that the criteria used to calculate the LOD values in these kits are rarely given in the commercial protocols. Moreover, the precision levels for these kits are around 10% or higher. Summarizing, it can be concluded that the analytical performance of the developed biosensor, covering a wide linear range of 3-HB concentrations and the clinically relevant interval, improves, in general terms, the performance claimed for other approaches.

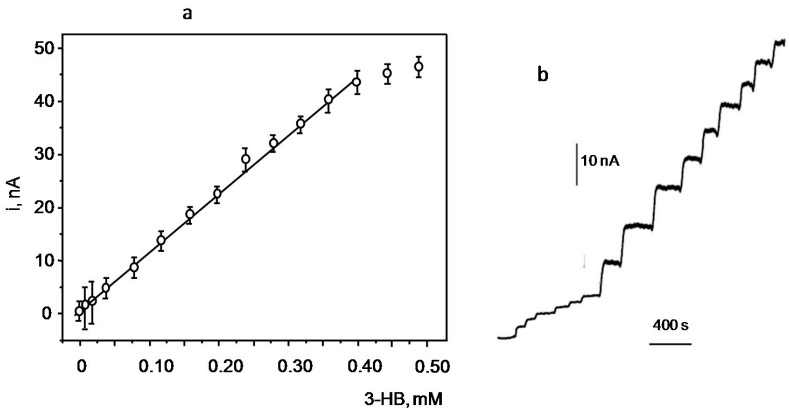

Figure 6. Calibration plot for 3-HB recorded with the 3-HBDH/THI/rGO/SPCE and some amperometric responses for additions of (**a**) 20 μM and (**b**) 100 μM 3-HB. Error bars are calculated according to ± s (n = 3).

The storage stability at 4 °C ofthe 3-HBDB/THI/rGO/SPCE biosensor was evaluated by measuring in different days the amperometric responses for 0.1 mM 3-HB solutions applying the procedure described in Section 2.4.1. The results obtained (not shown) revealed that the initial response of the biosensor kept within the limits of control set at three times the standard deviation of the measurements (n = 10) carried out in the first working day, during at least 20 days after the biosensor preparation, thus showing a good storage stability.

Regarding the selectivity of the biosensor, various compounds that can be present in the 3-HB serum samples, such as citrate, glutamine, glutamate, succinate, ascorbic acid, uric acid, and glucose, were tested as potential interfering substances. The effect of their presence was evaluated by measuring the currents under the optimal experimental conditions for the 3-HBDB/THI/rGO/SPCE biosensor in the absence of 3-HB. The concentration level checked for each interfering compound was that corresponding to the normal physiological levels in serum. Figure 7 shows the amperometric responses obtained compared to that measured for a low 3-HB concentration of 0.020 mM. This figure also allows for the background noise to be visualized. As can be seen, all the potential interfering compounds except ascorbic acid, produced very slight variations in the biosensor response, all of them within the range of two times the standard deviation for the background noise. In the case of ascorbic acid, a relatively high current was observed, probably as a consequence of its oxidation at the detection potential value used. Thus, for example, after the addition of 0.057 mM ascorbic acid, a current equivalent to a 0.040 mmol/L 3-HB concentration was measured. In spite of this interference, no significant current response was apparent from human serum components when the biosensor was used for the analysis of this type of sample, thus confirming the suitability of the developed method for the enzymatic determination of 3-HB in serum.

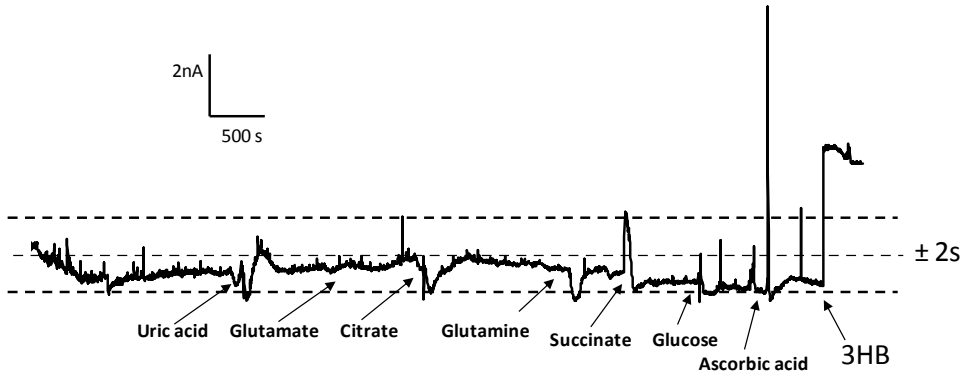

Figure 7. Amperometric responses obtained at the 3-HBDH/THI/rGO/SPCE biosensor for 0.178 mmol/L uric acid; 0.103 mmol/L glutamate; 0.060 mmol/L citrate; 0.067 mmol/L glutamine; 0.0083 mmol/L succinate; 0.0073 mmol/L glucose; 0.057 mmol/L ascorbic acid; 0.020 mmol/L 3-HB. Other conditions as in Figure 7.

3.3. Determination of 3-HB in Spiked Human Serum

The possible existence of matrix effects in human serum was evaluated by comparing the slope values of the calibration plots constructed with 3-HB standard solutions in a 0.1 M phosphate buffer, and in serum samples spiked with the analyte at concentrations ranging between 0.01 and 0.400 mM. As described in Section 2.4.2, the analytical procedure involved a 1:1 serum dilution with the 0.2 mM NAD^+ solution in phosphate buffer of pH 7.0. Under these conditions, the slope value of the linear calibration graph obtained for spiked serum samples was 66 ± 4 nAmM, which is significantly different from the slope of the calibration plot constructed with 3-HB standards in buffered solution (110 ± 4 nA mM). Therefore, it could be concluded that a significant matrix effect provoked by the serum components occurred. However, it is important to note that no unexpected increases in the biosensor response caused by the presence of potential interfering compounds were observed.

This was confirmed by the low level of the zero signal (0.4 ± 0.1 nA), which is even slightly lower than that of the calibration plot prepared with 3-HB solutions in phosphate buffer (0.6 ± 0.3 nA). Accordingly, the standard additions method wasemployed to quantify the analyte concentration is serum.

The analyzed samples were serum spiked with 3-HB at two concentration levels: 0.033 and 0.290 mM, which are lower than those expected for patients with health problems caused by hyperketonemia or diabetic ketoacidosis [1]. Other more concentrated samples could be analyzed by applying a proper sample dilution. The results obtained inquintuplicate provided 3-HB concentrations expressed as $\overline{x} \pm (t_{0.05} \times s)/\sqrt{n}$ of 0.032 ± 0.003 and 0.294 ± 0.015 mM, respectively, with mean recoveries of 98% ± 8% and 101% ± 5%. These results demonstrate fairly well the usefulness of the developed biosensor for the analysis of low 3-HB concentrations in human sera with minimal sample treatment.

4. Conclusions

A simple and facile method of preparing an electrochemical enzyme biosensor for the determination of the biomarker 3-HB in human serum has been constructed. The biosensor takes advantage of the well-known benefits provided by SPCEs modified with reduced graphene oxide, in terms of enhanced electron transfer rate of NADH oxidation, and the use of thionine as the redox mediator. The enzyme biosensor exhibits remarkably good analytical characteristics in terms of the range of linearity, high sensitivity, and low detection limit in comparison with theother biosensor configurations and commercial kits for 3-HB determination. Importantly, the enzyme electrode allows for the quantification of the analyte at clinically relevant levels in human sera involving minimal sample treatment (just an appropriate dilution with the working buffer solution).

Acknowledgments: The financial support of the CTQ2015-70023-R and CTQ2015-64402-C2-1-R (Spanish Ministerio de Economía y Competitividad Research Projects) and S2013/MT3029 (NANOAVANSENS Program from the Comunidad de Madrid) are gratefully acknowledged.

Author Contributions: G.M.-G. and E.P.-J. performed the experiments; L.A. and P.Y.-S. conceived and designed the experiments; N.C. and J.J. contributed materials/analysis tools; P.Y.-S. and J.M.P. analyzed the data and wrote the paper.

Conflicts of Interest: The authors declare no conflict of interest.

References

1. Wallace, T.M.; Matthews, D.R. Recent advances in the monitoring and management of diabetic ketoacidosis. *QJM* **2004**, *97*, 773–780. [CrossRef] [PubMed]
2. Laffel, L. Use of a point-of-care beta-hydroxybutyrate sensor for detection of ketonemia in dogs. *Diabetes/Metab. Res. Rev.* **1999**, *15*, 412–426. [CrossRef]
3. Rodríguez-Gallego, E.; Guirro, M.; Riera-Borrull, M.; Hernández-Aguilera, A.; Mariné-Casadó, R.; Fernández-Arroyo, S.; Beltrán-Debón, R.; Sabench, F.; Hernández, M.; Castillo, D.; et al. Mapping of the circulating metabolome reveals α-ketoglutarate as a predictor of morbid obesity-associated non-alcoholic fatty liver disease. *Int. J. Obes.* **2015**, *39*, 279–287. [CrossRef] [PubMed]
4. Wu, S.; He, Q.; Tan, C.; Wang, Y.; Zhang, H. Graphene-Based Electrochemical Sensors. *Small* **2013**, *9*, 1160–1172.
5. Lawal, A.T. Synthesis and utilisation of graphene for fabrication of electrochemical sensors. *Talanta* **2015**, *131*, 424–443. [CrossRef] [PubMed]
6. Di Bari, C.; Goñi-Urtiaga, A.; Pita, M.; Shleev, S.; Toscano, M.D.; Sainz, R.; De Lacey, A.L. Fabrication of high surface area graphene electrodes with high performance towards enzymatic oxygen reduction. *Electrochim. Acta* **2016**, *191*, 500–509. [CrossRef]
7. Pumera, M.; Ambrosi, A.; Bonanni, A.; Chng, E.L.K.; Poh, H.L. Graphene for electrochemical sensing and biosensing. *TrAC Trends Anal. Chem.* **2014**, *29*, 954–965. [CrossRef]
8. Zhang, J.; Yang, H.; Shen, G.; Cheng, P.; Zhang, J.; Guo, S. Reduction of graphene oxide via L-ascorbic acid. *Chem. Commun.* **2010**, *46*, 1112–1114. [CrossRef] [PubMed]

9. Tang, L.H.; Wang, Y.; Li, Y.M.; Feng, H.B.; Lu, J.; Li, J.H. Preparation structure and electrochemical properties of reduced graphene sheet films. *Adv. Funct. Mater.* **2009**, *19*, 2782–2789. [CrossRef]
10. Khorsand, F.; Azizi, M.D.; Naeemy, A.; Larijani, B.; Omidfar, K. An electrochemical biosensor for 3-hydroxybutyrate detection based on screen-printed modifed by coenzyme functionalized carbon nanotubes. *Mol. Biol. Rep.* **2013**, *40*, 2327–2334. [CrossRef] [PubMed]
11. Kwan, R.C.H.; Hon, P.Y.T.; Mak, W.C.; Law, L.Y.; Huc, J.; Renneberg, R. Biosensor for rapid determination of 3-hydrybutyrate using bienzyme system. *Biosens. Bioelectron.* **2006**, *21*, 1101–1106. [CrossRef] [PubMed]
12. Li, G.; Ma, N.Z.; Wang, Y. A new handheld biosensor for monitoring blood ketones. *Sens. Actuators B Chem.* **2005**, *109*, 285–290. [CrossRef]
13. Forrow, N.J.; Sanghera, G.S.; Walters, S.J.; Watkin, J.L. Development of a commercial amperometric biosensor electrodefor the ketone d-3-hydroxybutyrate. *Biosens. Bioelectron.* **2005**, *20*, 1617–1625. [CrossRef] [PubMed]
14. Shimomura, T.; Sumiya, T.; Ono, M.; Ito, T.; Hanaoka, T. A novel, disposable, screen-printed amperometric biosensor for ketone 3-β-hydroxybutyrate fabricated using a 3-β-hydroxybutyrate dehydrogenase—Mesoporous silica conjugate. *Anal. Bioanal. Chem.* **2013**, *405*, 297–305. [CrossRef] [PubMed]
15. Wang, C.C.; Hennek, J.W.; Ainla, A.; Kumar, A.A.; Lan, W.J.; Im, J.; Smith, B.S.; Zhao, M.; Whitesides, G.M. A paper-based "pop-up" electrochemical device for analysis of beta-hydroxybutyrate. *Anal. Chem.* **2016**, *88*, 6326–6333. [CrossRef] [PubMed]
16. Veerapandian, M.; Hunter, R.; Neethirajan, S. Ruthenium dye sensitized graphene oxide electrode for on-farm rapiddetection of beta-hydroxybutyrate. *Sens. Actuators B Chem.* **2016**, *228*, 180–184. [CrossRef]
17. Fang, L.; Wang, S.-H.; Liu, C.-C. An electrochemical biosensor of the ketone 3-β-hydroxybutyrate for potential diabetic patient management. *Sens. Actuators B Chem.* **2008**, *129*, 818–825. [CrossRef]
18. Shao, Y.; Wang, J.; Wu, H.; Liu, J.; Aksay, I.A.; Lin, Y. Graphene based electrochemical sensors and biosensors: A Review. *Electroanalysis* **2009**, *22*, 1027–1036. [CrossRef]
19. Chen, Y.; Zhang, X.; Yu, P.; Ma, Y. Stable dispersions of graphene and highly conducting graphene films: A new approach to creating colloids of graphene monolayers. *Chem. Commun.* **2009**, *30*, 4527–4529.
20. Huang, M.; Jiang, H.; Zhai, J.; Liu, B.; Dong, S. A simple route to incorporate redox mediator into carbon nanotubes/Nafion composite film and its application to determine NADH at low potential. *Talanta* **2007**, *74*, 132–139. [CrossRef] [PubMed]
21. Fernández-Merino, M.J.; Guardia, L.; Paredes, J.L.; Villar-Rodil, S.; Solís-Fernández, P.; Martínez-Alonso, A.; Tascón, J.M.D. Vitamin C is an ideal substitute for hydrazine in the reduction of graphene oxide suspensions. *J. Phys. Chem. C* **2010**, *114*, 6426–6432. [CrossRef]
22. Martínez-García, G.; Agüí, L.; Yáñez-Sedeño, P.; Pingarrón, J.M. Multiplexed electrochemical immunosensing of obesity-related hormones at grafted graphene-modified electrodes. *Electrochim. Acta* **2016**, *202*, 209–215. [CrossRef]
23. McNeil, C.J.; Spoors, J.A.; Cooper, J.M.; Alberti, K.G.M.M.; Mullen, W.H. Amperometric biosensor for rapid measurement of 3-hydroxybutyrate in undiluted whole blood and plasma. *Anal. Chim. Acta* **1990**, *237*, 99–105. [CrossRef]
24. Beta Hydroxybutyrate (beta HB) Assay Kit (Colorimetric) (ab83390). Available online: http://www.abcam.com/beta-hydroxybutyrate-beta-hb-assay-kit-colorimetric-ab83390.html (accessed on 10 November 2017).
25. Picoprobe β Hydroxybutyrate (beta HB) Assay Kit (Fluorometric) (ab180876). Available online: http://www.abcam.com/picoprobe-beta-hydroxybutyrate-beta-hb-assay-kit-fluorometric-ab180876.html (accessed on 10 November 2017).

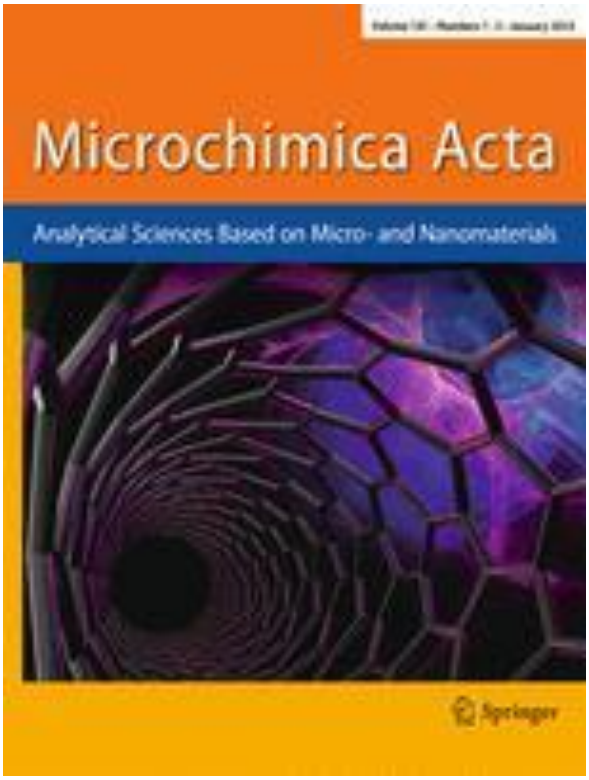

9.7.

AMPEROMETRIC IMMUNOASSAY FOR THE OBESITY BIOMARKER AMYLIN USING A SCREEN PRINTED CARBON ELECTRODE FUNCTIONALIZED WITH AN ELECTROPOLYMERIZED CARBOXYLATED POLYPYRROLE

Microchimica Acta
https://doi.org/10.1007/s00604-018-2863-x

ORIGINAL PAPER

Amperometric immunoassay for the obesity biomarker amylin using a screen printed carbon electrode functionalized with an electropolymerized carboxylated polypyrrole

Gonzalo Martínez-García[1] · Esther Sánchez-Tirado[1] · Araceli González-Cortés[1] · Paloma Yáñez-Sedeño[1] · José M. Pingarrón[1]

Received: 12 March 2018 / Accepted: 4 June 2018

Abstract
Amylin (the islet amyloid polypeptide) is a hormone related to adiposity, hunger and satiety. It is co-secreted with insulin from pancreatic B-cells. An amperometric immunosensor is presented here for the determination of amylin. It is making use of a screen printed carbon electrode (SPCE) functionalized with electropolymerized poly(pyrrole propionic acid) (pPPA) with abundant carboxyl groups that facilitate covalent binding of antibody against amylin. A competitive immunoassay was implemented using biotinylated amylin and streptavidin labeled with horse radish peroxidase (HRP-Strept) as the enzymatic tracer. The amperometric detection of H_2O_2 mediated by hydroquinone was employed as an electrochemical probe to monitor the affinity reaction. The variables involved in the preparation and function of the immunosensor were optimized and the electrodes were characterized by electrochemical impedance spectroscopy and cyclic voltammetry. The calibration graph for amylin, obtained by amperometry at −200 mV vs Ag pseudo-reference electrode, showed a range of linearity extending from 1.0 fg·mL^{-1} to 50 pg·mL^{-1}, with a detection limit of 0.92 fg·mL^{-1}. This is approximately 7000 times lower than the minimum detectable concentration reported for the ELISA immunoassays available for amylin. The assay has excellent reproducibility and good selectivity over potential interferents.

Keywords Screen-printed carbon electrodes · Electrochemical biosensor · Conducting polymer · Mix&Go™ · Urine · Serum

Introduction

Obesity, considered as being pandemic by the World Health Organization, is one of the most deadly diseases and causes more than 2.8 million deaths per year. The normal control of body weight and food intake by the brain relies upon the detection and integration of signals related with adiposity, hunger and satiety. Amylin (islet amyloid polypeptide, hIAPP or AMY) is a 37-residue peptide hormone co-secreted with insulin from pancreatic β-cells [1]. Human amylin is found as fibrillar deposits in pancreatic extracts of nearly all type-II diabetics. Both synthetic and endogenous AMY have significant cytotoxicity to islet cells. This effect is related to the death of such cells occurring in diabetes which results in the loss of blood glucose homeostasis and subsequent insulin dependence [2, 3]. Like insulin, plasma AMY levels are low during fasting and increase during meals and following glucose administration, the concentrations being directly proportional to body fat. AMY and insulin are normally co-secreted in a fixed molecular ratio between ten and one hundred insulin to AMY. However, obesity, diabetes mellitus, pancreatic cancer and certain pharmacological interventions tend to increase the amount of AMY relative to insulin [1]. Studies related to physiology of AMY [4, 5] revealed that individuals with type 1 diabetes are AMY deficient [6] whereas post-meal secretion of AMY seems to be defective in advanced type 2 diabetes [7]. Conversely, individuals who are insulin resistant and hyperinsulinemic have high concentrations of AMY in plasma [8]. The AMY levels in human serum oscillates around a few tens of pg·mL^{-1} [4, 9, 10].

Despite its importance, a scarce number of analytical methods for the determination of AMY have been described

✉ Paloma Yáñez-Sedeño
yseo@quim.ucm.es

[1] Department of Analytical Chemistry, Faculty of Chemistry, Complutense University of Madrid, Complutense Av., 28040 Madrid, Spain

Published online: 09 June 2018

in the literature. ELISA kits using competitive strategies with biotinylated antigen are commercially available. The RayBiotech (RayBio®) [https://www.raybiotech.com/files/manual/EIA/EIA-AMY.pdf] kit exhibits a dynamic range from 1 to 1000 ng·mL^{-1} with a minimum detectable concentration of 0.62 ng·mL^{-1}. In this assay, Biotin-AMY competes with AMY for anti-AMY, then interacting with HRP-Strept. A similar assay from LifeSpan BioSciences Inc. [https://www.lsbio.com/elisakits/manualpdf/ls-f9686.pdf] using HRP-Avidin provides a linear range between 6.17 and 500 pg·mL^{-1}, with detectable concentrations typically less than 6.17 pg·mL^{-1}. A sandwich-type immunoassay with fluorometric detection was also reported for the detection of AMY in plasma with a dynamic range between 2 and 100 pmol·L^{-1} and a minimum detectable concentration of 0.5 pmol·L^{-1} [4].

In this work, the first electrochemical immunosensor for the determination of AMY is reported. A screen printed carbon electrode (SPCE) functionalized with electropolymerized poly(pyrrole propionic acid) (pPPA) was used. This transducer provided a high content of surface confined carboxyl groups suitable for direct covalent binding of anti-AMY antibody after activation with Mix&Go™, a polymer containing several metallic complexes selected for their efficiency to bind proteins [11, 12]. Particularly, in the case of antibodies, Mix&Go uses small molecule ligands to bind Fc domains as an anchoring point, these ligands mimicking binding domains from proteins A and G, and extending as two adjacent sidechains from a polymer backbone [13]. In addition, metal complexes integrated into the polymer chains enhance binding of Fc domains providing a higher stability. The polymer also forms strong multivalent interactions with electron donating groups such as carboxylate [11]. Accordingly, coupling of pPPA with the use of Mix&Go™ for antibody immobilization resulted in a successful strategy suitable to be used as a general route for preparing electrochemical immunosensors with potential application in point-of-care devices. A competitive immunoassay involving biotinylated AMY and streptavidin labelled with horse radish peroxidase (HRP-Strept) as the enzymatic tracer was implemented (Fig. 1). The amperometric detection of H_2O_2 mediated by hydroquinone (HQ) was employed to monitor the affinity reaction. The variables involved in the preparation and functioning of the immunosensor were optimized and the modified electrodes were characterized by electrochemical impedance spectroscopy and cyclic voltammetry. The calibration graph for AMY shows a range of linearity extending from 0.001 to 50 pg·mL^{-1}, with a detection limit of 0.92 fg·mL^{-1}. This value is approximately seven thousand times lower than the minimum detectable concentration reported for the available ELISA immunoassays for AMY. An excellent reproducibility of the measurements carried out with different immunosensors as well as an excellent selectivity against other hormones was shown. In addition, good results were obtained by application to the AMY analysis in urine and serum.

Experimental

Reagents and solutions

Human monoclonal anti-amylin (anti-AMY) from mouse, human amylin (AMY) and biotinylated human amylin (Biotin-AMY) were the reagents included in the RayBio® Human/Mouse/Rat Amylin Enzyme Immunoassay Kit (EIA-AMY) from RayBiotech, Inc. (www.raybiotech.com) Solutions of the antigen and biotinylated antigen were prepared in Assay Diluent B pH 7.5 from RayBiotech. Anti-AMY capture antibody was reconstituted in the same solvent and diluted up to the working concentration with 25 mM 2-(*N*-morpholine) ethanosulfonic acid (MES) buffer of pH 5.0 (Gerbu, www.gerbu.de). 1H-pyrrole-1-propionic acid monomer (PPA) (Sigma-Aldrich, www.sigmaaldrich.com, 97%) and KCl (Scharlau, www.scharlab.com, 99.5%) were also used. 0.1 M PPA solutions were prepared in deionized water containing 0.5 M KCl. Mix&Go™ was from Anteo Diagnostics (www.anteotech.com). Streptavidin labeled with horseradish peroxidase (HRP-Strept) was from Roche (www.custombiotech.roche.com). Solutions of hydrogen peroxide (Aldrich, 30% (*w*/w)) and hydroquinone (HQ, Sigma) were prepared in 0.05 M phosphate buffer of pH 6.0. 0.05 M potassium ferro- and ferricyanide solutions were prepared in 0.1 M phosphate buffered saline (PBS) of pH 7.4 containing 2.002 g NaCl (Labkem, 99%), 0.050 g KCl (Probus), 0.287 g NaH_2PO_4 (Scharlau, 98%) and 0.051 g KH_2PO_4 (Merck, 99%) in 250 mL of deionized water. 2% (*w*/*v*) solutions of bovine serum albumin (BSA) in the same buffer were used as blocking agent. Ascorbic acid (AA, Fluka), uric acid (UA, Sigma), bilirubin (BR, Aldrich), cholesterol (Chol, Sigma), glucose (Glu, Panreac, www.itwreagents.com) and peptide YY (PYY, Phoenix Pharmaceuticals, Inc., www.phoenixpeptide.com.) were tested as interfering compounds. Deionized water was from a Millipore Milli - Q purification system (18.2 MΩ·cm at 25 °C).

Lyophilized human serum from Sigma reconstituted in deionized water, spiked with 0.75 and 4.0 pg·mL^{-1} amylin and diluted with Assay Diluent B from RayBio® was analyzed. Liquichek urine Chemistry Control (Level 1, BioRad 63,221, www.bio-rad.com) containing uric acid, amylase, cortisol, creatinine, glucose, albumin, urea, calcium, potassium, sodium, chloride and phosphorous, spiked with 1.50 and 8.00 pg·mL^{-1} amylin and diluted with the Assay Diluent B from RayBio® was also analyzed.

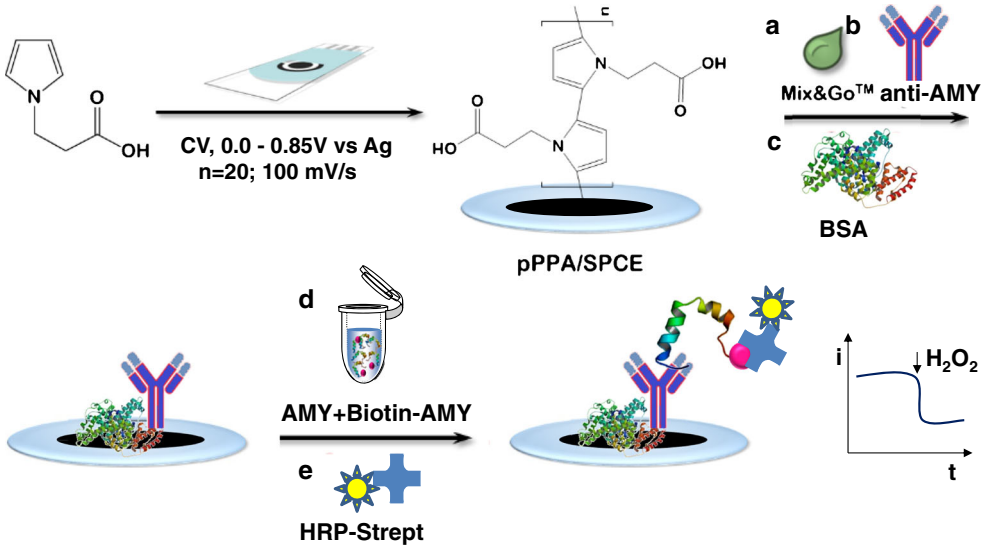

Fig. 1 Schematic display of the different steps involved in the construction of the amperometric immunosensor for AMY involving pPPA-modified SPCEs and covalent immobilization of anti-AMY: (**a**) Mix&Go™ addition; (**b**) covalent immobilization of anti-AMY antibody; (**c**) blocking step with BSA; (**d**) competitive immunoassay; (**e**) addition of HRP-Strept conjugate

Apparatus and electrodes

Amperometric measurements were performed using an INBEA potentiostat provided with the Ib Software. Voltammograms were registered using a μAutolab type III potentiostat controlled by the GPES 4.7 software (Ecochemie). EIS measurements were made using an Autolab type III controlled by FRA2 software (RcoChemie). Screen-printed carbon electrodes (SPCEs, 110DRP, ϕ 4 mm) from DropSens (Oviedo, Spain) were used as working electrodes. These electrodes are provided with a silver pseudo-reference electrode and a carbon counter electrode. pH measurements were made using a Crison Basic 20 + pH meter. An Elmasonic S-60 (Elma) ultrasonic bath, a Vortex (Velp Scientifica) shaker, and a centrifuge MPW-65R (MPW Med. Instruments) were also used. All experiments were performed at room temperature.

Procedures

Preparation of the electrochemical immunosensor

Electropolymerization of pPPA on the SPCE was accomplished by immersing the electrode into a 100 mM PPA monomer solution containing 0.5 M KCl and applying 20 successive voltammetric cycles between 0.0 and + 0.85 V at 100 mV s^{-1}. The resulting pPPA/SPCEs were immersed into 1 mM HQ solution in 0.1 M phosphate buffer of pH 7.4, and a control cyclic voltammogram was recorded between −0.2 and + 1.0 V (vs. the Ag pseudo-reference electrode of the SPCE) at 50 mV s^{-1}. Surface confined carboxyl groups were activated by adding 10 μL of Mix@Go™ on the pPPA/SPCEs and allowing incubation for 60 min at 25 °C. Thereafter, the electrodes were washed with the MES buffer of pH 5.0, and the capture antibody was covalently immobilized by dropping 5 μL of a 1/100 diluted anti-AMY solution prepared in 25 mM MES buffer of pH 5.0 and incubating during 60 min at 25 °C in a humid ambient chamber. After washing again with the same MES buffer, the un-reacted activated groups on the anti-AMY-pPPA/SPCEs were blocked by adding 7.5 μL of 2% BSA in 0.1 M phosphate buffer of pH 7.4, allowing incubation for 30 min, and washing again with the MES buffer. A competitive immunoassay was carried out by incubation of 5 μL of a solution containing 2.5 ng·mL^{-1} Biotin-AMY conjugate and the antigen, AMY, for 45 min. Then, 5 μL of a 1/500 HRP-Strept solution were added and, after 20 min incubation, the resulting HRP - Strept - Biotin - AMY - AMY- anti - AMY- pPPA / SPCE immunosensor was washed with 0.1 M phosphate buffer of pH 7.4 and kept in humid ambient until measurements were made.

Amperometric measurements

A volume of 45 μL of 0.05 M phosphate buffer of pH 6.0 and 1.0 mM hydroquinone (prepared just before the electrochemical measurement) was deposited onto the immunosensor and the current was recorded by applying a potential of −200 mV vs Ag pseudo-reference electrode. Once the background current was stabilized (after about 100 s) a 5-μL aliquot of a 50 mM hydrogen peroxide solution in 0.05 M PBS of pH 6.0 was added and the current was measured allowing 200 s for the enzymatic reaction to take place.

Determination of amylin

Analysis of spiked human serum and urine using the HRP-Strept-Biotin-AMY-AMY- anti-AMY-pPPA/SPCE immunosensor was performed after a simple sample treatment consisting of a five- or tenfold dilution, respectively, with the Assay Diluent B RayBio®.

Results and discussion

Fig. 1 illustrates schematically the different steps involved in the preparation and functioning of the HRP - Strept - Biotin - AMY- AMY - anti - AMY - pPPA / SPCE immunosensor. Upon modification of the SPCE by electropolymerization of pPPA, Mix & Go™ was used (step a) for covalent immobilization of capture antibodies on the surface confined carboxyl groups of the pPPA/SPCE (step b). Then, after a blocking step of the remaining activated un-reacted sites with a BSA solution (step c), a competitive immunoassay with target AMY and Biotin-AMY was implemented (step d). Finally, HRP-Strept conjugate was added (step e) and the amperometric responses at −0.20 V (vs the Ag pseudo-reference electrode) upon addition of H_2O_2 in the presence of HQ were measured.

Optimization of the experimental variables

The different variables affecting the preparation of pPPA/SPCEs and the performance of the resulting HRP-Strept-Biotin-AMY-AMY-anti-AMY-pPPA/SPCE immunosensors were evaluated. The ratio between the currents measured for the blank (0.0 pg·mL^{-1} AMY) and for 1.25 pg·mL^{-1} AMY was taken as the selection criterion for each tested variable. The optimization of variables involved evaluation of: a) the strategy for covalent immobilization of anti-AMY; b) anti-AMY loading on pPPA/SPCEs; c) concentration of the blocking agent BSA; d) time for competition between AMY and Biotin-AMY; e) HRP-Strept loading on Biotin-AMY-AMY-anti-AMY-pPPA/SPCEs. The results of these studies are summarized in Table 1. Other variables such as the number of voltammetric cycles carried out during PPA electropolymerization on SPCEs or the concentration of PPA monomer were the same than those optimized previously [14]. Furthermore, the reduction currents from benzoquinone (BQ) generated in the HRP enzyme reaction with HQ at the SPCE were measured at a detection potential of −200 mV vs Ag pseudo-reference electrode, which was that previously selected for this catalytic system [15].

Fig. 2a compares the amperometric responses of the HRP-Strept-Biotin-AMY-AMY-anti-AMY-pPPA/SPCE immunosensor prepared by covalent immobilization of the capture antibody, anti-AMY, by using two different strategies, the usual procedure based on activation of carboxylic moieties existing on the pPPA-modified SPCE by EDC/NHSS chemistry, and the methodology using Mix&Go™ polymer. As it can be seen, this latter approach allowed an enhanced response for the solution containing no AMY) and, therefore, a larger difference vs. the amperometric current measured for 1.25 pg·mL^{-1} AMY, thus demonstrating the suitability of coupling the use of pPPA with Mix&Go™ for the immobilization of the capture antibody.

Fig. 2b shows the effect of the HRP-Strept loading onto the Biotin-AMY-AMY-anti-AMY-pPPA/SPCE on the amperometric response of different immuno-sensors prepared from pPPA/SPCEs modified with 10 μL Mix&Go™, 5 μL 1/100 diluted anti-AMY, 7.5 μL 2% BSA, 0 (dark grey) or 1.25 (white) pg·mL^{-1} AMY, 5 μL 1 ng·mL^{-1} Biotin-AMY, and HRP-Strept dilution over the 1/250–1/2000 range. Both the current measured in the absence of AMY and in the presence of 1.25 pg·mL^{-1} antigen decreased with the conjugate dilution. Larger current ratios were obtained for a 1/500 dilution which, accordingly was chosen for further work. Regarding the time for competition between AMY and Biotin-AMY for the binding sites of the antibody, Fig. 2c shows a progressive increase in the amperometric response of the immunosensor for solutions with no AMY along with an almost constant current measured in the presence of 1.25 pg·mL^{-1} AMY. Considering the larger signals ratio as well as the shorter time for analysis, 45 min was selected to allow competition to proceed.

The step by step preparation of the immunosensor was monitored by electrochemical impedance spectroscopy (EIS) and cyclic voltammetry. Figure 3a shows the Nyquist plots recorded in a 2 mM $[Fe(CN)_6]^{4-/3-}$ solution in 0.05 M phosphate buffer of pH 6.0. As expected, pPPA/SPCE (curve 2) exhibited a larger charge transfer resistance (R_{CT} = 7835 Ω) than the bare SPCE (curve 1) with R_{CT} = 1226 Ω, due to both the lower conductivity of the polymer and the electrostatic repulsion between the dissociated pPPA carboxilic groups on the electrode surface at the working pH and the negatively charged redox probe [16]. The further addition of Mix&Go provoked a remarkable decrease in the R_{CT} value up to 978 Ω (curve 3) probably due to charges neutralization. Successive increases in the R_{CT} values were observed when anti-AMY (curve 4) and BSA (curve 5) were incorporated on the electrode, with R_{CT} values of 1723 Ω and 2342 Ω respectively, due to the insulating nature of the biomolecules. Interestingly, the incorporation of the biotinylated antigen (Biotin-AMY) and the subsequent formation of the complex with the HRP-

Table 1 Optimization of the different experimental variables involved in the functioning of the competitive immunosensor for the determination of AMY

Variable	Studied range	Selected value
Loading of anti-AMY, dilution	1/100–1/200	1/100
BSA concentration, %	1–5	2
Time for competition AMY-Biotin-AMY, min	15–60	45
HRP-Strept dilution	1/250–1/2000	1/500

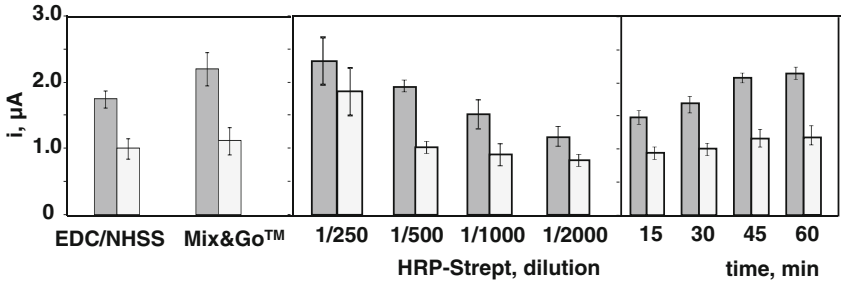

Fig. 2 Amperometric responses measured in the absence (dark grey) or in the presence of 1.25 pg·mL^{-1} AMY (white) as a function of the strategy used for covalent immobilization of anti-AMY (**a**), HRP-Strept dilution (**b**), and competition time between AMY and Biotin-AMY for the binding sites of antibody (**c**). 10 μL 100 mM EDC/NHSS, 30 min (**a**); 10 μL Mix&Go™, 60 min; 5 μL 1/100 diluted anti-AMY, 60 min; 7.5 μL 5% BSA, 30 min; 5 μL 1.25 AMY + 2.5 ng·mL^{-1} Biotin-AMY, 60 min (**a**,**b**); 1/500 diluted HRP-Strept, 20 min (**a**,**c**)

Strept conjugate (curves 6 and 7, respectively) produced Nyquist plots with a different shape similar to that of a conductive surface. This behavior can be explained by assuming the presence of positively charged biotin on the biotin-AMY-anti-AMY-pPPA/SPCE at the working pH (the pKa value of biotin is 4.51 [17]), thus leading to electrostatic attraction with the electrochemical probe and favoring the charge transfer. This effect seems to be sufficiently strong to avoid a noticeable increase in R_{CT} upon the incorporation of the streptavidin conjugate.

The behavior observed by EIS is corroborated by cyclic voltammetry (Fig. 3b). The voltammogram of the bare SPCE (curve 1) showed the characteristic oxidation and reduction peaks of the redox pair at potential values of +0.24 and + 0.16 V, respectively, with anodic and cathodic peak currents of 72 and 60 μA. The subsequent modification of SPCE with pPPA (curve 2) caused a decrease in the peak currents, and a larger peak potentials separation attributed to the low conductivity of the polymer and the electrostatic repulsion effect commented above. Incorporation of Mix&Go (curve 3) gave rise to a voltammetric behavior closer to that of the unmodified electrode due to minimization of charge repulsion. Voltammograms 4 and 5 corresponding to the successive incorporation of anti-AMY and Biotin-AMY, show slight changes towards a lesser reversible behavior as a consequence of the presence of insulating layers with increased thickness on the electrode surface. The behavior exhibited by voltammograms 6 and 7 is in agreement with that observed by EIS.

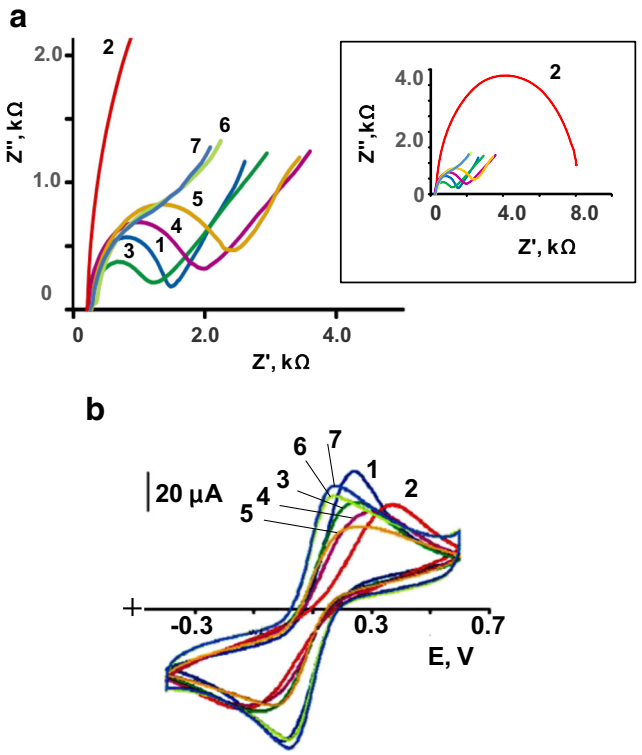

Fig. 3 Nyquist plots (**a**) and cyclic voltammograms (**b**) recorded in 2 mM $[Fe(CN)_6]^{3-/4-}$ in 0.05 M phosphate buffer of pH 3.0: SPCE (1); pPPA/SPCE (2); Mix&Go-pPPA/SPCE (3); anti-AMY-pPPA/SPCE (4); BSA/anti-AMY-pPPA/SPCE (5); Biotin-AMY-anti-AMY-pPPA/SPCE (6); HRP-Strept-Biotin-AMY-anti-AMY-pPPA/SPCE (7)

Analytical figures of merit

A calibration plot for AMY was constructed with the HRP-Strept-Biotin-AMY-anti-AMY-pPPA/SPCE immunosensor under the optimized working conditions at a potential of −200 mV vs Ag pseudo-reference electrode, over the 10^{-5} - 10^{4} pg·mL^{-1} range (Fig. 4). Current vs. AMY concentration curve was fitted by non-linear regression using the Sigma-Plot data analysis software. The adjusted equation ($R^2 = 0.994$) was:

$$i = i_{min} + \frac{i_{max} - i_{min}}{1 + \left(\frac{x}{EC_{50}}\right)^{-h}}$$

where i_{max} and i_{min} were the maximum and minimal current values of the calibration graph, 2.07 ± 0.05 μA and 0.26 ± 0.6 μA, respectively. The EC_{50} value, which is the AMY concentration corresponding to a 50 % competition, was 0.44 ± 0.1 pg·mL^{-1}, and the Hill slope at the inflection point of the sigmoid curve was h = −0.35 ± 0.04. The range of linearity ($R^2 = 0.99$) extended between 1.0 fg·mL^{-1} and 50 pg·mL^{-1}. This range is suitable for the determination of

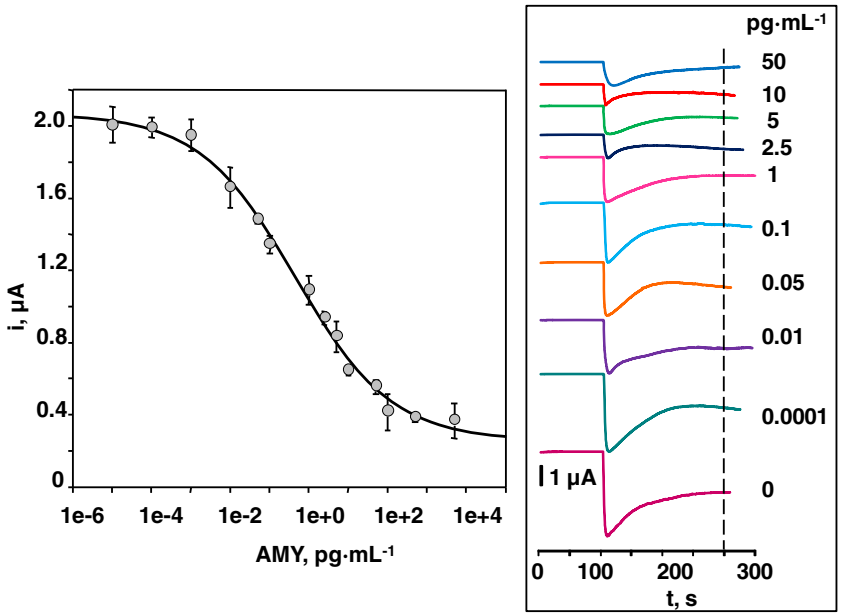

Fig. 4 Calibration plot for AMY and amperograms at HRP-Strept-Biotin-AMY-AMY-anti-AMY-pPPA/SPCE. Dotted line indicates the time of measurement. Working potential: −200 mV vs Ag pseudo.reference electrode. See the text for the other conditions

AMY in human serum since, as it was indicated in the Introduction section, serum concentration of AMY ranges around few tens of pg·mL^{-1} [4, 9, 10]. The limit of detection, 0.92 fg·mL^{-1}, was calculated from the equation:

$$LOD = EC_{50}\left(\frac{i_{max}-i_{min}}{i_{max}-i_{min}-3s}-1\right)^{-\frac{1}{h}}$$

where s is the standard deviation ($n = 10$) of the zero value (the amperometric current measured in the absence of AMY), ± 0.12 µA. It is important to remark that this LOD value is much lower than that claimed as the minimum detectable concentration of AMY for commercial ELISA kits using similar immunoreagents: 0.62 ng·mL^{-1} [https://www.raybiotech.com/files/manual/EIA/EIA-AMY.pdf] and 6.17 pg·mL^{-1} [https:// www.lsbio.com/elisakits/manualpdf/ls-f9686.pdf]. It is also worth to mention that the linear range extends over almost five orders of magnitude which is much wider than those claimed for the ELISA methods with dynamic ranges from 1 to 1000 ng·mL^{-1} [https://www.raybiotech.com/files/manual/EIA/EIA-AMY.pdf] and 6.17 to 500 pg·mL^{-1} [https://www.lsbio.com/elisakits/manualpdf/ls-f9686.pdf]. The high sensitivity achieved with this immunosensor is attributed to the presence of the polymer used as modifier of the electrode surface. The deposited porous conducting polymer allows large amperometric currents to be measured for the detection of the electroactive product, hydrogen peroxide mediated by the hydroquinone system. In addition, the polymer provides a high concentration of carboxyl groups confined on the electrode surface thus allowing the immobilization of a large capture antibody loading which, in turn, allows a high analyte concentration to compete with the biotinylated antigen for antibody binding. Therefore, the amount of HRP-Strept conjugate becomes high for very low amylin concentrations allowing large current signals as well as large current differences for different concentrations of antigen. Moreover, the time lasted for the assay is remarkably longer with the RayBiotech ELISA kit extending over 3 h 15 min and similar to the ELISA kit from LifeSpan BioSciences Inc. (the time needed with the immunosensor is 1 h 50 min counting in all cases since the immobilization of the capture antibody). In addition, the simplicity and ease of use, together with the possibility for developing multiplexed detection make the immunosensor highly attractive compared to ELISA conventional methodologies.

The reproducibility of the amperometric measurements for both 0 and 0.1 pg·mL^{-1} AMY was tested with five different immunosensors prepared on the same day. The relative standard deviation (RSD) values were 5.9 and 5.5%, respectively.

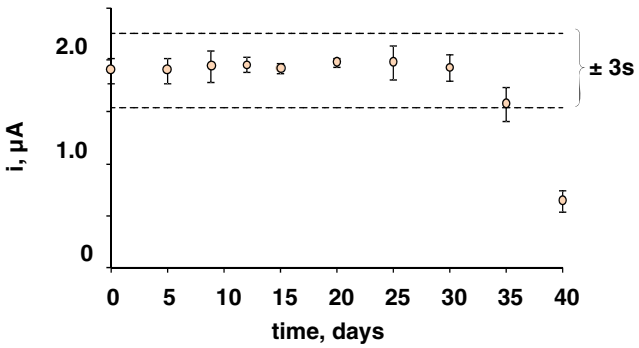

Fig. 5 Control chart constructed to check the storage stability of BSA/anti-AMY-pPPA/SPCE bioelectrodes upon storage at −20 °C in dry ambient. The central value was set as the average amperometric current for ten measurements of different solutions in absence of AMY. Upper and lower limits of control were set as three times the standard deviation of these measurements

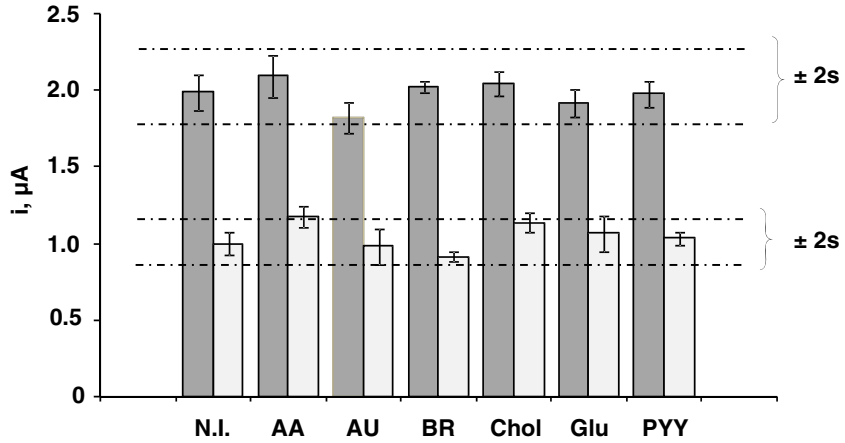

Fig. 6 Effect of the presence of 370 µg/mL ascorbic acid (AA), 50 µg/mL uric acid (UA), 3.4 µg/mL bilirubin (BR), 20 µg/mL cholesterol (Chol), 1.3 mg/mL glucose (Glu), and 100 pg·mL^{-1} peptide YY (PYY) on the amperometric responses measured with the HRP-Strept-Biotin-AMY-AMY-anti-AMY-pPPA/SPCE immunosensor for 0.0 (dark grey) or 1.0 (light grey) pg·mL^{-1} AMY. See the text for more information

Furthermore, RSD values of 6.8 and 7.4% were calculated from measurements made with five different immunosensors prepared in different days. The storage stability of BSA/anti-AMY-pPPA/SPCEs was checked by preparing different bioelectrodes on the same day and stored at −20 °C under dry ambient. Then measurements were made with the HRP-Strept-Biotin-AMY-anti-AMY-pPPA/SPCE immunosensor in the absence of AMY on different days according to the procedure described in Sections 2.3.1 and 2.3.2. The control chart constructed by setting ±3 s as control limits, where s was the standard deviation of the measurements ($n = 10$) carried out the first day of the assay (Fig. 5) shows that the immunosensor responses remained inside the control limits for 35 days, thus demonstrating a very good storage stability of the prepared bioelectrode.

Selectivity

The selectivity of the prepared immunosensor was tested by measuring the amperometric responses for 0.0 and 1.0 pg·mL^{-1} AMY in the absence and in the presence of potentially interfering compounds and non-target proteins. The species tested and their respective concentration level were: ascorbic acid (AA, 370 µg/mL), uric acid (UA, 50 µg·mL^{-1}), bilirubin, (BR, 3.4 µg·mL^{-1}), cholesterol (Chol, 20 µg·mL^{-1}), glucose (Glu, 1.3 mg·mL^{-1}), and peptide YY (PYY, 100 pg·mL^{-1}). These concentrations corresponded approximately to the normal physiological level of the tested compound in human serum. Figure 6 shows as no significant different currents were measured in all cases because all mean values of the measured steady state currents were within the ±2 x standard deviation range of the current measured in the absence of interferent.

Determination of AMY in urine and serum

The usefulness of the immunosensor was tested by analyzing AMY in urine and serum. The possibility of the existence of matrix effect was evaluated by measuring samples spiked with AMY in the range from 0.001 to 1 pg·mL^{-1} (urine) and from 0.001 to 10 pg·mL^{-1} (serum) diluted with different volumes of Assay Diluent B. The results (not shown) revealed that a 1/10 dilution for urine and 1/5 for serum were enough to avoid the matrix effect observed with the undiluted samples. The calibration plots for diluted urine and serum samples were very similar to that of standard AMY solutions with linear ranges between 0.001 and 10 pg·mL^{-1} and slope values of −327 ± 22 (urine) and − 336 ± 12 (serum) µA per decade of concentration. The comparison of these slopes with the slope value for the linear range of calibration for AMY standard solutions, 307 ± 8 µA per decade of concentration, was performed by application of the Student t test for $\alpha = 0.05$ and $n = 12$, obtaining $t_{exp} = 0.832$ and 2.005 for urine and serum, respectively, which are lower than the tabulated value, $t_{tab} = 2.179$. Therefore, the determination of AMY in urine and serum can be performed directly by interpolation of the amperometric current measured with the immunosensor for an aliquot of the diluted sample into the calibration plot constructed with standard solutions. Table 2 summarizes the results in the

Table 2 Determination of amylin in urine and serum samples

Sample	[AMY], pg·mL^{-1}	[AMY] found, pg·mL^{-1}*	Recovery, %
Urine	0.75	0.75 ± 0.05	100 ± 7
	4.0	4.1 ± 0.2	102 ± 4
Serum	1.5	1.4 ± 0.1	94 ± 7
	8.0	8.0 ± 0.4	100 ± 6

*$t_{tab} \cdot s / \sqrt{n}$; $n = 8$

analysis of urine spiked with AMY at 0.75 and 4.0 pg·mL^{-1} concentration levels, and serum spiked at 1.5 and 8.0 pg·mL^{-1} levels. Recoveries ranged between 93 and 102%, thus demonstrating the usefulness of the immunosensor for the analysis of AMY at low concentration levels in urine and serum with minimal sample treatment.

Conclusions

The first electrochemical immunosensor for the determination of the hormone related to adiposity amylin is reported in this work. The disposable immunosensor design implies SPCE functionalized with electropolymerized poly(pyrrole propionic acid) thus providing a high loading of surface confined carboxyl groups suitable for direct covalent binding of anti-AMY antibody upon activation with Mix&Go™ polymer. This design demonstrates to be a successful strategy to be used as a general route for preparing electrochemical immunosensors. The competitive immunoassay involving biotinylated AMY and streptavidin labelled with HRP as the enzymatic tracer was able to provide a calibration graph for AMY with a range of linearity extending from 1.0 fg·mL^{-1} to 50 pg·mL^{-1}, and a detection limit of 0.92 fg·mL^{-1}. It is important to mention that this value is around 7000 times lower than the minimum detectable concentration reported for the commercial ELISA immunoassays for this target hormone. In addition, the immunosensor exhibits an excellent selectivity and shows applicability for the analysis of AMY at low concentration levels in urine and serum with minimal sample treatment and in a shorter assay time that that required for ELISA kits.

Acknowledgements The financial support of projects CTQ2015-70023-R (Spanish Ministry of Economy and Competitivity Research Projects), and S2013/MT-3029 (NANOAVANSENS Program from the Comunidad de Madrid) are gratefully acknowledged.

Compliance with ethical standards The authors declare that they have no competing interest.

References

1. Cooper G, Willis A, Clark A, Turner R, Sim R, Reid K (1987) Purification and characterization of a peptide from amyloid-rich pancreases of type 2 diabetic patients. Proc Natl Acad Sci 84: 8628–8632. https://doi.org/10.1073/pnas.84.23.8628
2. Zhang J, Chen Y, Li D, Cao Y, Wang Z, Li G (2016) Colorimetric determination of islet amyloid polypeptide fibrils and their inhibitors using resveratrol functionalized gold nanoparticles. Microchim Acta 183:659–665
3. Konarkowska B, Aitken JF, Kistler J, Zhang S, Cooper GJ (2006) The aggregation potential of human amylin determines its cytotoxicity towards islet β-cells. FEBS J 273:3614–3624. https://doi.org/10.1111/j.1742-4658.2006.05367.x
4. Percy AJ, Trainor DA, Rittenhouse J, Phelps J, Koda JE (1996) Development of sensitive immunoassays to detect amylin and amylin-like peptides in unextracted plasma. Clin Chem 42:576–585
5. Castillo MJ, Scheen AJ, Lefèbre PJ (1995) Amylin/islet amyloid polypeptide: biochemistry, physiology, patho-physiology. Diabete Metab 21:3–25
6. Koda JE, Fineman M, Rink TJ, Dailey GE, Muchmore DB, Linarelli LG (1992) Amylin concentrations and glucose control. Lancet 339:1179–1180
7. Sanke T, Hanabusa T, Nakano Y, Oki C, Okai K, Nishimura S, Kondo M, Nanjo K (1991) Plasma islet amyloid polypeptide (amylin) levels and their responses to oral glucose in type-2 (non-insulin-dependent) diabetic patients. Diabetologia 34:129–132. https://doi.org/10.1007/BF00500385
8. Kautzky-Willer A, Thomaseth K, Pacini G, Clodi M, Ludvik B, Streli C, Waldhäusl W, Prager E (1994) Role of islet amyloid polypeptide secretion in insulin-resistant humans. Diabetologia 37:188–194. https://doi.org/10.1007/s001250050092
9. Harter E, Svoboda T, Ludvik B, Schuller M, Lell B, Kuenburg E, Brunnbauer M, Woloszcruk W, Prager E (1991) Basal and stimulated plasma levels of pancreatic amylin indicate its co-secretion with insulin in humans. Diabetologia 34:52–54
10. Butler PC, Chou J, Bradford Carter W, Wang Y-N, Bu B-H, Chang D, Chang J-K, Rizza RA (1990) Effects of meal ingestion on plasma amylin concentration in NIDDM and nondiabetic humans. Diabetes 29:752–756
11. Ooi HW, Cooper SJ, Huang C-Y, Jennins D, Chung E, Maeji NJ, Whittaker AK (2014) Coordination complexes as molecular glue for immobilization of antibodies on cyclic olefin copolymer surfaces. Anal Biochem 456:6–13. https://doi.org/10.1016/j.ab.2014.03.023.
12. Ojeda I, Barrejón M, Arellano LM, González-Cortés A, Yáñez-Sedeño P, Langa F, Pingarrón JM (2015) Grafted-double walled carbon nanotubes as electrochemical platforms for immobilization of antibodies using a metallic-complex chelating polymer: application to the determination of adiponectin cytokine in serum. Biosens Bioelectron 74:24–29. https://doi.org/10.1016/j.bios.2015.06.001
13. Muir W, Barden MC, Collett SP, Gorse A-D, Monteiro R, Yang L, McDougall NA, Gould S, Maeji NJ (2007) High-throughput optimization of surfaces for antibody immobilization using metal complexes. Anal Biochem 363:97–107. https://doi.org/10.1016/j.ab.2007.01.015
14. Serafín V, Torrente-Rodríguez RM, Batlle M, García de Frutos P, Campuzano S, Yáñez-Sedeño P, Pingarrón JM (2017) Electrochemical immunosensor for receptor tyrosine kinase AXL using poly(pyrrolepropionic acid)-modified disposable electrodes. Sensors Actuators B Chem 240:1251–1256. https://doi.org/10.1016/j.snb.2016.09.109
15. Eguílaz M, Moreno-Guzmán M, Campuzano S, González-Cortés A, Yáñez-Sedeño P, Pingarrón JM (2010) An electrochemical immunosensor for testosterone using functionalized magnetic beads and screen-printed carbon electrodes. Biosens Bioelectron 26:517–522. https://doi.org/10.1016/j.bios.2010.07.060
16. Dong H, Cao X, Li CM, Hu W (2008) An *in situ* electrochemical surface plasmon resonance immunosensor with polypyrrole propylic acid film: comparison between SPR and electrochemical responses from polymer formation to protein immunosensing. Biosens Bioelectron 23:1055–1062. https://doi.org/10.1016/j.bios.2007.10.026
17. Ball GM, in "Vitamins in foods: analysis, Bioavalaibility, and stability", CRC Taylor and Francis, Boca Raton FL (2006) p. 223.